Facile syntheses of silanols, and syntheses, structures, and properties of various siloxanes

Hisayuki Endo

2014

Department of Chemistry and Chemical Biology
Graduate School of Engineering
Gunma University

Contents

Part 1: General introduction ····· **1**

1.1 Introduction: the nature of silicon

1.2 Synthesis of organic silicon compounds

1.3 Siloxanes and silanols

1.4 Synthesis of silanols

1.5 Synthesis of laddersiloxanes

1.6 Cage-type silsesquioxanes

1.7 Synthesis of cage-type silsesquioxanes

1.8 Application to silicone products

1.9 References

Part 2: Facile syntheses of silanols ····· **17**

Abstract of part 2 ····· **17**

Chapter 1: Facile synthesis of disiloxanetetraols ····· **18**

2.1.1 Introduction

2.1.2 Results and discussion

2.1.3 Summary

2.1.4 Experimental section

2.1.5 References

2.1.6 Supporting information

Chapter 2: Facile synthesis of cyclotrisiloxanetriols ····· **62**

2.2.1 Introduction

2.2.2 Results and discussion

2.2.3 Summary

2.2.4 Experimental section

2.2.5 References

2.2.6 Supporting information

Chapter 3: Facile synthesis of stereoisomers of cyclic silanols ····· **81**

2.3.1 Introduction

2.3.2 Results and discussion

2.3.3 Summary

2.3.4 Experimental section

2.3.5 References

2.3.6 Supporting information
Conclusion of part 2 ····· **160**
2.4.1. Conclusion of part 2
2.4.2. References

Part 3: Syntheses, structures, and properties of various siloxanes ····· **172**
Abstract of part 3 ····· **172**
Chapter 1: Refractive indices of silsesquioxanes with various structures ·· **173**
3.1.1 Introduction
3.1.2 Results and discussion
3.1.3 Summary
3.1.4 Experimental section
3.1.5 References
3.1.6 Supporting information
Chapter 2: Synthesis and properties of phenylsilsesquioxanes with ladder and double-decker structures ····· **214**
3.2.1 Introduction
3.2.2 Results and discussion
3.2.3 Summary
3.2.4 Experimental section
3.2.5 References
3.2.6 Supporting information
Conclusion of part 3 ····· **311**
3.3.1. Conclusion of part 3
3.3.2. References

Acknowledgement ····· **315**

List of publications ····· **316**

Contribution to conferences and meetings ····· **317**

In this doctoral thesis, following abbreviations are used.

BzTMAH: benzyltrimethylammonium hydroxide
COP: cyclic olefin polymer
Cy: cyclohexyl
d: doublet
d: day
DCC: *N*,*N'*-dicyclohexylcarbodiimide
DCU: dicyclohexylurea
DMF: *N*,*N*-dimethylformamide
DMSO: dimethylsulfoxide
Et: ethyl
Et_3N: triethylamine
ether: diethyl ether
GC: gas chromatography
HPLC: high performance liquid chromatography
h : hour
i-Bu : isobutyl
i-Pr : isopropyl
IR: infrared spectroscopy
J: coupling constant of NMR
m: multiplet
*m*CPBA: *m*-chloroperoxybenzoic acid
Me : methyl
min : minute
MS: mass spectrometry
NCO: isocyanate
$NaHCO_3$: sodium bicarbonate
NMR: nuclear magnetic resonance
non: nonet
PC: polycarbonate
PMMA: polymethylmethacrylate
Pr: propyl
Ph : phenyl
ppm : parts per million
r.t. : room temperature

s: singlet
sext : sextet
t: triplet
TBAF: tetra-*n*-butylammonium fluoride
Thexyl: 1,1,2-trimethylpropyl
THF: tetrahydrofuran
Temp.: temperature
Vi: vinyl

Part 1: General introduction

Abstract of this part

This part summarizes properties of silicon element, reactions of silicon and organic silicon compounds, and syntheses and properties of various silanols and siloxanes.

1.1 Introduction: the nature of silicon

Silicon was isolated by J. J. Berzelius for the first time in 1823 [1]. Silicon is the Group 14 element and in the same group as carbon in the periodic table. The Clarke number of silicon is 25.8%, and silicon is the second most abundant element in the earth's crust, and exists as the inorganic silicate and as silicon dioxide [2,3]. Bond dissociation energies of silicon- and carbon-containing bonds is summarized in Table1. As seen from the table, Si-C or Si-Si bond is thermodynamically stable like C-C bond. Silicon also forms good connection to oxygen, giving very strong bonding. Because the electronegativity of silicon atom (1.8) is much smaller than that of oxygen (3.5), Si-O bonds are polarized with silicon positive and oxygen negative. It is estimated that Si-O is approximately 50% ionic bonding, and energetically stable. However, the ionic property of siloxane bonds means that siloxane bonds are vulnerable to ionic attack by acids or bases. The same tendency is observed in Si-Cl bond [4].

Table 1. Bond dissociation energy of various chemical bonds

	Bond dissociation energy / $kJmol^{-1}$
Si-C	270-376
Si-Si	308-332
Si-H	330-400
Si-Cl	450-470
Si-O	330-400
Si-N	400-430
C-C	334
C-H	420
C-Cl	335
C-O	340
C-N	335

Siloxane bond length (1.64 Å) is longer than that of carbon-carbon bonds (1.54 Å) and the bond angle of siloxane (140°) is greater than that of polyethylene (109°). Furthermore, compared to the rotation energy of carbon-carbon bonds (15.1 kJ/mol) or carbon-oxygen bonds (11.3 kJ/mol), the rotation energy of silicon-oxygen bonds is extremely low (less than 0.8 kJ/mol), so siloxane bonds can move easily. Several bond angles of siloxanes are shown in Figure 1 [4].

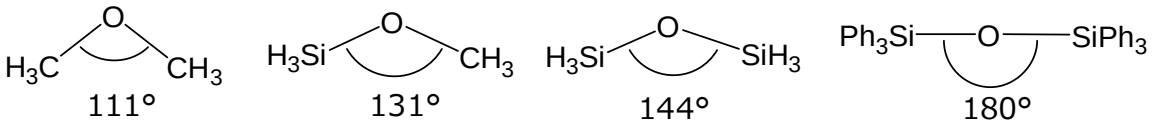

Figure 1

1.2 Synthesis of organic silicon compounds

Silicon metal is industrially prepared by the reaction of silica with carbon in the electric arc furnace at high temperature above 1000 ℃. Silicon metal is treated with halogen, hydrogen halide, and alcohol (e.g. Cl_2, HCl, ethanol, and methanol) to give various silicon compounds (Scheme 1) [4].

$$Si + 2Cl_2 \longrightarrow SiCl_4 \qquad Si + 4EtOH \longrightarrow Si(OEt)_4$$

$$Si + 3HCl \longrightarrow HSiCl_3 \qquad Si + 4MeOH \longrightarrow Si(OMe)_4$$

Scheme 1

Silicon metal reacts with alkyl halide (MeCl) in the presence of a Cu catalyst to give chlorosilanes (Me_2SiCl_2, $MeSiCl_3$, Me_3SiCl, and $MeSiHCl_2$) (Scheme 2) [4]. The importance of this reaction is recognized to be called “direct synthesis” or “direct process” which was discovered by E. G. Rochow. The direct synthesis method can offer various organic silicon compounds by changing alkyl halide and reaction conditions. In addition, most organic silicon compounds were made by Grignard reagents or organolithium reagents starting from chlorosilanes (Scheme 3) [4].

$$Si \xrightarrow{MeCl\ /\ Cu} Me_2SiCl_2 + Me_3SiCl + MeSiCl_3 + MeSiHCl_2 + other$$

Scheme 2

$$MeSiCl_3 \xrightarrow[-MgCl_2]{PhMgCl} PhMeSiCl_2 \qquad HSiCl_3 \xrightarrow[-MgBrCl]{EtMgBr} Et_3SiH$$

$$MeSiHCl_2 \xrightarrow[-MgCl_2]{PhMgCl} PhMeSiHCl \qquad MeSi(OEt)_3 \xrightarrow[-MgCl(OEt)]{PhMgCl} PhMeSi(OEt)_2$$

Scheme 3

Hydrosilanes react with various alkenes in the presence of platinum catalysts to give organic silicon compounds (Scheme 4). This reaction is called “hydrosilylation” [4].

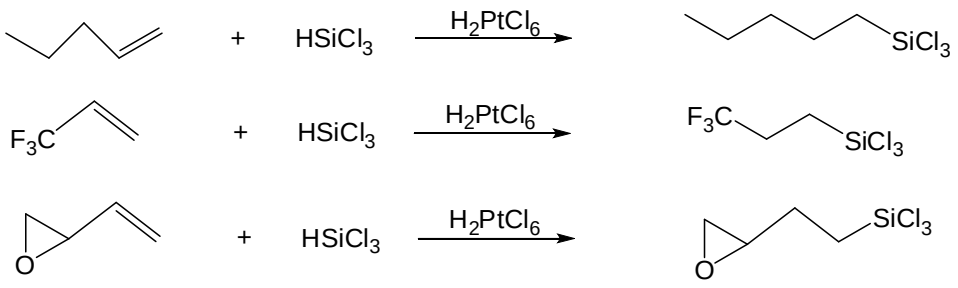

Scheme 4

1.3 Siloxanes and silanols

Primary siloxane ($R_3SiO_{1/2}$), secondary siloxane ($R_2SiO_{2/2}$), tertiary siloxane ($RSiO_{3/2}$) and quarterly siloxane ($SiO_{4/2}$) units are often referred as M (Mono-functional), D (Di-functional), T (Tri-functional) and Q (Quadra-functional) unit, respectively, which is widely accepted description for the building blocks of polyorganosiloxanes (Figure 2) [4].

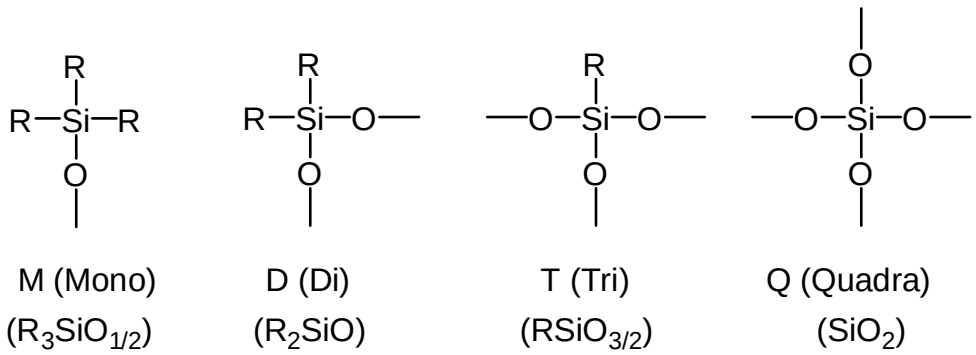

Figure 2

Siloxane compounds have several structures shown in Figure 3 [4]. Compounds containing only T structure are called silsesquioxanes. The structures of silsesquioxane have been reported as cage structures, parts of ladder structures, and random structures as illustrated in Figure 3.

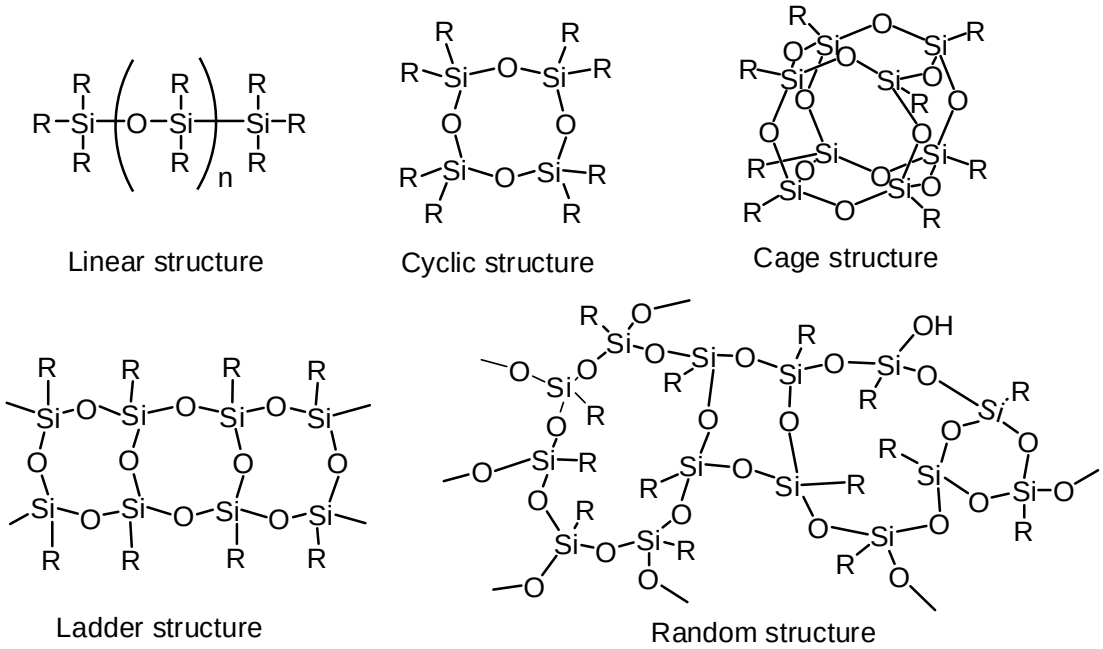

Figure 3

Silicon also forms stable compounds with multiple hydroxy groups. Therefore various silanols have been reported as shown in Figure 4 [5].

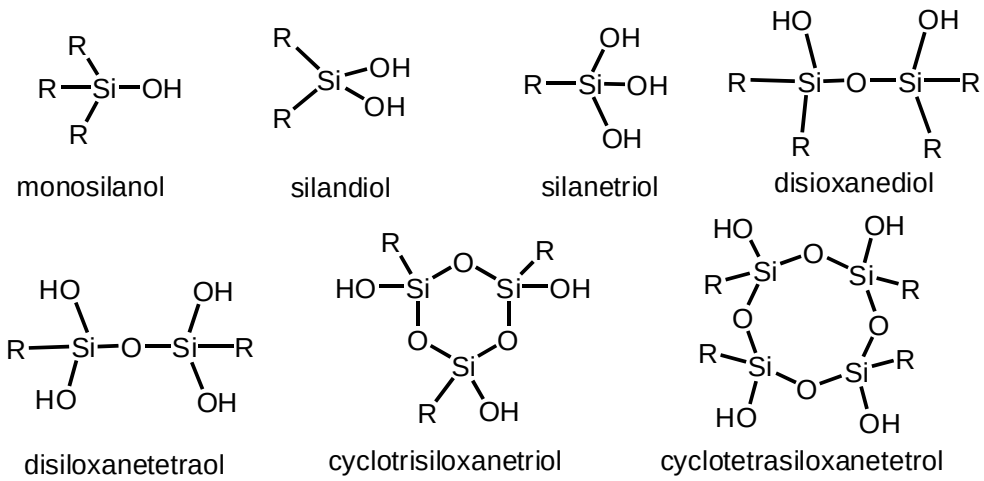

Figure 4

1.4 Synthesis of silanols

Usually, various silanols are synthesized by hydrolysis and following condensation from chlorosilanes ($RSiCl_3$, R_2SiCl_2, and R_3SiCl). Stability of these silanols depends on the bulkiness of substituents (Scheme 5) [5].

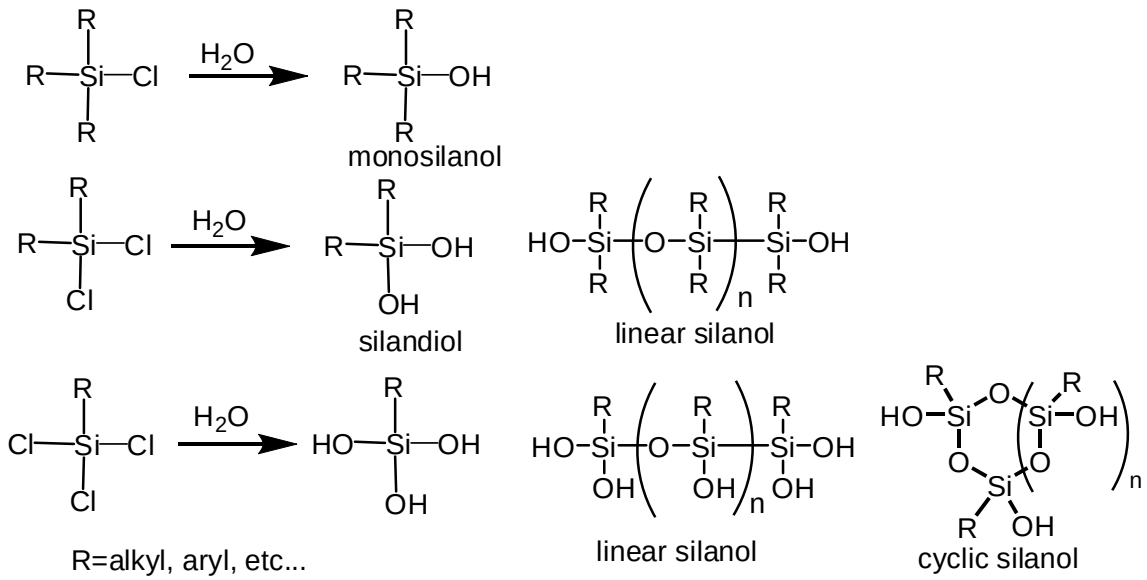

Scheme 5

All-*cis*-cyclotetrasiloxanetetraol $[RSiO(OH)]_4$ was synthesized from hydrolytic condensation of $RSiCl_3$ (R = *i*-Pr [6], Ph [7,8], *c*-C_6H_{11} [9]) (Scheme 6).

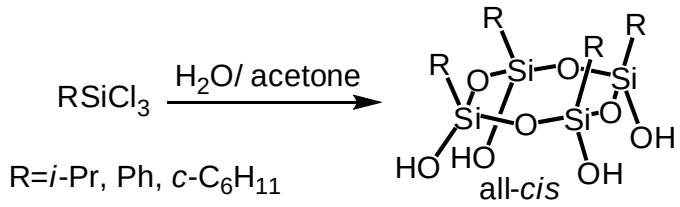

Scheme 6

Tetraisopropylcyclotetrasiloxanetetraols ($[i\text{-PrSiO(OH)}]_4$) (all-*cis*, *cis-trans-cis*, *cis-cis-trans*, all-*trans isomers*) were first synthesized by multi-step reaction [10]. As the first step, *i*-$PrPhD_4$ ($[i\text{-PrPhSiO}]_4$) was synthesized by hydrolytic condensation of *i*-$PrPhSiCl_2$, and four stereoisomers were separated by recycle-type HPLC. Then each isomer was converted to $[i\text{-PrSi(Cl)O}]_4$ by dephenylchlorination and following hydrolysis to afford the corresponding cyclic silanols. By this method, four isomers of the cyclic silanol were isolated and structures were determined by X-ray crystallographic analysis (Scheme 7).

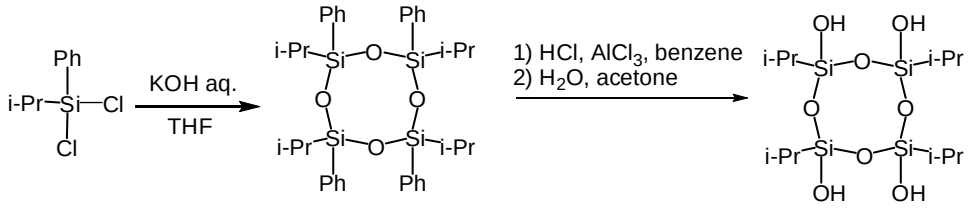

Scheme 7

Russian group and Kawakami group reported high-yield synthesis of all-*cis*-cyclotetorasiloxanolate [11,12]. These cyclotetorasiloxanolate can be converted to all-*cis*-cyclotetrasiloxanetetraols [12] (Scheme 8).

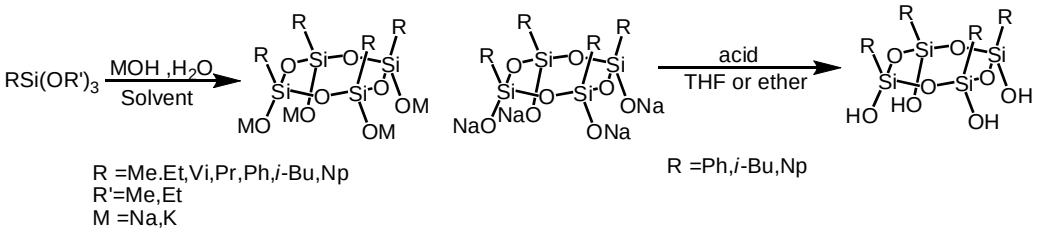

Scheme 8

Silsesquioxanes including oligocyclic laddersiloxanes (ladder-type silsesquioxanes with defined structure) and cage silsesquioxanes could be synthesized from cyclotetrasiloxanetetraols (Scheme 9) [13]. Therefore, in the syntheses of these silsesquioxanes with well-defined structures, all-*cis*-1,3,5,7-tetraisopropylcyclotetrasiloxane-1,3,5,7-tetraol ([*i*-PrSiO(OH)]$_4$) has been served as a key starting compound.

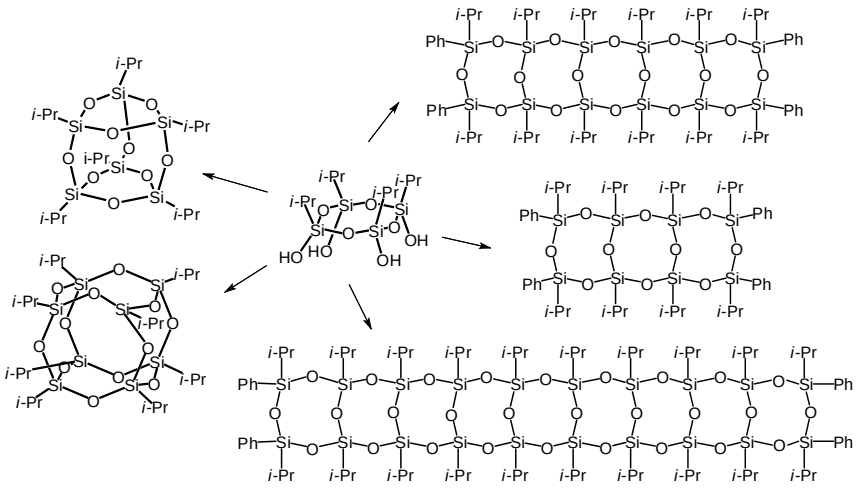

Scheme 9

1.5 Synthesis of laddersiloxanes

In 1960, Brown and co-workers first proposed the structure for phenyl-substituted ladder silsesquioxanes [14]. His group reported that the base-catalyzed polycondensation of the hydrolysate from phenyltrichlorosilane led to the formation of ladder polysilsesquioxanes $(PhSiO_{1.5})_n$ (Scheme 10). After this report, the synthesis of ladder polysilsesquioxanes was actively investigated. However, there has been no unequivocal evidence of *real* ladder structure. Now it is widely accepted that it is very difficult to obtain well-defined ladder polysilsesquioxanes from $RSiCl_3$. Because there are many possibilities to generate cage, ladder, and random structures in hydrolytic condensation reaction of $RSiCl_3$, and the ladder structure is entropically less favorable because of restricted structure.

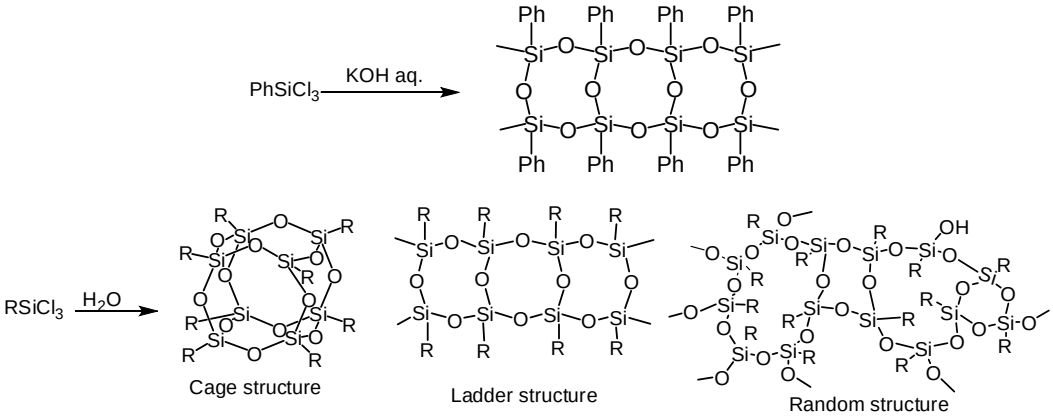

Scheme 10

In the last decade, synthesis, structure determination, and thermal properties of alkyl-substituted laddersiloxane up to nonacyclic one have been reported from our group [15]. The synthetic route into the laddersiloxane is shown in Scheme 11. All-*cis*-[*i*-PrSiO(OH)]$_4$ was treated with two equivalents of [*i*-PrPhSi(Cl)]$_2$O to give the corresponding tricyclic laddersiloxanes including five stereoisomers. *Syn*-type tricyclic laddersiloxanes were isolated by recycle-type HPLC for all five isomers. Then the tricyclic laddersiloxanes were converted to those with tetrachloro substituents, and the tetrachloro-tricyclic laddersiloxanes were converted to tricyclic laddersiloxane having four hydroxyl substituents. These processes were repeated several times to afford up to nonacyclic laddersiloxanes. We also reported methyl-substituted ladder polysilsesquioxane from *cis*- *trans*-*cis*-[MeSi(Br)O]$_4$.

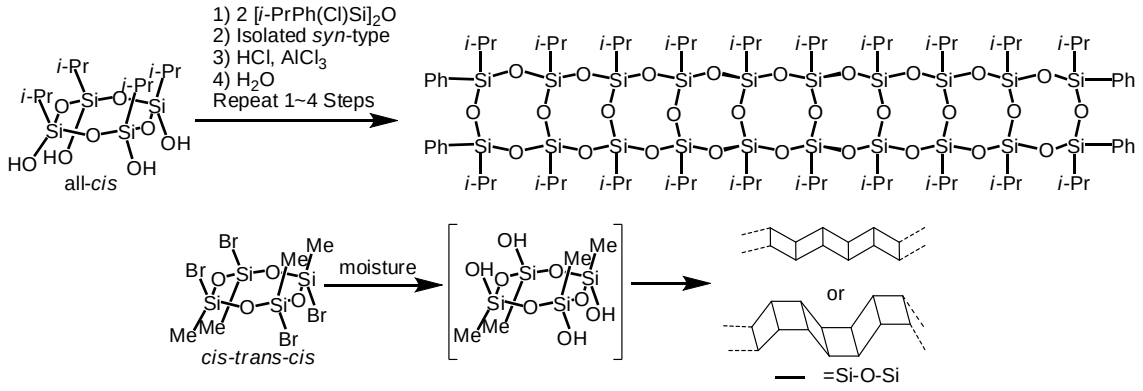

Scheme 11

Gunji's group reported synthesis of *cis-trans-cis*-[MeSi(NCO)O]$_4$. This *cis-trans-cis*-[MeSi(NCO)O]$_4$ is applied to the synthesis of bicyclic, tricyclic and pentacyclic laddersiloxanes (Scheme 12) [16,17].

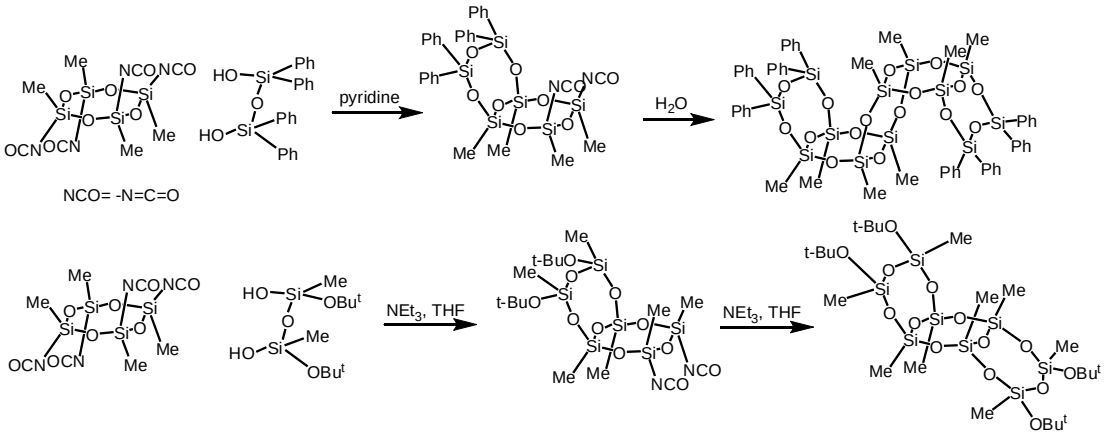

Scheme 12

Bicyclic, tricyclic and pentacyclic laddersiloxanes were also synthesized by oxidation of bicyclic, tricyclic and pentacyclic ladder polysilanes using excess amount of *m*CPBA (*m*-chloroperoxybenzoic acid) (Scheme 13) [18].

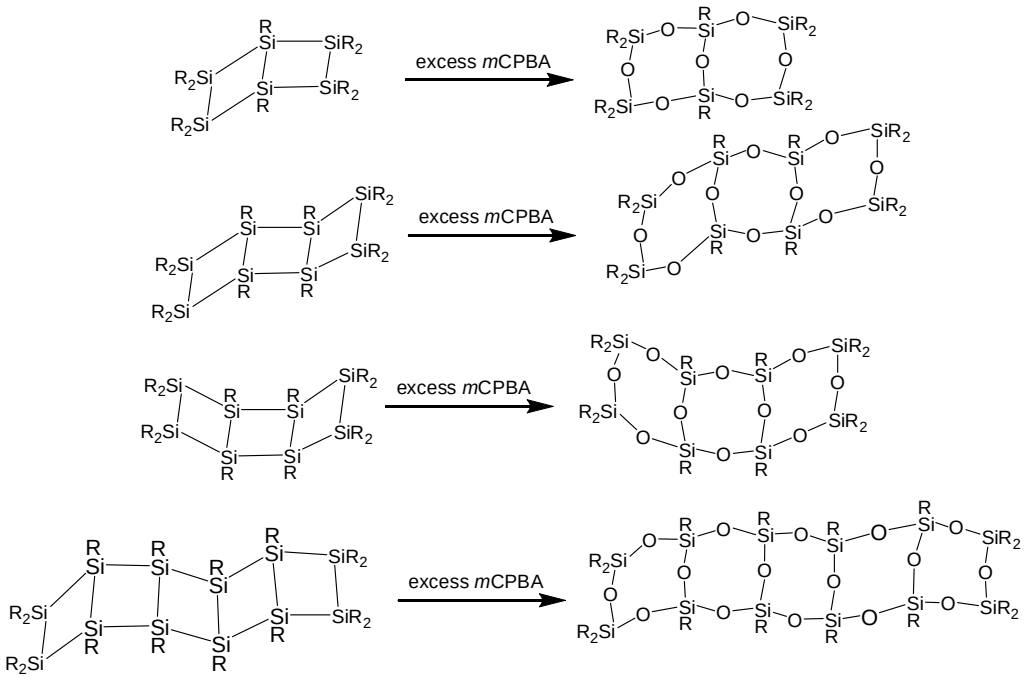

Scheme 13

1.6 Cage-type silsesquioxanes

Various cage type silsesquioxane were reported. In cage silsesquioxane, there are two types, that is, are closed-cage type and open-cage type (Figure 5) [4]. There are many synthetic reports on closed-cage type silsesquioxanes. In closed-cage type silsesquioxane, R_6T_6, R_8T_8, $R_{10}T_{10}$, and $R_{12}T_{12}$ are reported (R_nT_n, n: number of silicon atoms). The most studied type of closed-cage is the R_8T_8. Closed cage type silsesquioxane includes Q_8 which has siloxy substituents. Strictly speaking, the Q_8 cage should not be called silsesquioxane. The Q_8 cage can be synthesized from tetraalkoxysilanes. Structures of open-cage silsesquioxanes are sometimes referred as incompletely condensed silsesquioxanes. These open-cage silsesquioxane may have silanol moieties. Therefore, they are often utilized as precursors for siloxane polymer synthesis.

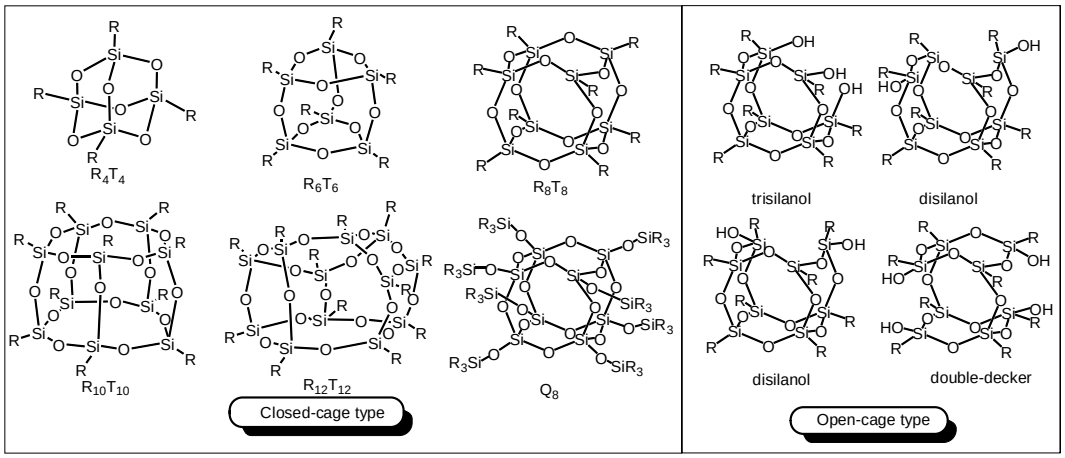

Figure 5

1.7 Synthesis of cage-type silsesquioxanes

Synthesis of R_4T_4 by hydrolysis and sequential condensation reaction of *t*-$BuSiCl_3$ or *i*-$PrSiCl_3$ was reported in 1950 (Scheme 14) [19]. However, there is no unequivocal evidence of the structure. Moreover, under in this reaction condition, cyclic silanols or silanetriols may be exclusively produced, and it is difficult to synthesize R_4T_4 under in this condition.

There are several synthetic methods of R_6T_6 (Scheme 15) [6,9,20,21,22]. Synthesis of Cy_6T_6 by hydrolysis and sequential condensation reaction of $CySiCl_3$ at room temperature for a few months was reported [9, 22]. We reported facile synthetic methods of R_6T_6 (Thexyl (1,1,2-trimethylpropyl), *t*-Bu, *i*-Pr) [6,20,21]. $RSi(OH)_3$ or $[RSi(OH)_2]_2O$ reacts with DCC (*N*,*N*-dicyclohexylcarbodiimide) in DMSO (dimethyl sulfoxide) or DMF (*N*,*N*-dimethylformamide) to give R_6T_6 (R = Thexyl, *t*-Bu). All-*cis*-[*i*-PrSiO(OH)]$_4$ was treated with (*i*-$PrCl_2Si)_2O$ in pyridine to give R_6T_6 (R = *i*-Pr) for drastically shorter reaction time.

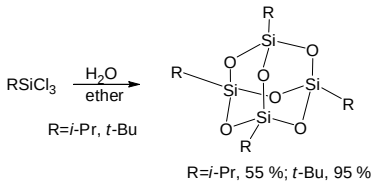

Scheme 14

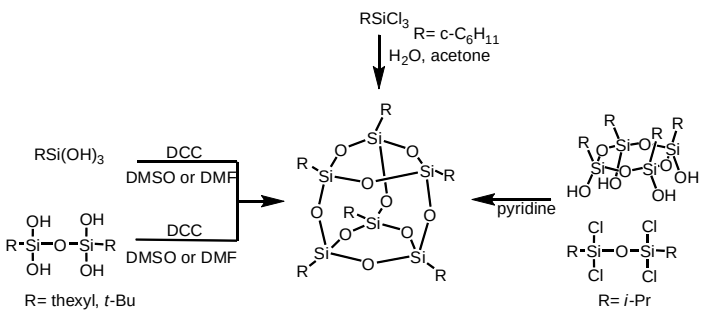

Scheme 15

R_8T_8 was synthesized by hydrolysis and sequential condensation reaction of $RSiCl_3$ or $RSi(OR')_3$ (Scheme 16). Recently, Kawakami's group reported the selective synthesis of R_8T_8 from all-*cis*-$[RSiO(OH)]_4$ by using catalytic amount of TBAF (tetra-*n*-butylammonium fluoride) or BzTMAH (benzyltrimethylammonium hydroxide) [23, 24].

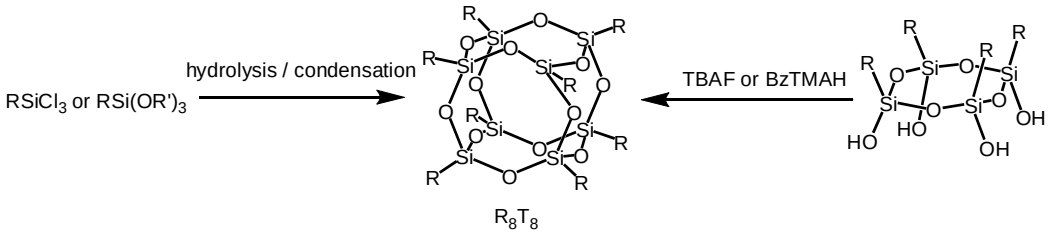

Scheme 16

Et_8T_8 was converted to $Et_{10}T_{10}$ or $Et_{12}T_{12}$ by using K_2CO_3 in acetone (Scheme 17) [25].

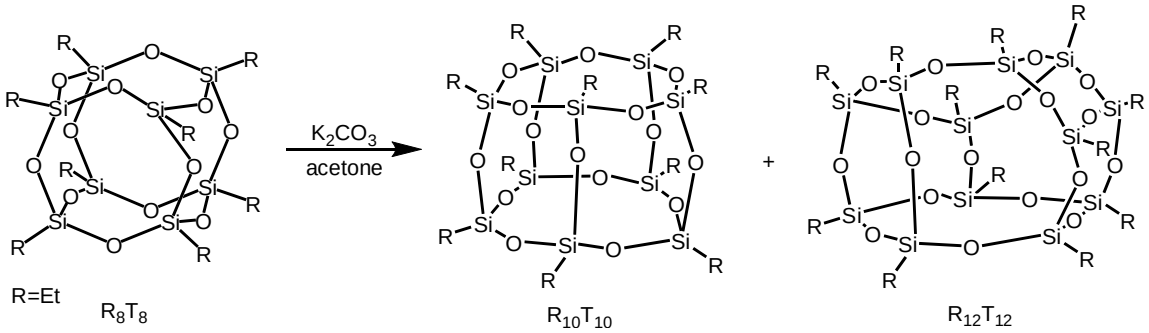

Scheme 17

Synthesis of chemical species encapsulated cage silsesquioxane was reported (Scheme 18) [26,27]. Bassindale *et al.* synthesized fluoride ion encapsulated Ph_8T_8 ($F^-@Ph_8T_8$) from triethoxyphenylsilane and TBAF as a catalyst in the presence of small amount of water. The structure was determined by X-ray crystallographic analysis. Hydrogen radical encapsulated Q_8 ($H\bullet@TMS_8Q_8$) was also synthesized by γ-ray irradiation of TMS_8Q_8.

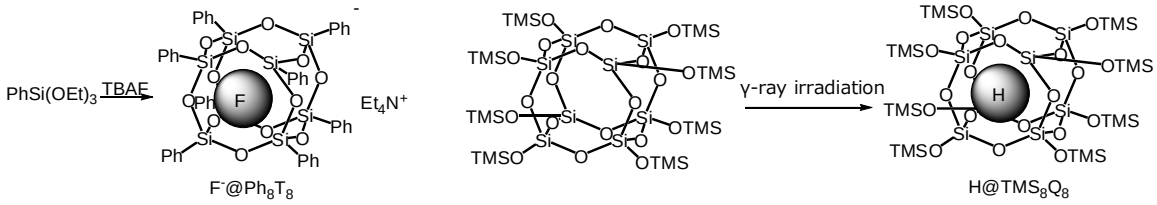

Scheme 18

1.8 Application to silicone products

Silicone composes a variety of materials by utilizing crosslinking and blending to other silicone. Silicone is classified roughly into three conformations (silicone oil, silicone rubber or elastomer, and silicone resin). Silicone oil is used as insulating oils, damper oil, and heat-transfer oil, etc. Silicone rubber or elastomer is used as parts for automobile, wire covering, keyboard and roller of printer. Silicone resin is used as heat resistant resin varnish and hard coating [28]. High-crosslinking silicone is used for resin. Low-crosslinking silicone is used oil. High-crosslinking silicone is high containing ratio of T and Q units. Low-crosslinking silicone is high ratio of D units.

There are various crosslinking methods in silicone. Popular crosslinking method is hydrolytic condensation to make siloxane bonds (Figure 6) [4]. Another method is hydrosilylation of hydrosilane and olefin. More recently, coupling reaction of a hydrosilane with a silanols or an alkoxysilane in the presence of catalytic amount of $B(C_6F_5)_3$ are well utilized [29a,b]. In these methods except hydrosilylation, usually byproducts are generated (e.g. alcohol, H_2O, H_2 gas, or alkane). These byproducts sometimes caused problems (cracking of resin, decomposition of protected substance) in process of manufacturing. Therefore, hydrosilylation is better crosslinking method because of no byproducts. Silicone may have several organic groups that can crosslink with other organic group.

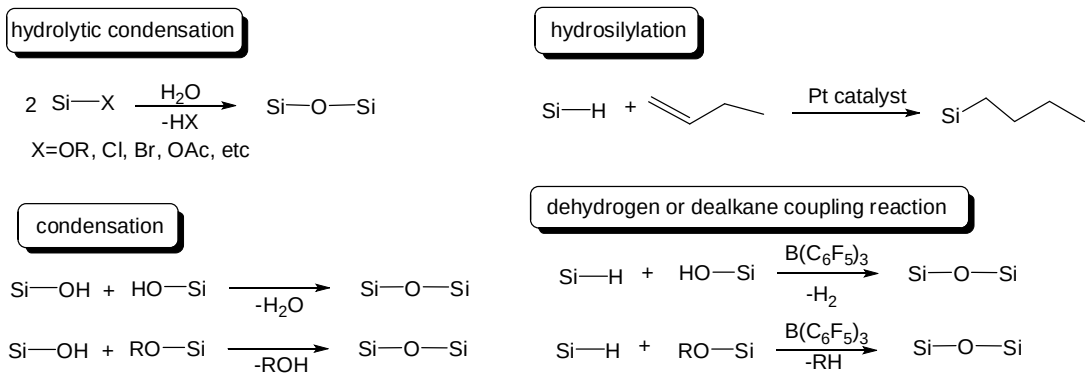

Figure 6

In these days, silicone is applied to LED encapsulate. LED (light emitting diode) is used as illumination lamp. LED needs little electricity to work, and longer operating life than fluorescent light. Structure of LED is shown in Figure 7 [30].

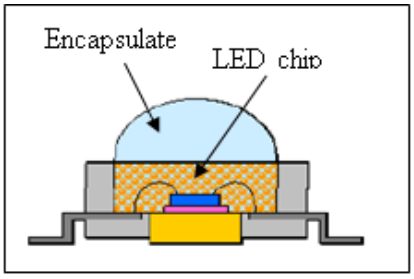

Figure 7. Pattern diagrams of LED (light emitting diode)

LED chip (semiconductor material: GaN) is unstable in moisture. Encapsulate protect LED chip from moisture. Encapsulates have several requirements including high transparency, high RI, chemical stability, weather resistance, high-temperature stability, and hermeticity [30]. In these days, silicone resin is used as encapsulate because silicone resin can accomplish most requirements [30]. However, usually RI of silicone resin is low (1.40~1.53). RI of LED chip (semiconductor material: GaN) is 2.5. The low RI of silicone resin caused deteriorating light-extraction efficiency [30]. Therefore, silicone resin having high RI is required. And if brighter LED chip is developed, LED encapsulate is required more high-temperature stability.

Usually, there are several methods for increasing RI: introduction of aromatic ring, halogen atom except fluorine, metal atom, sulfur atom, and phosphorus atom [31a]. In these methods, introduction of metal atom (e.g. Ti, Zr, Zn, and Sb) is better because RIs of these oxides are very high. For example, RI of organic polymer is about 1.4–1.6 (Table 2) while Ris of TiO_2, ZrO, and ZnO are 2.45–2.70, 2.2, and 2.2, respectively [31a].

Table 2. Refractive index of organic polymer [31a, b]

Compounds	Refractive index
PMMA (polymethylmethacrylate)	1.49
PC (polycarbonate)	1.59
COP (cyclic olefin polymer)	1.53
Epoxy resin	1.47–1.60
Silicone resin	1.40–1.53

1.9 References

[1]東芝シリコーン株式会社　“新シリコーンとその応用” 東芝シリコーン株式会社 (1994).
Toshiba Silicone Co., Ltd., “*Shin Silicone to sono ouyou*”, *Toshiba Silicone* Co., Ltd., Tokyo, Japan **1994**.
[2]岩波雄二郎　”岩波理化学事典　第 3 版” 岩波書店 (1971).
Y. Iwanami, “*Iwanami rikagaku jiten*”, 3rd Ed., *Iwanami Syoten*, Tokyo, Japan **1971**.
[3]岩崎岩次 “無機化学全集 12-2 ケイ素 Si”, 丸善株式会社 (1986).
I. Iwasaki, “Complete Book of Inorganic Chemistry, XII-2: Silicon (*Muki Kagaku Zensho, XII-2: Keiso*)”, Maruzen Co., Ltd., Tokyo, Japan.
[4] 技術情報協会　“ケイ素化合物の選定と最適利用技術　-応用事例集- <上巻>”　技術情報協会 (2006).
Gijyutu Jyouhou Kyoukai Ed., “*Keiso kagoubutsu no sentei to saiteki riyo gijyutsu –ouyou jirei shu jyoukan*”, *Gijyutu Jjyouhou Kyoukai*, Tokyo, Japan, **2006**.
[5] P. D. Lickiss, *Adv. Inorg. Chem.*, **1995**, *42*, 147.
[6] M. Unno, A. Suto, K. Takada, H. Matsumoto, *Bull. Chem. Soc. Jpn.*, **2000**, *73*, 215.
[7] J. F. Brown, Jr., L.H. Vogt, Jr., *J. Am. Chem. Soc.*, **1965**, *87*, 4317.
[8] F. J. Feher, J. J. Schwab, D. Soulivong, J. W. Ziller, *Main Group Chem.*, **1997**, *2*, 123.
[9] J. F. Brown, Jr., L.H. Vogt, Jr., *J. Am. Chem. Soc.*, **1965**, *87*, 4313.
[10] M. Unno, Y. Kawaguchi, Y. Kishimoto, H. Matsumoto, *J. Am. Chem. Soc.*, **2005,** *127*, 2256.
[11] O. I. Shchegolikhina, Yu. A. Pozdnyakova, A. A. Chetverikov, A. S. Peregudov,M. I. Buzin, E. V. Matukhina, *Russ. Chem. Bull. Int. Ed.*, **2007**, *56*, 83.
[12] R. Ito, Y. Kakihana, Y. Kawakami, *Chem. Lett.*, **2009**, *38*, 364.
[13] 伊藤真樹 “シルセスキオキサン材料の化学と応用展開”, 株式会社シーエムシー出版
(2007).
M. Itoh, Ed, “*Shirusesukiokisan Zairyo no Kagaku to Oyo Tenkai, CMC Shuppan”*, Tokyo, Japan, **2007.**
[14] J. F. Brown Jr, L. H. Vogt Jr, A. Katchman, J. W. Eustance, K. M. Kiser, K. W. Krantz, *J. Am. Chem. Soc*., **1960**, *82*, 6194.
[15] S. Chang, T. Matsumoto, H. Matsumoto, M. Unno, *Appl. Organomet., Chem.* **2010**, *24*, 241.
[16] K. Suyma, T. Gunji, K. Arimitsu, Y. Abe, *Organometallics*, **2006**, *25*, 5587.
[17] H. Seki, N. Abe, Y. Abe, T. Gunji, *Chem. Lett.*, **2011,** *40*, 722.

[18] M. Unno, R. Tanaka, S. Tanaka, T. Takeuchi, S. Kyushin, H. Matsumoto, *Organometallics*, **2005,** *24*, 765.
[19] E. Wiberg, W. Simmler, *Z. Anorg. Allg. Chem.* **1955,** *282*, 330.
[20] M. Unno, S. B. Alias, H. Saito, H. Matsumoto, *Organometallics*, **1996**, *15*, 2413.
[21] M. Unno, Y. Imai, H. Matsumoto, *Silicon Chem.*, **2003**, 2, 175.
[22] H. Behbehani, B. J. Brisdon, M. F. Mahon, K. C. Molloy, *J. Organomet. Chem.*, **1994**, *469*, 19.
[23] P. D. Lickiss, and F. Rataboul, *Adv. Organomet. Chem.*, **2008**, *57*, 1.
[24] S. Tateyama, Y. Kakihana, Y. Kawakami, *J. Organomet. Chem.*, **2010**, *695*, 898.
[25] E. Rikowski, H. C. Marsmann, *Polyhedron*, **1997**, *16*, 3357.
[26] R. Sasamori, Y. Okaue, T. Isobe, Y. Matsuda, *Science*, **1994**, *265*, 1691.
[27] A. R. Bassindale, M. Pourny, P. G. Taylor, M. B. Hursthouse, M. E. Light, *Angew. Chem., Int. Ed.*, **2003**, *42*, 3488.
[28]吉良満夫, 玉尾浩平, “現代ケイ素化学体系的な基礎概念と応用に向けて”, 化学同人 (2013). M. Kira, K. Tamao, Ed, “Gendai keiso kagaku – *taikeiteki na kisogainen to ouyou ni mukete*” *Kagaku* doujin, Tokyo, Japan, **2013**.
[29a] D. Zhou, Y. Kawakami, *Macromolecules*, **2005**, *38*, 6902.
[29b]D. B. Thompson, M. A. Brook, *J. Am. Chem. Soc.*, **2008**, *130*, 32.
[30] E. F. Schubert, “Light-emitting diodes, second edition”, Cambridge University Press, Cambridge, **2006**.
[31a] 渡辺敏行, 魚津吉弘 “光学材料の屈折率制御技術の最前線”, 株式会社シーエムシー出版 (2009). T. Watanabe, and Y. Uozu, Ed, “Frontiers of refractive index control in optical materials (*Kogaku zairyo no kussetsuritsu seigyo gijutsu no saizensen*)”, *CMC Shuppan*, Tokyo, Japan, **2009.**
[31b] LED 照明推進協議会 “LED 照明信頼性ハンドブック” 日刊工業新聞社 (2008). *LED shoumei suishin kyougikai, “LED syoumei shinraisei handobukku”, Nikkan kougyou shinbunsya*, Tokyo, Japan, **2008**.

Part 2: Facile syntheses of silanols

Abstract of part 2

In this part, we described a facile synthesis of disiloxanetetraols, cyclotrisiloxanetriols, and cyclotetrasiloxanetetraols by hydrolytic condensation of trichlorosilanes. We also described in a facile synthesis of four isomers of cyclotetrasiloxanetetraols by stereoisomerization reaction of all-*cis*-cyclotetrasiloxanetetraols. Suitable stereoisomerization reaction conditions could be found by carrying out the reactions under various conditions. A plausible mechanism of the stereoisomerization is also described.

Chapter 1: Facile synthesis of disiloxanetetraols

2.1.1 Introduction

Until now various structures of silanols have been known [1]. For example, there are silanetriol, disiloxanediol, disiloxanetetraol, cyclotetrasiloxanetetraol, and cage-like silanols. Among them, disiloxanetetraols are very useful as synthetic precursors for various siloxane compounds.

Our group reported the synthesis of cage octasilsesquioxanes R_8T_8 (R = Cy: cyclohexyl) [2] and hexasilsesquioxanes R_6T_6 (R = 1,1,2-trimethylpropyl, *t*-Bu, 2,4,6-triisopropylphenyl) from $[RSi(OH)_2]_2O$ with bulky substituents by using dicyclohexylcarbodiimide (DCC) in DMSO [3,4]. Other groups reported the synthesis of ladder-type silsesquioxanes from disiloxanetetraols as a useful parts of backbone construction [5]. More recently, synthesis of trigonal cage metallosiloxane complex from bis(*tert*-butyl)disiloxanetetraol and Te complex was reported by Chandrasekhar [6] as shown in Scheme 1.

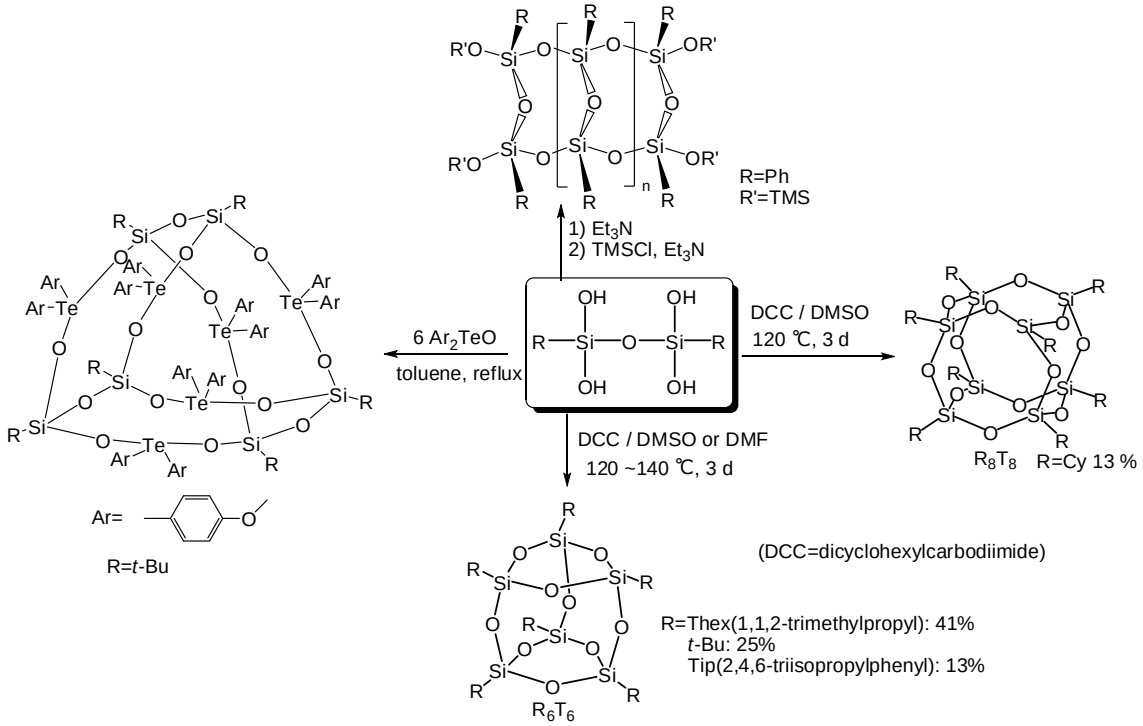

Scheme 1

Although a disiloxanetetraol has a simple structure, there have been few synthetic reports. Reported disiloxanetetraols bearing smaller alkyl or aryl substituents are summarized in Table 1 [5,7–13]. Disiloxanetetraols with larger substituents are also reported [14].

Table 1. Reported synthesis of various $[RSi(OH)_2]_2O$

R	Starting material	Yield / %	^{29}Si NMR / ppm	Ref.
C_6H_{13}	$C_6H_{13}SiCl_3$[a]	72.6	—	[7]
C_8H_{17}	$C_8H_{17}SiCl_3$[a]	75.2	—	[7]
$C_{10}H_{21}$	$C_{10}H_{21}SiCl_3$[a]	79.2	—	[7]
t-Bu	*t*-$BuSiCl_3$[a]	65	—	[8a]
t-Bu	*t*-$BuSiCl_3$[b]	90	–49.55	[8b]
1,1,2-trimethylpropyl	1,1,2-trimethylpropyltrichlorosilane [a]	47	–51.2	[9]
Cy	$CySiCl_3$[b]	84	—	[10]
Ph	$PhSi(OAc)_3$ [b]	9	—	[11a]
Ph	$[PhSiCl_2]O$ [c]	76	–62.1	[11b], [11c]
Ph	$[PhSi(OMe)_2]O$ [d]	47.9	–61	[5]
2,4,6-triisopropylphenyl	2,4,6-triisopropylphenyltrichlorosilane[b]	88	–63.07	[4, 12]
2-naphthyl	2-naphthyltrimethoxysilane[e]	88	–62.94	[13]
m-biphenyl	*m*-biphenyltrimethoxysilane [e]	84	–61.8	[13]

a: Hydrolytic condensation (HCl was trapped by base), b: Hydrolytic condensation , c: Hydrolysis (HCl was trapped by base), d: Hydrolysis（Acidic condition）, e: Hydrolytic condensation (In self-assembled coordination cages)

For structure analyses, there are only six crystallographic reports published for $[RSi(OH)_2]_2O$ (R = Ph [11c], *t*-Bu [8a], *m*-biphenyl [13], 2-naphthyl [13], Ph_3C [14a], *trans*,*trans*-1,2,3,4-tetraphenylbutadienyl [14b]). Generally, disiloxanetetraols are prone to self-condensation. This reaction is accelerated by the existence of acid or base. Usually silanols are prepared from the corresponding chlorosilanes or alkoxysilanes with acid or base, and therefore it is not easy to stop the reaction at the stage of disiloxanetetraol. For this reason, reported disiloxanetetraols are usually stabilized by bulky substituents. As another approach, dinapthyldisiloxanetetoraol and bisbiphenyldisiloxanetetoraol were isolated by stabilized in self-assembled coordination cages [13].

Generally for the preparation of disiloxanetetraols by hydrolytic condensation of chlorosilanes, it is difficult to obtain target compounds by controlling the reaction conditions. However, we have investigated the early stage of the reaction in detail, and

found out that disiloxanetetraols could be obtained by simple procedure.

In this chapter, we describe facile synthesis of disiloxanetetraols with middle size substituents from trichlorosilanes by only controlling reaction conditions (Scheme 2).

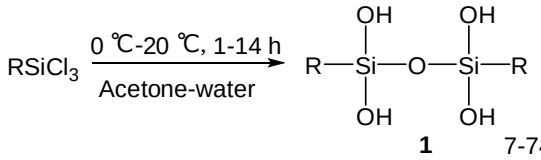

R=Pr (**1a**), C_6H_{13}(**1b**), *i*-Pr(**1c**), *i*-Bu(**1d**), Ph(**1e**), Cy(**1f**), C_5H_9(**1g**)

Scheme 2

2.1.2 Results and discussion

Ishikawa's group reported the elucidation of hydrolytic condensation mechanism from $PhSiCl_3$ monitored by ^{29}Si NMR [15]. In this paper, they indicated the existence of $[PhSi(OH)_2]_2O$ (**1e**) as an intermediate and it gradually transformed to all-*cis*-tetraphenylcyclotetorasiloxanetetraol ($[PhSiO(OH)]_4$). Thus, the disiloxanetetraol exists in the reaction mixture at initial stage of the hydrolytic condensation. Based on this result, we tried to obtain the disiloxanetetraol from hydrolytic condensation by modifying reaction conditions and work-up procedure (Scheme 2).

First, to examine the reaction conditions, we tried the reaction from *i*-$BuSiCl_3$ that possesses middle size substituent. When the reaction was performed at 0 ℃ for 1 h, the solution was colorless. To the solution was added NaCl (until saturated), and the mixture was extracted by ether. The organic layer was dried over anhydrous sodium sulfate, and concentrated to give crude solid. After washing it with $CHCl_3$, we obtained $[i\text{-}BuSi(OH)_2]_2O$ (**1d**) in 37% yield.

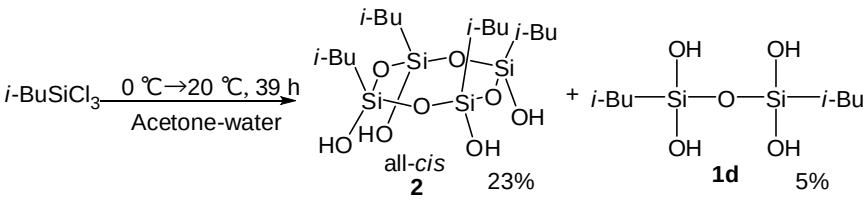

Scheme 3

We then tried the same reaction with longer reaction time and higher temperature (Scheme 3). White solid was precipitated from the solution. Solution was removed by decantation. The white solid was recrystallized to give all-*cis*-$[i\text{-}BuSiO(OH)]_4$ (**2**) in

23% yield. To the colorless solution was added NaCl (until saturated), and the mixture was extracted by ether. The organic layer was dried over anhydrous sodium sulfate, and concentrated to give crude solid. After washing it with $CHCl_3$, and we obtained **1d** in 5% yield.

Kawakami's group also reported the preparation of **2** in 2 steps from *i*-$BuSi(OMe)_3$ in 34% yield [16]. Considering one step reaction and moderate yield as well as facile separation, our synthesis method is more convenient. Previously, the synthesis of all-*cis*-$[RSiO(OH)]_4$ from $RSiCl_3$ (R = *i*-Pr [17a], Ph [17b]) in acetone-water solution was reported by Feher's group and our group in 22% (R = *i*-Pr) and 37% (R = Ph) yields respectively. In our case, cyclotetrasiloxanetetraols were easily isolated by collecting the precipitates from the reaction mixture like in the case of the isobutyl compound. From our results, cyclotetrasiloxanetetraols were gradually produced by further condensation reaction of the corresponding disiloxanetetraol as Ishikawa's group reported, and precipitated from the solution because of their less solubility. In this case, the yield of **2** is lower. This result indicates that the disiloxanetetraol and cyclotetrasiloxanetetraols can be synthesized from the corresponding trichlorosilanes by only changing quenching time and temperature of the reaction.

We also tried to synthesize $[RSi(OH)_2]_2O$ from trichlorosilanes with other substituents and confirmed that disiloxanetetraols with various substituents can be synthesized (Scheme 2). The results are summarized in Table 2.

In Tables 1 and 2, ^{29}Si NMR shifts of disiloxanetetraols are shown and they clearly indicate characteristics of structures of disiloxanetetraols. We could see the peaks around –50 ppm for dialkyldisiloxanetetraols, and –63 ppm for diaryldisiloxanetetraols.

Table 2. Various $[RSi(OH)_2]_2O$ prepared from $RSiCl_3$

Entry	Trichlorosilane	Temperature	Time / h	Yield / %	^{29}Si NMR / ppm
1	$MeSiCl_3$	0 ℃	1	—	—
2	$EtSiCl_3$	0 ℃	1	—	—
3	$PrSiCl_3$	0 ℃	1	7	–49.40
4	$C_6H_{13}SiCl_3$	0 ℃	1	18	–49.15
5	*i*-$PrSiCl_3$	0 ℃	1	7	–49.44
6	*i*-$BuSiCl_3$	0 ℃	1	37	–49.76
7	*i*-$BuSiCl_3$	0℃→ 20 ℃	39	5**	–49.76
8	$PhSiCl_3$	0 ℃	1	43	–62.20
9	$CySiCl_3$	0 ℃	1	mixture*	–42.32, –51.87
10	$CySiCl_3$	0℃→ 20 ℃	14	75	–51.87
11	$C_5H_9SiCl_3$	0℃→ 20 ℃	14	23	–49.32

*silanetriol and disiloxanetetraol ** **2** was also obtained as 23 % yield.

In entry 1, we could not obtain $[MeSi(OH)_2]_2O$. The crude product was analyzed by ^{29}Si NMR and no peaks were observed in -$OSiR(OH)_2$ region. Instead, many peaks were observed in -OSi(R)(OH)O- region. Under this reaction condition, the solution is acidic, and therefore $[MeSi(OH)_2]_2O$ which has small substituent is unstable in the solution to give further condensed oligosiloxanesilanols rapidly. In entry 2, the crude product was measured by ^{29}Si NMR. We observed many peaks in -$OSiR(OH)_2$ and -OSi(R)(OH)O- regions. The consequence indicates the possible existence of $[EtSi(OH)_2]_2O$. However, it is difficult to isolate it from the complex mixture of the products. Notably, $[PrSi(OH)_2]_2O$ (**1a**) and $[C_6H_{13}Si(OH)_2]_2O$ (**1b**) are unstable even in a solid state and the product was gradually transformed to insoluble solids. To the best of our knowledge, **1a** possesses the smallest substituents among disiloxanetetraols reported so far.

Cyclohexyl-substituted $[CySi(OH)_2]_2O$ (**1f**) was previously observed by Brown's group in the reaction of $CySiCl_3$ in acetone and water after 4 days [10]. As shown in entry 9, when we quenched the reaction after 1 h, we observed two peaks in ^{29}Si NMR. One peak was assigned to **1f** and the other peak which is located at –42.32 ppm was assigned to $CySi(OH)_3$. Cyclohexyl group is bulkier than methyl or ethyl group, which was effective for the isolation at the stage of the disiloxanetetraol. In entry 10, we selectively obtained **1f** as a precipitate by stirring longer time (14 h).

$[C_5H_9Si(OH)_2]_2O$ (**1g**) that has substituents with same bulkiness as cyclohexyl

group was synthesized in a similar manner to $[CySi(OH)_2]_2O$ (**1f**). Single crystal of $[C_5H_9Si(OH)_2]_2O$ (**1g**) was obtained by slow evaporation of its THF solution. The structure of **1g** is shown in Figure 1.

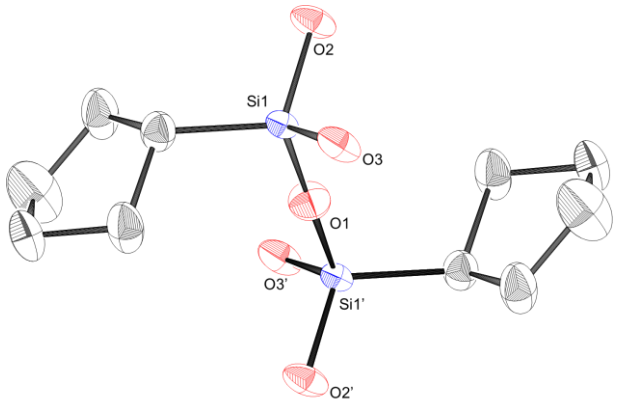

Figure 1. Crystal structure of **1g**. Black: Carbon; Blue: Silicon; Red: Oxygen. Thermal ellipsoids are shown in 50% probability level.

The cyclopentyl groups are arranged in *anti*-conformation. The space groups of *anti*-conformation was found to be $P2_1/a$ (monoclinic). The Si-O-Si bond angle was 180° . It is same bond angle as that reported for $[t\text{-}BuSi(OH)_2]_2O$ [8a]. There are intermolecular hydrogen bonding. Oxygen atom distances were O(2)･･･O(3) (2.674 Å), O(2)･･･O(3') (2.691 Å) respectively. These values are similar to those found in other disiloxanetetraols. Intermolecular hydrogen bonding occurs to give chains of molecules which are further connected to give sheetlike supramolecular structure.

The sheet structure is shown in Figure 2. Within a particular chain of molecules, the cyclopentyl groups locate above and below the sheets, thus giving a hydrophobic region between the sheet. The sheet structure was also observed in $[t\text{-}BuSi(OH)_2]_2O$ [8a].

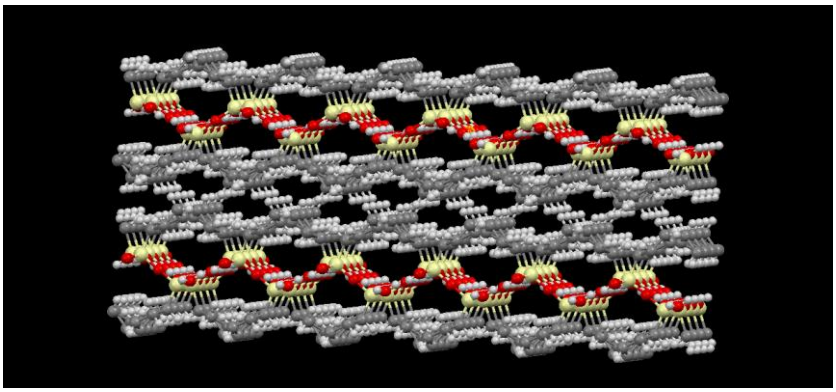

Figure 2. Packing structure of **1g**. Gray: Carbon; Yellow: Silicon; Red: Oxygen.

Compound **1e** was prepared by a multistep reaction from $PhSiCl_3$ or $PhSi(OMe)_3$ via $[PhSiCl_2]O$ or $[PhSi(OMe)_2]O$ [5, 11a, 11b]. $[PhSiCl_2]O$ was prepared from $PhSiCl_3$ in gas phase reaction by using custom-made device [18]. Compound **1e** was also prepared by a single-step reaction from $PhSi(OAc)_3$, but the yield was low (9%). On the other hand, it is reported that **1e** is a very effective precursor of laddersiloxanes [5]. Our new method of the syntheses of **1e** is a single-step reaction without custom-made device. And isolation is very easy without column chromatography. Therefore, our new method is thought to be versatile for a large-scale production.

2.1.3 Summary

We succeeded in a facile single-step synthesis of disiloxanetetraols with various substituents by hydrolytic condensation of trichlorosilanes by quenching the reactions in early stages. We also found that the disiloxanetetraol and cyclotetrasiloxanetetraols with isobutyl groups can be synthesized from isobutyltrichlorosilane by only changing quenching time and temperature of the reaction. $[PrSi(OH)_2]_2O$ **(1a)** possesses the smallest substituents among disiloxanetetraols reported so far. X-ray crystallography of $[C_5H_9Si(OH)_2]_2O$ (1**g**) is shown sheet super molecular structure by intermolecular hydrogen bonding.

2.1.4 Experimental section

The Fourier transform nuclear magnetic resonance (NMR) spectra were obtained using a JEOL JNM-ECS 300 (^1H at 300.53 MHz, ^{13}C at 75.57 MHz, and ^{29}Si at 59.71 MHz) NMR instruments and JEOL JNM-ECA 600 (^1H at 600.17 MHz) NMR instruments. Chemical shifts are reported as δ units (ppm) relative to $SiMe_4$, and residual solvents peaks were used for standards. For ^{29}Si NMR, $SiMe_4$ was used as an external standard. Electron impact mass spectrometry was performed on Shimadzu GCMS–QP2010SE/DI2010. Infrared spectra were measured using a Shimadzu FTIR-8400S spectrometer. All melting points were determined on a Yanaco micro melting point apparatus MP-J3 and are uncorrected. Elemental analyses were performed by the Center for Material Research by Instrumental Analysis (CIA), Gunma University.

General Procedure for the synthesis of $[RSi(OH)_2]_2O$ (R = Pr(**1a**), *i*-Pr(**1c**), *i*-Bu(**1d**), C_5H_9(**1g**))

A solution of $RSiCl_3$ and acetone was added dropwise into vigorously stirred cold water for 1 h at 0 ℃. Then, the reaction mixture was stirred for 1 h at 0 ℃. The

supernatant liquid solution was poured into another flask. NaCl and ether were added into the reaction mixture. Organic layer was extracted with ether over 3 times. The combined organic phase was washed with saturated aqueous $NaHCO_3$ solution and brine. The organic phase was dried over anhydrous sodium sulfate and concentrated. The crude product was washed by solvent ($CHCl_3$ or toluene (in the case of phenyl compound) to give analytically pure disiloxanetetraols (in the case of cyclopentyl compound, the crude product was recrystallized from THF).

Synthesis of $[PrSi(OH)_2]_2O$ (**1a**)

Compound **1a** (0.29 g, 1.3 mmol , 7 %) was prepared by following the general procedure employing $PrSiCl_3$ (6.3 g, 35 mmol), acetone (33 mL), water (400 mL) , and NaCl (125 g) as white solid.

Spectral data for **1a**: m.p. 87–90 ℃ (decomp.). ^{1}H NMR (300.53 MHz, acetone-d_6) δ 0.55 (*t*, *J* = 8.1 Hz, 4H), 0.93 (t, *J* = 8.1 Hz, 6H), 1.47 (sext, *J* = 8.1 Hz, 4H), 5.04 (br s, 4H) ppm. ^{13}C NMR (75.57 MHz, acetone-d_6) δ 16.67 (CH_2), 17.17 (CH_2), 17.92 (CH_3). ^{29}Si NMR (59.71 MHz, acetone-d_6) δ –49.40 ppm. DIMS (EI, 70eV) *m*/z (%) 183 ($[M–Pr]^+$,60) , 141 ($[M–Pr_2+H]^+$,100). IR (KBr) 871, 910, 1072, 1110, 1218, 2869, 2929, 2956, 3278 cm^{-1}. Anal. Calcd for $C_6H_{18}Si_2O_5$:C, 31.83; H, 8.01; Found C, 31.43 ; H, 7.78%.

Synthesis of $[i\text{-}PrSi(OH)_2]_2O$ (**1c**)

Compound **1c** (0.30 g, 1.3 mmol , 7 %) was prepared by following the general procedure employing *i*-$PrSiCl_3$ (6.2 g, 35 mmol), acetone (33 mL), water (400 mL) , and NaCl (125 g) as white solid.

Spectral data for **1c** : m.p. 160–164 ℃ (decomp.). ^{1}H NMR (600.17 MHz, acetone-d_6) δ 0.80 (sep, *J* = 7.2 Hz, 2H), 1.02 (d, *J* = 7.2 Hz, 12H), 4.96 (br s, 4H) ppm.^{13}C NMR (75.57 MHz, acetone-d_6) δ 13.36 (CH), 17.54 (CH_3) ppm. ^{29}Si NMR (59.71 MHz, acetone-d_6) δ –49.44 ppm. DIMS (EI, 70eV) *m*/z (%) 183 ($[M–i\text{-}Pr]^+$,86) ,155 (100), 141 ($[M–i\text{-}Pr_2+H]^+$, 13). IR (KBr) 844, 894, 1120, 1465, 2341, 2358, 2869, 3126 cm^{-1}. Anal. Calcd for $C_6H_{18}Si_2O_5$:C, 31.83; H, 8.01; Found C, 31.64; H, 7.82%.

Synthesis of $[i\text{-}BuSi(OH)_2]_2O$ (**1d**)

Compound **1d** (6.6 g, 26 mmol , 37%) was prepared by following the general procedure employing *i*-$BuSiCl_3$ (27 g, 140 mmol), acetone (132 mL), water (1600 mL) and NaCl (400 g) as white solid.

Spectral data for **1d**: m.p. 141–144 ℃ (decomp.). ^{1}H NMR (300.53 MHz, acetone-d_6) δ 0.56 (d, J = 6.9 Hz, 4H) , 0.95 (d, J = 6.9 Hz, 12H) , 1.91 (nonet, J = 6.9 Hz, 2H), 4.97 (br s, 4H) ppm. ^{13}C NMR (75.57 MHz, acetone-d_6) δ 24.59 (CH), 24.76 (CH_2), 26.19 (CH_3) ppm. ^{29}Si NMR (59.71 MHz, acetone-d_6) δ –49.76 ppm. DIMS (EI, 70eV) m/z (%) 197 ([M–i-Bu]$^+$,10.0), 141 ([M–i-Bu$_2$+H]$^+$, 27), 58 ([i-Bu], 27), 43 (100). IR (KBr) 476, 740, 819, 852, 896, 956, 1091, 1230, 1467, 2873, 2954, 3195 cm^{-1}. Anal. Calcd for $C_8H_{22}Si_2O_5$:C, 37.77; H, 8.72; Found C, 37.69; H, 8.50%.

Synthesis of [PhSi(OH)$_2$]$_2$O (**1e**)

Compound **1e** (2.2 g, 7.5 mmol , 43%) was prepared by following the general procedure employing $PhSiCl_3$ (7.4 g, 35 mmol), acetone (33 mL), water (400 mL) , and NaCl (125 g) as white solid.

Spectral date for **1e**: m.p. 115–118 ℃ (decomp.). ^{1}H NMR (300.53 MHz, acetone-d_6) δ 5.73 (br s, 4H) , 7.26–7.74 (m, 10H) ppm. ^{13}C NMR (75.57 MHz, acetone-d_6) δ 127.77 (CH), 129.88 (CH), 134.83 (CH), 136.05 (C) ppm. ^{29}Si NMR (59.71 MHz, acetone-d_6) δ –62.20 ppm. IR (KBr) 696, 738, 858, 906, 1117, 1138, 1429, 3195 cm^{-1}.

Synthesis of [C_5H_9Si(OH)$_2$]$_2$O (**1g**)

Compound **1g** (1.1 g, 4.0 mmol, 23 %) was prepared by following the general procedure employing $C_5H_9SiCl_3$ (7.2 g, 35 mmol), acetone (33 mL), water (400 mL) , and NaCl (125 g) as white solid.

Spectral data for **1g**: m.p. 183–187 ℃ (decomp.). ^{1}H NMR (300.53 MHz, acetone-d_6) δ 0.87–0.96 (m, 2H) , 1.38–1.63 (m, 12H) , 1.70–1.84 (m, 4H), 4.94 (br s, 4H) ppm. ^{13}C NMR (75.57 MHz, methanol-d_4) δ 25.05(CH), 27.92(CH_2), 28.62(CH_2) ppm. ^{29}Si NMR (59.71 MHz, methanol-d_4) δ –49.32 ppm. DIMS (EI, 70eV) m/z (%) 209 ([M–C_5H_9]$^+$,87) ,141 ([M–(C_5H_9)$_2$+H]$^+$, 100). IR (KBr) 842, 899, 1105, 2864, 2949, 3126 cm^{-1}. Anal. Calcd for $C_{10}H_{22}Si_2O_5$:C, 43.13; H, 7.96; Found C, 42.88; H,7.87 %.

Synthesis of [C_6H_{13}Si(OH)$_2$]$_2$O (**1b**)

Solution of $C_6H_{13}SiCl_3$ (7.7 g, 35 mmol) and acetone (33 mL) was added dropwise into vigorously stirred cold water (400 mL) for 1 h at 0 ℃. Then, the reaction mixture was stirred for 1 h at 0 ℃. Precipitated white solid was filtered and washed by water. The white solid was dried in reduced pressure. Insoluble in acetone was removed by filtration. $CHCl_3$ was added the acetone solution to precipitate. The white solid was filtered and dried in reduced pressure to give **1b** (1.0 g, 3.2 mmol, 18%).

Spectral data for **1b**: m.p. 94–96 ℃ (decomp.). ^{1}H NMR (300.53 MHz, acetone-d_6) δ 0.55 (t, J = 8.1 Hz, 4H) , 0.87 (t, J = 6.9 Hz, 6H) , 1.22-1.36 (m, 12H), 1.40-1.53 (m, 4H), 5.00 (br s, 4H) ppm. ^{13}C NMR (75.57 MHz, acetone-d_6) δ 14.41 (CH_3), 14.49 (CH_2), 23.26 (CH_2), 24.03 (CH_2), 32.42 (CH_2), 33.75 (CH_2). ^{29}Si NMR (59.71 MHz, acetone-d_6) δ –49.15 ppm. DIMS (EI, 70eV) m/z (%) 225 ([M– C_6H_{13}]$^+$, 19), 79 (100). IR (KBr) 874, 908, 1099, 2856, 2922, 2957, 3242 cm^{-1}.

Synthesis of [CySi(OH)$_2$]$_2$O (**1f**)

Solution of $CySiCl_3$(7.6 g, 35 mmol) and acetone (33 mL) was added dropwise into vigorously stirred cold water(400 mL) for 1 h at 0 ℃. Then, the reaction mixture was stirred for 14 h at 0 ℃ to 20 ℃. White solid was precipitated from the reaction solution. Precipitated white solid was filtered and washed by water. The white solid was dried in reduced pressure to give [CySi(OH)$_2$]$_2$O (**1f**) (4.0 g, 13 mmol, 75%).

Spectral data for **1f**: m.p. 205–208 ℃ (decomp). ^{1}H NMR (300.53 MHz, acetone-d_6) δ 0.63-1.86 (m, 22H), 4.87 (br s, 4H). ^{13}C NMR (75.57 MHz, DMSO-d_6) δ 25.21 (CH), 27.47 (CH_2), 28.36 (CH_2, overlapped) ppm. ^{29}Si NMR (59.71 MHz, DMSO-d_6) δ –51.87 ppm. DIMS (EI, 70eV) m/z (%), 223 ([M–Cy]$^+$,73), 141 ([M–Cy$_2$+H]$^+$,100). IR (KBr) 808, 852, 897, 999, 1038, 1094, 1121, 1196, 1447, 2848, 2920, 3147 cm^{-1}.

Synthesis of all-*cis*-[*i*-BuSiO(OH)]$_4$ (**2**)

Solution of *i*-$BuSiCl_3$ (6.7 g, 35 mmol) and acetone (33 mL) was added dropwise into vigorously stirred cold water (400 mL) for 1 h at 0 ℃. Then, the reaction mixture was stirred for 39 h at 0 ℃ to 20 ℃. White solid was precipitated from the reaction solution. The supernatant liquid solution was removed by decantation. The white solid was collected. Insoluble in $CHCl_3$ was removed by filteration. Filtrate was concentrated to give white solid. The solid was recrystallized from hexane to give **2** (0.94 g, 2.0 mmol, 23%) as white solid in. The decantated solution was poured into another flask. 125 g of NaCl and ether were added into the reaction mixture. Organic layer was extracted with ether over 3 times. The combined organic phase was washed with saturated aqueous $NaHCO_3$ solution and brine. The organic phase was dried over anhydrous sodium sulfate and concentrated. The crude product was washed by $CHCl_3$ gave **1d** (0.21 g, 0.83 mmol, 5%).

Spectral date for **2**: m.p. 148–151 ℃. ^{1}H NMR (300.53 MHz, $CDCl_3$) δ 0.61 (d, J = 6.9 Hz, 8H), 0.94 (d, J = 6.9 Hz, 24H), 1.84 (nonet, 4H), 6.36 (br s, 4H) ppm. ^{13}C NMR (75.57 MHz, $CDCl_3$) δ 23.04 (CH_2) , 23.87 (CH) , 25.74 (CH_3) ppm. ^{29}Si

NMR (59.71 MHz, $CDCl_3$) δ –58.14 ppm, MS (EI, 70 eV) *m*/z (%) 397 ([M–*i*-Bu–H_2O]$^+$, 100). IR (KBr) 879, 901, 926, 1087, 1229, 2955, 3240 cm^{-1}. Anal. Calcd for $C_{16}H_{40}Si_4O_8$:C, 40.64; H, 8.53; Found C, 40.40; H, 8.55%.

2.1.5 References

[1] P. D. Lickiss, *Adv. Inorg. Chem.*, **1995**, *42*, 147.

[2] M. Unno, S. B. Alias, M. Arai, K. Takada, R. Tanaka and H. Matsumoto, *Appl. Organomet. Chem.*, **1999**, *13*, 303.

[3] M. Unno, S. B. Alias, H. Saito, and H. Matsumoto, *Organometallics*, **1996**, *15*, 2413.

[4] M. Unno, Y. Imai and H. Matsumoto, *Silicon Chem*., **2003**, 2, 175.

[5] Z. X. Zhang, J. Hao, P. Xie, X. Zhang, C. C. Han, R. Zhang, *Chem. Mater.*, **2008**, *20*, 1322.

[6] V. Chandrasekhar, R. Thirumoorthi, *Inorg. Chem.*, **2009**, *48*, 6236.

[7] K. A. Andrianov, B. A. Izmailov, N. D. Petukhova, *Zh. Obshch. Khim.*, **1976**, *46*, 599.

[8a] P. D. Lickiss, S. A. Lister, A. D. Redhouse, P. D. Wisener, *J. Chem. Soc., Chem. Commun.*, **1991**, 173.

[8b] P. P. Pescarmona, J. C. Van der waal, T. Maschmeyer, *Chem. Eur. J.*, **2004**, *10*, 1657.

[9] M. Unno, S. B. Alias, H. Matsumoto, *Organometallics*, **1996**, *15*, 2413.

[10] J. F. Brown, Jr., L.H. Vogt, Jr., *J. Am. Chem. Soc.*, **1965**, *87*, 4313.

[11a] J. F. Brown, Jr., G. M. Slusarczuk, *J. Org. Chem.*, **1964**, *29*, 2809.

[11b] I. Seto, T. Gunji, K. Kumagai, K. Arimitsu, Y. Abe, *Bull. Chem. Soc. Jpn.*, **2003**, *76*, 1983.

[11c] K. Suyama, T. Nakatsuka, T. Gunji, Y. Abe, *J. Organomet. Chem.*, **2007**, *692*, 2028.

[12] M. Unno, T. Tanaka, H. Matsumoto, *J. Organomet. Chem.*, **2003**, *686*, 175.

[13] M. Yoshizawa. T. Kusukawa, M. Fujita, S. Sakamoto, K. Yamaguchi, *J. Am. Chem. Soc.*, **2001**, *123*, 10454.

[14a] J. H. Kim, J. S. Han, W. C. Lim, B. R. Yoo, *J. Ind. Eng. Chem.*, **2007**, *13*, 480.

[14b] I. Toulokhonova, R. Zhao, M. Kozee, R. West, *Main Group Met. Chem.* **2001**, *24*, 737.

[14c] R. Rulkens, M. P. Coles, T. D. Tilley, *J. Chem. Soc., Dalton Trans.*, **2000**, 627.

[14d] R. Murugavel, P. Bottcher, A. Voigt, M. G. Walawalker, H. W. Roesky, E. Parisini, M. Teichert, M. Noltemeyer, *Chem. Commun.*, **1996**, 2417.

[14e] C. E. F. Rickard, R. W. Roper, M. D. Salter, L. J. Wright, *J. Am. Chem. Soc*,. **1992**, *114*, 9682.
[14f] Z. Ren, D. Sun, H. Li, Q. Fu, D. Ma, J. Zhang, S. Yan, *Chem. Eur. J.*, **2012**, *18*, 4115.
[14g] Z. Ren, Z. Chen, W. Fu, R. Zhang, F. Shen, F. Wang, Y. Ma, S. Yan, *J. Mater. Chem.*, **2011**, *21*, 11306.
[14h] S. Perruchas, N. Desboeufs, S. Maron, X. F. L. Goff, A. Fagues, A. Garcia, T. Gacoin, J. P. Boilot, *Inorg. Chem.*, **2012**, *51*, 794.
[15] S. Yamamoto, N. Yasuda, A. Ueyama, H. Adachi, M. Ishikawa, *Macromolecules*, **2004**, *37*, 2775.
[16] R. Ito, Y. Kakihana, Y. Kawakami, *Chem. Lett.*, **2009**, *38*, 364.
[17a] M. Unno, A. Suto, K. Takada, H. Matsumoto, *Bull. Chem. Soc. Jpn.*, **2000**, *73*, 215.
[17b] F. J. Feher, J. J. Schwab, D.Soulivong, J. W. Ziller, *Main Group Chem.*, **1997**, *2*, 123.
[18] Y. Abe, K. Abe, M. Watanabe, T. Gunji, *Chem. Lett.*, **1999**, *28*, 259.

2.1.6 Supporting information

1. Spectral data

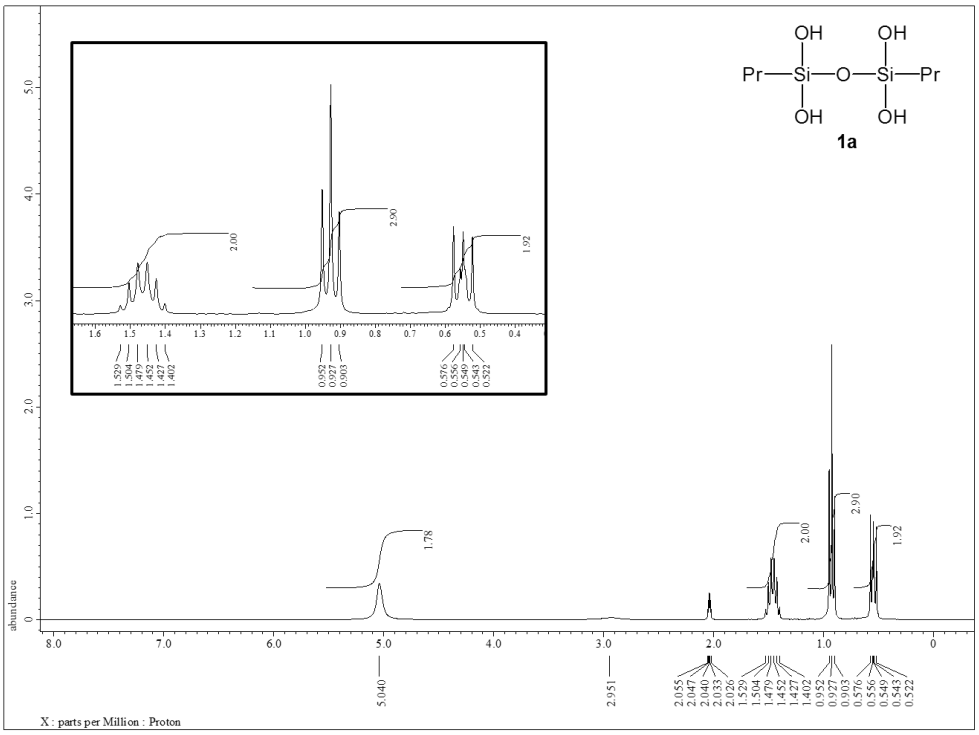

Figure 1. ^{1}H NMR spectrum of **1a** (300.53 MHz, acetone-d_6)

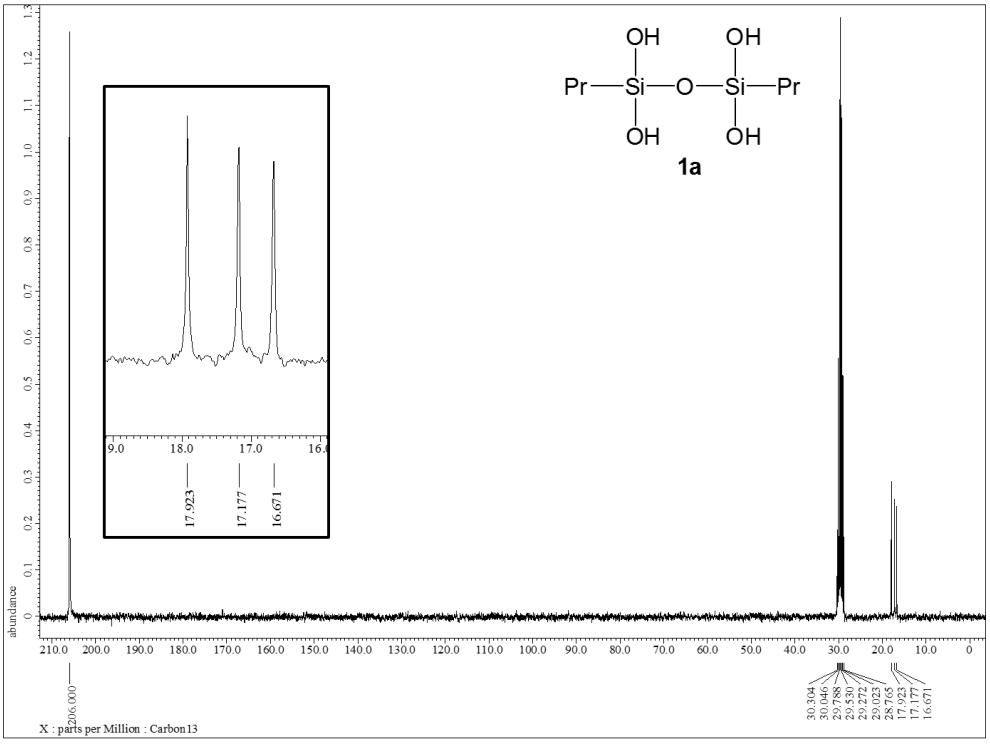

Figure 2. ^{13}C NMR spectrum of **1a** (75.57 MHz, acetone-d_6)

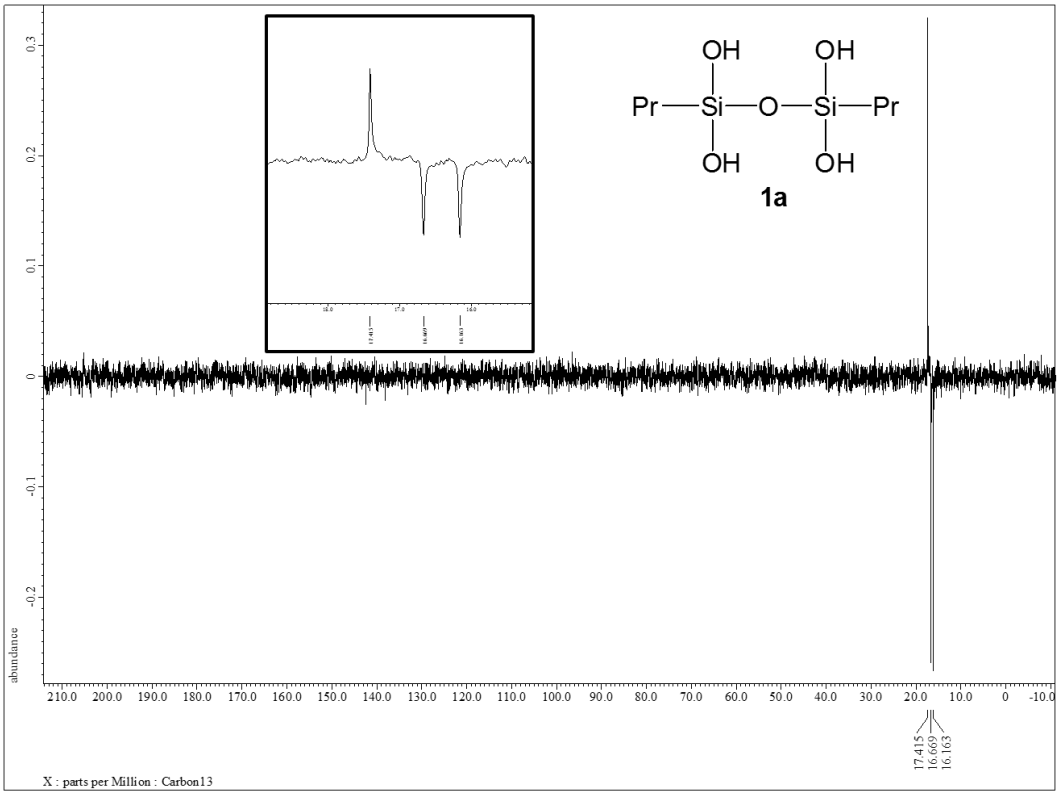

Figure 3. ^{13}C NMR (dept 135) spectrum of **1a** (75.57 MHz, acetone-d_6)

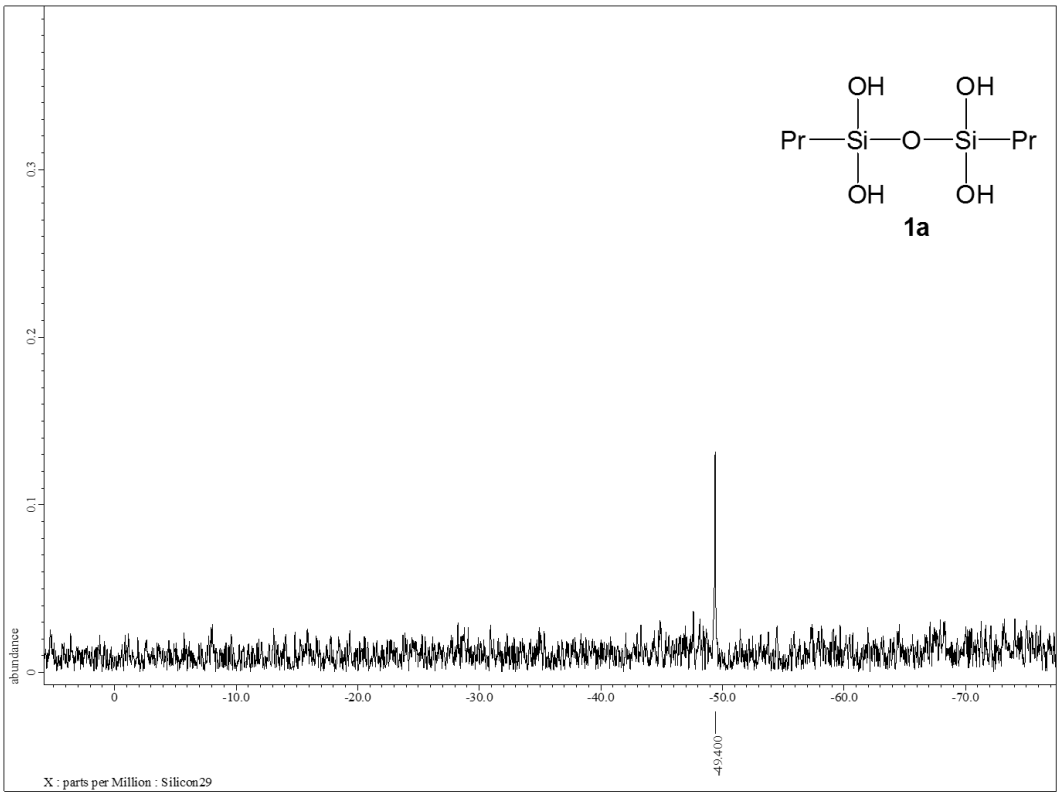

Figure 4. ^{29}Si NMR spectrum of **1a** (59.71 MHz, acetone-d_6)

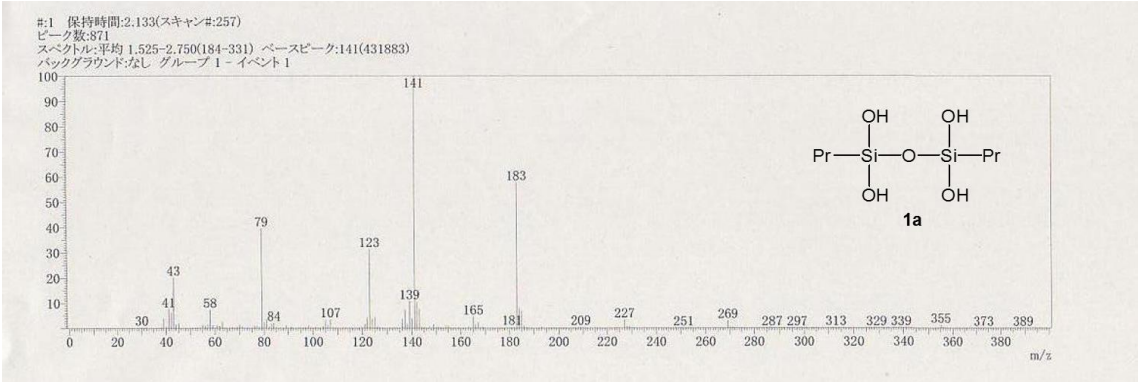

Figure 5. DIMS (EI, 70 eV) spectrum of **1a**

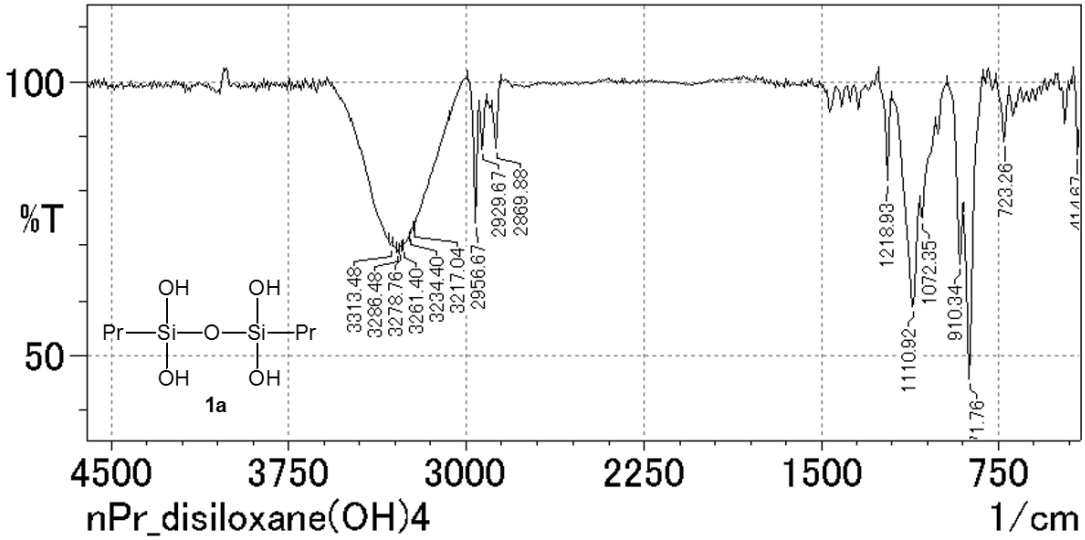

Figure 6. IR (KBr) spectrum of **1a**

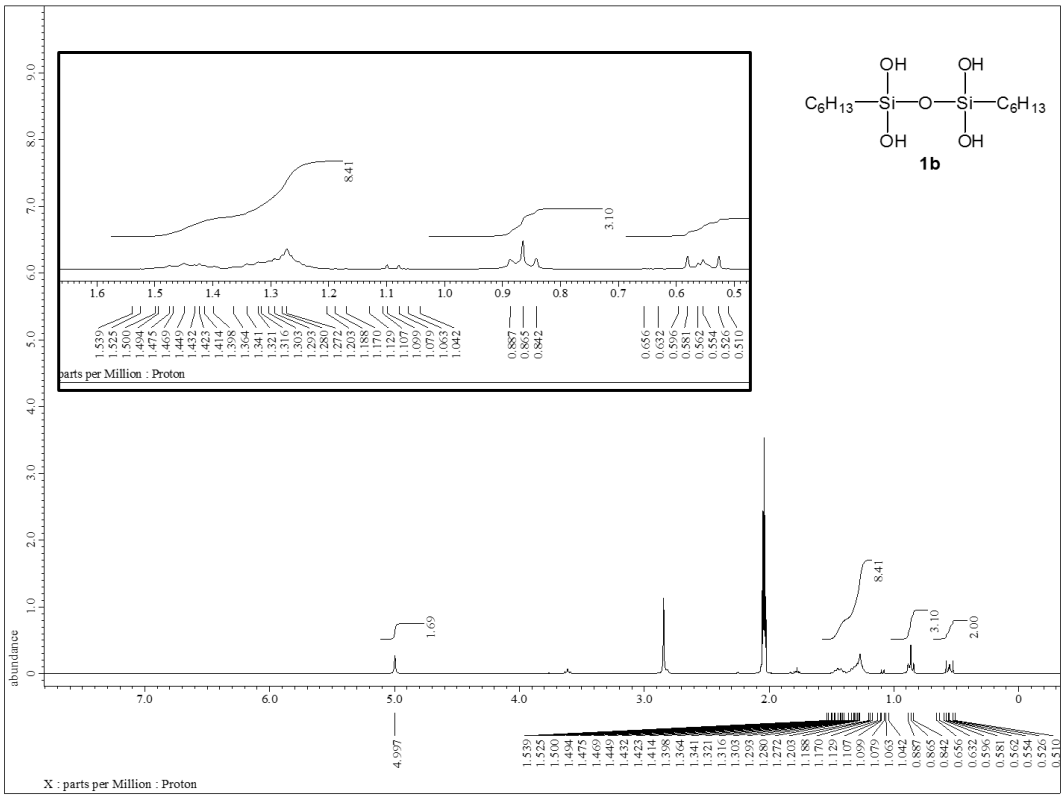

Figure 7. ^{1}H NMR spectrum of **1b** (300.53 MHz, acetone-d_6)

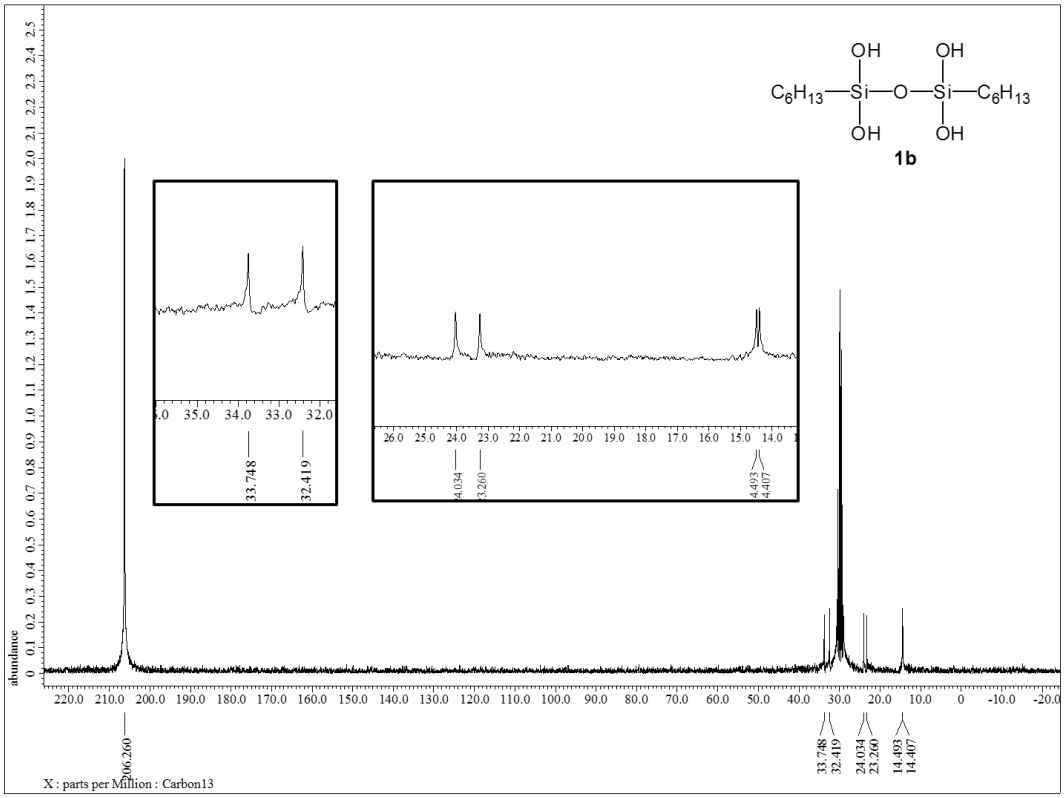

Figure 8. ^{13}C NMR spectrum of **1b** (75.57 MHz, acetone-d_6)

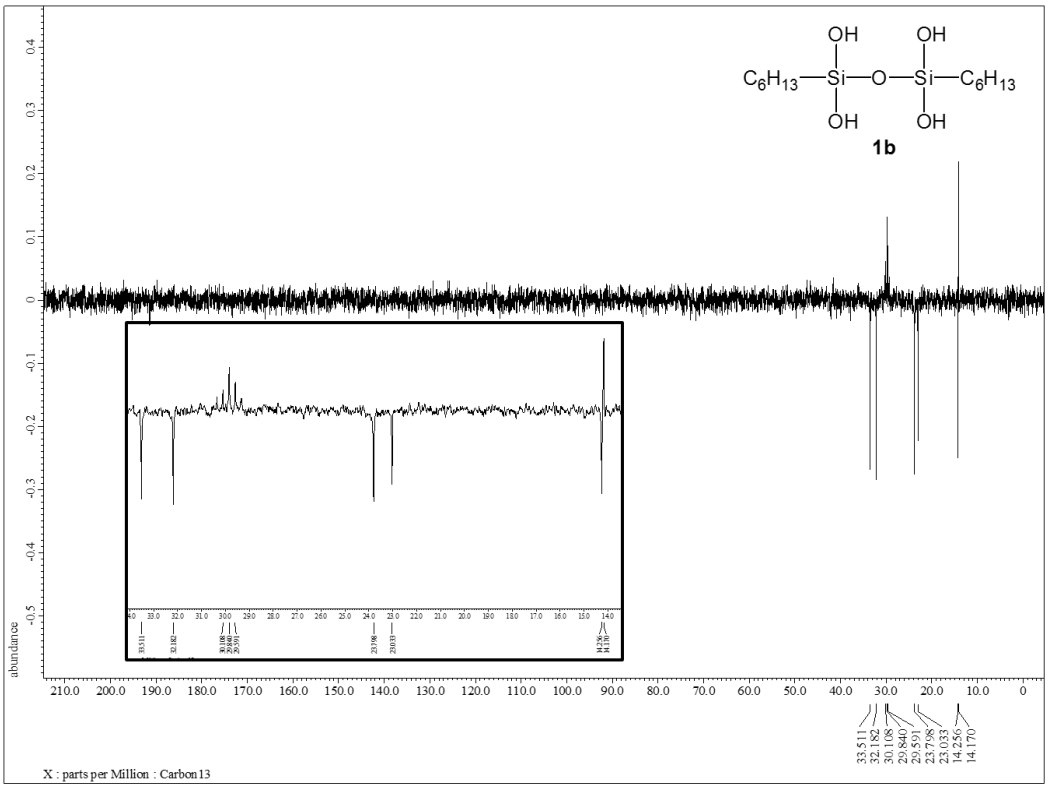

Figure 9. ^{13}C NMR (dept 135) spectrum of **1b** (75.57 MHz, acetone-d_6)

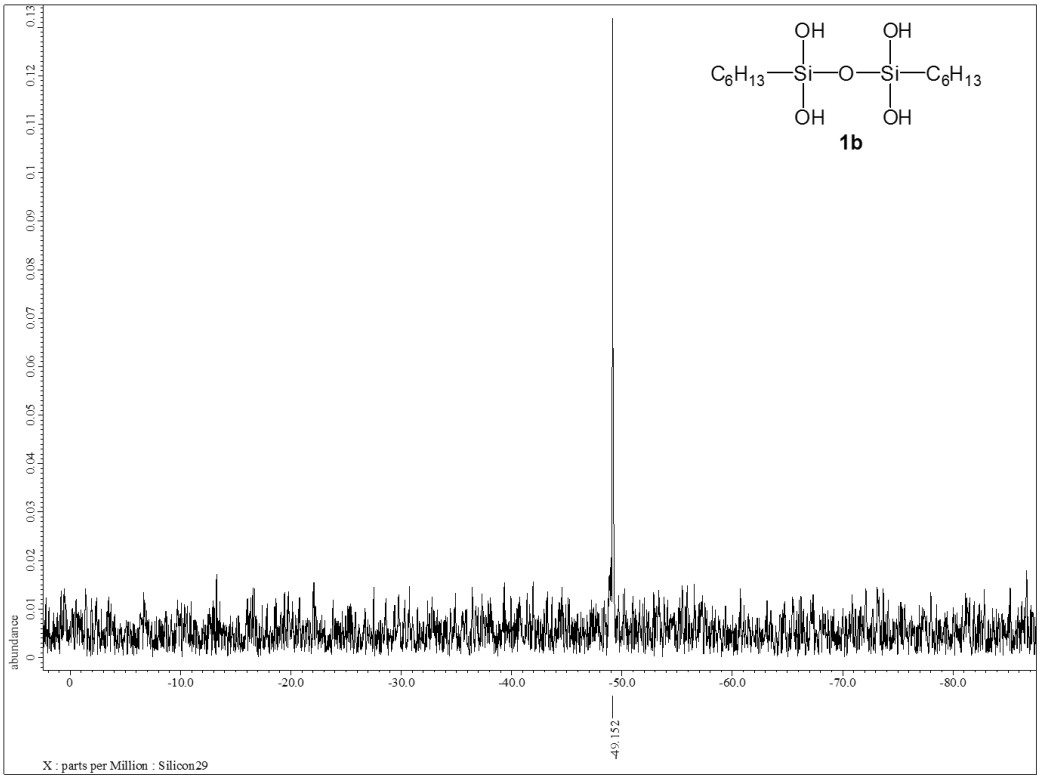

Figure 10. ^{29}Si NMR spectrum of **1b** (59.71 MHz, acetone-d_6)

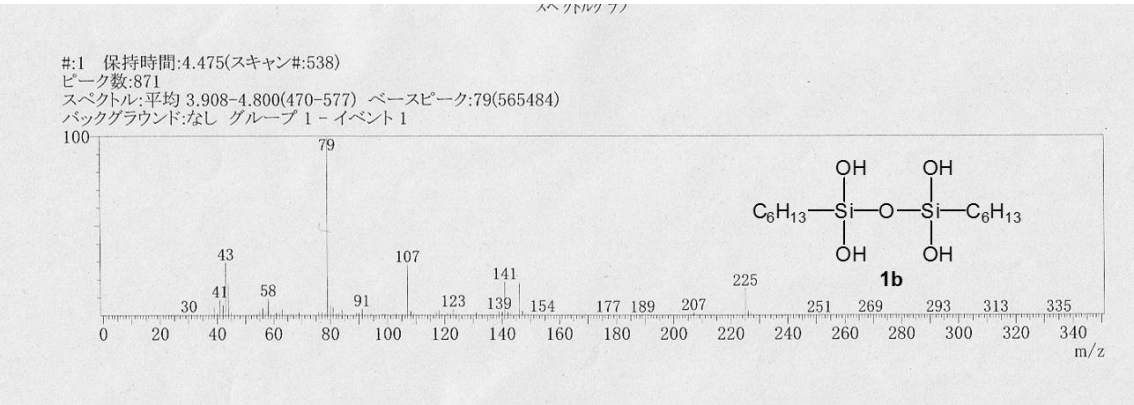

Figure 11. DIMS spectrum of **1b**

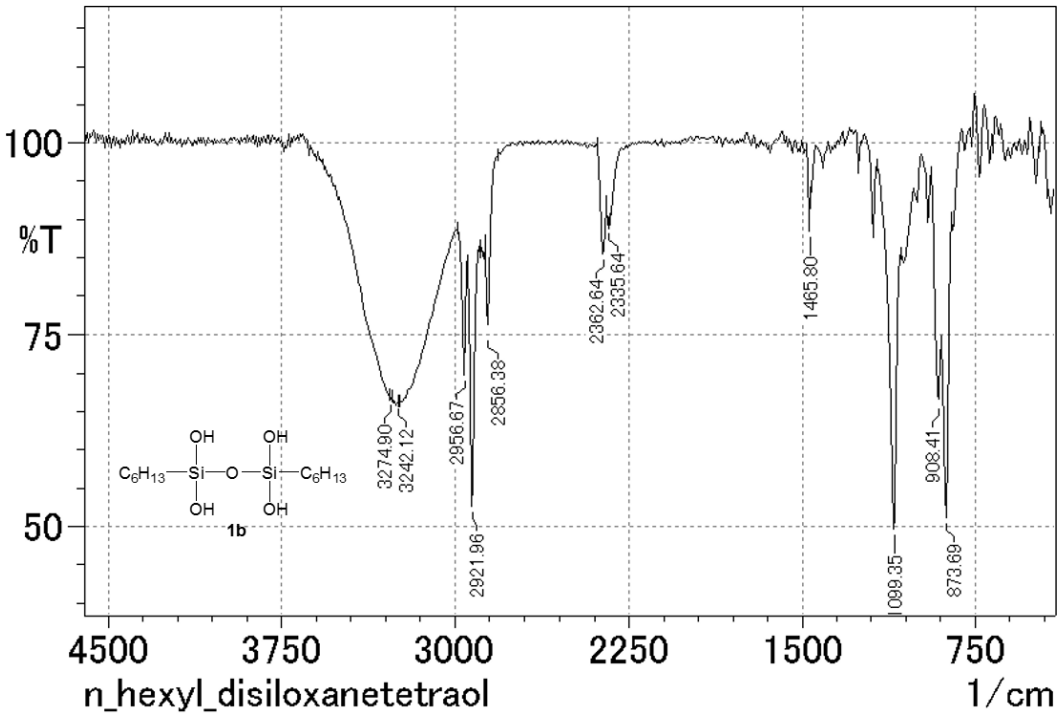

Figure 12. IR spectrum of **1b**

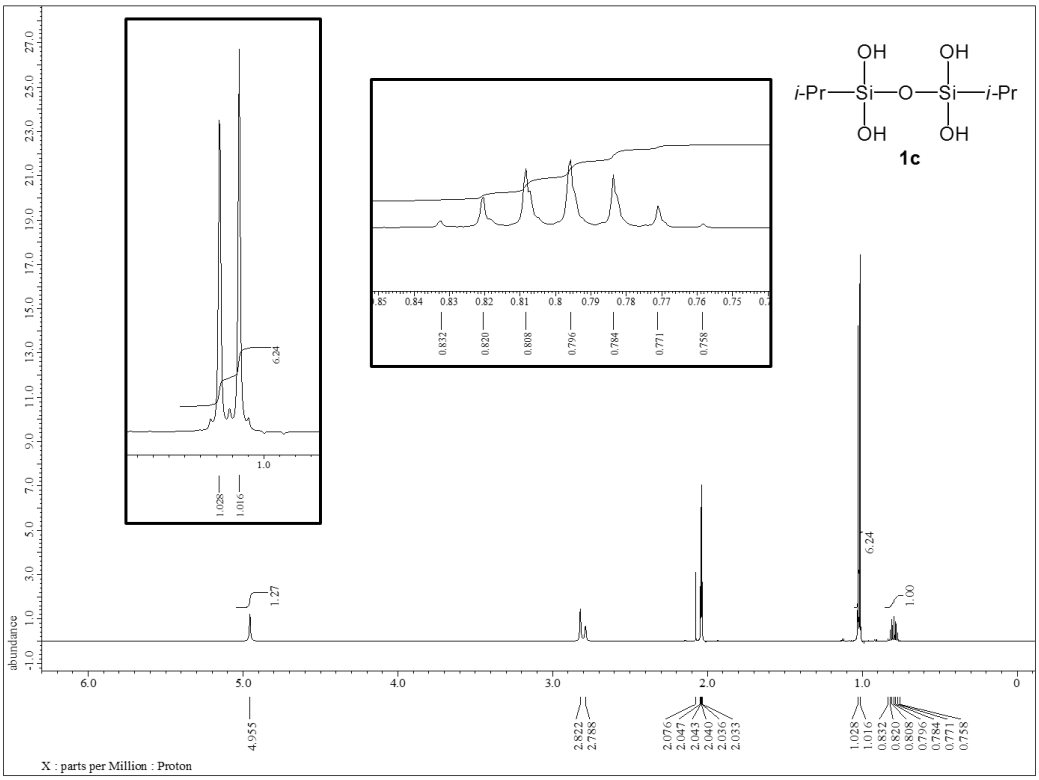

Figure 13. ^{1}H NMR spectrum of **1c** (600.17 MHz, acetone-d_6)

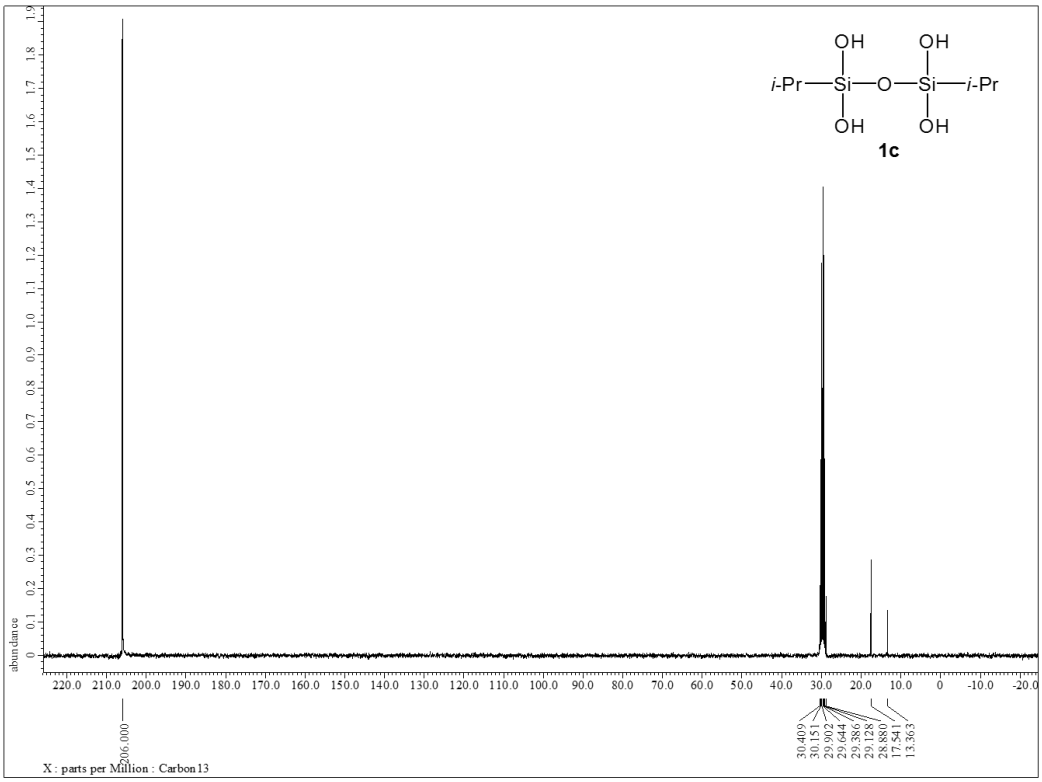

Figure 14. ^{13}C NMR spectrum of **1c** (75.57 MHz, acetone-d_6)

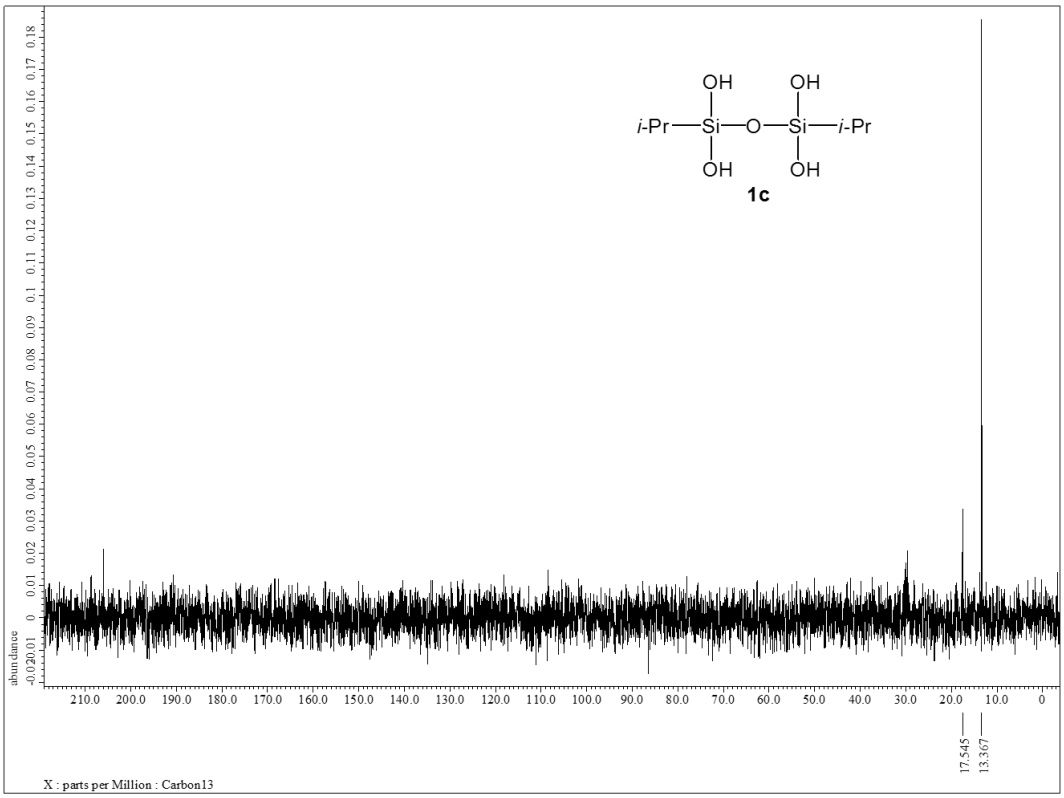

Figure 15. ^{13}C NMR (dept 90) spectrum of **1c** (75.57 MHz, acetone-d_6)

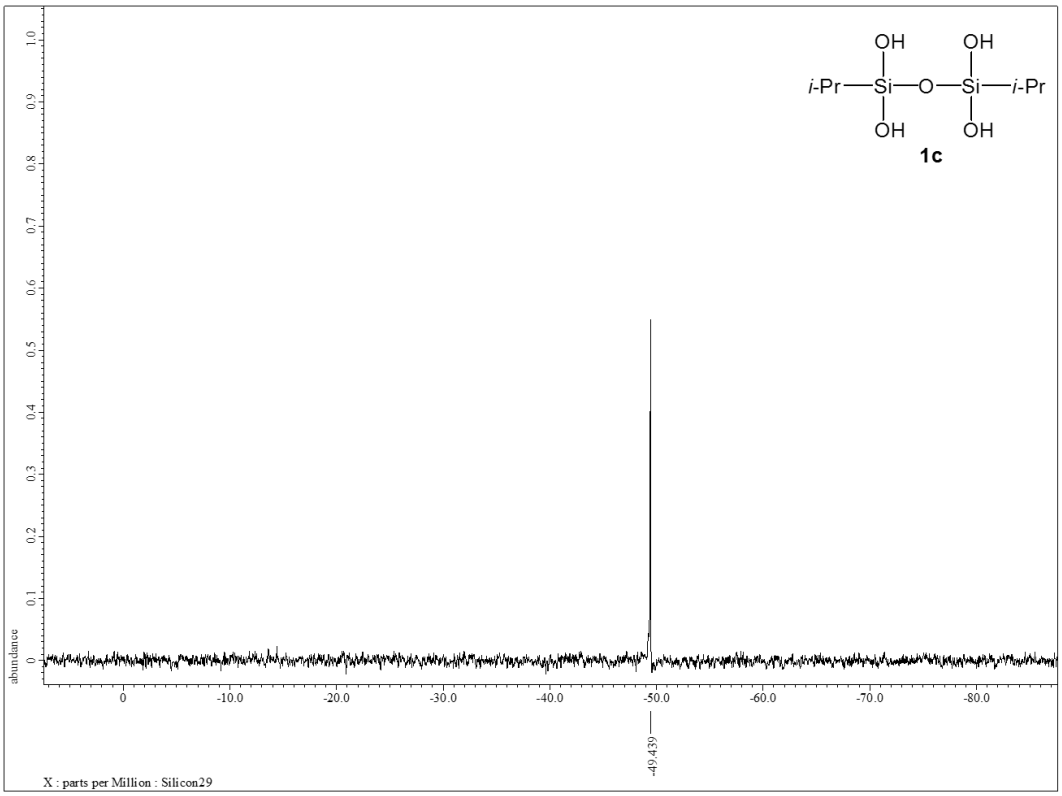

Figure 16. ^{29}Si NMR spectrum of **1c** (59.71 MHz, acetone-d_6)

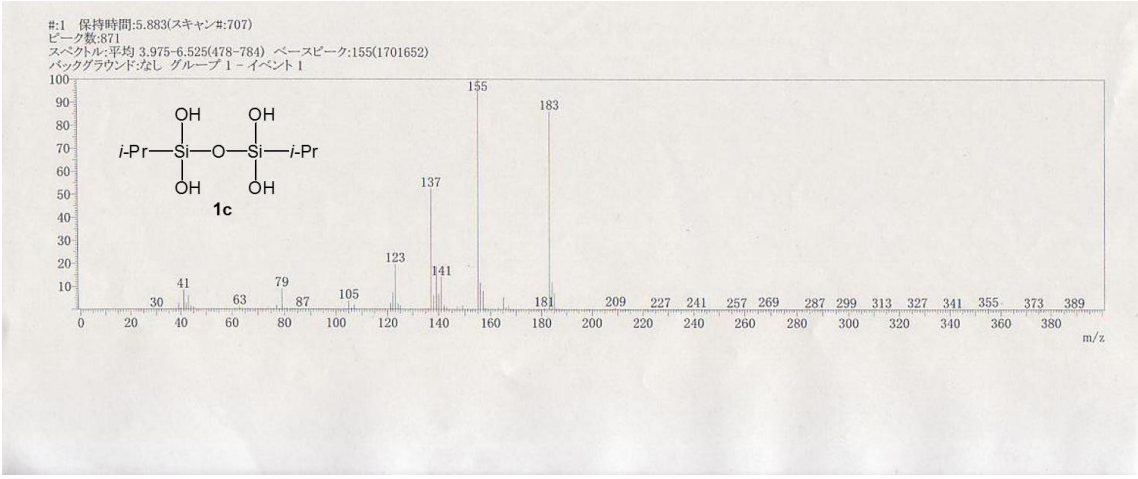

Figure 17. DIMS (EI, 70 eV) spectrum of **1c**

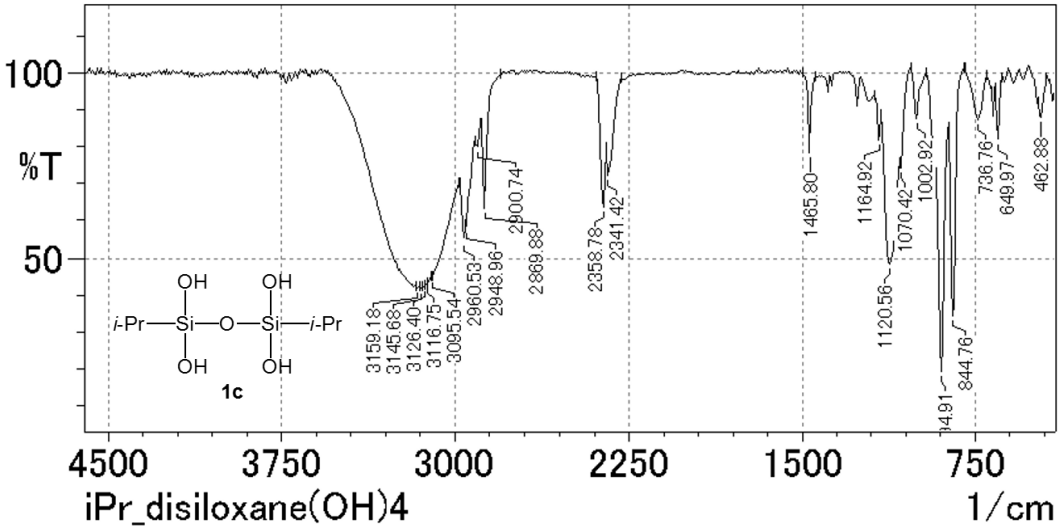

Figure 18. IR (KBr) spectrum of **1c**

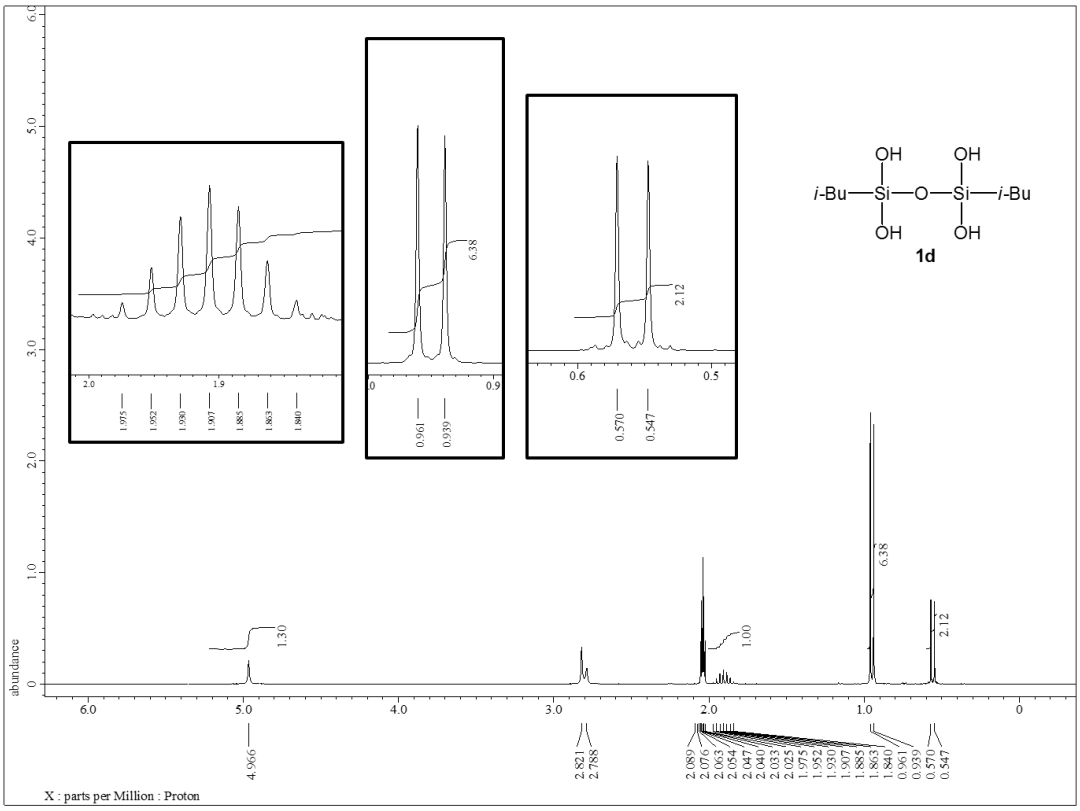

Figure 19. ^{1}H NMR spectrum of **1d** (300.53 MHz, acetone-d_6)

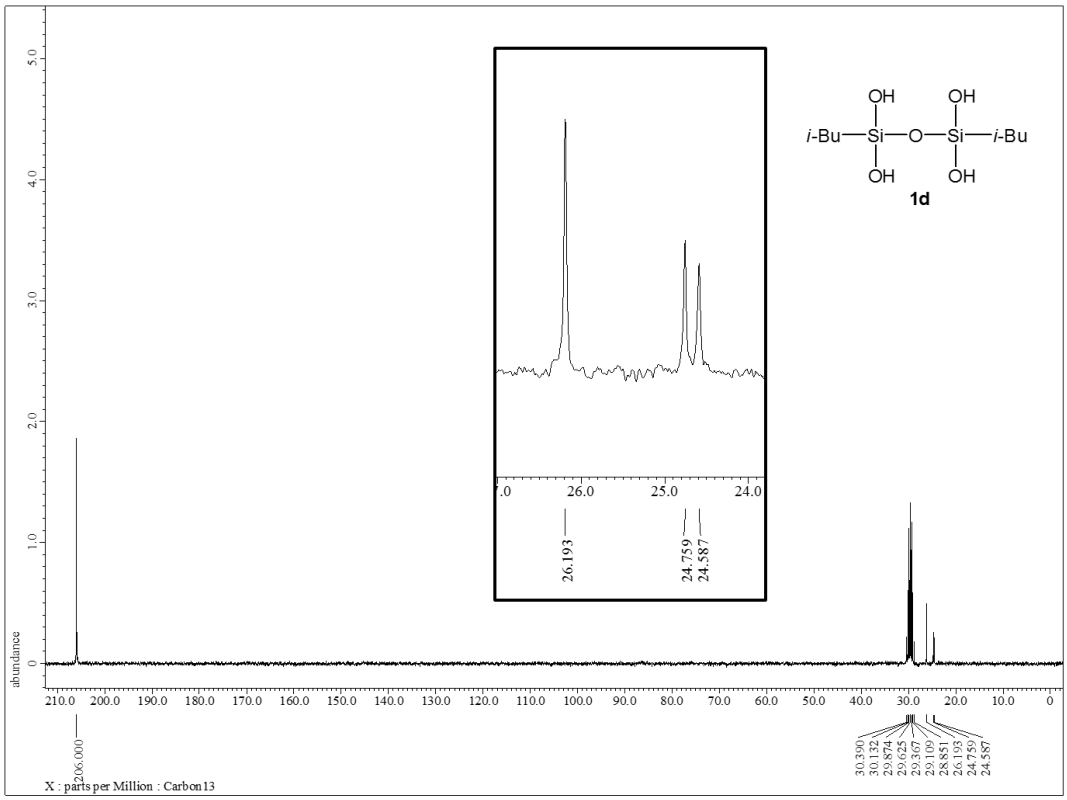

Figure 20. ^{13}C NMR spectrum of **1d** (75.57 MHz, acetone-d_6)

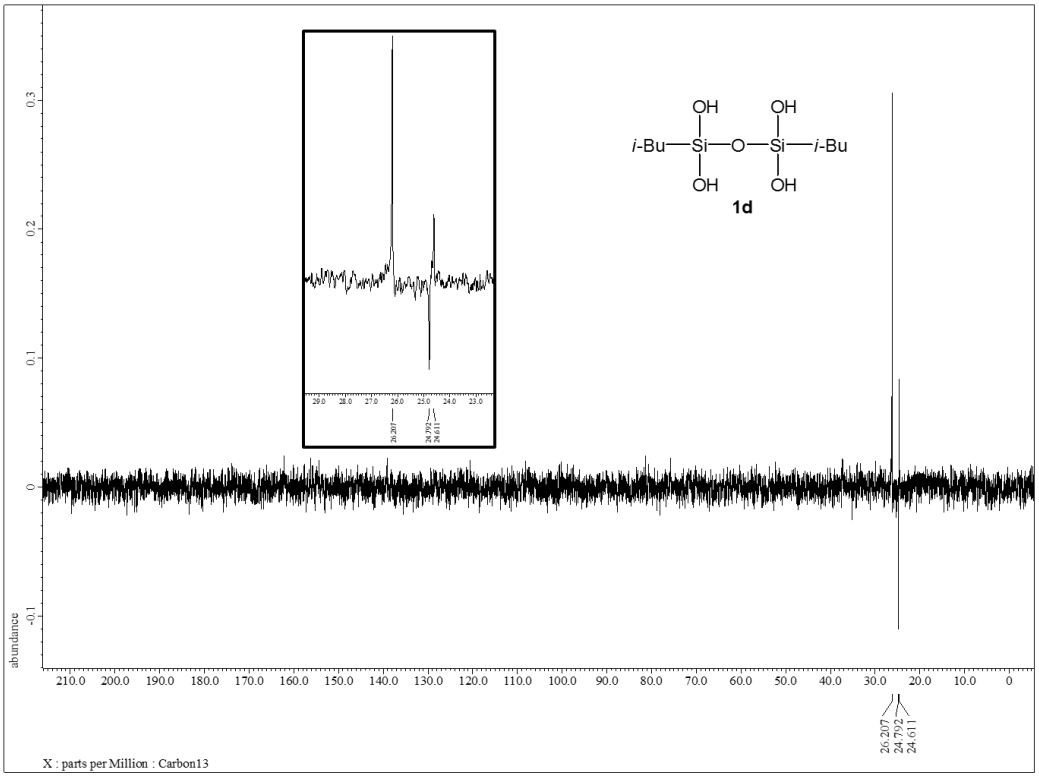

Figure 21. ^{13}C NMR (dept 135) spectrum of **1d** (75.57 MHz, acetone-d_6)

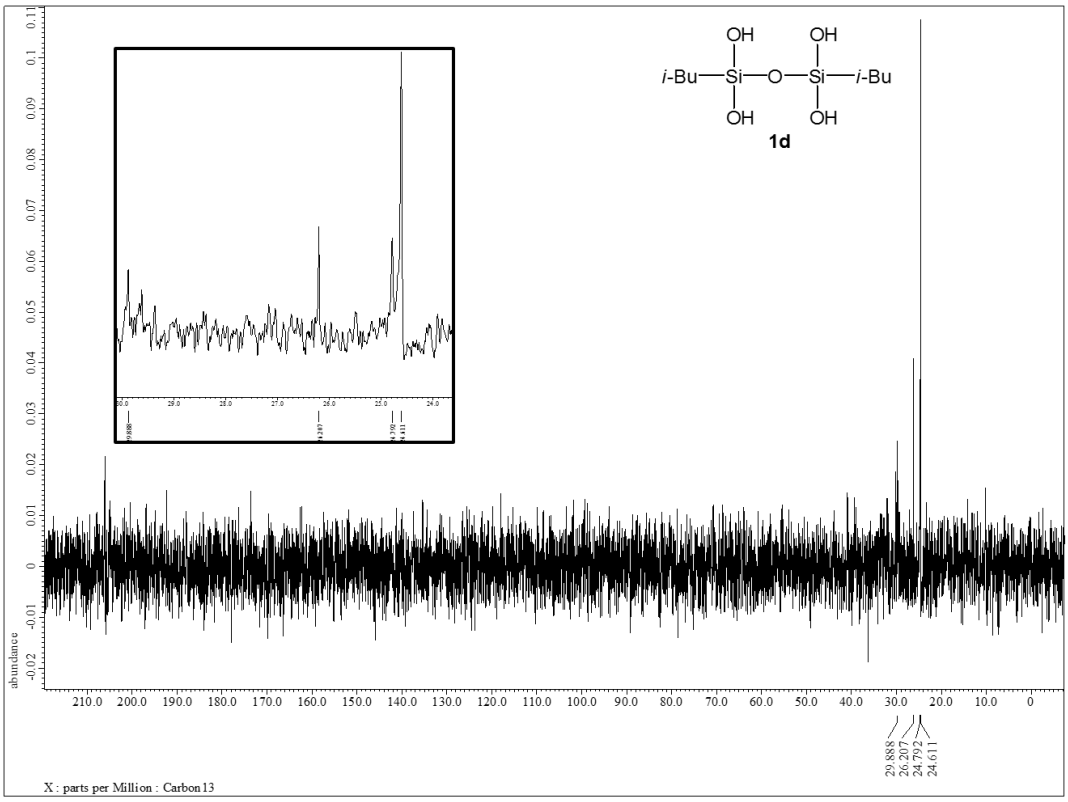

Figure 22. ^{13}C NMR (dept 90) spectrum of **1d** (75.57 MHz, acetone-d_6)

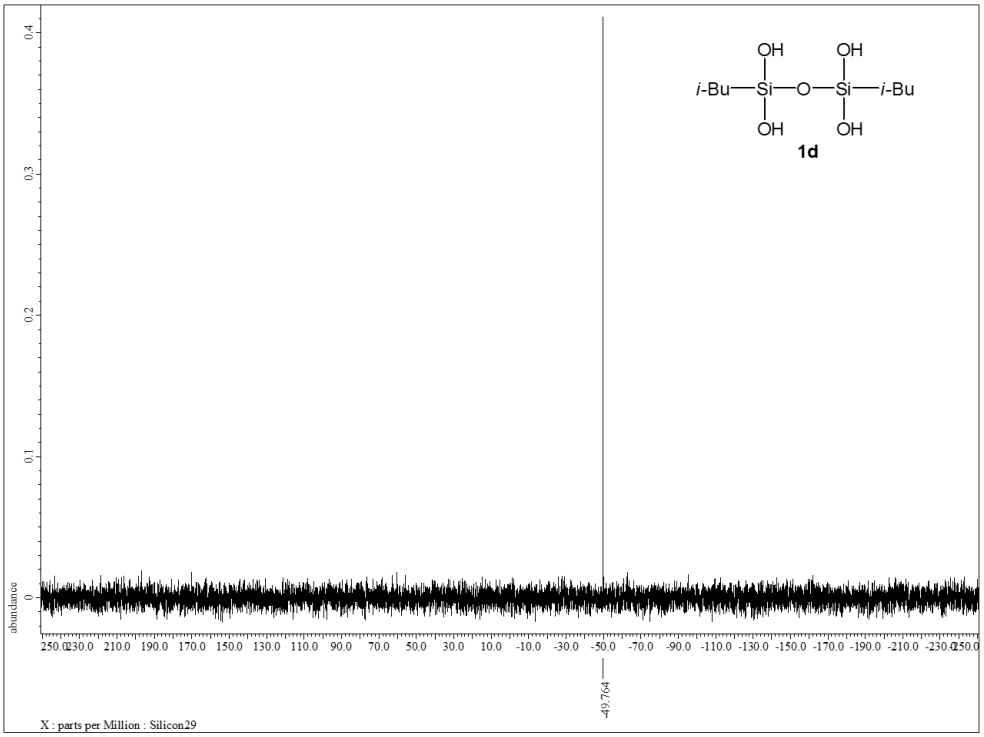

Figure 23. ^{29}Si NMR spectrum of **1d** (59.71 MHz, acetone-d_6)

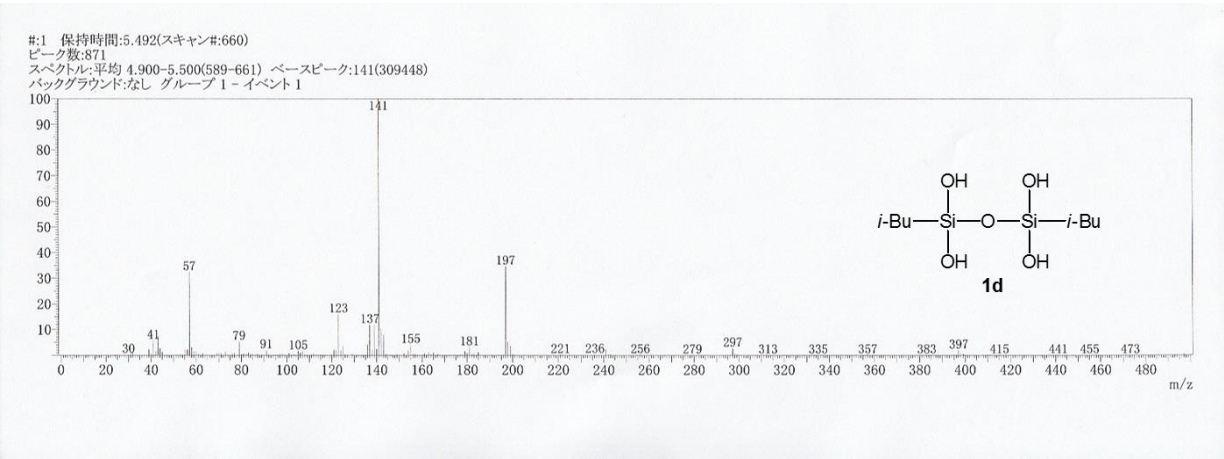

Figure 24. DIMS (EI, 70 eV) spectrum of **1d**

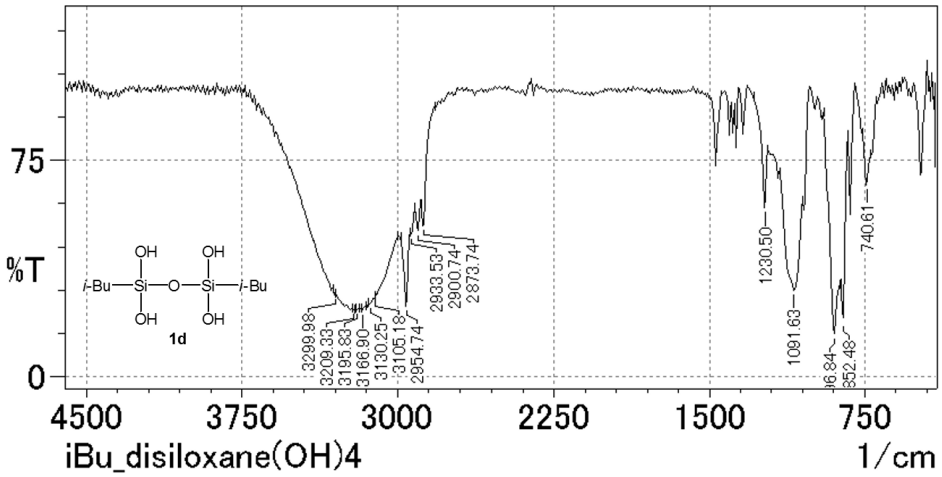

Figure 25. IR (KBr) spectrum of **1d**

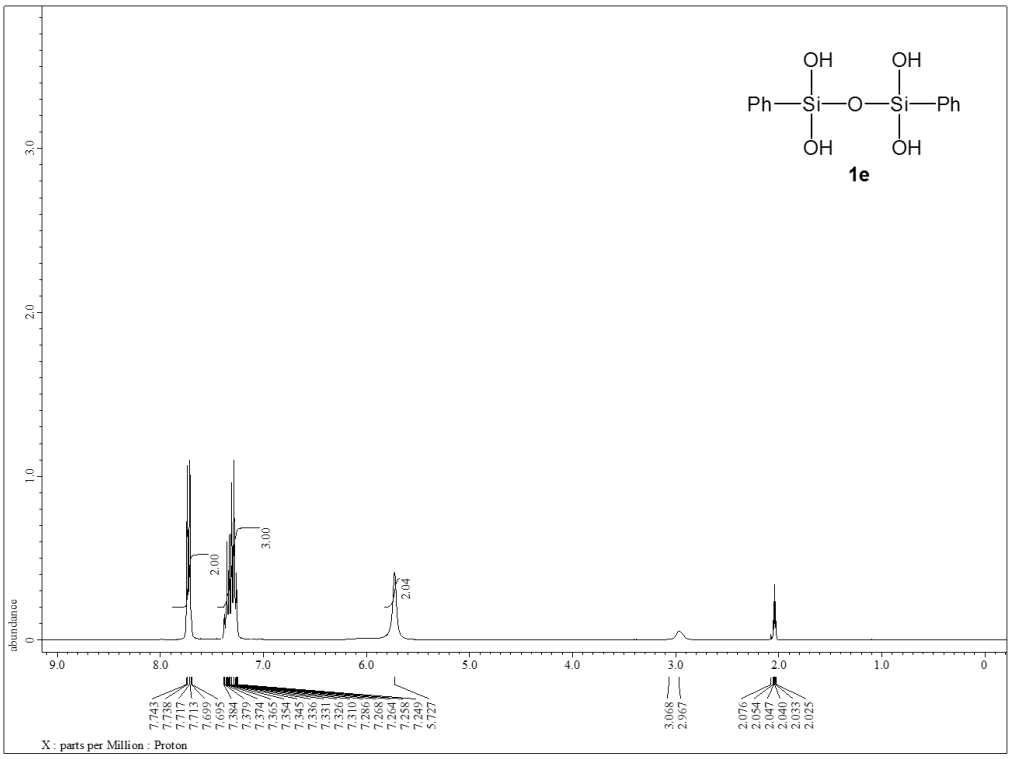

Figure 26. ^{1}H NMR spectrum of **1e** (300.53 MHz, acetone-d_6)

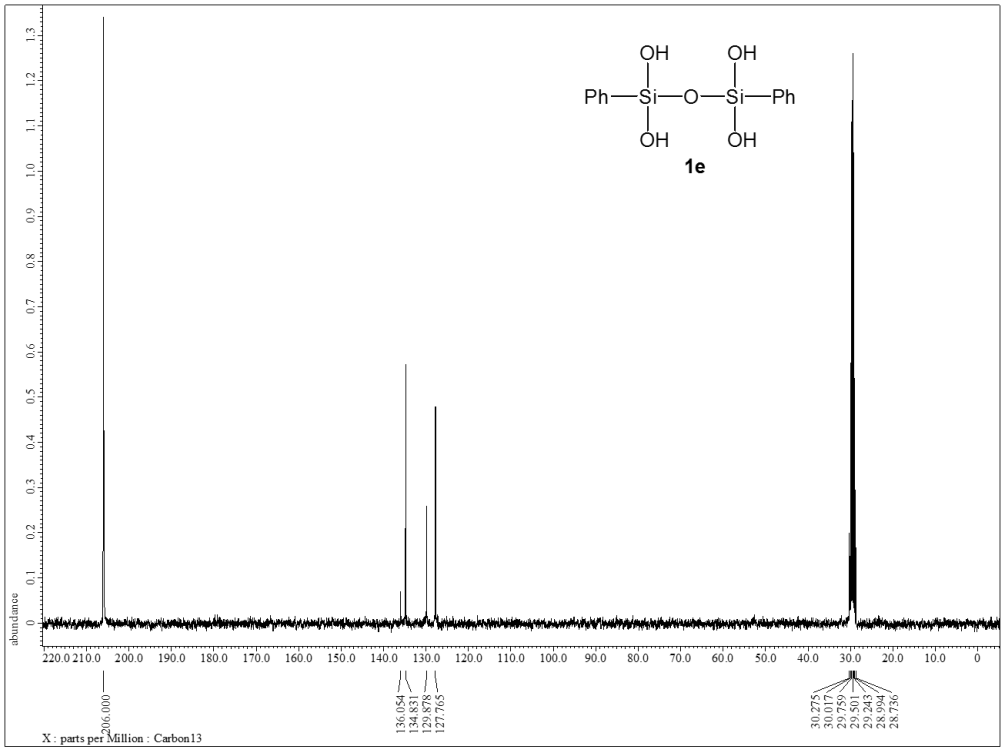

Figure 27. ^{13}C NMR spectrum of **1e** (75.57 MHz, acetone-d_6)

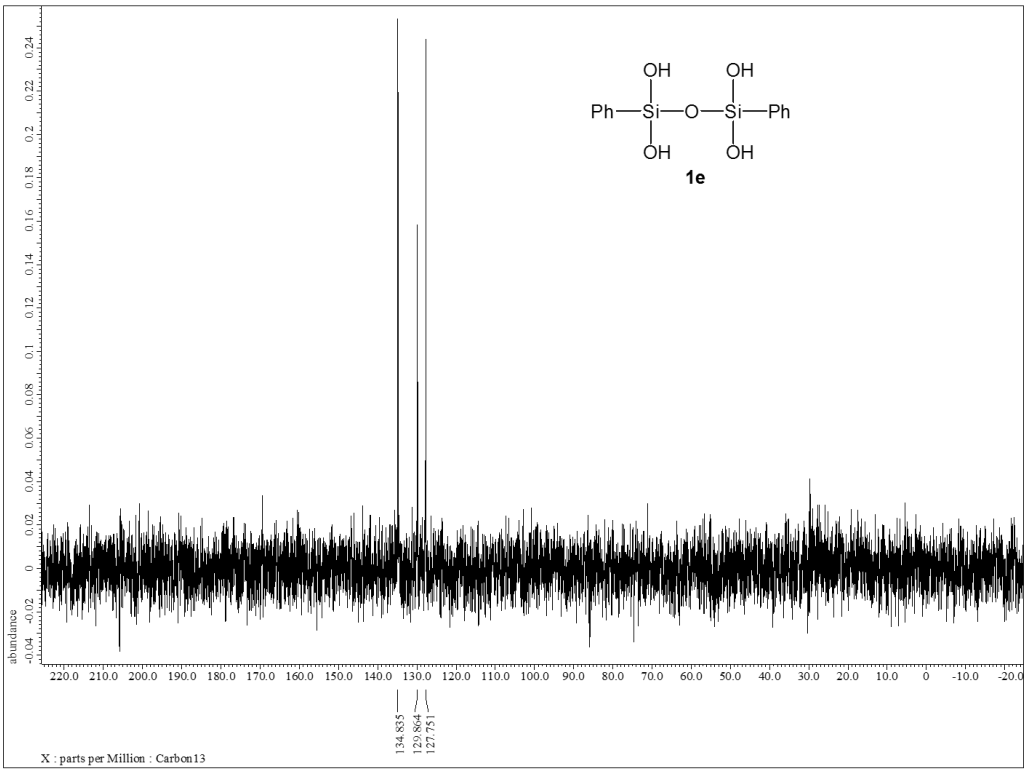

Figure 28. ^{13}C NMR (dept 90) spectrum of **1e** (75.57 MHz, acetone-d_6)

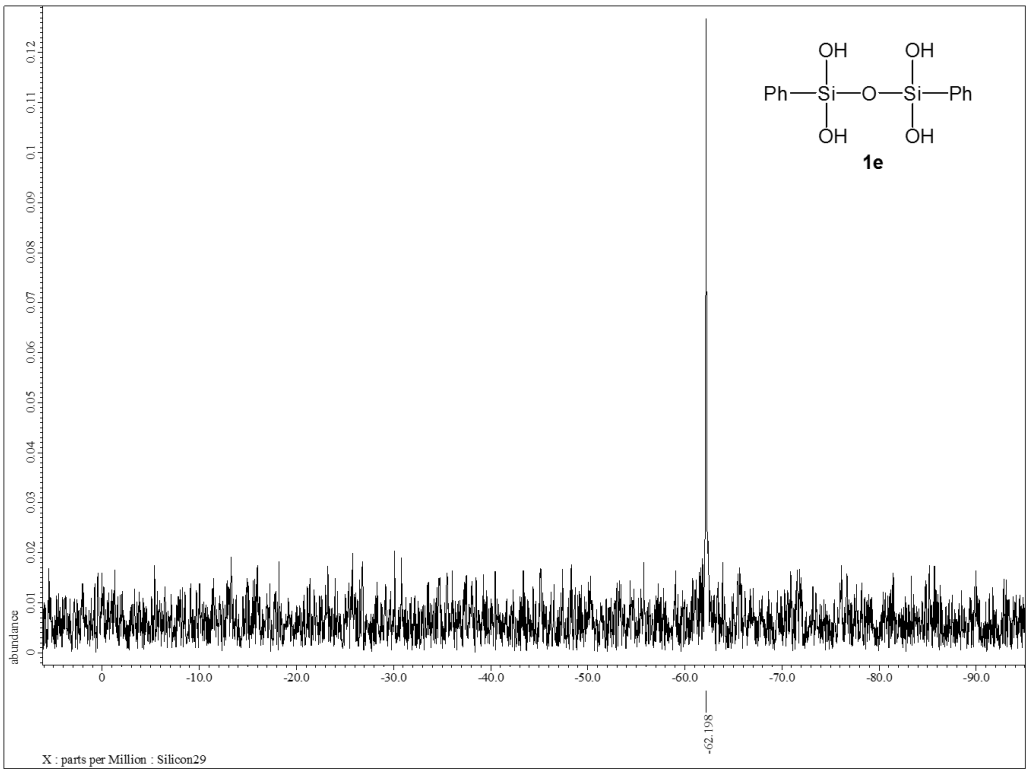

Figure 29. ^{29}Si NMR spectrum of **1e** (59.71 MHz, acetone-d_6)

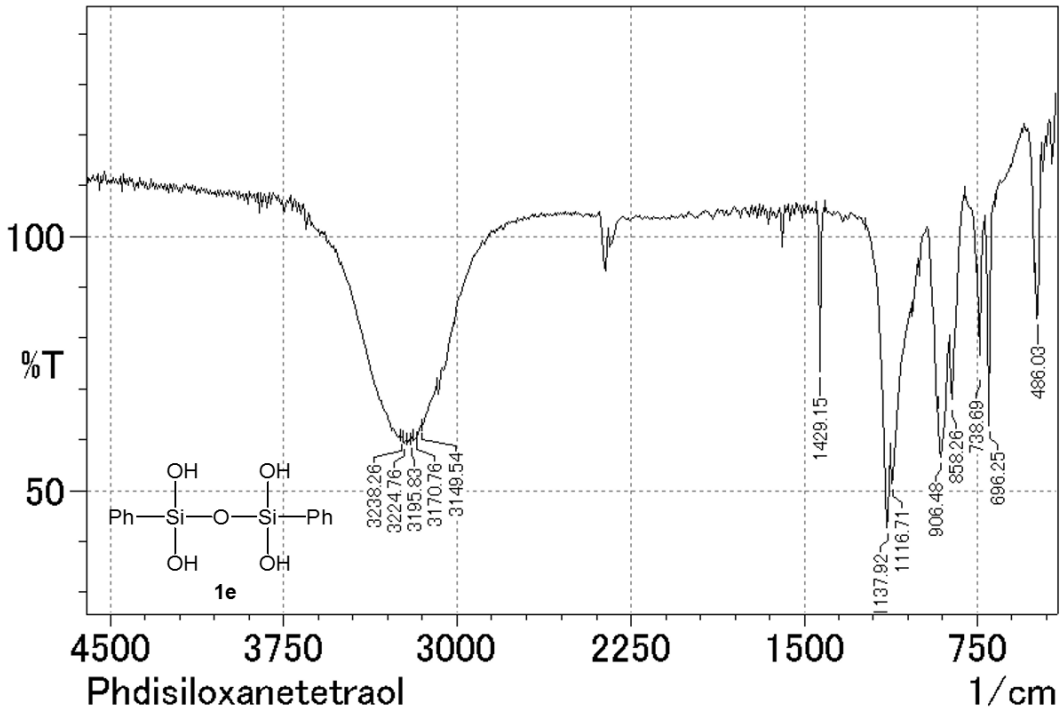

Figure 30. IR (KBr) spectrum of **1e**

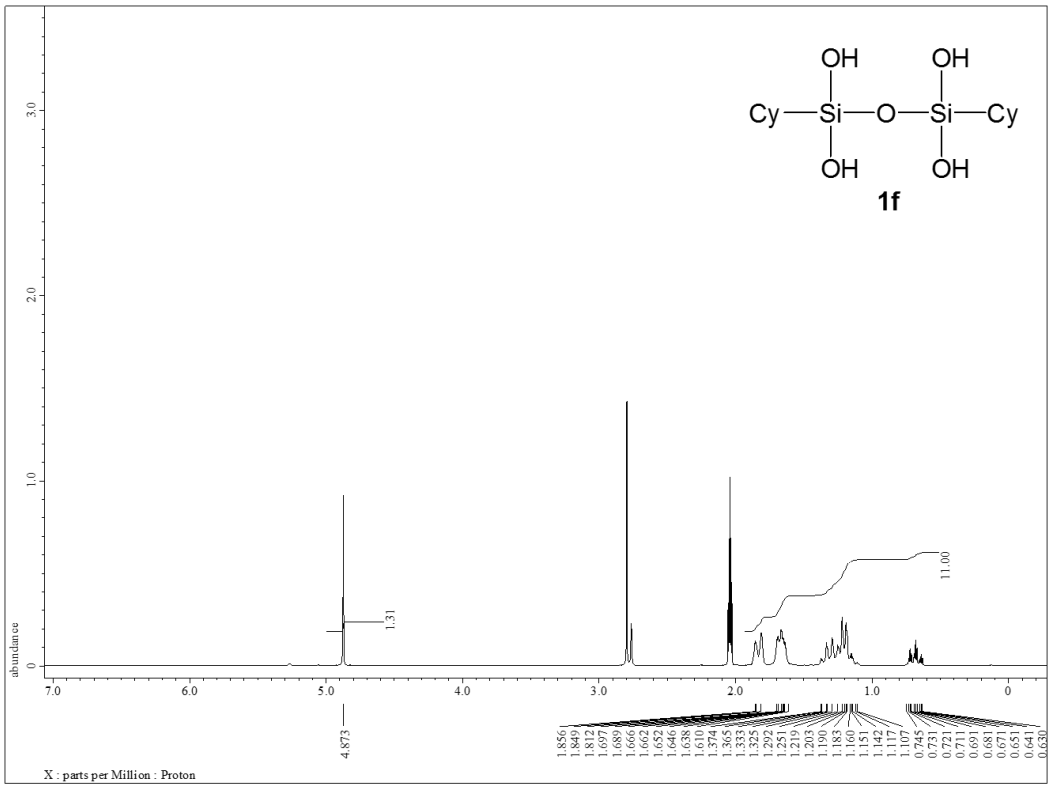

Figure 31. ^{1}H NMR spectrum of **1f** (300.53 MHz, acetone-d_6)

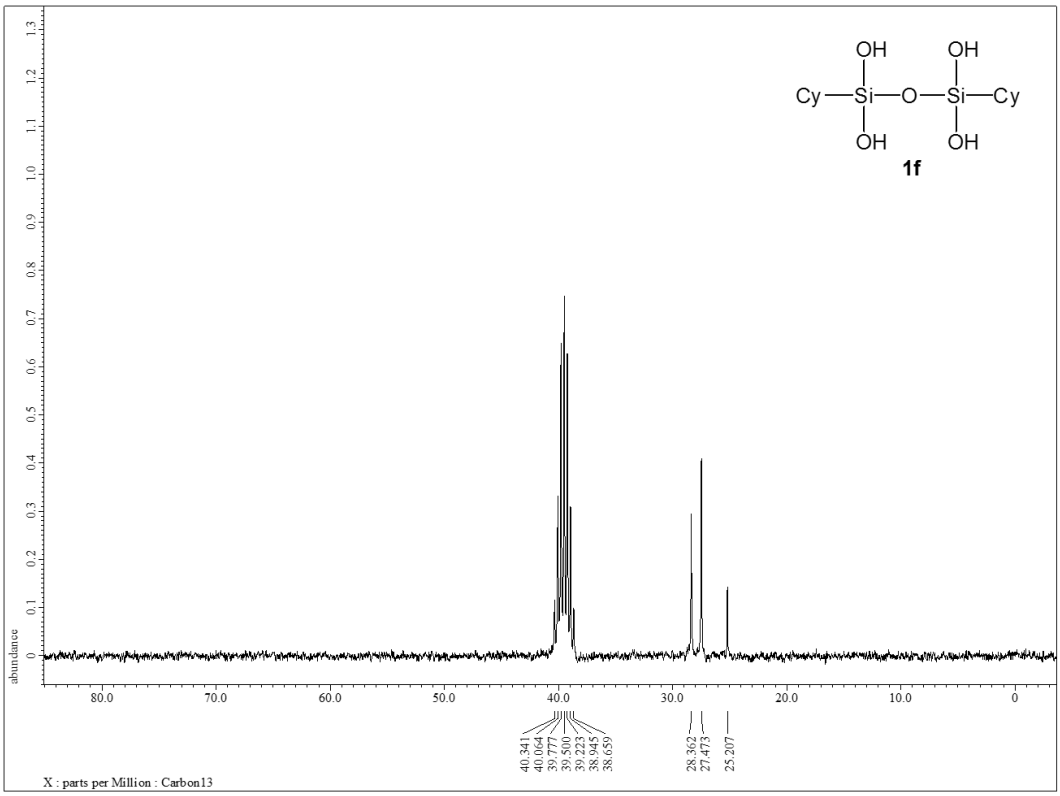

Figure 32. ^{13}C NMR spectrum of **1f** (75.57 MHz, acetone-d_6)

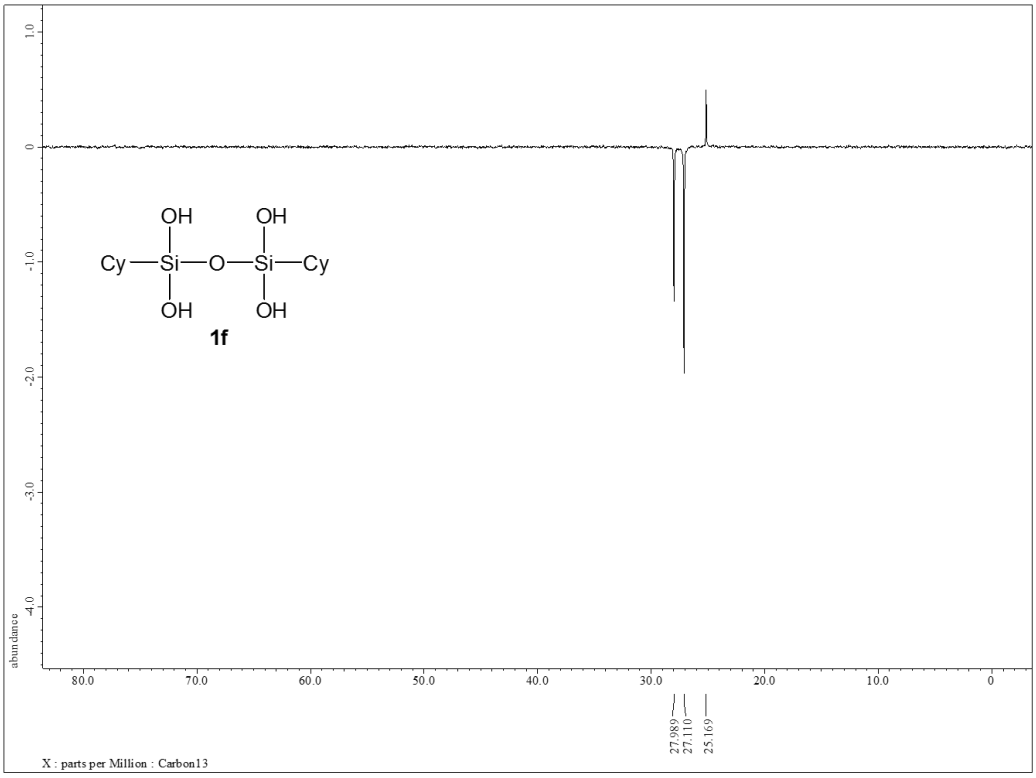

Figure 33. ^{13}C NMR (dept 135) spectrum of **1f** (75.57 MHz, acetone-d_6)

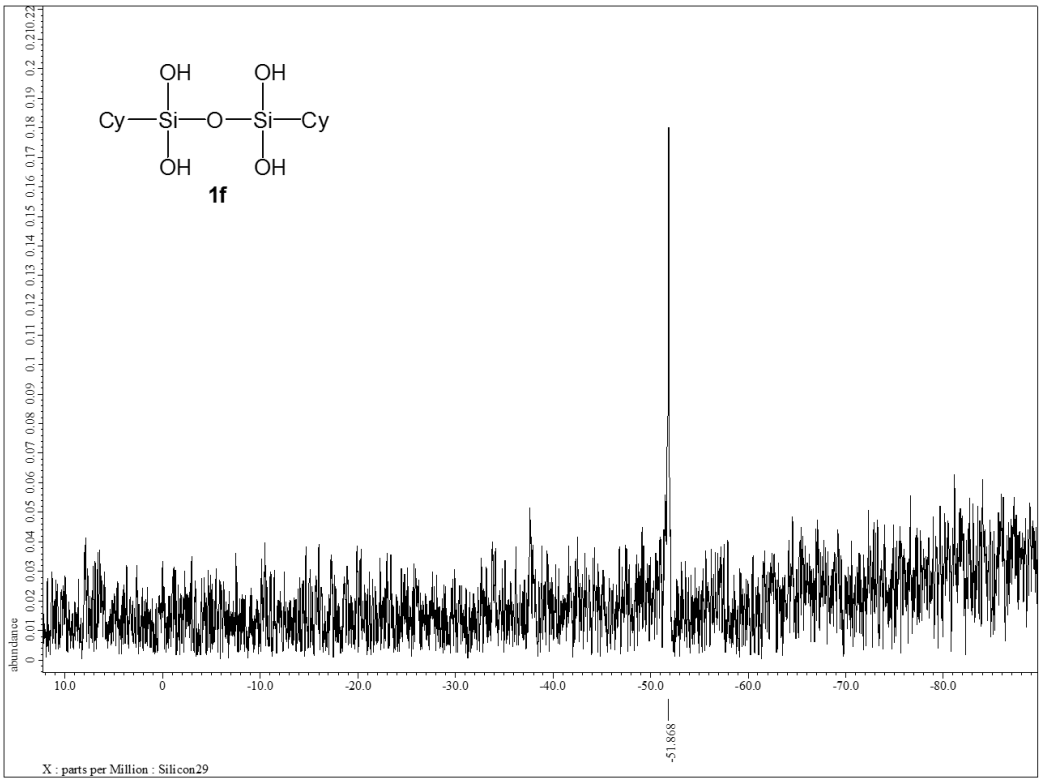

Figure 34. ^{29}Si NMR spectrum of **1f** (59.71 MHz, acetone-d_6)

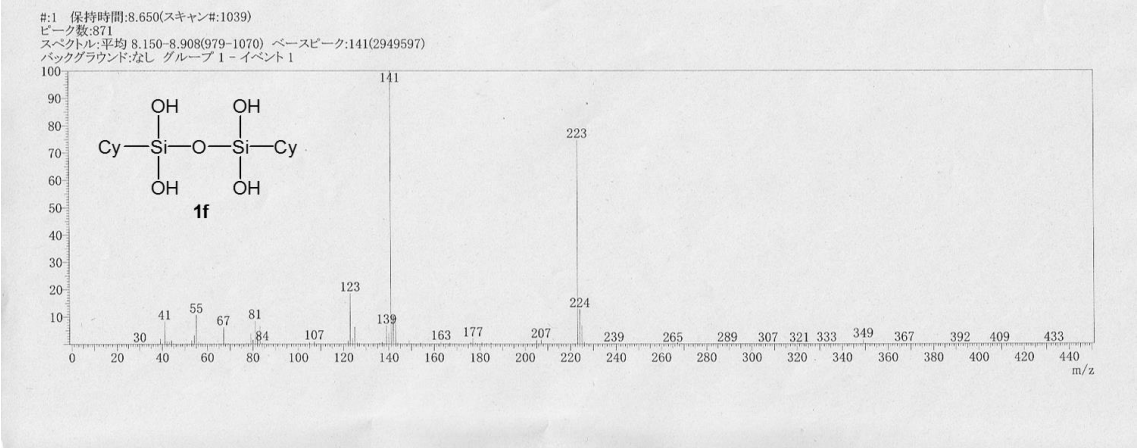

Figure 35. DIMS (EI, 70 eV) spectrum of **1f**

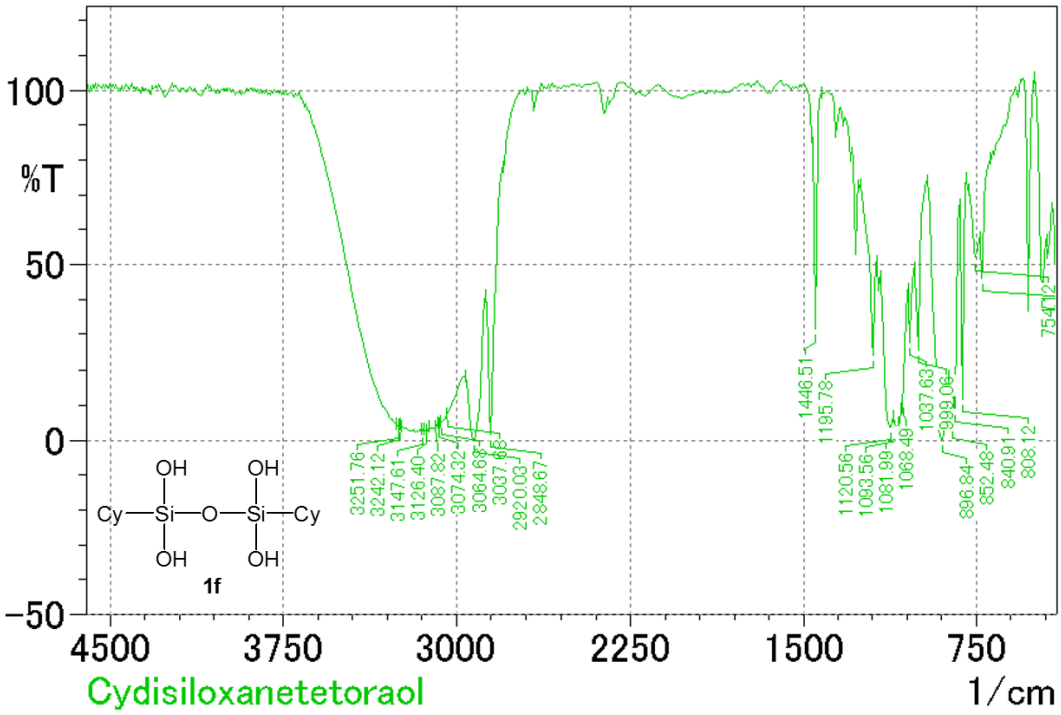

Figure 36. IR (KBr) spectrum of **1f**

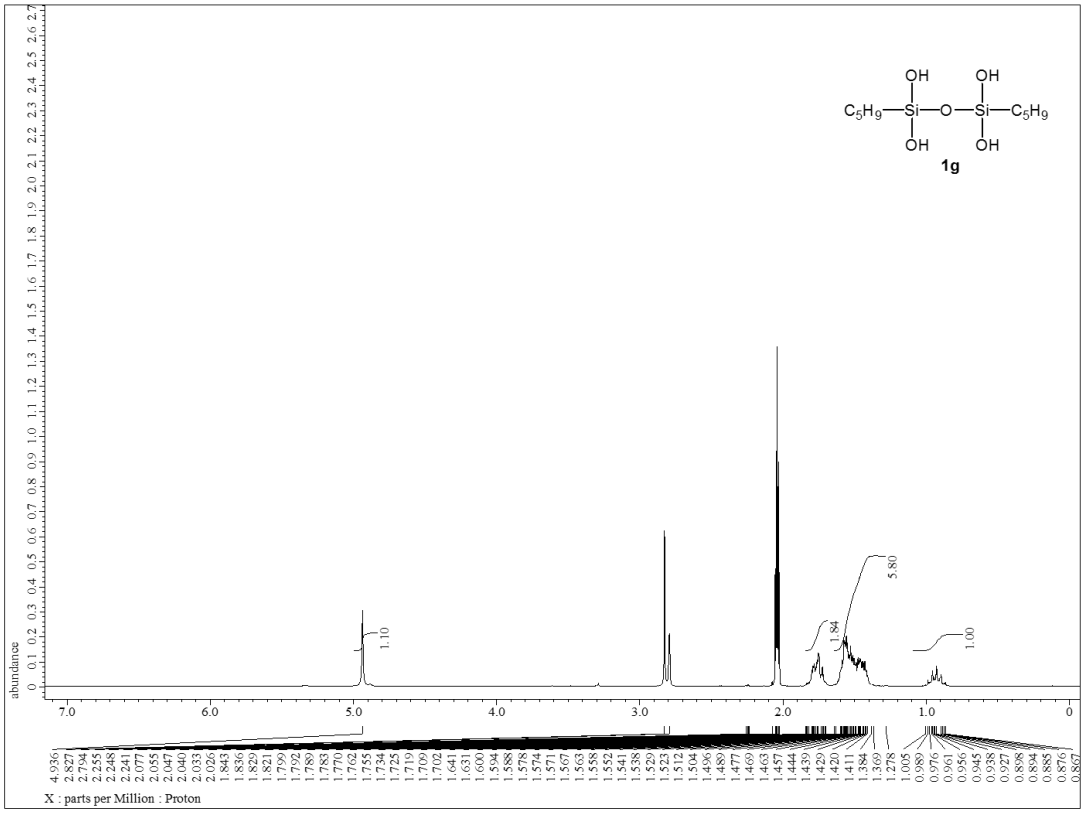

Figure 37. ^{1}H NMR spectrum of **1g** (300.53 MHz, acetone-d_6)

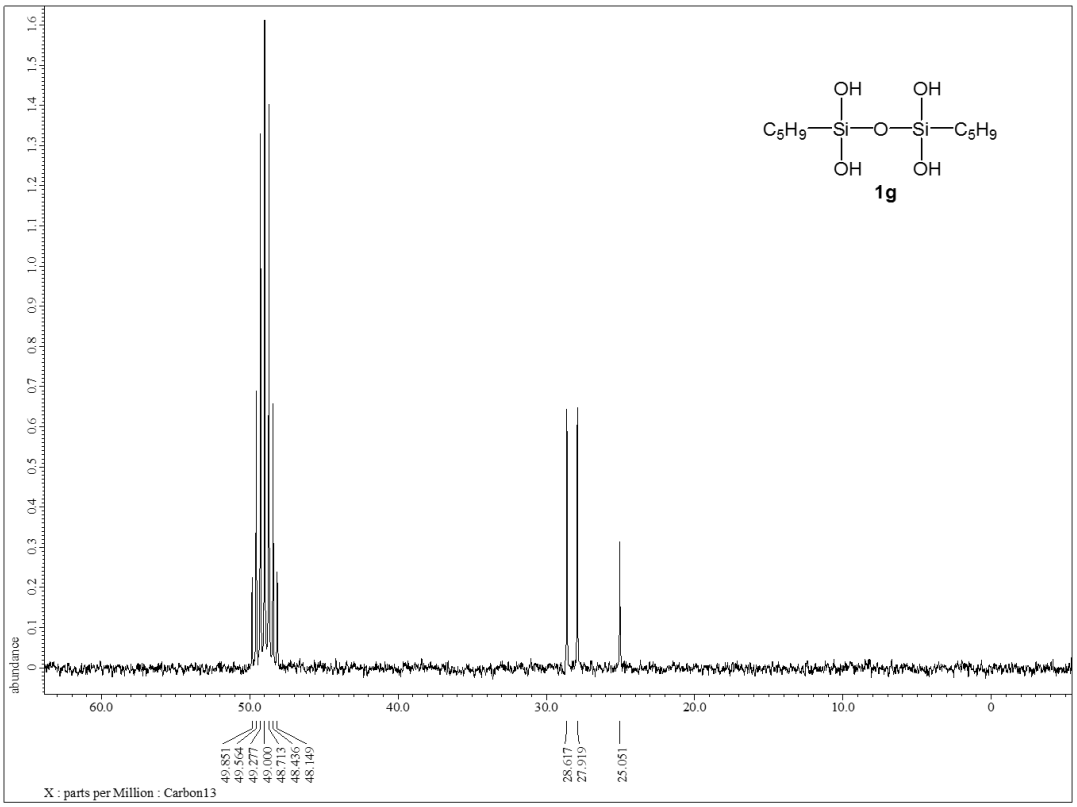

Figure 38. ^{13}C NMR spectrum of **1g** (75.57 MHz, methanol-d_4)

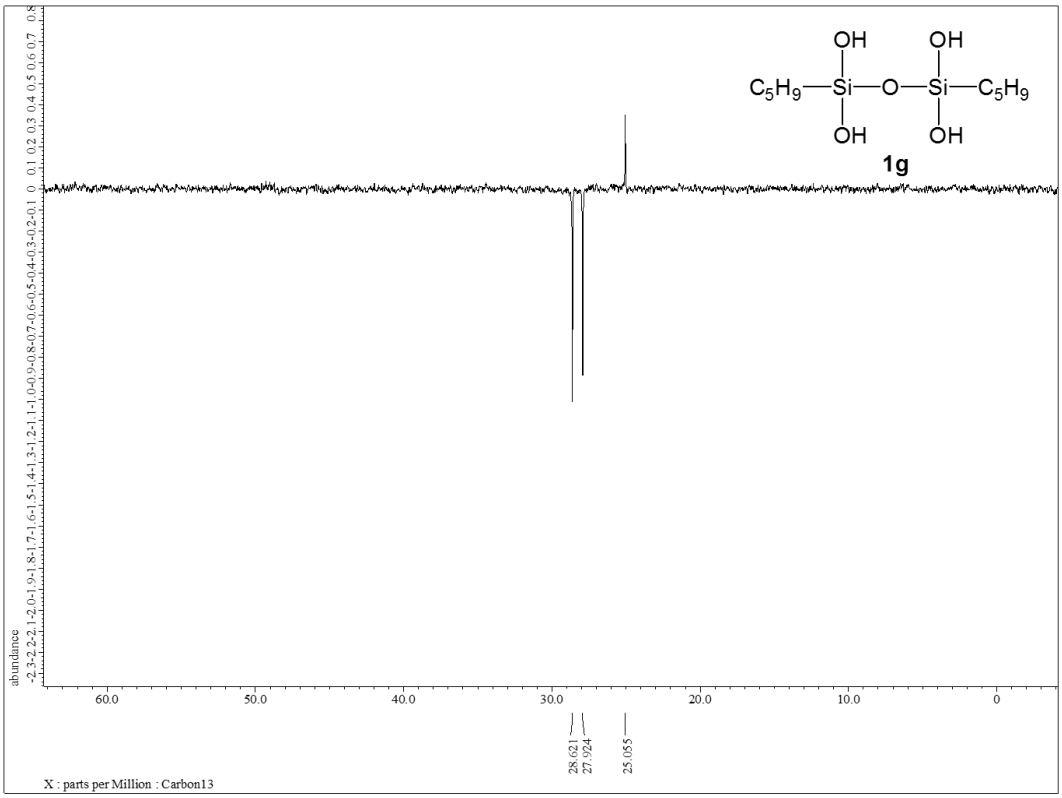

Figure 39. ^{13}C NMR (dept 135) spectrum of **1g** (75.57 MHz, methanol-d_4)

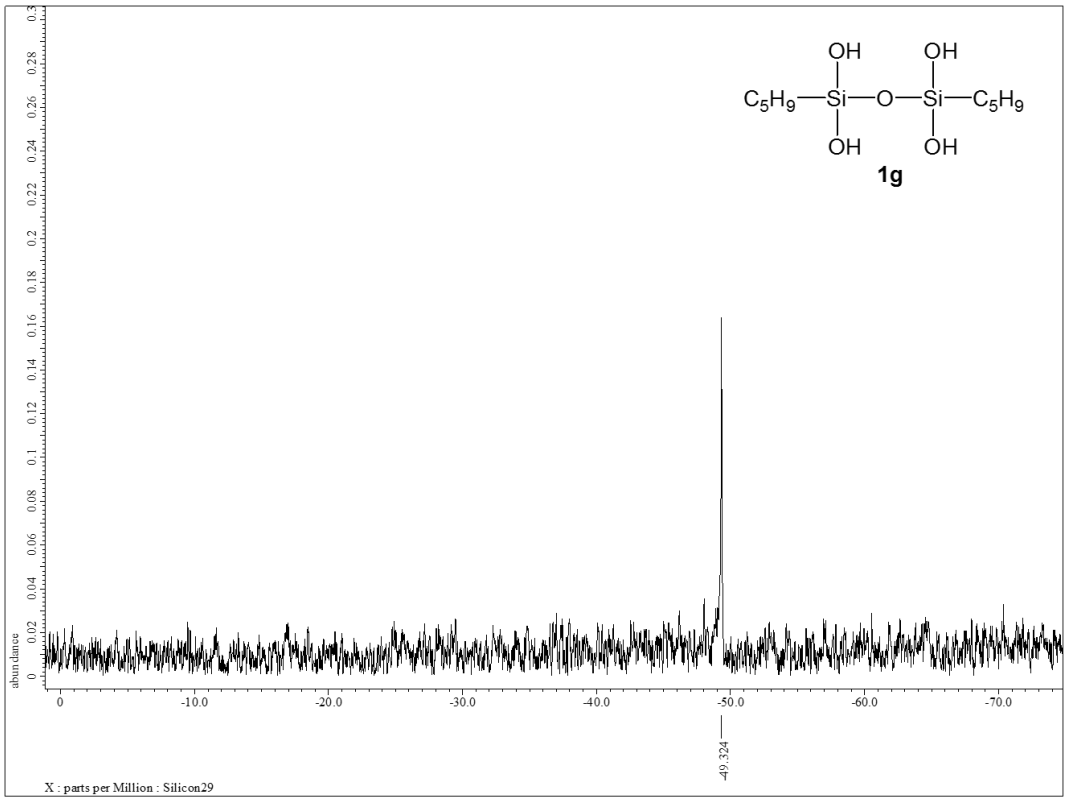

Figure 40. ^{29}Si NMR spectrum of **1g** (59.71 MHz, methanol-d_4)

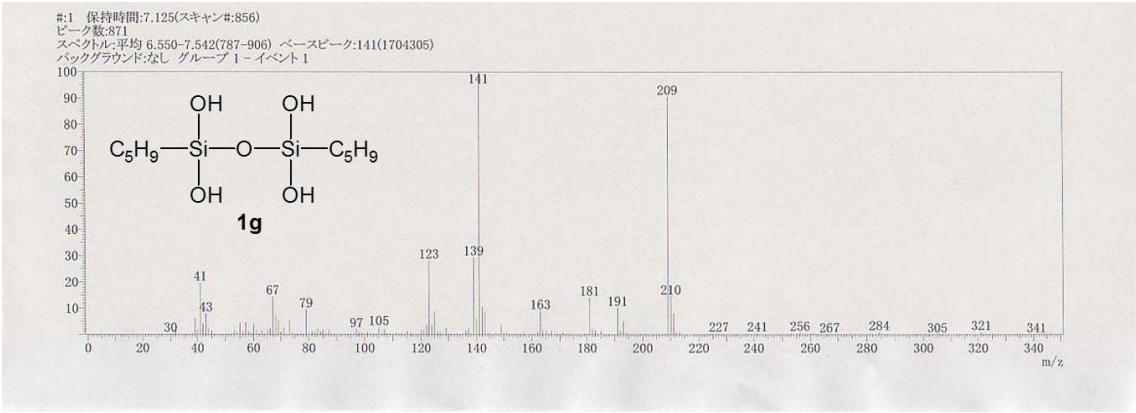

Figure 41. DIMS (EI, 70 eV) spectrum of **1g**

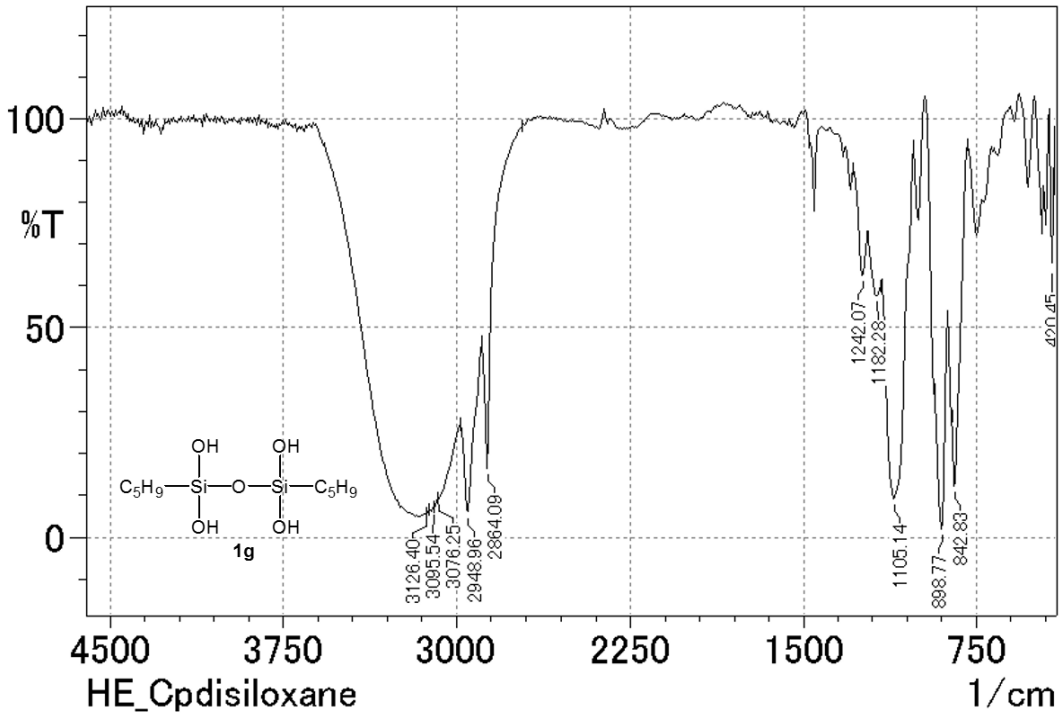

Figure 42. IR (KBr) spectrum of **1g**

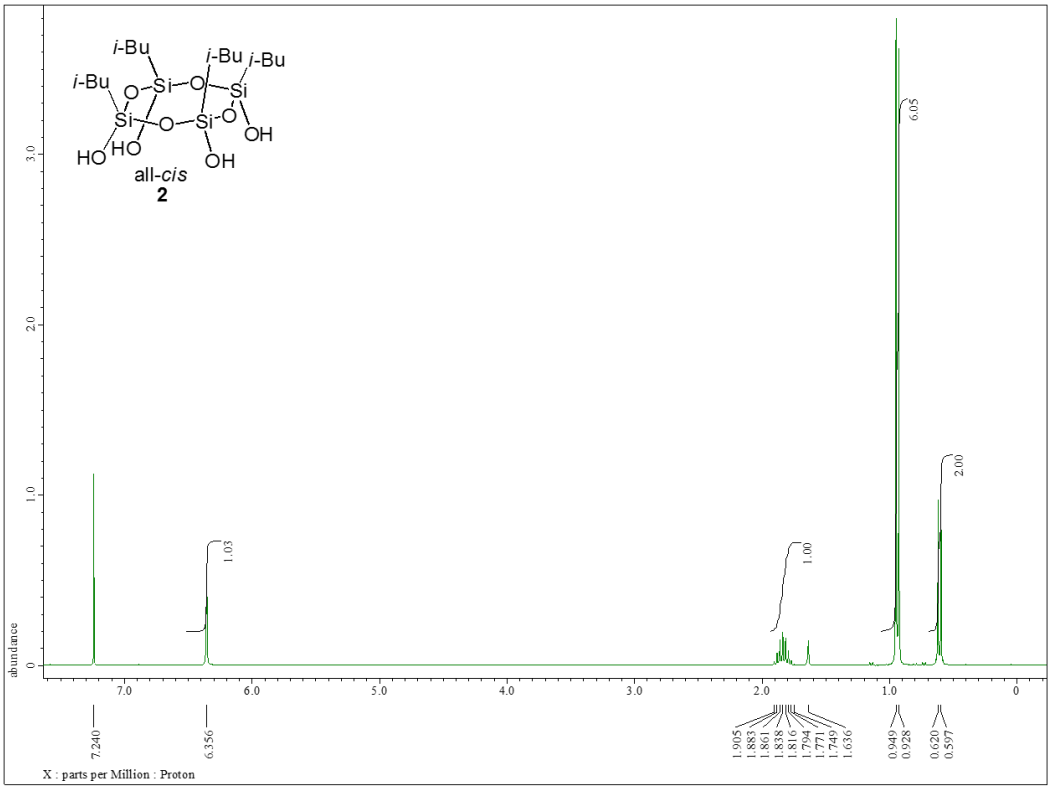

Figure 43. ^{1}H NMR spectrum of **2** (300.53 MHz, $CDCl_3$)

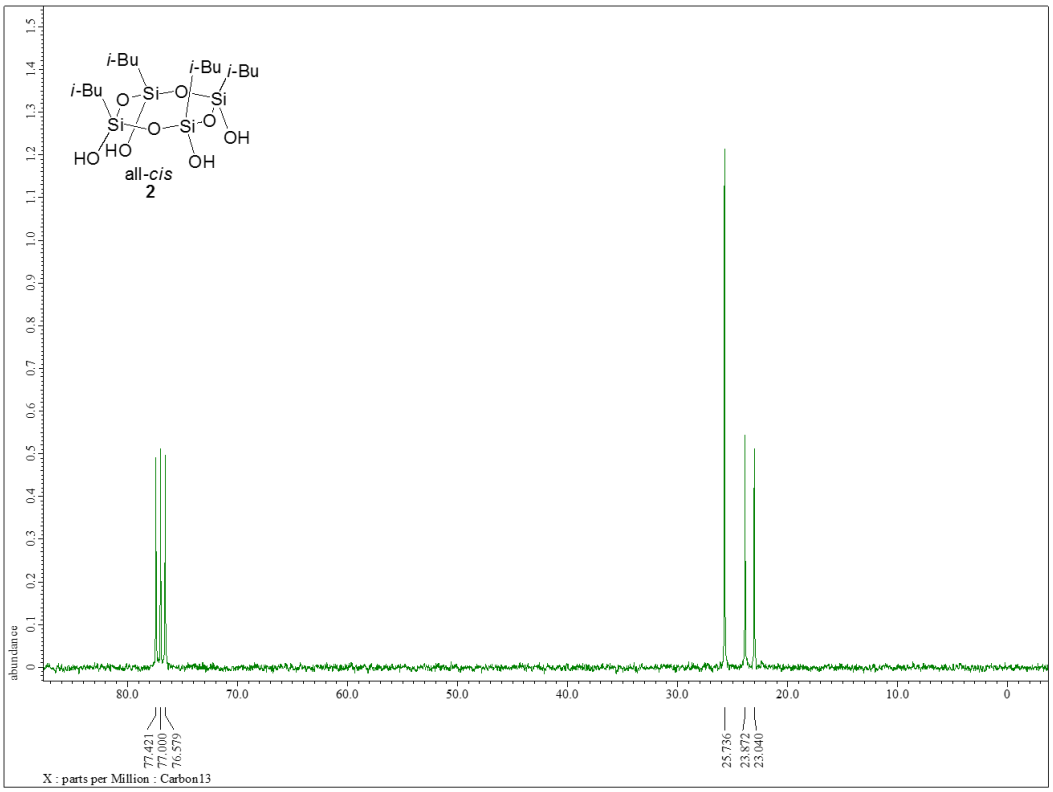

Figure 44. ^{13}C NMR spectrum of **2** (75.57 MHz, $CDCl_3$)

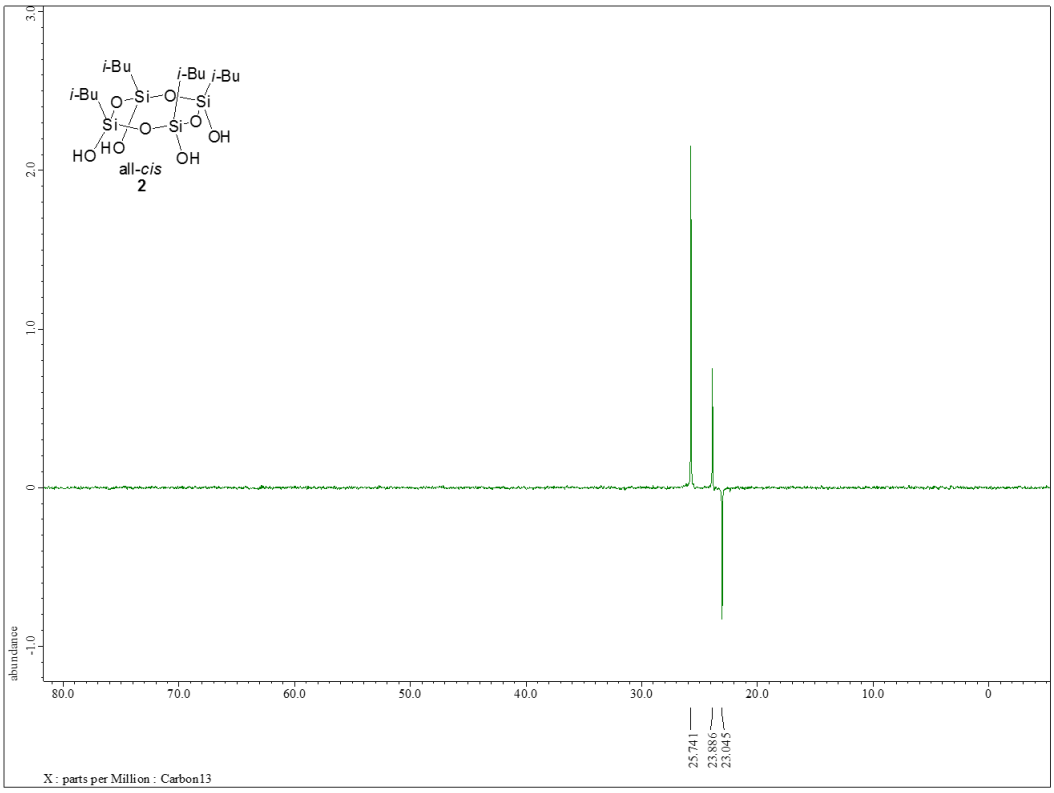

Figure 45. ^{13}C NMR (dept 135) spectrum of **2** (75.57 MHz, $CDCl_3$)

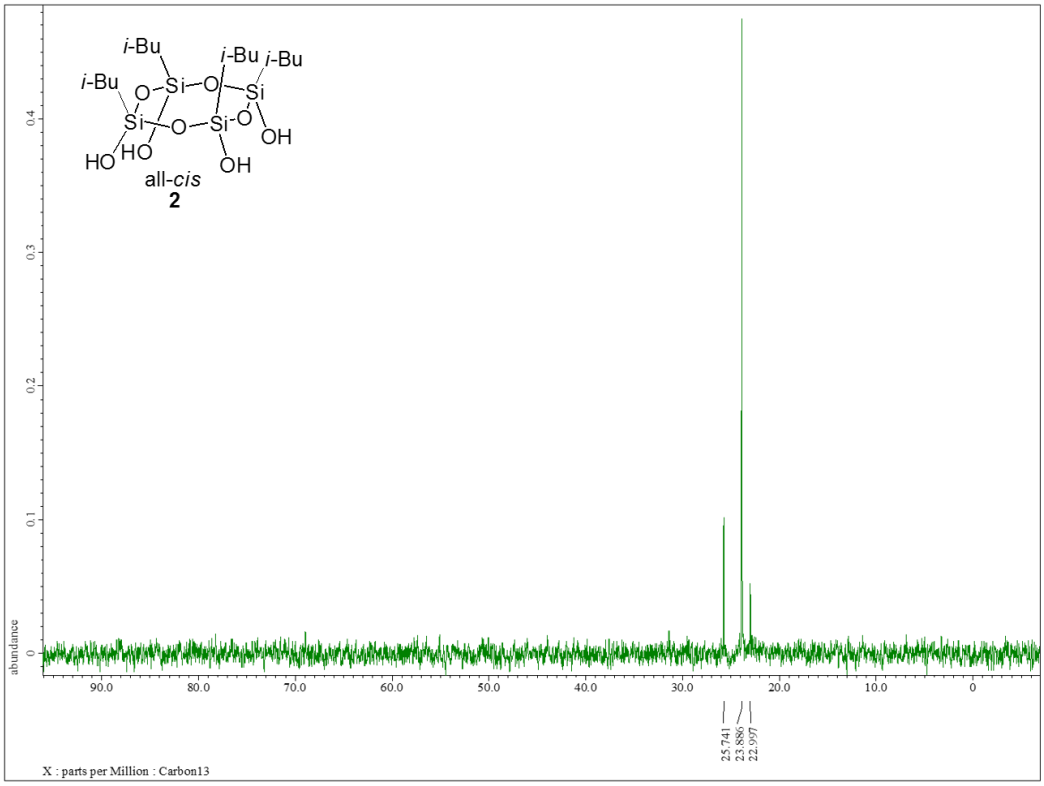

Figure 46. ^{13}C NMR (dept 90) spectrum of **2** (75.57 MHz, $CDCl_3$)

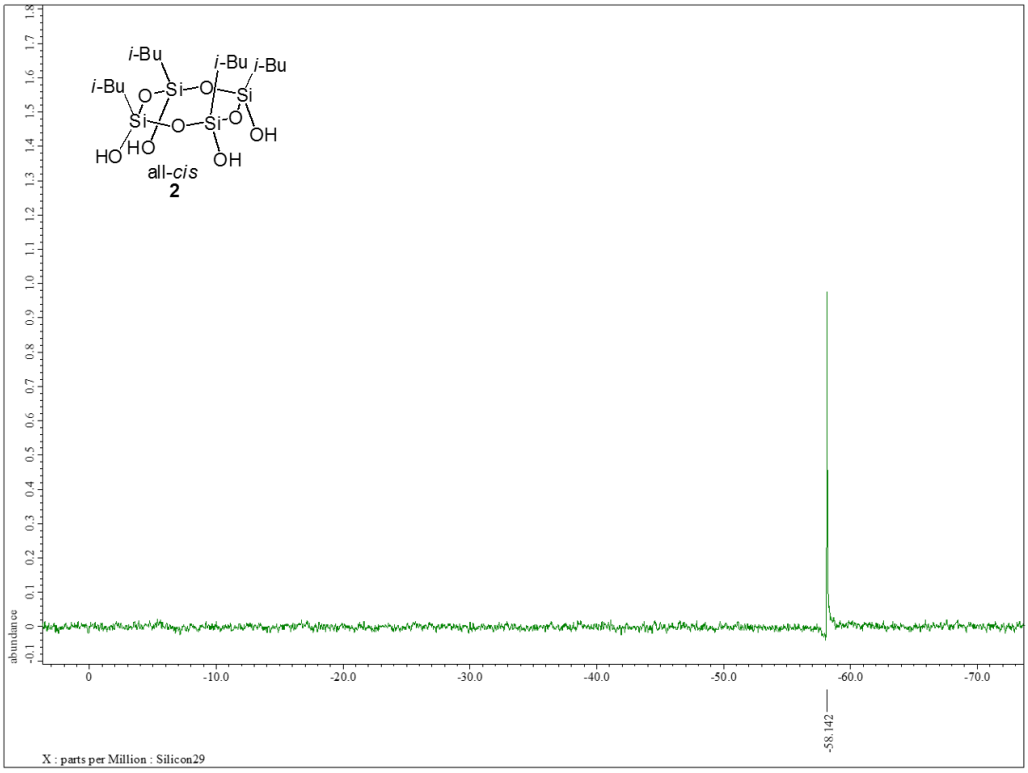

Figure 47. ^{29}Si NMR spectrum of **2** (59.71 MHz, $CDCl_3$)

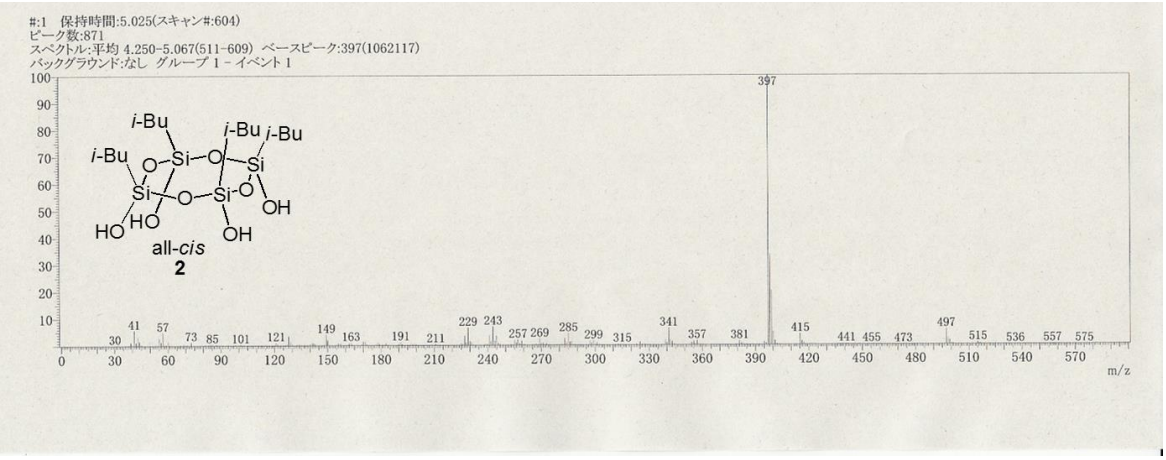

Figure 48. DIMS spectrum of **2**

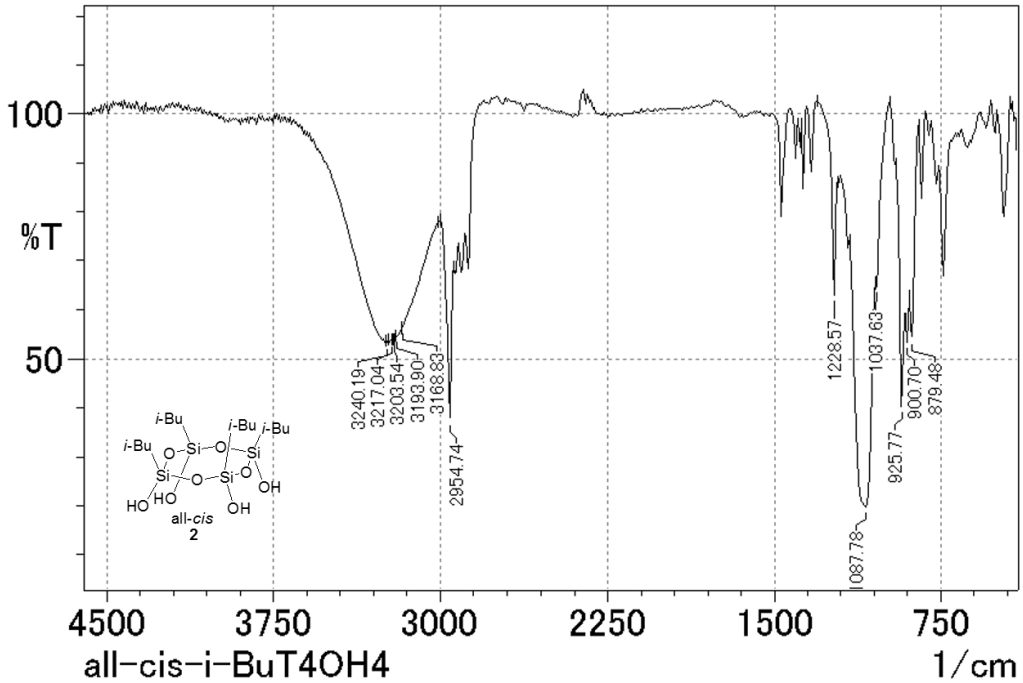

Figure 49. IR spectrum of **2**

2. X-ray analysis

2-1 X-ray analysis of **1g**

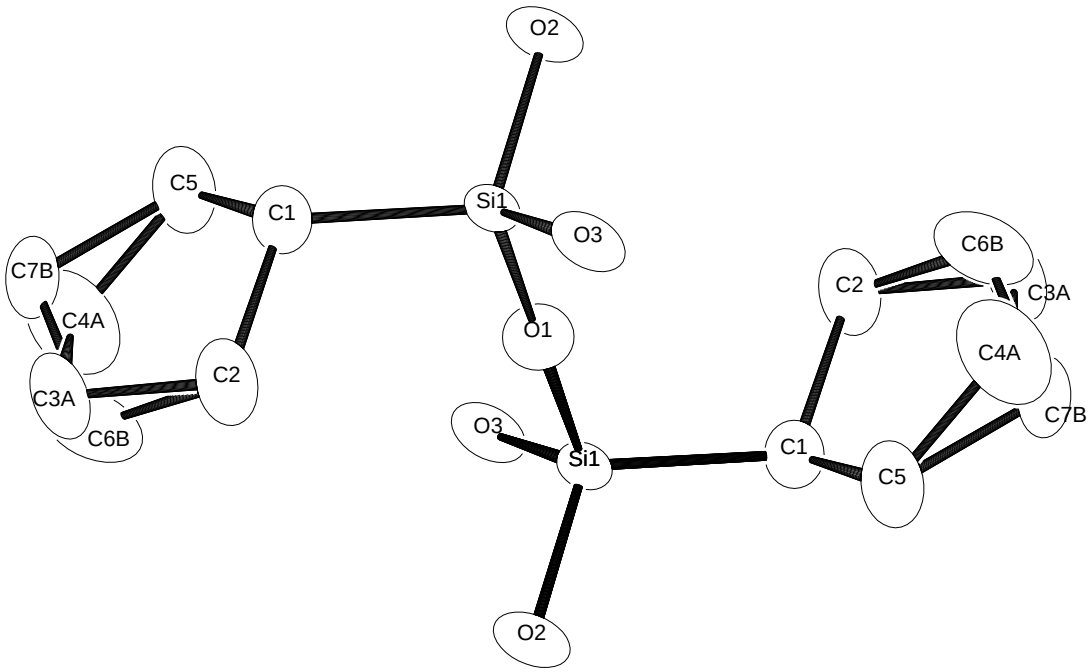

Figure 1. ORTEP drawing of **1g**

Table 1. Crystal data and structure refinement for **1g**.

Empirical formula	$C_{10}H_{22}O_5Si_2$	
Formula weight	278.46	
Temperature	173.1500 K	
Wavelength	0.71070 Å	
Crystal system	Monoclinic	
Space group	P 21/a	
Unit cell dimensions	a = 10.184(4) Å	α = 90.000(2)°.
	b = 6.7162(17) Å	β = 115.755(3)°.
	c = 11.612(5) Å	γ = 90.000(2)°.
Volume	715.3(5) $Å^3$	
Z	2	
Density (calculated)	1.293 g/mL	
Absorption coefficient	0.255 mm^{-1}	
F(000)	300	
Crystal size	0.4000 x 0.2000 x 0.1500 mm^3	
Theta range for data collection	3.61 to 25.50°.	
Index ranges	$-12<=h<=12$, $-7<=k<=8$, $-14<=l<=14$	
Reflections collected	3925	
Independent reflections	1263 [R(int) = 0.0207]	
Completeness to theta = 25.50°	94.7%	
Absorption correction	Semi-empirical from equivalents	
Max. and min. transmission	1.0000 and 0.3475	
Refinement method	Full-matrix least-squares on F^2	
Data / restraints / parameters	1263 / 1 / 100	
Goodness-of-fit on F2	1.130	
Final R indices [I>2sigma(I)]	$R1$ = 0.0544, $wR2$ = 0.1389	
R indices (all data)	$R1$ = 0.0549, $wR2$ = 0.1392	
Largest diff. peak and hole	0.380 and -0.574 e.$Å^{-3}$	

Table 2. Atomic coordinates (x 10^4) and equivalent isotropic displacement parameters ($Å^2$x 10^3) for **1g**. U(eq) is defined as one third of the trace of the orthogonalized U^{ij} tensor.

	x	y	z	U(eq)
Si(1)	4531(1)	1894(1)	4066(1)	20(1)
O(1)	5000	0	5000	36(1)
O(2)	5955(2)	3288(3)	4369(2)	33(1)
O(3)	3389(2)	3257(3)	4361(2)	33(1)
C(1)	3703(3)	1000(5)	2403(3)	32(1)
C(2)	2329(4)	-303(6)	2062(3)	48(1)
C(3A)	2243(16)	-1640(30)	983(12)	42(3)
C(4A)	3870(20)	-2110(30)	1450(30)	70(5)
C(5)	4729(4)	-311(6)	2061(3)	48(1)
C(6B)	2580(20)	-2130(30)	1430(30)	69(5)
C(7B)	3730(20)	-1660(30)	978(12)	43(3)

Table 3. Bond lengths [Å] for **1g**.

Si(1)-O(1)	1.6043(8)	C(2)-C(6B)	1.507(18)
Si(1)-O(3)	1.629(2)	C(2)-C(3A)	1.512(15)
Si(1)-O(2)	1.630(2)	C(3A)-C(4A)	1.54(3)
Si(1)-C(1)	1.839(3)	C(4A)-C(5)	1.48(2)
O(1)-Si(1)#1	1.6043(8)	C(5)-C(7B)	1.525(17)
C(1)-C(5)	1.545(4)	C(6B)-C(7B)	1.52(3)
C(1)-C(2)	1.549(4)		

Symmetry transformations used to generate equivalent atoms: #1 -x+1,-y,-z+1

Table 4. Bond angles [°] for **1g**.

O(1)-Si(1)-O(3)	109.45(9)	C(6B)-C(2)-C(3A)	22.5(9)
O(1)-Si(1)-O(2)	109.49(9)	C(6B)-C(2)-C(1)	105.1(7)
O(3)-Si(1)-O(2)	106.35(11)	C(3A)-C(2)-C(1)	105.5(7)
O(1)-Si(1)-C(1)	108.47(11)	C(2)-C(3A)-C(4A)	99.5(12)
O(3)-Si(1)-C(1)	111.12(13)	C(5)-C(4A)-C(3A)	108.7(14)
O(2)-Si(1)-C(1)	111.92(13)	C(4A)-C(5)-C(7B)	22.5(10)
Si(1)-O(1)-Si(1)#1	180.0	C(4A)-C(5)-C(1)	105.3(8)
C(5)-C(1)-C(2)	104.4(3)	C(7B)-C(5)-C(1)	105.6(7)
C(5)-C(1)-Si(1)	113.8(2)	C(2)-C(6B)-C(7B)	108.5(13)
C(2)-C(1)-Si(1)	113.9(2)	C(6B)-C(7B)-C(5)	100.0(12)

Symmetry transformations used to generate equivalent atoms: #1 -x+1,-y,-z+1

Table 5. Anisotropic displacement parameters ($Å^2 x 10^3$) for **1g**. The anisotropic displacement factor exponent takes the form: $-2 \pi^2 [h^2 a^{*2} U^{11} + ... + 2 h k a^* b^* U^{12}]$

	U^{11}	U^{22}	U^{33}	U^{23}	U^{13}	U^{12}
Si(1)	17(1)	16(1)	27(1)	-2(1)	10(1)	-1(1)
O(1)	43(2)	25(2)	35(2)	9(1)	14(1)	4(1)
O(2)	21(1)	25(1)	58(1)	-9(1)	23(1)	-5(1)
O(3)	24(1)	24(1)	57(1)	-12(1)	24(1)	-4(1)
C(1)	29(2)	37(2)	28(1)	-2(1)	10(1)	-1(1)
C(2)	28(2)	74(3)	43(2)	-25(2)	17(1)	-12(2)
C(3A)	36(5)	43(7)	34(5)	-14(4)	5(4)	-1(4)
C(4A)	47(7)	68(10)	97(15)	-31(10)	34(10)	0(6)
C(5)	34(2)	68(3)	45(2)	-23(2)	21(2)	-8(2)
C(6B)	68(12)	53(9)	105(15)	-25(8)	54(11)	-27(8)
C(7B)	47(6)	55(8)	34(5)	-17(4)	23(5)	-6(5)

Table 6. Torsion angles [°] for **1g**.

O(3)-Si(1)-O(1)-Si(1)#1	116(10)
O(2)-Si(1)-O(1)-Si(1)#1	-128(10)
C(1)-Si(1)-O(1)-Si(1)#1	-6(10)
O(1)-Si(1)-C(1)-C(5)	-59.4(3)
O(3)-Si(1)-C(1)-C(5)	-179.8(2)
O(2)-Si(1)-C(1)-C(5)	61.5(3)
O(1)-Si(1)-C(1)-C(2)	60.1(3)
O(3)-Si(1)-C(1)-C(2)	-60.3(3)
O(2)-Si(1)-C(1)-C(2)	-179.0(2)
C(5)-C(1)-C(2)-C(6B)	-5.7(12)
Si(1)-C(1)-C(2)-C(6B)	-130.3(12)
C(5)-C(1)-C(2)-C(3A)	-29.1(6)
Si(1)-C(1)-C(2)-C(3A)	-153.7(6)
C(6B)-C(2)-C(3A)-C(4A)	-53(3)
C(1)-C(2)-C(3A)-C(4A)	39.5(17)
C(2)-C(3A)-C(4A)-C(5)	-37(2)
C(3A)-C(4A)-C(5)-C(7B)	-74(3)
C(3A)-C(4A)-C(5)-C(1)	20(2)
C(2)-C(1)-C(5)-C(4A)	5.4(12)
Si(1)-C(1)-C(5)-C(4A)	130.1(12)
C(2)-C(1)-C(5)-C(7B)	28.8(7)
Si(1)-C(1)-C(5)-C(7B)	153.5(6)
C(3A)-C(2)-C(6B)-C(7B)	75(3)
C(1)-C(2)-C(6B)-C(7B)	-20(2)
C(2)-C(6B)-C(7B)-C(5)	37(2)
C(4A)-C(5)-C(7B)-C(6B)	53(3)
C(1)-C(5)-C(7B)-C(6B)	-39.6(17)

Symmetry transformations used to generate equivalent atoms: #1 -x+1,-y,-z+1

Chapter 2: Facile synthesis of cyclotrisiloxanetriols

2.2.1 Introduction

Our group has synthesized a series of silsesquioxanes including oligocyclic laddersiloxanes (ladder-type silsesquioxanes with defined structure) and cage silsesquioxanes, and determined the structures [1]. In the syntheses of these silsesquioxanes with well-defined structures, cyclotetrasiloxanetetraols ($[RSiO(OH)]_4$) have been served as the key starting compounds. In addition, cyclotrisiloxanetriol is also promising compound as a precursor to various siloxanes and silanol hosts. Cyclotrisiloxanetriol ($[RSiO(OH)]_3$) has reactive hydroxy groups and cyclic siloxane bonds.

There are only eight synthetic reports for $[RSiO(OH)]_3$ (R = $Ar(Me_3Si)N$ (Ar = 2,6-dimethylphenyl) [2a], $(Me_3Si)_2CH$ [2b], Ph [2c, d], *m*-tolyl [2e], 2-naphthyl [2f], Tip (2,4,6-triisopropylphenyl) [2g], 3,5-xylyl [2c], and *i*-Pr [2h]), because cyclotrisiloxanetriol has reactive hydroxyl groups and ring strain larger than that of cyclotetrasiloxanetetraol. Therefore, in many cases, $[RSiO(OH)]_3$ were kinetically stabilized by bulky substituents. For example, there are *cis*-*trans*-$[Ar(Me_3Si)NSiO(OH)]_3$ (Ar = 2,6-dimethylphenyl), all-*cis*- $[(Me_3Si)_2CHSiO(OH)]_3$ reported by Roesky et al., *cis*-*trans*-$[TipSiO(OH)]_3$ and *cis*-*trans*-$[i\text{-}PrSiO(OH)]_3$ by our group [2a,b,g,h]. As another approach, all-*cis*-$[RSiO(OH)]_3$ (R = Ph, *m*-tolyl, 2-naphthy, 3,5-xylyl) were isolated by stabilization in self-assembled coordination cages [2c,e,f]. In many cases, cyclotrisiloxanetriols have been synthesized by multi-step reaction.

In this chapter, we describe facile synthesis of *cis*-*trans*-$[RSiO(OH)]_3$ by simple hydrolytic condensation reaction from $RSiCl_3$ (R = Et, C_5H_9). Previous reports and the results for $[RSiO(OH)]_3$ are summarized in Table 1.

Table 1. Various silanotriols

$[RSiO(OH)]_3$	Type of substituents	^{29}Si NMR / ppm	Ref.
cis-trans-$[Ar(Me_3Si)NSiO(OH)]_3$*	Heteroatom	–75.5, –76.5, 7.6, 7.9	[2a]
all-*cis*- $[(TMS)_2CHSiO(OH)]_3$	Alkyl	–21.8, –0.2	[2b]
all-*cis*-$[PhSiO(OH)]_3$**	Aryl	–64.1	[2c]
all-*cis*-$[PhSiO(OH)]_3$**	Aryl	–64.1	[2c]
cis-trans-$[PhSiO(OH)]_3$	Aryl	−62.59, −62.31	[2d]
all-*cis*-[*m*-tolylSiO(OH)]$_3$**	Aryl	–63.32	[2e]
all-*cis*-[2-naphthylSiO(OH)]$_3$**	Aryl	–63.05	[2f]
cis-trans -$[TipSiO(OH)]_3$	Aryl	–60.00, –60.84	[2g]
all-*cis*-[3, 5-xylylSiO(OH)]$_3$**	Aryl	–63.3	[2c]
all-*cis*-[3, 5-xylylSiO(OH)]$_3$**	Aryl	–63.5	[2c]
cis-trans -[*i*-PrSiO(OH)]$_3$	Alkyl	–50.60, –49.75	[2h]
cis-trans -$[EtSiO(OH)]_3$(**1a**)	Alkyl	–48.43, –49.06	This work
cis-trans -$[C_5H_9SiO(OH)]_3$ (**1b**)	Alkyl	–49.50, –50.07	This work

*Ar = 2,6-dimethylphenyl, ** In self-assembled coordination cages

2.2.2 Results and discussion

We already succeeded in a facile single-step synthesis of disiloxanetetraols ($[RSi(OH)_2]_2O$) with various middle-size substituents by hydrolytic condensation of trichlorosilanes ($RSiCl_3$) by quenching the reactions in early stages (Scheme 1) [3].

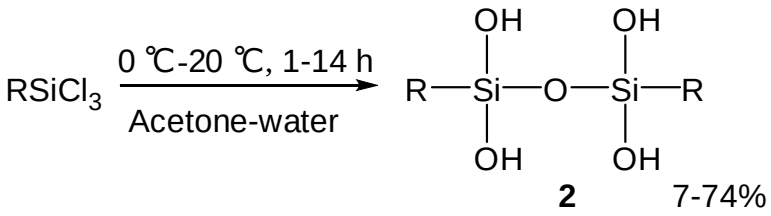

R=Pr , C_6H_{13}, *i*-Pr, *i*-Bu, Ph, Cy, C_5H_9 (**2a**)

Scheme 1

In this procedure, we also attempted the synthesis of $[EtSi(OH)_2]_2O$ and $[C_5H_9Si(OH)_2]_2O$ (**2a**). We could prepare **2a**, however we could not obtain

$[EtSi(OH)_2]_2O$. With several times attempts of these reactions, we serendipitously isolated *cis-trans*-$[EtSi(OH)O]_3$ (**1a**) and *cis-trans*-$[C_5H_9SiO(OH)]_3$ (**1b**). The reaction scheme is shown in Scheme 2.

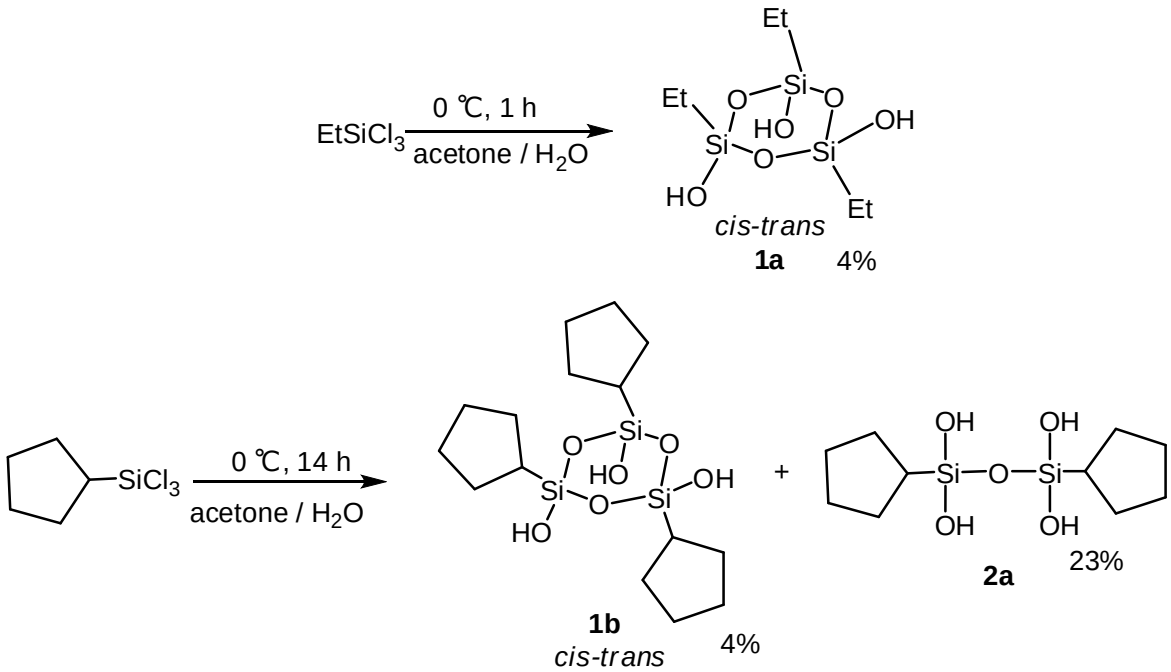

Scheme 2

Hydrolytic condensation reaction of $EtSiCl_3$ was performed at 0 ℃ for 1 h in mixture of acetone and water. The solution was extracted by ether. The organic layer was dried over anhydrous sodium sulfate, and concentrated to give crude solid; that was washed by $CHCl_3$, and we obtained *cis-trans*-$[EtSiO(OH)]_3$ (**1**) in 4% yield.

In ^{1}H NMR spectrum, there are two peaks attributed to OH groups. In ^{13}C NMR spectrum there are four peaks attributed to Et groups. In ^{29}Si NMR spectrum there are two peaks at –48.43, –49.06 ppm. The ^{29}Si NMR peaks are similar to those of *cis-trans*-[*i*-PrSiO(OH)]$_3$ which is also trialkylcyclotrisiloxanetriol [2h]. This information allows us to determine the structure to be *cis-trans* conformation. ^{29}Si spectrum of crude product is shown in Figure 1.

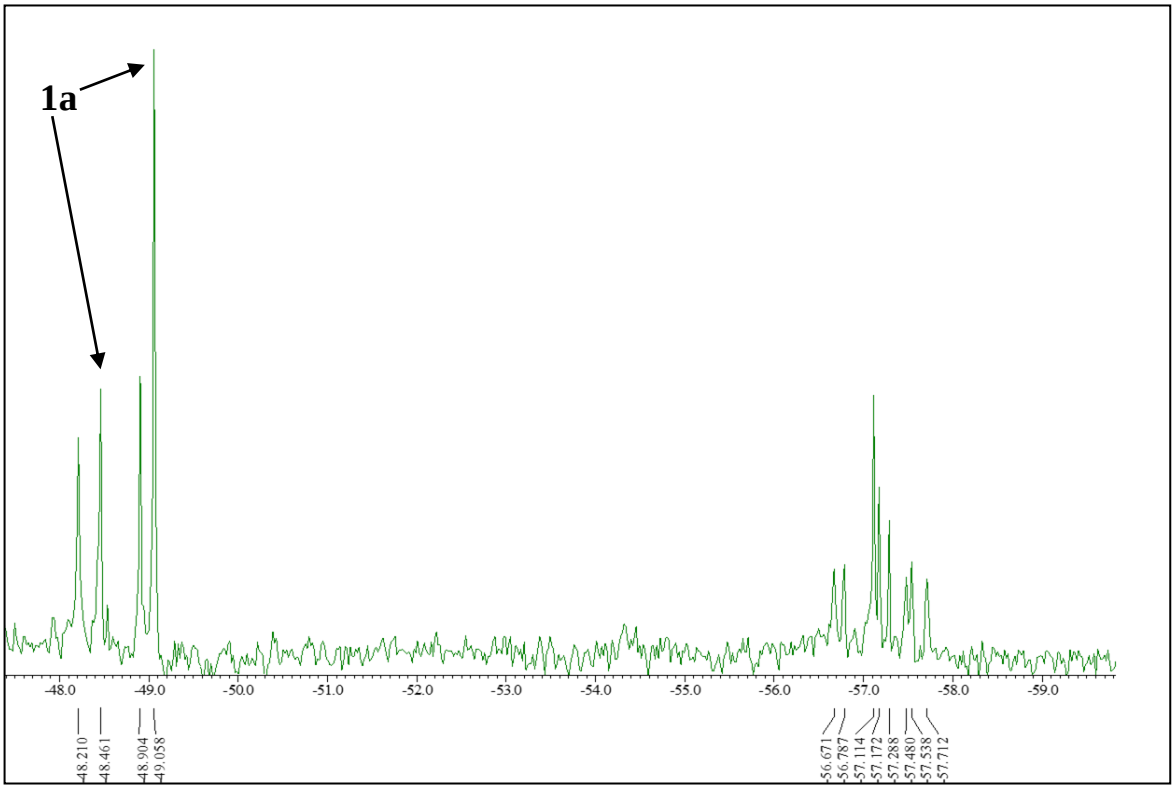

Figure 1. ^{29}Si NMR spectrum of crude product in reaction of $EtSiCl_3$ (119.4 MHz, acetone-d_6)

There are multiple peaks in two regions around –48 to –49 ppm and –56 to –58 ppm. Our group reported isolation of all isomers of [*i*-PrSiO(OH)]$_4$ (all-*cis*, *cis*-*trans*-*cis*, *cis*-*cis*-*trans*, all-*trans*) [4]. These ^{29}Si NMR peaks are observed at –59.7 to –58.5 ppm. Therefore, the peaks of –56 to –58 ppm are ascribed to four isomers of [EtSiO(OH)]$_4$ or related oligomers. There are four peaks around –48 to –49 ppm. Two peaks of those are assigned to *cis*-*trans*-[EtSiO(OH)]$_3$. On the other hand, all-*cis*-[RSiO(OH)]$_3$ shows one peak around –48 to –49 ppm. ^{29}Si signals for dialkyldisiloxanetetoraol [*t*-BuSi(OH)$_2$]$_2$O was reported to be observed at –49.55 ppm [5]. Similarly, [EtSi(OH)$_2$]$_2$O shows one peak around –48 to –49 ppm. Therefore, it is assumed that crude product included aforementioned compounds. However, we could isolate only *cis*-*trans*-[EtSiO(OH)]$_3$ from the mixture because of good crystallinity. Notably, **1a** is unstable even in a solid state and the product was gradually transformed to insoluble solid. So far, **1a** possesses the smallest substituents in cyclotrisiloxanetriols reported.

We then tried the hydrolytic condensation of $C_5H_9SiCl_3$ with longer reaction time and higher temperature because cyclopentyl group is bulkier than ethyl groups. White solid was precipitated from the reaction solution. The solid was recrystallized from THF

and hexane to give *cis-trans*-$[C_5H_9SiO(OH)]_3$ (**1b**) in 4% yield. In ^{1}H NMR spectrum, there are two peaks for OH groups. In ^{29}Si NMR spectrum there are two peaks at –49.50 and –50.07 ppm. These data indicates *cis-trans* conformation. Compound **1b** is more stable than **1a** because cyclopentyl group is bulkier than ethyl groups. After filtration, the colorless solution was extracted by ether. The organic layer was concentrated to give crude solid. After recrystallization from THF, we also obtained $[C_5H_9Si(OH)_2]_2O$ (**2a**) in 23% yield.

Shimada and Yagihashi group synthesized *cis-trans*-$[PhSiO(OH)]_3$, from $PhSi(OH)_3$ in 10% yield [2d]. In our reaction, $EtSiCl_3$ is immediately converted to $EtSi(OH)_3$ by hydrolysis. And the reaction solution is acidic by generated hydrogen chloride, therefore the generation mechanism of **1a** and **1b** is assumed similar to that of *cis-trans*-$[PhSiO(OH)]_3$ (Scheme 3).

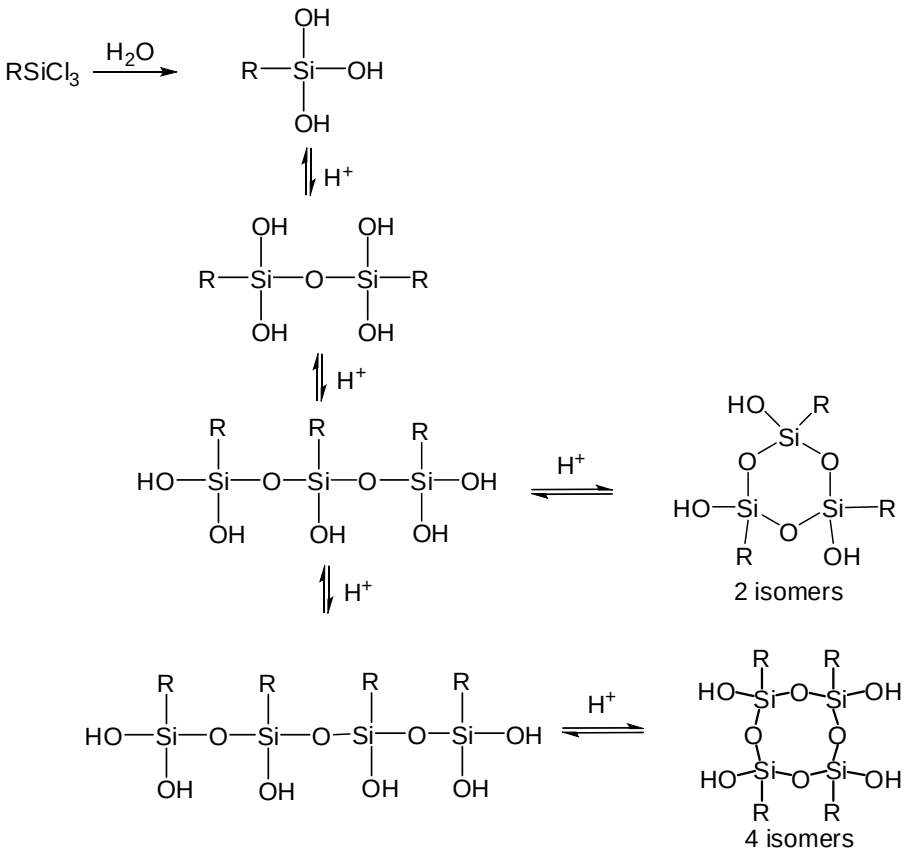

Scheme 3

In the cases with small substituents R, $RSiCl_3$ is immediately converted to $RSi(OH)_3$ by hydrolysis. $RSi(OH)_3$ is very unstable in this case, then condensation reaction of $RSi(OH)_3$ spontaneously occurred to give $[RSi(OH)_2]_2O$. Two molecules of

$[RSi(OH)_2]_2O$ further react to afford four isomers of $[RSiO(OH)]_4$. $[RSi(OH)_2]_2O$ reacts with $RSi(OH)_3$ or remained $EtSiCl_3$ to give two isomers of $[RSiO(OH)]_3$.

2.2.3 Summary

We succeeded in a facile single-step synthesis of *cis-trans* cyclotrisiloxanetriol with ethyl and cyclopentyl substituents by hydrolytic condensation of corresponding trichlorosilanes. *Cis-trans*-$[EtSiO(OH)]_3$ (**1a**) possesses the smallest substituents in cyclotrisiloxanetriols reported so far.

2.2.4 Experimental section

The Fourier transform nuclear magnetic resonance (NMR) spectra were obtained using a JEOL JNM-ECS 300 (^{1}H at 300.53 MHz, ^{13}C at 75.57 MHz, and ^{29}Si at 59.71 MHz) NMR instruments and JEOL JNM-ECA 600 (^{1}H at 600.17 MHz and ^{29}Si at 119.4 MHz) NMR instruments. Chemical shifts are reported as δ units (ppm) relative to $SiMe_4$, and residual solvents peaks were used for standards. For ^{29}Si NMR, $SiMe_4$ was used as an external standard. Electron impact mass spectrometry was performed on Shimadzu GCMS–QP2010SE/DI2010. Infrared spectra were measured using a Shimadzu FTIR-8400S spectrometer. All melting points were determined on a Yanaco micro melting point apparatus MP-J3 and are uncorrected. Elemental analyses were performed by the Center for Material Research by Instrumental Analysis (CIA), Gunma University.

Synthesis of *cis-trans*-$[EtSiO(OH)]_3$ (**1a**)

Solution of $EtSiCl_3$ (5.8 g, 35 mmol) and acetone (33 mL) was added dropwise into vigorously stirred cold water (400 mL) for 1 h at 0 ℃. Then, the reaction mixture was stirred for 1 h at 0 ℃ and poured into another flask. About 125 g of NaCl (for making saturated solution) and 100 mL ether were added into the flask. Organic layer was extracted with ether 3 times. The combined organic phase was washed with saturated aqueous $NaHCO_3$ solution and brine. The organic phase was dried over anhydrous sodium sulfate and concentrated. The crude product was washed by $CHCl_3$ to afford **1a** as white solid (0.14 g, 0.52 mmol, 4%).

Spectral data for **1**: ^{1}H NMR (600.17 MHz, acetone-d_6) δ 0.54–0.59 (m, 6H), 0.99 (t, J = 7.8 Hz, 9H), 5.71 (br s, 2H), 5.74 (br s, 1H) ppm. ^{13}C NMR (75.57 MHz, acetone-d_6) δ 5.19, 5.24, 6.33, 6.45 ppm. ^{29}Si NMR (59.71 MHz, acetone-d_6) δ –48.43, –49.06 ppm. DIMS (EI, 70eV) m/z (%) 241 ($[M–Et]^+$,100) ,141 ($[M–Et–H_2O]^+$, 47). IR (KBr) 700, 779, 881, 1038, 1254, 2881, 2961, 3215 cm^{-1}.

Synthesis of *cis-trans*-$[C_5H_9SiO(OH)]_3$ (**1b**) and $[C_5H_9Si(OH)_2]_2O$ (**2**)

Solution of $C_5H_9SiCl_3$ (7.2 g, 35 mmol) and acetone (33 mL) was added dropwise into vigorously stirred cold water (400 mL) for 1 h at 0 ℃. Then, the reaction mixture was stirred for 14 h at 0 ℃ to 20 ℃. White solid was precipitated from the solution. The supernatant liquid solution was removed by decantation, and white solid was collected. The solid was recrystallized from THF / hexane to give **1b** as white solid in (0.18 g, 0.46 mmol 4 %). The decanted solution was poured into another flask. 125 g of NaCl and ether were added into the mixture. Organic layer was extracted with ether more than 3 times. The combined organic phase was washed with saturated aqueous $NaHCO_3$ solution and brine. The organic phase was dried over anhydrous sodium sulfate and concentrated. The solid was recrystallized from THF to give **2a** as white solid in (1.1 g, 4.0 mmol, 23 %).

Spectral data for **1b**: m.p. 178–180 ℃. ^{1}H NMR (300.53 MHz, acetone-d_6) δ 0.89–1.05 (*m*, 3H), 1.41–1.63 (*m*, 18H), 1.71–1.84 (m, 6H) 5.62 (br s, 2H), 5.68 (br s, 1H) ^{13}C NMR (75.57 MHz, acetone-d_6) δ 24.23 (CH, overlapped), 27.25 (CH_2, overlapped), 27.37 (CH_2), 27.86(CH_2), 27.93(CH_2), 28.02 (CH_2) ppm. ^{29}Si NMR (59.71 MHz, acetone-d_6) δ –49.50, –50.07 ppm. DIMS (EI, 70eV) *m*/z (%) 321 ($[M–C_5H_9]^+$,100) , 253 ($[M–(C_5H_9)_2+H]^+$, 38), 67 (66). IR (KBr) 876, 1032, 2341, 2359, 2868, 2951, 3312 cm^{-1}.

Spectral data for **2a**: m.p. 183–187 ℃ (decomp.). ^{1}H NMR (300.53 MHz, acetone-d_6) δ 0.87–0.96 (m, 2H), 1.38–1.63 (m, 12H), 1.70–1.84 (m, 4H), 4.94 (br, 4H) ppm. ^{13}C NMR (75.57 MHz, methanol-d_4) δ 25.05(CH), 27.92(CH_2), 28.62(CH_2) ppm. ^{29}Si NMR (59.71 MHz, methanol-d_4) δ –49.32 ppm. DIMS (EI, 70eV) *m*/z (%) 209 ($[M–C_5H_9]^+$,87) ,141 ($[M–(C_5H_9)_2+H]^+$, 100). IR (KBr) 842, 899, 1105, 2864, 2949, 3126 cm^{-1}. Anal. Calcd for $C_{10}H_{22}Si_2O_5$:C, 43.13; H, 7.96; Found C, 42.88; H,7.87 %.

2.2.5 References

[1] M. Unno, A. Suto, T. Matsumoto, *Russ. Chem. Rev.*, **2013**, *82*, 289.

[2a] R. Murugavel, P. Bottcher, A. Voigt, M. G. Walawalkar, H. W. Roesky, E. Parisini, M. Teichert, M. Noltemeyer, *Chem. Commun.*, **1996**, 2417.

[2b] C. Ackerhans, H. W. Roesky, Th. Labahn, J. Magull, *Organometallics*, **2002**, *21*, 3671.

[2c] M. Yoshizawa, T. Kusukawa, M. Fujita, K. Yamaguchi, *J. Am. Chem. Soc.*, **2000**, *122*, 6311.

[2d] F. Yagihashi, M. Igarashi, Y. Nakajima, W. Ando, K. Sato, Y. Yumoto, C. Matsui, S. Shimada, *Organometallics*, **2014**, *33*, 6278.

[2e] T. Kusukawa, M. Yoshizawa, M. Fujita, *Angew. Chem. Int. Ed.*, **2001**, *40* 1879.

[2f] M. Yoshizawa, T. Kusukawa, M. Fujita, S. Sakamoto, K. Yamaguchi, *J. Am. Chem. Soc.*, **2001**, *123*, 10454.
[2g] M. Unno, T. Tanaka, H. Matsumoto, *J. Organomet. Chem.*, **2003**, *686*, 175.
[2h] M. Unno, Y. Kishimoto, H. Matsumoto, *Organometallics*, **2004**, *23*, 6221.
[3] In this thesis part 2, chapter 1.
[4] M. Unno, Y. Kawaguchi, Y. Kishimoto, H. Matsumoto, *J. Am. Chem. Soc.*, **2005,** *127*, 2256.
[5] P. P. Pescarmona, J. C. Van der waal, T. Maschmeyer, *Chem. Eur. J.*, **2004**, *10*, 1657.

2.2.6 Supporting information

1. Spectral data

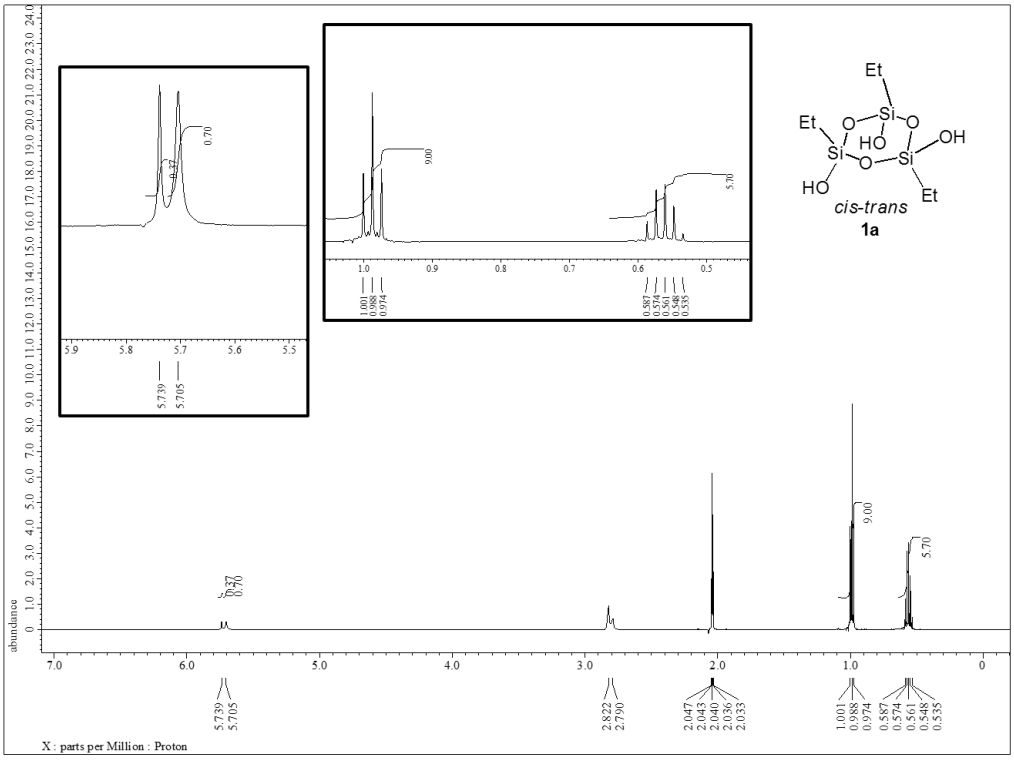

Figure 1. ^{1}H NMR spectrum of **1a** (600.17 MHz, acetone-d_6)

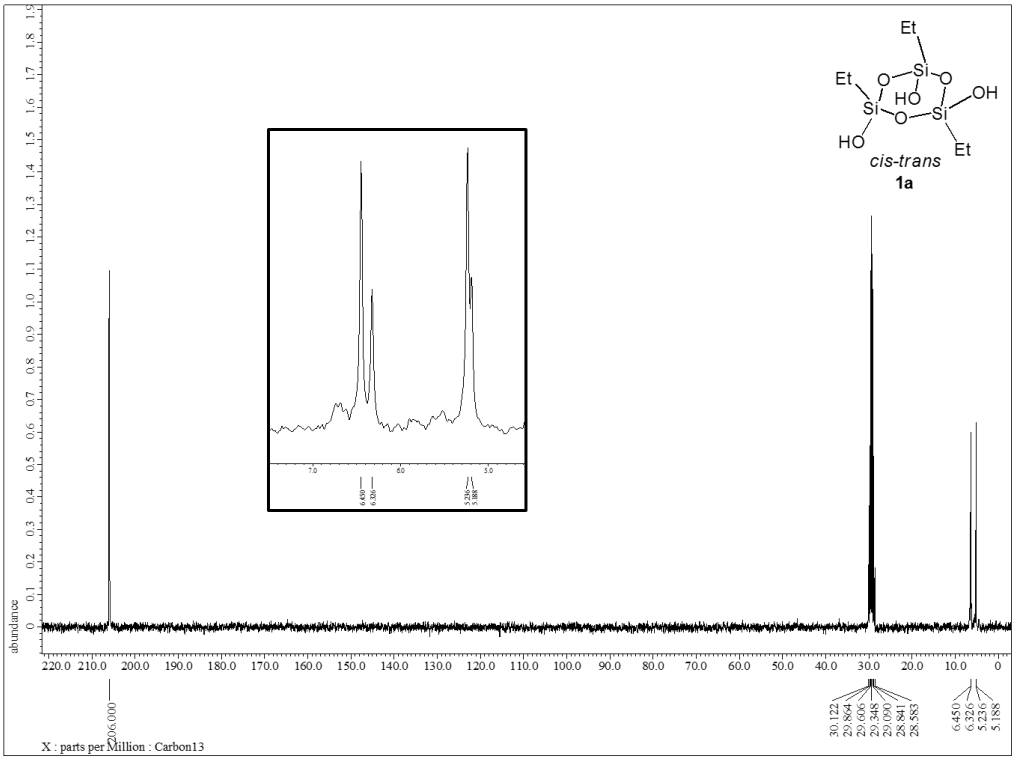

Figure 2. ^{13}C NMR spectrum of **1a** (75.57 MHz, acetone-d_6)

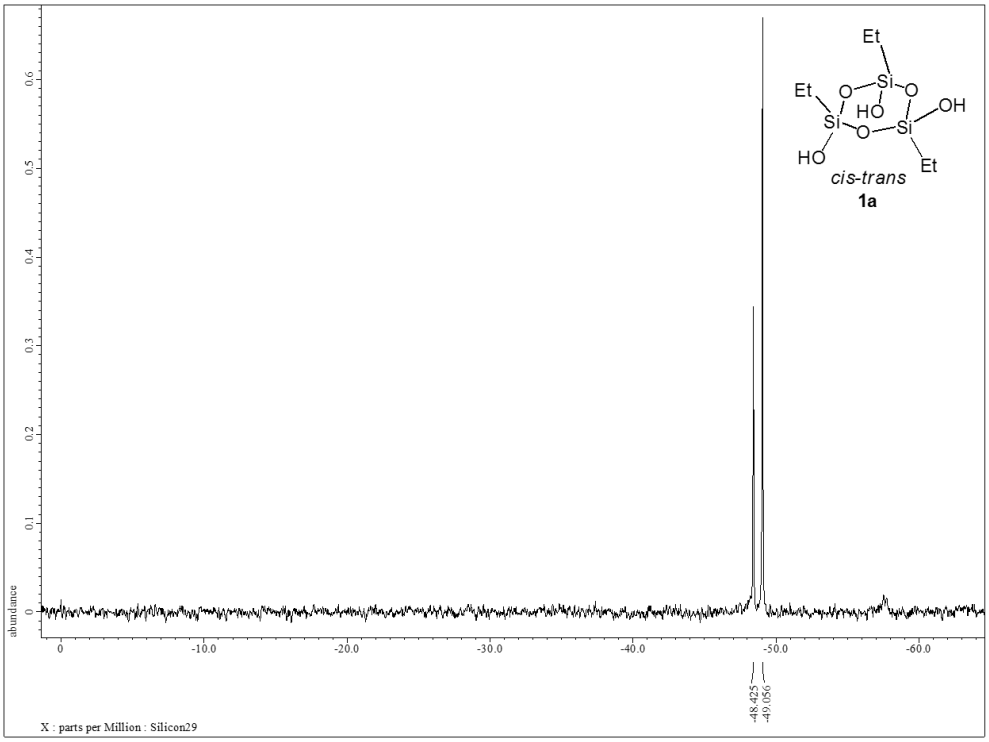

Figure 3. ^{29}Si NMR spectrum of **1a** (59.71 MHz, acetone-d_6)

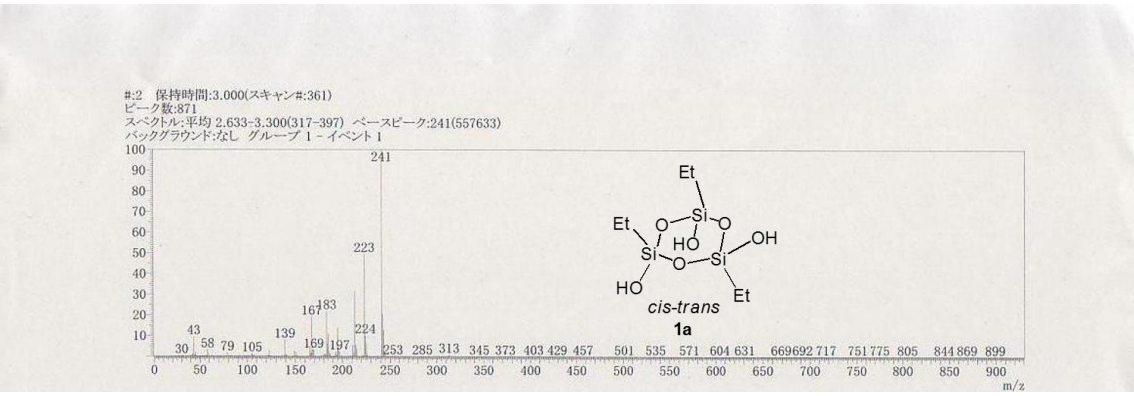

Figure 4. DIMS (EI, 70 eV) spectrum of **1a**

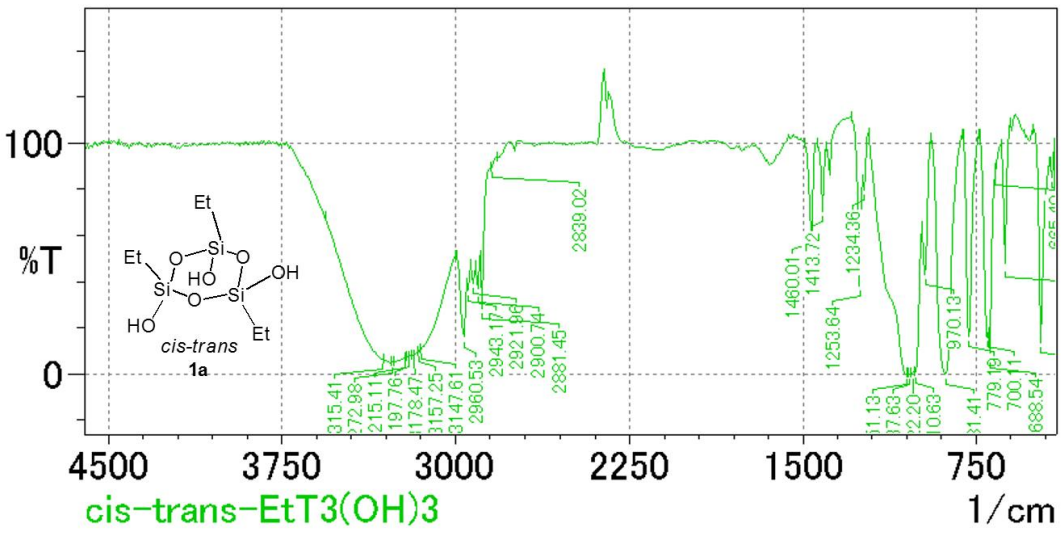

Figure 5. IR (KBr) spectrum of **1a**

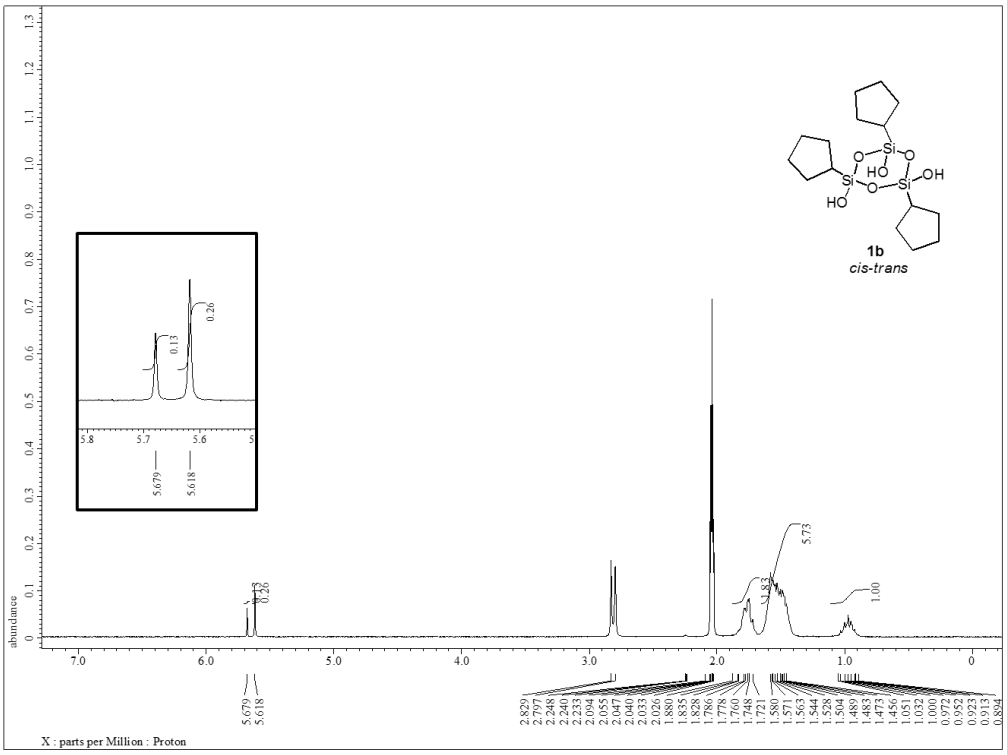

Figure 6. ^{1}H NMR spectrum of **1b** (300.53 MHz, acetone-d_6)

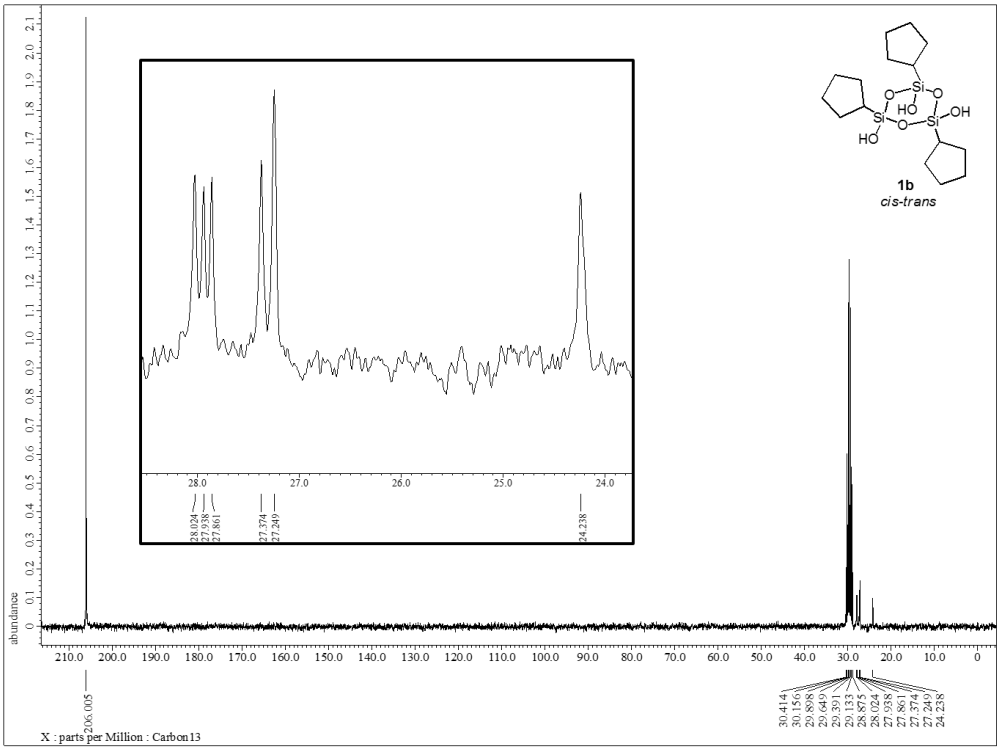

Figure 7. ^{13}C NMR spectrum of **1b** (75.57 MHz, acetone-d_6)

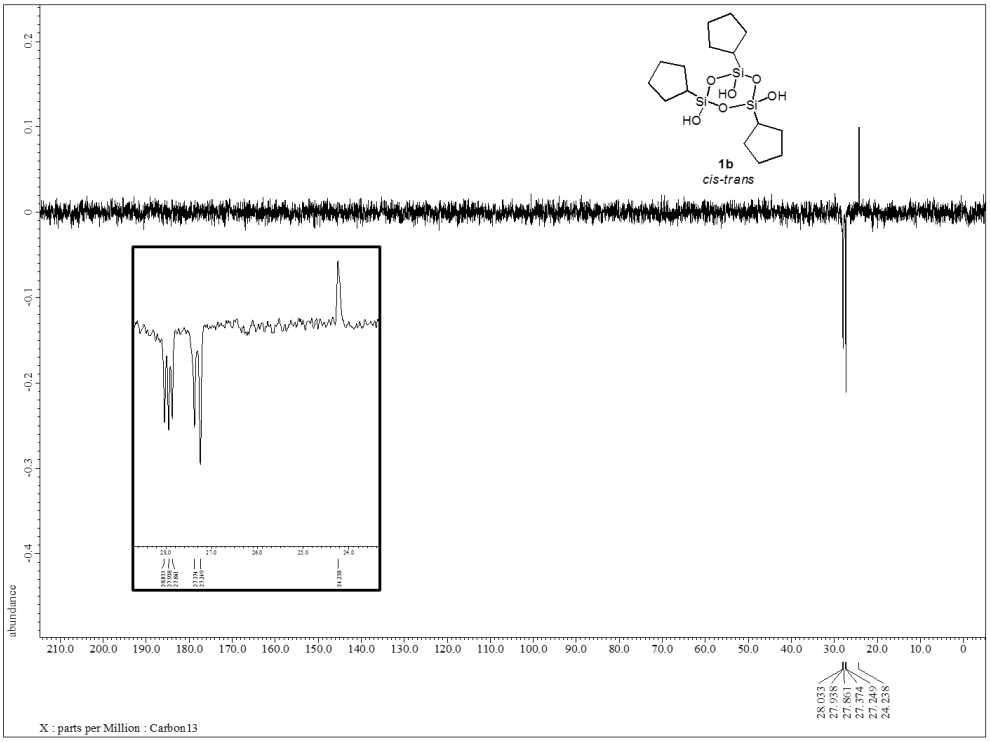

Figure 8. ^{13}C NMR (dept 135) spectrum of **1b** (75.57 MHz, acetone-d_6)

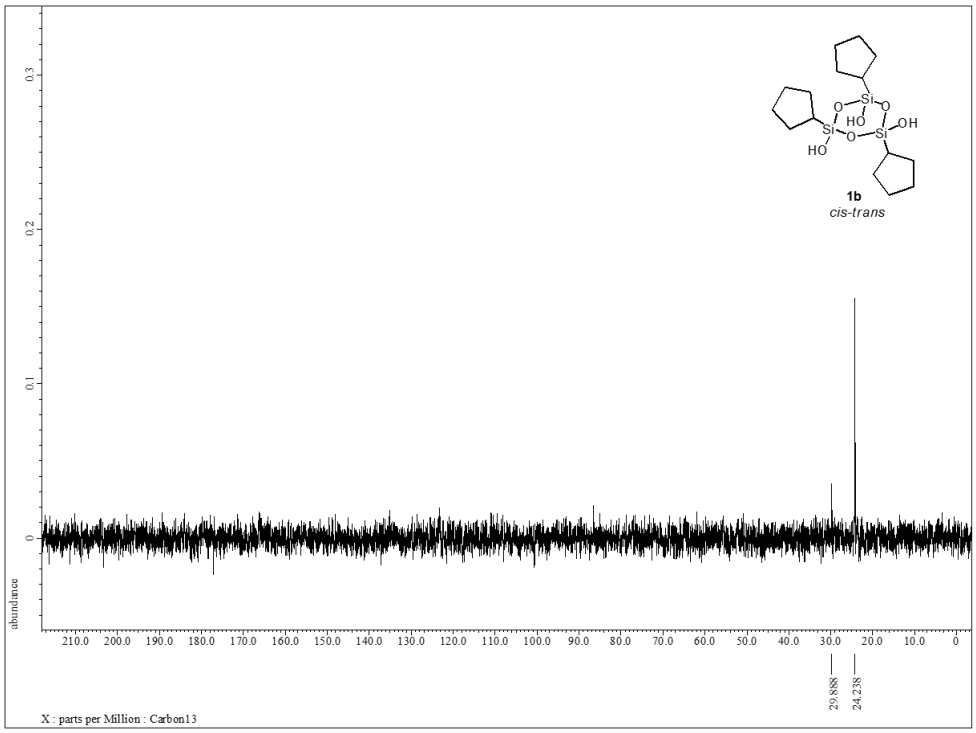

Figure 9. ^{13}C NMR (dept 90) spectrum of **1b** (75.57 MHz, acetone-d_6)

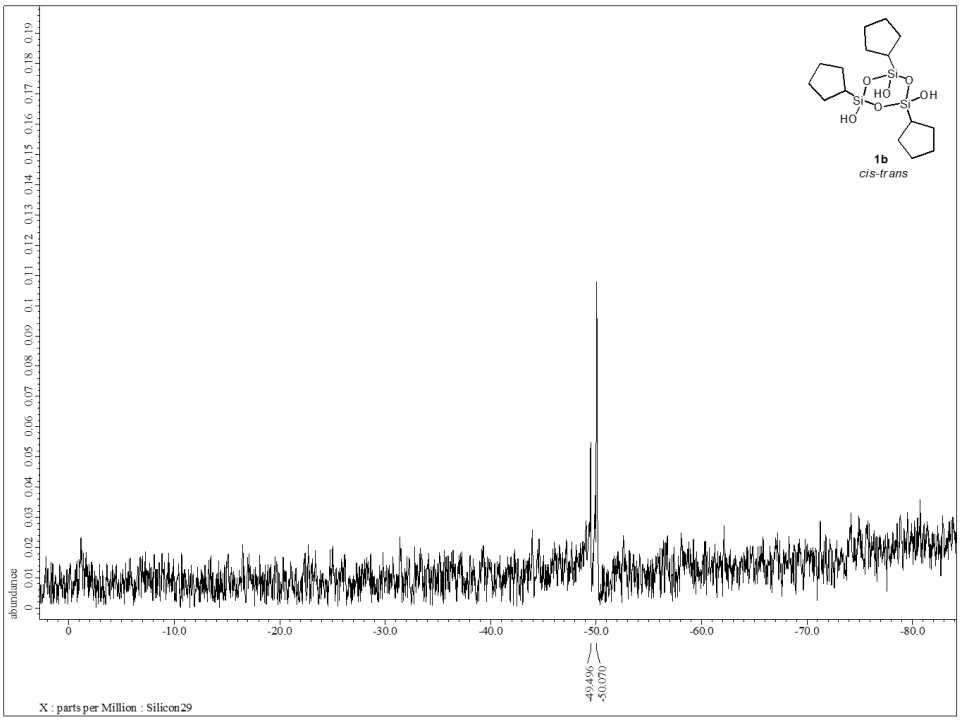

Figure 10. ^{29}Si NMR spectrum of **1b** (59.71 MHz, acetone-d_6)

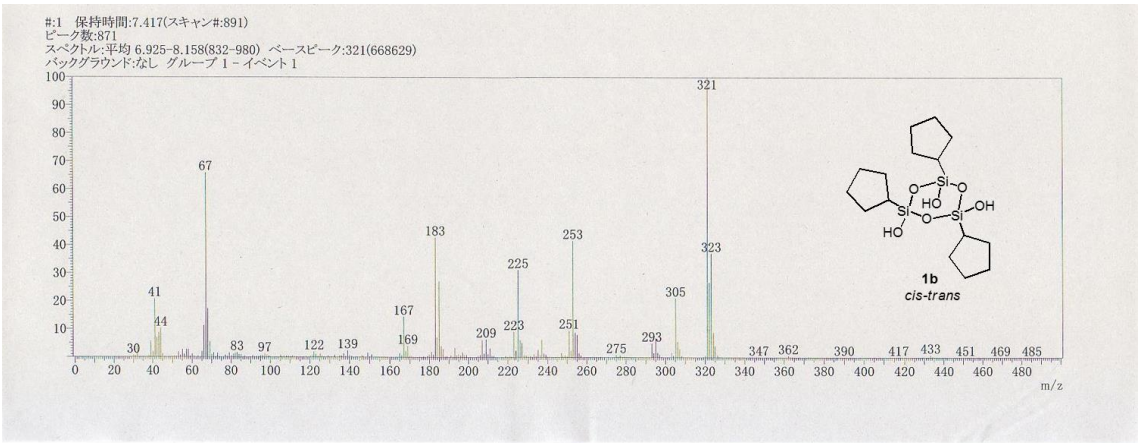

Figure 11. DIMS (EI, 70 eV) spectrum of **1b**

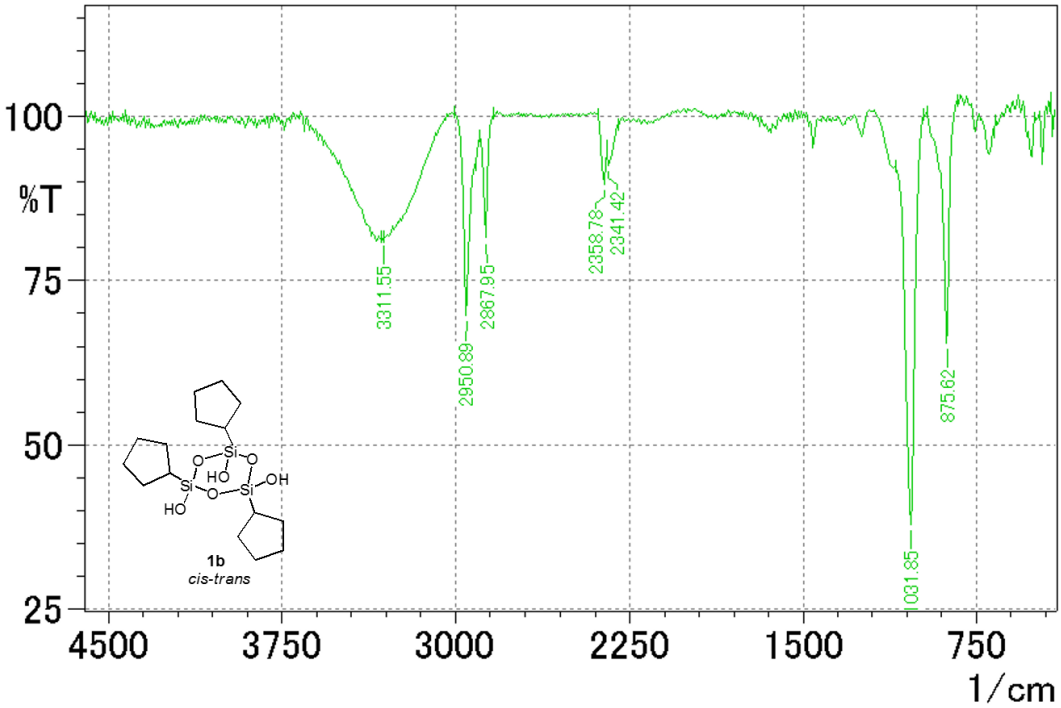

Figure S1. IR (KBr) spectrum of **1b**

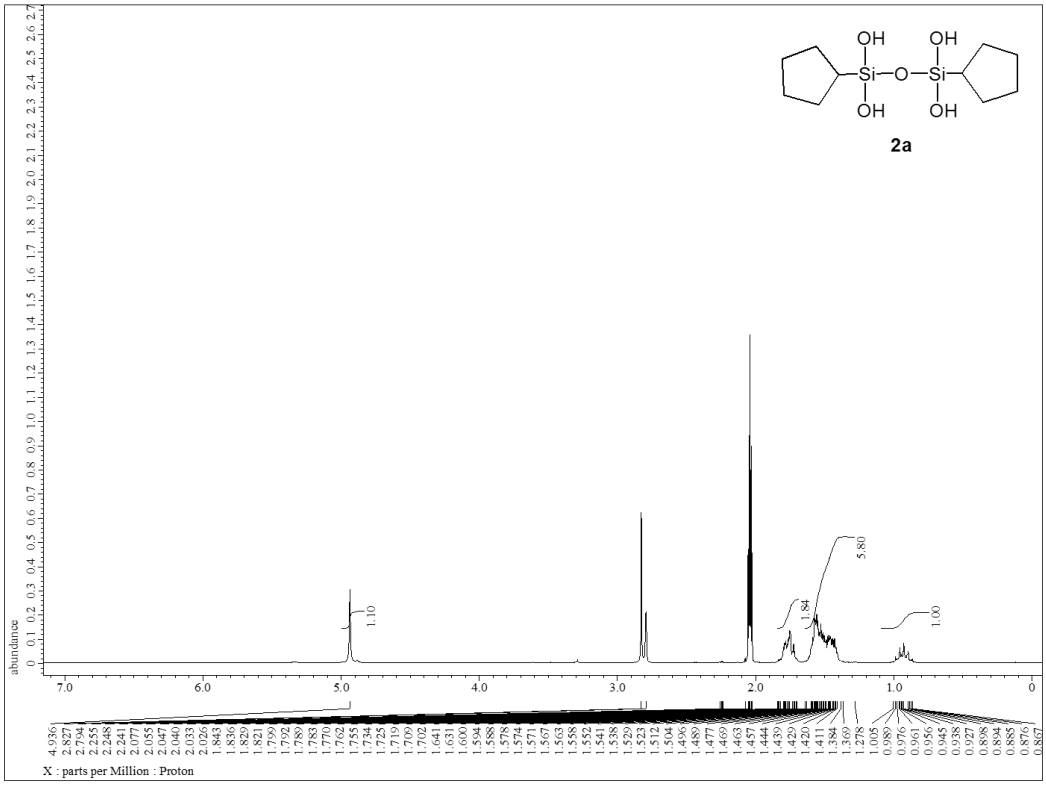

Figure 13. ^{1}H NMR spectrum of **2a** (300.53 MHz, acetone-d_6)

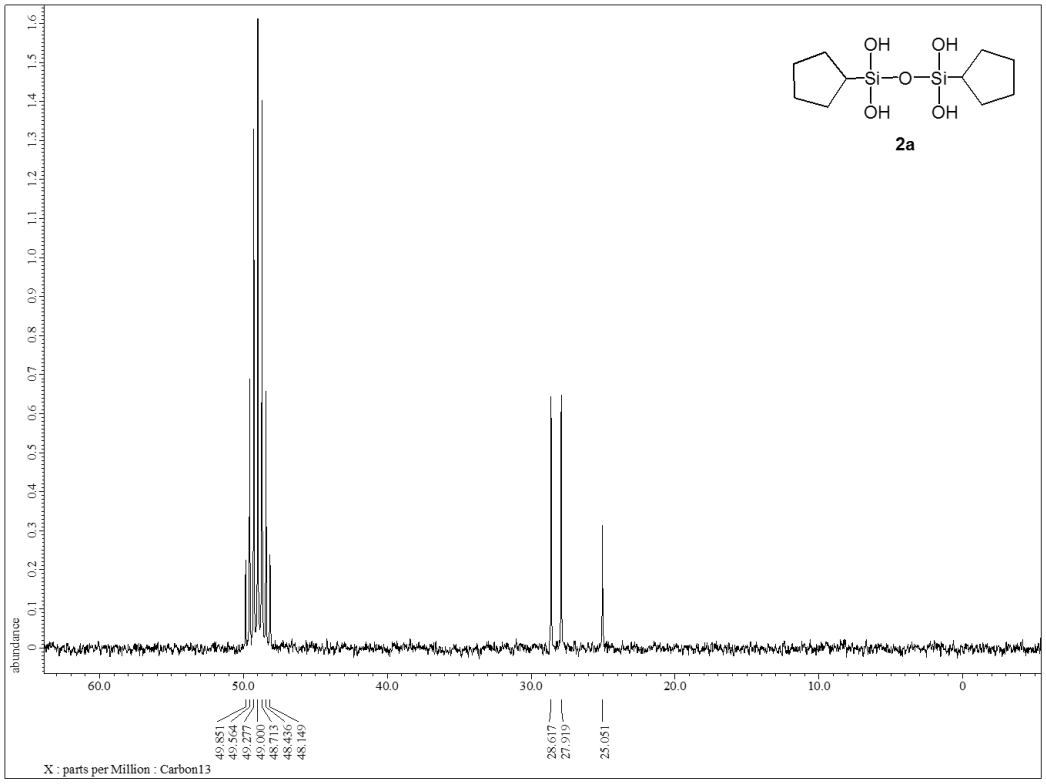

Figure 14. ^{13}C NMR spectrum of **2a** (75.57 MHz, methanol-d_4)

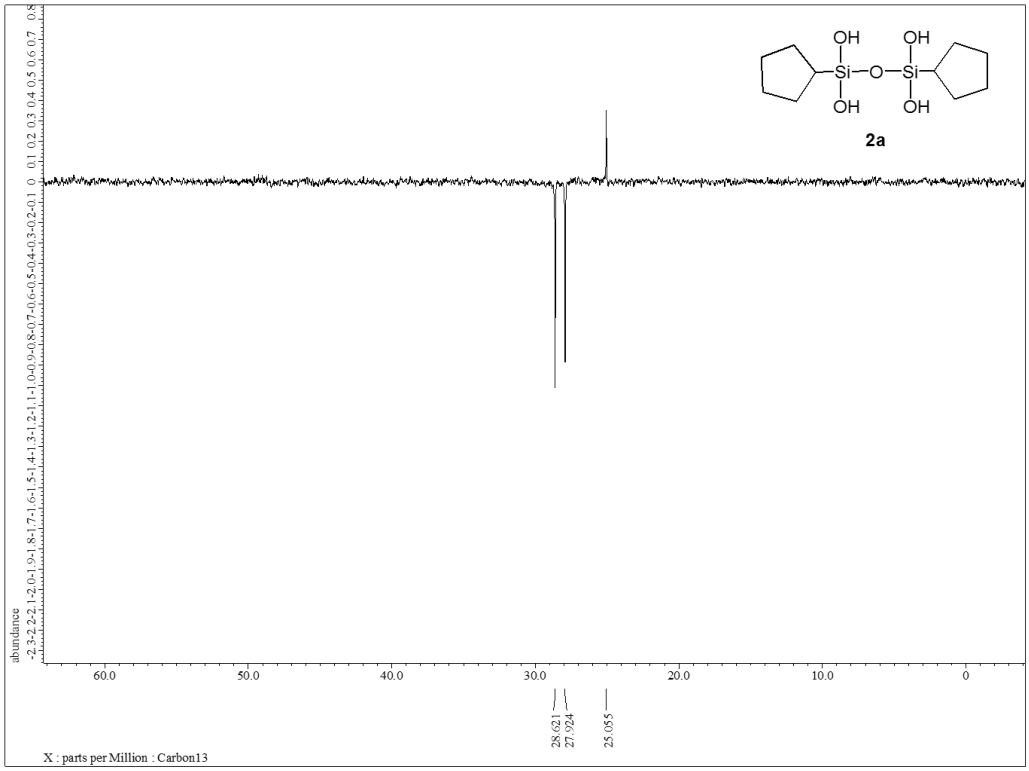

Figure 15. ^{13}C NMR (dept 135) spectrum of **2a** (75.57 MHz, methanol-d_4)

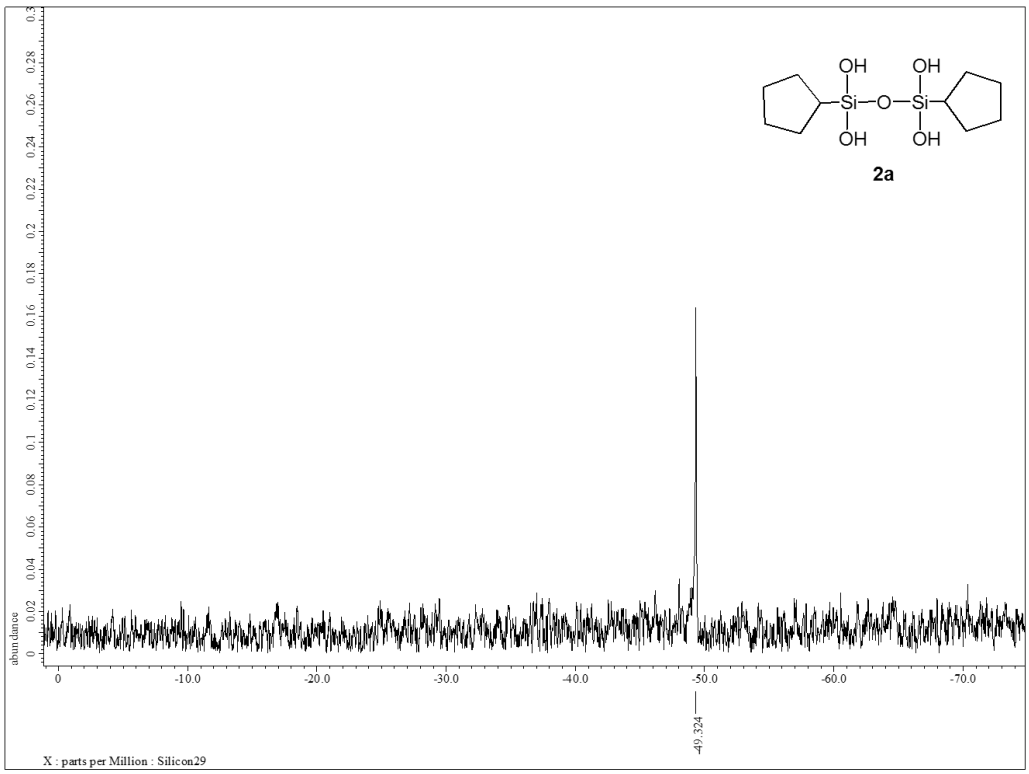

Figure 16. ^{29}Si NMR spectrum of **2a** (59.71 MHz, methanol-d_4)

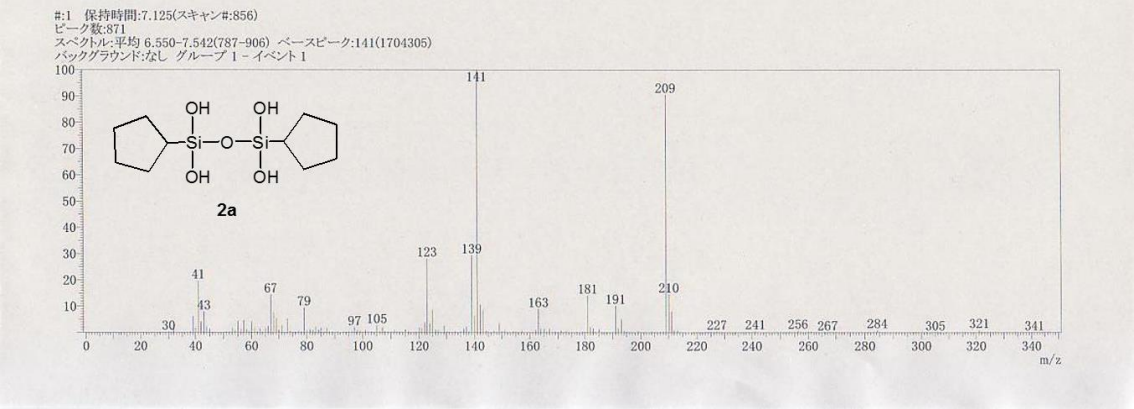

Figure 17. DIMS (EI, 70 eV) spectrum of **2a**

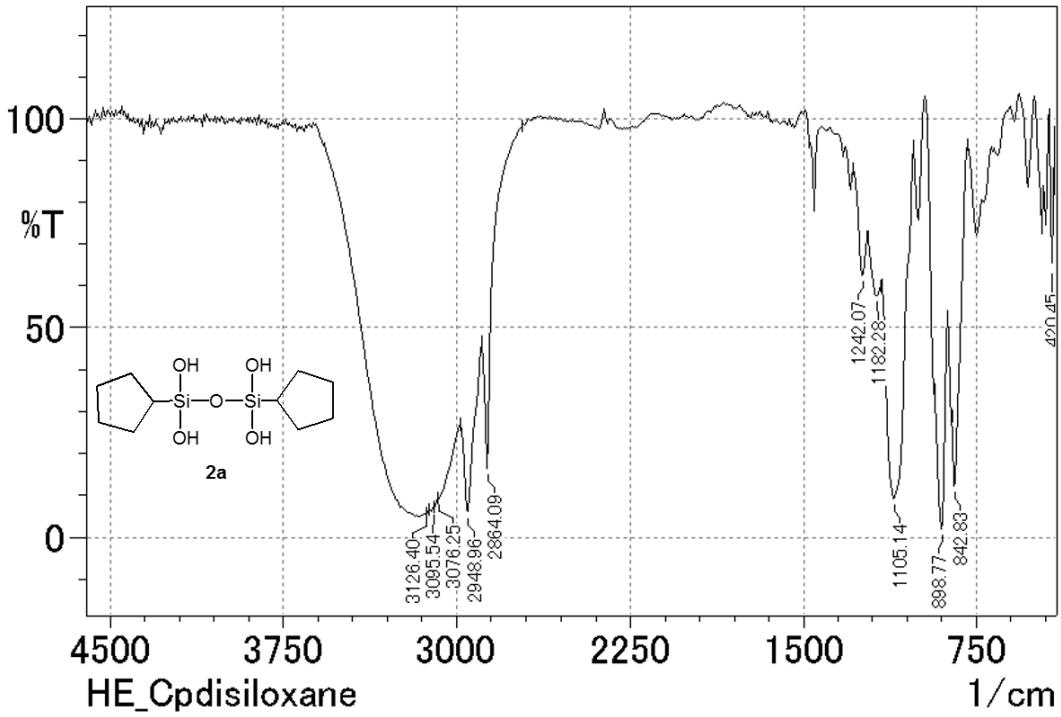

Figure 18. IR (KBr) spectrum of **2a**

Chapter 3: Facile synthesis of stereoisomers of cyclic silanols

2.3.1 Introduction

Our group has synthesized a series of silsesquioxanes including oligocyclic laddersiloxanes (ladder-type silsesquioxanes with defined structure) and cage silsesquioxanes, and determined the structures [1]. These well-defined structures significantly affect the physical properties. For example our ladder polysilsesquioxane possesses high regularity than any of the previously reported ladder-like silsesquioxanes directly synthesized from $RSiCl_3$ [2]. And the 5% weight loss temperatures of the previously reported ladder-like polymers are all well below that of our ladder polysilsesquioxane.

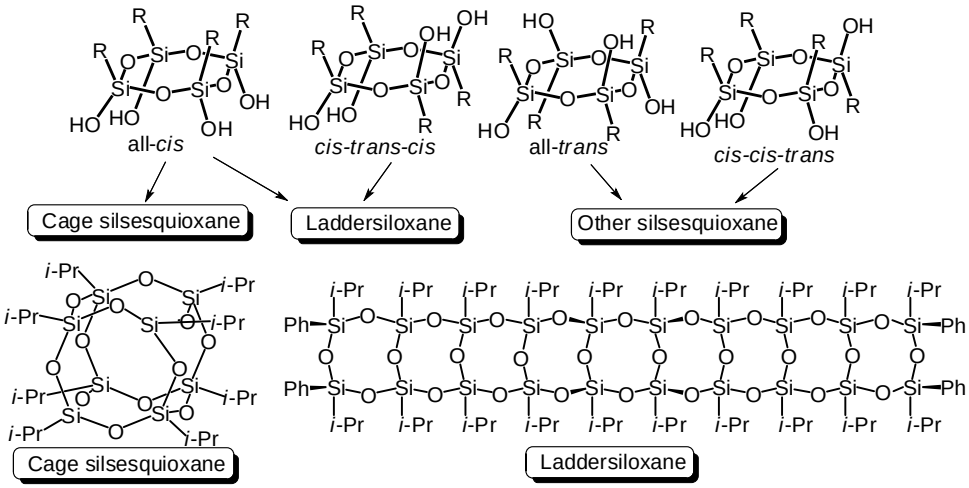

Scheme 1

In the syntheses of these silsesquioxanes with well-defined structures, all-*cis*-cyclotetrasiloxanetetraols ($[RSiO(OH)]_4$) have been served as the key starting compounds. In cyclotetrasiloxanetetraols, there are four stereoisomers (all-*cis*, *cis-trans-cis*, all-*trans*, *cis-cis-trans*) as shown in Scheme 1. Each isomer is also a potential precursor of various well-defined siloxanes. As shown in our previous reports, all-*cis*-cyclotetrasiloxanetetraol can be utilized as starting materials for cage silsesquioxanes and *syn*-type laddersiloxane [3a,b]. In this isomer, four substituents can be arranged in the same direction and that gives rise to several interesting properties [4a,b,c]. *Cis-trans-cis*-cyclotetrasiloxanetetraols can be utilized as precursors of *anti*-type laddersiloxanes that can be formed as infinite length polymers [2]. In all-*trans*, and *cis-cis-trans*-cyclotetrasiloxanetetraols are promising as the building blocks of cage molecules or surface treating agents.

There are several known synthetic methods of cyclotetrasiloxanetetraols [4a, 5a-j].

In most cases, all-*cis* isomer is the single product when hydrolytic condensation of $RSiCl_3$ was employed [5a–d]. The first synthesis of $[RSiO(OH)]_4$ with phenyl [5a] or cyclohexyl [5b] substituents were reported by Brown's group in early 60s. More recently, Feher's group and our group reported the synthesis and structure determination of all-*cis*-$[RSiO(OH)]_4$ from $RSiCl_3$ (R = Ph [5c], *i*-Pr [5d], *i*-Bu (in part2, chapter 1)) in acetone-water solution.

We also reported hydrolytic condensation of $(i\text{-}PrSiCl_2)_2O$ to give all-*cis*-$[i\text{-}PrSiO(OH)]_4$ [5d]. Russian group and Kawakami group reported synthesis of all-*cis*- cyclotetorasiloxanolate which can be converted to all-*cis*-cyclotetrasiloxanetetraols [5e,f,g].

For other stereoisomers, there are several methods of synthesis of *cis-trans-cis*, *cis-cis-trans*, and all-*trans* isomers [4a, 5f-j]. Our group has synthesized four stereoisomers of tetraisopropylcyclotetrasiloxanetetraols ($[i\text{-}PrSiO(OH)]_4$) (all-*cis*, *cis-trans-cis*, *cis-cis-trans*, all-*trans* isomers) [5h]. The compounds were synthesized by multi-step reaction. As the first step, $i\text{-}PrPhD_4$ ($[i\text{-}PrPhSiO]_4$) was synthesized by dehydrative coupling from $i\text{-}PrPhSiCl_2$, and four stereoisomers were separated by recycle-type HPLC. Then each isomer was converted to $[i\text{-}PrSiOCl]_4$ by dephenylchlorination and following hydrolysis to afford cyclic silanols. By this method, four isomers of cyclotetrasiloxanetetraol were isolated and structures were determined by X-ray crystallographic analysis. *Cis-trans-cis*-$[MeSiO(OH)]_4$ was synthesized from all-*cis*-$[MeSiO(K)]_4$ with excess amount of acetic acid then fractional crystallization [5g]. *Cis-trans-cis*-$[MeSiO(OH)]_4$ is also synthesized from oxidation reaction of four isomers mixture of $[MeSiO(H)]_4$ then fractional crystallization [5i].

Another report regarding the isolation of isomers is stereoisomerization of cyclotetrasiloxanetetraols. Russian group reported the isomerization of all-*cis*-$[PhSiO(OH)]_4$ with catalytic amount of organochlorosilane (Me_3SiCl, Me_2SiCl_2), HCl or CH_3COOH to afford an equilibrium mixture of all isomers [5j]. This is first report of stereoisomerization. Other Russian group reported synthesis of mixture of all isomers by pH-controlled hydrolytic condensation of $PhSiCl_3$ [4a]. And these isomers were isolated by recrystallization. Kawakami's group also reported that isomerization of all-*cis*-$[PhSiO(OH)]_4$ to give other three stereoisomers (*cis-trans-cis*, *cis-cis-trans*, all-*trans*) in hydrochloric acid at room temperature for 10 minutes [5f] (Scheme 2).

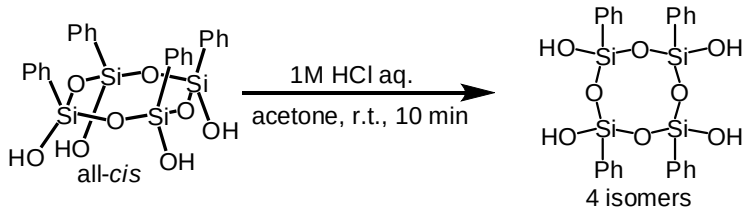

Scheme 2

In order to obtain large amount of isomers, stereoisomerization is more preferable because of less reaction steps, availability of aryl substituents, and no need for the handling of chlorosilanes. However, only isomerization from phenyl-substituted cyclic silanols is known to date, and optimized reaction condition and reaction mechanism are not available so far. If stereoisomerization can be commonly applied to other cyclotetrasiloxanetetraols, we can easily obtain isomers of cyclotetrasiloxanetetraols starting from readily available all-*cis* one. It is also beneficial to know the reaction condition and mechanism, because we can avoid unnecessary isomerization in the reactions using cyclotetrasiloxanetetraol.

In this chapter, we describe elucidated stereoisomerization of alkyl-substituted cyclotetrasiloxanetetraol, which is commonly applied to those with other substituents. And we proposed the reaction mechanism of isomerization.

2.3.2 Results and discussion

Part 1: Synthesis and determined structure of all-*cis*-[*i*-BuSiO(OH)]$_4$ (**1a**)

Overall yield of all-*cis*-[RSiO(OH)]$_4$ were not very high except phenyl compound [5a-g]. In several synthetic reports need multi-step reaction. Then it is difficult to obtain enough amounts of cyclic silanols capable of serving as starting material. On the other hand, we dramatically improved the yield of all-*cis*-[*i*-BuSiO(OH)]$_4$ (**1a**) than the reported yield (34%) [5f]. Therefore, we decided to use **1a** for a starting compound for isomerization. The reaction scheme is shown in Scheme 3.

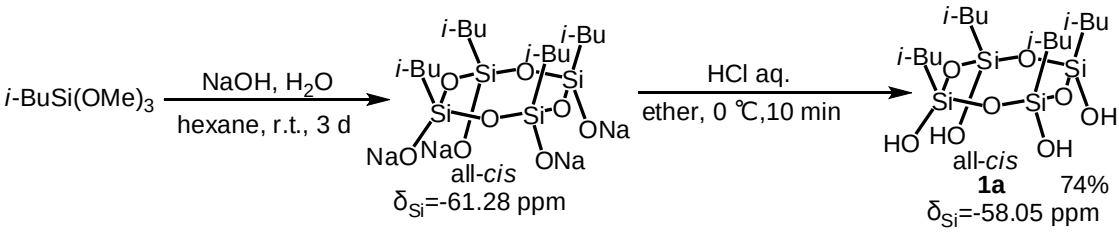

Scheme 3

The reaction procedure is almost same as literature [5f]. ^{29}Si NMR of sodium salt was shown only one peak at –61.28 ppm in DMSO-d_6. The sodium salt react with diluted hydrochloric acid in ether at 0 ℃ in 10 min to give **1a** (74%). ^{29}Si NMR of **1a** showed only one peak at –58.14 ppm in $CDCl_3$ and –58.05 ppm in acetone-d_6. Kawakami's group reported ^{29}Si signal of **1a** was observed at –57.9 ppm [5f] that is very close to our observed value. Thus **1a** seems to be all-*cis* structure. However, NMR chemical shift cannot assure all-*cis* structure. Because *cis*-*cis*-*trans* and all-*trans* structures also show only one peak in ^{29}Si NMR. Therefore we tried to determine the structure by X-ray crystallographic analysis. However, unfortunately we could not obtained suitable crystal of **1a** for X-ray analysis.

By the way, in several cases, we determine the stereostructure of cyclic silanols by a transformation to tricyclic laddersiloxanes [6a,b,c]. Therefore, to determine the structure of **1a**, we tried the reaction of **1a** with dichlorodiphenylsilane to give *syn*-type laddersiloxane (**2a**). The reaction scheme is shown in Scheme 4.

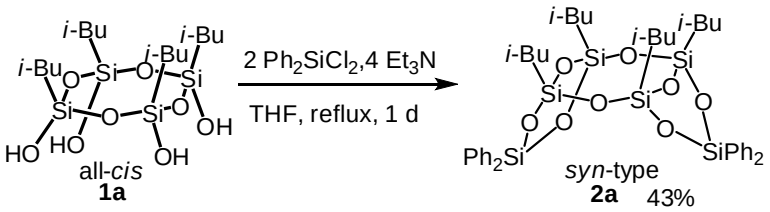

Scheme 4

In THF, **1a** was treated with dichlorodiphenylsilane in the presence of triethylamine as HCl scavenger to give target *syn*-laddersiloxane (**2a**) in 43% yield after the crystallization of the crude product. Compound **2a** was further recrystallized from toluene by slow evaporation at room temperature to give crystals suitable for X-ray analysis. Molecular structure is shown in Figure 1. Because the product **2a** has *syn*-type structure, **1a** is all-*cis* conformation.

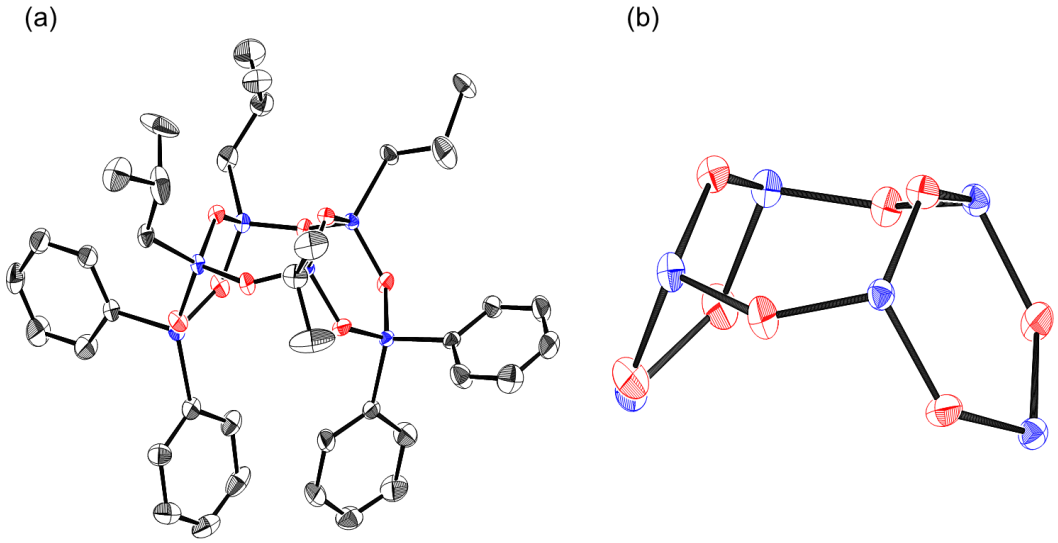

Figure 1. Crystal structure of **2a**. Black: Carbon; Blue: Silicon; Red: Oxygen. Thermal ellipsoids are shown in 50% probability level. (a) All H atoms have been omitted for clarity. (b) All H and C atoms have been omitted for clarity.

Part 2: Stereoisomerization of **1a** (identification and isolation of each isomer)

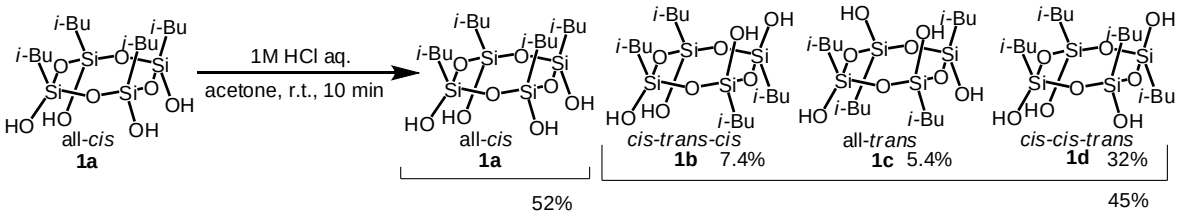

Scheme 5

By analogous process in the literature [5f], isomerization of **1a** was carried out in acetone with 1 M hydrochloric acid at room temperature for 10 min (Scheme 5). The crude product showed 4 peaks (−58.01, −58.31, −58.53, −58.66 ppm) in ^{29}Si NMR in acetone-d_6. Reported ^{29}Si NMR chemical shifts of four isomers of $[RSiO(OH)]_4$ are summarized in Table 1. Four stereoisomers of $[i\text{-PrSiO(OH)}]_4$ showed ^{29}Si signals from –58.5 to –59.7 ppm in DMSO-d_6 [5d, 5h], and four stereoisomers of $[PhSiO(OH)]_4$ showed ^{29}Si signals from –69.7 to –70.5 ppm [4a, 5f]. From these report, stereoisomer of $[RSiO(OH)]_4$ show ^{29}Si signals in a range about 1 ppm. In addition, in

^{1}H NMR, we observed six pair of doublet peaks having same coupling constant that were attributed to CH_2 of isobutyl group. This fact also indicates that stereoisomerization was occurred in **1a**. If there are four isomers and do not overlap signals, there should be 6 peaks. But there were only four peaks including **1a** because of overlap of stereoisomers as shown in the literatures.

Table 1. ^{29}Si NMR of $[RSiO(OH)]_4$ (ppm)

R	Solvent	all-*cis*	*cis-trans-cis*	all-*trans*	*cis-cis-trans*
Ph [5f]	not listed	–69.7	–70.4	–70.5	–70.5, –70.2, –70.1
Ph [4a]	acetone-d_6	–69.79	–69.94	–70.52	–70.08, –70.12, –70.31
i-Pr [5d, h]	DMSO-d_6	–59.7	–59.0	–58.5	–59.7, –59.1, –59.0
i-Bu (This work)	acetone-d_6	–58.05	–58.66	–58.12	–58.33, –58.51

Compound **1a** was soluble in $CHCl_3$. However, crude product was almost insoluble in $CHCl_3$. Soluble in $CHCl_3$ portion were analyzed by ^{29}Si NMR and ^{1}H NMR to identify **1a**. Insoluble in $CHCl_3$ portion was also analyzed by ^{29}Si NMR and ^{1}H NMR (Figure 2 and Figure 3). The ^{29}Si spectrum showed 4 peaks (−58.10, −58.31, −58.53, −58.66 ppm) in acetone-d_6 (Figure 2). In ^{1}H NMR, we observed five pairs of doublet peaks having same coupling constant that were attributed to CH_2 of isobutyl group and five singlet peaks attributed to OH group (Figure 3). And results of elemental analysis and DIMS of insoluble in $CHCl_3$ portion was also attributed to $[i\text{-BuSiO(OH)}]_4$. These facts indicate insoluble in $CHCl_3$ portion is mixture of **1b**, **1c**, and **1d** except **1a**. Therefore mixture of **1a-1d** can very easily divide into **1a** and mixture of **1b**, **1c**, **1d** by using chloroform. In this reaction, recovered **1a** was 52%. Conversion rate into mixture of **1b**, **1c**, and **1d** was 45%.

Kawakami's group reported the separation of stereoisomers of $[PhSiO(OH)]_4$ by re-precipitation and column chromatography [5f]. We observed 3 spots (component A: R_f = 0.13, component B: R_f = 0.38, component C: R_f = 0.61) in TLC (SiO_2, $CHCl_3$: AcOEt = 3:1) by using *p*-anisaldehyde as an indicator. We separated each component by flash chromatography with gradient conditions (SiO_2, $CHCl_3$: AcOEt = 3:1) using Biotage Isolera with ELSD detector. Each component was analyzed by ^{29}Si NMR and showed at –58.33, –58.51 ppm (component A : R_f = 0.13), –58.66 ppm (component B : R_f = 0.38), –58.12 ppm (component C : R_f = 0.61). In ^{1}H NMR of the component A (R_f = 0.13), we observed three pair of doublet peaks having same coupling constant that were attributed to CH_2 of isobutyl group. ^{1}H NMR of the component B (R_f = 0.38), we observed two pair of doublet peaks having same coupling constant which were

attributed to CH_3 of isobutyl group. ^{13}C NMR of the component B (R_f = 0.38), we observed two peaks which were attributed to CH_3 of isobutyl group. These facts indicate that *cis-trans-cis* isomer (**1b**) was component B (R_f = 0.38), *cis-cis-trans* isomer (**1d**) was component A (R_f = 0.13), and, all-*trans* isomer (**1c**) was component C (R_f = 0.61). This result coincide reported $[PhSiO(OH)]_4$ of R_f = 0.05 (all-*cis*), 0.29 (*cis-cis-trans*), 0.53 (*cis-trans-cis*), 0.64 (all-*trans*) (toluene : ether = 1 : 1) [5f]. In ^1H NMR spectrum of mixture of **1b**, **1c**, and **1d**, observed five OH peaks were attributed to each isomer (Figure 3). Each ratio was calculated based on OH integration of ^1H NMR. (**1b**: 7.4%, **1c**: 5.4%, **1d**: 32%).

Compound **1b** was recrystallized from ethyl acetate and $CHCl_3$ by slow evaporation at room temperature to give crystals suitable for X-ray analysis. The molecular structure is shown in Figures 4. The structure of *cis-trans-cis* was confirmed.

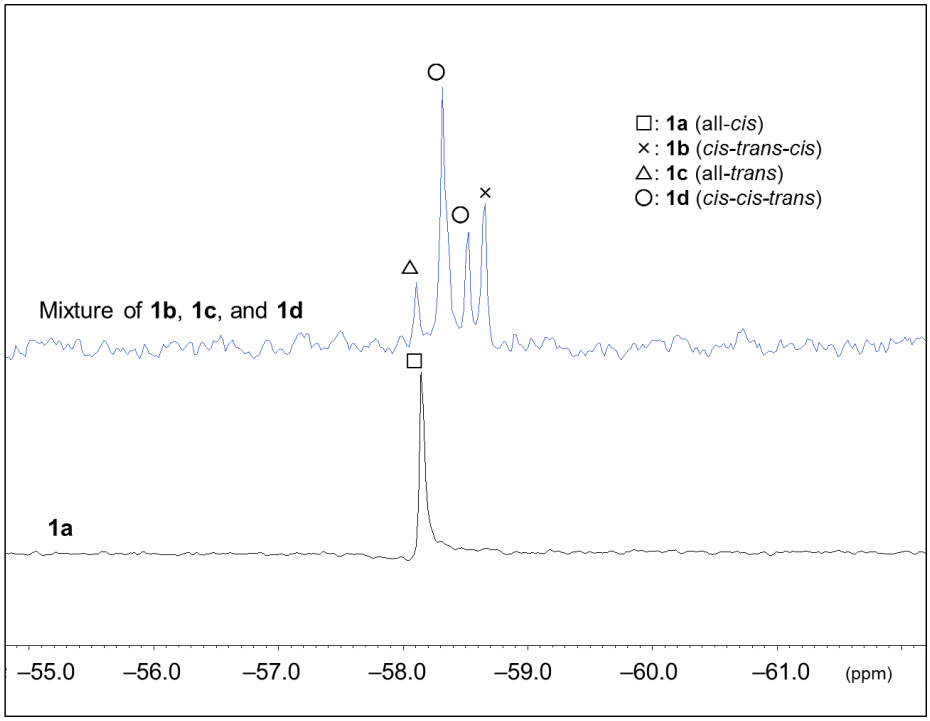

Figure 2. ^{29}Si NMR spectra of **1a**, and mixture of **1b**, **1c**, and **1d** (59.7 MHz, acetone-d_6).

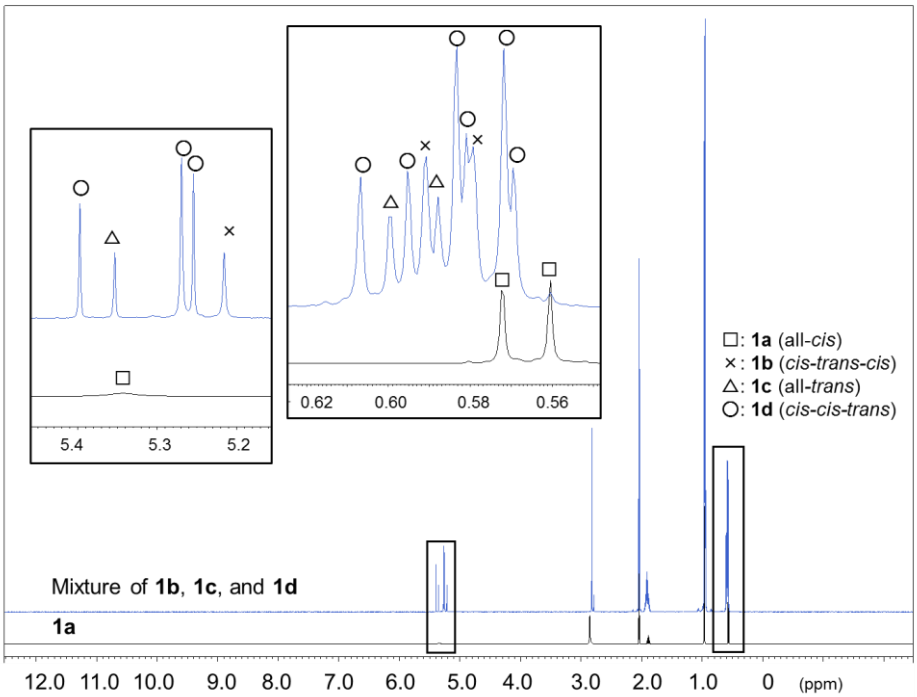

Figure 3. ^{1}H NMR spectra of **1a**, and mixture of **1b**, **1c**, and **1d** (600.17 MHz, acetone-d_6).

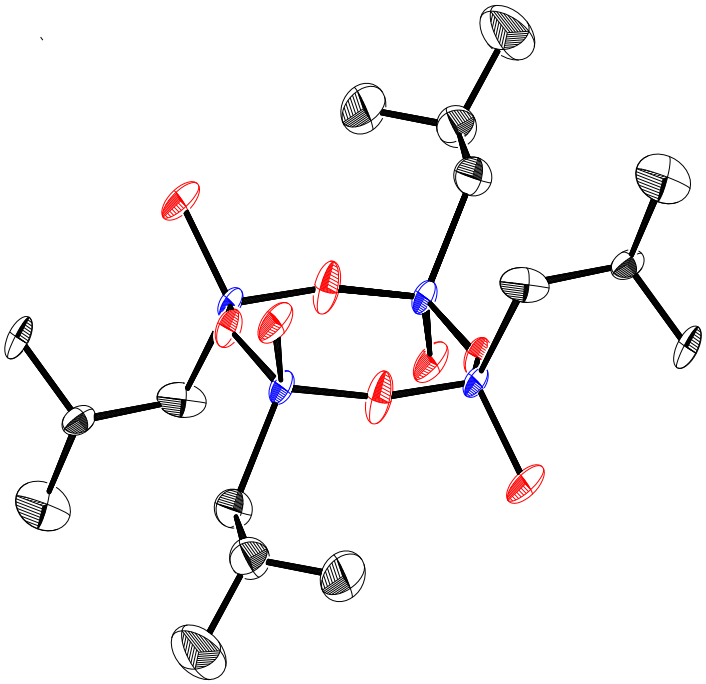

Figure 4. Crystal structure of **1b**. Black: Carbon; Blue: Silicon; Red: Oxygen. Thermal ellipsoids are shown in 50% probability level.

Part 3: Synthesis of *anti*-type laddersiloxane (**2a**)

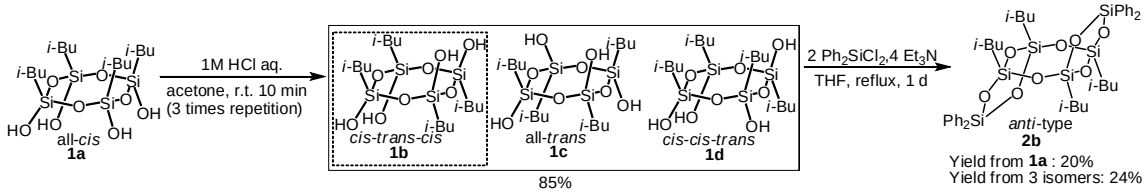

Scheme 6

Within all-*trans*, *cis-trans-cis*, *cis-cis-trans* compounds, only *cis-trans-cis* isomer (**1b**) can be converted to *anti*-laddersiloxane (**2b**). Therefore, we tried to transfer to *anti*-laddersiloxane (**2b**) (Scheme 6). Firstly, **1a** was converted to a mixture of **1b**, **1c**, and **1d**. Compound **1a**, which was soluble in $CHCl_3$ portion, was salvaged and reused. Then the stereoisomerization was repeated 3 times. Total conversion rate of mixture of **1b**, **1c**, and **1d** was 85%. In THF, the mixture of **1b**, **1c**, and **1d** was treated with dichlorodiphenylsilane in the presence of triethylamine as HCl scavenger. Then, water was added to reaction mixture to quench the reaction. After work up, crude solid was obtained. The solid was filtrated, and washed by methanol to give **2b** (24%, overall yield from **1a**: 20%). Compound **2a** could not be obtained in this reaction. Compound **2b** was further recrystallized from $CHCl_3$ and hexane by slow evaporation at room temperature to give crystals suitable for X-ray analysis. The molecular structure is shown in Figures 5. Compound **2b** have *anti*-structure. This synthetic method of **2b** is very useful in order to selectively synthesize *anti*-type laddersiloxane exclusively.

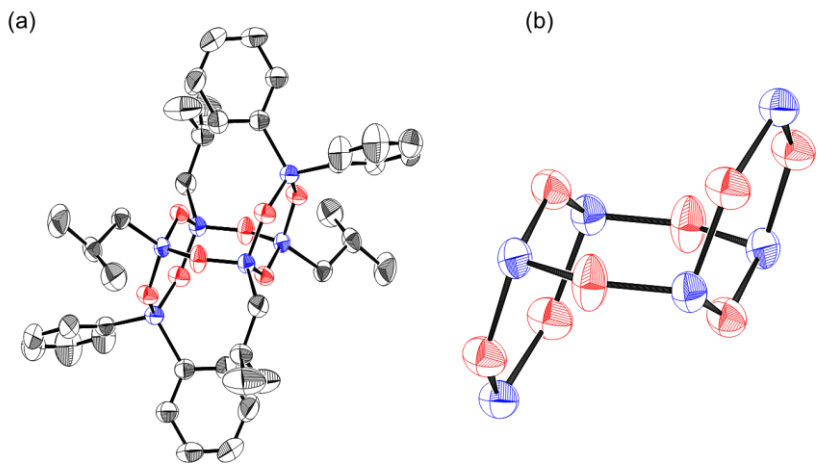

Figure 5. Crystal structure of **2b**. Black: Carbon; Blue: Silicon; Red: Oxygen. Thermal ellipsoids are shown in the 50% probability level. (a) All H atoms have been omitted for clarity. (b) All H and C atoms have been omitted for clarity.

Part 4: Elucidation of suitable reaction condition

We tried to elucidate suitable condition of the reaction (Scheme 7).

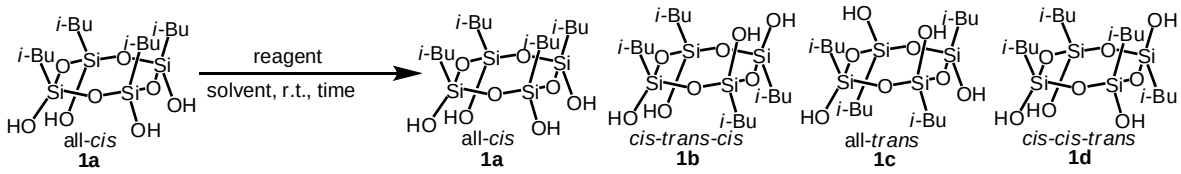

Scheme 7

Firstly, we investigated relationship with conversion rate and reaction time. The result is shown in Table 2. Conversion rates were almost same value (≒40%) until 3 h. However after 12 h, conversion rate dropped to a lower value. In addition, after 12 h, condensation or decomposition product peak were observed (−54 to −55 ppm and −62 ppm) in ^{29}Si NMR. Therefore, the reason of decreasing conversion rate is attributed to the side reactions.

Table 2. Relationship with reaction time and yield (Reagent: 1M HCl aq. Solvent: acetone)

Entry	Time	Conv. (%)	Yield (%)*			Recov. of **1a** / %
			1b	**1c**	**1d**	
1	10 min	45	7.4	5.4	32	52
2	30 min	45	7.3	4.6	33	52
3	1 h	43	6.9	4.6	32	57
4	3 h	41	6.1	4.7	31	53
5	12 h	36	4.4	3.4	28	Complex mixture
6	2 day	27	4.2	2.7	20	Complex mixture**
7	3 day	25	3.6	2.7	19	Complex mixture**

* Yield based on OH integration ratio of ^{1}H NMR. ****1a**, decomposed products peaks (e.g. disiloxane) and condensed products peaks were observed in ^{29}Si NMR.

Secondly, we investigated relationship with conversion rate and acid or base concentration. The result is shown in Table 3. Conversion rates were almost same value (≒40%) in entries 1, 2, 3, and 5. Stereoisomerization occurred by catalytic amount of acid (0.32 eq. or 0.032 eq.). However, conversion rate was only 1% by using 0.01 M HCl aq. in 10 min and we could not obtain compound **1c**. Stereoisomerization rate depends on the acid concentration. Condensation or decomposition product peaks were

observed by using 1 M NaOH in 10 min. And we could not obtain a mixture of **1b**, **1c**, and **1d** by using 1 M NaOH in 10 min.

Table 3. Relationship with acid or base and yield (Solvent: acetone)

Entry	Reagent	Eq.	Time	Conv. (%)	Yield (%)*			Recov. of **1a** / %
					1b	**1c**	**1d**	
1	5 M HCl aq.	16	10 min	39	5.8	3.8	29	55
2	1 M HCl aq.	3.2	10 min	45	7.4	5.4	32	52
3	0.1 M HCl aq.	0.32	10 min	39	6.6	4.3	28	55
4	0.01 M HCl aq.	0.032	10 min	1	0.2	—	0.8	96
5	0.01 M HCl aq.	0.032	3 day	41	6.6	4.4	30	53
6	1 M NaOH aq.	3.2	10 min	—	—	—	—	Complex mixture**
7	0.1 M NaOH aq.	0.32	10 min	—	—	—	—	97

* Yield based on OH integration of ^{1}H NMR. **Decomposed products peaks and condensed products peaks were observed in ^{29}Si NMR.

Thirdly we investigated the relationship of conversion rate with kinds of acid. The result is shown in Table 4. Conversion rates were almost same value (≒40%) by using HCl and CF_3COOH aqueous solution. However, conversion could not be observed by using CH_3COOH in 10 min. And conversion rate is low by using H_3PO_4 in 10 min or CH_3COOH in 3 days. Therefore we think stereoisomerization also depends on acidity.

Table 4. Relationship with kind of acid and yield (Solvent: acetone)

Entry	Reagent	Eq.	pK_a	Time	Conv. (%)	Yield (%)*			Recov. of **1a** / %
						1b	**1c**	**1d**	
1	1 M HCl aq.	3.2	−3.7	10 min	45	7.4	5.4	32	52
2	1M CF_3COOH aq.	3.2	−0.3	10 min	44	6.8	4.8	32	52
3	1 M H_3PO_4 aq.	3.2	1.8	10 min	17	2.6	1.5	13	77
4	1 M CH_3COOH aq.	3.2	4.8	10 min	—	—	—	—	96
5	1 M CH_3COOH aq.	3.2	4.8	3 day	21	3.9	2.2	15	71

* Yield based on OH integration of ^{1}H NMR.

Fourthly, we investigated the relationship of conversion rate with kinds of solvents. The result is shown in Table 5. Reactions were observed in entries 1, 2, 3, 5, and 6. However, conversion could not be observed by using diethyl ether in 10 min and $CHCl_3$

in 3 days. Commonly, $CHCl_3$ and diethyl ether relatively show low miscibility in water. Therefore we think stereoisomerization depends on the solvents miscibility in water. We think reaction rate of stereoisomerization is fast for the solvents with high miscibility in water and vice versa. By the way, in entry 2, we observed methoxylated product peak in ^{1}H NMR. In addition, we could not observed stereoisomerization in no-solvent condition.

Abundance ratio of **1b, 1c**, and **1d** were almost constant (0.2 : 0.2 : 1) in part 3. And these products did not converged only one isomer.

Table 5. Relationship with solvent and yield (Reagent: 1M HCl aq.)

Entry	Solvent	Miscibility in water***	Time	Conv. (%)	Yield (%)*			Recov. of **1a** / %
					1b	**1c**	**1d**	
1	Acetone	○	10 min	45	7.4	5.4	32	52
2	MeOH	○	10 min	32	5.6	3.3	23	Complex mixture**
3	THF	○	10 min	41	6.8	4.3	30	57
4	Ether	△	10 min	—	—	—	—	99
5	Ether	△	12 h	36	5.9	4.2	26	58
6	Ether	△	3 d	43	7.5	5.3	30	50
7	$CHCl_3$	×	3 d	—	—	—	—	98
8	Non	—	3 d	—	—	—	—	97

* Yield based on OH integration of ^{1}H NMR. ****1a**, and methoxylated products peaks were observed in ^{1}H NMR., ***○: high miscibility to water, △: middle miscibility to water, ×: low miscibility to water

Finally, we investigated stereoisomerization with nucleophiles. Gunji's group reported synthesis of *cis-trans-cis*-$[MeSiO(NCO)]_4$ and its stereoisomerization with nucleophiles [7]. They performed the reaction with pyridine and HMPT: hexamethylphosphorous triamide in $CDCl_3$. We also tried stereoisomerization of **1a** with nucleophiles (HMPT, DMF: dimethyl formamide, pyridine, and acetonitrile) at room temperature in acetone-d_6 (because stereoisomerization could not occur in $CHCl_3$). However, we could not observed stereoisomerization after 10 min elapsed by ^{1}H NMR. After 10 min, we added water, however we could not observed stereoisomerization after 12 h elapsed by ^{1}H NMR.

Part 5: Elucidation of reaction mechanism

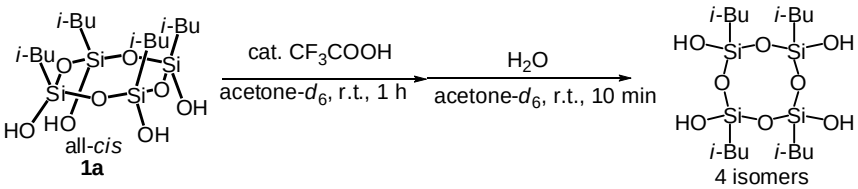

Scheme 8

We investigated whether water is necessary or not in stereoisomerization. We carried out reaction of **1a** with CF_3COOH in acetone-d_6 excluding water (Scheme 8). The reaction was traced by ^{29}Si NMR measurement. The result is shown in Figure 6. After 1 h, other isomers signals could not be observed. Then we added water and new four signals were observed. After usual workup of stereoisomerization, we measured ^{29}Si NMR to show four signals attributed to each stereoisomer. When added water, we could observe five peaks to be expected including four isomers in this solution. This result indicates that water is necessary in stereoisomerization.

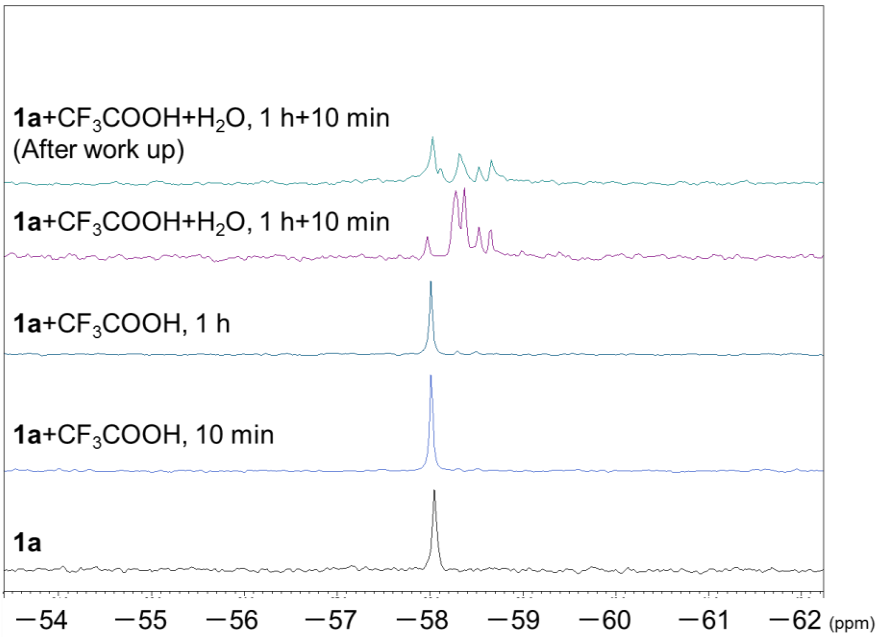

Figure 6. ^{29}Si NMR spectra of mixture of **1a**, CF_3COOH, and water (119.4 MHz, acetone-d_6, r.t.).

There are two plausible mechanisms of stereoisomerization i) siloxane bond cleavage reaction then recombination occurs, ii) substitution reaction for silicon center

without siloxane bond cleavage (Scheme 9).

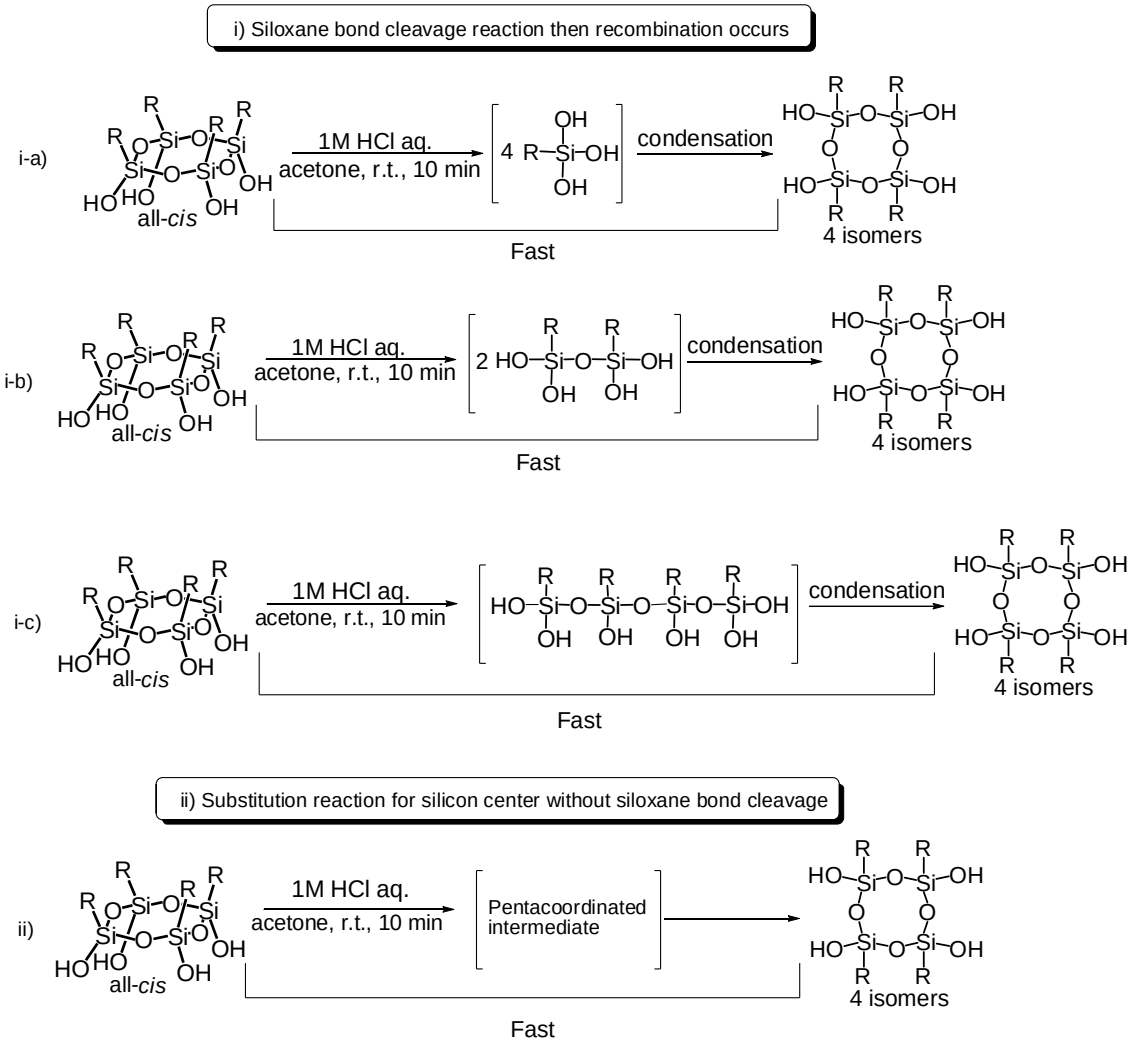

Scheme 9

Up to now, there are only two reports for stereoisomerization of all-*cis*-$[RSiO(OH)]_4$ (R = Ph, *i*-Bu). We carried out stereoisomerization of each all-*cis*-$[RSiO(OH)]_4$ (R = Ph, *i*-Bu) (Scheme 10, eq.1), eq.2)). The result is shown in Figure 6 (eq.1), eq.2)). All-*cis*-$[PhSiO(OH)]_4$ was synthesized by known procedure [5f]

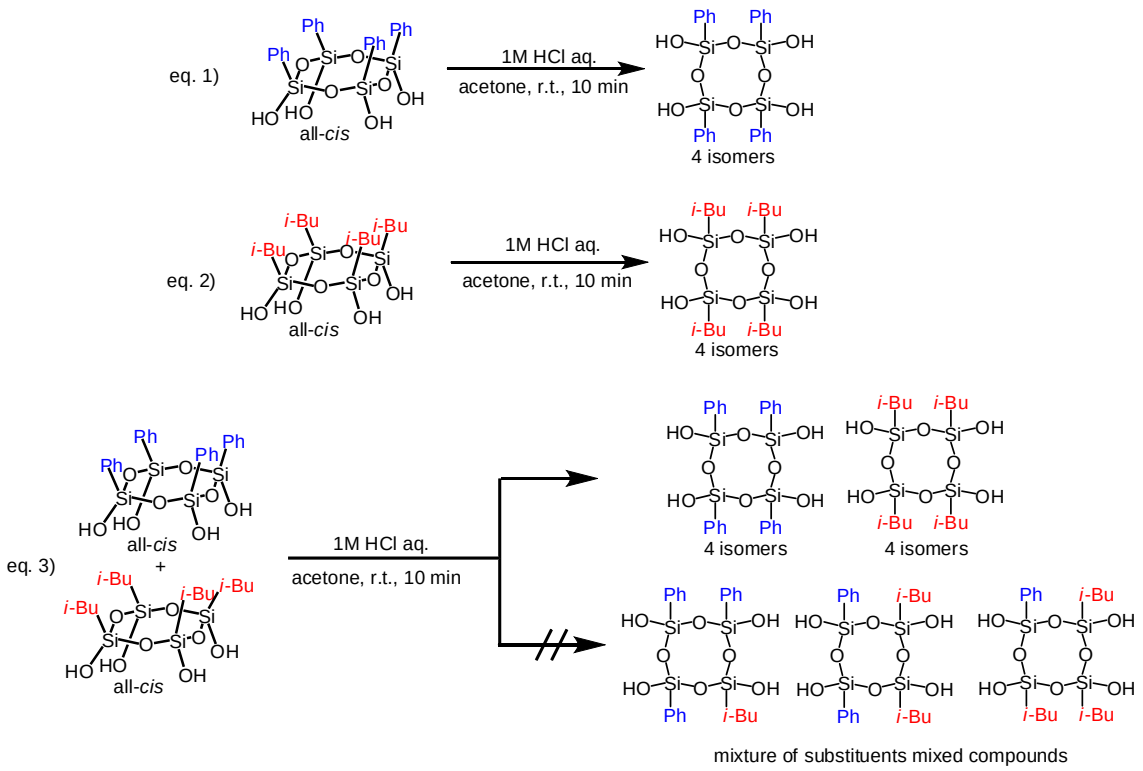

Scheme 10

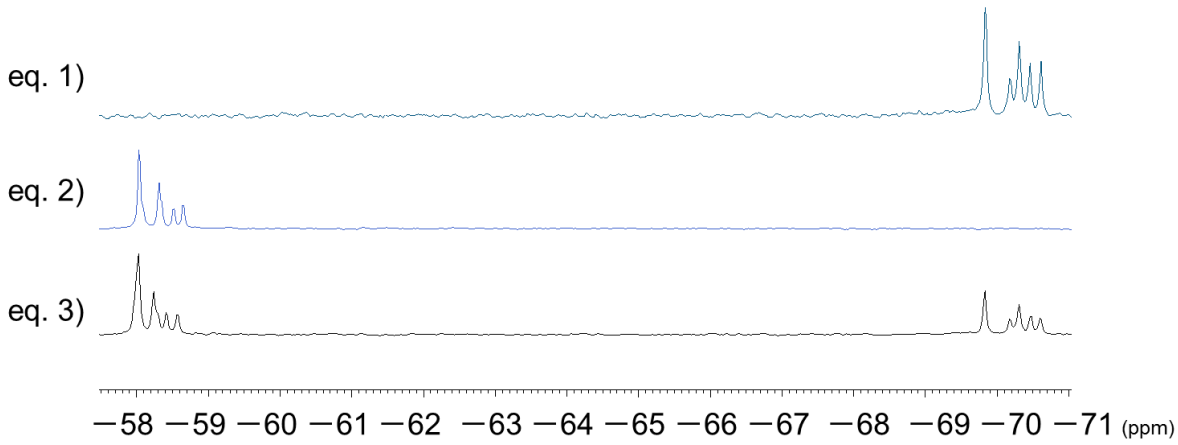

Figure 6. Summarized ^{29}Si NMR spectra of Scheme 10 procedures (59.71 MHz, acetone-d_6,).

In reaction of all-*cis*-[PhSiO(OH)]$_4$, the crude product showed 5 peaks (–69.83, –70.17, –70.31, –70.46, –70.61 ppm) attributed to 4 isomers of cyclotetrasiloxanetetraols in ^{29}Si NMR in acetone-d_6 as reported [4a, 5f]. In reaction of all-*cis*-[*i*-BuSiO(OH)]$_4$, the crude product showed 4 peaks (–58.10, –58.31, –58.53, –58.66 ppm) attributed to 4 isomers of cyclotetrasiloxanetetraols in ^{29}Si NMR in

acetone-d_6. Other signals were not observed, therefore, there are no siloxane bond cleavage products or cyclooctasiloxaneoctaols in crude product.

In mechanism i), siloxane bond cleavage and following recombination is very fast and must be completed before 10 min. If siloxane bond cleavage occurred, mixture of all-*cis*-$[PhSiO(OH)]_4$ and all-*cis*-$[i\text{-}BuSiO(OH)]_4$ disproportionation resulted in the generation of mixed-substituents cyclotetrasiloxanetetraols is expected (Scheme 10, eq.3)). The result is shown in Figure 6 (eq.3). The crude product may show many peaks in ^{29}Si NMR attributed to substituents in mixed cyclotetrasiloxanetetraols. However, the crude product showed only 9 peaks in ^{29}Si NMR attributed to 4 isomers of $[PhSiO(OH)]_4$ and 4 isomers of $[i\text{-}BuSiO(OH)]_4$. In the reaction of all-*cis*-$[RSiO(OH)]_4$, the crude product showed only 4 isomers of cyclotetrasiloxanetetraols. If siloxane bond cleavage occurred, bond cleavage product must regenerate only cyclotetrasiloxanetetraol immediately in the reaction condition (1M HCl, acetone, r.t., 10 min).

Then we tried the reaction starting from $PhSi(OH)_3$ or $[i\text{-}BuSi(OH)_2]_2O$ in order to examine that they can afford the cyclotetrasiloxanetetraol in 10 minutes in a similar condition (1M HCl, acetone, r.t., 10 min) (Scheme 11). These compound were synthesized by known procedure [8a, 8b].

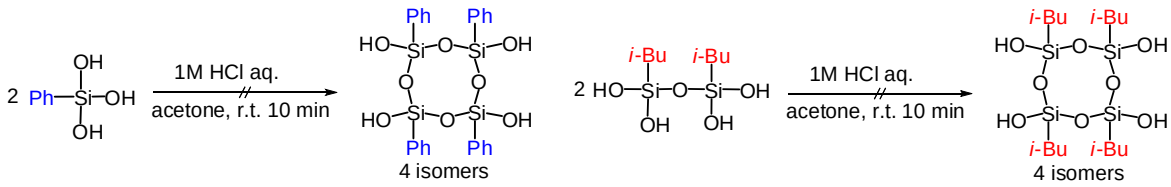

Scheme 11

Reaction from $PhSi(OH)_3$ gave complex mixture. The crude product showed –53.19 ppm peak attributed to $PhSi(OH)_3$, −61.68, −61.89, −62.13 ppm peaks attributed to $[PhSiO(OH)]_3$ or $[PhSi(OH)_2]_2O$ as major peaks, −71.03 , −71.16 ppm including broad peak (−69 to −72 ppm) attributed to $[PhSiO(OH)]_4$ and broad peak (−76 to −82 ppm) attributed to $RSiO_3$ region. This reaction resulted in the similar manner to that of Shimada and Yagihashi group that reported synthesis of *cis-trans*-$[PhSiO(OH)]_3$ from $PhSi(OH)_3$ [9]. Reaction of $[i\text{-}BuSi(OH)_2]_2O$ (δ_{Si} = –49.76 ppm) did not give $[i\text{-}BuSiO(OH)]_4$ and only recovered $[i\text{-}BuSi(OH)_2]_2O$.

If cyclic siloxane bond cleavage occurred without elimination of OH group, stereoisomerization may also occur for cyclic siloxanes without OH group. We already reported synthesis of *cis-trans-cis*-$[PhSiO(Me)]_4$ with similar bulkiness as

phenyl-substituted cyclotetrasiloxanetetraol [6c]. We attempted to carry out stereoisomerization in NMR tube (catalytic amount of 1M HClaq., acetone-d_6, r.t.) (Scheme 12).

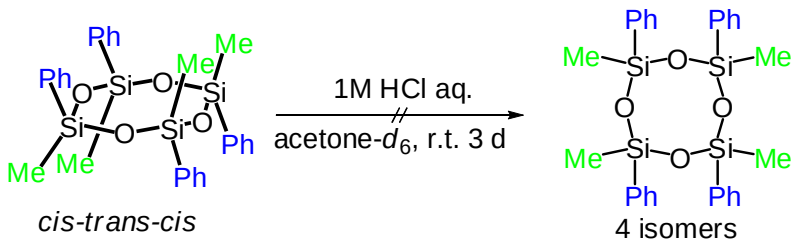

Scheme 12

However, we could not observe stereoisomerization after 3 days. Therefore, we think stereoisomerization only occurs for cyclotetrasiloxanes bearing OH groups. These results indicate that mechanism i) is unlikely. Thus we propose the mechanism ii) substitution reaction for silicon center without cyclic siloxane bond cleavage.

Based on the above results, plausible reaction mechanism is shown in Scheme 13.

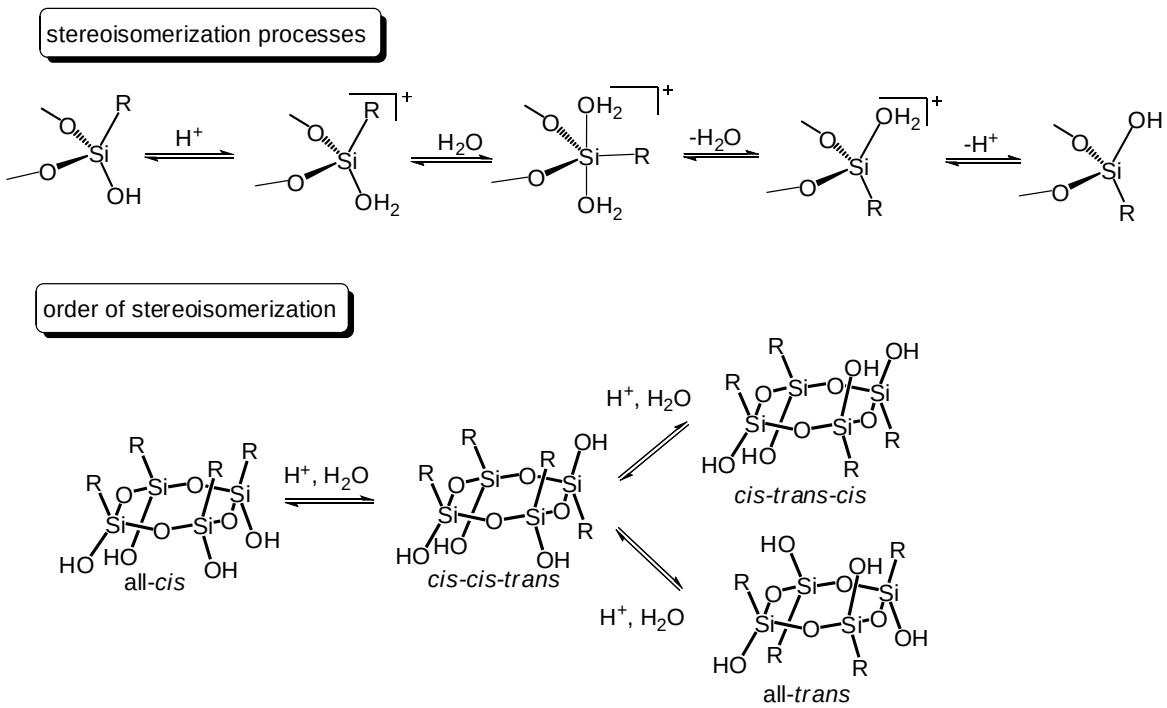

Scheme 13

The key intermediate is pentacoordinated silicon species formed by addition of water to the silicon atom in acidic condition. Therefore, *cis-cis-trans*, *cis-cis-trans*, and

all-*trans* isomers are generated step by step. If the reaction rate is slow, ratio of all-*trans* or *cis-trans-cis* isomers is low in the early stage. In our result, conversion rate was only 1 % by using 0.01 M HCl in 10 min and we could not obtain compound **1c** (all-*trans* isomer) (Table 3, entry 4). The result supported above hypothesis.

Part 6: Re-investigation of synthesis of **1a** from hydrolysis and condensation of *i*-$BuSiCl_3$

We already reported synthesis of **1a** from *i*-$BuSiCl_3$ in acetone-water solution in 23% yield [8b]. In the reaction, we also obtained insoluble product in $CHCl_3$. However, we did not analyze it before. Therefore, the reaction was re-investigated. The reaction was carried out in a similar manner (Scheme 14) [8b].

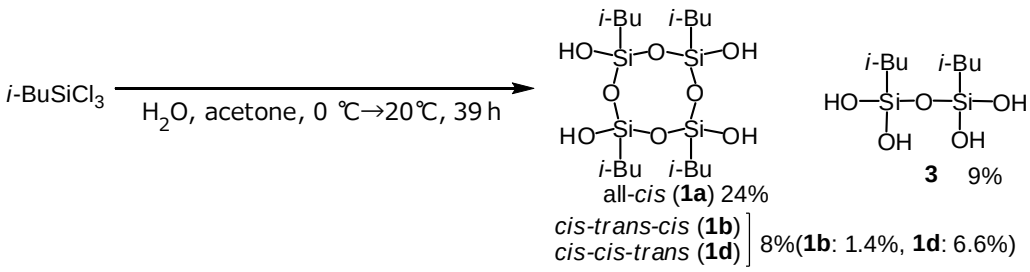

Scheme 14

We obtained white solid was precipitated from the solution. The white solid was collected. Insoluble compounds in chloroform were filtrated to give mixture of **1b** and **1d** except **1c** (8%, NMR yield of **1b**: 1.4%, NMR yield of **1d**: 6.6%). Filtrate was concentrated to give white solid then recrystallized from hexane to give **1a** (24%). From the solution removed precipitated, we also obtained [*i*-$BuSi(OH)_2]_2O$ (**3**) in 9% yield.

We reported that stereoisomerization did not occur in non-organic solvent condition (Table 5, entry 8). Therefore it assumed that stereoisomerization did not occur (or very slow), because **1a** was precipitated and eliminated from the solution by hydrolysis and condensation of *i*-$BuSiCl_3$. As a result, synthesis of all-*cis*-$[RSiO(OH)]_4$ from $RSiCl_3$ needs careful operation and analysis for the presence of other isomers.

Part 7: Stereoisomerization of all-*cis*-[*i*-$PrSiO(OH)]_4$ and double-decker silanol

We also attempted to carry out stereoisomerization of two cyclic siloxanes in NMR tube (catalytic amount of 1M HClaq., acetone-d_6, r.t.) (Scheme 15). These silanols were synthesized by known procedure [5d,10]. And the structures were already determined

by X-ray crystallographic analysis [10,11a,b].

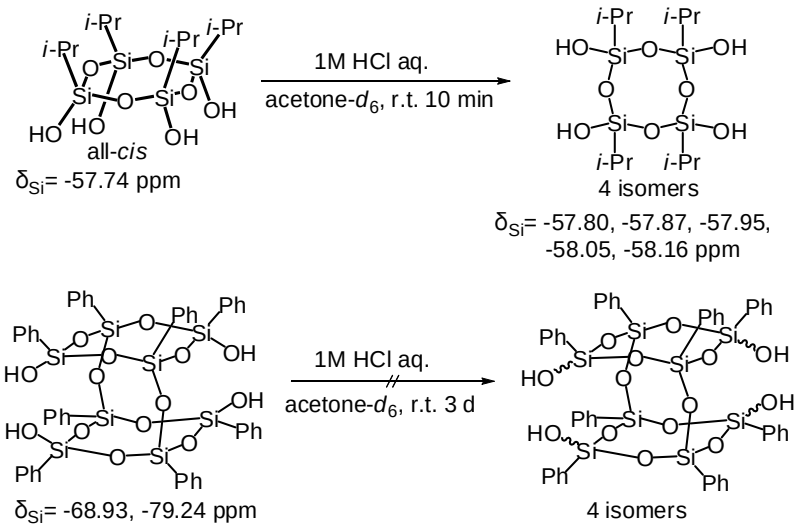

Scheme 15

In all-*cis*-[*i*-PrSiO(OH)]$_4$ (δ_{Si} = −57.74 ppm in acetone-d_6), after 10 min, new five signals (−57.80, −57.87, −57.95, −58.05, −58.16 ppm) were observed attributed to four isomers of [*i*-PrSiO(OH)]$_4$. However, in double-decker silanols (δ_{Si} = −68.93,−79.24 ppm in aceton-d_6), we could not observe new peak after 3 days. Therefore in double-decker silanol, stereoisomerization was not observed. The reason may be attributed to the bulkiness of cage-like structure that interrupted substitution reaction of silicon center.

2.3.3 Summary

Stereoisomerization of all-*cis*-1,3,5,7-tetrahydroxy-1,3,5,7-tetraisobutylcyclotetrasiloxane (**1a**) was carried out in acidic condition to give *cis-trans-cis* isomer (**1b**), all-*trans* isomer (**1c**), and *cis-cis-trans* isomer (**1d**). Mixture of **1b**, **1c**, and **1d** were isolated and identified by nuclear magnetic resonance spectra. *Cis-trans-cis* structure of **1b** was perfectly determined by X-ray crystallographic analysis. And **1a** and a mixture of **1b**, **1c**, and **1d** reacted with dichlorodiphenylsilane in the presence of triethylamine to give *syn*-type laddersiloxane selectively (**2a**) and *anti*-type laddersiloxane (**2b**), respectively. Suitable stereoisomerization condition was investigated in various conditions (reaction time, concentration of reagents, kind of reagents, and kind of solvents). As a result, best conditions is that using 3.2 equivalent amount of strong acid aqueous solutions (e.g. HCl aq.) in mixable solvent with water (e.g. acetone) at room temperature in 10 min. Stereoisomerization mechanism was

investigated by various experiments. The experimental results indicated that the most plausible mechanism is substitution reaction for silicon center without siloxane bond cleavage. Re-investigation of synthesis of **1a** from hydrolysis and condensation of *i*-$BuSiCl_3$ was performed to give **1a**, **1b**, **1d**, and [*i*-$BuSi(OH)_2]_2O$ (**3**). Stereoisomerization of all-*cis*-[*i*-$PrSiO(OH)]_4$ and double-decker silanols are performed. As a result, stereoisomerization of all-*cis*-[*i*-$PrSiO(OH)]_4$ is also observed.

2.3.4 Experimental section

All reagents were obtained from commercial sources and used without additional purification. Tetrahydrofuran was distilled from sodium benzophenone ketyl under argon. The Fourier transform nuclear magnetic resonance (NMR) spectra were obtained using a JEOL JNM-ECS 300 (^{1}H at 300.53 MHz, ^{13}C at 75.57 MHz, and ^{29}Si at 59.71 MHz) NMR instruments and JEOL JNM-ECA 600 (^{1}H at 600.17 MHz and ^{29}Si at 119.4 MHz) NMR instruments. Chemical shifts are reported as δ units (ppm) relative to $SiMe_4$, and residual solvents peaks were used for standards. For ^{29}Si NMR, $SiMe_4$ was used as an external standard. Electron impact mass spectrometry was performed on Shimadzu GCMS–QP2010SE/DI2010. Infrared spectra were measured using a Shimadzu FTIR-8400S spectrometer. All melting points were determined on a Yanaco micro melting point apparatus MP-J3 and are uncorrected. Elemental analyses were performed by the Center for Material Research by Instrumental Analysis (CIA), Gunma University. Flash chromatography were performed by Biotage Isolera with ELSD detector (ELSD1080) in gradient conditions (SiO_2, $CHCl_3$: AcOEt = 3 : 1).

General procedure of stereoisomerization

Acidic or basic aqueous solution (6 mL) was added to a solution of **1a** (0.90 g, 1.9 mmol) in various solvents (15 mL). The mixture was stirred. Saturated sodium bicarbonate aqueous solution (in acidic condition) or saturated ammonium chloride aqueous solution (in basic condition) was added to the reaction mixture to quench the reaction. Then ether was added to the mixture and organic phase was washed with brine. The organic phase was dried over anhydrous sodium sulfate and evaporated to give crude solid. Generated solid was filtrated, and washed by chloroform to give white solid (mixture of **1b**, **1c**, and **1d**). The chloroform solution was concentrated to afford **1a**.

Spectral data for a mixture of **1b, 1c,** and **1d**,: ^{1}H NMR (600.17 MHz, acetone-d_6) δ 0.57–0.61 (m, 8H), 0.94–0.97 (m, 24H), 1.86–1.96 (m, 4H), 5.22–5.40 (m, 4H) ppm. ^{29}Si NMR (59.71 MHz, acetone-d_6) δ –58.10, –58.31, –58.53, –58.66 ppm. MS (EI, 70 eV) m/z (%) 397 ([M–*i*-Bu–$H_2O]^+$, 100). Anal. Calcd for $C_{16}H_{40}Si_4O_8$:C, 40.64; H,

8.53; Found C, 40.39; H, 8.50%.

Spectral data for **1a** (all-*cis*): m.p. 148–151 ℃. ^{1}H NMR (600.17 MHz, acetone-d_6) δ 0.57 (d, J = 7.2 Hz, 8H), 0.97 (d, J = 7.2 Hz, 24H), 1.89 (nonet, J = 7.2 Hz, 4H), 5.34 (br s, 4H) ppm. ^{13}C NMR (75.57 MHz, acetone-d_6) δ 24.93 (CH_2), 25.22 (CH), 26.71 (CH_3) ppm. ^{29}Si NMR (59.71 MHz, acetone-d_6) δ –58.05 ppm. MS (EI, 70 eV) m/z (%) 397 ([M–*i*-Bu–H_2O]$^+$, 100). IR (KBr) 925, 1087, 2955, 3203 cm^{-1}. Anal. Calcd for $C_{16}H_{40}Si_4O_8$:C, 40.64; H, 8.53; Found C, 40.40; H, 8.55%.

Spectral data for **1b** (*cis*-*trans*-*cis*): m.p. 172–175 ℃ (decomp.). ^{1}H NMR (600.17 MHz, acetone-d_6) δ 0.59 (d, J = 6.6 Hz, 8H), 0.95 (d, J = 6.6 Hz, 12H), 0.95 (d, J = 6.6 Hz, 12H), 1.91 (nonet, J = 6.6 Hz, 4H), 5.29 (br s, 4H) ppm. ^{13}C NMR (75.57 MHz, acetone-d_6) δ 25.19 (CH), 25.26 (CH_2), 26.77 (CH_3), 26.80 (CH_3) ppm. ^{29}Si NMR (59.71 MHz, acetone-d_6) δ –58.66 ppm. DIMS (EI, 70eV) *m*/z (%) 415 ([M–*i*-Bu]$^+$, 3) , 397 ([M–*i*-Bu–H_2O]$^+$, 100). IR (KBr) 899, 1068, 1144, 2955, 3258 cm^{-1}. Anal. Calcd for $C_{16}H_{40}Si_4O_8$:C, 40.64; H, 8.53; Found C, 40.61; H, 8.57%.

Spectral data for **1c** (all-*trans*): m.p. 197–200 ℃ (decomp.). ^{1}H NMR (600.17 MHz, acetone-d_6) δ 0.59 (d, J = 6.6 Hz, 8H), 0.95 (d, J = 6.6 Hz, 24H), 1.93 (nonet, J = 6.6 Hz, 4H), 5.37 (s, 4H) ppm. ^{13}C NMR (75.57 MHz, acetone-d_6) δ 25.16 (CH), 25.27 (CH_2), 26.81 (CH_3) ppm. ^{29}Si NMR (59.71 MHz, acetone-d_6) δ –58.12 ppm. DIMS (EI, 70eV) *m*/z (%) 415 ([M–*i*-Bu]$^+$,3),397 ([M–*i*-Bu–H_2O]$^+$, 79), 43 (100). IR (KBr) 879, 895, 1061, 2955, 3273 cm^{-1}. Anal. Calcd for $C_{16}H_{40}Si_4O_8$:C, 40.64; H, 8.53; Found C, 40.49; H, 8.63%.

Spectral data for **1d** (*cis*-*cis*-*trans*): m.p. 153–156 ℃ (decomp.). ^{1}H NMR (600.17 MHz, acetone-d_6) δ 0.57 (d, J = 7.2 Hz, 8H), 0.58 (d, J = 7.2 Hz, 8H), 0.60 (d, J = 7.2 Hz, 8H), 0.94–0.96 (m, 24H), 1.86–1.95 (m, 4H), 5.31 (br s, 3H), 5.41 (s, 1H) ppm. ^{13}C NMR (75.57 MHz, acetone-d_6) δ 25.11 (CH_2), 25.17 (CH), 25.24 (CH), 25.32 (CH_2), 26.75 (CH_3) (5 peaks are overlapped) ppm. ^{29}Si NMR (59.71 MHz, acetone-d_6) δ –58.33, –58.51 ppm. DIMS (EI, 70eV) *m*/z (%) 415 ([M–*i*-Bu]$^+$,4) , 397 ([M–*i*-Bu–H_2O]$^+$, 100). IR (KBr) 881, 899, 1078, 2955, 3256 cm^{-1}. Anal. Calcd for $C_{16}H_{40}Si_4O_8$:C, 40.64; H, 8.53; Found C, 40.97; H, 8.57%.

Synthesis of **2a** (*syn*-type laddersiloxane)

Under argon atmosphere, dichlorodiphenylsilane (3.8 g, 15 mmol) in THF (22.5 mL) was added to a solution of **1a** (3.5 g, 7.4 mmol) and triethylamine (3.0 g, 30 mmol) in THF (22.5 mL) at 0 ℃. Then the mixture was refluxed for 24 h. Hexane was added to the reaction mixture and organic phase was washed with saturated ammonium chloride aqueous solution and brine. The organic phase was dried over anhydrous

sodium sulfate and evaporated to give crude solid. The solid was filtrated, and washed by methanol. Then the resulted solid was recrystallized from isopropyl alcohol to give tricyclic laddersiloxane **2a** (2.7 g, 3.2 mmol, 43%).

Spectral data for **2a**: m.p.111–113 ℃. ^{1}H NMR (300.53 MHz, $CDCl_3$) δ 0.70 (d, *J* = 6.9 Hz, 8H), 0.92 (d, 16H), 1.87 (nonet, *J* = 6.9 Hz, 4H), 6.90 (t, *J* = 7.2 Hz, 4H), 7.14 (t, *J* = 7.2 Hz, 2H), 7.34-7.45 (m, 10H), 7.63 (d, *J* = 7.2 Hz, 4H) ppm. ^{13}C NMR (75.57 MHz, $CDCl_3$) δ 23.12 (CH_2), 23.70 (C), 25.73 (CH_3) overlapped, 127.55 (CH), 127.75 (CH), 130.19 (CH) overlapped, 132.90 (C), 134.05 (CH), 134.21 (CH), 134.89 (C) ppm. ^{29}Si NMR (59.71 MHz, $CDCl_3$) δ –34.17, –55.01 ppm. DIMS (EI, 70eV) *m*/z (%) 775 ([M–*i*-Bu]$^{+}$,10) ,699 (100). IR (KBr) 513, 698, 717, 737, 991, 1005, 1022, 1040, 1051, 1080, 1128, 2955 cm^{-1}. Anal. Calcd for $C_{40}H_{56}Si_6O_8$:C, 57.65; H, 6.77; Found C, 57.54; H, 6.88%.

Synthesis of **2b** (*anti*-type laddersiloxane)

In order to obtain a sufficient amount of **1b**, **1c**, and **1d,** isomerization reaction was repeated several times. Thus, similar reaction condition was applied to **1a** (6.3 g, 13 mmol), 1M HCl aq. (42 mL) and acetone (105 mL). After the reaction, remained **1a** was separated by dissolving in $CHCl_3$, and treated with 1M HCl aq. This procedure was repeated three times. Total amount of mixture of **1b**, **1c**, and **1d** was 5.2 g (11 mmol), and conversion was 85%. Under argon atmosphere, dichlorodiphenylsilane (5.5 g, 22 mmol) in THF (33 mL) was added to a solution of mixture of **1b**, **1c**, and **1d** (5.2 g, 11 mmol) and triethylamine (4.5 g, 44 mmol) in THF (32 mL) at 0 ℃. The mixture was refluxed for 24 h. Water (20 mL) was added to reaction mixture to quench the reaction. Then chloroform was added to the reaction mixture and organic phase was washed with saturated ammonium chloride aqueous solution and brine. The organic phase was dried over anhydrous sodium sulfate and evaporated to give crude solid. The solid was filtrated, and washed by methanol to give **2b** (2.2 g, 2.6 mmol, 24%, and overall yield from **1a**: 20%)

Spectral data for **2b**: m.p. 104–105 ℃. ^{1}H NMR (300.53 MHz, $CDCl_3$) δ 0.62 (d, *J* = 6.6 Hz, 8H), 0.83 (d, *J* = 6.6 Hz, 12H), 0.85 (d, *J* = 6.6 Hz, 12H), 1.76 (nonet, *J* = 6.6 Hz, 4H), 7.27–7.46 (m, 12H), 7.61–7.68 (m, 8H) ppm. ^{13}C NMR (75.57 MHz, $CDCl_3$) δ 22.72 (CH_2), 23.50 (CH), 25.49 (CH_3), 25.77 (CH_3), 127.53 (CH), 127.78 (CH), 130.25 (CH), 130.32 (CH), 134.01 (CH), 134.18 (C), 134.35 (CH) ppm one C peak overlapped. ^{29}Si NMR (59.71 MHz, $CDCl_3$) δ –35.76, –54.68 ppm. DIMS (EI, 30eV) *m*/z (%) 775 ([M–*i*-Bu]$^{+}$, 100). IR (KBr) 698, 995, 1009, 1034, 1057, 1084, 1121, 1229, 2953 cm^{-1}. Anal. Calcd for $C_{40}H_{56}Si_6O_8$:C, 57.65; H, 6.77; Found C, 57.61; H,

6.86%.

Synthesis of **1a** from isobutyltrimethoxysilane

Isobutyltrimethoxysilane (4.5 g, 25 mmol) was added to hexane (25 mL), water (0.47 g, 26 mmol) and sodium hydroxide (1.0 g, 25 mmol) at room temperature. The mixture was stirred for 3 days and white solid generated. The solvent was removed by decantation, and resulting solid was washed with hexane. The product was dried under reduced pressure to give cyclic silanol sodium salt (3.6 g). A mixture of concentrated hydrochloric acid (35%) (4.3 g, 41 mmol), and water (190 mL) was added to the suspension of sodium salt in ether (36 mL) at 0 ℃. The mixture was stirred for 10 minutes. Saturated sodium bicarbonate aqueous solution was added to the mixture for neutralization. Ether was added to the mixture and separated organic phase was washed with water and brine. The organic phase was dried over anhydrous sodium sulfate and concentrated. The resulted solid was recrystallized from hexane and washed with cold hexane. The product was dried under reduced pressure to give **1a** (2.2 g, 74%).

Synthesis of **1a**, **1b**, and **1d**, and 1,3-diisobutyldisiloxane-1,1,3,3-tetrol (**3**) from isobutyltrichlorosilane

Solution of isobutyltrichlorosilane (6.7 g, 35 mmol) and acetone (33 mL) was added dropwise into vigorously stirred cold water (400 mL) for 1 h at 0 ℃. Then, the reaction mixture was stirred for 39 h at 0℃ to 20 ℃. White solid was precipitated from the solution. The supernatant liquid solution was removed by decantation. The white solid was collected. Insoluble compounds in chloroform were removed by filtration to give mixture of **1b** and **1d** (0.35 g, 8%, NMR yield of **1b**: 1.4%, NMR yield of **1d**: 6.6%). Filtrate was concentrated to afford white solid. The solid was recrystallized from hexane to give **1a** (1.0 g, 24%). The decanted solution was poured into another flask. Sodium chloride (125 g) and ether were added into the reaction mixture. Organic layer was extracted with ether 3 times. The combined organic phase was washed with saturated sodium bicarbonate aqueous solution and brine. The organic phase was dried over anhydrous sodium sulfate and concentrated. The crude product was washed by chloroform to afford 1,3-diisobutyldisiloxane-1,1,3,3-tetrol (**3**) (0.37 g, 9%).

Spectral data for **3**: m.p. 141–144 ℃ (decomp.). ^{1}H NMR (300 MHz, acetone-d_6) δ 0.56 (d, J = 6.9 Hz, 4H), 0.95 (d, J = 6.9Hz, 12H), 1.91 (nonet, J = 6.9 Hz, 2H), 4.97 (br s, 4H) ppm. ^{13}C NMR (75.3 MHz, acetone-d_6) δ 24.59(CH), 24.76(CH_2), 26.19(CH_3). ^{29}Si NMR (59.7 MHz, acetone-d_6) δ –49.76 ppm. DIMS (EI, 70eV) *m/z*

(%) 197 ([M–*i*-Bu]$^+$, 33) ,141 ([M–*i*-Bu$_2$+H]$^+$, 100), 58 ([*i*-Bu–H]$^+$, 27). IR (KBr) 740, 852, 896, 1091, 1230, 2873, 2954, 3195 cm^{-1}. Anal. Calcd for $C_8H_{22}Si_2O_5$: C, 37.77; H, 8.72; Found C, 37.69; H, 8.50%.

2.3.5 References

[1] M. Unno, A. Suto, T. Matsumoto, *Russ. Chem. Rev.*, **2013**, *82*, 289.

[2] S. Chang, T. Matsumoto, H. Matsumoto, M. Unno, *Appl. Organomet., Chem.* **2010**, *24*, 241.

[3a] M. Unno, A. Suto, K. Takada, H. Matsumoto, *Bull. Chem. Soc. Jpn.*, **2000**, *73*, 215.

[3b]S. Tateyama, Y. Kakihana, Y. Kawakami, *J. Organomet. Chem.*, **2010**, *695*, 898.

[4a] N. N. Makarova, I. M. Petrova, P. V. Petrovskii, A. V. Kaznacheev, L. M. Volkova, M. A. Shcherbina, N. P. Bessonova, S. N. Chvalun, Yu. K. Godovskiib, *Russ. Chem. Bull. Int. Ed.*, **2004**, *53*, 1983.

[4b] R. Panisch, A. R. Bassindale, A. A. Korlyukov, M. B. Pitak, S. J. Coles, P. G. Taylor, *Organometallics*, 2013, **32**, 1732.

[4c] W. Mróz, J. P. Bombenger, C. Botta, A. O. Biroli, M. Pizzotti, F. D. Angelis, L. Belpassi, R. Tubino, F. Meinardi, *Chem. Eur. J.*, **2009**, *15*, 12791.

[5a] J. F. Brown, Jr., L.H. Vogt, Jr., *J. Am. Chem. Soc.*, **1965**, *87*, 4317.

[5b] J. F. Brown, Jr., L.H. Vogt, Jr., *J. Am. Chem. Soc.*, **1965**, *87*, 4313.

[5c] F. J. Feher, J. J. Schwab, D. Soulivong, J. W. Ziller, *Main Group Chem.*, **1997**, *2*, 123.

[5d] M. Unno, A. Suto, K. Takada, H. Matsumoto, *Bull. Chem. Soc. Jpn.*, **2000**, *73*, 215.

[5e] O. I. Shchegolikhina, Y. A. Pozdnyakova, Y. A. Molodtsova, S. D. Korkin, S. S. Bukalov, L. A. Leites, K. A. Lyssenko, A. S. Peregudov, N. Auner, and D. E. Katsoulis, *Inorg. Chem.*, **2002**, *41*, 6892.

[5f] R. Ito, Y. Kakihana, Y. Kawakami, *Chem. Lett.*, **2009**, *38*, 364.

[5g] Y. A. Pozdnyakova, A. A. Korlyukov, E. G. Kononova, K. A. Lyssenko, A. S. Peregudov, and O. I. Shchegolikhina, *Inorg. Chem.*, **2010**, *49*, 572.

[5h] M. Unno, Y. Kawaguchi, Y. Kishimoto, H. Matsumoto, *J. Am. Chem. Soc.*, **2005**, *127*, 2256.

[5i] H. S. Lee, S. S. Choi, K. Y. Baek, S. M. Hong, E. C. Lee, J. C. Lee , S. S. *Hwang, European Polymer Journal*, **2012**, *48*, 1073.

[5j] I. Yu. Klement'ev, V. E. Shklover, M. A. Kulish, V. S. Tikhonov, E. V. Volkova, *Dokl. Akad. Nauk SSSR*, **1981**, *259*, 1371.

[6a] M. Unno, A. Suto, H. Matsumoto, *J. Am. Chem. Soc.*, **2002,** *124*, 1574.

[6b]M. Unno, T. Matsumoto, H. Matsumoto, *J. Organomet., Chem.* **2007**, *692*, 307.

[6c] M. Unno, S. Chang, H. Matsumoto, *Bull. Chem. Soc. Jpn.*, **2005**, *78*, 1105.
[7]H. Seki, Y. Abe, T. Gunji, *J. Organomet. Chem..*, **2011**, *696*, 846.
[8a] S. D. Korkin, M. I. Buzin, E. V. Matukhina, L. N. Zherlitsyna, N. Auner, O. I. Shchegolikhina, *J. Organomet. Chem.* **2003**, *686*, 313.
[8b] In this thesis part 2, chapter 1.
[9] F. Yagihashi, M. Igarashi, Y. Nakajima, W. Ando, K. Sato, Y. Yumoto, C. Matsui, and S. Shimada, *Organometallics*, *Organometallics*, **2014**, *33*, 6278.
[10] D. W. Lee, Y. Kawakami, *Polym. J.*, **2007**, *39*, 230.
[11a] M. Unno, K.Takada, H. Matsumoto, *Chem. Lett.* **1998**, *27*, 489.
[11b] M. Unno, K.Takada, H. Matsumoto, *Chem. Lett.* **2000**, *29*, 242.

2.3.6 Supporting information

1. Spectral data

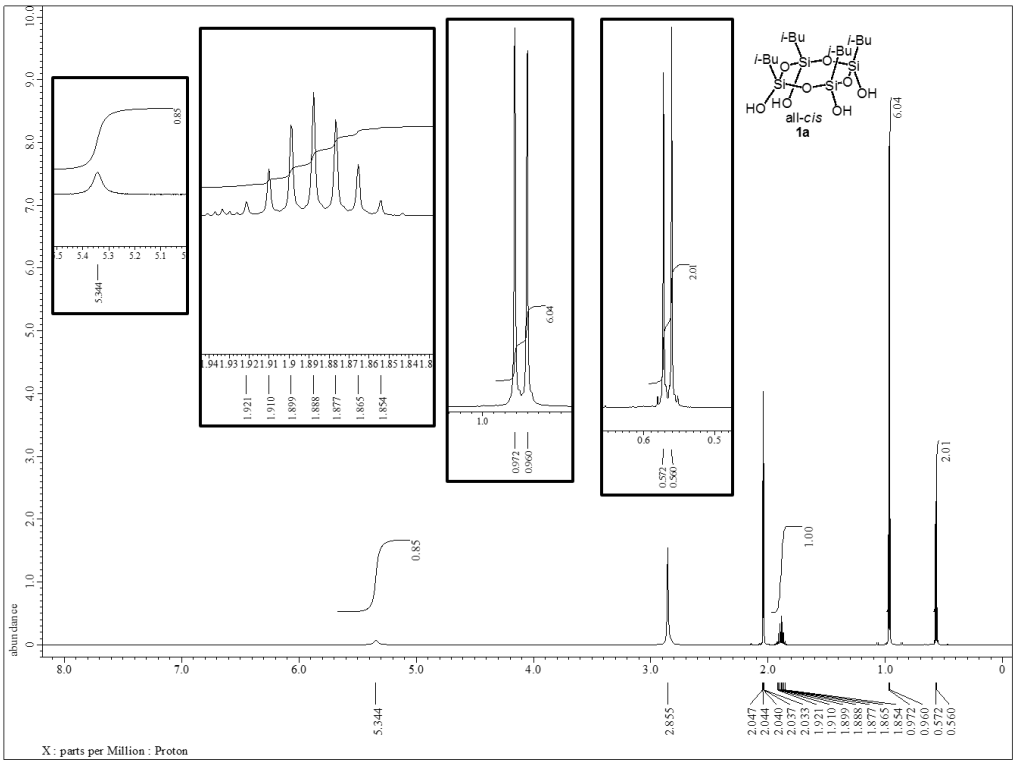

Figure 1. ^{1}H NMR spectrum of **1a** (600.17 MHz, acetone-d_6)

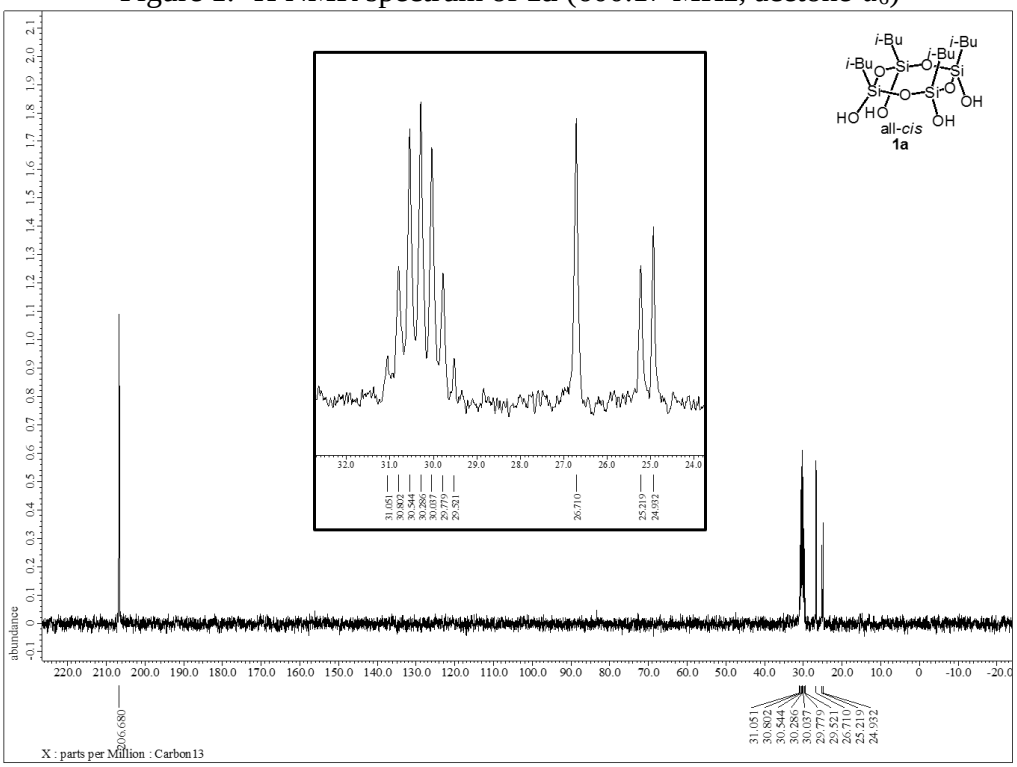

Figure 2. ^{13}C NMR spectrum of **1a** (75.57 MHz, acetone-d_6)

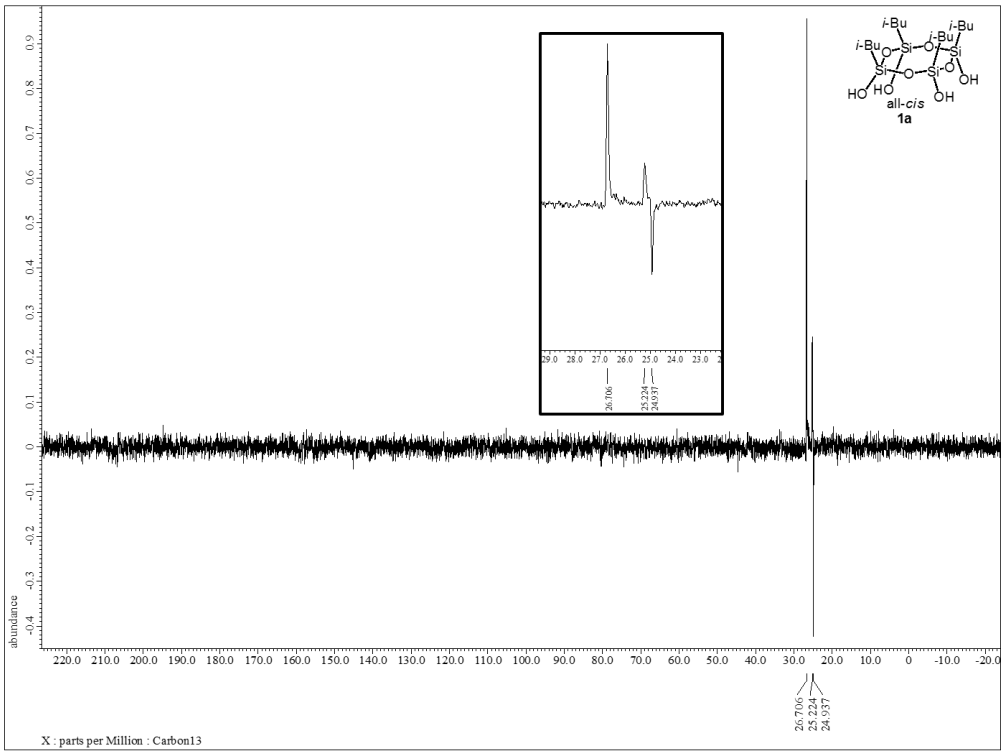

Figure 3. ^{13}C NMR (dept 135) spectrum of **1a** (75.57 MHz, acetone-d_6)

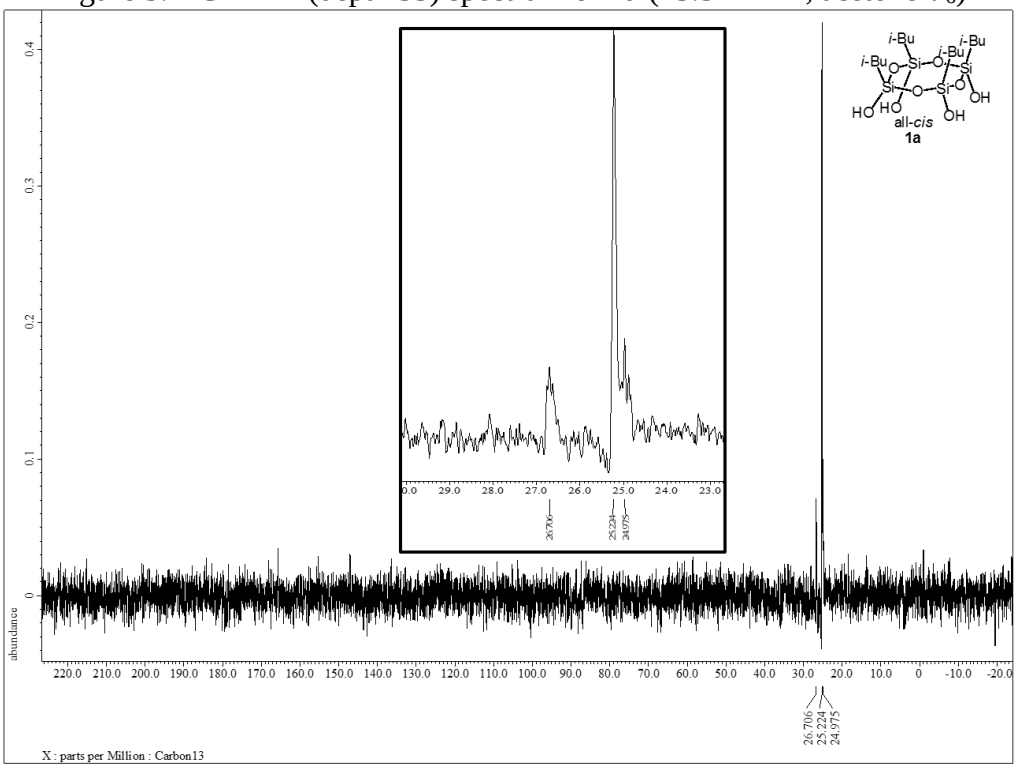

Figure 4. ^{13}C NMR (dept 90) spectrum of **1a** (75.57 MHz, acetone-d_6)

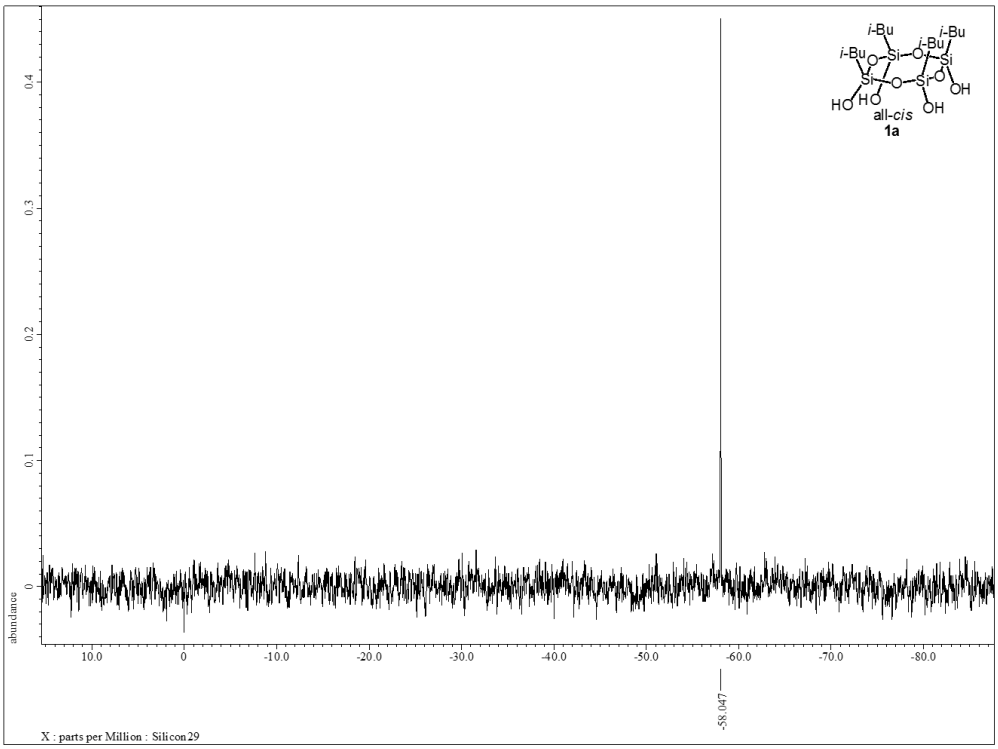

Figure 5. ^{29}Si NMR spectrum of **1a** (59.71 MHz, acetone-d_6)

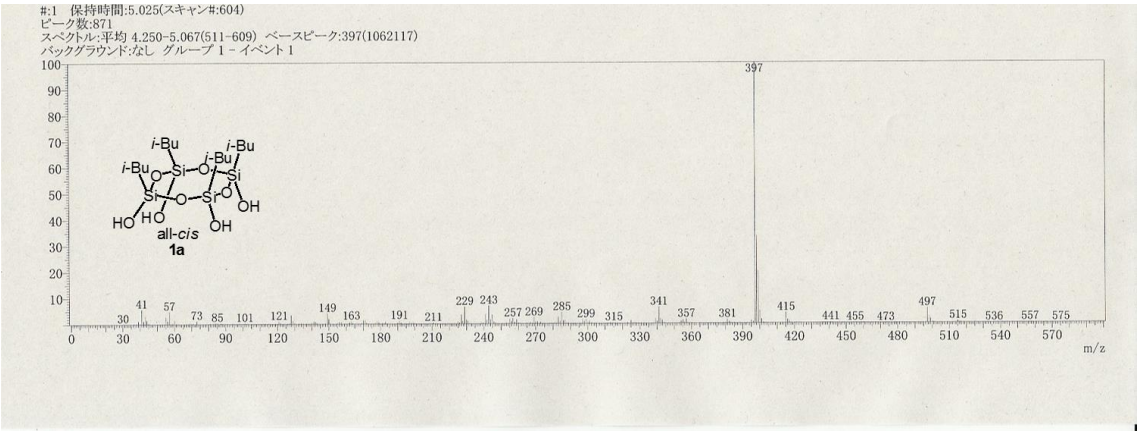

Figure 6. DIMS (EI, 70 eV) spectrum of **1a**

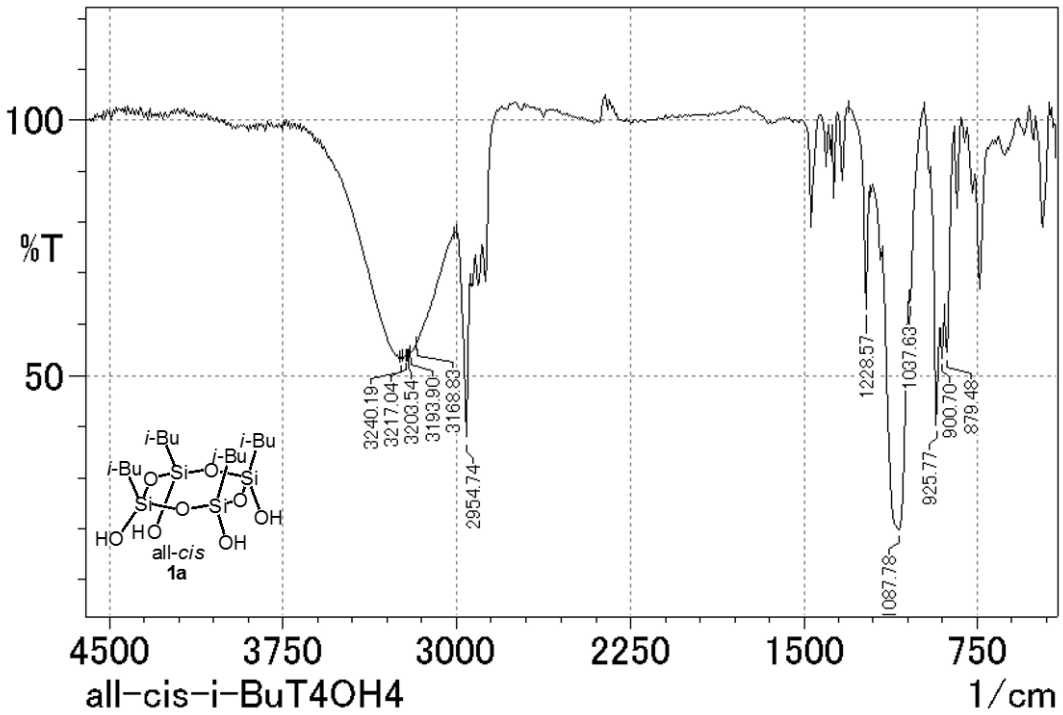

Figure 7. IR (KBr) spectrum of **1a**

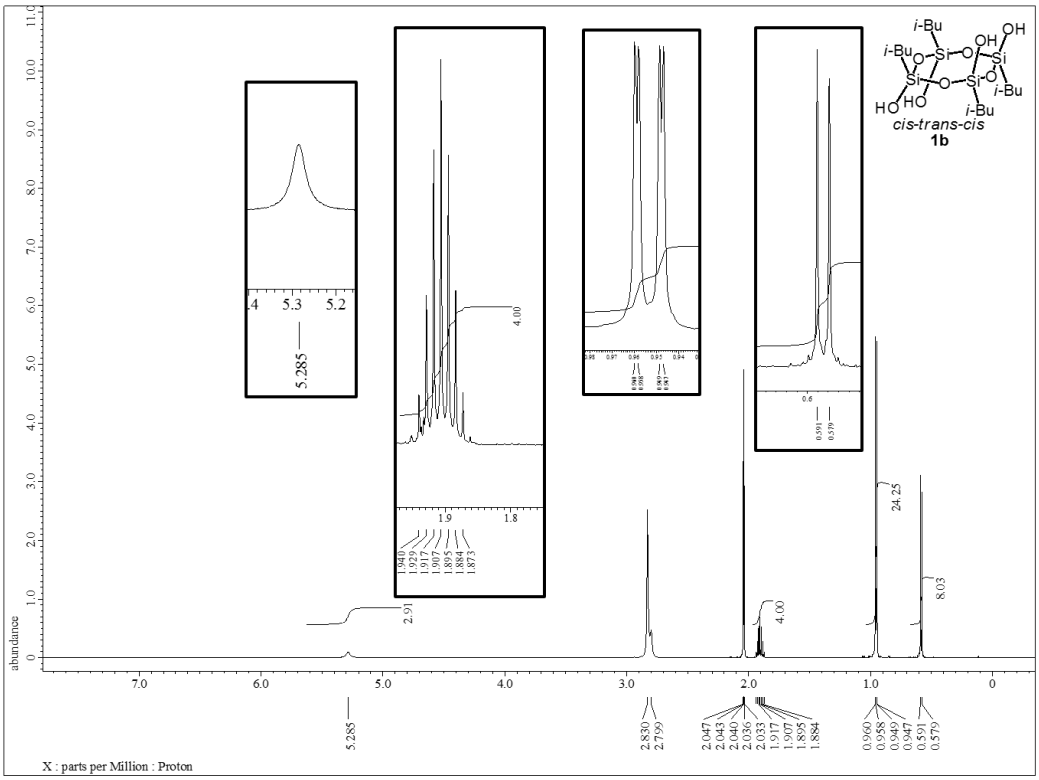

Figure 8. ^{1}H NMR spectrum of **1b** (600.17 MHz, acetone-d_6)

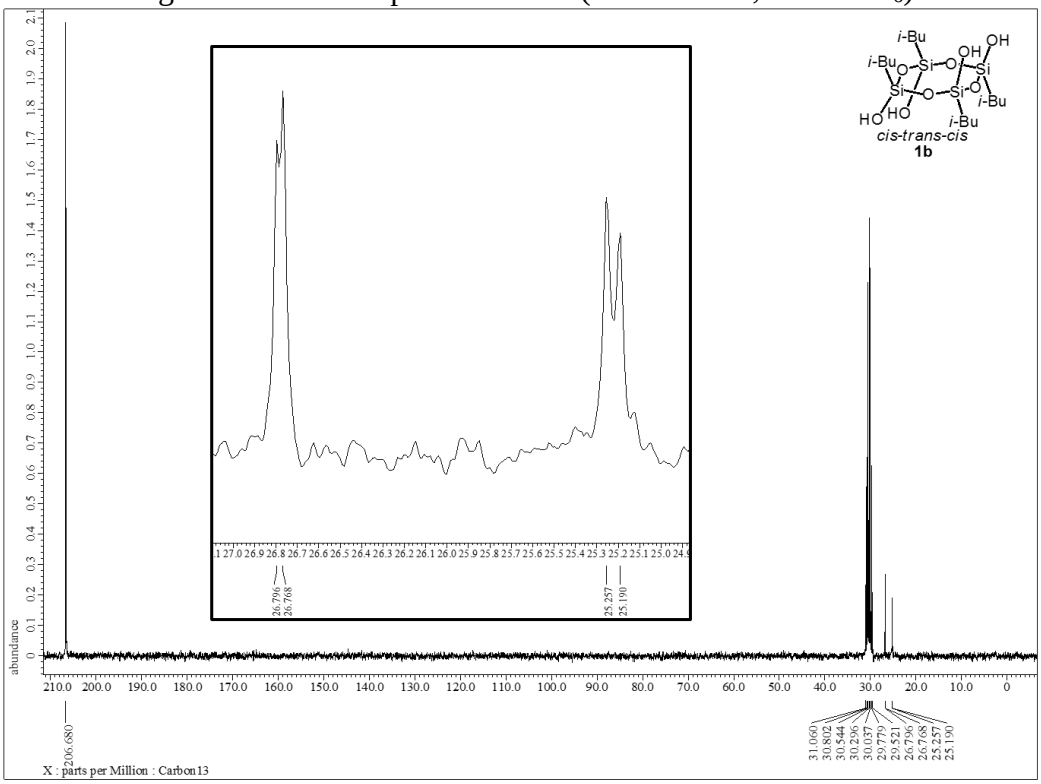

Figure 9. ^{13}C NMR spectrum of **1b** (75.57 MHz, acetone-d_6)

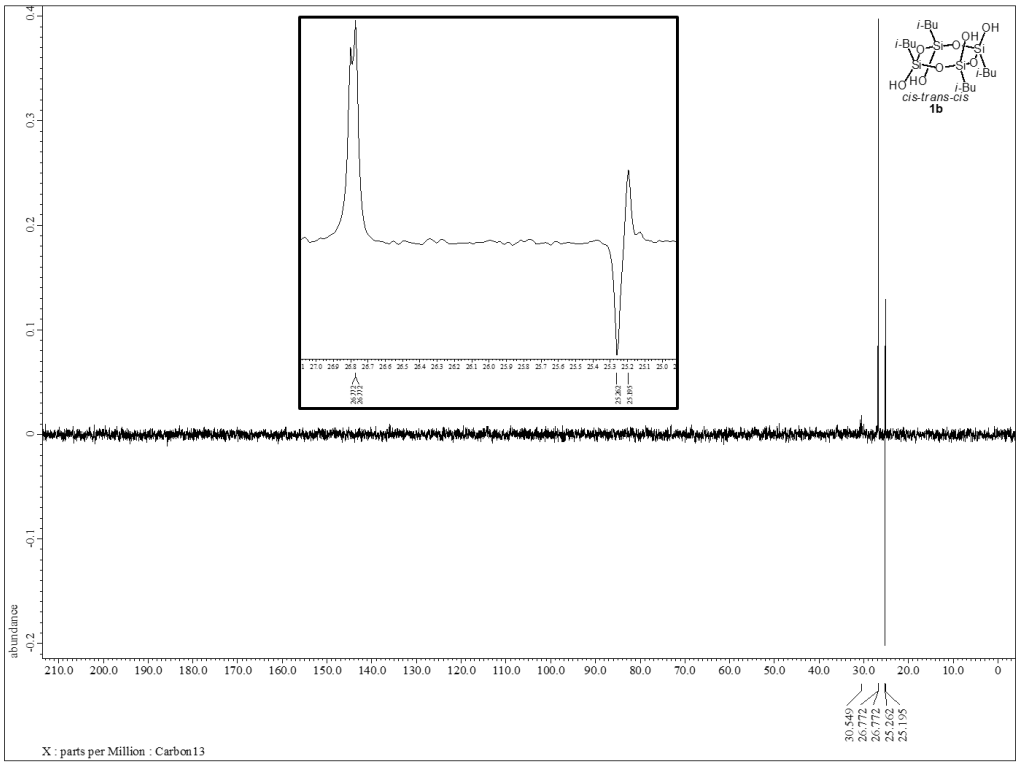

Figure 10. ^{13}C NMR (dept 135) spectrum of **1b** (75.57 MHz, acetone-d_6)

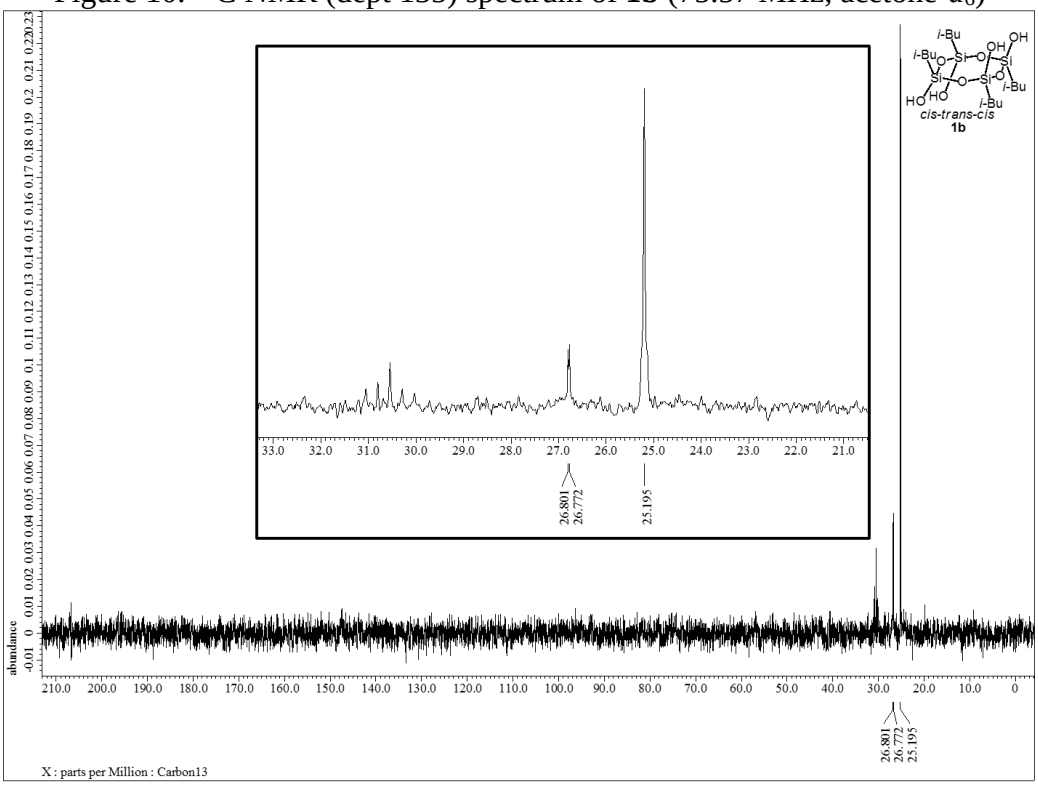

Figure 11. ^{13}C NMR (dept 90) spectrum of **1b** (75.57 MHz, acetone-d_6)

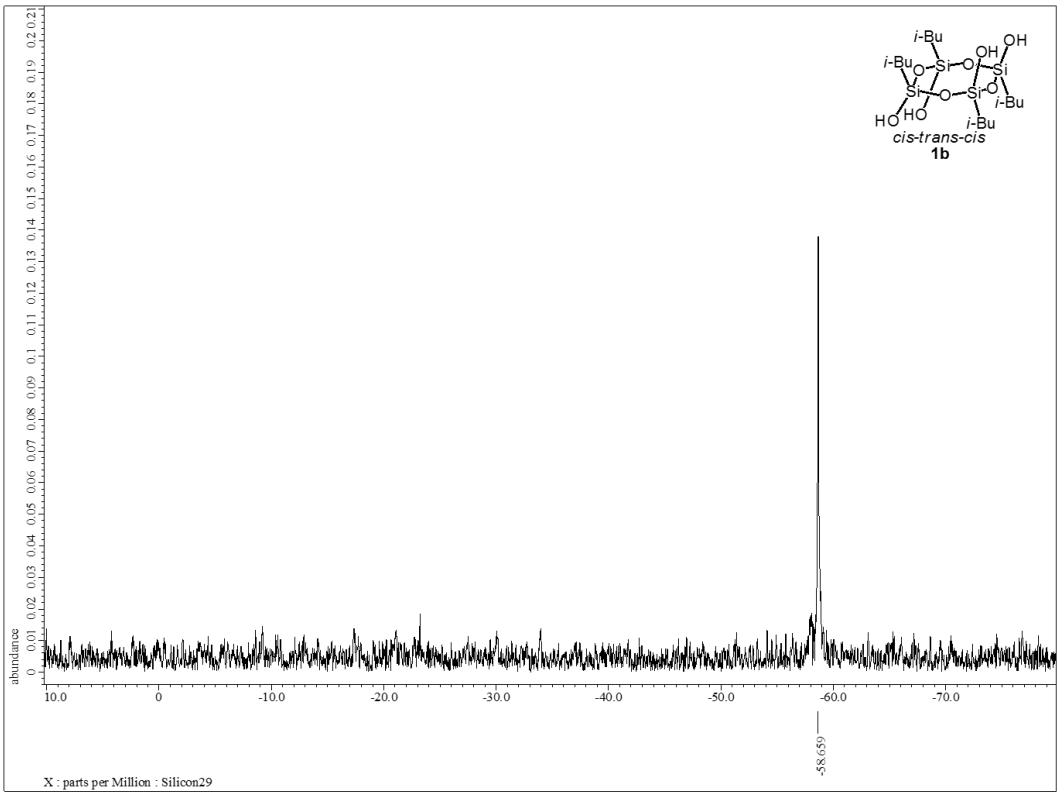

Figure 12. ^{29}Si NMR spectrum of **1b** (59.71 MHz, acetone-d_6)

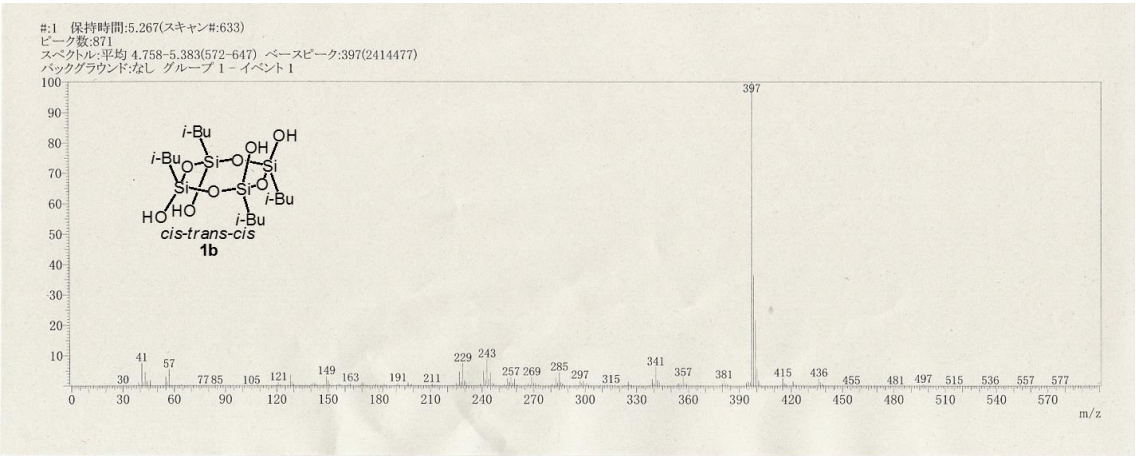

Figure 13. DIMS (EI, 70 eV) spectrum of **1b**

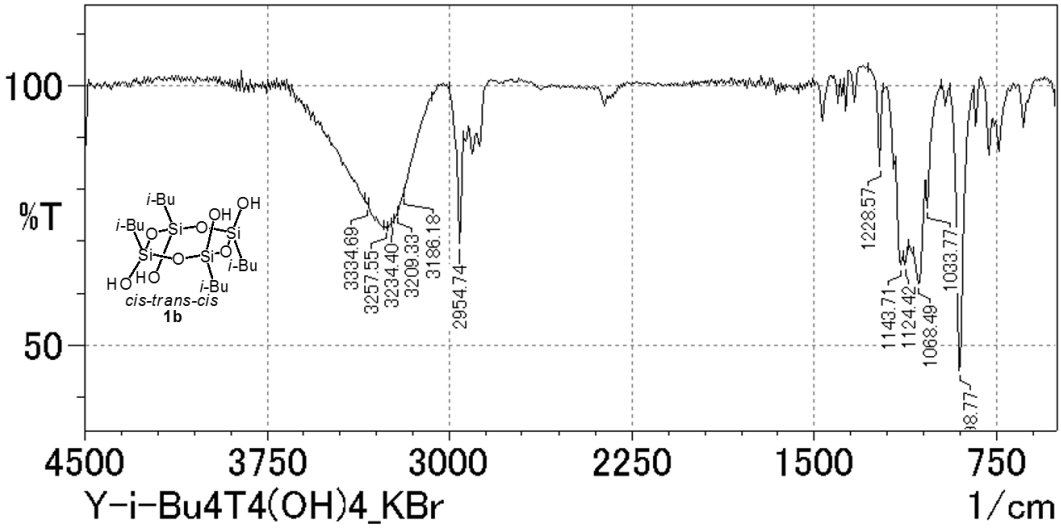

Figure 14. IR (KBr) spectrum of **1b**

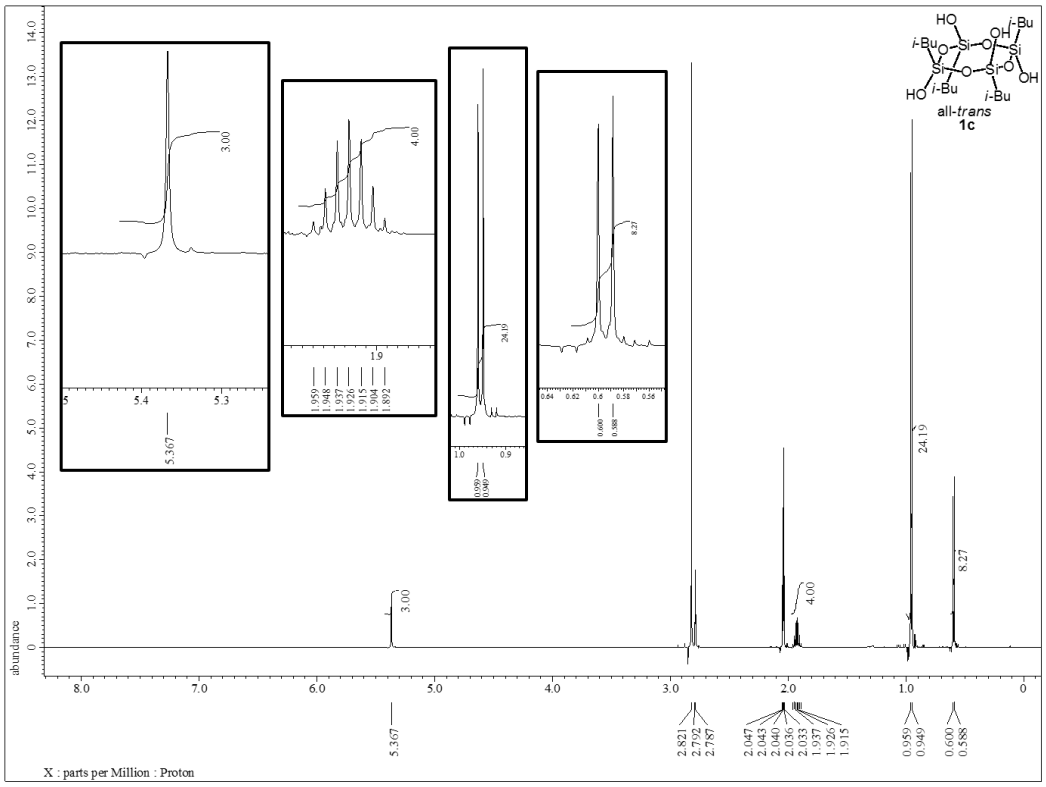

Figure 15. ^{1}H NMR spectrum of **1c** (600.17 MHz, acetone-d_6)

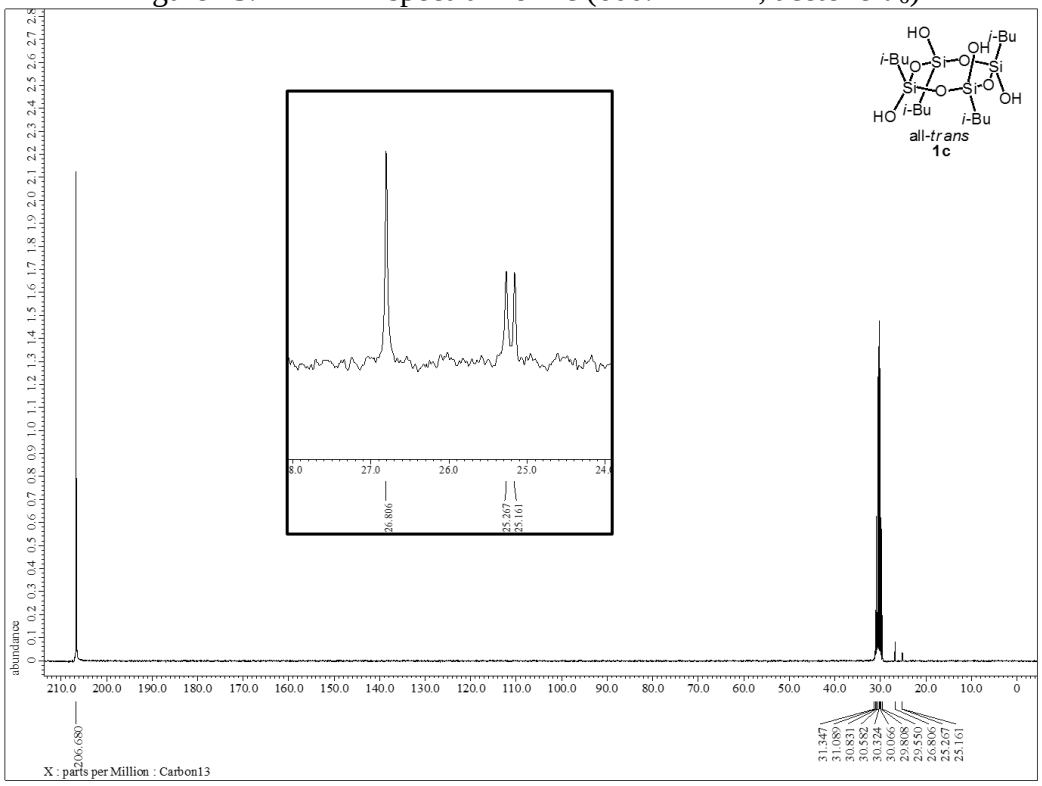

Figure 16. ^{13}C NMR spectrum of **1c** (75.57 MHz, acetone-d_6)

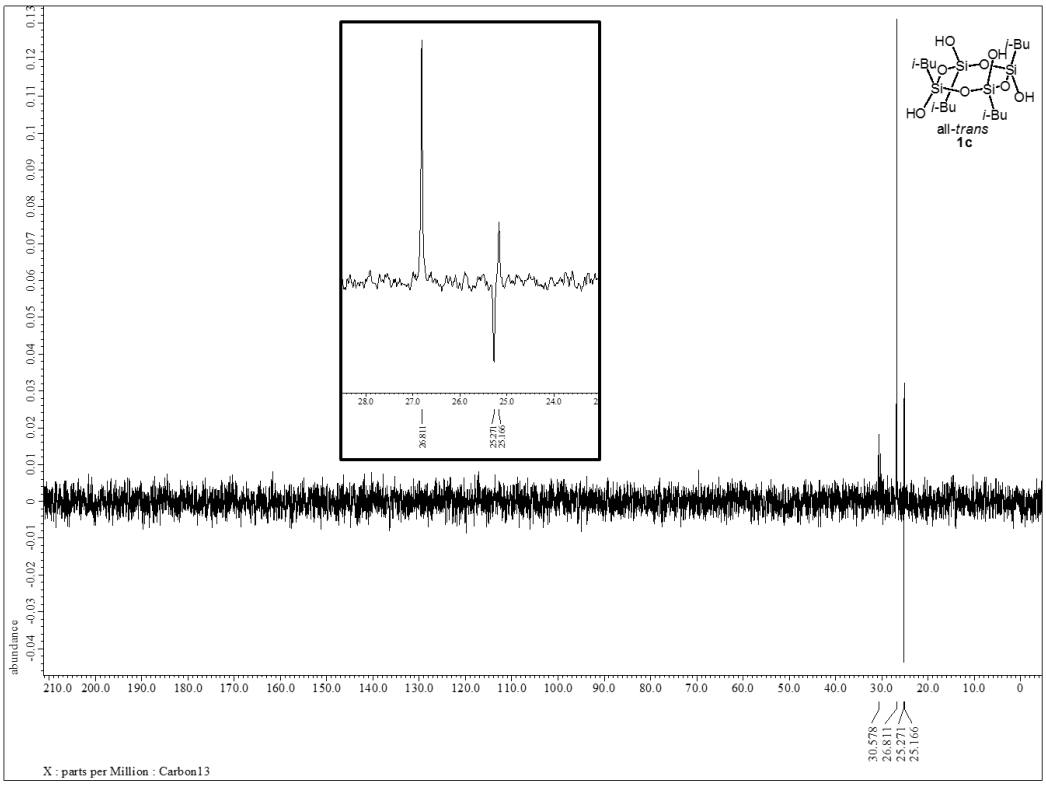

Figure 17. ^{13}C NMR (dept 135) spectrum of **1c** (75.57 MHz, acetone-d_6)

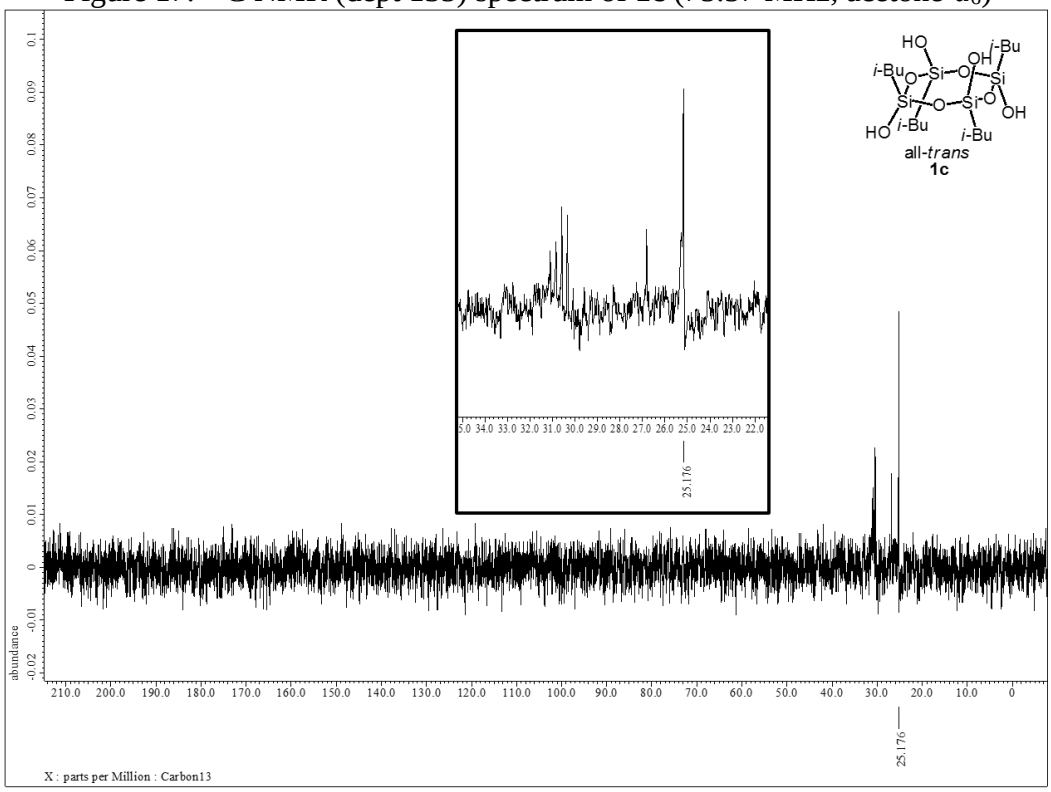

Figure 18. ^{13}C NMR (dept 90) spectrum of **1c** (75.57 MHz, acetone-d_6)

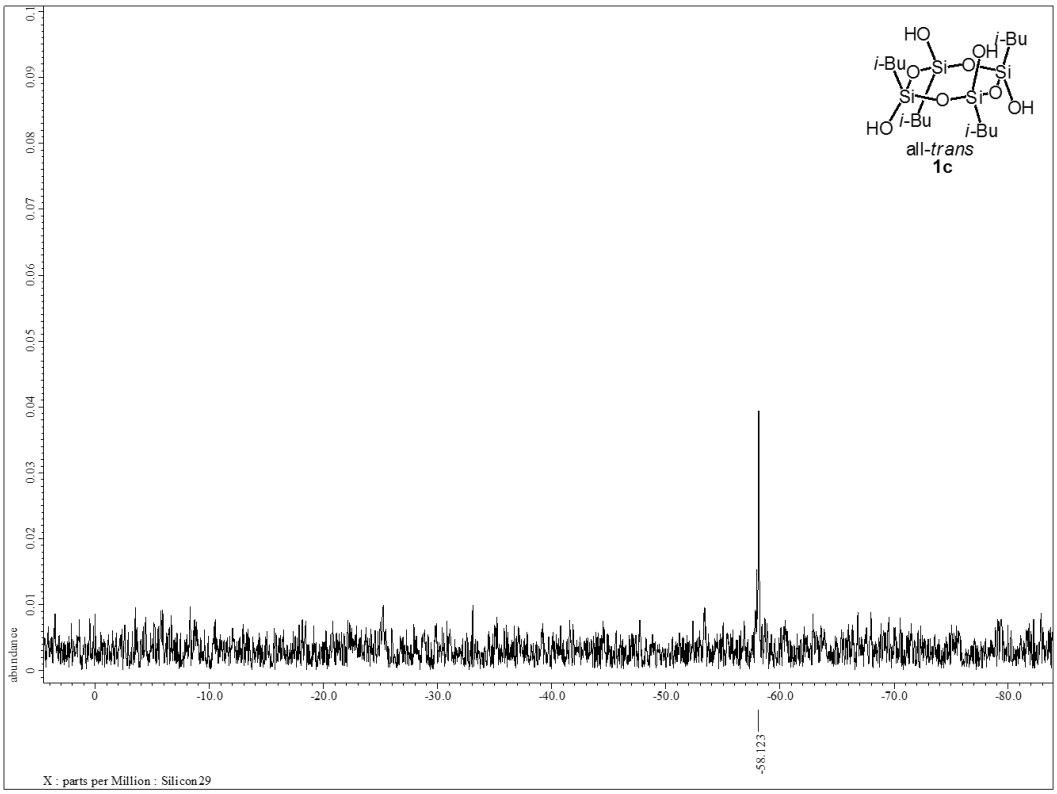

Figure 19. ^{29}Si NMR spectrum of **1c** (59.71 MHz, acetone-d_6)

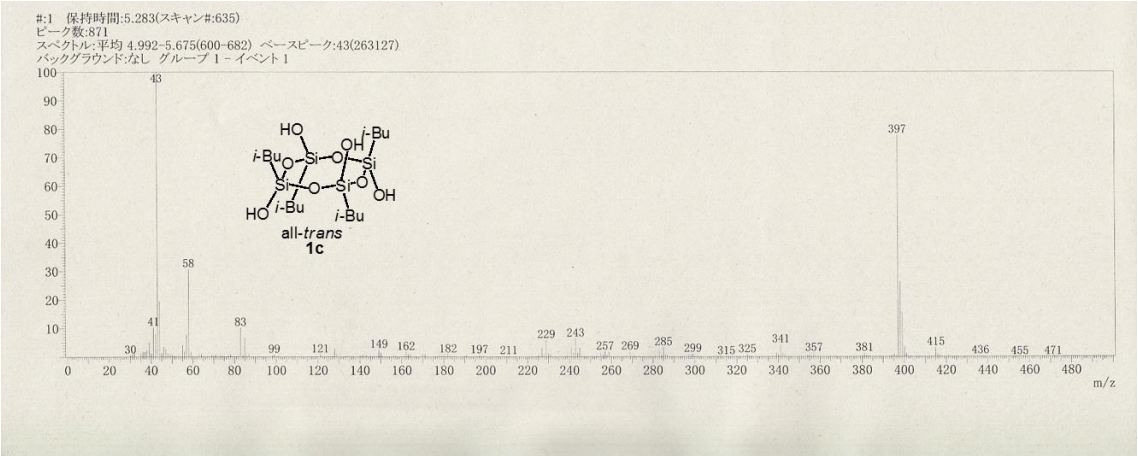

Figure 20. DIMS (EI, 70 eV) spectrum of **1c**

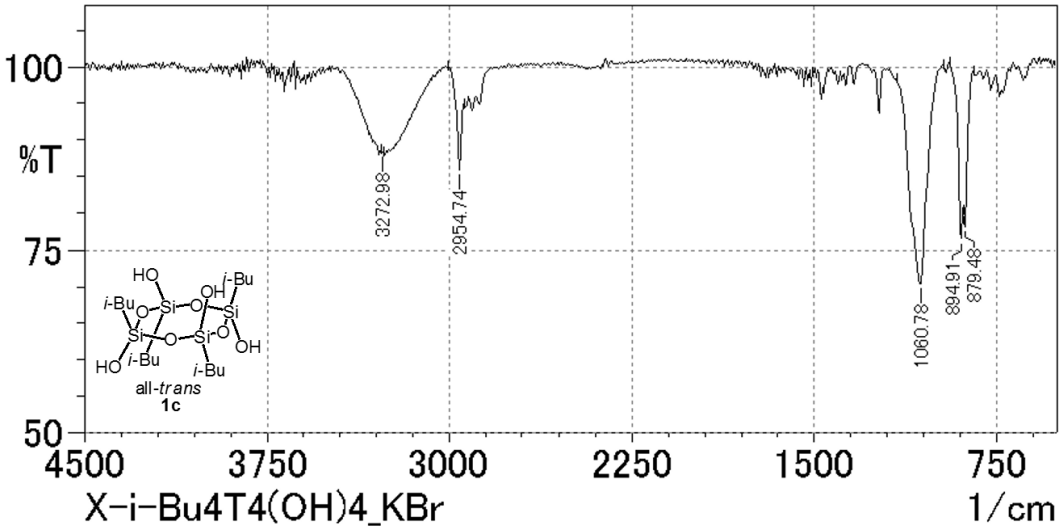

Figure 21. IR (KBr) spectrum of **1c**

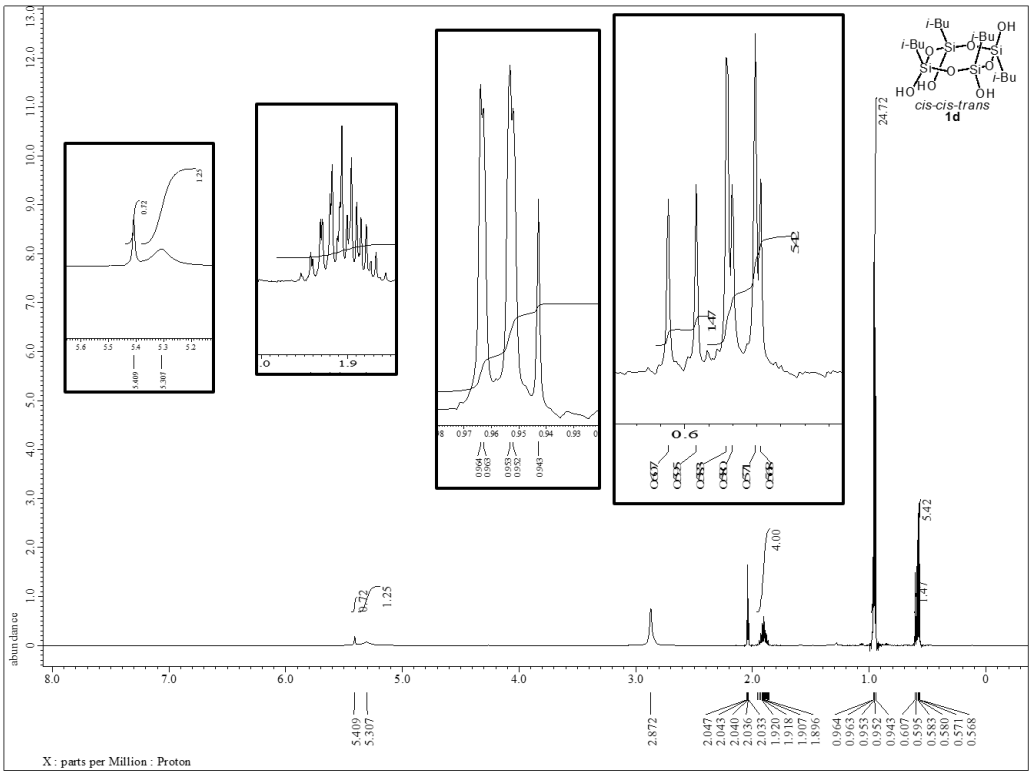

Figure 22. ^{1}H NMR spectrum of **1d** (600.17 MHz, acetone-d_6)

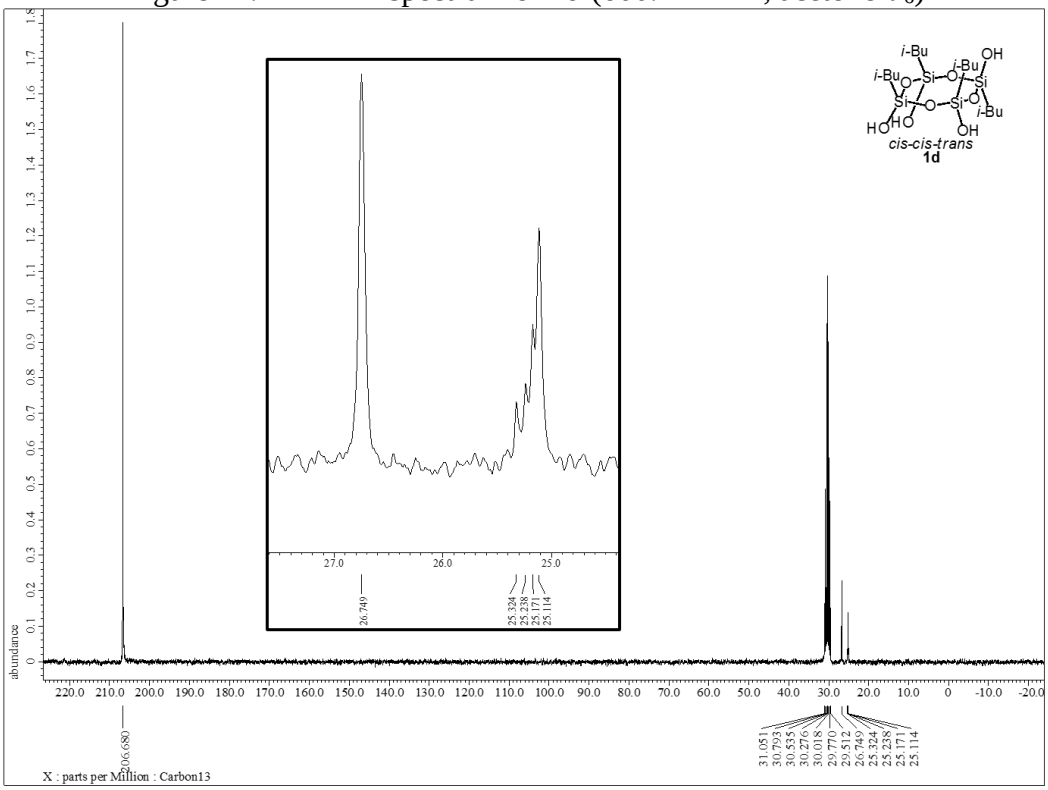

Figure 23. ^{13}C NMR spectrum of **1d** (75.57 MHz, acetone-d_6)

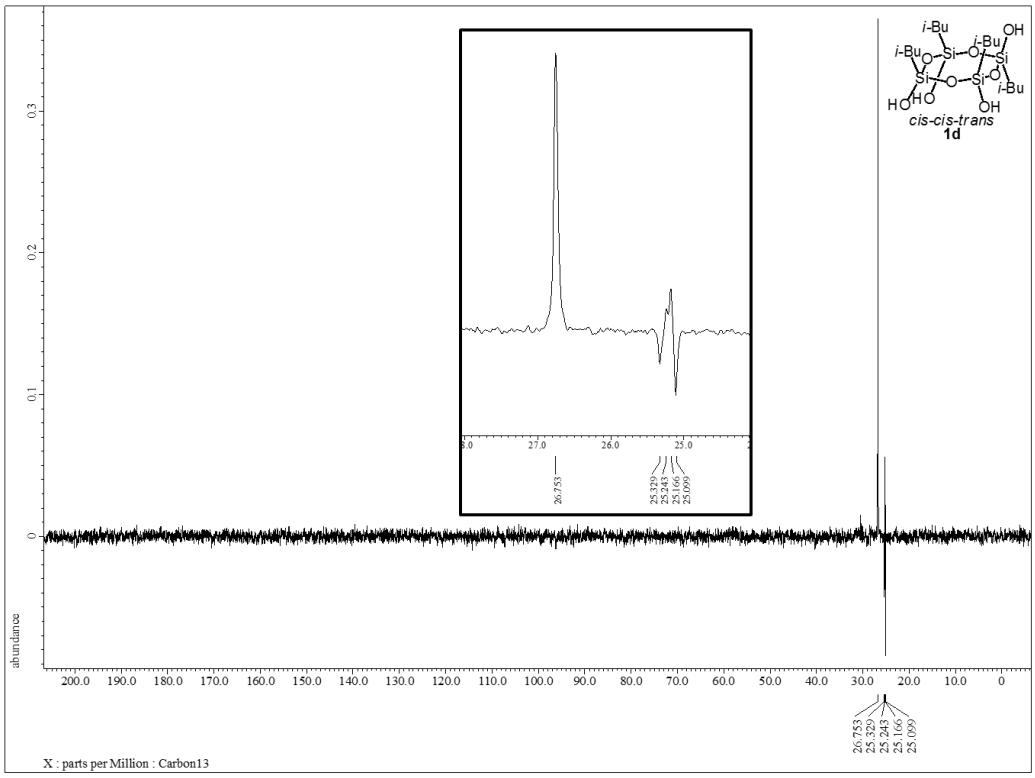

Figure 24. ^{13}C NMR (dept 135) spectrum of **1d** (75.57 MHz, acetone-d_6)

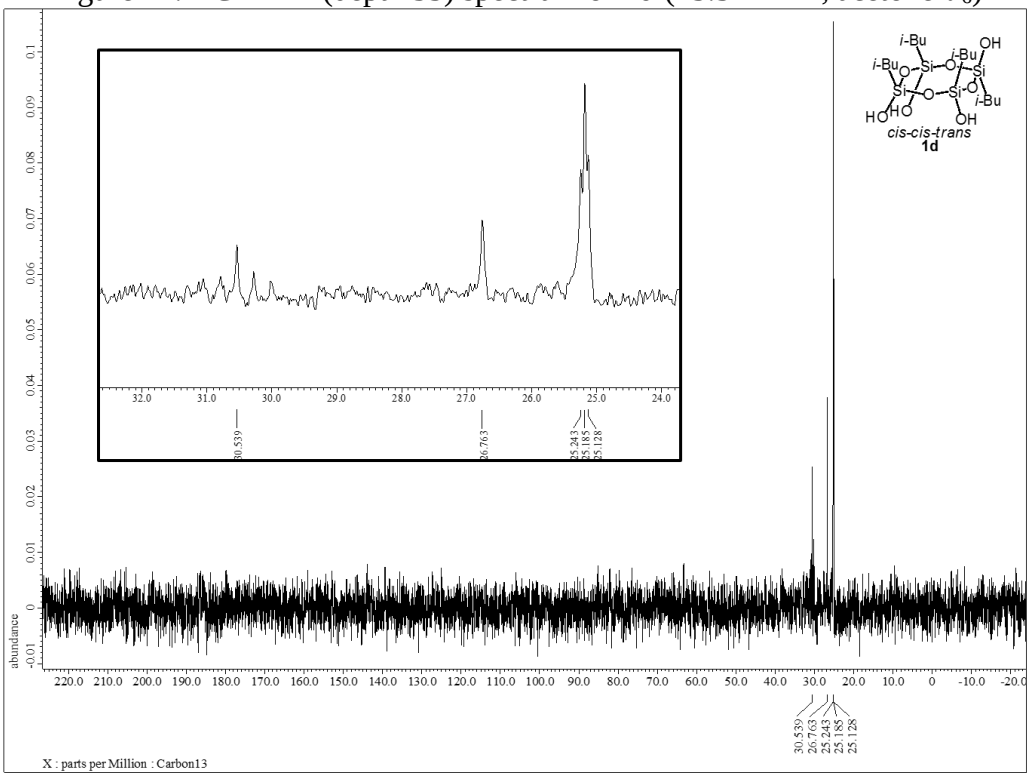

Figure 25. ^{13}C NMR (dept 90) spectrum of **1d** (75.57 MHz, acetone-d_6)

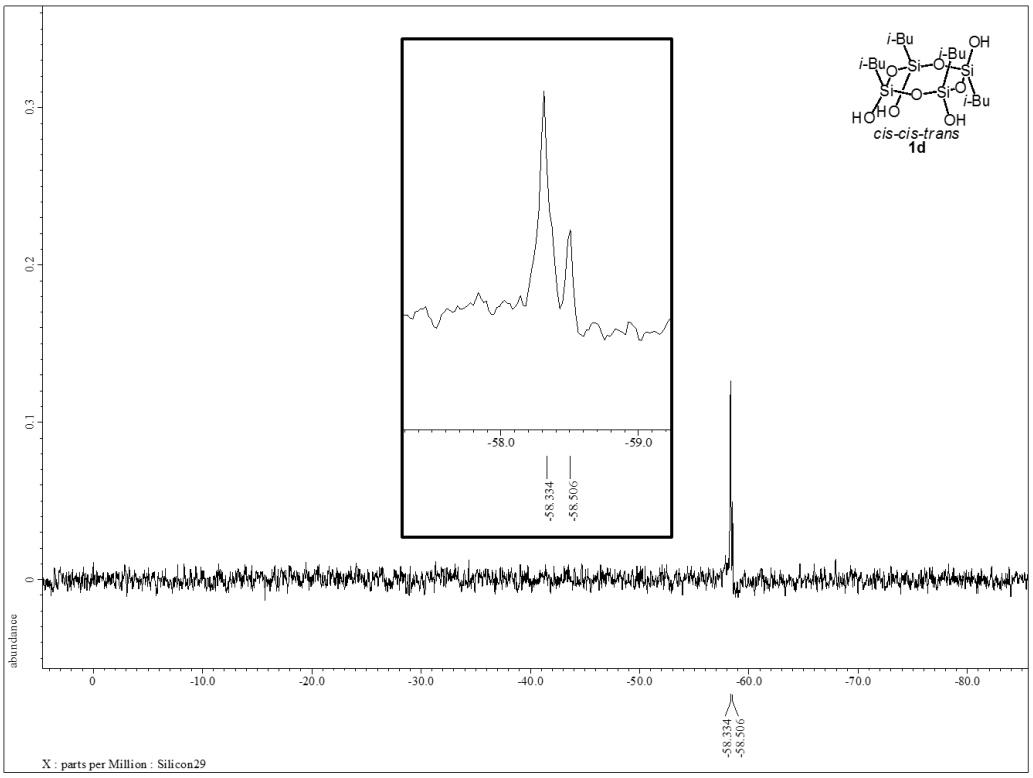

Figure 26. ^{29}Si NMR spectrum of **1d** (59.71 MHz, acetone-d_6)

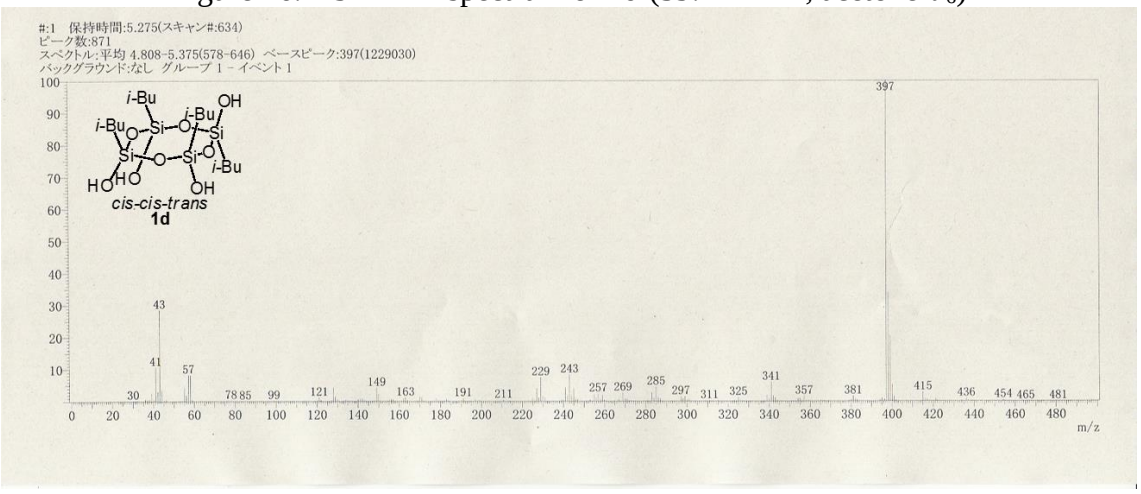

Figure 27. DIMS (EI, 70 eV) spectrum of **1d**

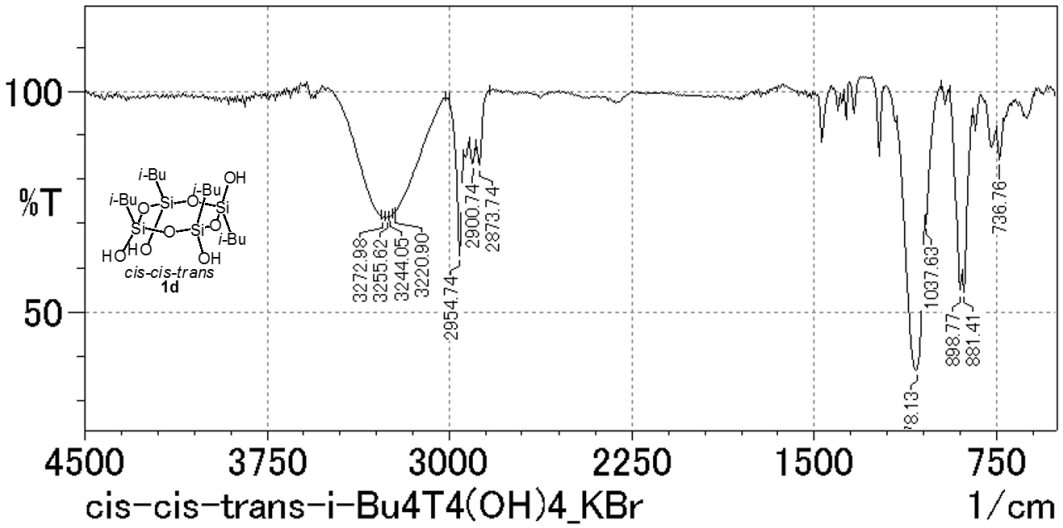

Figure 28. IR (KBr) spectrum of **1d**

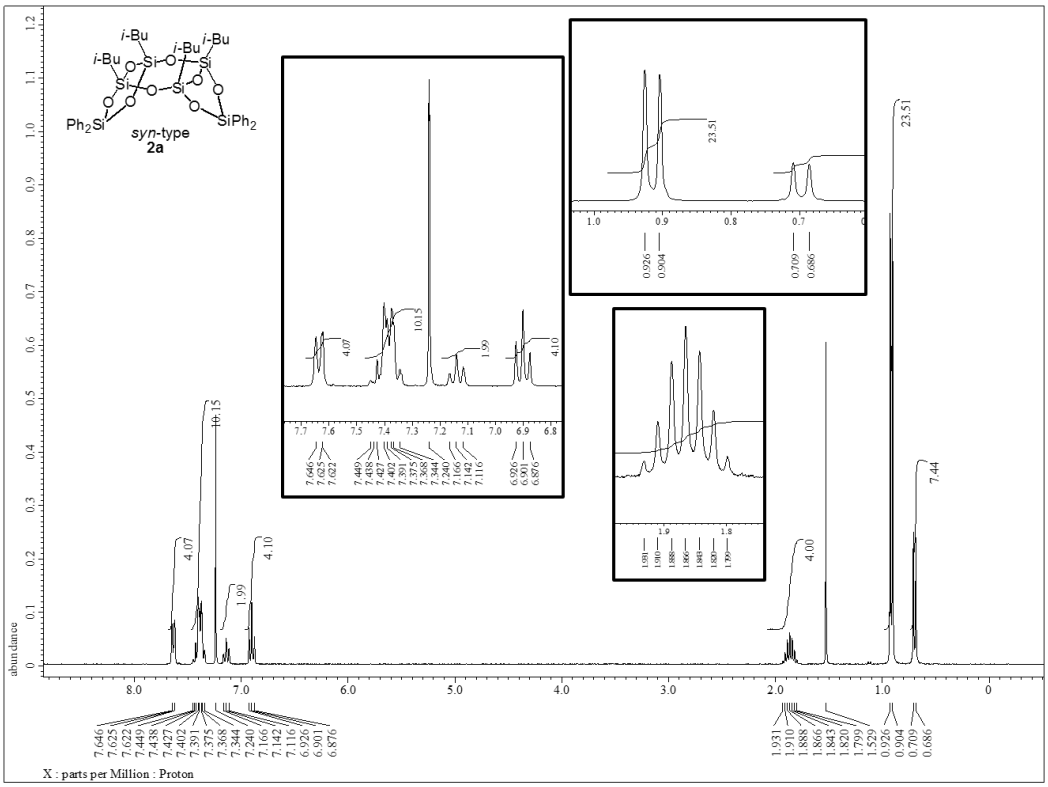

Figure 29. ^{1}H NMR spectrum of **2a** (300.53 MHz, $CDCl_3$)

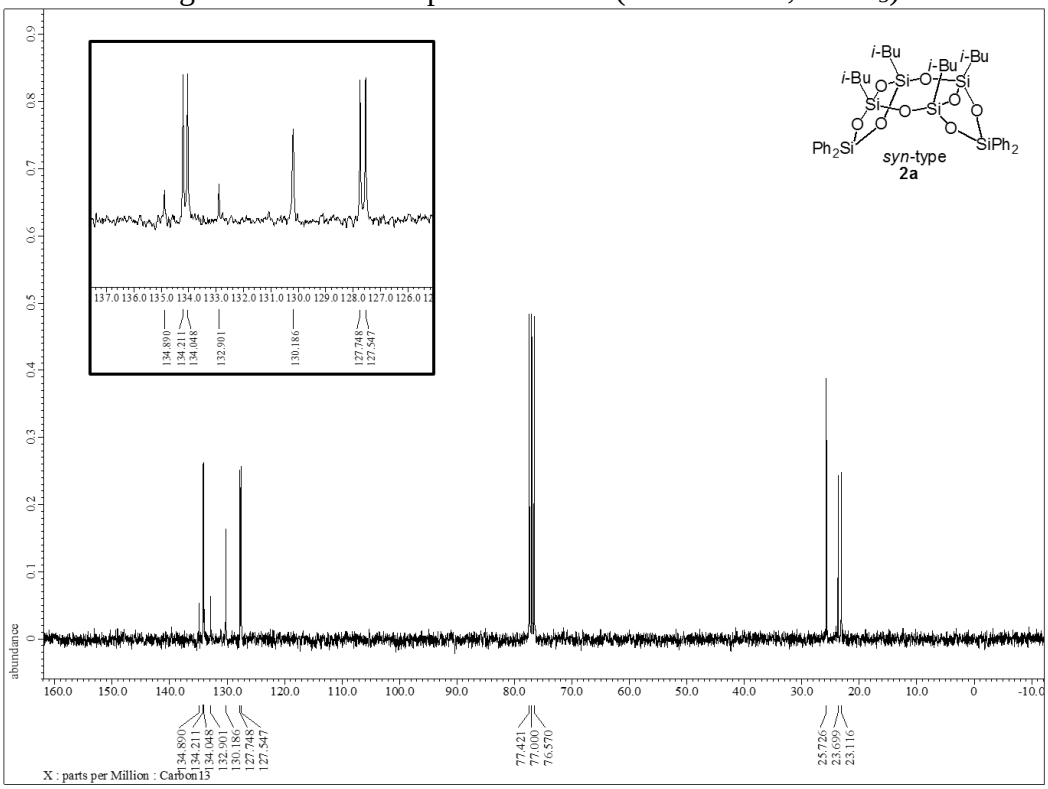

Figure 30. ^{13}C NMR spectrum of **2a** (75.57 MHz, $CDCl_3$)

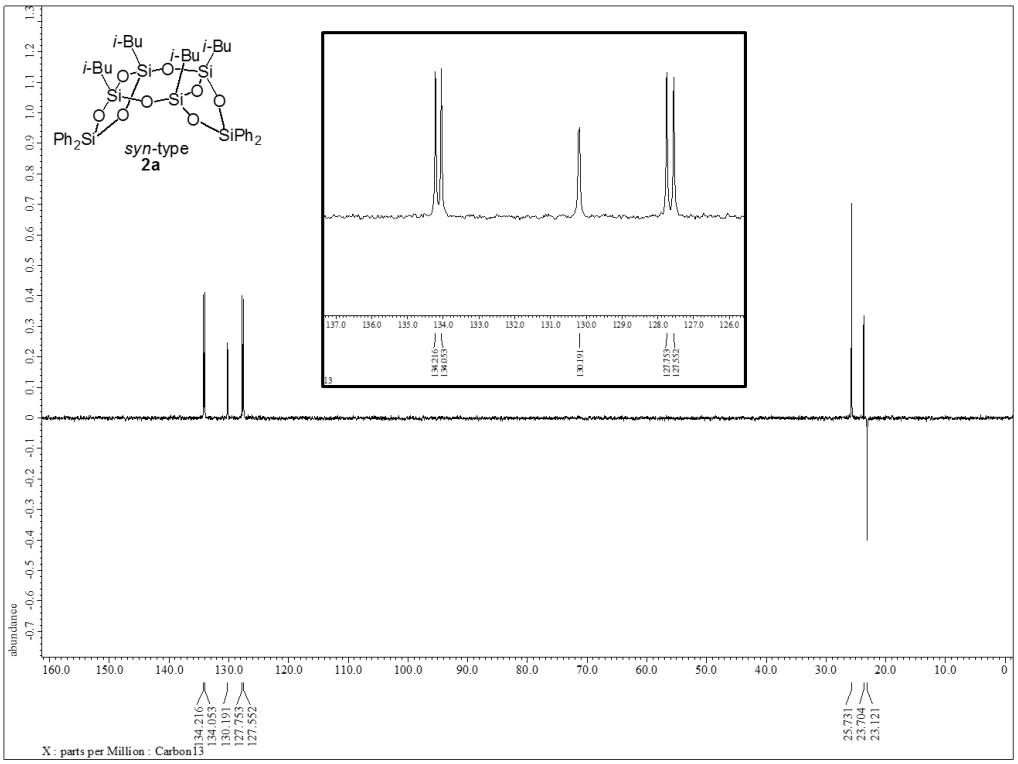

Figure 31. ^{13}C NMR (dept 135) spectrum of **2d** (75.57 MHz, $CDCl_3$)

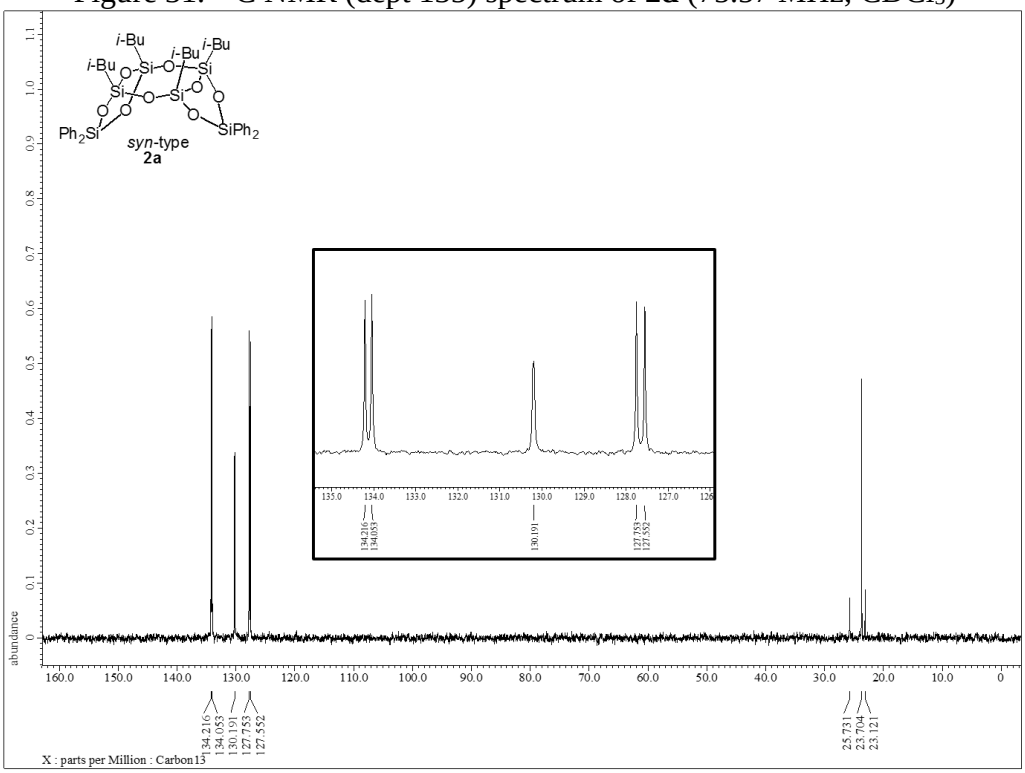

Figure 32. ^{13}C NMR (dept 90) spectrum of **2d** (75.57 MHz, $CDCl_3$)

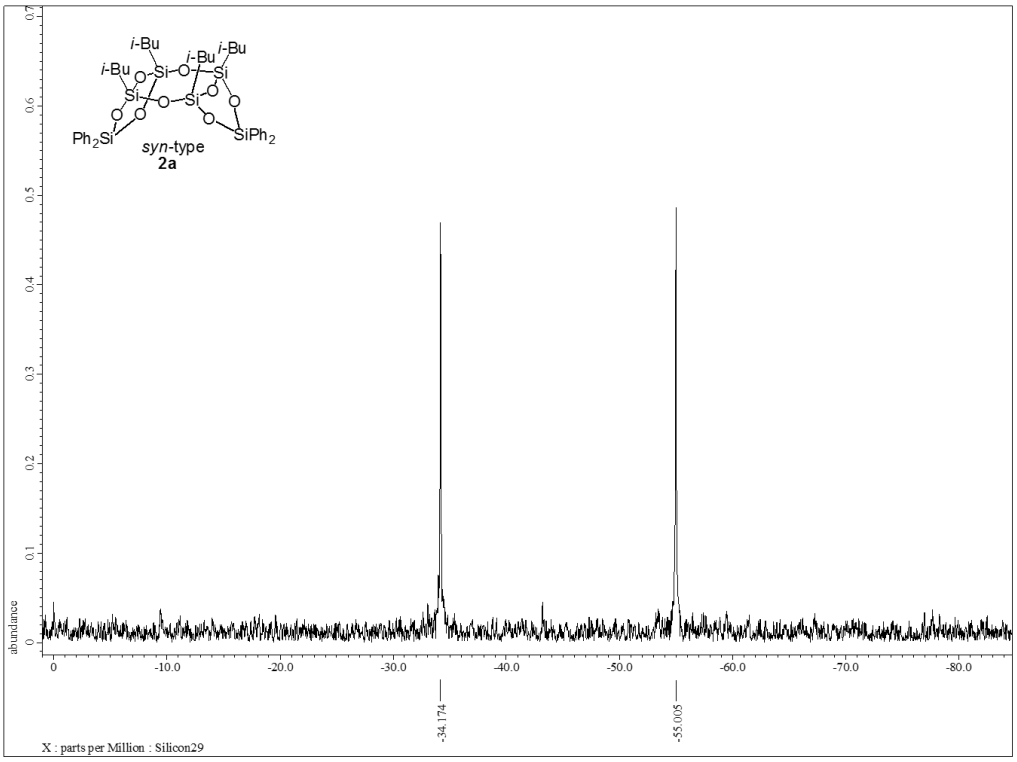

Figure 33. ^{29}Si NMR spectrum of **2a** (59.71 MHz, $CDCl_3$)

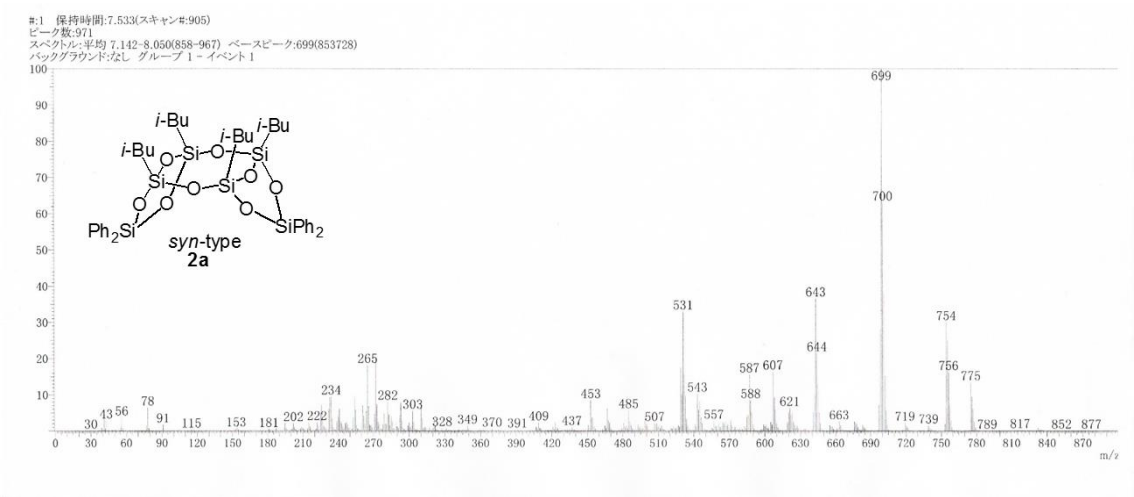

Figure 34. DIMS (EI, 70 eV) spectrum of **2a**

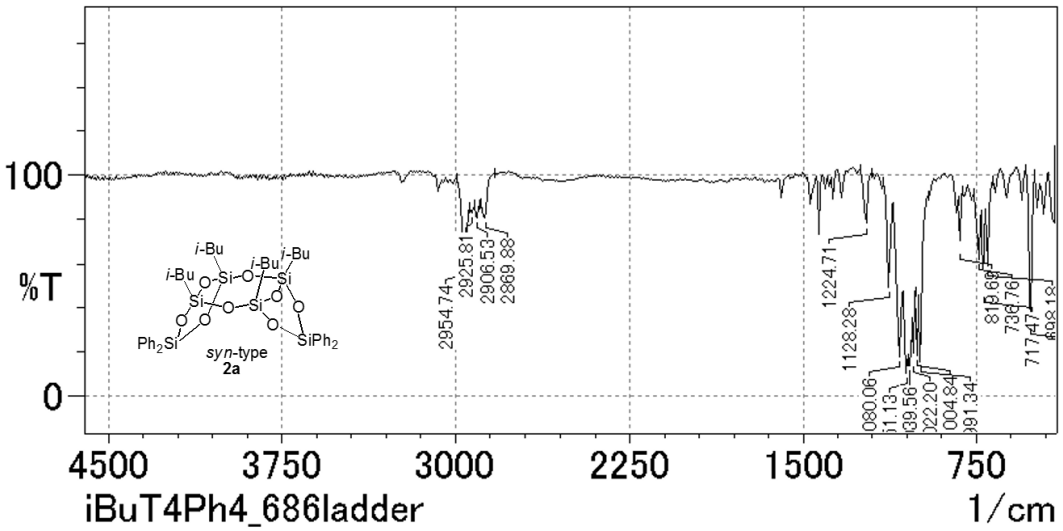

Figure 35. IR (KBr) spectrum of **2a**

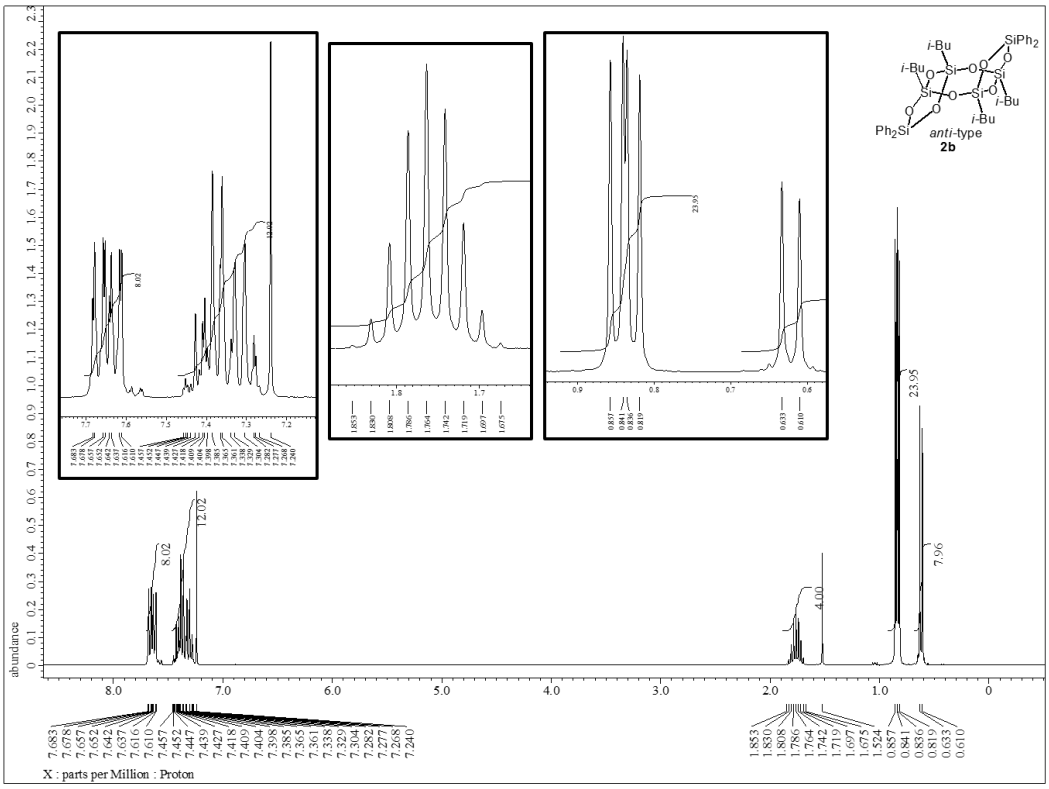

Figure 36. ^{1}H NMR spectrum of **2b** (300.53 MHz, $CDCl_3$)

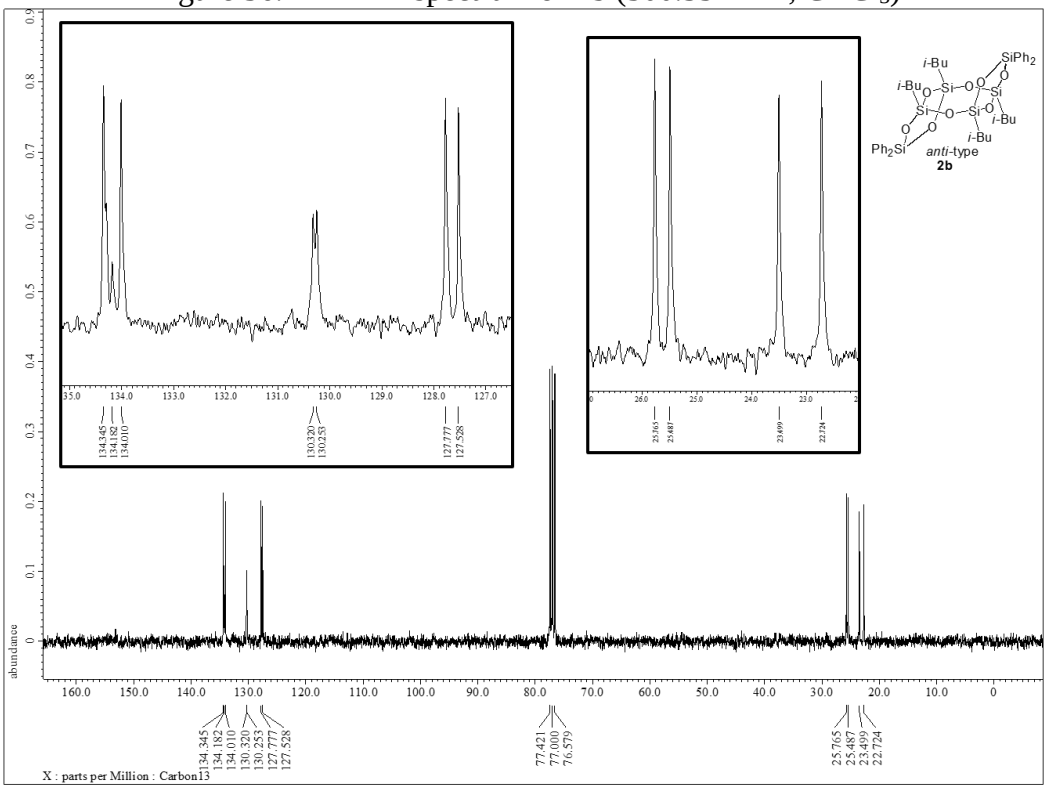

Figure 37. ^{13}C NMR spectrum of **2b** (75.57 MHz, $CDCl_3$)

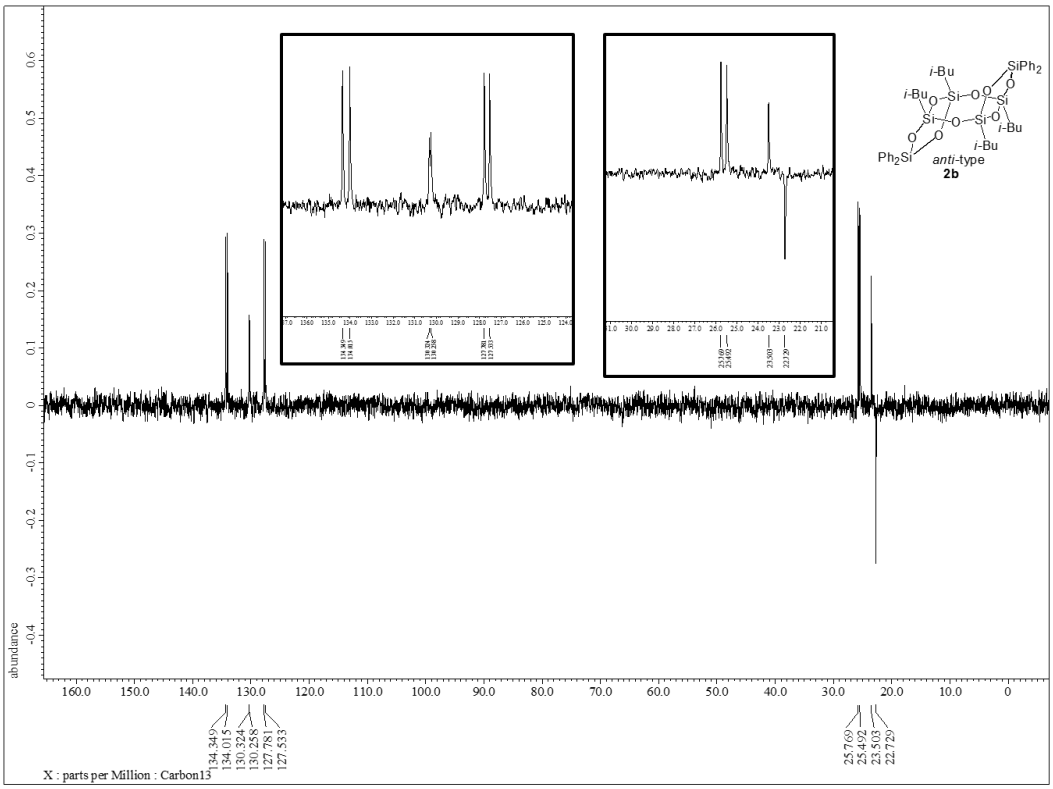

Figure 38. ^{13}C NMR (dept 135) spectrum of **2b** (75.57 MHz, $CDCl_3$)

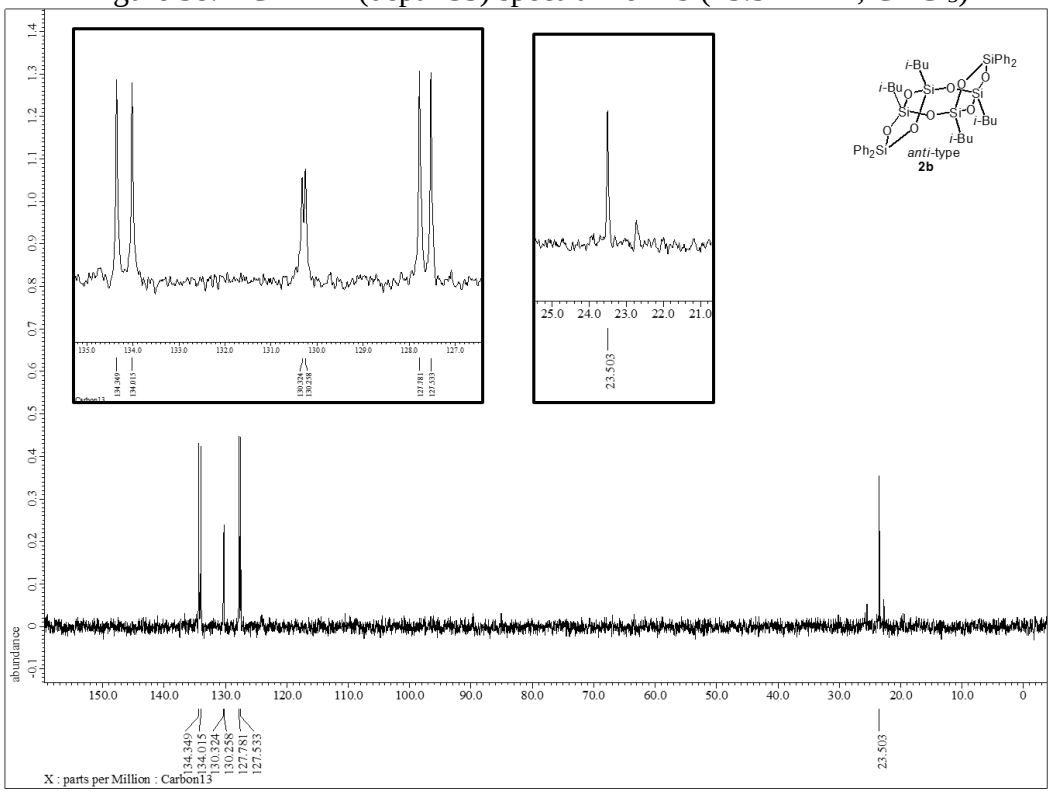

Figure 39. ^{13}C NMR (dept 90) spectrum of **2b** (75.57 MHz, $CDCl_3$)

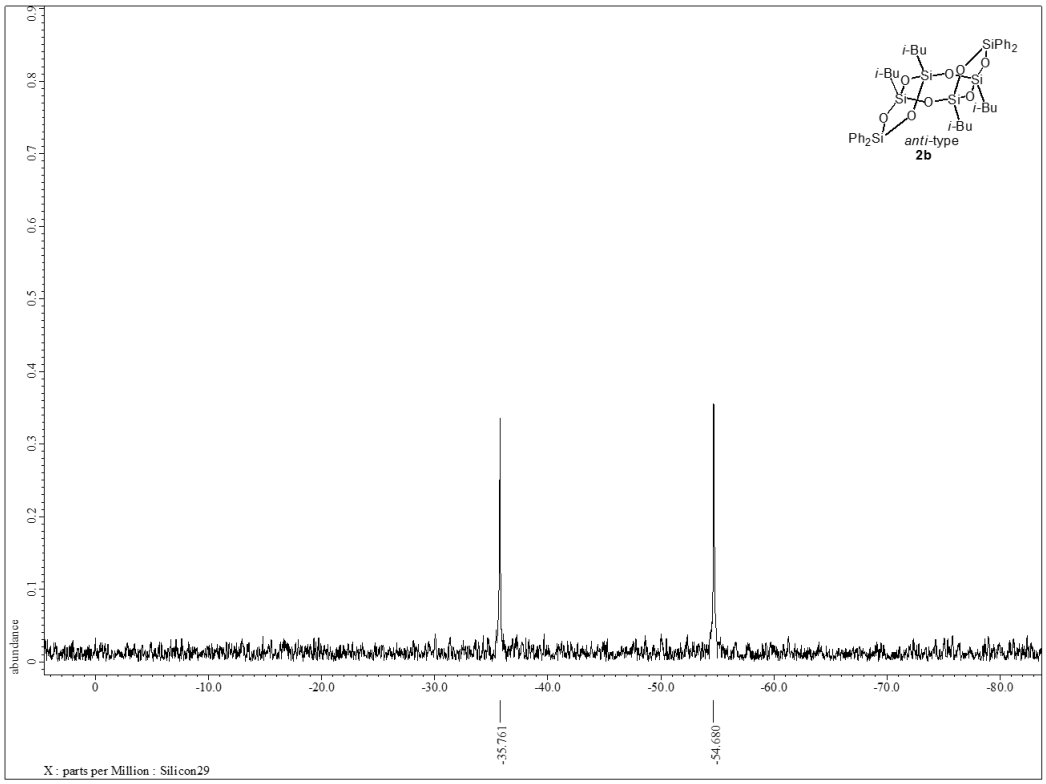

Figure 40. ^{29}Si NMR spectrum of **2b** (59.71 MHz, $CDCl_3$)

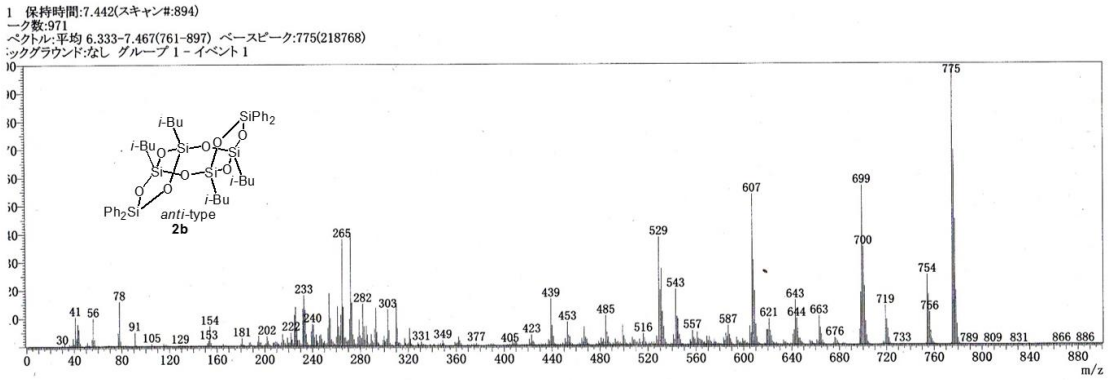

Figure 41. DIMS (EI, 70 eV) spectrum of **2b**

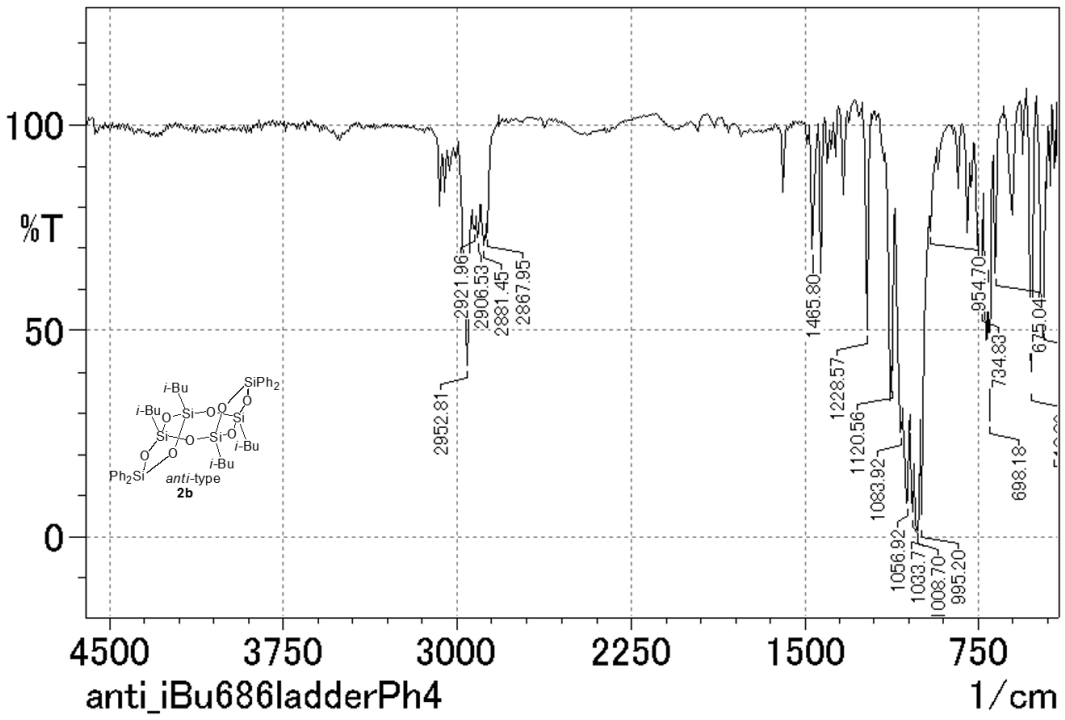

Figure 42. IR (KBr) spectrum of **2b**

2. X-ray analysis

2-1 X-ray analysis of **1b**

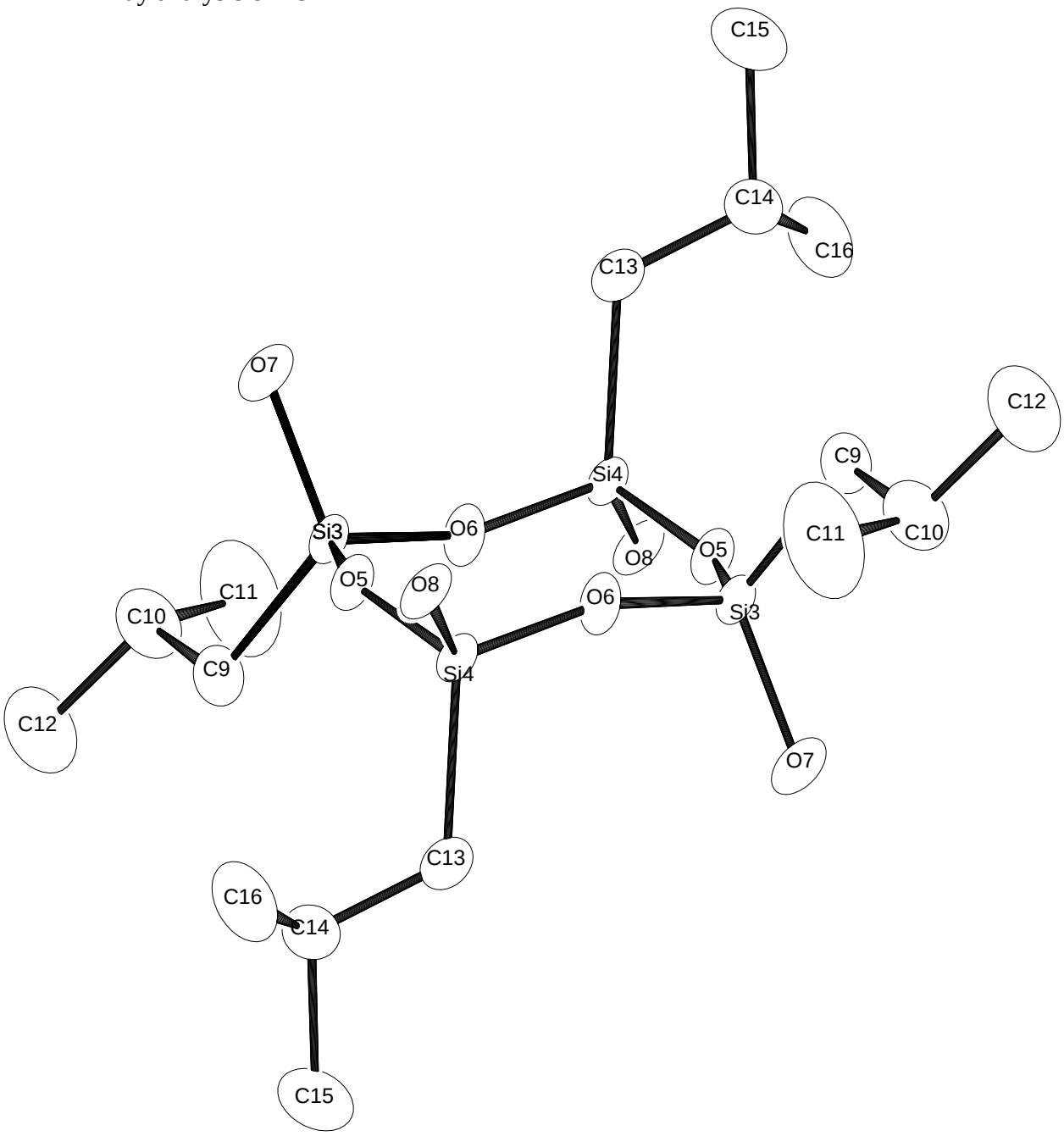

Figure 1. ORTEP drawing of **1b**.

Table 1. Crystal data and structure refinement for **1b**.

Empirical formula	$C_{16}H_{40}O_8Si_4$	
Formula weight	472.84	
Temperature	123 K	
Wavelength	0.71075 Å	
Crystal system	Triclinic	
Space group	*P* -1	
Unit cell dimensions	a = 10.332(2) Å	α = 102.023(6)°.
	b = 10.659(2) Å	β = 92.628(6)°.
	c = 12.080(3) Å	γ = 90.142(6)°.
Volume	1299.7(5) $Å^3$	
Z	2	
Density (calculated)	1.208 g/mL	
Absorption coefficient	0.263 mm^{-1}	
F(000)	512	
Crystal size	0.10 x 0.10 x 0.02 mm^3	
Theta range for data collection	2.56 to 27.50°.	
Index ranges	-13<=*h*<=13, -13<=*k*<=13, -15<=*l*<=15	
Reflections collected	42244	
Independent reflections	5945 [*R*(int) = 0.0453]	
Completeness to theta = 27.50°	99.5%	
Absorption correction	Numerical	
Max. and min. transmission	1.000 and 0.928	
Refinement method	Full-matrix least-squares on F^2	
Data / restraints / parameters	5945 / 0 / 294	
Goodness-of-fit on F^2	1.086	
Final R indices [*I*>2sigma(*I*)]	*R*1 = 0.0482, *wR*2 = 0.1142	
R indices (all data)	*R*1 = 0.0579, *wR*2 = 0.1228	
Largest diff. peak and hole	0.807 and -0.403 e.$Å^{-3}$	

Table 2. Atomic coordinates (x 10^4) and equivalent isotropic displacement parameters ($Å^2$x 10^3) for **1b**. U(eq) is defined as one third of the trace of the orthogonalized U^{ij} tensor.

	x	y	z	U(eq)
Si(1)	-1862(1)	-461(1)	3993(1)	18(1)
O(1)	-1195(1)	925(1)	3991(1)	21(1)
Si(2)	201(1)	1655(1)	4191(1)	17(1)
O(2)	1009(2)	1200(2)	5203(2)	33(1)
O(3)	-3281(1)	-146(1)	4509(2)	28(1)
O(4)	-108(1)	3172(1)	4600(2)	27(1)
C(1)	-2005(3)	-1422(2)	2524(2)	34(1)
C(2)	-3067(3)	-2489(3)	2274(2)	42(1)
C(3)	-3166(5)	-3105(4)	1011(3)	80(1)
C(4)	-2841(4)	-3486(3)	2983(3)	56(1)
C(5)	1130(3)	1331(2)	2902(2)	37(1)
C(6A)	100(30)	1720(18)	1790(20)	26(5)
C(6B)	469(11)	1312(15)	1772(5)	66(3)
C(7A)	900(30)	1360(30)	720(30)	52(7)
C(7B)	1410(15)	917(18)	807(7)	131(6)
C(8A)	-370(20)	3058(17)	1950(20)	26(5)
C(8B)	-101(11)	2617(19)	1748(11)	94(5)
Si(3)	-3118(1)	4981(1)	5974(1)	17(1)
O(5)	-3781(1)	6371(1)	6001(1)	21(1)
Si(4)	-5163(1)	7032(1)	5808(1)	17(1)
O(6)	-5955(1)	6151(1)	4736(1)	23(1)
O(7)	-1774(1)	5040(1)	5330(1)	25(1)
O(8)	-4821(1)	8405(1)	5488(1)	22(1)
C(9)	-2808(2)	4746(2)	7437(2)	28(1)
C(10)	-1776(3)	3739(3)	7593(2)	40(1)
C(11)	-2191(4)	2399(3)	7020(3)	72(1)
C(12)	-1396(4)	3833(4)	8840(3)	59(1)
C(13)	-6120(2)	7232(2)	7088(2)	26(1)
C(14)	-5403(3)	7766(3)	8231(2)	35(1)
C(15)	-6245(4)	7666(4)	9217(3)	65(1)
C(16)	-4938(4)	9141(3)	8324(3)	58(1)

Table 3. Bond lengths [Å] for **1b**.

Si(1)-O(2)#1	1.6082(16)	C(6B)-C(7B)	1.544(9)
Si(1)-O(3)	1.6276(15)	Si(3)-O(6)#2	1.6118(15)
Si(1)-O(1)	1.6289(14)	Si(3)-O(5)	1.6290(15)
Si(1)-C(1)	1.855(3)	Si(3)-O(7)	1.6293(15)
O(1)-Si(2)	1.6211(15)	Si(3)-C(9)	1.849(2)
Si(2)-O(2)	1.6074(16)	O(5)-Si(4)	1.6225(15)
Si(2)-O(4)	1.6261(15)	Si(4)-O(6)	1.6184(15)
Si(2)-C(5)	1.838(2)	Si(4)-O(8)	1.6313(14)
O(2)-Si(1)#1	1.6082(16)	Si(4)-C(13)	1.849(2)
C(1)-C(2)	1.552(3)	O(6)-Si(3)#2	1.6118(15)
C(2)-C(4)	1.510(4)	C(9)-C(10)	1.549(3)
C(2)-C(3)	1.529(4)	C(10)-C(11)	1.504(4)
C(5)-C(6B)	1.494(10)	C(10)-C(12)	1.522(4)
C(5)-C(6A)	1.79(3)	C(13)-C(14)	1.535(3)
C(6A)-C(8A)	1.48(2)	C(14)-C(16)	1.522(4)
C(6A)-C(7A)	1.55(3)	C(14)-C(15)	1.527(4)
C(6B)-C(8B)	1.517(10)		

Symmetry transformations used to generate equivalent atoms:
#1 -x,-y,-z+1 #2 -x-1,-y+1,-z+1

Table 4. Bond angles [°] for **1b**.

O(2)#1-Si(1)-O(3)	109.63(9)	O(1)-Si(2)-O(4)	105.90(8)
O(2)#1-Si(1)-O(1)	109.90(8)	O(2)-Si(2)-C(5)	109.70(12)
O(3)-Si(1)-O(1)	105.82(8)	O(1)-Si(2)-C(5)	111.68(10)
O(2)#1-Si(1)-C(1)	110.62(11)	O(4)-Si(2)-C(5)	112.05(10)
O(3)-Si(1)-C(1)	111.29(11)	Si(2)-O(2)-Si(1)#1	167.29(13)
O(1)-Si(1)-C(1)	109.46(10)	C(2)-C(1)-Si(1)	116.46(18)
Si(2)-O(1)-Si(1)	141.07(10)	C(4)-C(2)-C(3)	111.1(3)
O(2)-Si(2)-O(1)	109.27(8)	C(4)-C(2)-C(1)	111.9(2)
O(2)-Si(2)-O(4)	108.09(10)	C(3)-C(2)-C(1)	110.6(3)

C(6B)-C(5)-C(6A)	17.5(7)	O(6)-Si(4)-O(5)	109.07(8)
C(6B)-C(5)-Si(2)	120.2(5)	O(6)-Si(4)-O(8)	108.40(8)
C(6A)-C(5)-Si(2)	106.6(8)	O(5)-Si(4)-O(8)	105.93(8)
C(8A)-C(6A)-C(7A)	111.2(19)	O(6)-Si(4)-C(13)	110.25(9)
C(8A)-C(6A)-C(5)	117.5(19)	O(5)-Si(4)-C(13)	111.08(9)
C(7A)-C(6A)-C(5)	104.1(16)	O(8)-Si(4)-C(13)	111.96(9)
C(5)-C(6B)-C(8B)	109.9(6)	Si(3)#2-O(6)-Si(4)	159.34(11)
C(5)-C(6B)-C(7B)	111.2(6)	C(10)-C(9)-Si(3)	116.13(17)
C(8B)-C(6B)-C(7B)	110.6(7)	C(11)-C(10)-C(12)	111.8(3)
O(6)#2-Si(3)-O(5)	110.27(8)	C(11)-C(10)-C(9)	112.4(3)
O(6)#2-Si(3)-O(7)	109.98(8)	C(12)-C(10)-C(9)	111.2(2)
O(5)-Si(3)-O(7)	104.72(8)	C(14)-C(13)-Si(4)	117.06(16)
O(6)#2-Si(3)-C(9)	110.24(10)	C(16)-C(14)-C(15)	110.7(3)
O(5)-Si(3)-C(9)	109.87(9)	C(16)-C(14)-C(13)	111.9(2)
O(7)-Si(3)-C(9)	111.64(10)	C(15)-C(14)-C(13)	111.1(2)
Si(4)-O(5)-Si(3)	142.00(9)		

Symmetry transformations used to generate equivalent atoms:
#1 -x,-y,-z+1 #2 -x-1,-y+1,-z+1

Table 5. Anisotropic displacement parameters ($Å^2 x 10^3$) for **1b**. The anisotropic displacement factor exponent takes the form: $-2 \pi^2 [h^2 a^{*2} U^{11} + ... + 2 h k a^* b^* U^{12}]$

	U^{11}	U^{22}	U^{33}	U^{23}	U^{13}	U^{12}
Si(1)	14(1)	14(1)	27(1)	9(1)	2(1)	-1(1)
O(1)	17(1)	17(1)	33(1)	12(1)	0(1)	-3(1)
Si(2)	14(1)	11(1)	26(1)	7(1)	3(1)	0(1)
O(2)	26(1)	27(1)	52(1)	24(1)	-14(1)	-9(1)
O(3)	21(1)	18(1)	49(1)	14(1)	13(1)	1(1)
O(4)	17(1)	13(1)	53(1)	9(1)	10(1)	0(1)
C(1)	39(1)	29(1)	33(1)	5(1)	7(1)	-8(1)
C(2)	57(2)	29(1)	38(1)	4(1)	-2(1)	-12(1)
C(3)	125(4)	61(2)	46(2)	-3(2)	-11(2)	-37(2)
C(4)	75(2)	32(2)	61(2)	10(1)	-4(2)	-14(2)
C(5)	37(1)	33(1)	38(1)	-6(1)	19(1)	-16(1)

C(6A)	35(11)	16(9)	29(8)	6(6)	20(7)	4(6)
C(6B)	53(5)	113(8)	24(2)	-5(4)	7(3)	-59(5)
C(7A)	43(13)	60(14)	50(11)	2(8)	18(10)	-23(9)
C(7B)	92(8)	247(14)	31(3)	-29(6)	31(4)	-97(9)
C(8A)	23(8)	16(9)	44(9)	16(6)	0(6)	1(5)
C(8B)	60(5)	174(13)	69(6)	84(8)	-28(4)	-36(7)
Si(3)	13(1)	12(1)	26(1)	4(1)	1(1)	0(1)
O(5)	16(1)	13(1)	32(1)	3(1)	1(1)	1(1)
Si(4)	14(1)	10(1)	27(1)	5(1)	3(1)	-1(1)
O(6)	20(1)	15(1)	33(1)	4(1)	-4(1)	-2(1)
O(7)	18(1)	13(1)	45(1)	7(1)	9(1)	2(1)
O(8)	16(1)	12(1)	41(1)	9(1)	7(1)	1(1)
C(9)	32(1)	24(1)	28(1)	5(1)	0(1)	3(1)
C(10)	51(2)	37(1)	33(1)	13(1)	1(1)	18(1)
C(11)	105(3)	32(2)	77(3)	14(2)	-22(2)	17(2)
C(12)	71(2)	69(2)	43(2)	23(2)	-7(2)	18(2)
C(13)	23(1)	23(1)	33(1)	10(1)	7(1)	1(1)
C(14)	34(1)	41(1)	29(1)	4(1)	7(1)	7(1)
C(15)	70(2)	93(3)	33(2)	9(2)	15(2)	-9(2)
C(16)	74(2)	55(2)	37(2)	-8(1)	-1(2)	-17(2)

Table 6. Torsion angles [°] for **1b**.

O(2)#1-Si(1)-O(1)-Si(2)	25.32(19)
O(3)-Si(1)-O(1)-Si(2)	143.61(16)
C(1)-Si(1)-O(1)-Si(2)	-96.37(18)
Si(1)-O(1)-Si(2)-O(2)	-37.44(19)
Si(1)-O(1)-Si(2)-O(4)	-153.65(16)
Si(1)-O(1)-Si(2)-C(5)	84.11(19)
O(1)-Si(2)-O(2)-Si(1)#1	75.3(5)
O(4)-Si(2)-O(2)-Si(1)#1	-169.9(5)
C(5)-Si(2)-O(2)-Si(1)#1	-47.5(5)
O(2)#1-Si(1)-C(1)-C(2)	82.5(2)
O(3)-Si(1)-C(1)-C(2)	-39.6(2)
O(1)-Si(1)-C(1)-C(2)	-156.21(19)
Si(1)-C(1)-C(2)-C(4)	-61.3(3)
Si(1)-C(1)-C(2)-C(3)	174.1(3)
O(2)-Si(2)-C(5)-C(6B)	162.6(7)
O(1)-Si(2)-C(5)-C(6B)	41.3(7)
O(4)-Si(2)-C(5)-C(6B)	-77.3(7)
O(2)-Si(2)-C(5)-C(6A)	174.6(7)
O(1)-Si(2)-C(5)-C(6A)	53.3(7)
O(4)-Si(2)-C(5)-C(6A)	-65.4(7)
C(6B)-C(5)-C(6A)-C(8A)	-157(5)
Si(2)-C(5)-C(6A)-C(8A)	59.6(19)
C(6B)-C(5)-C(6A)-C(7A)	-33(3)
Si(2)-C(5)-C(6A)-C(7A)	-176.9(13)
C(6A)-C(5)-C(6B)-C(8B)	20(3)
Si(2)-C(5)-C(6B)-C(8B)	61.7(6)
C(6A)-C(5)-C(6B)-C(7B)	143(4)
Si(2)-C(5)-C(6B)-C(7B)	-175.5(5)
O(6)#2-Si(3)-O(5)-Si(4)	18.58(19)
O(7)-Si(3)-O(5)-Si(4)	136.84(16)
C(9)-Si(3)-O(5)-Si(4)	-103.14(18)
Si(3)-O(5)-Si(4)-O(6)	-39.53(19)
Si(3)-O(5)-Si(4)-O(8)	-156.02(16)
Si(3)-O(5)-Si(4)-C(13)	82.19(18)

O(5)-Si(4)-O(6)-Si(3)#2	84.6(3)
O(8)-Si(4)-O(6)-Si(3)#2	-160.5(3)
C(13)-Si(4)-O(6)-Si(3)#2	-37.6(3)
O(6)#2-Si(3)-C(9)-C(10)	79.1(2)
O(5)-Si(3)-C(9)-C(10)	-159.17(18)
O(7)-Si(3)-C(9)-C(10)	-43.5(2)
Si(3)-C(9)-C(10)-C(11)	-66.1(3)
Si(3)-C(9)-C(10)-C(12)	167.7(2)
O(6)-Si(4)-C(13)-C(14)	166.07(16)
O(5)-Si(4)-C(13)-C(14)	45.04(19)
O(8)-Si(4)-C(13)-C(14)	-73.17(19)
Si(4)-C(13)-C(14)-C(16)	65.3(3)
Si(4)-C(13)-C(14)-C(15)	-170.4(2)

Symmetry transformations used to generate equivalent atoms:

#1 -x,-y,-z+1 #2 -x-1,-y+1,-z+1

2-2 X-ray analysis of **2a**

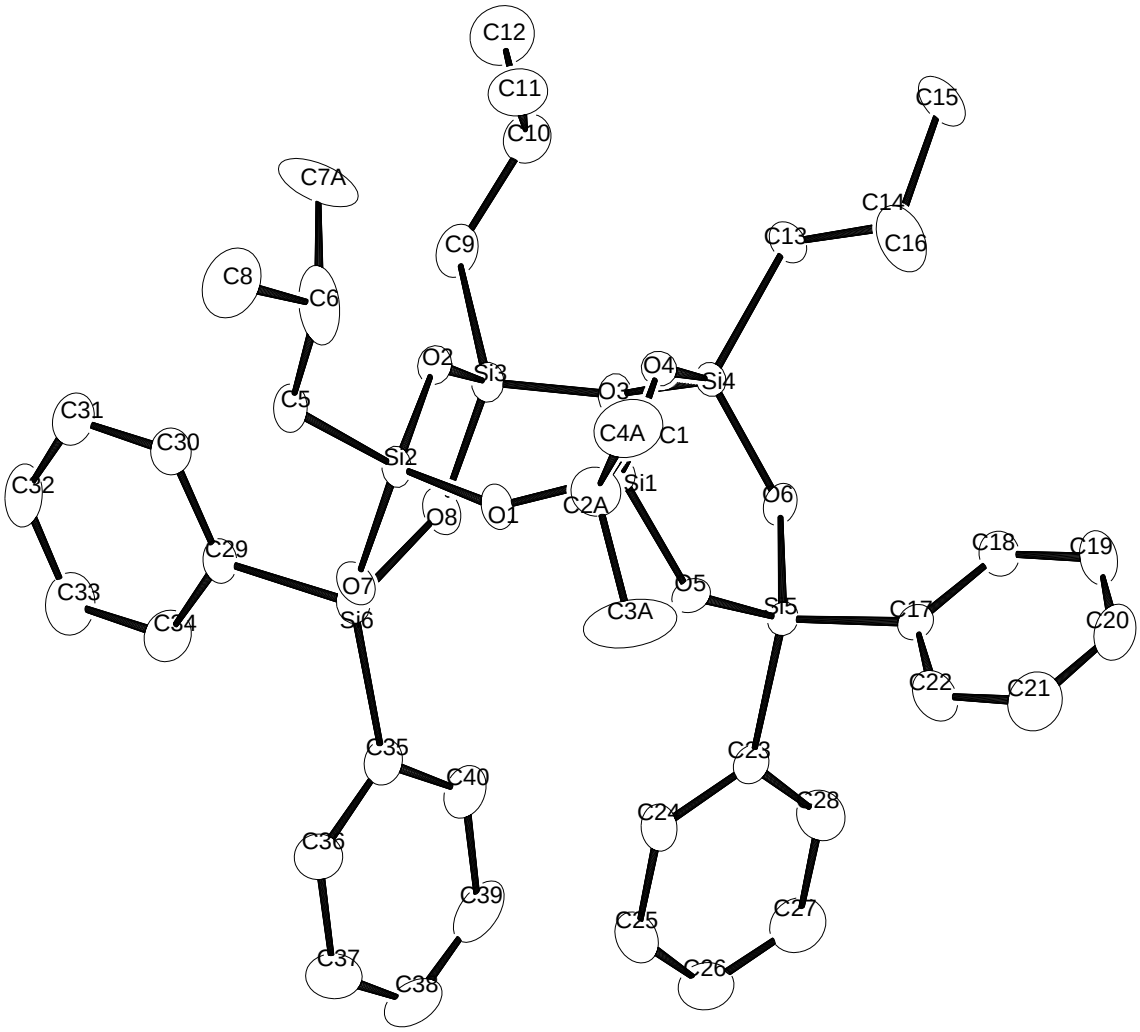

Figure 1. ORTEP drawing of **2a**.

Table 1. Crystal data and structure refinement for **2a**.

Empirical formula	$C_{40}H_{56}O_8Si_6$	
Formula weight	833.39	
Temperature	173(2) K	
Wavelength	0.71070 Å	
Crystal system	Monoclinic	
Space group	P 21	
Unit cell dimensions	a = 14.1890(16) Å	α = 90.0000(10)°.
	b = 10.6638(11) Å	β = 94.6151(11)°.
	c = 14.9667(15) Å	γ =90.0000(10)°.
Volume	2257.2(4) $Å^3$	
Z	2	
Density (calculated)	1.226 g/mL	
Absorption coefficient	0.232 mm^{-1}	
F(000)	888	
Crystal size	0.40 x 0.40 x 0.40 mm^3	
Theta range for data collection	2.39 to 25.50°.	
Index ranges	-17<=h<=16, -12<=k<=12, -18<=l<=18	
Reflections collected	15484	
Independent reflections	8360 [R(int) = 0.0527]	
Completeness to theta = 25.50°	99.8%	
Absorption correction	Semi-empirical from equivalents	
Max. and min. transmission	1.0000 and 0.4195	
Refinement method	Full-matrix least-squares on F^2	
Data / restraints / parameters	8360 / 7 / 524	
Goodness-of-fit on F^2	1.030	
Final R indices [I>2sigma(I)]	R1 = 0.0376, wR2 = 0.0905	
R indices (all data)	R1 = 0.0379, wR2 = 0.0908	
Absolute structure parameter	0.02(7)	
Largest diff. peak and hole	0.288 and -0.424 e.$Å^{-3}$	

Table 2. Atomic coordinates (x 10^4) and equivalent isotropic displacement parameters ($Å^2$x 10^3) for **2a**. U(eq) is defined as one third of the trace of the orthogonalized U^{ij} tensor.

	x	y	z	U(eq)
Si(1)	8452(1)	5527(1)	3258(1)	14(1)
O(1)	7454(1)	5129(1)	3643(1)	20(1)
Si(2)	6448(1)	5709(1)	3895(1)	16(1)
O(2)	6404(1)	7189(1)	3614(1)	17(1)
Si(3)	6080(1)	7854(1)	2653(1)	16(1)
O(3)	6974(1)	7932(2)	2041(1)	18(1)
Si(4)	8115(1)	7746(1)	2086(1)	15(1)
O(4)	8444(1)	7021(1)	3025(1)	17(1)
O(5)	8553(1)	4797(2)	2313(1)	21(1)
Si(5)	8632(1)	5317(1)	1291(1)	16(1)
O(6)	8353(1)	6809(2)	1274(1)	20(1)
O(7)	5586(1)	5034(2)	3288(1)	21(1)
Si(6)	4817(1)	5634(1)	2528(1)	19(1)
O(8)	5293(1)	6918(2)	2157(1)	23(1)
C(1)	9458(2)	5202(2)	4078(2)	23(1)
C(2A)	9520(3)	3960(3)	4562(2)	29(1)
C(3A)	9534(7)	2865(9)	3922(6)	67(3)
C(4A)	10426(4)	3947(5)	5200(3)	45(1)
C(2B)	9896(5)	3813(9)	4018(6)	31(3)
C(3B)	9143(11)	2851(17)	4056(17)	52(5)
C(4B)	10719(7)	3620(14)	4722(11)	59(4)
C(5)	6314(2)	5489(2)	5100(1)	23(1)
C(6)	7112(2)	5980(4)	5754(2)	59(1)
C(7A)	6895(18)	7507(9)	5794(6)	92(6)
C(7B)	7445(14)	7188(19)	5685(11)	101(7)
C(8)	7010(2)	5512(4)	6706(2)	53(1)
C(9)	5630(2)	9451(2)	2823(2)	28(1)
C(10)	6408(2)	10447(3)	3001(2)	35(1)
C(11)	7056(2)	10145(3)	3834(2)	45(1)
C(12)	5994(3)	11757(3)	3085(3)	57(1)
C(13)	8693(2)	9289(2)	2034(2)	24(1)

C(14)	9727(2)	9371(2)	1814(2)	30(1)
C(15)	10055(2)	10735(3)	1877(2)	44(1)
C(16)	10381(2)	8545(3)	2393(2)	46(1)
C(17)	9862(1)	5179(2)	963(1)	20(1)
C(18)	10328(2)	6176(2)	592(2)	27(1)
C(19)	11250(2)	6054(3)	344(2)	37(1)
C(20)	11710(2)	4918(3)	459(2)	38(1)
C(21)	11271(2)	3919(3)	812(2)	44(1)
C(22)	10350(2)	4050(3)	1071(2)	35(1)
C(23)	7795(2)	4389(2)	548(1)	21(1)
C(24)	7189(2)	3521(3)	888(2)	31(1)
C(25)	6572(2)	2821(3)	325(2)	42(1)
C(26)	6549(2)	2974(3)	-591(2)	41(1)
C(27)	7143(2)	3829(3)	-944(2)	43(1)
C(28)	7767(2)	4528(3)	-382(2)	36(1)
C(29)	3710(2)	6046(2)	3058(1)	20(1)
C(30)	3730(2)	6728(3)	3858(2)	29(1)
C(31)	2899(2)	7067(3)	4230(2)	35(1)
C(32)	2040(2)	6730(3)	3809(2)	38(1)
C(33)	1998(2)	6059(3)	3020(2)	46(1)
C(34)	2830(2)	5723(3)	2649(2)	36(1)
C(35)	4528(2)	4545(2)	1583(2)	24(1)
C(36)	4114(2)	3388(3)	1737(2)	31(1)
C(37)	3823(2)	2582(3)	1040(2)	40(1)
C(38)	3919(2)	2935(3)	168(2)	40(1)
C(39)	4331(2)	4063(3)	-3(2)	43(1)
C(40)	4641(2)	4866(3)	696(2)	31(1)

Table 3. Bond lengths [Å] for **2a**.

Si(1)-O(1)	1.6267(14)	C(6)-C(8)	1.527(4)
Si(1)-O(5)	1.6304(15)	C(6)-C(7A)	1.660(13)
Si(1)-O(4)	1.6310(15)	C(9)-C(10)	1.539(4)
Si(1)-C(1)	1.839(2)	C(10)-C(11)	1.522(4)
O(1)-Si(2)	1.6280(15)	C(10)-C(12)	1.525(4)
Si(2)-O(7)	1.6311(15)	C(13)-C(14)	1.533(3)
Si(2)-O(2)	1.6330(16)	C(14)-C(16)	1.502(4)
Si(2)-C(5)	1.844(2)	C(14)-C(15)	1.527(4)
O(2)-Si(3)	1.6360(14)	C(17)-C(18)	1.391(3)
Si(3)-O(3)	1.6246(14)	C(17)-C(22)	1.391(3)
Si(3)-O(8)	1.6310(16)	C(18)-C(19)	1.394(3)
Si(3)-C(9)	1.844(3)	C(19)-C(20)	1.380(4)
O(3)-Si(4)	1.6271(14)	C(20)-C(21)	1.362(4)
Si(4)-O(6)	1.6297(15)	C(21)-C(22)	1.399(4)
Si(4)-O(4)	1.6384(14)	C(23)-C(24)	1.387(3)
Si(4)-C(13)	1.843(2)	C(23)-C(28)	1.397(3)
O(5)-Si(5)	1.6400(15)	C(24)-C(25)	1.384(4)
Si(5)-O(6)	1.6391(16)	C(25)-C(26)	1.379(4)
Si(5)-C(23)	1.848(2)	C(26)-C(27)	1.376(4)
Si(5)-C(17)	1.857(2)	C(27)-C(28)	1.389(4)
O(7)-Si(6)	1.6409(15)	C(29)-C(34)	1.388(3)
Si(6)-O(8)	1.6431(17)	C(29)-C(30)	1.399(3)
Si(6)-C(35)	1.850(2)	C(30)-C(31)	1.392(3)
Si(6)-C(29)	1.869(2)	C(31)-C(32)	1.375(4)
C(1)-C(2A)	1.509(4)	C(32)-C(33)	1.378(4)
C(1)-C(2B)	1.612(9)	C(33)-C(34)	1.390(3)
C(2A)-C(3A)	1.511(9)	C(35)-C(40)	1.394(3)
C(2A)-C(4A)	1.539(5)	C(35)-C(36)	1.394(4)
C(2B)-C(3B)	1.485(16)	C(36)-C(37)	1.388(4)
C(2B)-C(4B)	1.523(11)	C(37)-C(38)	1.375(4)
C(5)-C(6)	1.529(3)	C(38)-C(39)	1.370(5)
C(6)-C(7B)	1.379(14)	C(39)-C(40)	1.396(4)

Table 4. Bond angles [°] for **2a**.

O(1)-Si(1)-O(5)	108.82(8)	C(23)-Si(5)-C(17)	111.78(9)
O(1)-Si(1)-O(4)	109.88(8)	Si(4)-O(6)-Si(5)	130.38(10)
O(5)-Si(1)-O(4)	106.28(8)	Si(2)-O(7)-Si(6)	129.85(10)
O(1)-Si(1)-C(1)	111.39(9)	O(7)-Si(6)-O(8)	106.91(8)
O(5)-Si(1)-C(1)	111.79(10)	O(7)-Si(6)-C(35)	112.30(10)
O(4)-Si(1)-C(1)	108.55(9)	O(8)-Si(6)-C(35)	109.68(10)
Si(1)-O(1)-Si(2)	141.91(10)	O(7)-Si(6)-C(29)	109.42(9)
O(1)-Si(2)-O(7)	109.61(8)	O(8)-Si(6)-C(29)	109.26(10)
O(1)-Si(2)-O(2)	108.90(8)	C(35)-Si(6)-C(29)	109.21(10)
O(7)-Si(2)-O(2)	105.79(8)	Si(3)-O(8)-Si(6)	129.86(10)
O(1)-Si(2)-C(5)	109.85(9)	C(2A)-C(1)-C(2B)	38.0(3)
O(7)-Si(2)-C(5)	110.87(9)	C(2A)-C(1)-Si(1)	119.9(2)
O(2)-Si(2)-C(5)	111.72(10)	C(2B)-C(1)-Si(1)	114.7(3)
Si(2)-O(2)-Si(3)	130.29(9)	C(1)-C(2A)-C(3A)	112.2(5)
O(3)-Si(3)-O(8)	108.17(8)	C(1)-C(2A)-C(4A)	108.6(3)
O(3)-Si(3)-O(2)	109.96(8)	C(3A)-C(2A)-C(4A)	109.5(5)
O(8)-Si(3)-O(2)	105.61(8)	C(3B)-C(2B)-C(4B)	113.3(11)
O(3)-Si(3)-C(9)	108.96(10)	C(3B)-C(2B)-C(1)	110.5(8)
O(8)-Si(3)-C(9)	113.31(10)	C(4B)-C(2B)-C(1)	111.3(8)
O(2)-Si(3)-C(9)	110.75(9)	C(7B)-C(6)-C(8)	115.7(7)
Si(3)-O(3)-Si(4)	142.14(10)	C(7B)-C(6)-C(5)	120.8(6)
O(3)-Si(4)-O(6)	108.05(8)	C(8)-C(6)-C(5)	111.3(2)
O(3)-Si(4)-O(4)	107.88(8)	C(7B)-C(6)-C(7A)	31.9(7)
O(6)-Si(4)-O(4)	106.74(8)	C(8)-C(6)-C(7A)	104.8(4)
O(3)-Si(4)-C(13)	109.52(10)	C(5)-C(6)-C(7A)	103.2(7)
O(6)-Si(4)-C(13)	113.35(9)	C(10)-C(9)-Si(3)	114.19(17)
O(4)-Si(4)-C(13)	111.10(9)	C(11)-C(10)-C(12)	109.7(3)
Si(1)-O(4)-Si(4)	129.86(9)	C(11)-C(10)-C(9)	111.9(2)
Si(1)-O(5)-Si(5)	131.68(10)	C(12)-C(10)-C(9)	111.8(2)
O(6)-Si(5)-O(5)	107.94(8)	C(14)-C(13)-Si(4)	119.82(16)
O(6)-Si(5)-C(23)	111.58(9)	C(16)-C(14)-C(15)	110.6(2)
O(5)-Si(5)-C(23)	106.92(9)	C(16)-C(14)-C(13)	113.6(2)
O(6)-Si(5)-C(17)	107.68(9)	C(15)-C(14)-C(13)	109.5(2)
O(5)-Si(5)-C(17)	110.89(9)	C(18)-C(17)-C(22)	117.3(2)

C(18)-C(17)-Si(5)	122.15(18)	C(34)-C(29)-Si(6)	120.79(18)
C(22)-C(17)-Si(5)	120.50(18)	C(30)-C(29)-Si(6)	121.64(17)
C(17)-C(18)-C(19)	121.4(2)	C(31)-C(30)-C(29)	121.2(2)
C(20)-C(19)-C(18)	119.5(2)	C(32)-C(31)-C(30)	119.8(3)
C(21)-C(20)-C(19)	120.5(2)	C(31)-C(32)-C(33)	120.2(2)
C(20)-C(21)-C(22)	119.7(3)	C(32)-C(33)-C(34)	119.8(2)
C(17)-C(22)-C(21)	121.4(2)	C(29)-C(34)-C(33)	121.4(2)
C(24)-C(23)-C(28)	117.9(2)	C(40)-C(35)-C(36)	117.2(2)
C(24)-C(23)-Si(5)	121.57(17)	C(40)-C(35)-Si(6)	122.6(2)
C(28)-C(23)-Si(5)	120.53(18)	C(36)-C(35)-Si(6)	120.03(17)
C(25)-C(24)-C(23)	121.1(2)	C(37)-C(36)-C(35)	121.9(2)
C(26)-C(25)-C(24)	120.3(3)	C(38)-C(37)-C(36)	119.8(3)
C(27)-C(26)-C(25)	119.6(3)	C(39)-C(38)-C(37)	119.6(3)
C(26)-C(27)-C(28)	120.2(3)	C(38)-C(39)-C(40)	120.8(3)
C(27)-C(28)-C(23)	120.8(3)	C(35)-C(40)-C(39)	120.7(3)
C(34)-C(29)-C(30)	117.5(2)		

Table 5. Anisotropic displacement parameters ($Å^2 x 10^3$) for **2a**. The anisotropic displacement factor exponent takes the form: $-2 \pi^2 [h^2 a^{*2} U^{11} + ... + 2 h k a^* b^* U^{12}]$

	U^{11}	U^{22}	U^{33}	U^{23}	U^{13}	U^{12}
O(1)	16(1)	20(1)	24(1)	7(1)	2(1)	1(1)
Si(2)	14(1)	20(1)	13(1)	5(1)	0(1)	1(1)
O(2)	20(1)	19(1)	13(1)	3(1)	-2(1)	2(1)
Si(3)	16(1)	17(1)	16(1)	4(1)	-1(1)	3(1)
O(3)	19(1)	19(1)	17(1)	4(1)	1(1)	3(1)
Si(4)	17(1)	12(1)	15(1)	2(1)	1(1)	0(1)
O(4)	21(1)	14(1)	14(1)	2(1)	-3(1)	0(1)
O(5)	33(1)	14(1)	15(1)	-1(1)	3(1)	1(1)
Si(5)	18(1)	16(1)	14(1)	-1(1)	2(1)	-1(1)
O(6)	26(1)	17(1)	17(1)	4(1)	5(1)	5(1)
O(7)	19(1)	21(1)	23(1)	5(1)	-5(1)	-3(1)
Si(6)	15(1)	24(1)	17(1)	1(1)	-3(1)	-1(1)
O(8)	20(1)	28(1)	20(1)	7(1)	-6(1)	-3(1)

C(1)	19(1)	23(1)	24(1)	4(1)	-7(1)	1(1)
C(2A)	37(2)	23(2)	26(2)	9(2)	-7(2)	5(2)
C(3A)	107(7)	30(4)	56(4)	-11(3)	-45(5)	29(5)
C(4A)	59(3)	36(2)	36(3)	6(2)	-22(2)	19(2)
C(2B)	22(4)	35(6)	35(6)	17(4)	-3(4)	18(4)
C(3B)	61(10)	19(6)	73(10)	14(6)	-9(8)	21(7)
C(4B)	29(5)	71(9)	75(10)	32(8)	-15(6)	17(5)
C(5)	24(1)	30(1)	16(1)	5(1)	2(1)	-1(1)
C(6)	39(2)	116(3)	20(1)	3(2)	-1(1)	-31(2)
C(7A)	187(16)	68(6)	20(3)	-2(3)	-2(6)	-90(8)
C(7B)	91(10)	164(15)	44(6)	22(7)	-13(6)	-99(11)
C(8)	64(2)	75(2)	19(1)	3(2)	-8(1)	3(2)
C(9)	30(1)	28(1)	26(1)	6(1)	2(1)	11(1)
C(10)	42(1)	22(1)	41(1)	0(1)	7(1)	7(1)
C(11)	54(2)	34(2)	46(2)	-10(1)	-4(1)	1(1)
C(12)	69(2)	25(2)	78(2)	-1(2)	11(2)	16(2)
C(13)	27(1)	16(1)	29(1)	4(1)	4(1)	-4(1)
C(14)	32(1)	24(1)	36(1)	-3(1)	8(1)	-8(1)
C(15)	50(2)	31(2)	53(2)	0(1)	11(1)	-22(1)
C(16)	28(1)	48(2)	62(2)	10(2)	-1(1)	-4(1)
C(17)	18(1)	23(1)	18(1)	-7(1)	-1(1)	0(1)
C(18)	26(1)	26(1)	30(1)	-1(1)	2(1)	-1(1)
C(19)	27(1)	47(2)	36(1)	-4(1)	6(1)	-11(1)
C(20)	18(1)	58(2)	36(1)	-13(1)	1(1)	0(1)
C(21)	29(1)	41(2)	62(2)	-6(2)	0(1)	15(1)
C(22)	29(1)	22(1)	54(2)	2(1)	6(1)	0(1)
C(23)	19(1)	23(1)	21(1)	-4(1)	1(1)	2(1)
C(24)	26(1)	41(2)	27(1)	-8(1)	6(1)	-11(1)
C(25)	29(1)	52(2)	46(2)	-14(2)	5(1)	-17(1)
C(26)	32(1)	49(2)	42(2)	-18(1)	-11(1)	-2(1)
C(27)	50(2)	54(2)	25(1)	-6(1)	-9(1)	-2(1)
C(28)	44(2)	39(2)	23(1)	2(1)	-4(1)	-9(1)
C(29)	18(1)	23(1)	19(1)	5(1)	0(1)	1(1)
C(30)	25(1)	35(1)	28(1)	-4(1)	1(1)	-3(1)
C(31)	40(1)	33(1)	32(1)	0(1)	10(1)	2(1)
C(32)	25(1)	46(2)	45(2)	3(1)	13(1)	6(1)

C(33)	19(1)	64(2)	54(2)	-12(2)	-2(1)	3(1)
C(34)	22(1)	49(2)	35(1)	-12(1)	-5(1)	1(1)
C(35)	17(1)	33(1)	20(1)	-2(1)	-4(1)	2(1)
C(36)	34(1)	32(1)	26(1)	-2(1)	-6(1)	-1(1)
C(37)	40(2)	32(2)	45(2)	-10(1)	-7(1)	0(1)
C(38)	37(1)	46(2)	36(1)	-19(1)	-9(1)	14(1)
C(39)	44(2)	64(2)	19(1)	-10(1)	0(1)	13(2)
C(40)	33(1)	39(2)	23(1)	-1(1)	3(1)	5(1)

Table 6. Torsion angles [°] for **2a**.

O(5)-Si(1)-O(1)-Si(2)	-117.35(16)
O(4)-Si(1)-O(1)-Si(2)	-1.36(19)
C(1)-Si(1)-O(1)-Si(2)	118.97(17)
Si(1)-O(1)-Si(2)-O(7)	119.73(16)
Si(1)-O(1)-Si(2)-O(2)	4.43(19)
Si(1)-O(1)-Si(2)-C(5)	-118.21(17)
O(1)-Si(2)-O(2)-Si(3)	85.33(13)
O(7)-Si(2)-O(2)-Si(3)	-32.42(14)
C(5)-Si(2)-O(2)-Si(3)	-153.17(12)
Si(2)-O(2)-Si(3)-O(3)	-86.70(13)
Si(2)-O(2)-Si(3)-O(8)	29.79(14)
Si(2)-O(2)-Si(3)-C(9)	152.82(13)
O(8)-Si(3)-O(3)-Si(4)	-125.75(17)
O(2)-Si(3)-O(3)-Si(4)	-10.9(2)
C(9)-Si(3)-O(3)-Si(4)	110.67(18)
Si(3)-O(3)-Si(4)-O(6)	128.40(17)
Si(3)-O(3)-Si(4)-O(4)	13.3(2)
Si(3)-O(3)-Si(4)-C(13)	-107.70(18)
O(1)-Si(1)-O(4)-Si(4)	-91.02(13)
O(5)-Si(1)-O(4)-Si(4)	26.56(14)
C(1)-Si(1)-O(4)-Si(4)	146.95(12)
O(3)-Si(4)-O(4)-Si(1)	83.73(13)
O(6)-Si(4)-O(4)-Si(1)	-32.19(14)
C(13)-Si(4)-O(4)-Si(1)	-156.22(12)

O(1)-Si(1)-O(5)-Si(5)	117.99(13)
O(4)-Si(1)-O(5)-Si(5)	-0.29(15)
C(1)-Si(1)-O(5)-Si(5)	-118.56(14)
Si(1)-O(5)-Si(5)-O(6)	-12.78(16)
Si(1)-O(5)-Si(5)-C(23)	-132.96(13)
Si(1)-O(5)-Si(5)-C(17)	104.96(14)
O(3)-Si(4)-O(6)-Si(5)	-102.46(13)
O(4)-Si(4)-O(6)-Si(5)	13.34(15)
C(13)-Si(4)-O(6)-Si(5)	135.97(13)
O(5)-Si(5)-O(6)-Si(4)	4.93(15)
C(23)-Si(5)-O(6)-Si(4)	122.12(13)
C(17)-Si(5)-O(6)-Si(4)	-114.86(13)
O(1)-Si(2)-O(7)-Si(6)	-116.18(12)
O(2)-Si(2)-O(7)-Si(6)	1.08(14)
C(5)-Si(2)-O(7)-Si(6)	122.38(13)
Si(2)-O(7)-Si(6)-O(8)	23.00(15)
Si(2)-O(7)-Si(6)-C(35)	143.34(13)
Si(2)-O(7)-Si(6)-C(29)	-95.21(14)
O(3)-Si(3)-O(8)-Si(6)	122.69(13)
O(2)-Si(3)-O(8)-Si(6)	4.99(15)
C(9)-Si(3)-O(8)-Si(6)	-116.40(14)
O(7)-Si(6)-O(8)-Si(3)	-26.69(15)
C(35)-Si(6)-O(8)-Si(3)	-148.69(13)
C(29)-Si(6)-O(8)-Si(3)	91.63(14)
O(1)-Si(1)-C(1)-C(2A)	45.9(3)
O(5)-Si(1)-C(1)-C(2A)	-76.1(2)
O(4)-Si(1)-C(1)-C(2A)	167.0(2)
O(1)-Si(1)-C(1)-C(2B)	88.5(4)
O(5)-Si(1)-C(1)-C(2B)	-33.5(4)
O(4)-Si(1)-C(1)-C(2B)	-150.4(4)
C(2B)-C(1)-C(2A)-C(3A)	-34.0(6)
Si(1)-C(1)-C(2A)-C(3A)	58.8(5)
C(2B)-C(1)-C(2A)-C(4A)	87.2(6)
Si(1)-C(1)-C(2A)-C(4A)	179.9(3)
C(2A)-C(1)-C(2B)-C(3B)	54.6(11)
Si(1)-C(1)-C(2B)-C(3B)	-52.9(12)

C(2A)-C(1)-C(2B)-C(4B)	-72.2(8)
Si(1)-C(1)-C(2B)-C(4B)	-179.7(6)
O(1)-Si(2)-C(5)-C(6)	53.9(3)
O(7)-Si(2)-C(5)-C(6)	175.2(2)
O(2)-Si(2)-C(5)-C(6)	-67.0(3)
Si(2)-C(5)-C(6)-C(7B)	50.5(13)
Si(2)-C(5)-C(6)-C(8)	-168.7(2)
Si(2)-C(5)-C(6)-C(7A)	79.4(6)
O(3)-Si(3)-C(9)-C(10)	-40.9(2)
O(8)-Si(3)-C(9)-C(10)	-161.34(17)
O(2)-Si(3)-C(9)-C(10)	80.19(19)
Si(3)-C(9)-C(10)-C(11)	-59.6(3)
Si(3)-C(9)-C(10)-C(12)	176.9(2)
O(3)-Si(4)-C(13)-C(14)	-163.77(18)
O(6)-Si(4)-C(13)-C(14)	-43.0(2)
O(4)-Si(4)-C(13)-C(14)	77.2(2)
Si(4)-C(13)-C(14)-C(16)	-51.9(3)
Si(4)-C(13)-C(14)-C(15)	-176.11(19)
O(6)-Si(5)-C(17)-C(18)	-12.4(2)
O(5)-Si(5)-C(17)-C(18)	-130.32(18)
C(23)-Si(5)-C(17)-C(18)	110.5(2)
O(6)-Si(5)-C(17)-C(22)	168.48(19)
O(5)-Si(5)-C(17)-C(22)	50.6(2)
C(23)-Si(5)-C(17)-C(22)	-68.6(2)
C(22)-C(17)-C(18)-C(19)	-0.5(4)
Si(5)-C(17)-C(18)-C(19)	-179.59(19)
C(17)-C(18)-C(19)-C(20)	0.7(4)
C(18)-C(19)-C(20)-C(21)	0.0(4)
C(19)-C(20)-C(21)-C(22)	-0.9(4)
C(18)-C(17)-C(22)-C(21)	-0.4(4)
Si(5)-C(17)-C(22)-C(21)	178.7(2)
C(20)-C(21)-C(22)-C(17)	1.1(5)
O(6)-Si(5)-C(23)-C(24)	-112.6(2)
O(5)-Si(5)-C(23)-C(24)	5.2(2)
C(17)-Si(5)-C(23)-C(24)	126.7(2)
O(6)-Si(5)-C(23)-C(28)	68.6(2)

O(5)-Si(5)-C(23)-C(28)	-173.6(2)
C(17)-Si(5)-C(23)-C(28)	-52.0(2)
C(28)-C(23)-C(24)-C(25)	-0.5(4)
Si(5)-C(23)-C(24)-C(25)	-179.3(2)
C(23)-C(24)-C(25)-C(26)	0.1(5)
C(24)-C(25)-C(26)-C(27)	-0.2(5)
C(25)-C(26)-C(27)-C(28)	0.6(5)
C(26)-C(27)-C(28)-C(23)	-1.0(5)
C(24)-C(23)-C(28)-C(27)	0.9(4)
Si(5)-C(23)-C(28)-C(27)	179.7(2)
O(7)-Si(6)-C(29)-C(34)	-133.9(2)
O(8)-Si(6)-C(29)-C(34)	109.3(2)
C(35)-Si(6)-C(29)-C(34)	-10.7(2)
O(7)-Si(6)-C(29)-C(30)	48.5(2)
O(8)-Si(6)-C(29)-C(30)	-68.2(2)
C(35)-Si(6)-C(29)-C(30)	171.82(19)
C(34)-C(29)-C(30)-C(31)	0.2(4)
Si(6)-C(29)-C(30)-C(31)	177.8(2)
C(29)-C(30)-C(31)-C(32)	-0.1(4)
C(30)-C(31)-C(32)-C(33)	0.0(4)
C(31)-C(32)-C(33)-C(34)	-0.1(5)
C(30)-C(29)-C(34)-C(33)	-0.2(4)
Si(6)-C(29)-C(34)-C(33)	-177.9(2)
C(32)-C(33)-C(34)-C(29)	0.2(5)
O(7)-Si(6)-C(35)-C(40)	-123.60(19)
O(8)-Si(6)-C(35)-C(40)	-4.9(2)
C(29)-Si(6)-C(35)-C(40)	114.8(2)
O(7)-Si(6)-C(35)-C(36)	61.4(2)
O(8)-Si(6)-C(35)-C(36)	-179.86(18)
C(29)-Si(6)-C(35)-C(36)	-60.2(2)
C(40)-C(35)-C(36)-C(37)	0.1(4)
Si(6)-C(35)-C(36)-C(37)	175.3(2)
C(35)-C(36)-C(37)-C(38)	-1.8(4)
C(36)-C(37)-C(38)-C(39)	2.3(4)
C(37)-C(38)-C(39)-C(40)	-1.1(4)
C(36)-C(35)-C(40)-C(39)	1.2(4)

Si(6)-C(35)-C(40)-C(39)	-173.90(19)
C(38)-C(39)-C(40)-C(35)	-0.7(4)

2-3 X-ray analysis of **2b**.

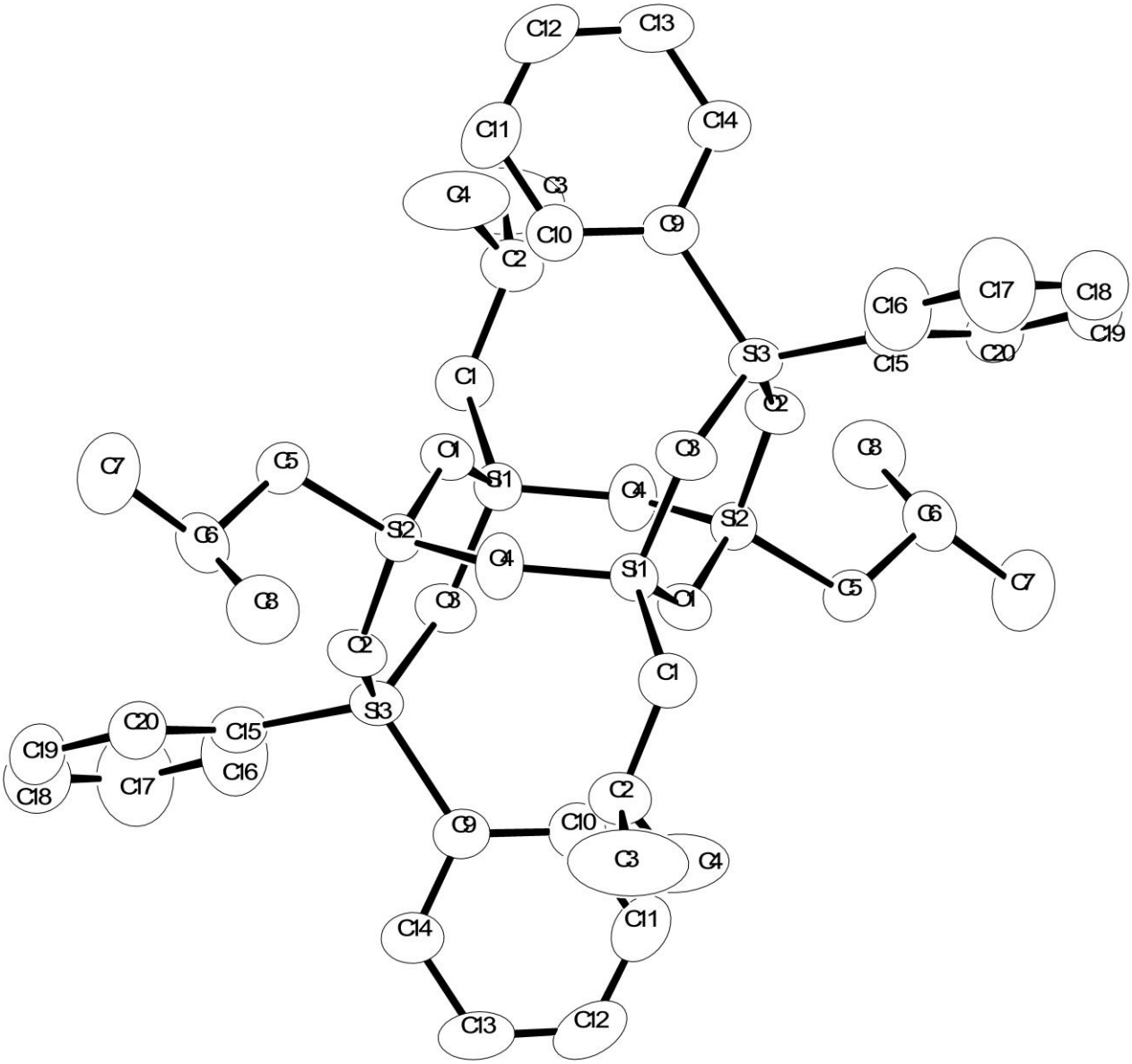

Figure 1. ORTEP drawing of **2b**.

Table 1. Crystal data and structure refinement for **2b**.

Empirical formula	$C_{40}H_{56}O_8Si_6$	
Formula weight	833.39	
Temperature	258.1500 K	
Wavelength	0.71070 Å	
Crystal system	Orthorhombic	
Space group	*Pbca*	
Unit cell dimensions	a = 10.8140(11) Å	α = 90°.
	b = 20.212(2) Å	β = 90°.
	c = 20.661(2) Å	γ = 90°.
Volume	4516.0(8) $Å^3$	
Z	4	
Density (calculated)	1.226 g/mL	
Absorption coefficient	0.232 mm^{-1}	
F(000)	1776	
Crystal size	0.3000 x 0.2000 x 0.1000 mm^3	
Theta range for data collection	4.39 to 25.50°.	
Index ranges	$-12<=h<=13$, $-24<=k<=24$, $-25<=l<=25$	
Reflections collected	28115	
Independent reflections	4111 [R(int) = 0.0364]	
Completeness to theta = 25.50°	97.9%	
Absorption correction	Semi-empirical from equivalents	
Max. and min. transmission	1.0000 and 0.4481	
Refinement method	Full-matrix least-squares on F^2	
Data / restraints / parameters	4111 / 0 / 248	
Goodness-of-fit on F^2	1.184	
Final R indices [I>2sigma(I)]	$R1$ = 0.0470, $wR2$ = 0.1060	
R indices (all data)	$R1$ = 0.0539, $wR2$ = 0.1080	
Largest diff. peak and hole	0.462 and -0.550 e.$Å^{-3}$	

Table 2. Atomic coordinates (x 10^4) and equivalent isotropic displacement parameters ($Å^2$x 10^3) for **2b**. U(eq) is defined as one third of the trace of the orthogonalized U^{ij} tensor.

	x	y	z	U(eq)
Si(1)	5587(1)	408(1)	4095(1)	33(1)
O(1)	4654(1)	-218(1)	4212(1)	37(1)
Si(2)	3286(1)	-258(1)	4547(1)	32(1)
O(2)	2687(1)	481(1)	4491(1)	41(1)
Si(3)	3279(1)	1199(1)	4294(1)	37(1)
O(3)	4723(1)	1072(1)	4093(1)	43(1)
O(4)	6542(1)	448(1)	4695(1)	46(1)
C(1)	6471(2)	368(1)	3338(1)	44(1)
C(2)	7406(2)	-190(1)	3256(1)	56(1)
C(3)	8291(4)	-47(2)	2701(2)	125(2)
C(4)	6802(4)	-842(2)	3153(2)	104(1)
C(5)	2321(2)	-883(1)	4140(1)	41(1)
C(6)	920(2)	-829(1)	4229(1)	48(1)
C(7)	252(3)	-1360(2)	3838(2)	80(1)
C(8)	547(3)	-872(2)	4936(2)	71(1)
C(9)	3260(2)	1794(1)	4981(1)	40(1)
C(10)	4287(3)	1874(1)	5382(1)	57(1)
C(11)	4275(3)	2316(1)	5897(1)	68(1)
C(12)	3239(3)	2685(1)	6017(1)	65(1)
C(13)	2215(3)	2621(1)	5630(1)	63(1)
C(14)	2229(2)	2178(1)	5113(1)	52(1)
C(15)	2413(2)	1545(1)	3599(1)	43(1)
C(16)	2877(3)	2097(2)	3283(2)	72(1)
C(17)	2260(4)	2392(2)	2776(2)	94(1)
C(18)	1165(4)	2145(2)	2568(1)	79(1)
C(19)	673(3)	1602(2)	2863(1)	69(1)
C(20)	1289(2)	1303(1)	3379(1)	55(1)

Table 3. Bond lengths [Å] for **2b**.

Si(1)-O(4)	1.6159(16)	C(5)-C(6)	1.529(3)
Si(1)-O(3)	1.6349(15)	C(6)-C(8)	1.518(4)
Si(1)-O(1)	1.6352(14)	C(6)-C(7)	1.526(4)
Si(1)-C(1)	1.835(2)	C(9)-C(14)	1.386(3)
O(1)-Si(2)	1.6354(14)	C(9)-C(10)	1.395(3)
Si(2)-O(4)#1	1.6232(16)	C(10)-C(11)	1.389(4)
Si(2)-O(2)	1.6328(15)	C(11)-C(12)	1.369(4)
Si(2)-C(5)	1.841(2)	C(12)-C(13)	1.372(4)
O(2)-Si(3)	1.6384(14)	C(13)-C(14)	1.393(3)
Si(3)-O(3)	1.6358(15)	C(15)-C(16)	1.387(3)
Si(3)-C(15)	1.851(2)	C(15)-C(20)	1.388(3)
Si(3)-C(9)	1.861(2)	C(16)-C(17)	1.378(4)
O(4)-Si(2)#1	1.6232(16)	C(17)-C(18)	1.354(5)
C(1)-C(2)	1.524(3)	C(18)-C(19)	1.365(5)
C(2)-C(4)	1.487(4)	C(19)-C(20)	1.394(4)
C(2)-C(3)	1.519(4)		

Symmetry transformations used to generate equivalent atoms: #1 -x+1,-y,-z+1

Table 4. Bond angles [°] for **2b**.

O(4)-Si(1)-O(3)	109.04(9)	C(4)-C(2)-C(3)	109.7(3)
O(4)-Si(1)-O(1)	108.61(8)	C(4)-C(2)-C(1)	112.4(2)
O(3)-Si(1)-O(1)	106.39(7)	C(3)-C(2)-C(1)	111.2(3)
O(4)-Si(1)-C(1)	108.83(10)	C(6)-C(5)-Si(2)	117.26(16)
O(3)-Si(1)-C(1)	109.42(9)	C(8)-C(6)-C(7)	110.1(2)
O(1)-Si(1)-C(1)	114.42(9)	C(8)-C(6)-C(5)	112.0(2)
Si(1)-O(1)-Si(2)	131.24(9)	C(7)-C(6)-C(5)	110.8(2)
O(4)#1-Si(2)-O(2)	109.21(9)	C(14)-C(9)-C(10)	117.3(2)
O(4)#1-Si(2)-O(1)	108.47(8)	C(14)-C(9)-Si(3)	121.36(18)
O(2)-Si(2)-O(1)	106.46(7)	C(10)-C(9)-Si(3)	121.31(17)
O(4)#1-Si(2)-C(5)	110.13(9)	C(11)-C(10)-C(9)	121.5(2)
O(2)-Si(2)-C(5)	111.72(9)	C(12)-C(11)-C(10)	119.8(3)
O(1)-Si(2)-C(5)	110.73(9)	C(11)-C(12)-C(13)	120.3(2)
Si(2)-O(2)-Si(3)	132.32(9)	C(12)-C(13)-C(14)	119.9(2)
O(3)-Si(3)-O(2)	107.24(8)	C(9)-C(14)-C(13)	121.3(2)
O(3)-Si(3)-C(15)	110.24(9)	C(16)-C(15)-C(20)	116.5(2)
O(2)-Si(3)-C(15)	109.26(9)	C(16)-C(15)-Si(3)	119.09(19)
O(3)-Si(3)-C(9)	107.79(9)	C(20)-C(15)-Si(3)	124.36(19)
O(2)-Si(3)-C(9)	112.20(9)	C(17)-C(16)-C(15)	122.1(3)
C(15)-Si(3)-C(9)	110.05(10)	C(18)-C(17)-C(16)	120.3(3)
Si(1)-O(3)-Si(3)	132.41(9)	C(17)-C(18)-C(19)	119.8(3)
Si(1)-O(4)-Si(2)#1	143.34(10)	C(18)-C(19)-C(20)	120.2(3)
C(2)-C(1)-Si(1)	118.29(16)	C(15)-C(20)-C(19)	121.1(3)

Symmetry transformations used to generate equivalent atoms: #1 -x+1,-y,-z+1

Table 5. Anisotropic displacement parameters ($Å^2$x 10^3) for **2b**. The anisotropic displacement factor exponent takes the form: $-2\pi^2[h^2a^{*2}U^{11} + ... + 2 h k a^* b^* U^{12}]$

	U^{11}	U^{22}	U^{33}	U^{23}	U^{13}	U^{12}
Si(1)	29(1)	37(1)	33(1)	1(1)	4(1)	-2(1)
O(1)	31(1)	33(1)	46(1)	0(1)	5(1)	0(1)
Si(2)	28(1)	33(1)	36(1)	-1(1)	1(1)	-4(1)
O(2)	32(1)	34(1)	59(1)	-3(1)	9(1)	-2(1)
Si(3)	34(1)	32(1)	45(1)	-4(1)	5(1)	0(1)
O(3)	35(1)	35(1)	59(1)	-1(1)	10(1)	-3(1)
O(4)	36(1)	65(1)	37(1)	7(1)	-2(1)	-13(1)
C(1)	47(1)	49(1)	38(1)	5(1)	8(1)	1(1)
C(2)	50(1)	69(2)	51(1)	-10(1)	9(1)	12(1)
C(3)	111(3)	115(3)	150(4)	-17(3)	92(3)	4(3)
C(4)	117(3)	62(2)	133(3)	-22(2)	49(3)	2(2)
C(5)	39(1)	40(1)	45(1)	-5(1)	0(1)	-5(1)
C(6)	37(1)	39(1)	67(2)	5(1)	-8(1)	-5(1)
C(7)	60(2)	87(2)	93(2)	-13(2)	-15(2)	-28(2)
C(8)	46(2)	85(2)	82(2)	-6(2)	17(1)	-10(1)
C(9)	44(1)	32(1)	45(1)	0(1)	4(1)	-2(1)
C(10)	58(2)	50(1)	63(2)	-9(1)	-12(1)	7(1)
C(11)	83(2)	59(2)	62(2)	-13(1)	-18(2)	-3(2)
C(12)	91(2)	52(2)	53(2)	-16(1)	11(1)	-9(2)
C(13)	61(2)	53(2)	74(2)	-19(1)	22(1)	3(1)
C(14)	45(1)	47(1)	62(2)	-12(1)	7(1)	0(1)
C(15)	44(1)	42(1)	43(1)	-8(1)	6(1)	4(1)
C(16)	72(2)	75(2)	69(2)	22(2)	-4(2)	-18(2)
C(17)	109(3)	98(3)	76(2)	40(2)	-5(2)	-14(2)
C(18)	99(2)	90(2)	47(2)	5(2)	-7(2)	24(2)
C(19)	66(2)	79(2)	60(2)	-20(2)	-17(1)	14(2)
C(20)	55(2)	51(1)	60(2)	-9(1)	-7(1)	1(1)

Table 6. Torsion angles [°] for **2b**.

O(4)-Si(1)-O(1)-Si(2)	93.65(13)
O(3)-Si(1)-O(1)-Si(2)	-23.61(14)
C(1)-Si(1)-O(1)-Si(2)	-144.55(13)
Si(1)-O(1)-Si(2)-O(4)#1	-93.63(13)
Si(1)-O(1)-Si(2)-O(2)	23.78(14)
Si(1)-O(1)-Si(2)-C(5)	145.41(13)
O(4)#1-Si(2)-O(2)-Si(3)	105.18(14)
O(1)-Si(2)-O(2)-Si(3)	-11.74(16)
C(5)-Si(2)-O(2)-Si(3)	-132.74(14)
Si(2)-O(2)-Si(3)-O(3)	3.37(16)
Si(2)-O(2)-Si(3)-C(15)	122.86(14)
Si(2)-O(2)-Si(3)-C(9)	-114.81(14)
O(4)-Si(1)-O(3)-Si(3)	-105.62(14)
O(1)-Si(1)-O(3)-Si(3)	11.34(16)
C(1)-Si(1)-O(3)-Si(3)	135.44(14)
O(2)-Si(3)-O(3)-Si(1)	-3.14(16)
C(15)-Si(3)-O(3)-Si(1)	-121.99(14)
C(9)-Si(3)-O(3)-Si(1)	117.87(14)
O(3)-Si(1)-O(4)-Si(2)#1	89.9(2)
O(1)-Si(1)-O(4)-Si(2)#1	-25.7(2)
C(1)-Si(1)-O(4)-Si(2)#1	-150.81(18)
O(4)-Si(1)-C(1)-C(2)	56.9(2)
O(3)-Si(1)-C(1)-C(2)	175.99(18)
O(1)-Si(1)-C(1)-C(2)	-64.8(2)
Si(1)-C(1)-C(2)-C(4)	72.2(3)
Si(1)-C(1)-C(2)-C(3)	-164.4(3)
O(4)#1-Si(2)-C(5)-C(6)	80.09(19)
O(2)-Si(2)-C(5)-C(6)	-41.5(2)
O(1)-Si(2)-C(5)-C(6)	-159.94(16)
Si(2)-C(5)-C(6)-C(8)	-59.3(3)
Si(2)-C(5)-C(6)-C(7)	177.3(2)
O(3)-Si(3)-C(9)-C(14)	156.80(18)
O(2)-Si(3)-C(9)-C(14)	-85.3(2)
C(15)-Si(3)-C(9)-C(14)	36.5(2)

O(3)-Si(3)-C(9)-C(10)	-22.8(2)
O(2)-Si(3)-C(9)-C(10)	95.0(2)
C(15)-Si(3)-C(9)-C(10)	-143.10(19)
C(14)-C(9)-C(10)-C(11)	0.5(4)
Si(3)-C(9)-C(10)-C(11)	-179.8(2)
C(9)-C(10)-C(11)-C(12)	-0.2(4)
C(10)-C(11)-C(12)-C(13)	-0.1(4)
C(11)-C(12)-C(13)-C(14)	0.0(4)
C(10)-C(9)-C(14)-C(13)	-0.6(4)
Si(3)-C(9)-C(14)-C(13)	179.8(2)
C(12)-C(13)-C(14)-C(9)	0.3(4)
O(3)-Si(3)-C(15)-C(16)	-51.8(2)
O(2)-Si(3)-C(15)-C(16)	-169.5(2)
C(9)-Si(3)-C(15)-C(16)	66.9(2)
O(3)-Si(3)-C(15)-C(20)	130.40(19)
O(2)-Si(3)-C(15)-C(20)	12.8(2)
C(9)-Si(3)-C(15)-C(20)	-110.8(2)
C(20)-C(15)-C(16)-C(17)	0.1(4)
Si(3)-C(15)-C(16)-C(17)	-177.8(3)
C(15)-C(16)-C(17)-C(18)	-0.2(6)
C(16)-C(17)-C(18)-C(19)	0.0(6)
C(17)-C(18)-C(19)-C(20)	0.4(5)
C(16)-C(15)-C(20)-C(19)	0.3(4)
Si(3)-C(15)-C(20)-C(19)	178.09(19)
C(18)-C(19)-C(20)-C(15)	-0.5(4)

Symmetry transformations used to generate equivalent atoms: #1 -x+1,-y,-z+1

Conclusion of part 2

2.4.1. Conclusion of part 2

We described in a facile single-step synthesis of disiloxanetetraols ($[RSi(OH)_2]_2O$) with various substituents (R = Pr, C_6H_{13}, *i*-Pr, *i*-Bu, Ph, Cy, C_5H_9,) in chapter 1 and cyclotrisiloxanetriols (*cis-trans*-$[RSiO(OH)]_3$) with ethyl and cyclopentyl substituents in chapter 2 by hydrolytic condensation of trichlorosilanes by quenching the reactions in early stages (Scheme 1, and Scheme 2).

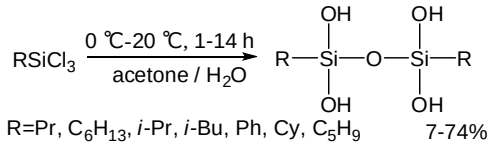

Scheme 1

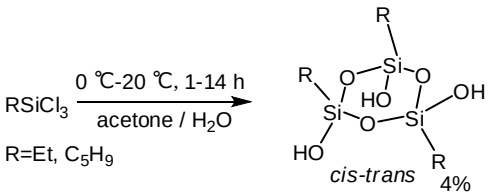

Scheme 2

Moreover, $[PrSi(OH)_2]_2O$, and *cis-trans*-$[EtSiO(OH)]_3$ possesses the smallest substituents in disiloxanetetraols or cyclotrisiloxanetetraols reported so far. Generally, silanols bearing small substituents are prone to self-condensation. This reaction is accelerated by the existence of acid or base. Usually silanols are prepared from chlorosilanes or alkoxysilanes with acid or base, therefore it is not easy to obtain disiloxanetetraols or cyclotrisiloxanetriols from $RSiCl_3$. Therefore, commonly multi step reactions are used like Scheme 3, and Scheme 4.

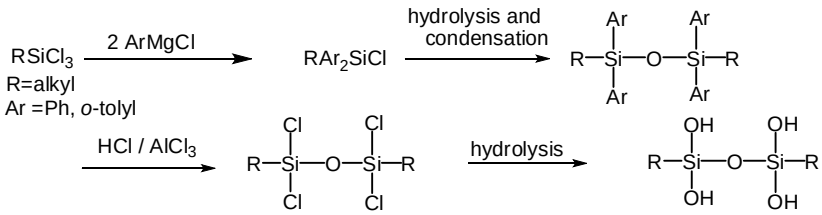

Scheme 3

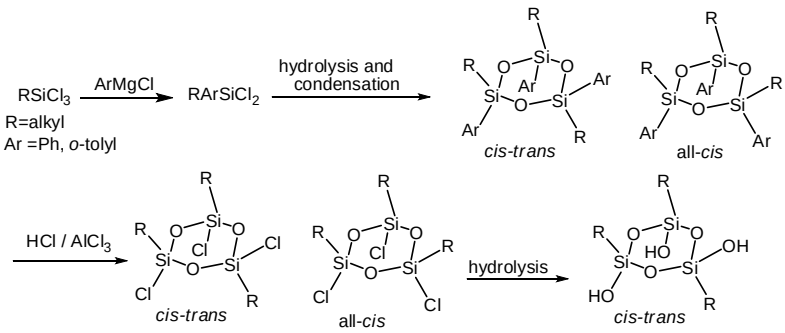

Scheme 4

Our new method of syntheses of disiloxanetetraols and cyclotrisiloxanetriols is a single-step. And isolation is very easy without column chromatography. Therefore, our new method is promising to be versatile for a large-scale production, although these yield are low at present.

Especially, in the case of isobutyl substituted compound, we elucidated that we could perform the synthesis of both disiloxanetetraol and all-*cis*-cyclotetrasiloxanetetraol from the same starting material simply by changing the quenching time by hydrolytic condensation of trichlorosilanes in chapter 2 (Scheme 5).

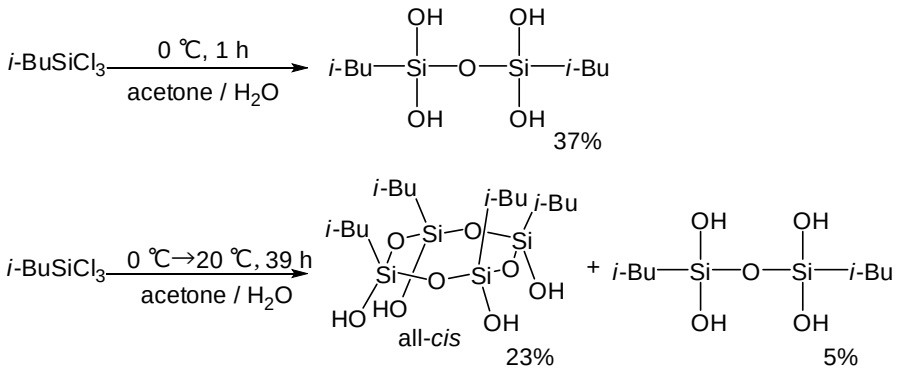

Scheme 5

In chapter 3, we dramatically improved yield (73%) of all-*cis*-[*i*-BuSiO(OH)]$_4$ than the reported yield (34%) [1f] (Scheme 6). The overall yield of all-*cis*-[[*i*-BuSiO(OH)]$_4$ is highest in previously reported all-*cis*-[RSiO(OH)]$_4$ from trialkoxysilane or trichlorosilane except phenyl substituent so far [1a-k].

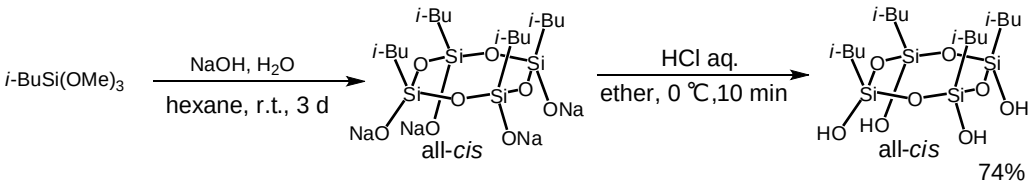

Scheme 6

For isomers of cyclotetrasiloxanetetraol except all-*cis* type, there are several methods of synthesis of *cis*-*trans*-*cis*, *cis*-*cis*-*trans*, and all-*trans* isomers [1f–k]. However, these methods need multi step reactions, for the handling chlorosilanes and are restricted the product substituents. Another report regarding the isolation of isomers is stereoisomerization of cyclotetrasiloxanetetraols [1j, 1f, 1k]. However, only isomerization from phenyl-substituted cyclic silanols was known to date, and optimized

reaction condition and reaction mechanism are not available so far. Therefore, in chapter 3, stereoisomerization reaction of all-*cis*-1,3,5,7-tetrahydroxy-1,3,5,7- tetraisobutyl-cyclotetrasiloxane was carried out in acidic condition to give *cis-trans-cis* isomer, all-*trans* isomer, and *cis-cis-trans* isomer (Scheme 7).

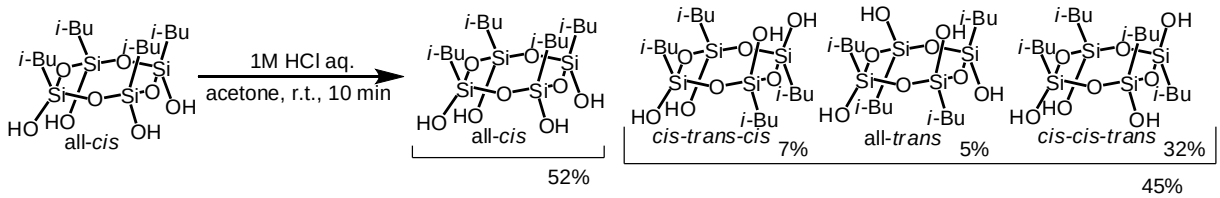

Scheme 7

This result indicates stereoisomerization can be commonly applied to other cyclotetrasiloxanetetraols. Mixture of the four isomers of [*i*-BuSiO(OH)]$_4$ can very easily divide into all-*cis*-isomer and mixture of *cis-trans-cis*, all-*trans*, *cis-cis-trans* isomers by using chloroform. Therefore, this method is promising to be versatile for a large-scale production.

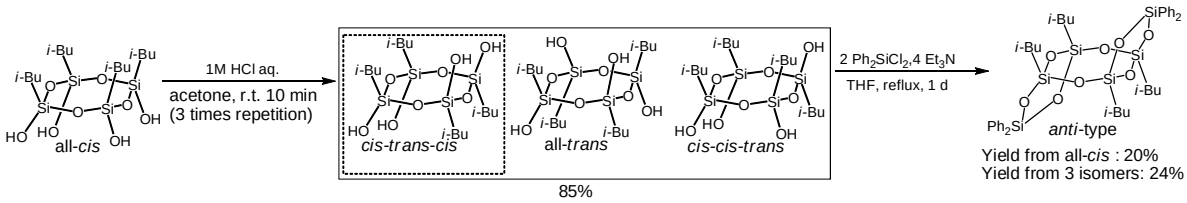

Scheme8

By salvaged and reused all-*cis*-isomer, stereoisomerization reaction was repeated 3 times to give mixture of three isomers in 85% conversion rate. Within all-*trans*, *cis-trans-cis*, *cis-cis-trans*, only *cis-trans-cis* isomer can be converted to *anti*-laddersiloxane. Therefore, in THF, the mixture of three isomers was treated with dichlorodiphenylsilane in the presence of triethylamine as HCl scavenger to give *anti*-type laddersiloxane. This synthetic method of *anti*-type laddersiloxane is very useful when selectively synthesize *anti*-type laddersiloxane structure without generation of *syn*-type laddersiloxane structure.

Each cyclotetrasiloxanetetraol isomer (*cis-trans-cis*, all-*trans*, *cis-cis-trans* isomers) was also isolated from mixture of three isomers and identified by nuclear magnetic resonance spectra. And structure of *cis-trans-cis* isomer was determined by X-ray

crystallographic analysis.

Suitable stereoisomerization condition was investigated in various conditions (reaction time, concentration of reagents, kind of reagents, and kind of solvents). As a result, best conditions are that using 3.2 equivalent amount of strong acid aqueous solutions (e.g. HCl aq.) in mixable solvent with water (e.g. acetone) at room temperature in 10 min. Stereoisomerization mechanism was investigated by various experiments. The experimental results indicated that the most plausible mechanism is substitution reaction for silicon center without siloxane bond cleavage.

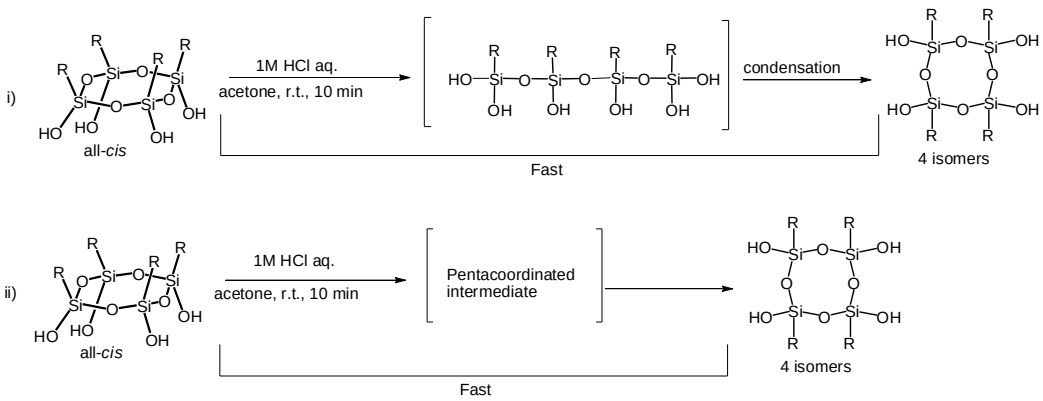

Scheme 9

However, in chapter 3, currently experimental results cannot perfectly deny the mechanism in which one of siloxane bonds cleaved then recombination occurs. For example, O^{18} labeling experiment by using H_2O^{18} (Scheme 10) and siloxane bond formation reaction for linear silanol (**1**) in the stereoisomerization reaction condition (1M HCl, acetone, r.t., 10 min) (Scheme 11) more clearly elucidate the reaction mechanism. Synthetic scheme is shown in Scheme 12.

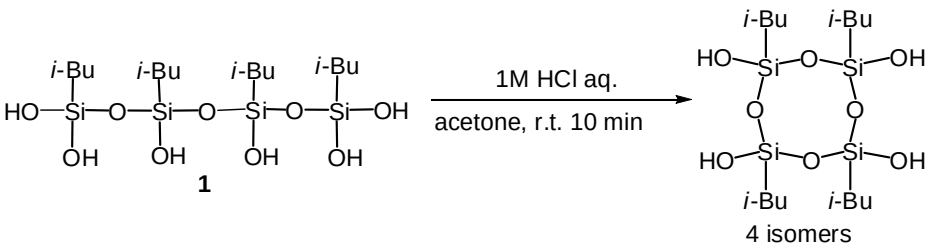

Scheme10

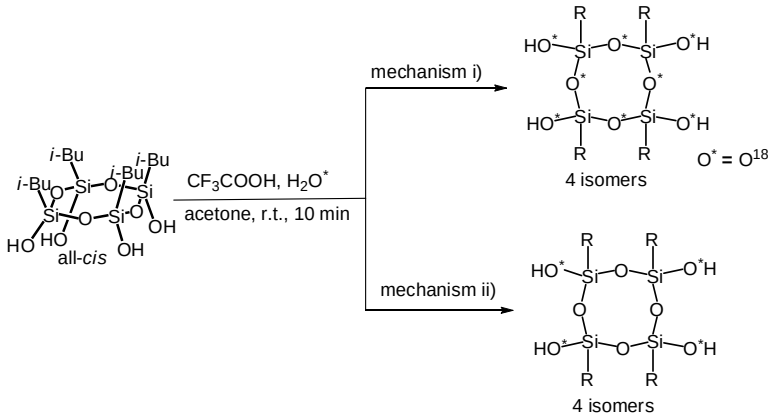

Scheme11

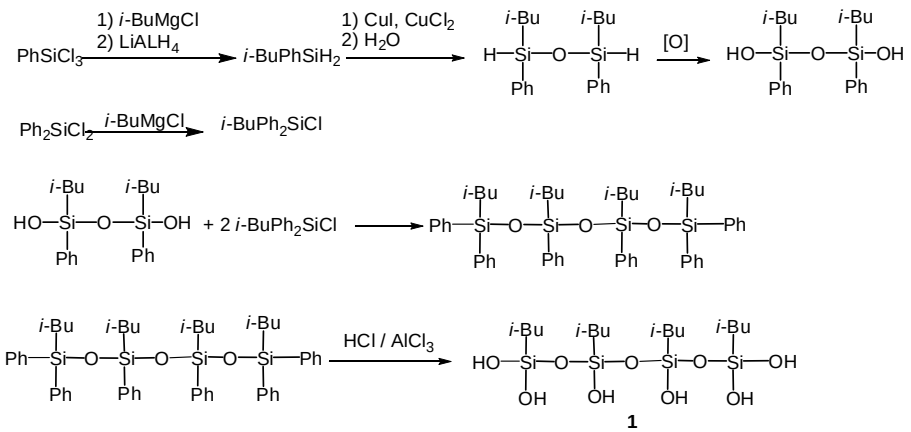

Scheme12

Previously, synthesis of all-*cis*-[RSiO(OH)]$_4$ from RSiCl$_3$ (R = *i*-Pr [1c], Ph [1d]) in acetone-water solution were reported by Feher's group and our group in 22% (R = *i*-Pr) and 37% (R = Ph) yields respectively. In these reports, other stereoisomer were not observed in spite of using acetone as solvent and acidic reaction solution because of no HCl scavenger. We reported synthesis of all-*cis*-[*i*-BuSiO(OH)]$_4$ from *i*-BuSiCl$_3$ in 24% yield (part 2, chapter 3). However, we also obtained *cis*-*cis*-*trans* (1.4%), and *cis*-*trans*-*cis* isomer (6.6%) in this reaction. In these cases, cyclotetrasiloxanetetraols were isolated by collecting the precipitates from the solution because of less solubility. In chapter 3, we reported that stereoisomerization is not occurred in non-organic solvent condition. Therefore it assumed that stereoisomerization did not occur (or very slow), because all-*cis*-[RSiO(OH)]$_4$ was precipitated and eliminated from the solution by hydrolysis and condensation of RSiCl$_3$. In either case, synthesis of all-*cis*-[RSiO(OH)]$_4$ from RSiCl$_3$ needs careful operation and analysis for the generation of other isomers [1c,

1d]. The same holds true for other synthetic method of cyclotetrasiloxanetetraols as summarized in Scheme 13 [1e-h].

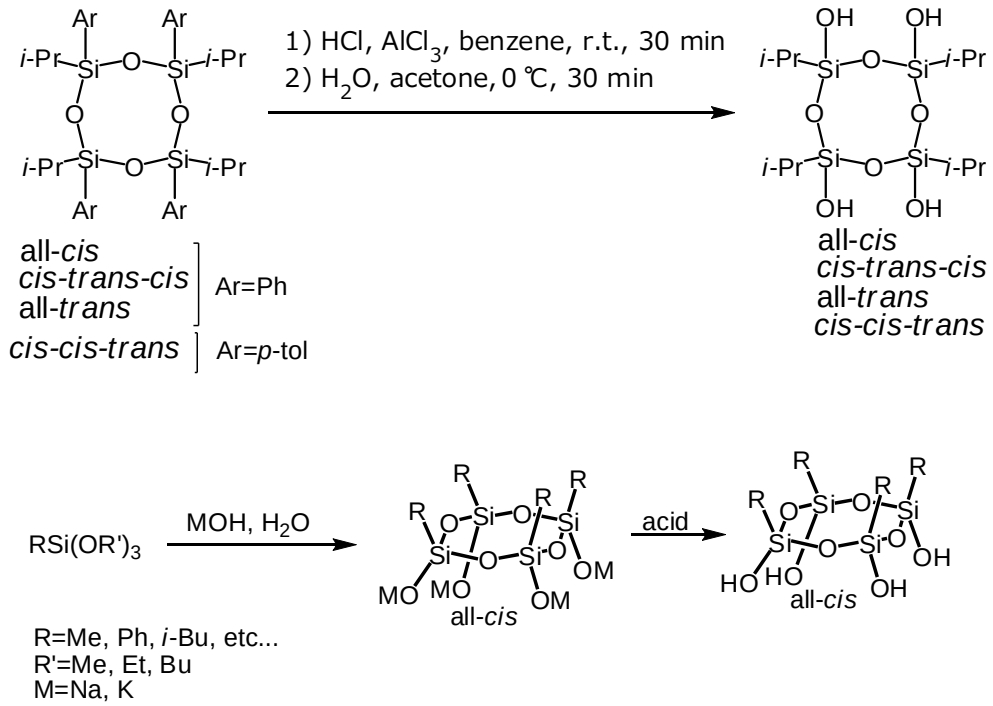

Scheme 13

Stereoisomerization caused unnecessary isomerization in the reactions reported by Gunji's group [2]. They reported stereoisomerization of *cis*-*trans*-*cis*-[MeSiO(NCO)]$_4$ by pyridine. The *cis*-*trans*-*cis*-[MeSiO(NCO)]$_4$ reacted with triphenylsilanol in the presence of pyridine to give all-*cis*-triphenylsilylated product (57%). In this reaction, *cis*-*trans*-*cis*-triphenylsilylated product was not obtained. The *cis*-*trans*-*cis*-[MeSiO(NCO)]$_4$ also reacted with tetraphenyldisiloxanediol in the presence of pyridine to give *syn*-type laddersiloxane (52%). In this reaction, *anti*-type laddersiloxane was not obtained. Therefore, stereoisomerization is very important phenomenon when we synthesize well-defined siloxane structures.

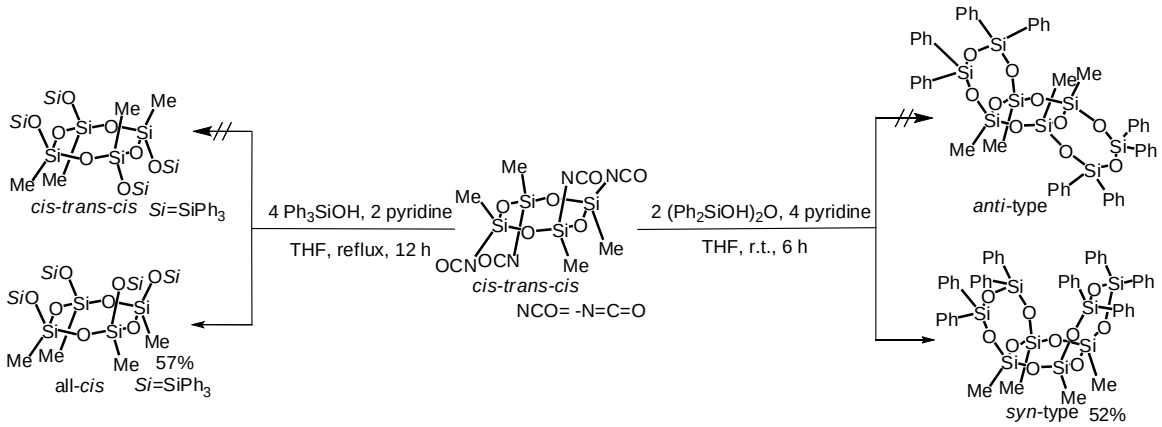

Scheme14

By the way, there are several synthetic reports regarding synthesis of ladder polysilsesquioxanes from $RSiCl_3$. However, there has been no unequivocal evidence of *real* ladder structure. The fact of stereoisomerization taking place in acidic condition indicates that it is impossible to obtain well-defined ladder polysilsesquioxanes from hydrolysis and condensation of $RSiCl_3$ in acidic conditions. We also reported siloxane bond of all-*cis*-[*i*-BuSiO(OH)]$_4$ were cleaved by excess amount of strong base to give complex mixture in 10 min. Therefore, to obtain well-defined ladder polysilsesquioxanes from *cis*-*trans*-*cis*-[RSiO(OH)]$_4$ or all-*cis*-[RSiO(OH)]$_4$, condensation should be operated in neutral condition. In the next part, we described condensation of all-*cis*-[*i*-BuSiO(OH)]$_4$ in DMSO at reflux temperature (Scheme 15). The reaction condition is perfectly neutral condition.

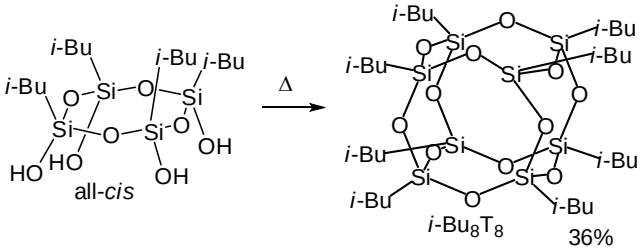

Scheme15

Therefore, condensation of *cis*-*trans*-*cis*-[*i*-BuSiO(OH)]$_4$ in DMSO at reflux temperature is promising to synthesize well-defined ladder polysilsesquioxanes (Scheme 16). Reaction of *cis*-*trans*-*cis*-[RSiO(OH)]$_4$ and *cis*-*trans*-*cis*-[RSiO(H)]$_4$ in the presence of $B(C_6F_5)_3$ is also promising to synthesize well-defined ladder polysilsesquioxanes [3] (Scheme16).

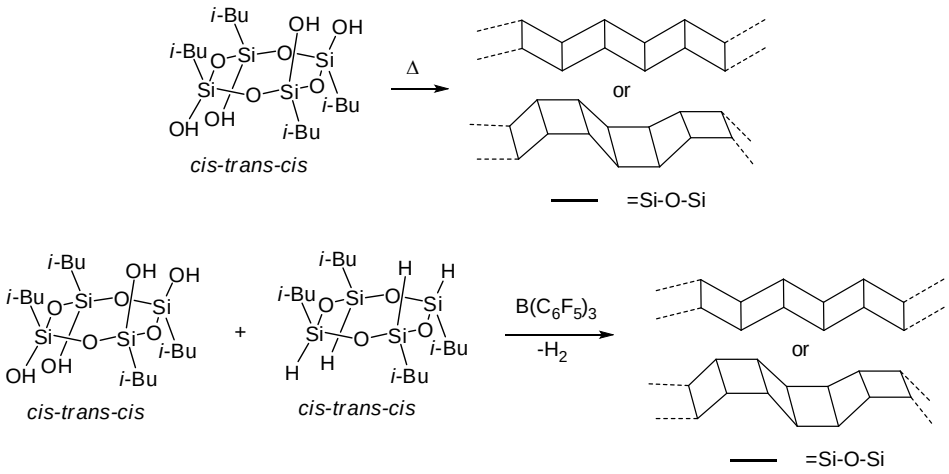

Scheme16

Hydrolysis and condensation of Cl_3Si-R-$SiCl_3$ may form disiloxanetetraols with four hydroxyl groups arranged and this is a promising precursor laddersiloxane (Scheme 17).

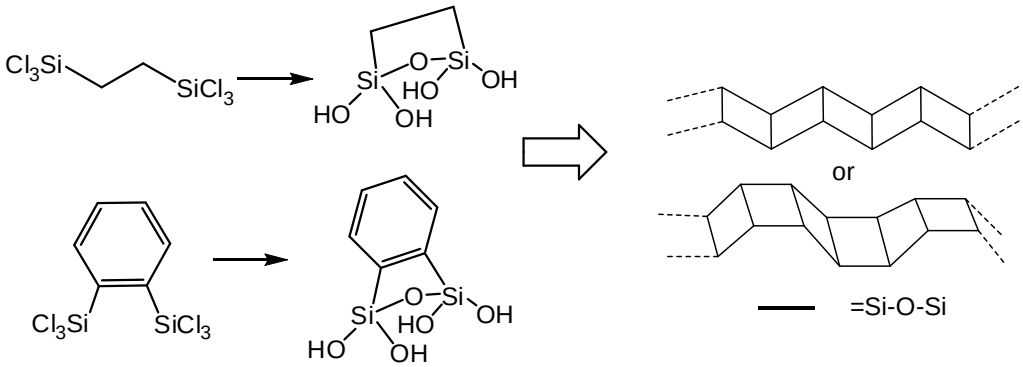

Scheme17

The possibility of 2 molar disiloxanetetoraol to form all-*cis*-cyclotetrasiloxanetetraols indicates possibility to synthesis of asymmetrical all-cis-cyclotetrasiloxanetetraols ($[R_{0.5}R'_{0.5}SiO(OH)]_4$) (Scheme 18).

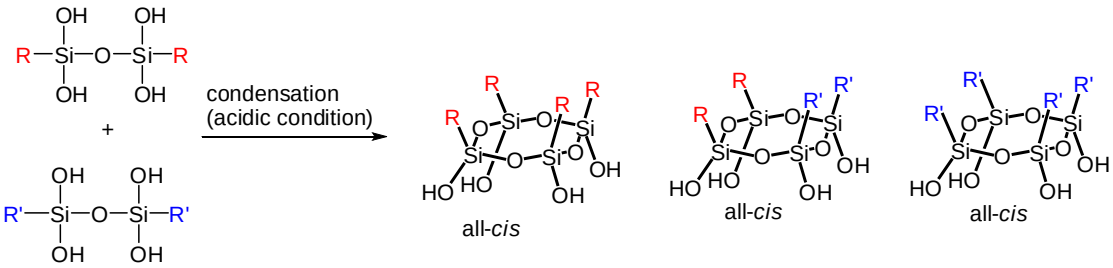

Scheme18

Asymmetrical all-*cis*-cyclotetrasiloxanetetraols is good precursor to Janus cube [4] or asura prism (Scheme 19).

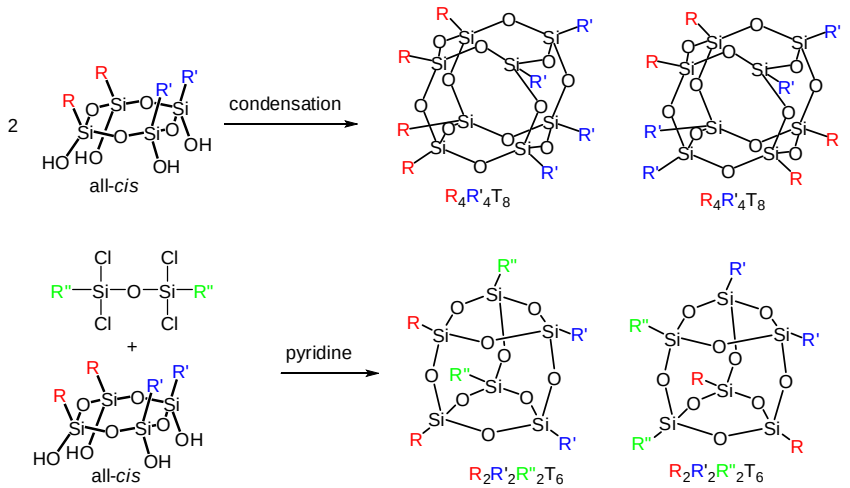

Scheme19

Attempt to stereoisomerization reaction of *cis-trans*-cyclotrisiloxanetriols $[RSiO(OH)]_3$ is promising to synthesize all-*cis*-cyclotrisiloxanetriols (Scheme 20).

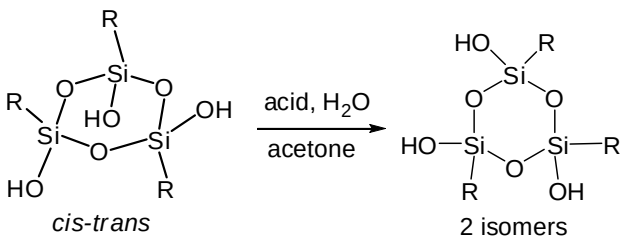

Scheme 20

All-*cis*-$[RSiO(OH)]_3$ is promising to synthesize cage compounds (R_6T_6 or R_4T_4) (Scheme 21).

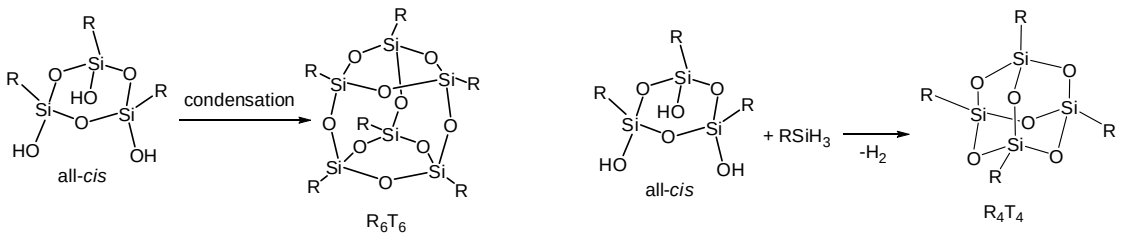

Scheme 21

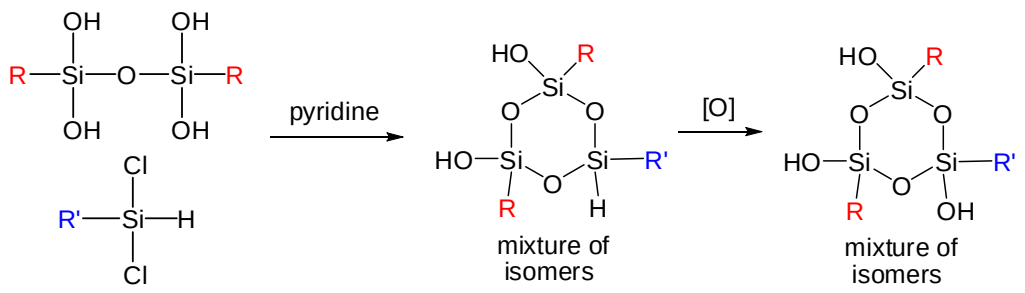

Scheme 22

Disiloxanetetoraol is promising to synthesize asymmetrical cyclotrisiloxanetriols (Scheme 22).

As stated above, we elucidated several experimental facts are promising synthesis of various well-defined siloxane compound.

2.4.2. References

[1a] J. F. Brown, Jr., L.H. Vogt, Jr., *J. Am. Chem. Soc.*, **1965**, *87*, 4317.

[1b] J. F. Brown, Jr., L.H. Vogt, Jr., *J. Am. Chem. Soc.*, **1965**, *87*, 4313.

[1c] F. J. Feher, J. J. Schwab, D. Soulivong, J. W. Ziller, *Main Group Chem.*, **1997**, *2*, 123.

[1d] M. Unno, A. Suto, K. Takada, H. Matsumoto, *Bull. Chem. Soc. Jpn.*, **2000**, *73*, 215.

[1e] O. I. Shchegolikhina, Y. A. Pozdnyakova, Y. A. Molodtsova, S. D. Korkin, S. S. Bukalov, L. A. Leites, K. A. Lyssenko, A. S. Peregudov, N. Auner, D. E. Katsoulis, *Inorg. Chem.*, **2002**, *41*, 6892.

[1f] R. Ito, Y. Kakihana, Y. Kawakami, *Chem. Lett.*, **2009**, *38*, 364.

[1g] Y. A. Pozdnyakova, A. A. Korlyukov, E. G. Kononova, K. A. Lyssenko, A. S. Peregudov, O. I. Shchegolikhina, *Inorg. Chem.*, **2010**, *49*, 572.

[1h] M. Unno, Y. Kawaguchi, Y. Kishimoto, H. Matsumoto, *J. Am. Chem. Soc.*, **2005**, *127*, 2256.

[1i] H. S. Lee, S. S. Choi, K. Y. Baek, S. M. Hong, E. C. Lee, J. C. Lee , S. S. *Hwang*, *European Polymer Journal*, **2012**, *48*, 1073.

[1j] I. Yu. Klement'ev, V. E. Shklover, M. A. Kulish, V. S. Tikhonov, E. V. Volkova, *Dokl. Akad. Nauk SSSR*, **1981**, *259*, 1371.

[1k] N. N. Makarova, I. M. Petrova, P. V. Petrovskii, A. V. Kaznacheev, L. M. Volkova, M. A. Shcherbina, N. P. Bessonova, S. N. Chvalun, and Yu. K. Godovskiib, *Russ. Chem. Bull. Int. Ed.*, **2004**, *53*, 1983.

[2]H. Seki, Y. Abe, and T. Gunji, *J. Organomet. Chem..*, **2011**, *696*, 846.

[3] D. Zhou, Y. Kawakami, *Macromolecules*, **2005**, *38*, 6902.

[4] M. Z. Asuncion, M. Ronchi, H. A. Seir, R. M. Laine, *C. R. Chimie*, **2010**, *13*, 270.

Part 3: Syntheses, structures, and properties of various siloxanes

Abstract of this part

Siloxane compounds with various structures are now widely applied to commercially products. However, relationship of well-defined siloxane structures with properties is almost unknown because there are few synthetic reports of siloxanes with well-defined structure. In this chapter, we synthesized several siloxanes with various structures and elucidate relationship of structure and properties (refractive index and thermal stability). These results will make a valuable contribution in the material design.

Chapter 1: Refractive indices of silsesquioxanes with various structures

3.1.1 Introduction

Although LED (light emitting diode) is widely used because of longer operating life and low electric power consumption, high photo-thermal stability is required for LED encapsulants that epoxy resins can not withstand due to the still low efficiency to generate the high intensity blue light and low ability to resist excessive heat [1].

On the other hand, polysiloxanes or silicones, often quoted as organic-inorganic hybrid materials, are promising because of their thermal and mechanical stabilities and UV resistance. Among silicones, silsesquioxanes show superior light and thermal stability and mechanical properties [2]. In addition, compared to carbon materials, structure modification of silsesquioxanes is relatively easier.

We have reported the syntheses of a series of silsesquioxanes including oligocyclic laddersiloxanes (ladder-type silsesquioxanes with defined structure) [3–10] and cage silsesquioxanes [11–16], and determined the structures. These well-defined structures significantly affect the physical properties. For example, laddersiloxanes show higher Td_5 (5% weight loss) temperatures with increasing ring numbers [3]. These properties of silsesquioxanes are ideal for the usage as LED encapsulant, thus recently silicone resin has been intensively investigated to overcome the weak points of epoxy resin.

The current problem of silicone resins is that they generally show lower refractive index (RI). This reduces low light-extraction efficiency and results in the lower LED performance. For this reason, high performance LED usually needs silicone resin with high RI values although the geometry of the encapsulant and design of LED packages are also important [17]. To improve RI values, introduction of titanium [18, 19] and sulfur [20] atoms, or incorporation of phenyl groups has been examined [21]. However, comparison of the optical properties in connection with the stereostructures has not been investigated to the best of our knowledge.

In this chapter, we focused on the alkyl-containing siloxanes, and relationship of structure and RI values are investigated. These results will make a valuable contribution in the material design for LED encapsulants.

3.1.2 Results and discussion

In this study, we synthesized linear, cyclic, cage, and ladder siloxanes with alkyl groups as shown in Scheme 1.

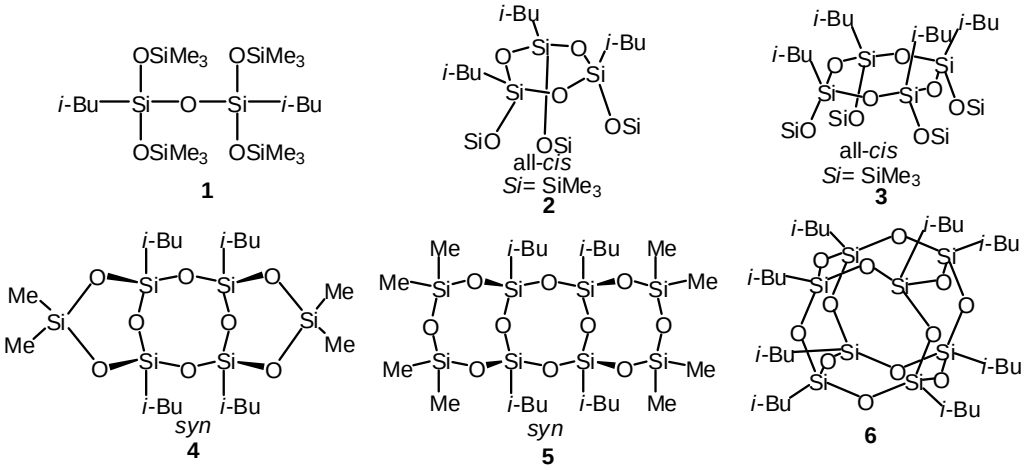

Scheme 1

In order to construct ladder and cage silsesquioxanes, we chose the isobutyl group as a substituent because it gave the highest yields for the synthesis of precursors. Previously, all-*cis*-$[RSiO(OH)]_4$ from trichlorosilanes, $RSiCl_3$ (R = *i*-Pr, Ph) following the reports by our group (R = *i*-Pr, 22% yield) [5] and Feher's group (R = Ph, 37% yield) [22]. In part 2, chapter 1, we reported all-*cis*-[*i*-BuSiO(OH)]$_4$ (**7**) and [*i*-BuSi(OH)$_2$]$_2$O (**8**) can be prepared from *i*-BuSiCl$_3$ by only changing reaction time and temperature (Scheme 2). Kawakami's group also reported the preparation of **7** from *i*-BuSi(OMe)$_3$ in 34% yield [23]. In part 2, chapter 3, we also modified the reaction condition and better yield (74%) was accomplished (Scheme 3).

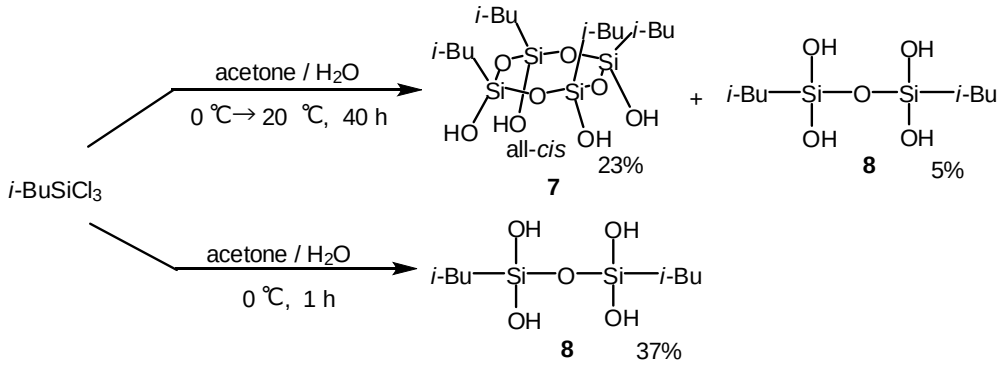

Scheme 2

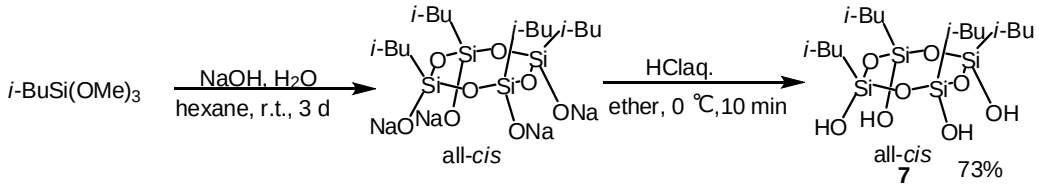

Scheme 3

The reaction of **8** with chlorotrimethylsilane in the presence of triethylamine as an HCl scavenger under reflux in THF gave a linear siloxane (**1**) as a colorless solid (Scheme 4).

Scheme 4

Cyclic siloxane (**2**) and (**3**) could be synthesized from isobutyltrimethoxysilane via cyclic silanolate all-*cis*-[*i*-BuSiO(ONa)]$_3$ or all-*cis*-[*i*-BuSiO(ONa)]$_4$ (Scheme 5).

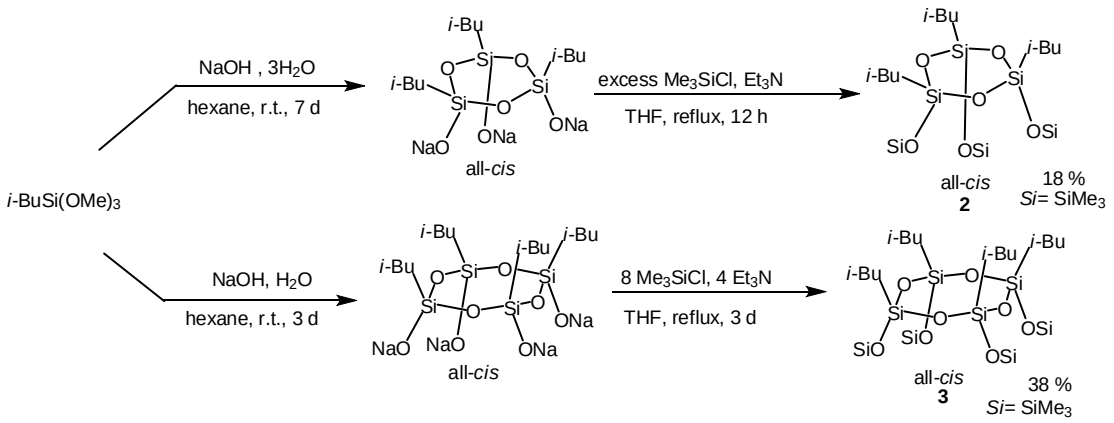

Scheme 5

In 2004, Shchegolikhina's group reported the synthesis of all-*cis*-[RSiO(OM)]$_3$ from phenyltrialkoxysilane (R = Ph, M = Na, K) [24]. They also applied this reaction to the silanolate with various substituents (R = Me, Et, Pr, Vi, M = Na, K) [25]. In reference to their results, we synthesized all-*cis*-cyclotrisiloxanesilanolate by using isobutyltrimethoxysilane, sodium hydroxide and 3 eq. of water. Compound **2** was obtained by the reaction of all-*cis*-[*i*-BuSiO(ONa)]$_3$ with chlorotrimethylsilane in the presence of triethylamine. In ^{29}Si NMR, compound **2** shows only 2 peaks at –59.29 ppm and 9.04 ppm. This result indicates the structure of **2** is all-*cis* type. Compound **3** was obtained by reaction of all-*cis*-[*i*-BuSiO(ONa)]$_4$ with chlorotrimethylsilane in the presence of triethylamine under reflux in THF.

The reaction of **7** with dichlorodimethylsilane or 1,3-dichloro-1,1,3,3-tetramethyldisiloxane in the presence of triethylamine afforded tricyclic laddersiloxane **4** or **5**. Compounds **4** and **5** were isolated as a colorless liquid in 31% and 60% yield, respectively (Scheme 6). All the previously reported tricyclic laddersiloxanes were solid [3], but isobutyl-substituted **4** and **5** are liquid.

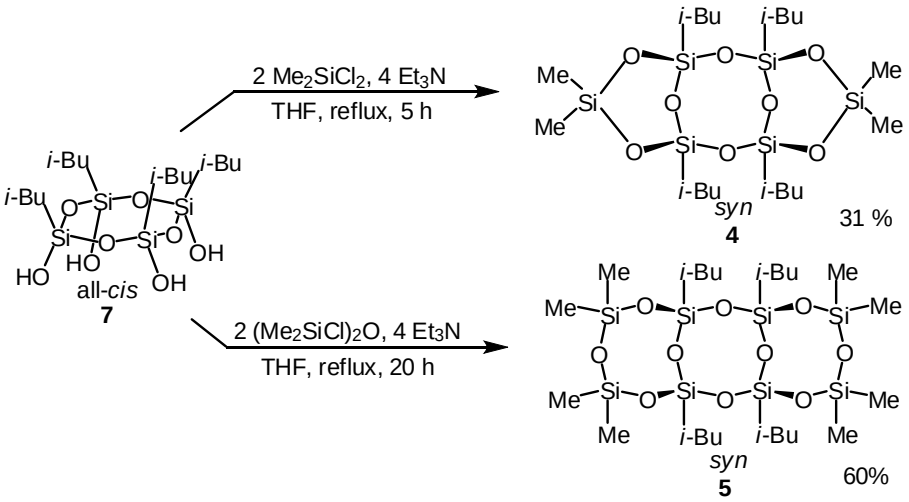

Scheme 6

Several synthetic methods of octaisobutyloctasilsesquioxane (**6**) have been reported [26]. We reported that siloxanes could be obtained by the reaction of silanol with DMSO [5,11,14]. The reaction of **7** under reflux in DMSO gave **6** in 36% yield. Kawakami's group reported that reaction of **7** with tetrabutylammonium fluoride (TBAF) as catalyst afforded **6** in 93% yield [27]. Applying a similar manner, we obtained **6** in high yield from disiloxanetetraol **8** (Scheme 7). The structures of all the siloxanes were unequivocally determined by spectroscopic methods.

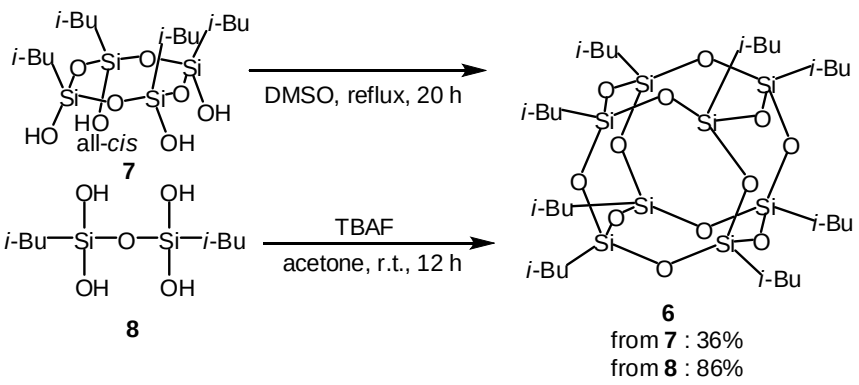

Scheme 7

The values of ^{29}Si NMR are summarized in Table 1. In ^{29}Si NMR, **7** shows one peak at −58.2 ppm. This value is in good agreement with that of all-*cis*-[*i*-PrSiO(OH)]$_4$ (−59.7 ppm) whose structure was determined by X-ray analysis [28]. Linear disiloxanetetraol **8** showed 8 ppm lower-field shift from cyclic **7**, which is a further condensed product from **8**. The same tendency can be observed for all-*cis*-[PhSiO(OH)]$_4$ (−69.84 ppm) [22] and [PhSi(OH)$_2$]$_2$O (−62.1 ppm) [29]. Higher-field shift was observed by siloxylation of silanol **7** or **8**. The value of ^{29}Si NMR for T part (RSiO$_{1.5}$) of laddersiloxanes, different chemical shifts were observed for six-membered ring and eight-membered ring. Basically, silicon atoms in six-membered rings of **2** and **4** were observed about 10 ppm lower field than eight-membered ring silicon atoms of **3**, **5**, and **6**. A similar relationship was also observed for all-*cis*-[PhSiO(OSiMe$_3$)]$_4$ and all-*cis*-[PhSiO(OSiMe$_3$)]$_3$ [24]. These data are useful to predict siloxane structures with unknown siloxane compounds (e.g. ring size, and number of siloxane bond).

Table 1. ^{29}Si NMR data of various siloxanes (δ , ppm)

Silsesquioxanes	R$_3$SiO$_{0.5}$	R$_2$SiO	RSiO$_{1.5}$
1	6.9		–68.3
2	9.0		–59.3
3	8.1		–69.5
4		–6.2	–56.2
5		–19.3	–67.4
6			–67.9
7			–58.2
8			–49.8
9		–20.98, –21.38, –21.51	–55.96, –56.08, –56.13

The result of RI analysis is summarized in Table 2. Liquid compounds were measured in neat, and solid compounds were measured in film. Unfortunately, **6** could not be measured because we could not make a suitable film for RI analysis because **6** has high melting point and good crystallinity. As model compounds, we also measured PDMS (polydimethylsiloxane) and *i*-BuSi(OMe)$_3$. The results showed that RI of *i*-BuSi(OMe)$_3$, PDMS, and **1** without ring structures showed lower values than that of **2**–**5** with ring structure. RI values of **4** and **5** were higher than those of **2** and **3**. However, against our expectations, we observed no significant differences in RI values

by the structures. Although silicon compounds containing aliphatic substituents show similar RI values, the isobutyl group usually shows slightly higher RI values than those with methyl groups. Among compounds **1**–**5**, tricyclic laddersiloxane **4** possesses the highest *i*-Bu/Me ratio (1.0) while that of compound **1** is the lowest (0.17). In addition, our previous results [7] indicated that laddersiloxanes show higher density with increasing ring numbers. This may be the reason for slightly higher RI values. Nonetheless, the results of Abbe numbers indicated the promising property of laddersiloxanes. Usually lower values (high dispersion for visible light) are observed by increasing refractive indices, however a different tendency was observed for our compounds. Thus, laddersiloxane **4** showed the highest refractive index value, whereas Abbe number of **4** is also the highest. This is a promising result because laddersiloxane structure can afford materials with high refractive index with low dispersion. Cyclic and linear silsesquioxanes showed Abbe numbers in inverse proportion to refractive index values, as usually observed.

Table 2. RI data of alkyl silsesquioxane compounds

Compound	PDMS	*i*-BuSi(OMe)$_3$	**1**	**2**	**3**	**4**	**5**
Structure	linear	monomer	linear	cyclic	cyclic	ladder	ladder
State	liquid	liquid	solid	liquid	solid	liquid	liquid
Ring numbers	0	0	0	1	1	3	3
n_D (589nm)*	1.4030	1.3908	1.4001	1.4179	1.4181	1.4306	1.4281
Abbe No: ν_D	54	62	56	54	46	64	59

* n_D= refractive index

These synthesized compounds are difficult to apply to siloxane resin because these compounds do not have reactive substituents. The structures of tricyclic laddersiloxane having six-eight-six-membered ring an be easily modified by dichlorosilane bearing various substituents because there are many dichlorosilanes commercially available. Therefore, we attempted to synthesize six-eight-six membered ring type tricyclic laddersiloxane bearing vinyl groups as reactive substituents (Scheme 8).

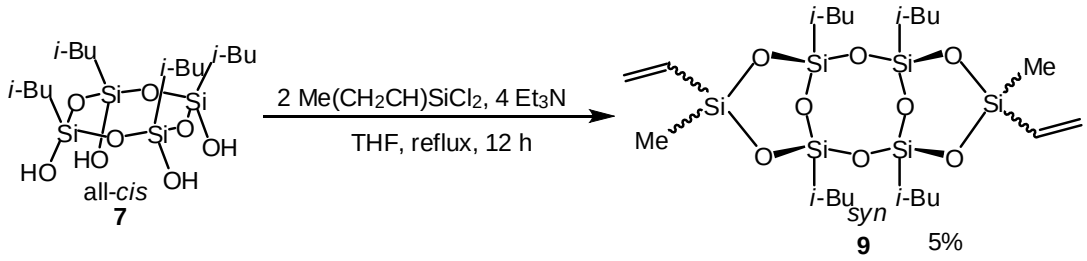

Scheme 8

The reaction of **7** with dichloromethylvinylsilane in the presence of triethylamine as an HCl scavenger under reflux in THF gave 5,11-diethenyl-5,11-dimethyl-1,3,7,9-tetraisobutyl-tricyclo[7.3.1.1^{3,7}]hexasiloxane (**9**). GC chart of **9** shows 3 peaks. And ^{29}Si NMR spectrum of **9** shows 3 peaks in –56 ppm region. This fact indicates **9** including 3 isomers.

3.1.3 Summary

We selectively synthesized isobutyl-substituted cyclic and linear silanols from *i*-BuSiCl$_3$ by only changing reaction time and temperature. These silanols were converted to linear, cyclic, cage, and ladder silsesquioxanes by reaction with corresponding chlorosilanes. We elucidated that RI values of these siloxane compounds slightly increase as ring number increases. Among the compounds we investigated, laddersiloxanes afforded best results for both refractive index and Abbe number. We also synthesized six-eight-six membered ring type tricyclic laddersiloxane bearing vinyl substituents as reactive substituents that can be applied to siloxane resin.

3.1.4 Experimental section

The Fourier transform nuclear magnetic resonance (NMR) spectra were obtained using a Jeol ECS-300 (^{1}H at 300.53 MHz, ^{13}C at 75.57 MHz, and ^{29}Si at 59.71 MHz) NMR instruments. Chemical shifts are reported as δ units (ppm) relative to SiMe$_4$, and residual solvents peaks were used for standards. For ^{29}Si NMR, SiMe$_4$ was used as an external standard. Electron impact mass spectrometry was performed on a Shimadzu GCMS-QP2010SE / DI2010. Infrared spectra were measured with a Shimadzu FTIR-8400S. High resolution mass spectrometry was performed on a JEOL AccuTOF-CS. Refractive indexes were measured by Multi-wavelength Abbe Refractometer DR-M2/1550 (ATAGO Co., Ltd.) at 25 ℃.

Synthesis of 1,1,1,7,7,7-Hexamethyl-3,5-diisobutyl-3,5-bis(trimethylsilyloxy)tetrasiloxane (**1**)

Under argon atmosphere, chlorotrimethylsilane (5.5 g, 51 mmol) in THF (20 mL) was added to a solution of **7** (2.5 g, 9.8 mmol) and triethylamine (5.1 g, 50 mmol) in THF (30 mL) at 0 ℃. The mixture was refluxed for 1 day. Hexane was added to reaction mixture and organic phase was washed with saturated ammonium chloride aqueous solution and brine. The organic phase was dried over anhydrous sodium sulfate and evaporated to give crude solid. The solid was filtrated, and washed by methanol. And the solid was more purified by HPLC to give **1** (2.4 g, 45%).

Spectral data for **1**: m.p. 131–135 ℃. ^{1}H NMR (300.53 MHz, $CDCl_3$) δ 0.08 (s, 36H), 0.45 (d, *J* = 6.6 Hz, 4H), 0.92 (d, *J* = 6.6 Hz, 12H), 1.79 (nonet, *J* = 6.6 Hz, 2H) ppm. ^{13}C NMR (75.57 MHz, $CDCl_3$) δ 25.98(CH_3), 25.04(CH_2), 24.09 (CH), 1.79 (CH_3) ppm. ^{29}Si NMR (59.71 MHz, $CDCl_3$) δ 6.93, –68.34 ppm. GCMS (EI, 70eV) *m*/z (%) 527 ([M–Me]$^+$, 21) ,485 ([M–*i*-Bu]$^+$, 19), 73 (100) . IR (KBr) 756, 843, 866, 1061, 1109, 1252, 2957 cm^{-1}. HRMS (m/z) [M＋Na]$^+$ calcd. for $C_{20}H_{54}NaO_5Si_6$, 565.24845; found, 565.25012.

Synthesis of all-*cis*-2,4,6-triisobutyl-2,4,6-tris[trimethylsiloxy]-cyclotrisiloxane (**2**)

Isobutyltrimethoxysilane (4.5 g, 25 mmol) was added to a solution of sodium hydroxide (1.1 g, 28 mmol), hexane (25 mL) and water (1.4 g, 78 mmol) at room temperature. The reaction mixture was stirred for 7 days. Most of the solvents (ca. 75%) were removed by a rotary evaporator until precipitate generated. The formed solid was filtrated and washed with hexane and ether, and dried under reduced pressure to give sodium salt (2.4 g). Under argon atmosphere, chlorotrimethylsilane (5.5 g, 51 mmol) in THF (20 mL) was added to a solution of sodium salt (2.4 g) and triethylamine (5.0 g, 49 mmol) in THF (20 mL) at 0 ℃. The mixture was refluxed for 5 h. Hexane was added to the reaction mixture and organic phase was washed with saturated ammonium chloride aqueous solution and brine. The organic phase was dried over anhydrous sodium sulfate and evaporated to give crude liquid. And the liquid was more purified by HPLC and bulb to blub distillation to give **2** (0.85 g, 18%)

Spectral data for **2**: b.p. 140 ℃ (0.25 mmHg). ^{1}H NMR (300.53 MHz, $CDCl_3$) δ 0.12 (s, 27H), 0.53 (d, *J* = 6.9 Hz, 6H), 0.93 (d, *J* = 6.9 Hz, 18H), 1.80 (nonet, *J* = 6.9 Hz, 3H) ppm. ^{13}C NMR (75.57 MHz, $CDCl_3$) δ 1.76(CH_3) 23.93 (CH), 24.29 (CH_2), 25.89 (CH_3) ppm. ^{29}Si NMR (59.71 MHz, $CDCl_3$) δ 9.04, –59.29 ppm. GCMS (EI, 70eV) *m*/z (%) 555 ([M–Me]$^+$,11) ,513 ([M–*i*-Bu]$^+$, 7), 73 (100) . IR (NaCl) 757, 843, 863, 1023, 1110, 1254, 1466, 2871, 2903, 2957 cm^{-1}. HRMS (m/z) [M＋H]$^+$ calcd. for

$C_{21}H_{55}O_6Si_6$, 571.26142; found, 571.26119.

Synthesis of all-*cis*-2,4,6,8-tetraisobutyl-2,4,6,8-tetrakis[trimethylsiloxy]-cyclotetrasiloxane (**3**)

Isobutyltrimethoxysilane (4.5 g, 25 mmol) was added to a solution of sodium hydroxide (1.0 g, 25 mmol), hexane (25 mL) and water (0.46 g, 26 mmol) at room temperature. The reaction mixture was stirred for 3 days. The formed precipitate was filtrated and washed with hexane and dried under reduced pressure to give sodium salt (2.5 g). Under argon atmosphere, chlorotrimethylsilane (3.3 g, 30 mmol) in THF (20 mL) was added to a solution of sodium salt (2.5 g) and triethylamine (3.1 g, 31 mmol) in THF (20 mL) at 0 ℃. The mixture was refluxed for 3 days. The reaction was traced by GCMS, but the reaction did not complete. Further chlorotrimethylsilane (3.1 g, 31 mmol) was added and the mixture was refluxed for 3 h. Hexane was added to reaction mixture and organic phase was washed with saturated ammonium chloride aqueous solution and brine. The organic phase was dried over anhydrous sodium sulfate and evaporated to give crude solid. The solid was filtrated, and washed by methanol to give **3** (1.8 g, 38 %).

Spectral data for **3**: m.p. 167–170 ℃. ^{1}H NMR (300.53 MHz, $CDCl_3$) δ 0.11 (s, 36H), 0.47 (d, J = 6.9 Hz, 8H), 0.92 (d, J = 6.9 Hz, 24H), 1.78 (nonet, J = 6.9 Hz, 4H) ppm. ^{13}C NMR (75.57 MHz, $CDCl_3$) δ 1.84 (CH_3), 24.11 (CH), 24.68 (CH_2), 25.95 (CH_3) ppm. ^{29}Si NMR (59.71 MHz, $CDCl_3$) δ 8.10, –69.49 ppm. GCMS (EI, 70eV) *m*/z (%) 745 ([M–Me]$^+$, 9), 73 (100) . IR (KBr) 756, 843, 866, 1057, 1113, 1254, 2957 cm^{-1}. HRMS (m/z) [M＋Na]$^+$ calcd. for $C_{28}H_{72}NaO_8Si_8$, 783.32790; found, 783.32580.

Synthesis of 1,1,7,7-Tetramethyl-3,5,9,11-tetraisobutyltricyclohexasiloxane (**4**)

Under argon atmosphere, dichlorodimethylsilane (1.9 g, 15 mmol) in THF (25 mL) was added to a solution of **7** (3.6 g, 7.6 mmol) and triethylamine (3.0 g, 30 mmol) in THF (25 mL) at 0 ℃. The mixture was refluxed for 5 h. Hexane was added to reaction mixture and organic phase was washed with saturated ammonium chloride aqueous solution and brine. The organic phase was dried over anhydrous sodium sulfate and evaporated to give crude liquid. The liquid was purified by bulb to blub distillation to give **4** (1.4 g, 32 %).

Spectral data for **4**: b.p. 135 ℃ (0.25 mmHg). ^{1}H NMR (300.53 MHz, $CDCl_3$) δ 0.17 (s, 6H), 0.22 (s, 6H), 0.63 (d, J = 6.6 Hz, 8H), 0.95 (d, J = 6.6 Hz, 24H), 1.85 (nonet, J = 6.6 Hz, 4H) ppm. ^{13}C NMR (75.57 MHz, $CDCl_3$) δ 25.70 (CH_3), 23.69 (CH), 22.94 (CH_2), 0.95 (CH_3), 0.93 (CH_3) ppm. ^{29}Si NMR (59.71 MHz, $CDCl_3$) δ –6.15,

–56.19 ppm. GCMS (EI, 70eV) *m*/z (%) 569 ([M–Me]$^+$,88) ,527 ([M–*i*-Bu]$^+$, 100) . IR (NaCl) 800, 822, 1009, 1028, 1043, 1090, 1229, 1261, 1466, 2361, 2872 cm^{-1}. HRMS (m/z): [M＋H]$^+$ calcd. for $C_{20}H_{49}O_8Si_6$, 585.20430; found, 585.20469.

Synthesis of 5,5,7,7,13,13,15,15-octamethyl-1,3,9,11-tetraisobutyl-tricyclo[9.5.1.1^{3,9}]octasiloxane (**5**)

Under argon atmosphere, 1,3-dichloro-1,1,3,3-tetramethyldisiloxane (3.1 g, 15 mmol) in THF (25 mL) was added to a solution of **7** (3.5 g, 7.4 mmol) and triethylamine (3.1 g, 31 mmol) in THF (25 mL) at 0℃. The mixture was refluxed for 20 h. Hexane was added to reaction mixture and organic phase was washed with saturated ammonium chloride aqueous solution and brine. The organic phase was dried over anhydrous sodium sulfate and evaporated to give crude liquid. The liquid was purified by HPLC to give **5** (3.3 g, 61%)

Spectral data for **5**: b.p. 155 ℃ (0.25 mmHg). ^{1}H NMR (300.53 MHz, $CDCl_3$) δ 0.08 (s, 12H), 0.12 (s, 12H), 0.54 (d, *J* = 6.6 Hz, 8H), 0.93 (d, *J* = 6.6 Hz, 24H), 1.81 (nonet, *J* = 6.6 Hz, 4H) ppm. ^{13}C NMR (75.57 MHz, $CDCl_3$) δ 25.82(CH_3), 25.77(CH_3), 24.03(CH), 23.59(CH_2), 0.78(CH_3), 0.69(CH_3) ppm. ^{29}Si NMR (59.71 MHz, $CDCl_3$) δ –19.31, –67.44 ppm. GCMS (EI, 70eV) *m*/z (%) 717 ([M–Me]$^+$,11) ,675 ([M–*i*-Bu]$^+$, 38), 73 (100) . IR (NaCl) 802, 1059, 1099, 1261, 2870, 2905, 2955 cm^{-1}. HRMS (m/z): [M＋Na]$^+$ calcd. for $C_{24}H_{60}NaO_{10}Si_8$, 755.22383; found, 755.23222.

Synthesis of octaisobutyloctasilsesquioxane (**6**) from **7**

Compound **7** (0.20 g, 0.42 mmol) and DMSO (15 mL) were charged in a flask. The reaction mixture was refluxed for 20 h. White solid was precipitated. The solid was filtrated, and washed by DMSO and water. The product was dried under reduced pressure to give **6** (0.067 g, 36 %).

Synthesis of octaisobutyloctasilsesquioxane (**6**) from **8**

Compound **8** (0.50 g, 2.0 mmol) and acetone (15 mL) were charged in a flask. 1M THF solution of TBAF (22 μl, 22 μmol) was added with stirring. The reaction mixture was stirred for 12 h. White solid was precipitated. The solid was filtrated, and washed by acetone and methanol. The product was dried under reduced pressure to give **6** (0.37 g, 84%).

Spectral data for **6**: m.p. 246–249 ℃. ^{1}H NMR (300.53 MHz, $CDCl_3$) δ 0.57 (d, *J*

= 6.9 Hz, 16H), 0.93 (d, J = 6.9 Hz, 48H), 1.83 (nonet, J = 6.9 Hz, 8H) ppm. ^{13}C NMR (75.57 MHz, $CDCl_3$) δ 22.50 (CH_2), 23.86 (CH), 25.69 (CH_3) ppm. ^{29}Si NMR (59.71 MHz, $CDCl_3$) δ –67.86 ppm. DIMS (EI, 70eV) *m*/z (%) 815 ([M–*i*-Bu]$^+$,100). IR (KBr) 486, 748, 1105, 1117, 1231, 2872, 2905, 2928, 2955 cm^{-1}.

Synthesis of all-*cis*-1,3,5,7-tetrahydroxy-1,3,5,7-tetraisobutyl-cyclotetrasiloxane (**7**) and synthesis of 1,3-diisobutyldisiloxane-1,1,3,3-tetrol (**8**) were described in this thesis (Part 2, Chapter 1).

Synthesis of 5,11-divinyl-5,11-dimethyl-1,3,7,9-tetraisobutyl-tricyclo[7.3.1.1^{3,7}]hexasiloxane (**9**)

Dichloromethylvinylsilane (2.1 g, 15 mmol) in THF (23 mL) was added to a solution of **7** (3.6 g, 7.6 mmol) and triethylamine (3.0 g, 30 mmol) in THF (25 mL) at 0 ℃. The mixture was refluxed for 12 h. Hexane was added to the reaction mixture and organic phase was washed with saturated ammonium chloride aqueous solution and brine. The organic phase was dried over anhydrous sodium sulfate and evaporated to give crude liquid. And the liquid was further purified by HPLC and bulb to blub distillation to give **9** (0.22 g, 5%).

Spectral data for **9**: b.p. 150 ℃ (0.18 mmHg). ^{1}H NMR (300.53 MHz, $CDCl_3$) δ 0.25–0.30 (m, 6H), 0.62–0.67 (m, 8H), 0.93–0.97 (m, 24H), 1.79–1.94 (m, 4H), 5.79–6.14 (m, 6H) ppm. ^{13}C NMR (75.57 MHz, $CDCl_3$) δ –1.24 (CH_3), –0.97 (CH_3), –0.71 (CH_3), –0.60 (CH_3), 22.94 (CH_2) overlapped, 23.70 (CH) overlapped, 25.70 (CH_3) overlapped, 134.07 (CH_2), 134.26 (CH_2), 134.75 (CH), 135.07 (CH), 135.14 (CH_2), 135.48 (CH, CH_2) overlapped, 135.67 (CH) ppm. ^{29}Si NMR (59.71 MHz, $CDCl_3$) δ –20.98, –21.38, –21.51, –55.96, –56.08, –56.13 ppm. GCMS (EI, 70eV) *m*/z (%) 608 ([M]$^+$, 8) ,551 ([M–*i*-Bu]$^+$,100) , 537 ([M–*i*-Bu–Me+H]$^+$, 80) . IR (NaCl) 744, 785, 822, 1007-1090, 1229, 1261, 2872, 2907, 2930, 2955 cm^{-1}. HRMS (m/z): [M＋H]$^+$ calcd. for $C_{17}H_{57}O_6Si_9$, 609.20785; found, 609.20513.

3.1.5 References

[1] E. F. Schubert, “Light-emitting diodes, second edition”, Cambridge University Press, Cambridge, **2006**.

[2] R. H. Baney, M. Itoh, A. Sakakibara, T. Suzuki, *Chem. Rev.*, **1995**, *95*, 1409.

[3] M. Unno, A. Suto, T. Matsumoto, *Russ. Chem. Rev.*, **2013**, *82*, 289.

[4] M. Unno, B. A. Shamsul, M. Arai, K. Takada, R. Tanaka, H. Matsumoto, *Appl. Organomet. Chem.* **1999**, *13*, 303.

[5] M. Unno, A. Suto, K. Takada, H. Matsumoto, *Bull. Chem. Soc. Jpn.*, **2000**, *73*, 215.

[6] M. Unno, A. Suto, H. Matsumoto, *J. Am. Chem. Soc.*, **2002,** *124*, 1574.
[7] M. Unno, R. Tanaka, S. Tanaka, T. Takeuchi, S. Kyushin, H. Matsumoto, *Organometallics*, **2005,** *24*, 765.
[8] M. Unno, T. Matsumoto, H. Matsumoto, *J. Organomet., Chem.* **2007**, *692*, 307.
[9] S. Chang, T. Matsumoto, H. Matsumoto, M. Unno, *Appl. Organomet., Chem.* **2010**, *24*, 241.
[10] M. Unno, T. Matsumoto, H. Matsumoto, *Int. J. Polym. Sci.*, **2012**, ID 723892.
[11] M. Unno, S. B. Alias, H. Saito, H. Matsumoto, *Organometallics*, **1996**, *15*, 2413.
[12] M. Unno, T. Matsumoto, K. Mochizuki, K. Higuchi, M. Goto, H. Matsumoto, *J. Organomet. Chem.*, **2003**, *685*, 156.
[13] M. Unno, T. Tanaka, H. Matsumoto, *J. Organomet. Chem.*, **2003**, *686*, 175.
[14] M. Unno, Y. Imai, H. Matsumoto, *Silicon Chem.*, **2003**, 2, 175.
[15] H. Liu, S. Kondo, N. Takeda, M. Unno, *J. Am. Chem. Soc.*, **2008**, *130*, 10074.
[16] H. Liu, S. Kondo, N. Takeda, M. Unno, *Eur. J. Inorg. Chem.*, **2009**, 1317.
[17] K. T. Kim, S. H. Park, K. T. Kim, K. Jo, J. H. Hwang, H. K. Kwon, *J. Korean Phys. Soc.*, **2010**, *57*, 1779.
[18] W. Chen, W. Liu, P. Wu, P. Chen, *Mater. Chem. Phys.*, **2004**, *83*, 71.
[19] H. Mori, Y. Miyamura, T. Endo, *Mater. Chem. Phys.*, **2009**, *115*, 287.
[20] H. Mori, K. Takahashi, R. Koizumi, K. Ohmori, M. Hidaka, *Colloid. Polym. Sci.*, **2013**, *291*: 1085.
[21] J. S. Kim, S. C. Yang, B. S. Bae, *Chem. Mater.*, **2010**, *22*, 3549.
[22] F. J. Feher, J. J. Schwab, D. Soulivong, J. W. Ziller, *Main Group Chem.*, **1997**, *2*, 123.
[23] R. Ito, Y. Kakihana, Y. Kawakami, *Chem. Lett.*, **2009**, *38*, 364.
[24] Yu. A. Pozdniakova, K. A. Lyssenko, A. A. Korlyukov, I. V. Blagodatskikh, N. Auner, D. Katsoulis, O. I. Shchegolikhina, *Eur. J. Inorg. Chem.*, **2004**, *6*, 1253.
[25]Y. A. Pozdnyakova, A. A. Korlyukov, K. A. Lyssenko, L. Zherlitsyna, N. Auner , O. I. Shchegolikhina, *J. Organomet. Chem.*, **2013**, *729*, 86.
[26] D. B. Cordes, P. D. Lickiss, F. Rataboul, *Chem. Rev.*, **2010**, *110*, 2081.
[27] S. Tateyama, Y. Kakihana, and Y. Kawakami, *J. Organomet. Chem.*, **2010**, *695*, 898.
[28] M. Unno, K. Takada, H. Matsumoto, *Chem. Lett.*, **1998**, 489.
[29] K. Suyama, T. Nakatsuka, T. Gunji, Y. Abe, *J. Organomet. Chem.*, **2007**, *692*, 2028.

3.1.6 Supporting information

1. Spectral data

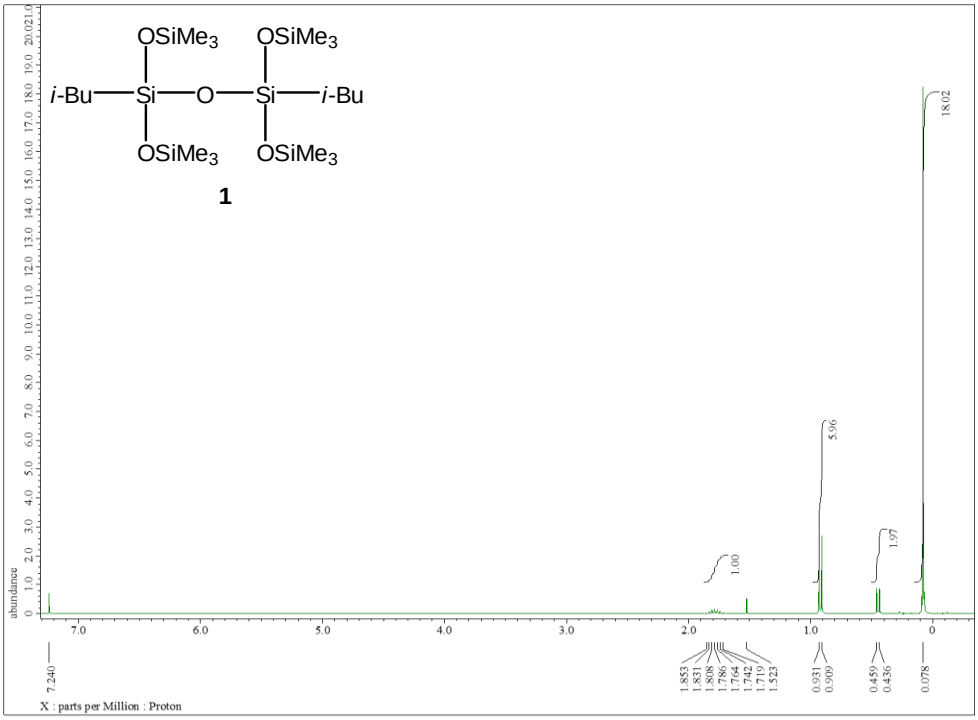

Figure 1. ^{1}H NMR spectrum of **1** (300.53 MHz, $CDCl_3$)

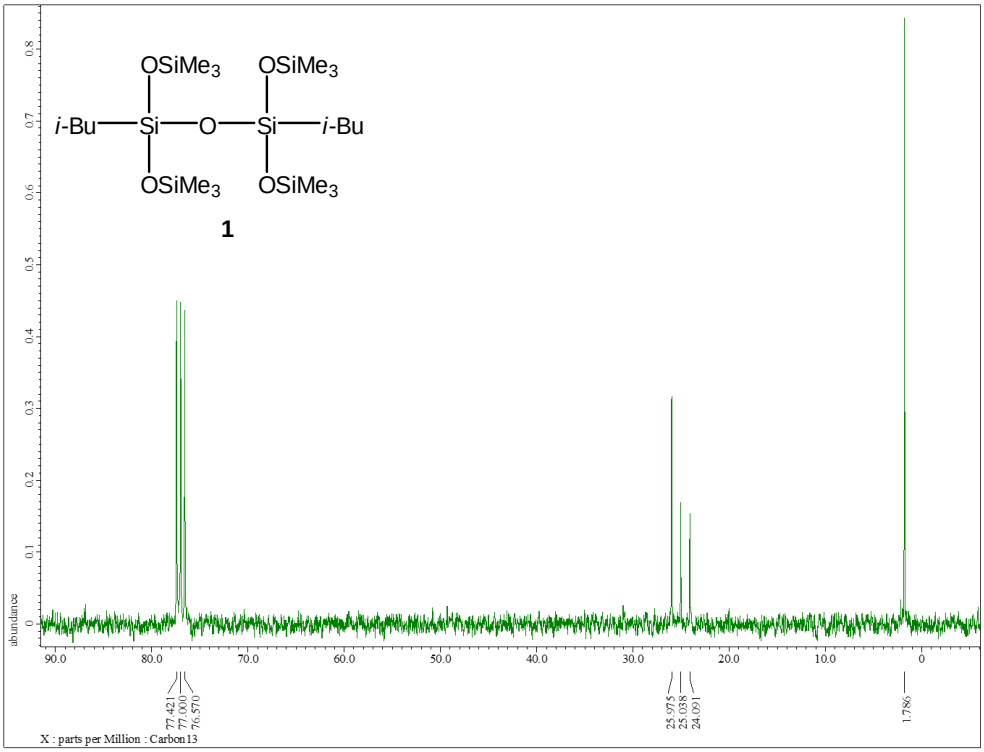

Figure 2. ^{13}C NMR spectrum of **1** (75.57 MHz, $CDCl_3$)

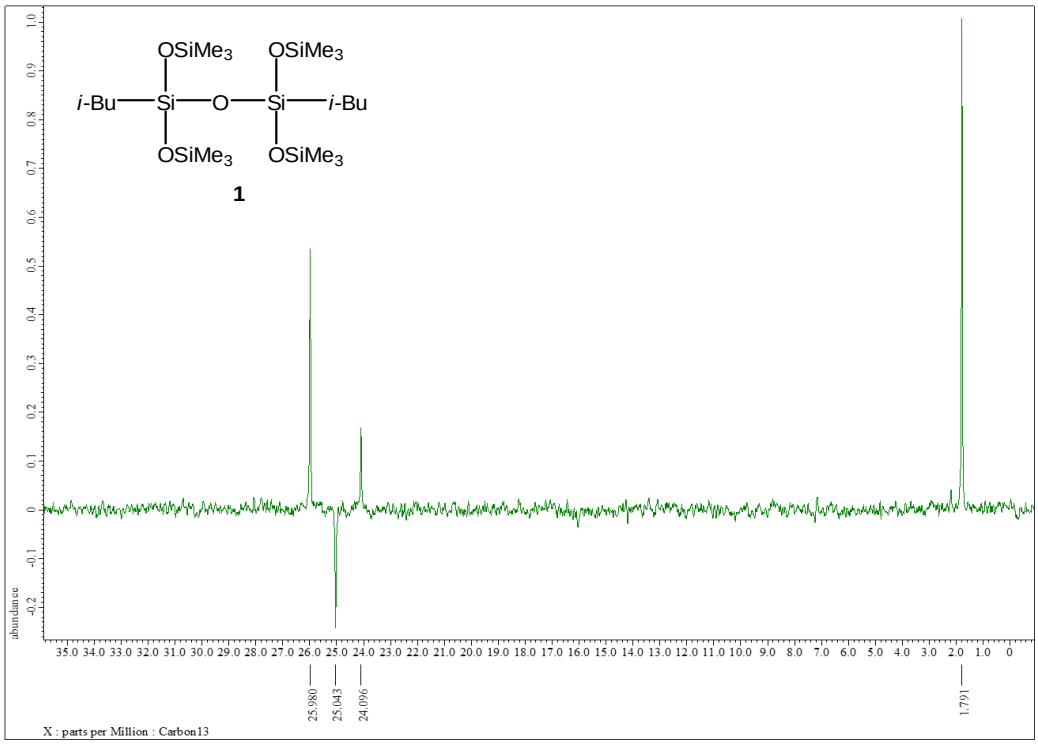

Figure 3. ^{13}C NMR (dept 135) spectrum of **1** (75.57 MHz, $CDCl_3$)

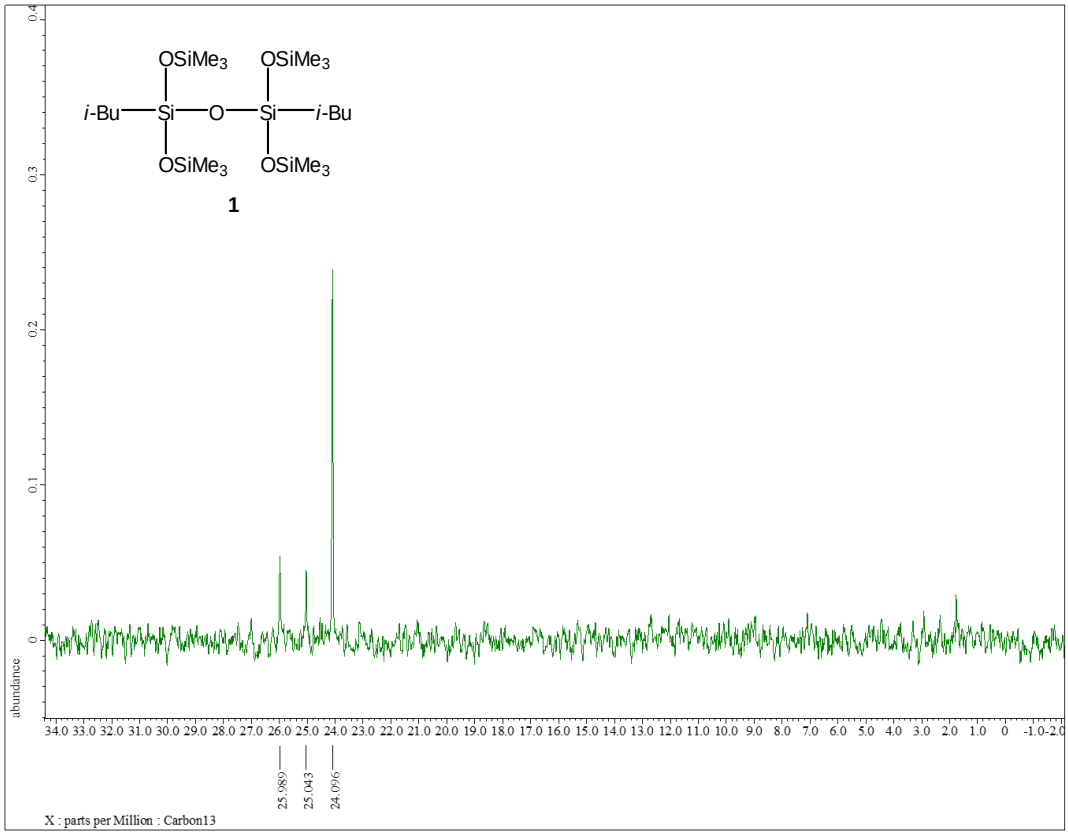

Figure 4. ^{13}C NMR (dept 90) spectrum of **1** (75.57 MHz, $CDCl_3$)

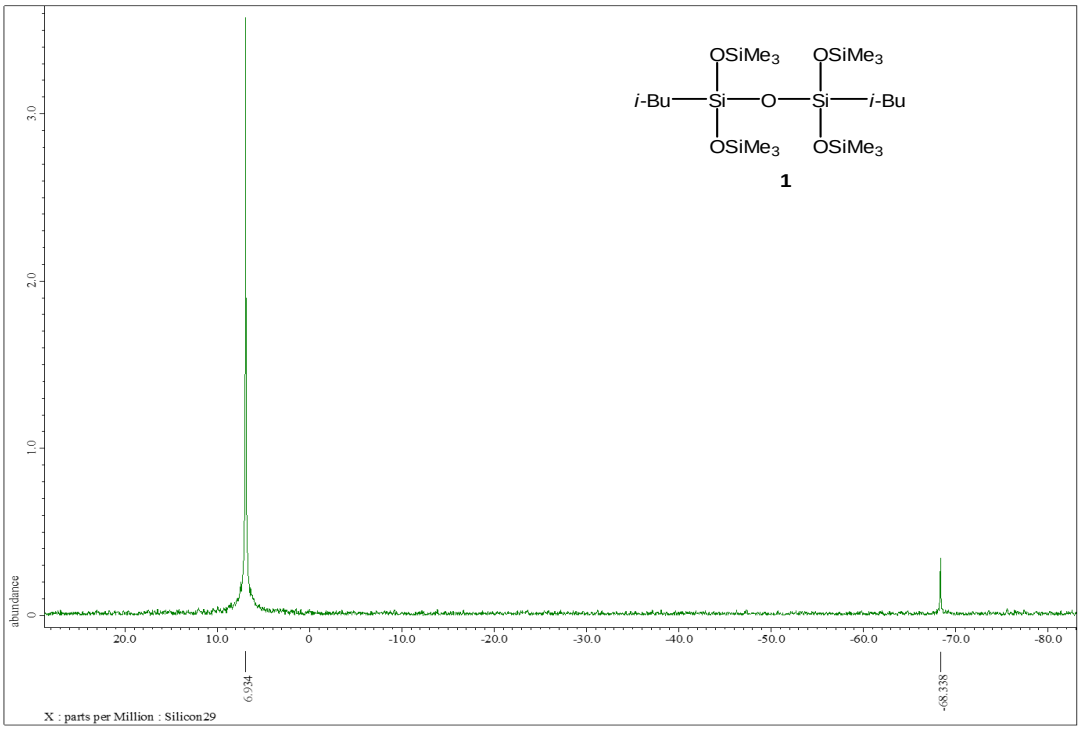

Figure 5. ^{29}Si NMR spectrum of **1** (59.71 MHz, $CDCl_3$)

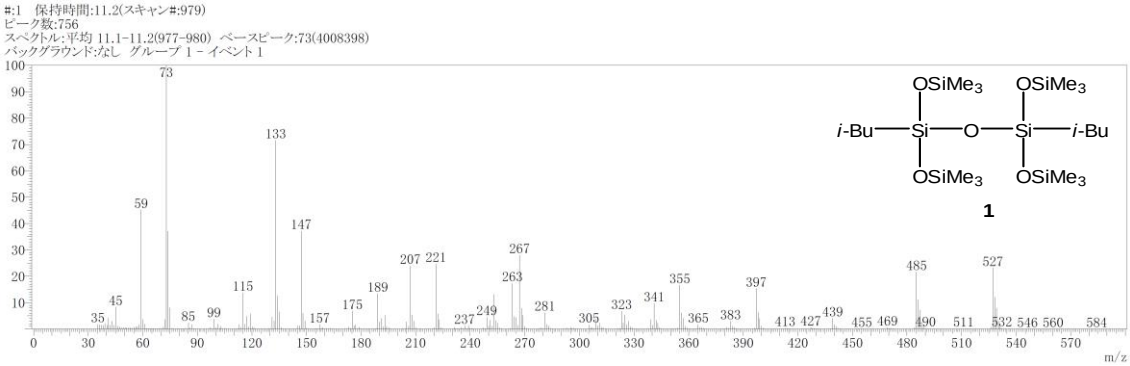

Figure 6. GCMS (EI, 70 eV) spectrum of **1**

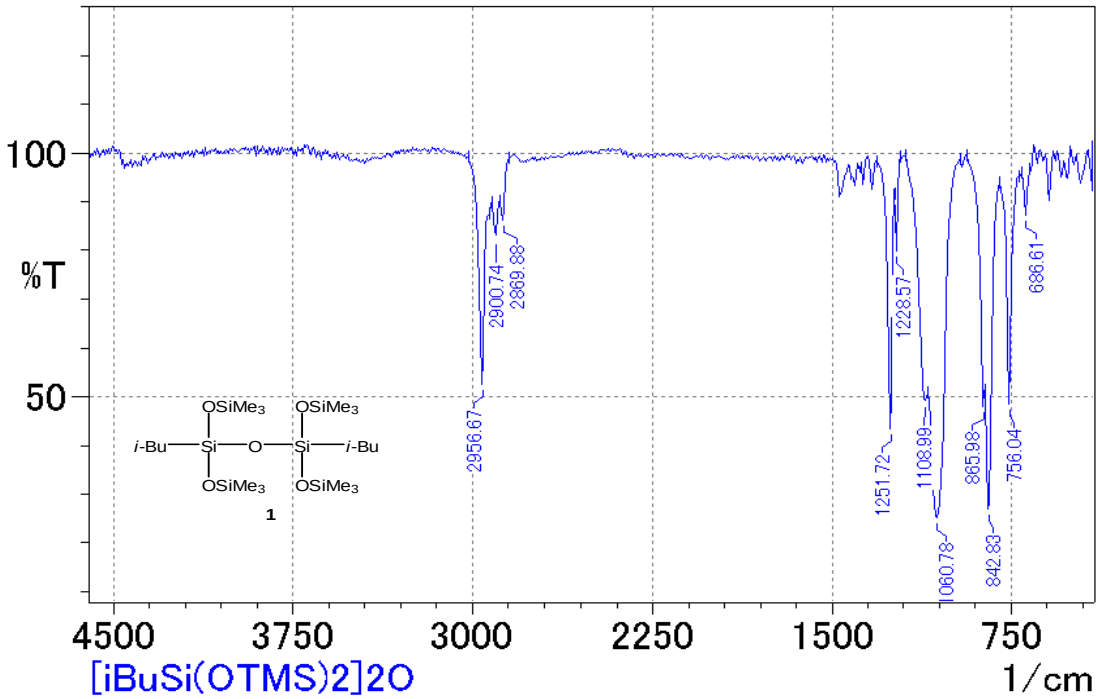

Figure 7. IR spectrum (KBr) of **1**

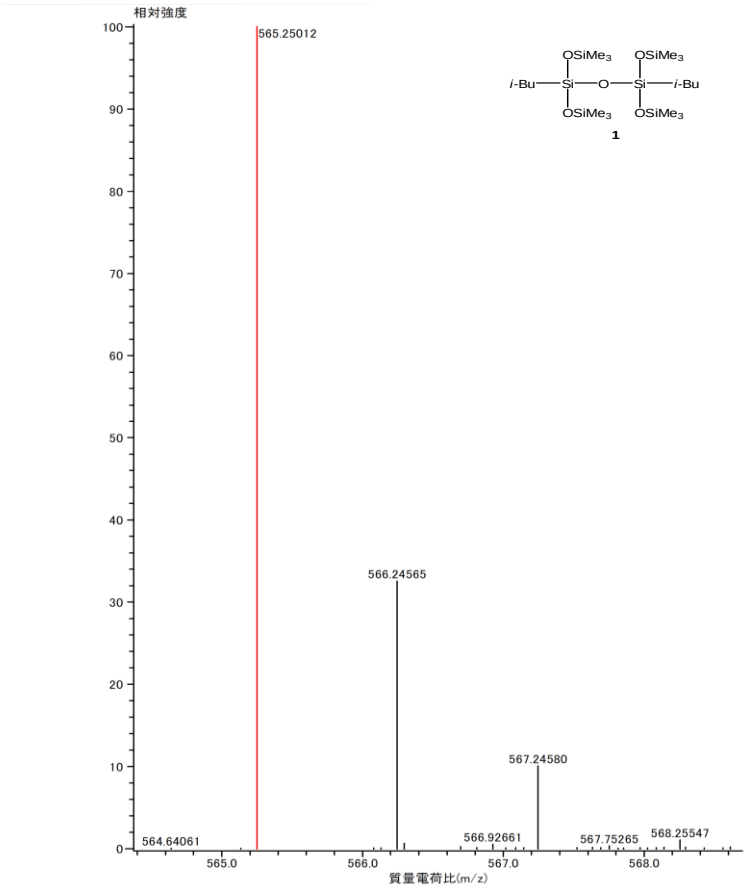

Figure 8. MALDITOFMS spectrum of **1**

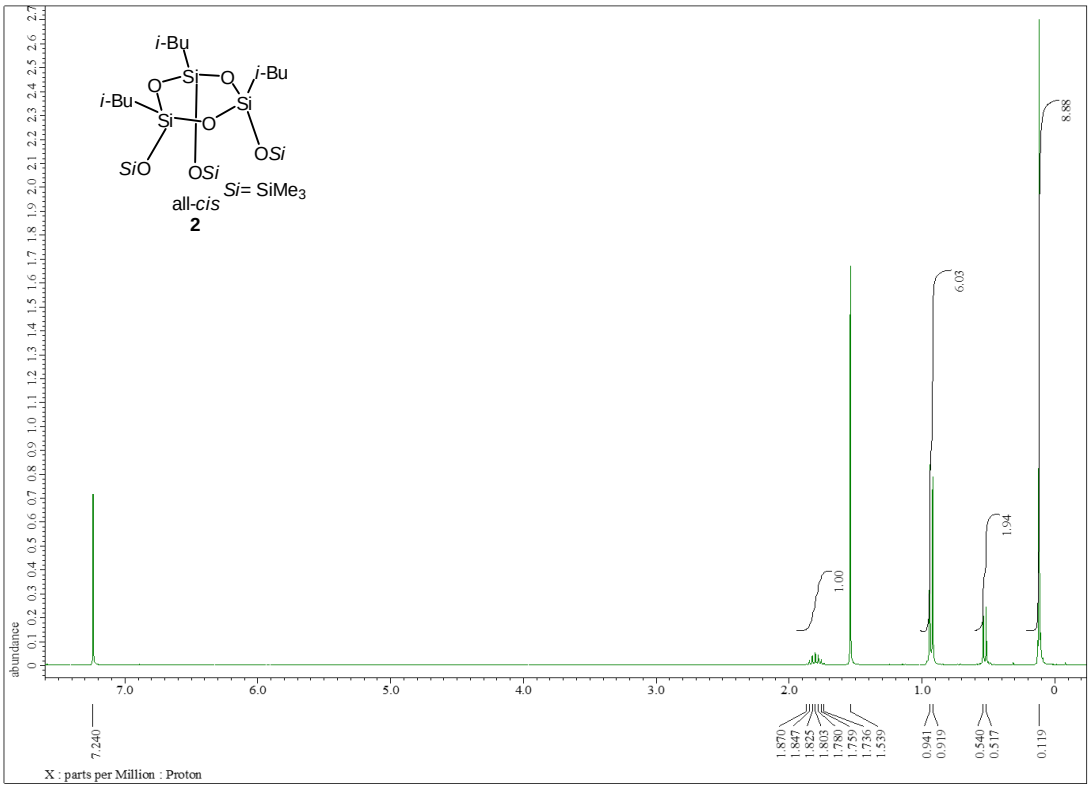

Figure 9. ^{1}H NMR spectrum of **2** (300.53 MHz, $CDCl_3$)

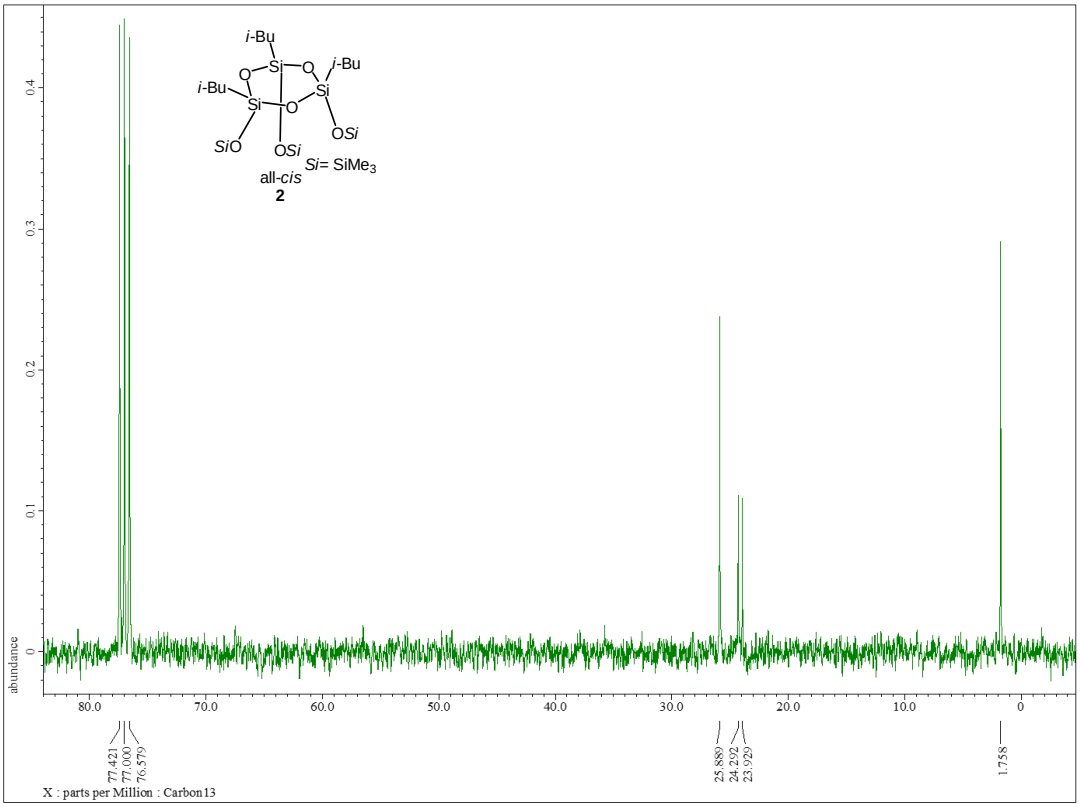

Figure 10. ^{13}C NMR spectrum of **2** (75.57 MHz, $CDCl_3$)

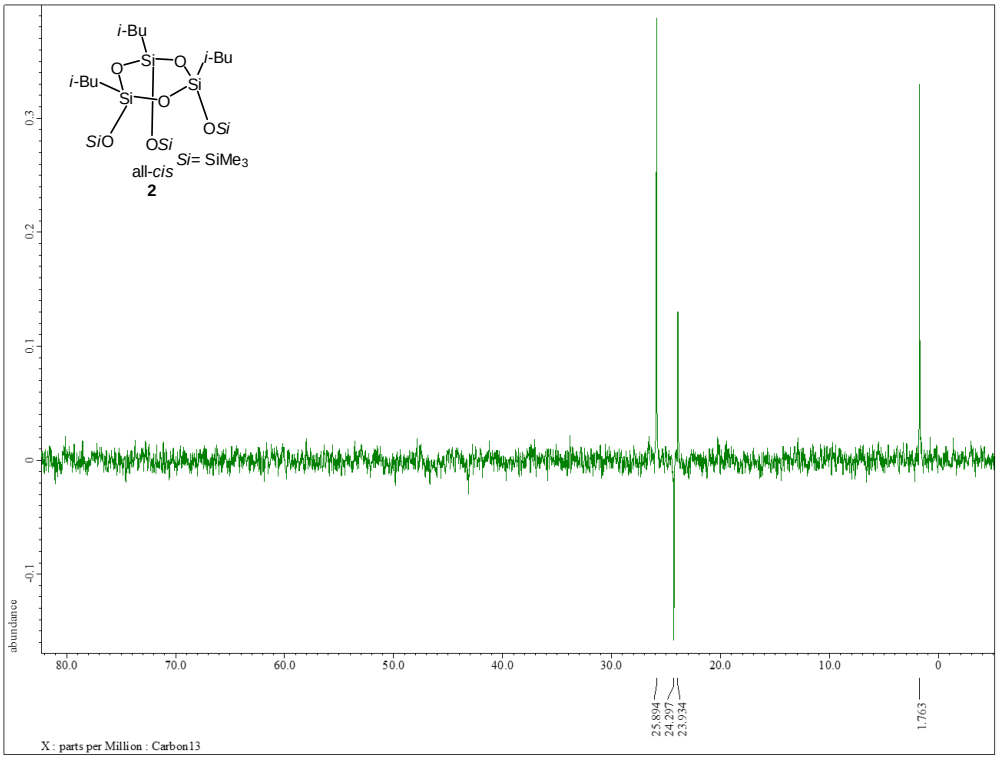

Figure 11. ^{13}C NMR (dept 135) spectrum of **2** (75.57 MHz, $CDCl_3$)

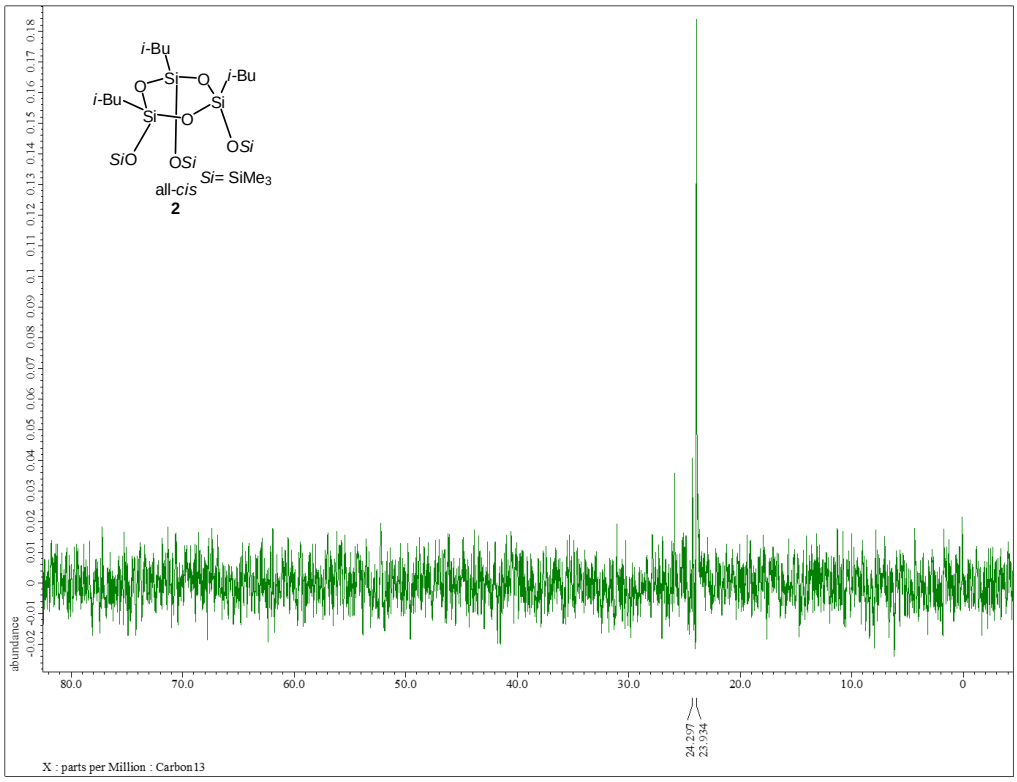

Figure 12. ^{13}C NMR (dept 90) spectrum of **2** (75.57 MHz, $CDCl_3$)

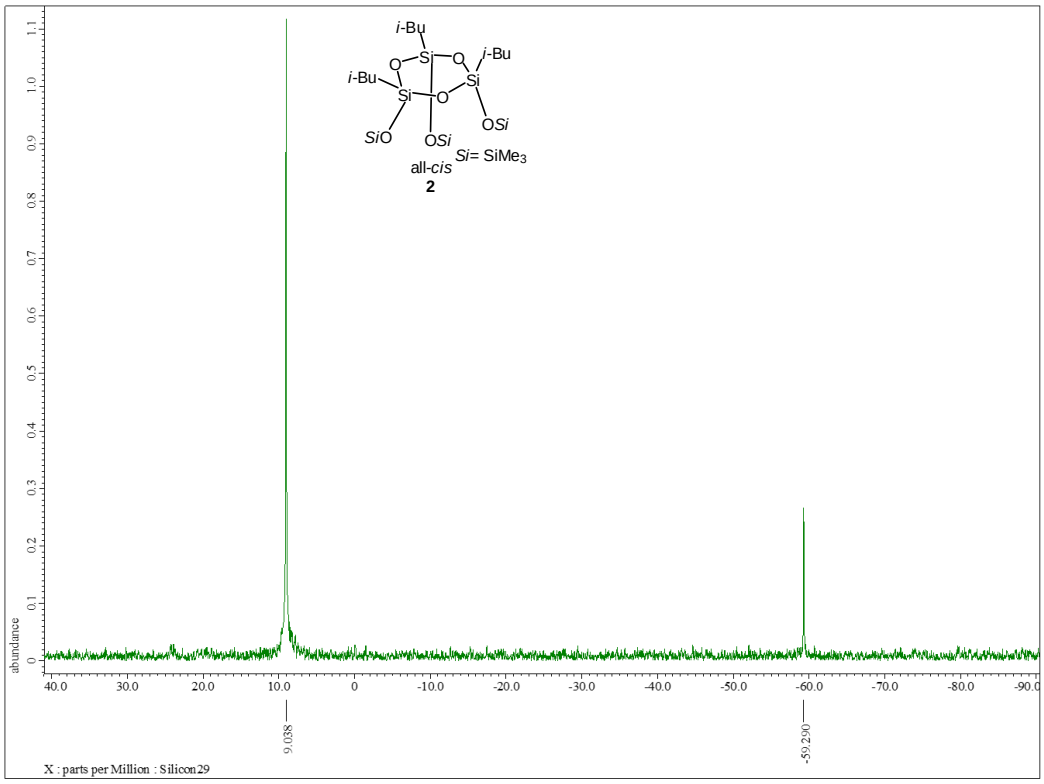

Figure 13. ^{29}Si NMR spectrum of **2** (59.71 MHz, $CDCl_3$)

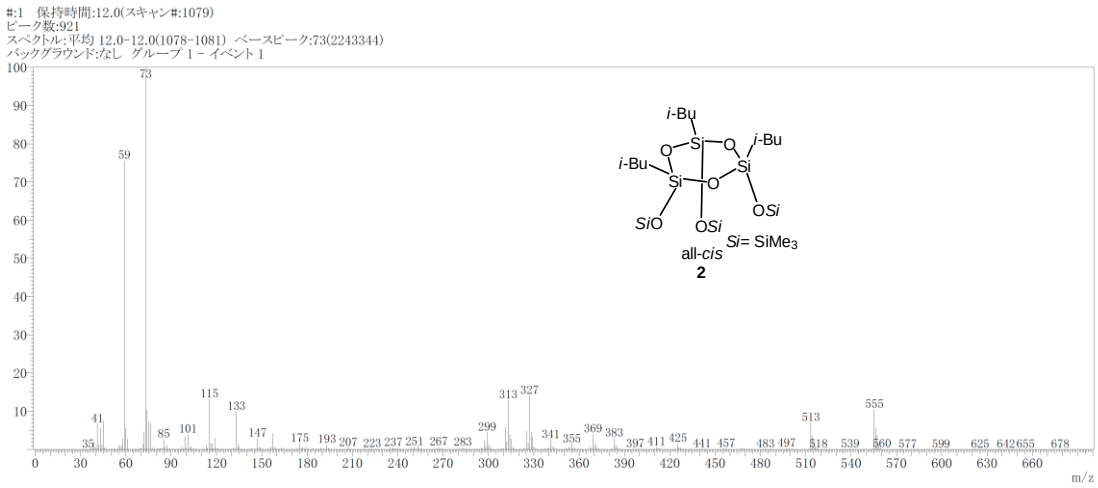

Figure 14. GCMS spectrum of **2**

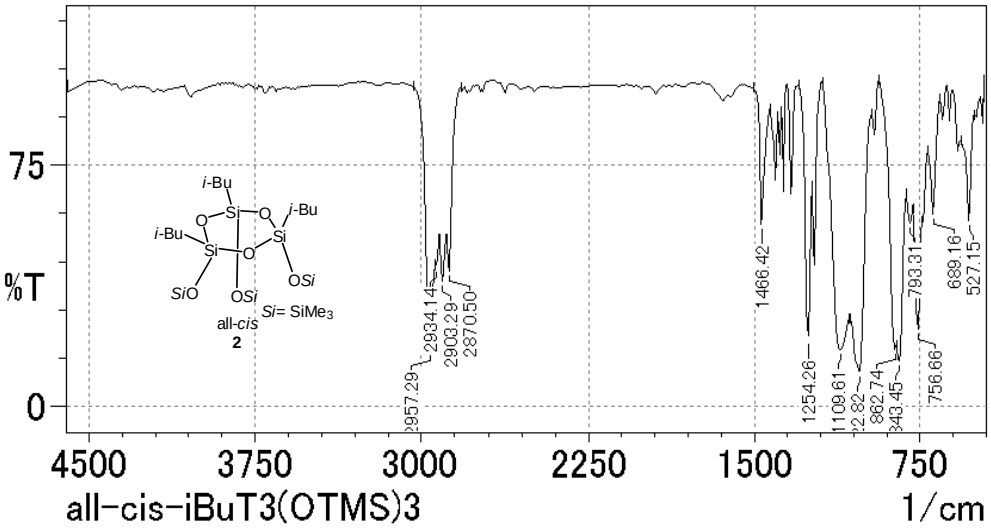

Figure 15. IR spectrum of **2**

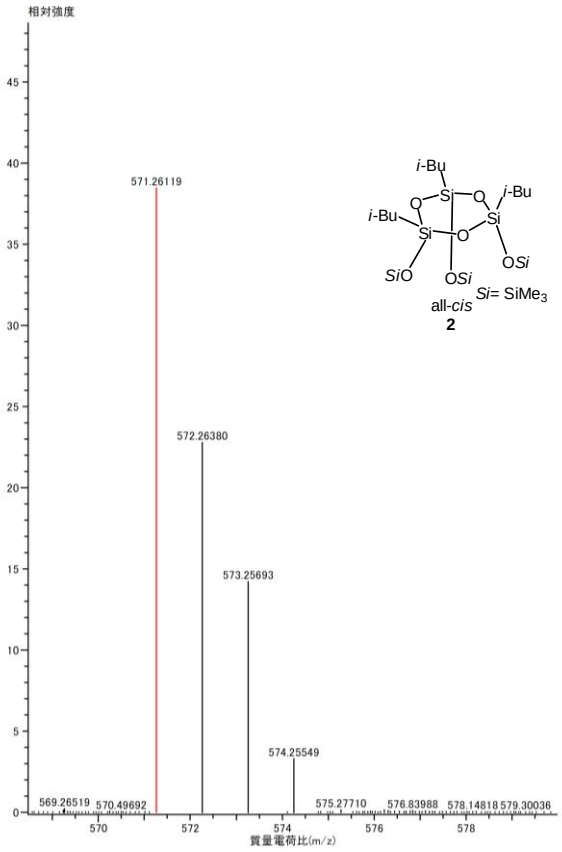

Figure 16. MALDITOFMS spectrum of **2**

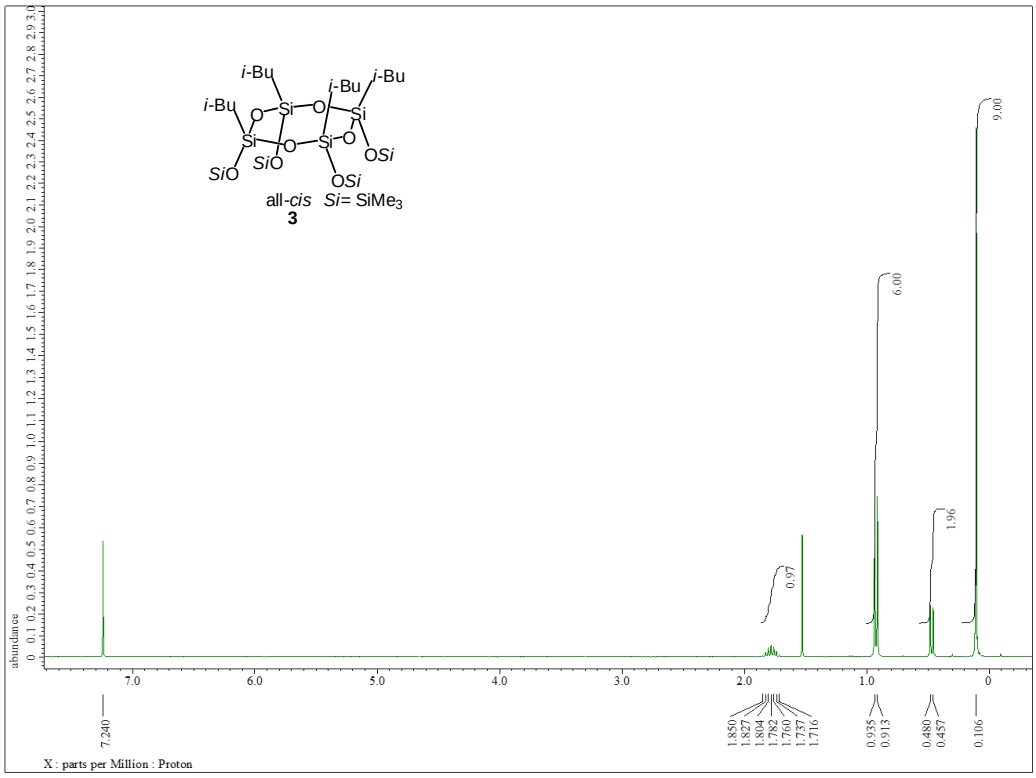

Figure 17. ^{1}H NMR spectrum of **3** (300.53 MHz, $CDCl_3$)

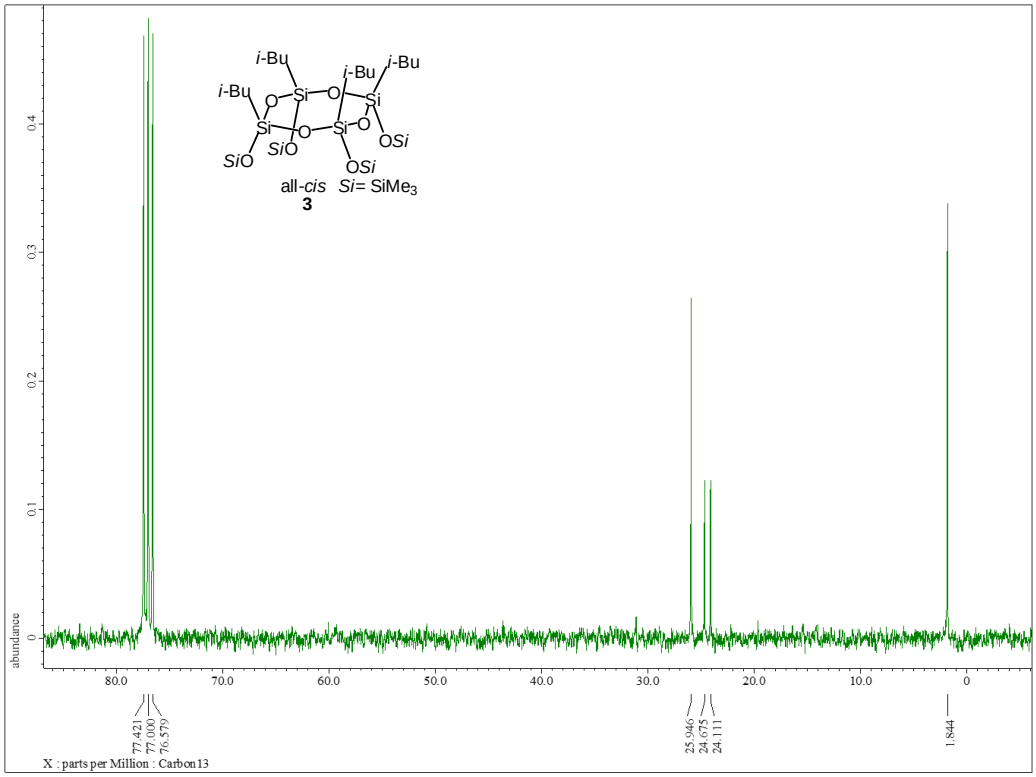

Figure 18. ^{13}C NMR spectrum of **3** (75.57 MHz, $CDCl_3$)

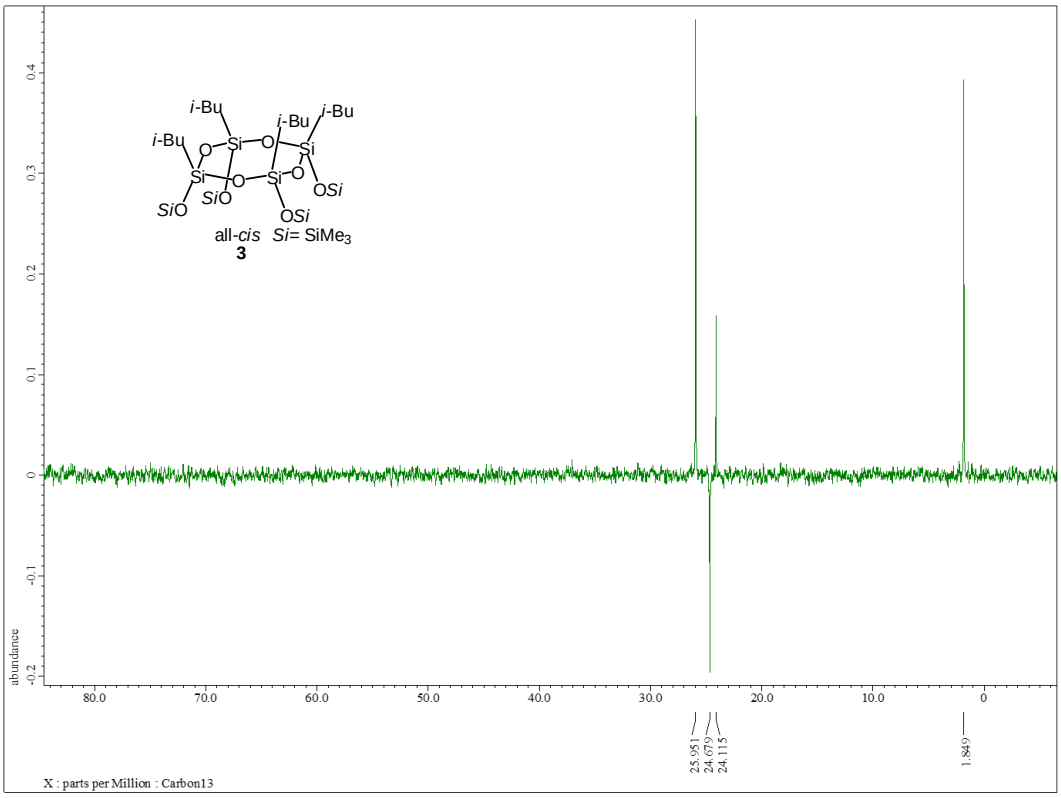

Figure 19. ^{13}C NMR (dept 135) spectrum of **3** (75.57 MHz, $CDCl_3$)

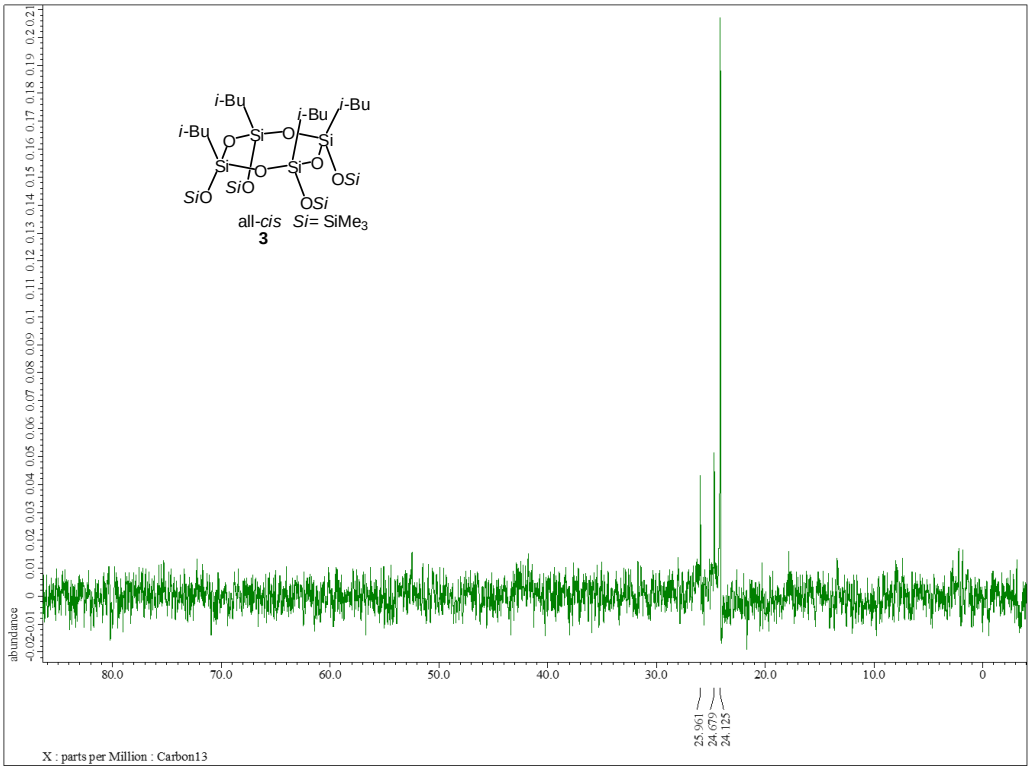

Figure 20. ^{13}C NMR (dept 90) spectrum of **3** (75.57 MHz, $CDCl_3$)

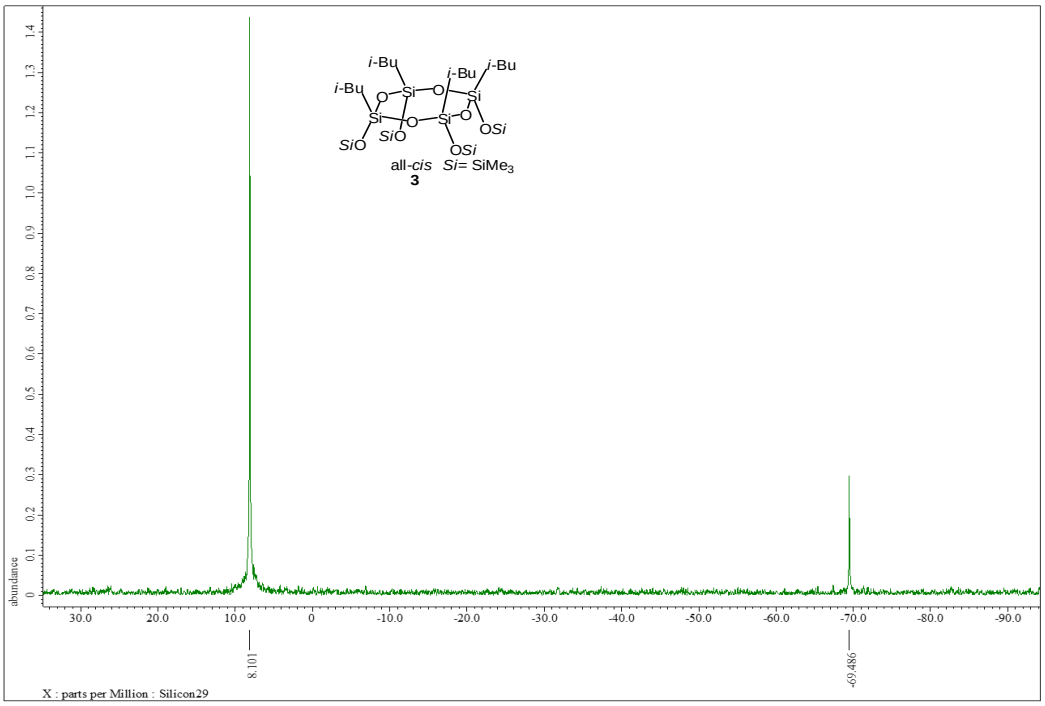

Figure 21. ^{29}Si NMR spectrum of **3** (59.71 MHz, $CDCl_3$)

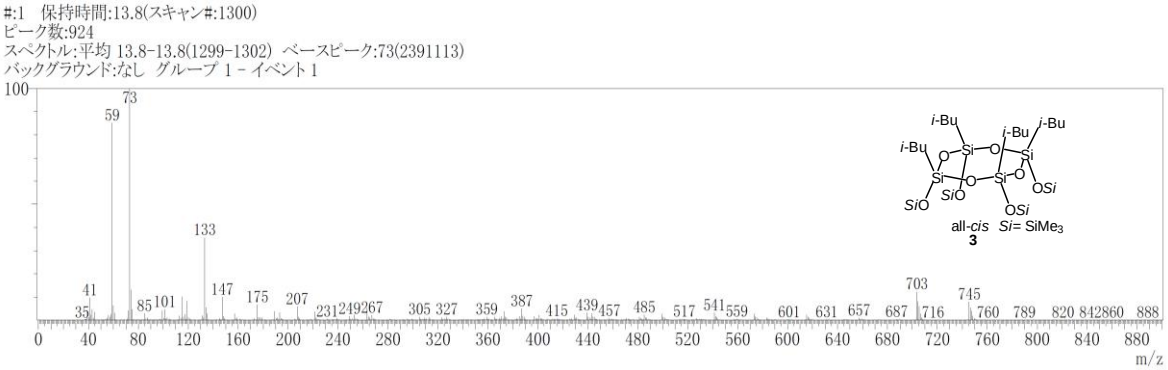

Figure 22. GCMS spectrum of **3**.

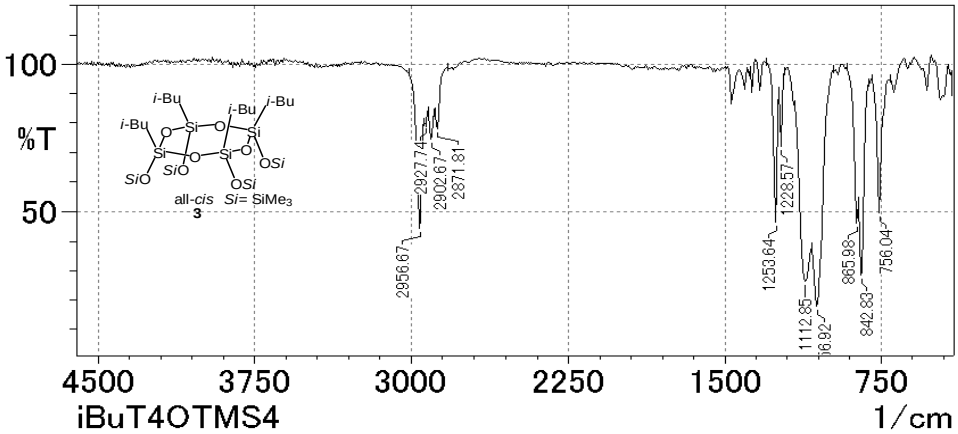

Figure 23. IR spectrum of **3.**

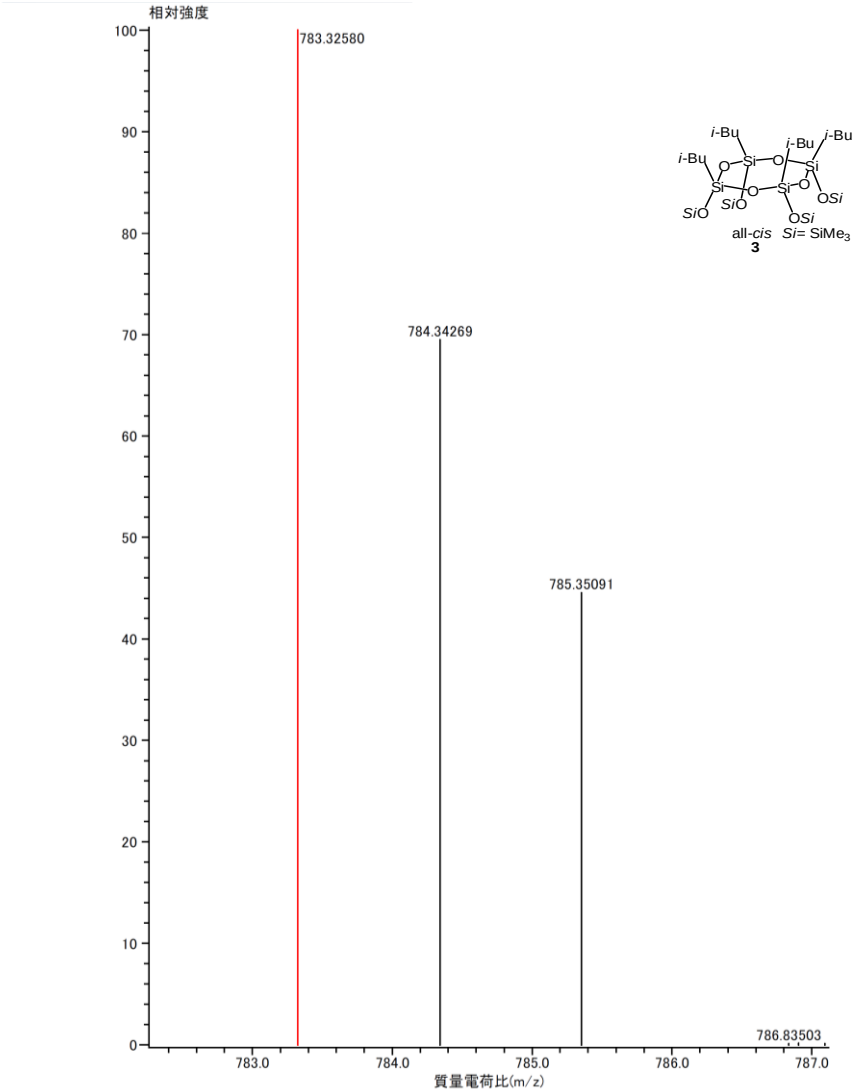

Figure 24. MALDITOFMS spectrum of **3**

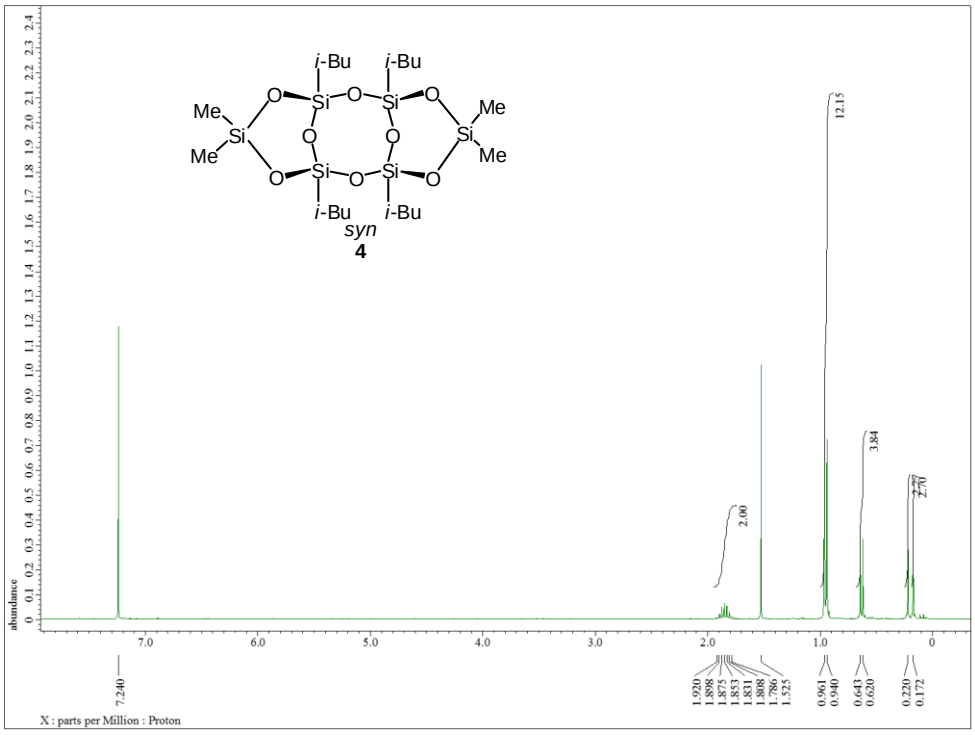

Figure 25. ^{1}H NMR spectrum of **4** (300.53 MHz, $CDCl_3$)

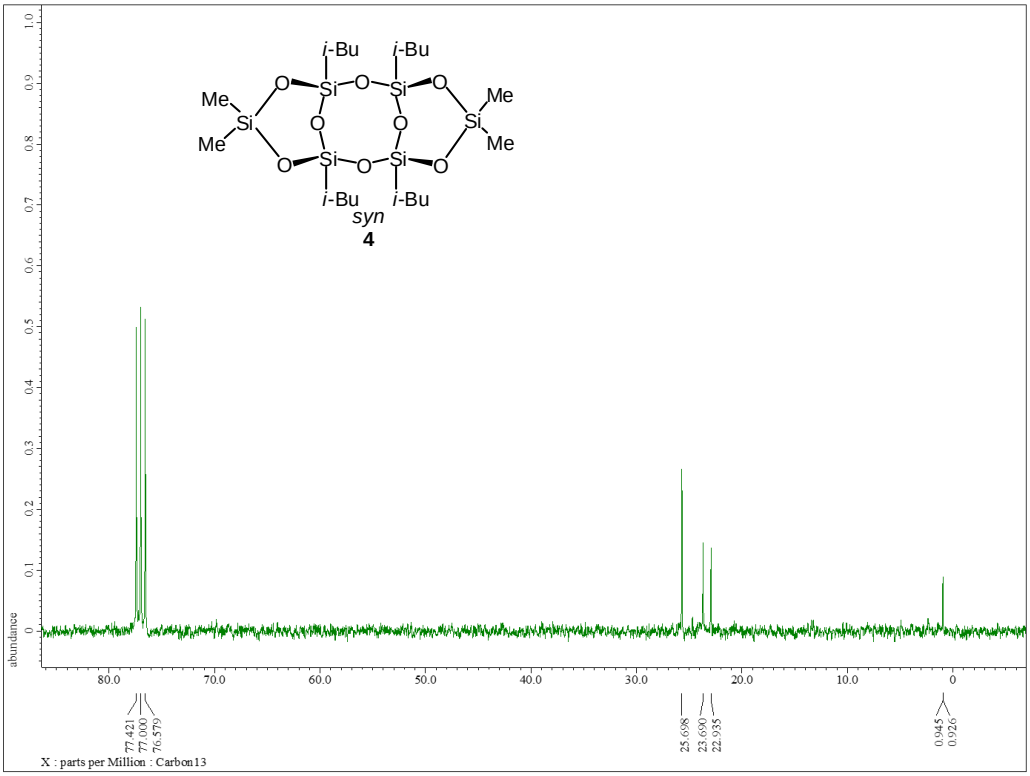

Figure 26. ^{13}C NMR spectrum of **4** (75.57 MHz, $CDCl_3$)

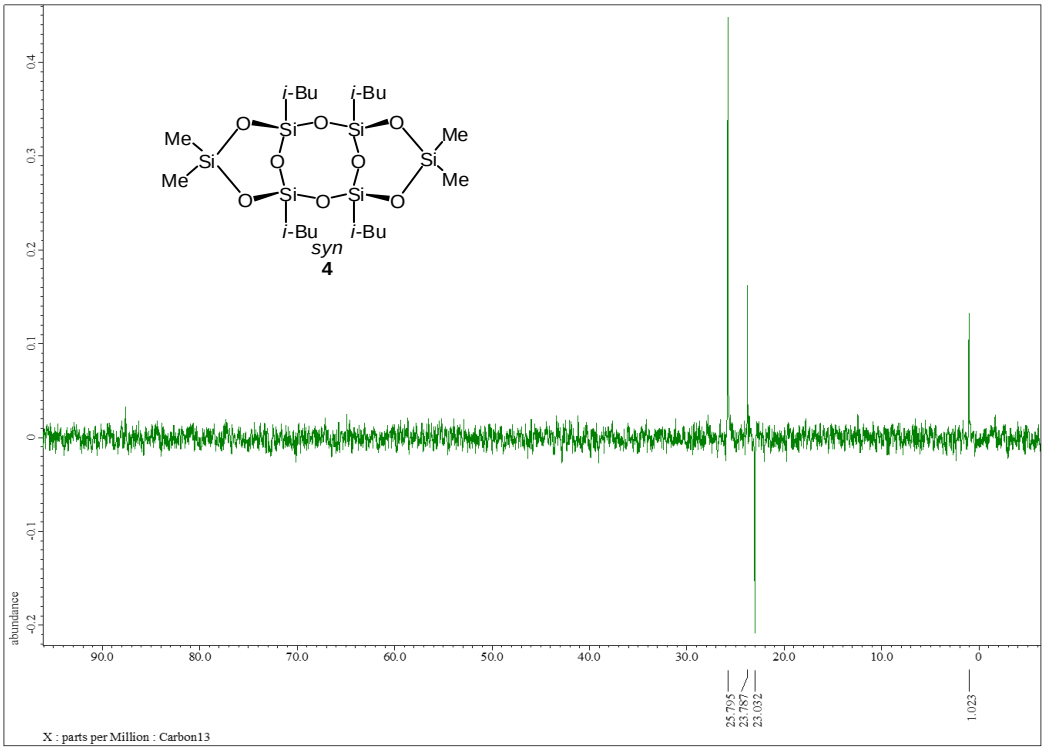

Figure 27. ^{13}C NMR (dept 135) spectrum of **4** (75.57 MHz, $CDCl_3$)

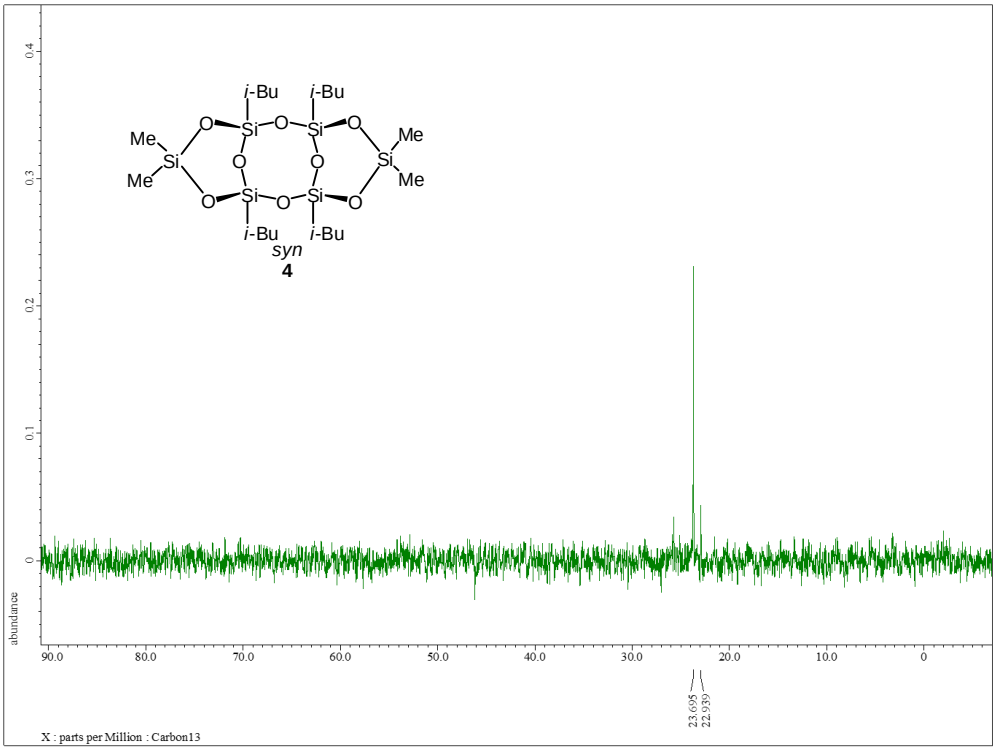

Figure 28. ^{13}C NMR (dept 90) spectrum of **4** (75.57 MHz, $CDCl_3$)

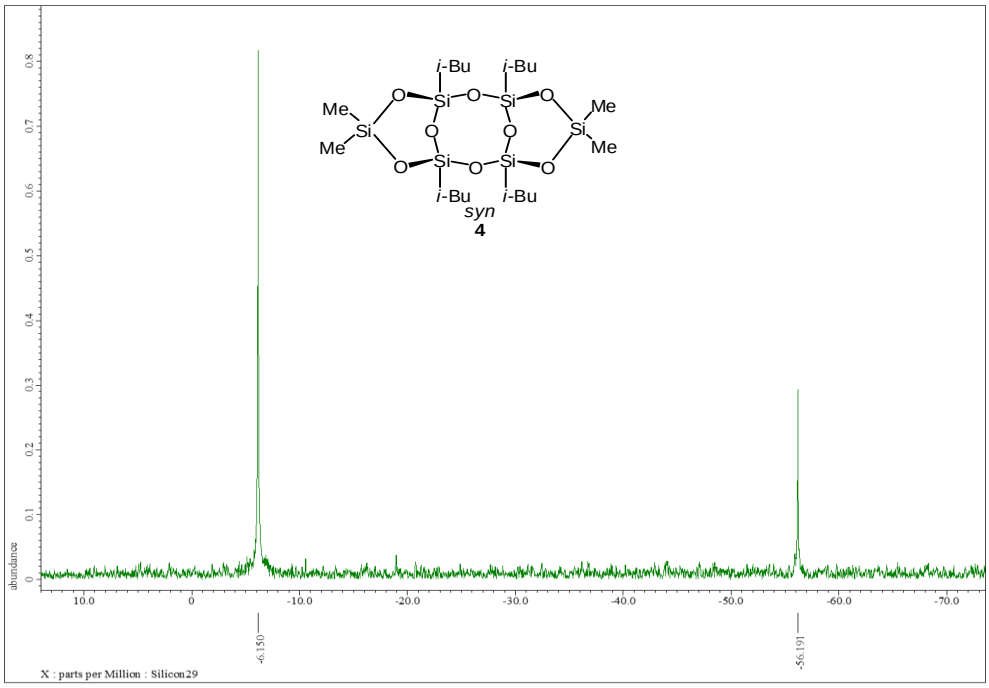

Figure 29. ^{29}Si NMR spectrum of **4** (59.71 MHz, $CDCl_3$)

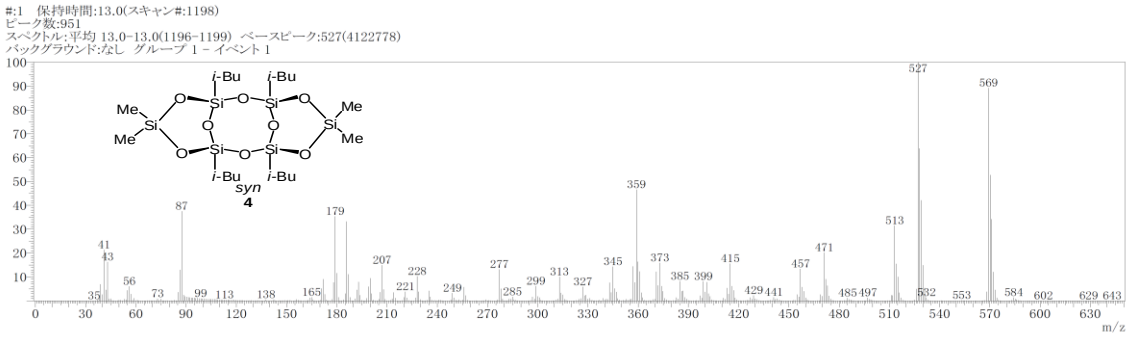

Figure S30. GCMS spectrum of **4**

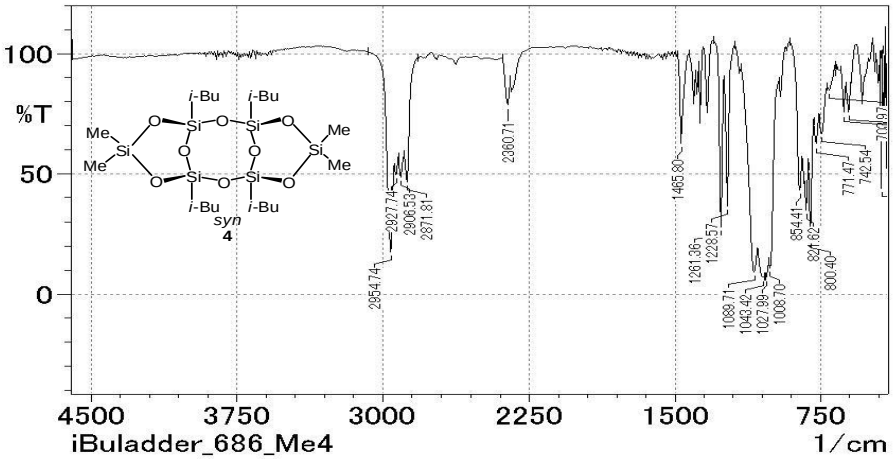

Figure 31. IR spectrum of **4**

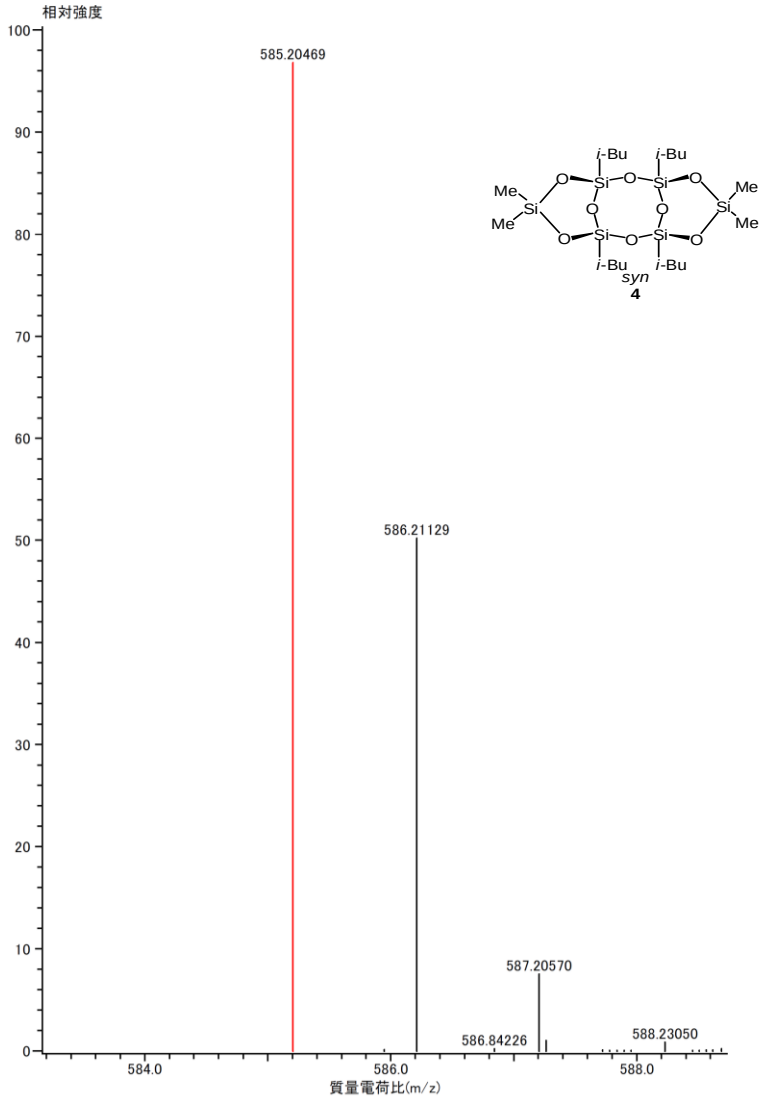

Figure 32. MALDITOFMS spectrum of **4**

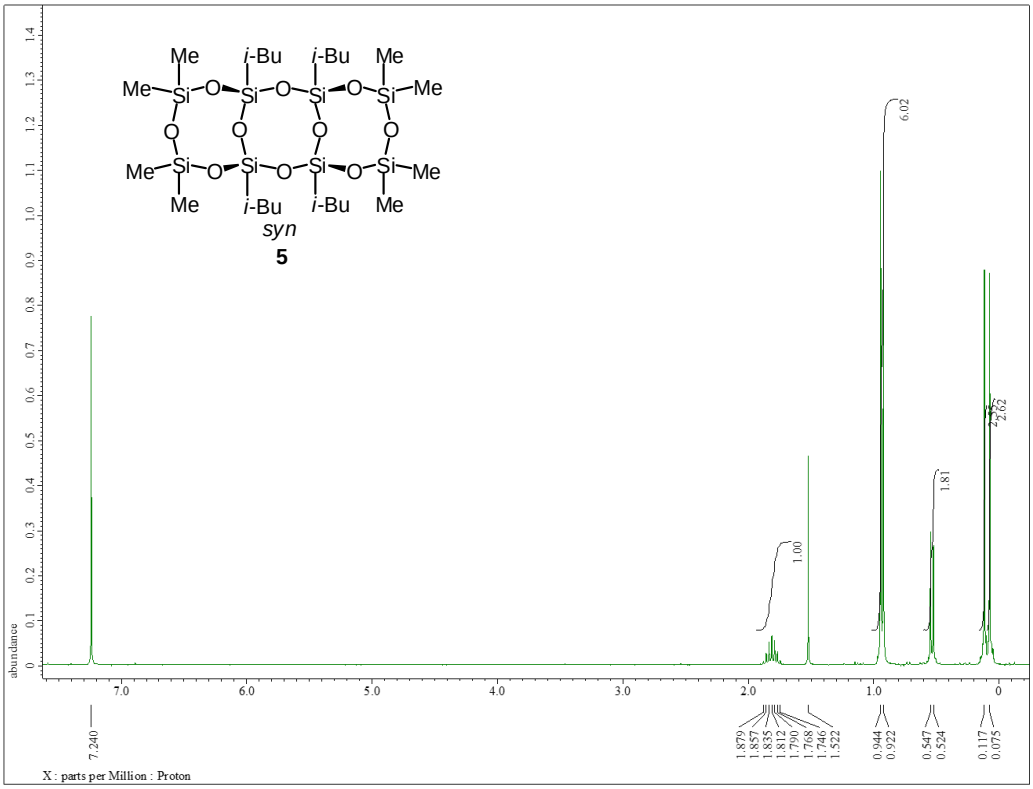

Figure 33. ^{1}H NMR spectrum of **5** (300.53 MHz, $CDCl_3$)

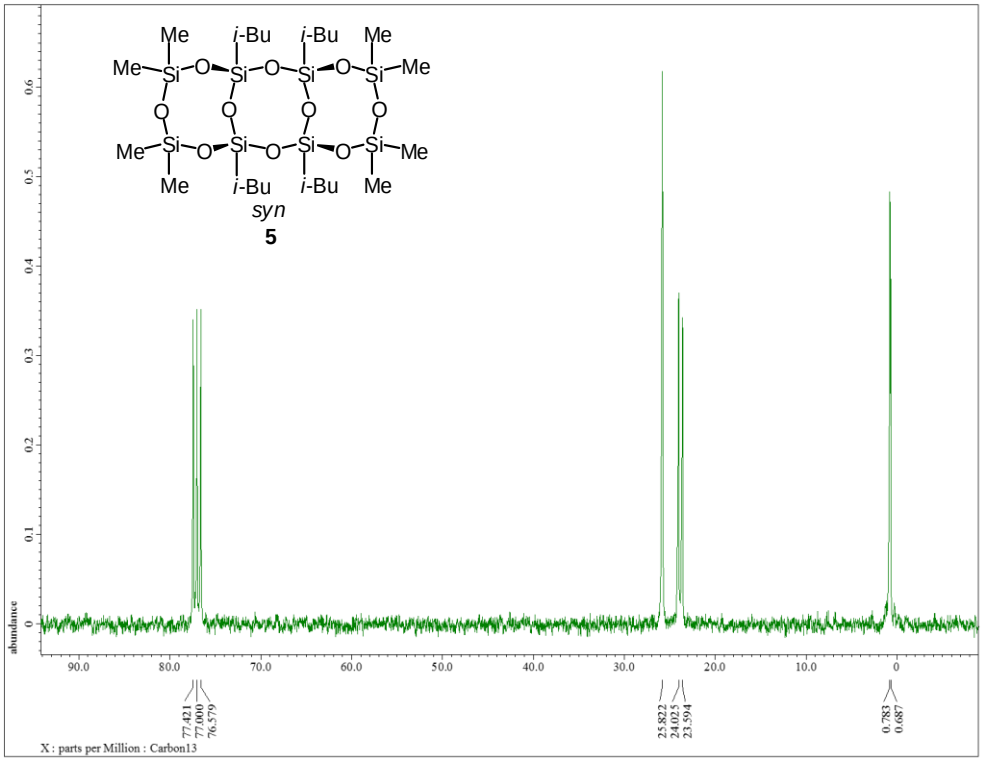

Figure 34. ^{13}C NMR spectrum of **5** (75.57 MHz, $CDCl_3$)

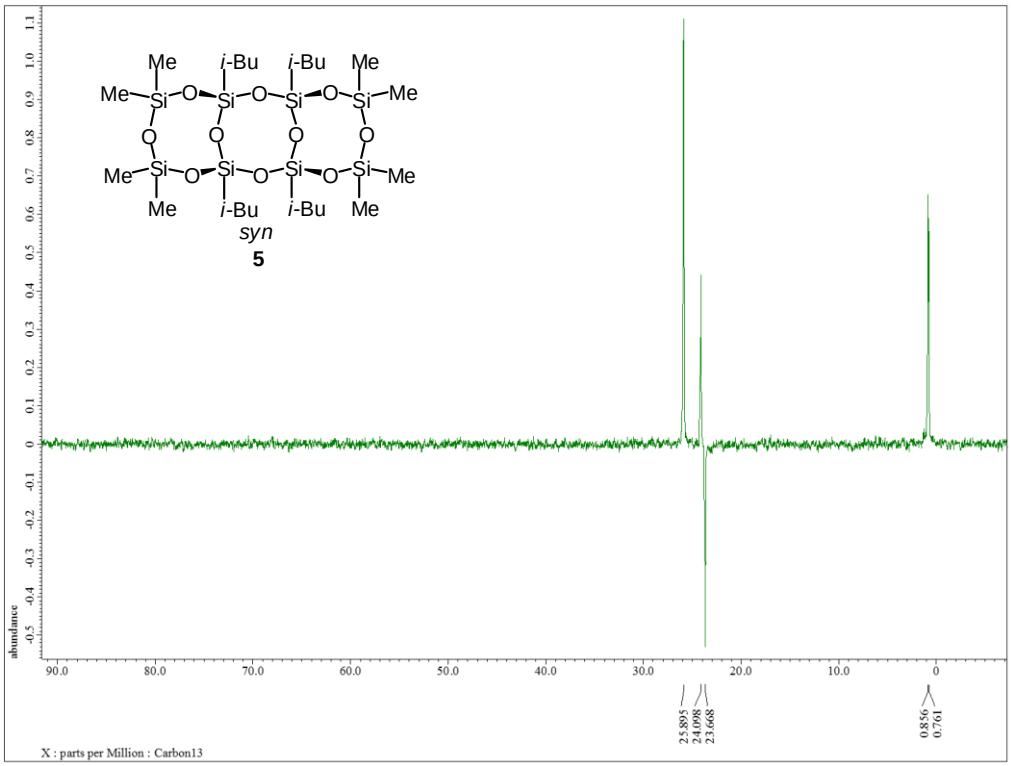

Figure 35. ^{13}C NMR (dept 135) spectrum of **5** (75.57 MHz, $CDCl_3$)

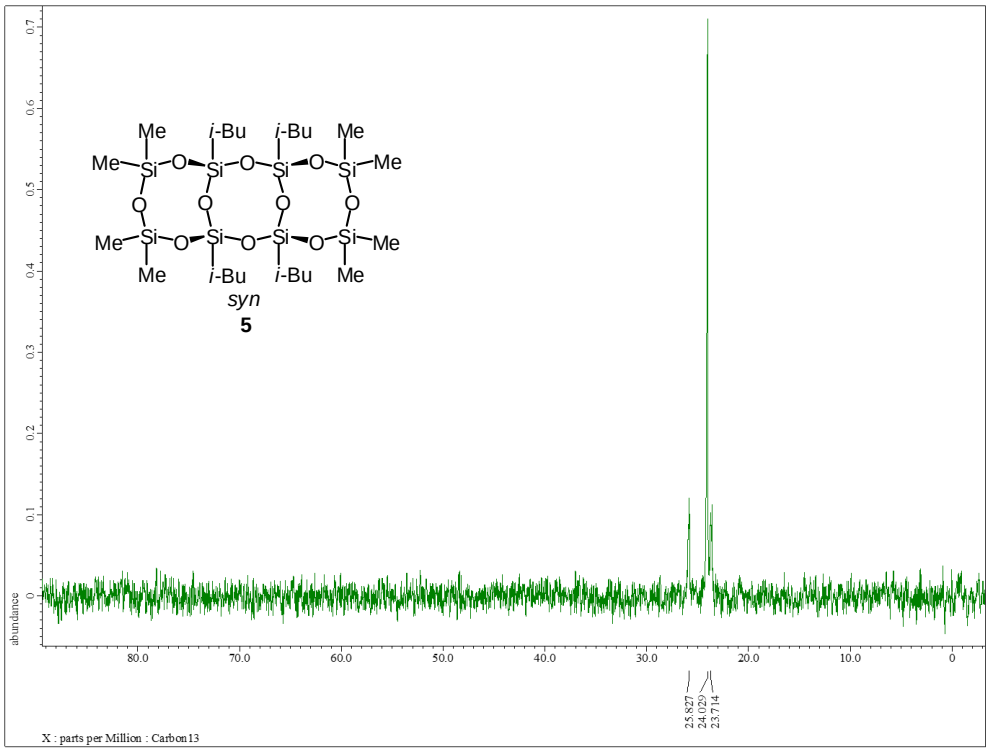

Figure 36. ^{13}C NMR (dept 90) spectrum of **5** (75.57 MHz, $CDCl_3$)

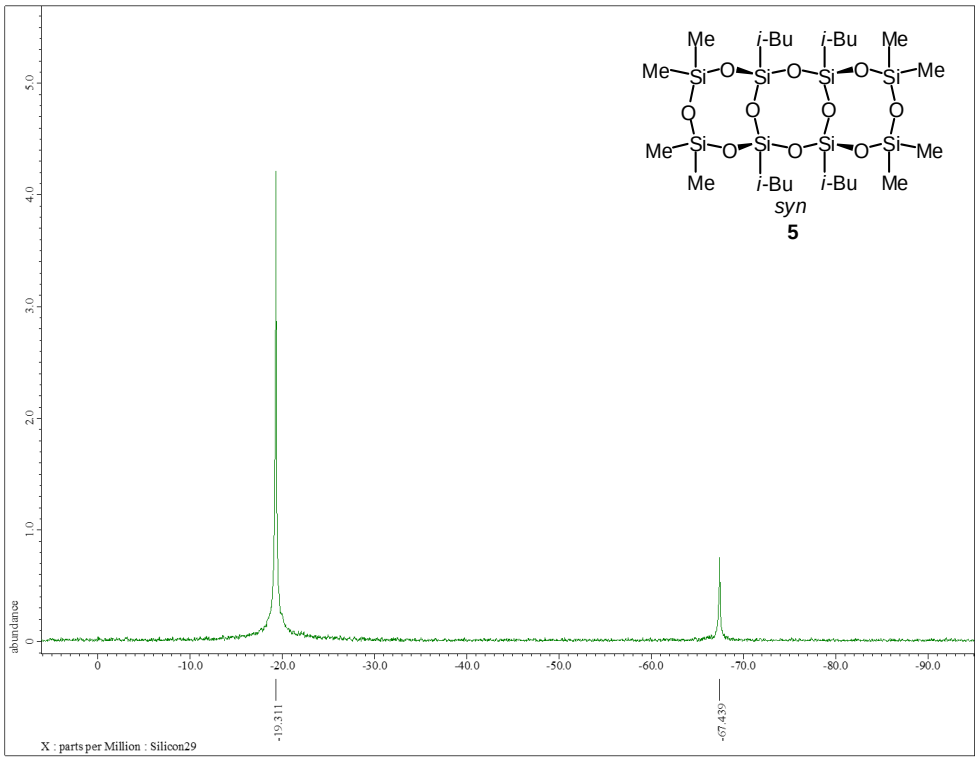

Figure 37. ^{29}Si NMR spectrum of **5** (59.71 MHz, $CDCl_3$)

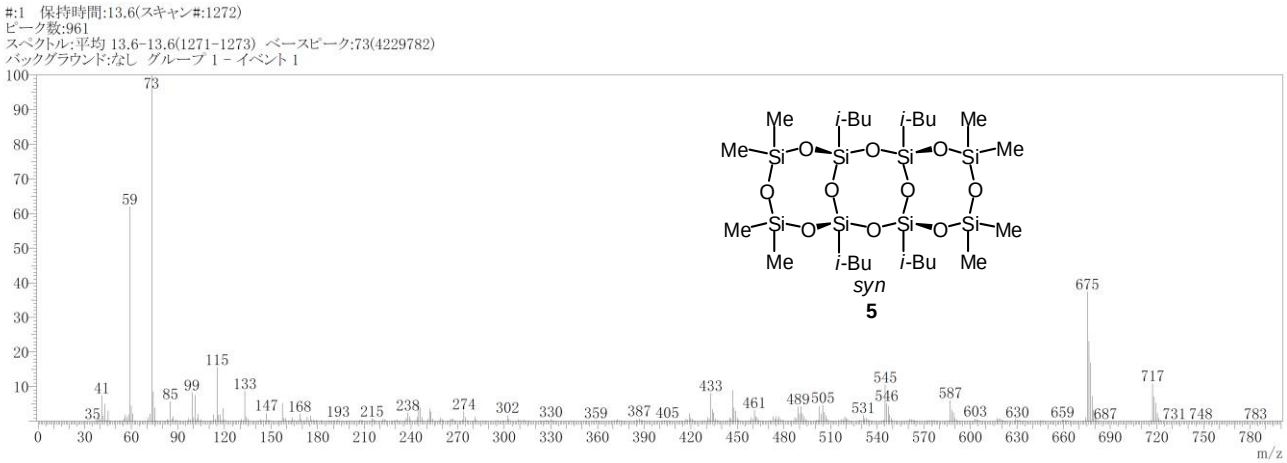

Figure 38. GCMS spectrum of **5**

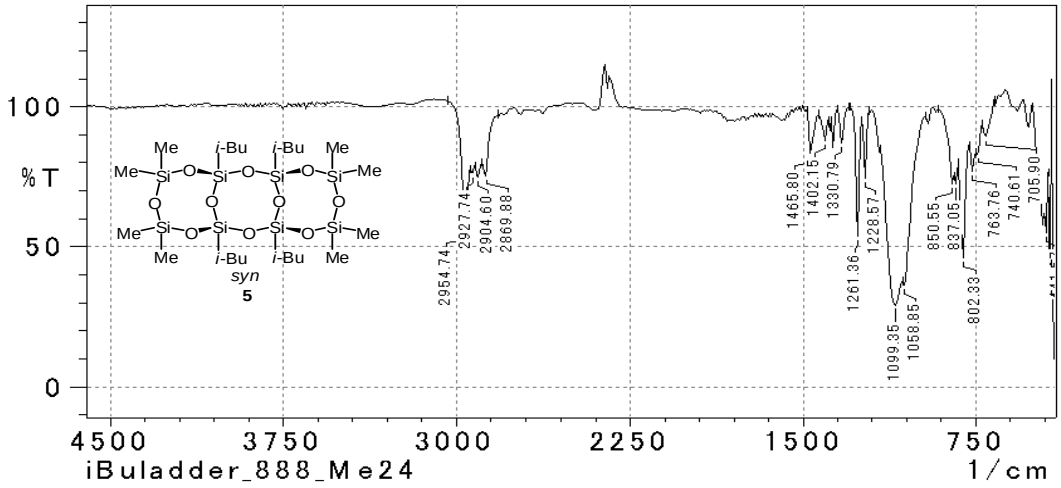

Figure 39. IR spectrum of **5**

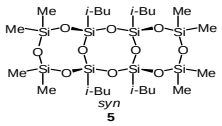

Figure S40. MALDITOFMS spectrum of **5**

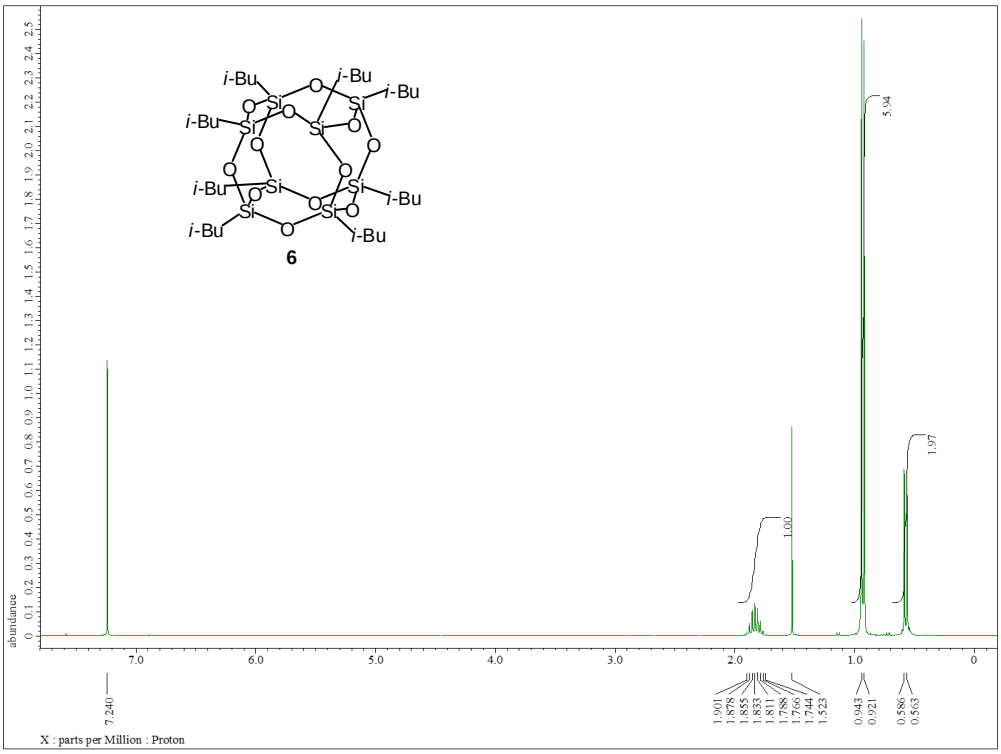

Figure 41. ^{1}H NMR spectrum of **6** (300.53 MHz, $CDCl_3$)

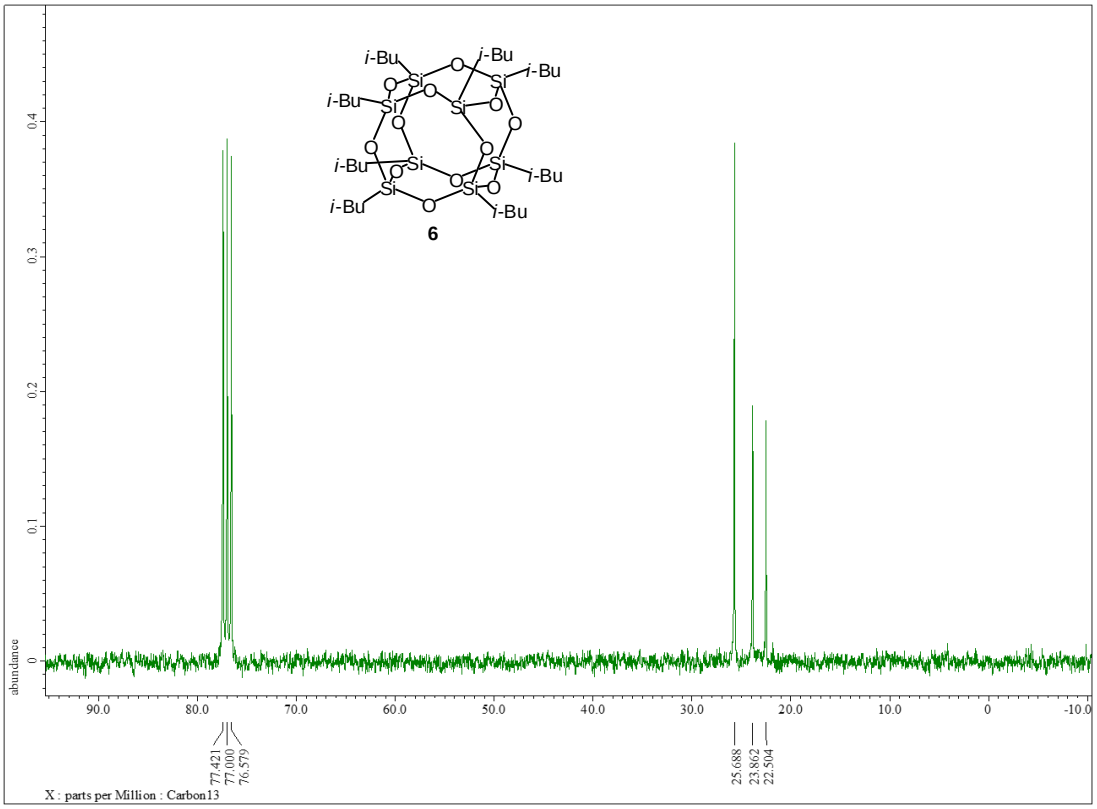

Figure 42. ^{13}C NMR spectrum of **6** (75.57 MHz, $CDCl_3$)

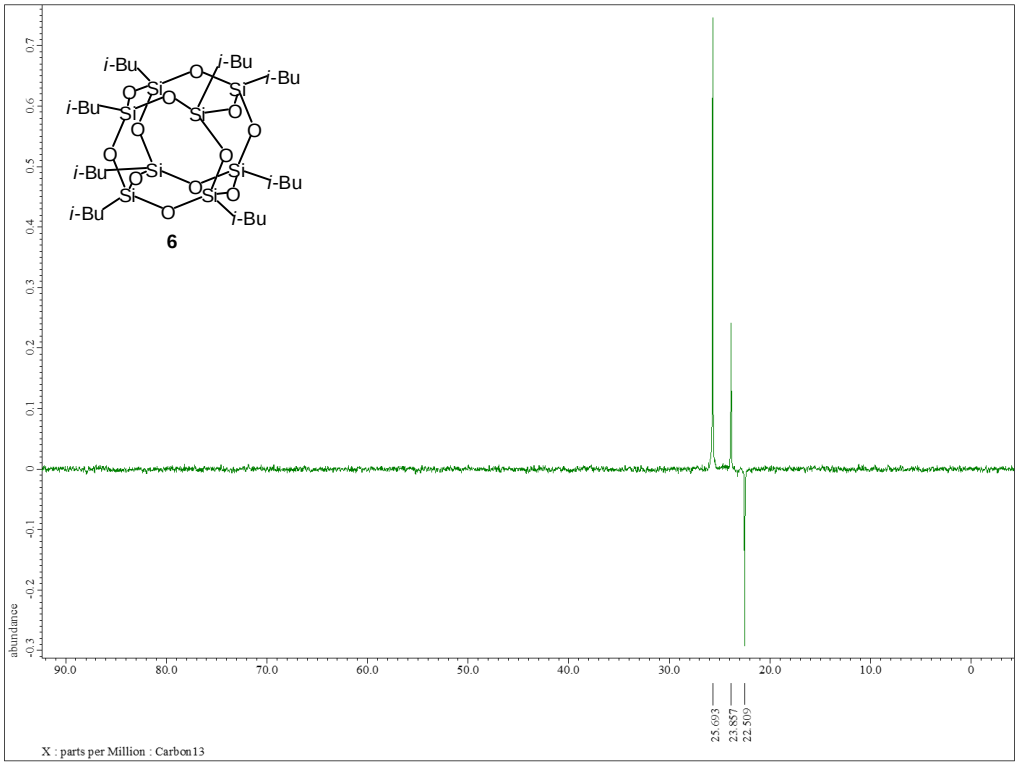

Figure 43. ^{13}C NMR (dept 135) spectrum of **6** (75.57 MHz, $CDCl_3$)

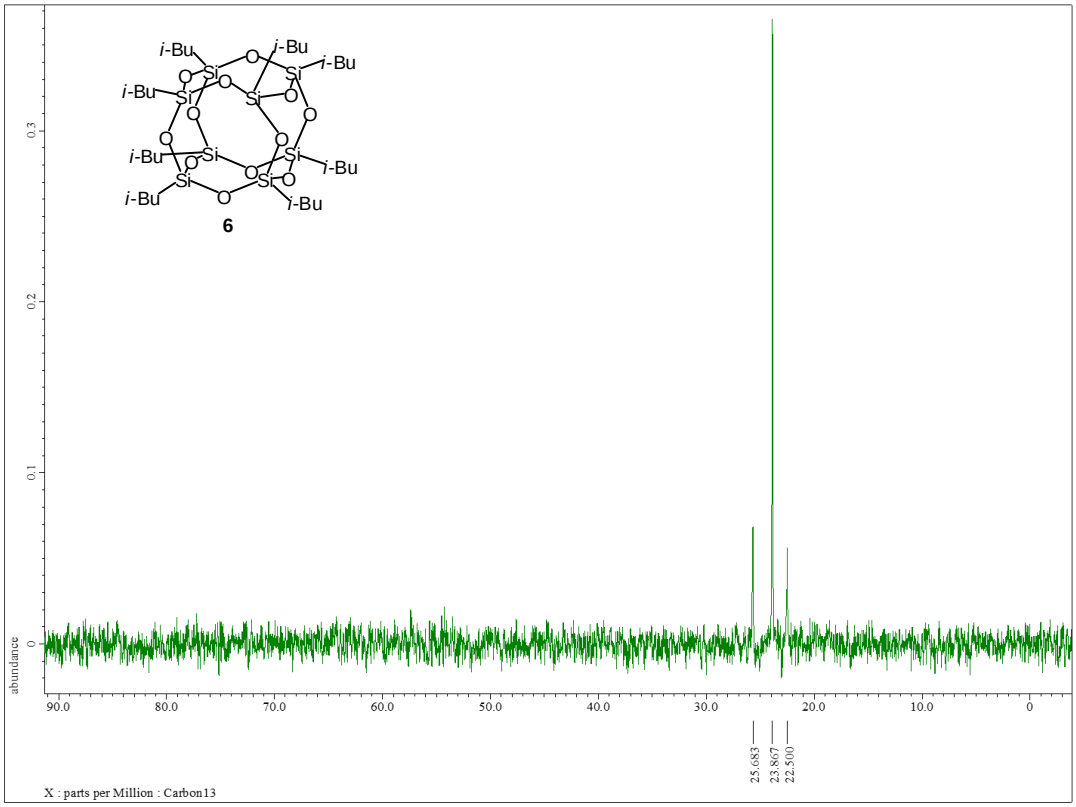

Figure 44. ^{13}C NMR (dept 90) spectrum of **6** (75.57 MHz, $CDCl_3$)

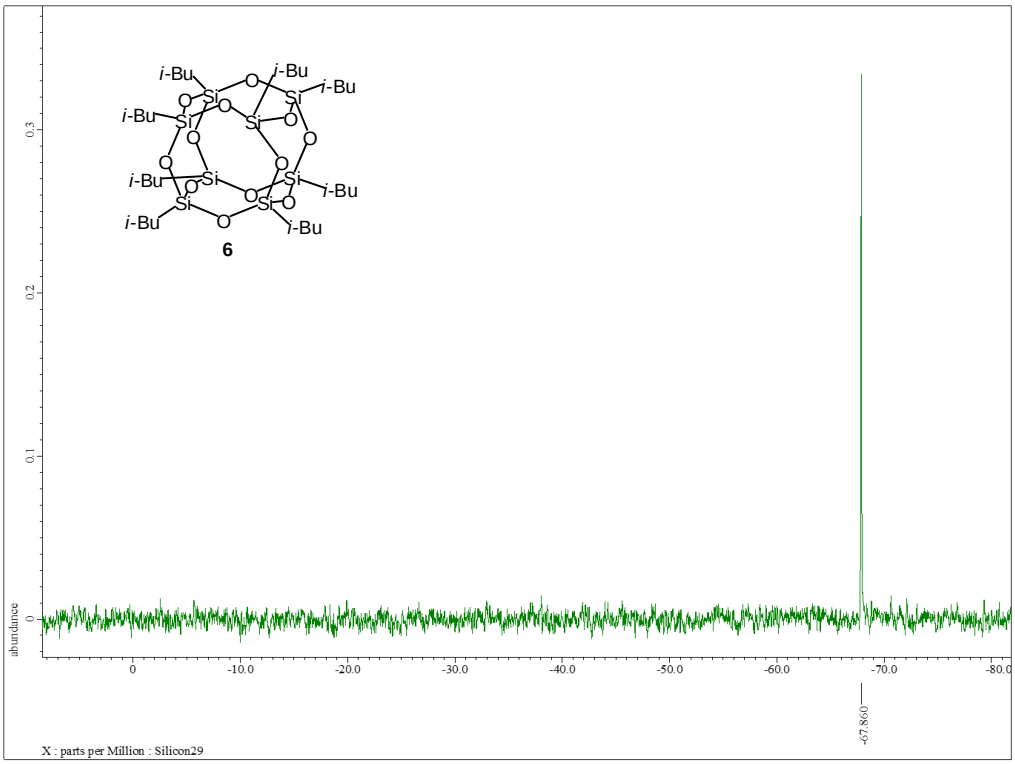

Figure 45. ^{29}Si NMR spectrum of **6** (59.71 MHz, $CDCl_3$)

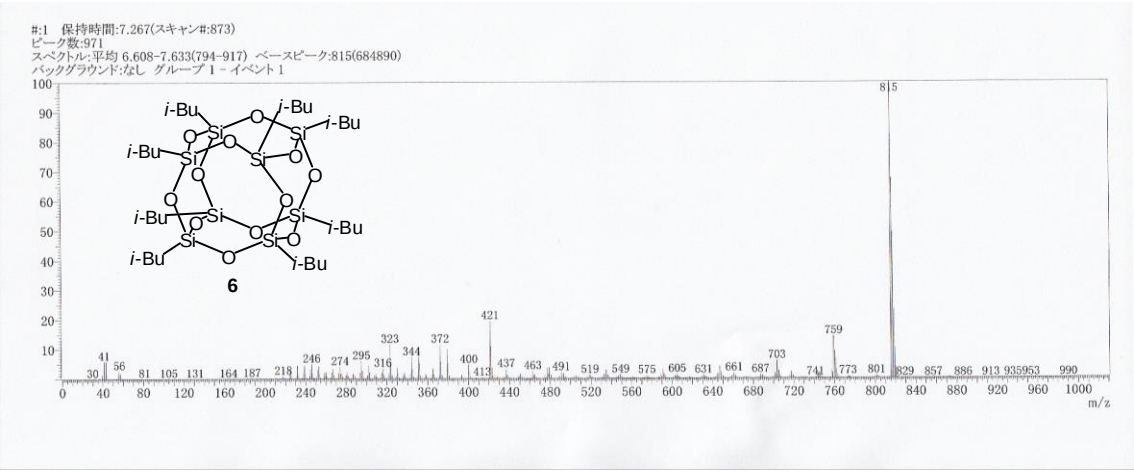

Figure 46. DIMS spectrum of **6**

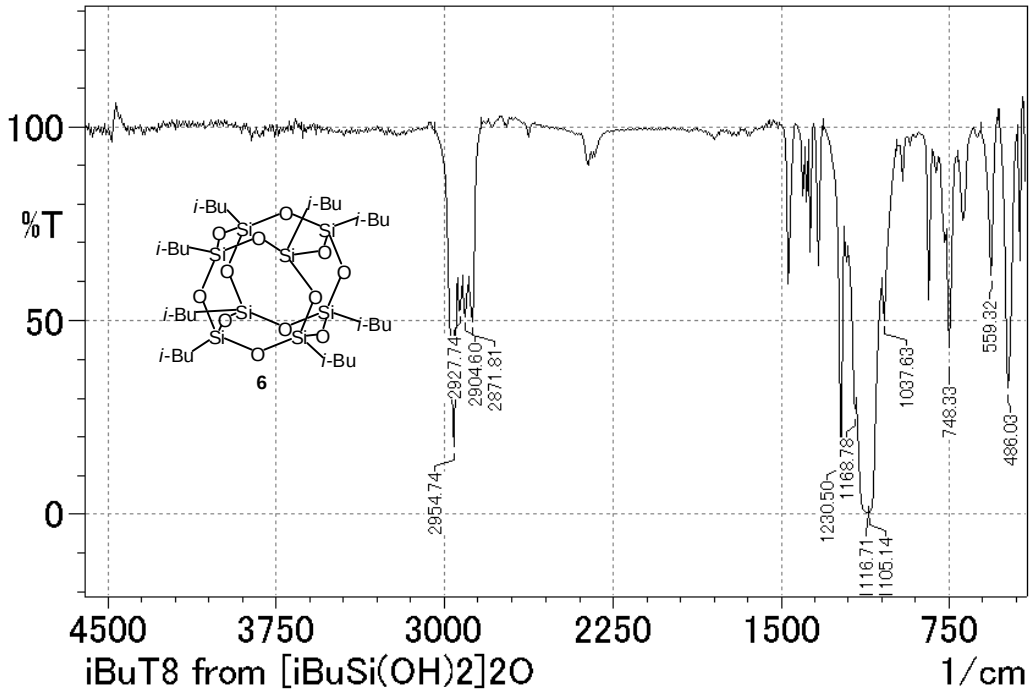

Figure 47. IR spectrum of **6**

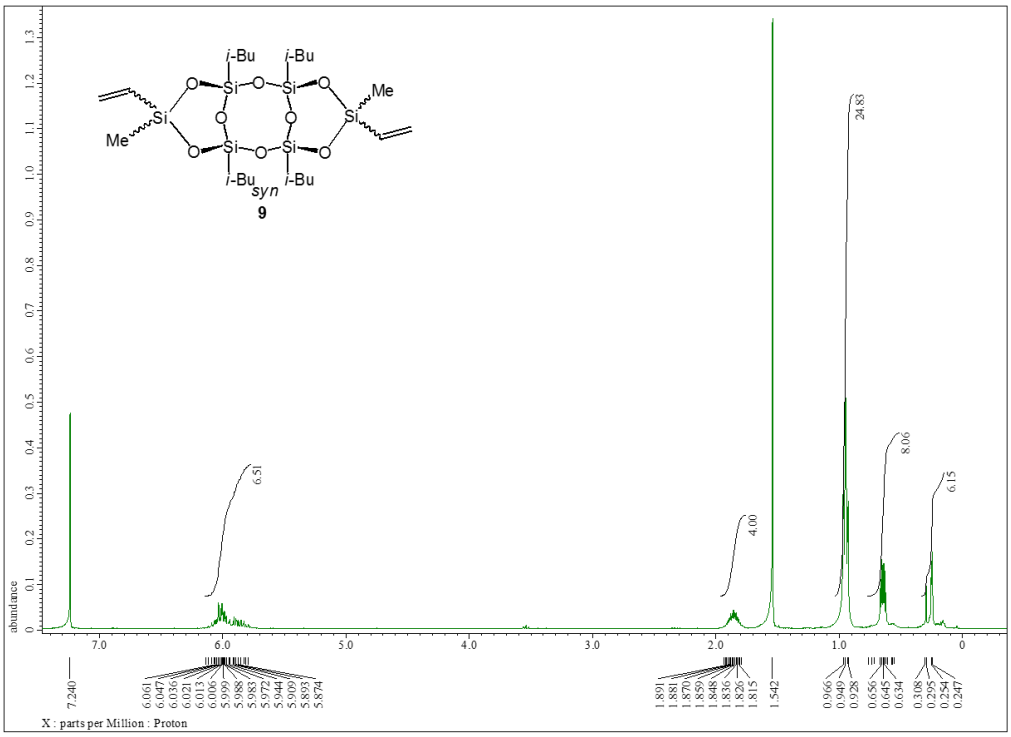

Figure 48. ^{1}H NMR spectrum of **9** (300.53 MHz, $CDCl_3$)

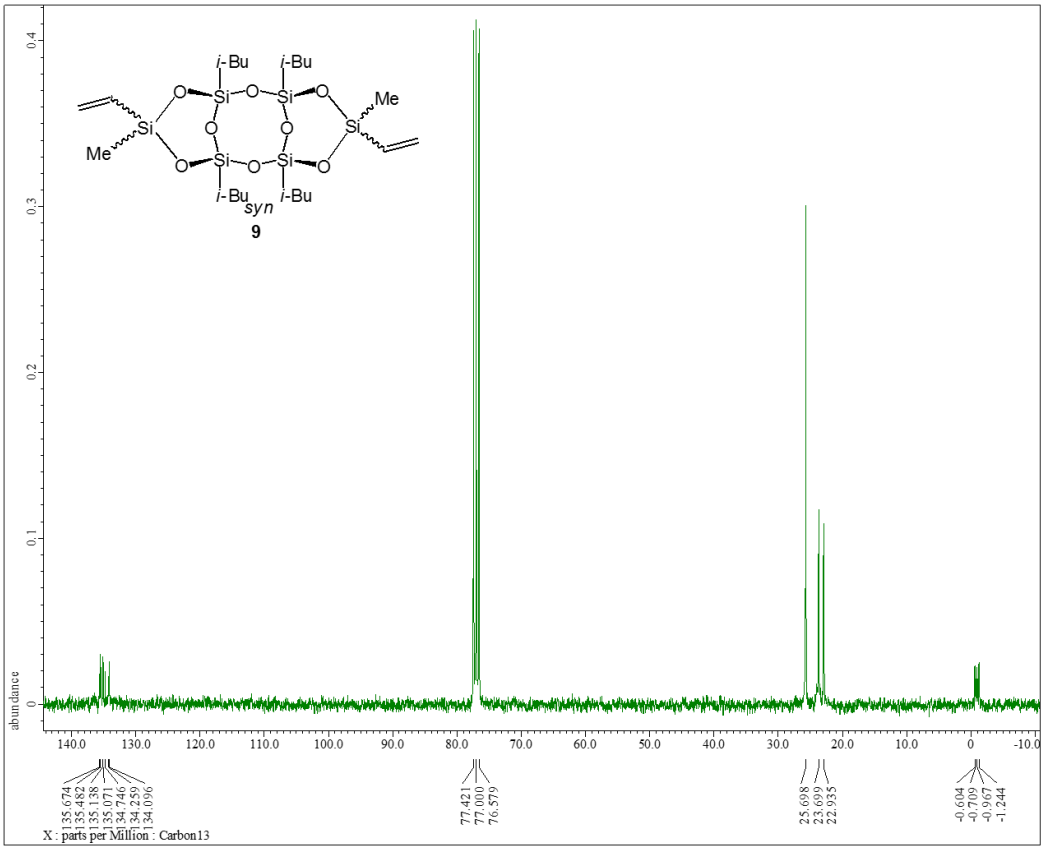

Figure 49. ^{13}C NMR spectrum of **9** (75.57 MHz, $CDCl_3$)

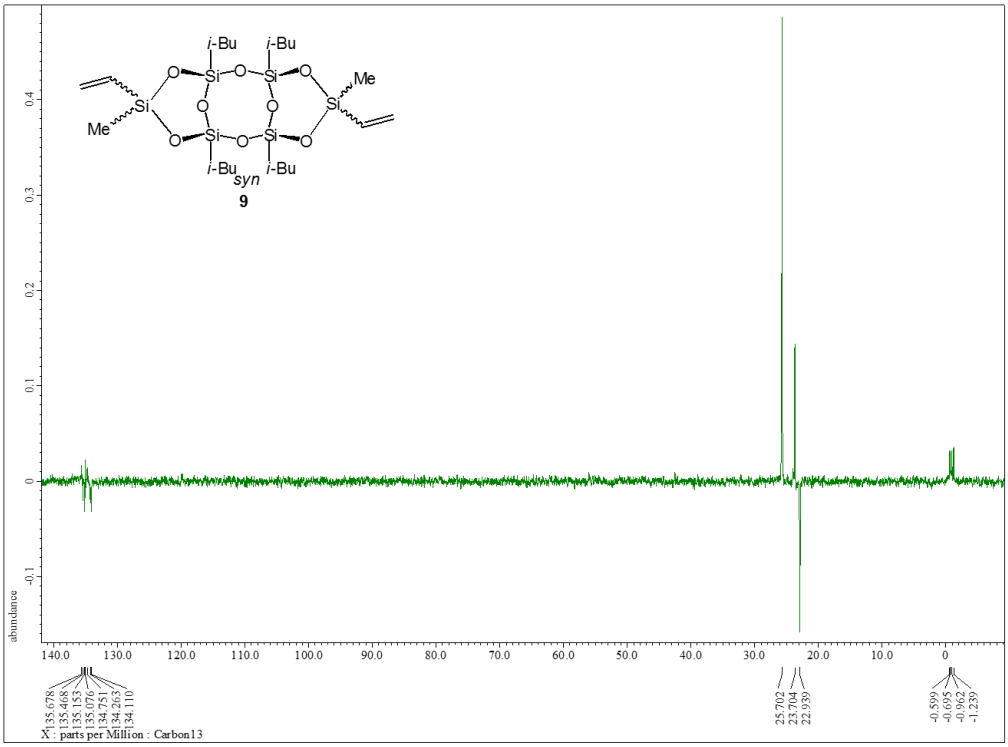

Figure 50. ^{13}C (dept 135) NMR spectrum of **9** (75.57 MHz, $CDCl_3$)

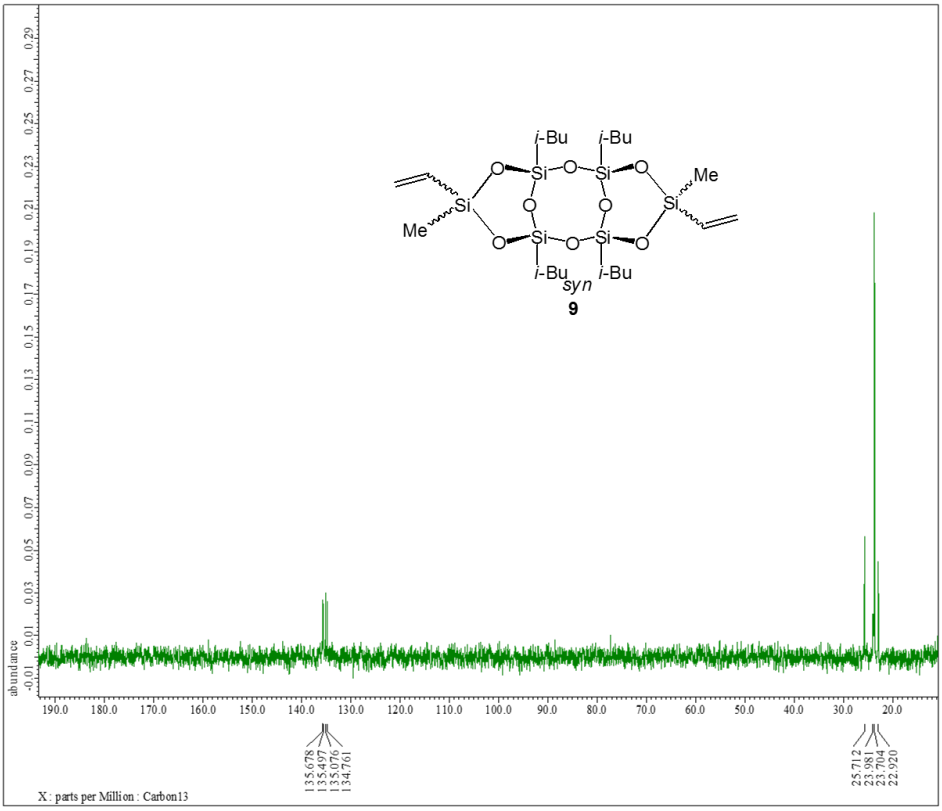

Figure 51. ^{13}C (dept 90) NMR spectrum of **9** (75.57 MHz, $CDCl_3$)

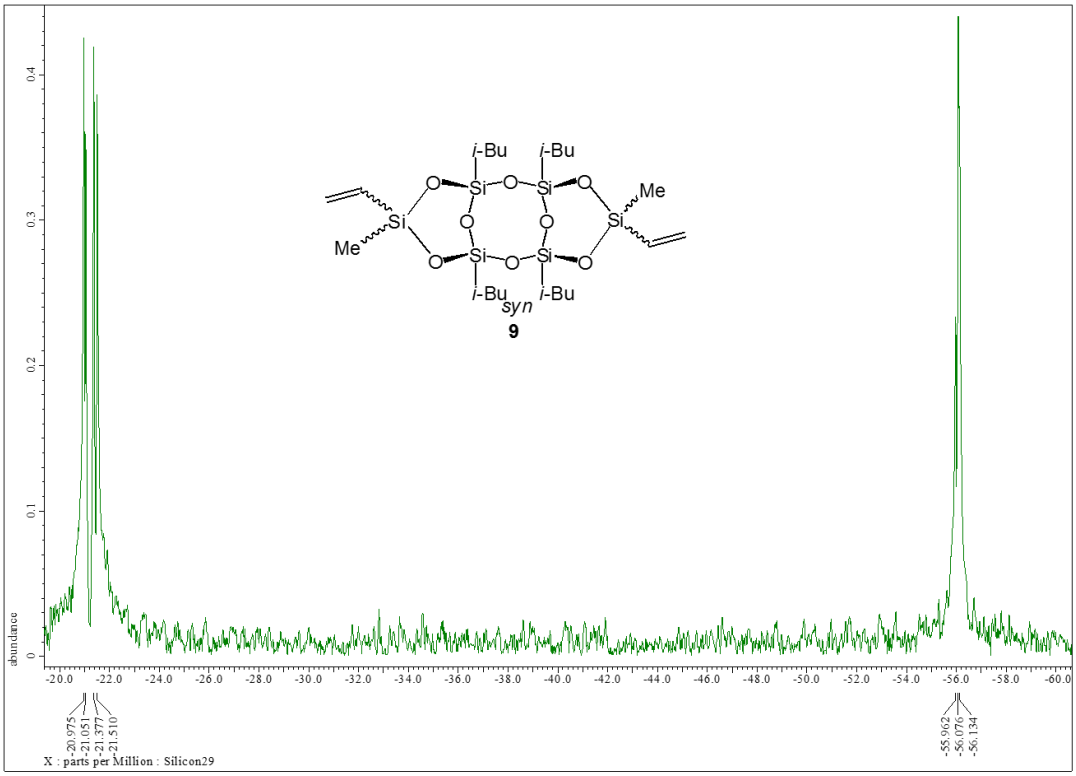

Figure 52. ^{29}Si NMR spectrum of **9** (59.71 MHz, $CDCl_3$)

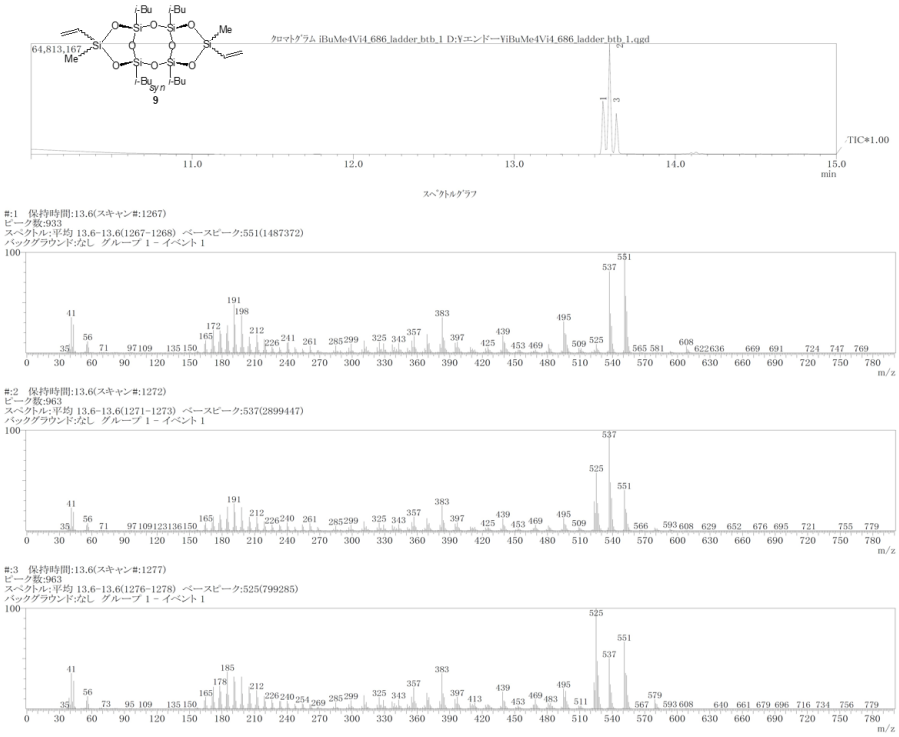

Figure 53. GCMS spectrum of **9** (EI, 70 ev)

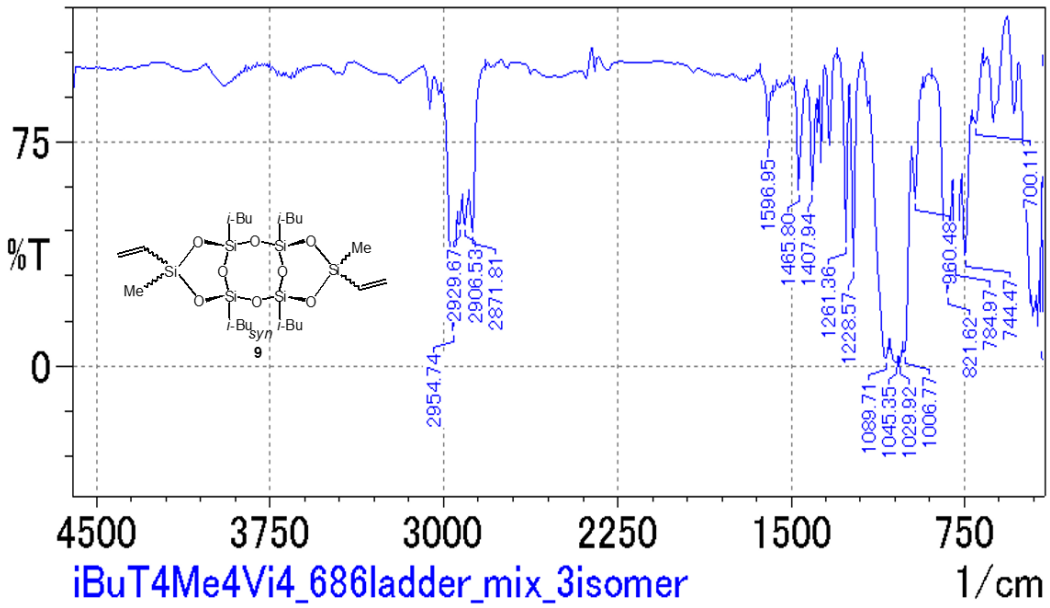

Figure 54. IR spectrum of **9** (KBr)

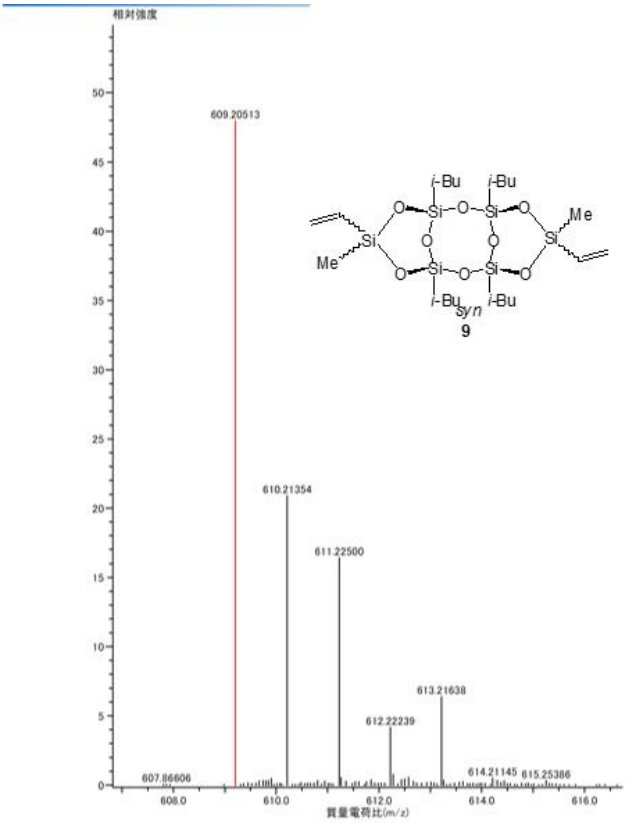

Figure 55. MALDITOFMS spectrum of **9**

Chapter 2: Synthesis and properties of phenylsilsesquioxanes with ladder and double-decker Structures

3.2.1 Introduction

A recent increase in the demand for thermally stable materials has highlighted the importance of silsesquioxanes with well-defined structures. Among them, the cage-type octasilsesquioxanes (T_8) have been the most intensively studied for numerous applications [1]. On the other hand, siloxanes and silsesquioxanes with other structures have not been as extensively studied, and comparison of cage silsesquioxane properties to the properties of compounds (ladder, double-decker, or partial cage) has not been sufficiently studied.

In the last decade, the synthesis, structure determination, and thermal properties of alkyl-substituted ladder oligosilsesquioxanes with defined structures (called "laddersiloxanes") up to nonacyclic one have been reported [2–13]. Thermal stability of these compounds increases with the numbers of rings. For application purposes, phenyl-substituted silsesquioxanes are more promising than alkyl-substituted silsesquioxanes. For example, a phenyl-substituted silsesquioxane has a higher refractive index and thermal stability [14,15]. Therefore, the substituents were fixed to phenyl groups, and their properties were measured. In this chapter, to clarify the properties of laddersiloxanes and examine the structure–thermal property relationship with various structures, new ladder and double-decker silsesquioxanes were synthesized. The spectral features and thermal properties of silsesquioxanes, cyclic siloxanes, and acyclic siloxanes were investigated.

In 1960, Brown reported that the base-catalyzed polycondensation of the hydrolysate from phenyl-trichlorosilane led to the formation of polyphenylsilsesquioxane $(PhSiO_{1.5})_n$ [16]. Additionally, the selective synthesis of phenyl-substituted cage silsesquioxanes with various cage sizes (Ph_6T_6, Ph_8T_8, $Ph_{10}T_{10}$, and $Ph_{12}T_{12}$) was recently reported [17–20]. Their structures were determined by X-ray crystallographic analysis [19-25]. In addition, the synthesis of double-decker–type silanol derivatives have also been reported [26,27].

Brown and coworkers first proposed the structure of ladder polysilsesquioxanes for phenyl-substituted ladder silsesquioxanes [16]; however, only a few compounds were unequivocally determined by crystallographic analysis. Andrianov and coworkers reported the synthesis and structure determination of tricyclic ladder siloxanes [28–30]. Additionally, the structures of ladder siloxanes containing phenyl groups in part have been established [6,9,10,11,13].

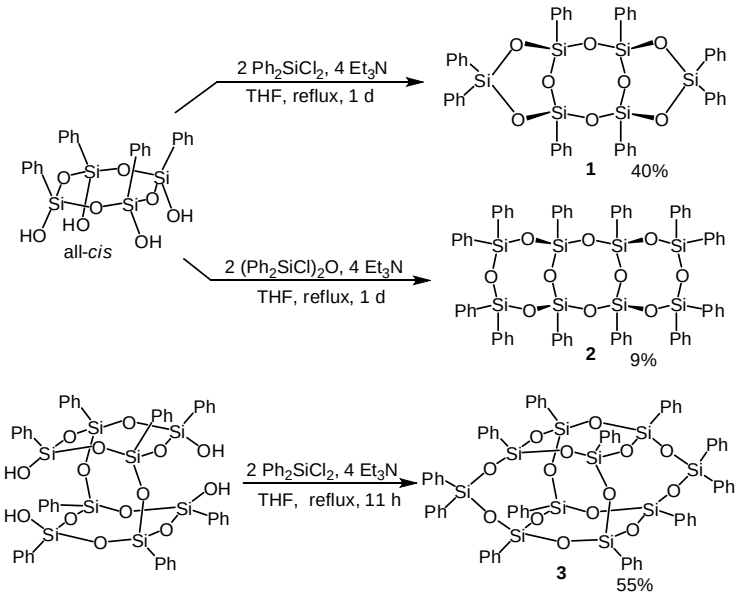

Scheme 1

In this chapter, we describe syntheses of phenyl-substituted tricyclic ladder siloxanes with 6-8-6– and 8-8-8–membered fused rings (Scheme 1: **1** and **2**) and novel phenyl-substituted double-decker–type silsesquioxane **3** (Scheme 1). In addition to these new compounds, the NMR spectra and thermal properties of known phenyl-substituted siloxane compounds were measured and compared.

3.2.2 Results and discussion

The syntheses of **1**, **2**, and **3** were performed as shown in Scheme 1. All-*cis*-tetraphenylcyclotetrasiloxanetetraol, a precursor of **1** and **2**, was synthesized according to the procedure by Kawakami et al [31]. Double-decker tetraol, the precursor of **3**, was also synthesized by a known procedure [27]. All-*cis*-tetraphenylcyclotetrasiloxanetetraol was treated with dichlorodiphenylsilane in the presence of triethylamine, and the target tricyclic laddersiloxane **1** was obtained in 40% yield after the crystallization of the crude product. Tricyclic laddersiloxane **2** was prepared in a similar manner from cyclic silanol with dichlorodisiloxane. At the stage of purification, we observed compounds with silanol groups, thus the generation of incompletely condensed products is the reason of low yield of **2**. The reaction of the double-decker tetraol with dichlorodiphenylsilane afforded **3** in 55% yield. The obtained solid was further recrystallized from toluene (**1** and **2**) or $CHCl_3$ and isopropyl alcohol (**3**) by slow evaporation at room temperature to afford crystals suitable for X-ray analysis.

Molecular structures are shown in Figures 1–3. Toluene was observed in the crystals of **1** and **2**. Reflecting the conformation of the starting cyclic silanol, both the compounds adopt a *syn*-conformation of the rings. The Si–O bond lengths were in the ranges of 1.619(2)–1.648(1) Å (average 1.631(1) Å) for **1**, 1.603(3)–1.635(3) Å (average 1.617(3) Å) for **2**, and 1.606(2)–1.631(2) Å (average 1.616(2) Å) for **3**. In compound **1**, the Si–O–Si bond angles in the six-membered ring have similar values (127.4(1)°–132.8(1)°), and the two center Si–O–Si bond angles in the eight-membered ring have larger values (141.1(1)° and 142.7(1)°). In compound **2**, the Si–O–Si bond angles for the terminal rings are wider (150.0(2)°–162.3(2)°) than the average Si–O–Si bond angles in the central ring (147.7(2)°) because of the steric congestion of the two phenyl groups. In compound **3**, the Si–O–Si bond angles vary considerably (140.1(1)°–165.2(1)°) because of the presence of both eight- and ten-membered rings.

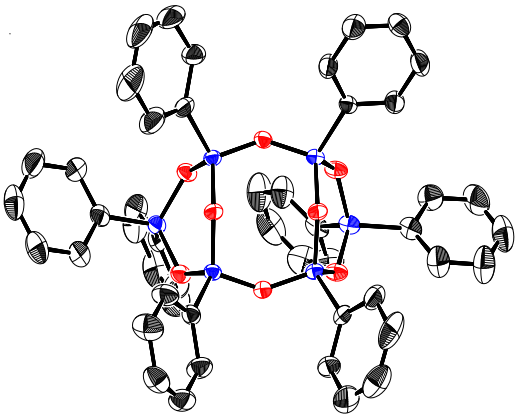

Figure 1. Crystal structure of **1**. Black: Carbon; Blue: Silicon; Red: Oxygen. Thermal ellipsoids are shown in 50% probability level.

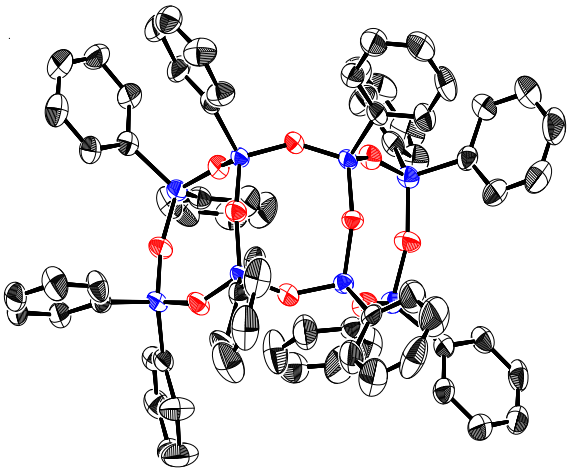

Figure 2. Crystal structure of **2**. Black: Carbon; Blue: Silicon; Red: Oxygen. Thermal ellipsoids are shown in 50% probability level.

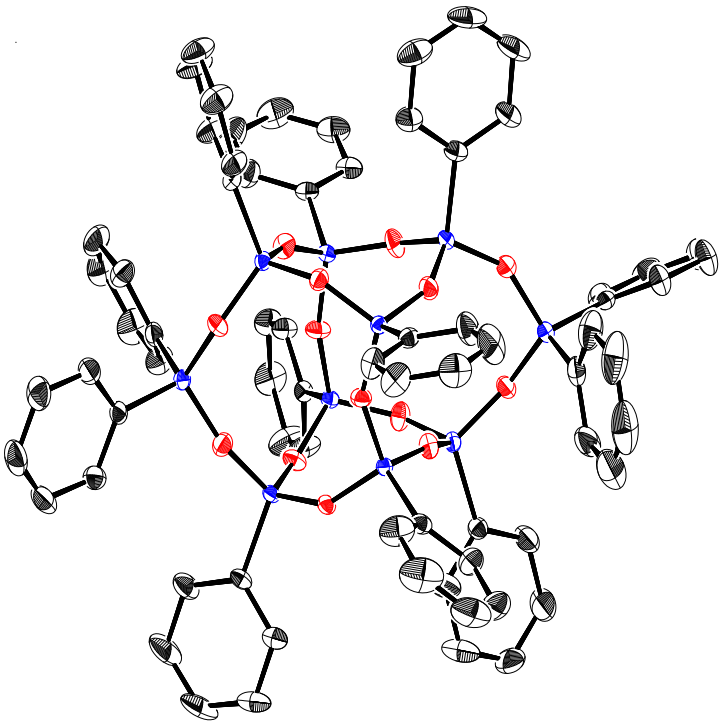

Figure 3. Crystal structure of **3**. Black: Carbon; Blue: Silicon; Red: Oxygen. Thermal ellipsoids are shown in 50% probability level.

To compare the spectral and thermal properties of **1**–**3**, hexaphenyldisiloxane, hexaphenylcyclotrisiloxane, octaphenylcyclotetrasiloxane, and octaphenyloctasilsesquioxane were synthesized according to known procedures [32-34]. The values from ^{29}Si NMR are summarized in Table 1.

Table 1. ^{29}Si NMR Data of Phenyl Siloxanes (in $CDCl_3$)

Compounds	Structure	^{29}Si NMR / ppm
$Ph_3SiOSiPh_3$	M	–18.5
$(Ph_2SiO)_3$	D	–33.9
$(Ph_2SiO)_4$	D	–43.0
1	D, T	–32.0, –66.7
2	D, T	–43.6, –76.3
3	D, T	–45.4, –78.1, –79.4
$(PhSiO_{1.5})_6$	T	–66.9 [17]
$(PhSiO_{1.5})_8$ [18]	T	–78.4
$(PhSiO_{1.5})_{12}$	T	–77.0, –80.6 [18]*

*Data by MAS NMR

From these results, the chemical shifts in the ^{29}Si NMR can be estimated on the basis of ring size and the number of oxygen atoms bonded to silicon atoms. For example, the D (connected to two oxygen atoms) silicon atom in six-membered rings shows a peak between –32 and –34 ppm, regardless of the other molecule components. An eight-membered D silicon atom has a signal around –43 ppm, which is a magnetic field shift of about 10 ppm higher than that seen in six-membered ring silicon atoms. A similar tendency is also observed for T (silicon atoms connecting three oxygen atoms) silicon. Thus, silicon atoms contained in eight-membered rings show peaks in the region varying from –76 to –79 ppm, and those in six-membered rings have signals at –67 ppm, a shift about 10 ppm lower. In contrast, the chemical shift of silicon atoms incorporated in ten-membered rings is similar to that of the eight-membered ring atoms (–78.1 and –79.4 ppm).

The results of thermogravimetric (TG) analysis in N_2 are summarized in Table 2. The results show that a higher Td_5 (5% weight loss) temperature was observed with a higher inorganic component ratio (Si and O, %ratio). The Td_5 temperatures of **2**, **3**, and Ph-T_8 are all over 400 °C, showing their high thermal stability.

The Td_5 of the isopropyl-substituted heptacyclic laddersiloxane was reported to be 326 °C [9]. With phenyl groups as substituents, even tricyclic **1** and **2** show higher Td_5 temperatures. The Td_5 of $(Ph_2SiO)_4$, **2**, and PhT_8 are significantly higher than that of isopropyl-substituted siloxane compounds with the same structure (Table 3) [10]. These results clearly show the advantage of phenyl siloxanes for thermal stability. TG measurements in air were also performed. The Td_5 temperatures were almost unchanged, showing the high anti-oxidation ability of phenyl siloxanes.

Table 2. TG Measurement Data under N_2 atmosphere

Compounds	Si+O ratio / %	Td_5 /℃	Comment
$Ph_3SiOSiPh_3$	13	281	Sublimed at 369 ℃
$(Ph_2SiO)_3$	22	296	Sublimed at 372 ℃
$(Ph_2SiO)_4$	22	343	Sublimed at 429 ℃
1	32	355	20% Residue at 1000 ℃
2	29	404	Sublimed at 488 ℃
3	35	425	Sublimed at 526 ℃
$(PhSiO_{1.5})_8$	40	439	50% residue at 1000 ℃

Table 3. TG Measurement Data of *i*-Pr or Ph substituted siloxanes under N_2 atmosphere [10]

R	Structure	Si+O ratio	TG measurement data
i-Pr	R_8D_4	34	Td_5 (N_2): 205 ℃ Sublimed at 345 ℃
i-Pr	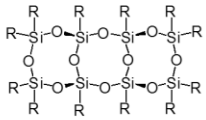	43	Td_5 (N_2): 260 ℃ Sublimed at 390 ℃
i-Pr	R_8T_8	55	Td_5 (N_2):200 ℃ Sublimed at 282 ℃
Ph	R_8D_4	22	Td_5 (N_2): 343 ℃ Sublimed at 429 ℃
Ph	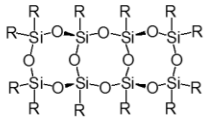	29	Td_5 (N_2): 404 ℃ Sublimed at 488 ℃
Ph	R_8T_8	40	Td_5 (N_2): 439 ℃ Residue 50% at 1000 ℃

3.2.3 Summary

In summary, phenyl-substituted tricyclic ladder siloxane and double-decker–type siloxanes were synthesized and their structures clarified by crystallographic analysis. Thermal analysis of the phenyl-substituted siloxane compounds showed their high thermal stability.

3.2.4 Experimental section

The Fourier transform nuclear magnetic resonance (NMR) spectra were obtained using a Jeol ECS-300 (^{1}H at 300.53 MHz, ^{13}C at 75.57 MHz, and ^{29}Si at 59.71 MHz) NMR instrument. Chemical shifts are reported as δ units (ppm) relative to $SiMe_4$, and the residual solvents peaks were used as standards. For ^{29}Si NMR, $SiMe_4$ was used as an external standard. Electron impact mass spectrometry was performed on Shimadzu GCMS-QP2010SE/DI2010. Infrared spectra were measured with Shimadzu FTIR-8400S. All melting points were determined on Yanaco micro melting point apparatus MP-J3 and are uncorrected. MALDI-TOF mass analysis was carried out with a Shimadzu AXIMA Performance instrument using 2,5-dihydroxybenzoic acid (dithranol) as the matrix and $AgNO_3$ as the ion source. Elemental analyses were performed by the Center for Material Research by Instrumental Analysis (CIA), Gunma University, Japan. A Rigaku thermal gravimetric analyzer (Thermoplus TG-8120) was used to investigate the thermal stability of siloxane compounds. All samples were

heated in N_2 and the air rose from the ambient temperature to 1000 °C at a heating rate of 10 °C min^{-1} in all cases. All reagents used were of analytical grade. Tetrahydrofuran was dried over Na/benzophenone.

Synthesis of phenyl-substituted 6-8-6–membered fused rings tricyclic ladder siloxane (**1**)

Under argon atmosphere, dichlorodiphenylsilane (2.6 g, 10 mmol) in THF (25 mL) was added to a solution of all *cis*-1,3,5,7-tetrahydroxy-1,3,5,7-tetraphenylcyclotetrasiloxane (2.8 g, 5.1 mmol) and triethylamine (2.1 g, 21 mmol) in THF (15 mL) at 0 °C . The mixture was refluxed for one day. Trichloromethane was added to the reaction mixture, and the organic phase was washed with a saturated ammonium chloride aqueous solution and brine. The organic phase was dried over anhydrous sodium sulfate and evaporated to afford a crude solid, which was washed with methanol and ethanol. The solid was further purified by reprecipitation from trichloromethane and hexane to afford **1** (1.8 g, 40%) as a white solid.

Spectral data for **1**: m.p. over 300 ℃. ^{1}H NMR (300.53 MHz, $CDCl_3$) δ 7.01 (t, *J* = 7.5 Hz, 4H), 7.22–7.28 (m, 14H), 7.35–7.43 (m, 6H), 7.52–7.58 (m, 16H) ppm. ^{13}C NMR (75.57 MHz, $CDCl_3$) δ 127.78 (CH), 129.72 (C), 130.46 (CH), 130.56 (CH), 130.93 (CH), 132.26 (C), 133.91 (C), 134.27 (CH), 134.33 (CH), 134.38 (CH) ppm two CH peaks were overlapped. ^{29}Si NMR (59.71 MHz, $CDCl_3$) δ –32.01, –66.69 ppm. DIMS (EI, 70eV) *m*/z (%) 912 (M^+, 16), 835 ($[M–Ph]^+$, 80), 757 (100) . MALDI-TOF MS (*m/z*) 1021.6 ($[M+Ag]^+$, calc.: 1021.0). IR (KBr) 517, 698, 995, 1009, 1024, 1040, 1095, 1134 cm^{-1}. Anal. Calcd for $C_{48}H_{40}Si_6O_8 \cdot H_2O$:C, 61.90; H, 4.55; Found C, 62.04; H, 4.41%.

Synthesis of phenyl-substituted 8-8-8–membered fused rings tricyclic ladder siloxane (**2**)

Under argon atmosphere, 1,3-dichloro-1,1,3,3-tetraphenyldisiloxane (2.9 g, 6.4 mmol) in THF (10 mL) was added to a solution of all *cis*-1,3,5,7-tetrahydroxy-1,3,5,7-tetraphenylcyclotetrasiloxane (1.7 g, 3.1 mmol) and triethylamine (1.2 g, 12 mmol) in THF (10 mL) at 0 °C. The mixture was refluxed for one day. Trichloromethane was added to the reaction mixture, and the organic phase was washed with a saturated ammonium chloride aqueous solution and brine. The organic phase was dried over anhydrous sodium sulfate and evaporated to afford a crude solid. The solid was washed by methanol and ethanol, and it was recrystallized from acetone. The solid was the further purified by reprecipitation from trichloromethane and

hexane to afford **2** (0.37 g, 9%) as a white solid.

Spectral data for **2**: m.p. 227–229 ℃. ^{1}H NMR (300.53 MHz, $CDCl_3$) δ 6.94 (t, *J* = 7.8 Hz, 8H) , 7.02 (t, *J* = 7.8 Hz, 8H) , 7.06 (t, *J* = 7.8 Hz, 8H) , 7.12-7.25 (m, 12H) , 7.30 (dd, *J* = 7.8 Hz, 0.9 Hz, 8H), 7.37 (dd, *J* = 7.8 Hz, 0.9 Hz, 8H) ,7.56 (dd, *J* = 7.8 Hz, 0.9 Hz, 8H) ppm. ^{13}C NMR (75.57 MHz, $CDCl_3$) δ 127.35 (CH), 127.41 (CH), 127.61 (CH), 129.85 (CH), 129.92(CH), 130.01(CH), 131.09 (C), 133.75 (C), 133.99 (CH), 134.19 (CH), 134.31 (CH), ppm one C peak overlapped. ^{29}Si NMR (59.71 MHz, $CDCl_3$) δ –43.64, –76.26 ppm. MALDI-TOF MS (*m/z*) 1417.0 ([M+Ag]$^{+}$, calc.: 1417.1). IR (KBr) 490, 523, 696, 717, 739, 1061, 1130, 1429, 3072 cm^{-1}. Anal. Calcd for $C_{72}H_{60}Si_8O_{10}$:C, 66.02; H, 4.62; Found C, 65.82; H, 4.76%.

Synthesis of phenyl-substituted double-decker–type silsesquioxane (**3)**

Under argon atmosphere, dichlorodiphenylsilane (1.5 g, 5.9 mmol) in THF (15 mL) was added to a solution of 3,9,14,17-tetrahydroxy-1,3,5,7,9,11,14,16-octaphenyltricyclo[7.3.3^{7,10}]octasilsesquioxane (3.1 g, 2.9 mmol) and triethylamine (1.2 g, 12 mmol) in THF (15 mL) at 0 °C . The mixture was refluxed for 11 h. Trichloromethane was added to the reaction mixture, and the organic phase was washed with saturated ammonium chloride aqueous solution and brine. The organic phase was dried over anhydrous sodium sulfate and evaporated to afford a crude solid, which was washed by methanol and ethanol. The solid was further purified by reprecipitation from trichloromethane and hexane to afford **3** (2.3 g, 55%) as a white solid.

Spectral data for **3**: m.p. over 300 ℃. ^{1}H NMR (300.53 MHz, $CDCl_3$) δ 7.06 (t, *J* = 7.5 Hz, 8H), 7.13–7.30 (m, 28H), 7.33–7.39 (m, 8H), 7.49–7.51 (m, 8H), 7.64–7.67 (m, 8H) ppm. ^{13}C NMR (75.57 MHz, $CDCl_3$) δ 127.39 (CH), 127.77 (CH), 127.81 (CH), 130.10 (CH), 130.19 (CH), 130.40 (C), 130.48 (C), 131.54 (C), 134.01 (CH), 134.09 (CH), 134.25 (CH), 134.57 (C) ppm. ^{29}Si NMR (59.71 MHz, $CDCl_3$) δ –45.42, –78.09, –79.36 ppm. MALDI-TOF MS (*m/z*) 1536.8 ([M+Ag]$^{+}$, calc.: 1537.1). IR (KBr) 490, 519, 698, 729, 1088, 1132, 1429, 3072 cm^{-1}. Anal. Calcd for $C_{72}H_{60}Si_{10}O_{14}$:C, 60.47; H, 4.23; Found C, 60.50; H, 4.63%.

3.2.5. References

[1] D. B. Cordes, P. D. Lickiss, F. Rataboul, *Chem. Rev.*, **2010**, *110*, 2081.

[2] M. Unno, A. Suto, T. Matsumoto, *Russ. Chem. Rev.*, **2013**, *82*, 289.

[3] M. Unno, B. A. Shamsul, M. Arai, K. Takada, R. Tanaka, H. Matsumoto, *Appl.*

Organomet. Chem. **1999**, *13*, 303.
[4] F. J. Feher, R. Terroba, J. W. Ziller, *Chem. Commun.*, **1999**, 2153.
[5] M. Unno, A. Suto, K. Takada, H. Matsumoto, *Bull. Chem. Soc. Jpn.*, **2000**, *73*, 215.
[6] M. Unno, A. Suto, H. Matsumoto, *J. Am. Chem. Soc.*, **2002,** *124*, 1574.
[7] M. Unno, R. Tanaka, S. Tanaka, T. Takeuchi, S. Kyushin, H. Matsumoto, *Organometallics*, **2005**, *24*, 765.
[8] K. Suyama, T. Gunji, K. Arimitsu, Y. Abe, *Organometallics*, **2006**, *25*, 5587.
[9] M. Unno, T. Matsumoto, H. Matsumoto, *J. Organomet., Chem.* **2007**, *692*, 307.
[10] S. Chang, T. Matsumoto, H. Matsumoto, M. Unno, *Appl. Organomet., Chem.* **2010**, *24*, 241.
[11] H. Seki, Y. Abe, T. Gunji, *J. Organomet. Chem.*, **2011**, *696*, 846.
[12] H. Seki, N. Abe, Y. Abe, T. Gunji, *Chem. Lett.*, **2011**, *40*, 722.
[13] M. Unno, T. Matsumoto, H. Matsumoto, *Int. J. Polym. Sci.*, **2012**, ID 723892.
[14] L. H. Brown, "Silicones in protective coatings," in *Treatise on Coatings*, R. Myers and J. S. Long, Eds., vol. 1, part 3, chapter 13, p. 513, Marcel Dekker, New York, NY, USA, 1972.
[15] J. S. Kim, S. C. Yang, B. S. Bae, *Chem. Mater.*, **2010**, *22*, 3549.
[16] Jr. J. F. Brown, *J. Am. Chem. Soc.*, **1965**, *87*, 4317.
[17] A. R. Bassindale, I. A. MacKinnon, M. G., Maesano P. G. Taylor, *Chem. Comm.*, **2003**, 1382.
[18] M. Kozelj, B. Orel, *Dalton Trans.* **2008**, 5072.
[19] M. F. Roll, J. W. Kampf, Y. Kim, E. Yi, R. M. Laine, *J. Am. Chem. Soc.*, **2010**, *132*, 10171.
[20] R. M. Laine, M. F. Roll, *Macromolecules*, **2011**, *44*, 1073.
[21] V. E. Shklover, Yu. T. Struchkov, N. N. Makarova, K.A. Andrianov, *Zh. Strukt. Khim.*, **1978**, *19*, 1107.
[22] A. R. Bassindale, M. Pourny, P. G. Taylor, M. B. Hursthouse, M. E. Light, *Angew. Chem., Int. Ed.*, **2003**, *42*, 3488.
[23] M. A. Hossain, M. B. Hursthouse, K. M. A. Malik, *Acta Crystallogr., Sect.B: Struct. Crystallogr. Cryst. Chem.*, **1979**, *35***,** 2258.
[24] V. E. Shklover, Yu. E. Ovchinnikov, Yu. T. Struchkov, M. M. Levitskii, A. A. Zhdanov, *Metalloorg. Khim.*, **1988**, *1***,** 1273.
[25] W. Clegg, G. M. Sheldrick, N. Vater, *Acta Crystallogr., Sect.B: Struct. Crystallogr. Cryst. Chem.*, **1980**, *36*, 3162.
[26] K. Yoshida, Y. Ookuma, Y. Morimoto, K. Watanabe, N. Ootake, R. Tanaka, H. Matumoto, *Polym. Prep. Jpn.*, **2003**, *52*, 316.

[27] D. W. Lee, Y. Kawakami, *Polym. J.*, **2007**, *39*, 230.
[28] K. A. Andrianov, I. Yu. Klement'ev, G. N. Kartsev, V. S. Tikhonov, *Izvestiya Akademii Nauk SSSR, Seriya Khimicheskaya*, **1975**, *11*, 2554.
[29] I. I. Dubovik, N. N. Makarova, G. L. Slonimskii, *Vysokomol. Soedin. A+*, **1981**, *23*, 1066.
[30] K. A. Andrianov, I. Yu. Klement'ev, G. N. Kartsev, V. S. Tikhonov, *Zh. Obshch. Khim.*, **1972**, *42*, 1342.
[31] R. Ito, Y. Kakihana, Y. Kawakami, *Chem. Lett.*, **2009**, *38*, 364.
[32] K. Goto, T. Okumura, T. Kawashima, *Chem. Lett.*, **2001**, *12*, 1258.
[33] M. Unno, R. Tanaka, D. Obinata, M. Endo, T. Sakurai, S. Ojima, T. Katayama, K. Fugami, *Key. Eng. Mater.*, **2011**, *459*, 43
[34] S. Tateyama, Y. Kakihana, Y. Kawakami, *J. Organomet. Chem.*, **2010**, *695*, 898.

2.3.6 Supporting information

1. Spectral data

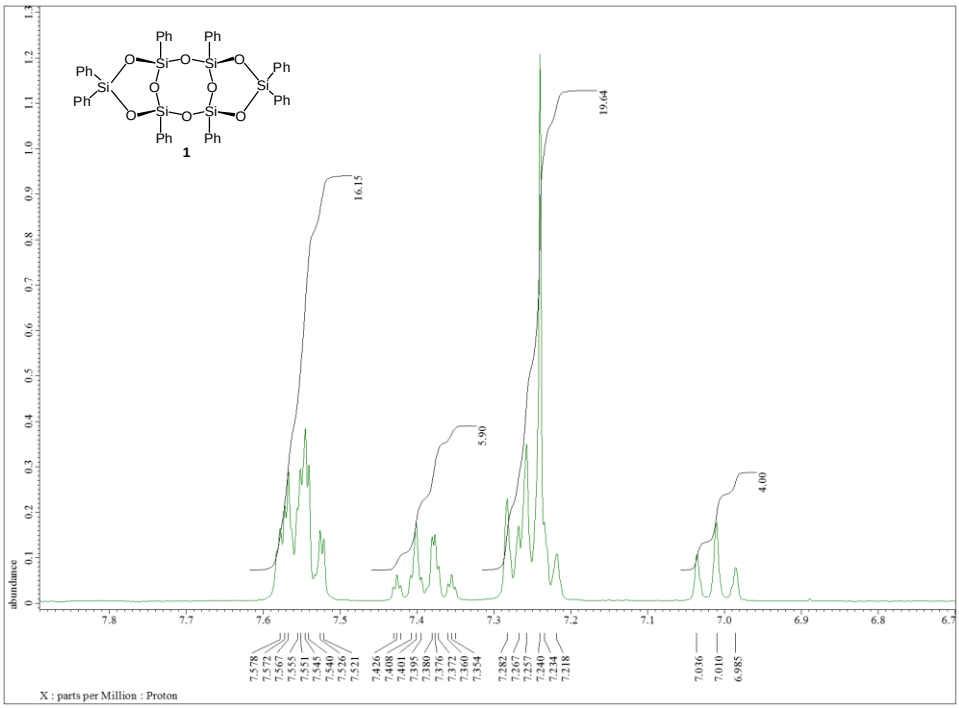

Figure 1. ^{1}H NMR spectrum of **1** (300.53 MHz, $CDCl_3$)

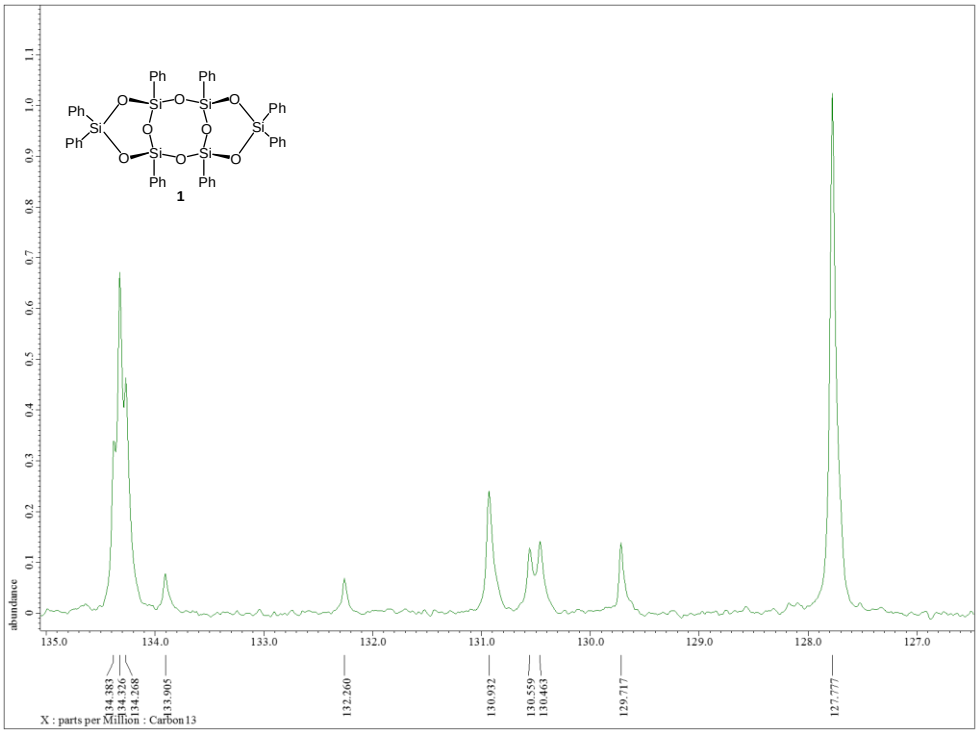

Figure 2. ^{13}C NMR spectrum of **1** (75.57 MHz, $CDCl_3$)

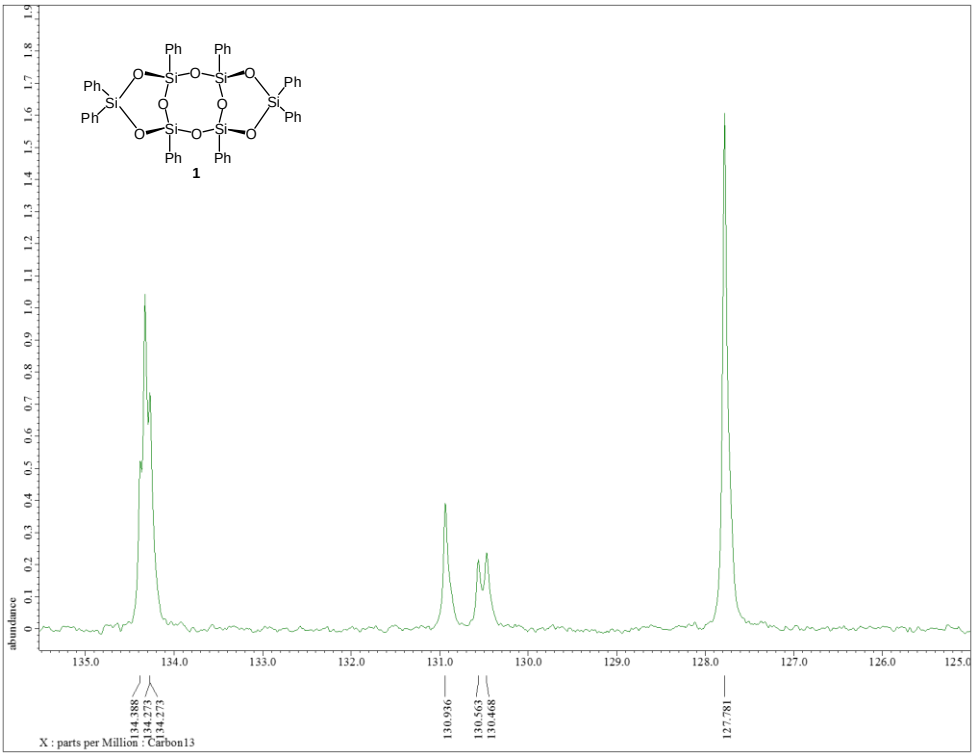

Figure 3. ^{13}C NMR (dept 135) spectrum of **1** (75.57 MHz, $CDCl_3$)

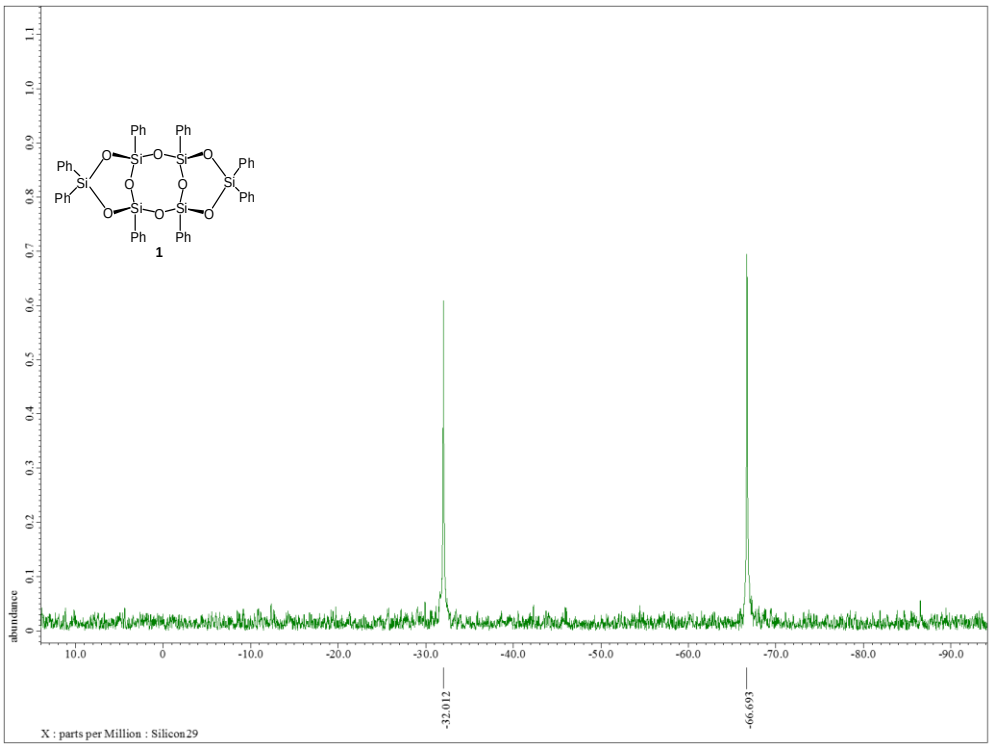

Figure 4. ^{29}Si NMR spectrum of **1** (59.71 MHz, $CDCl_3$)

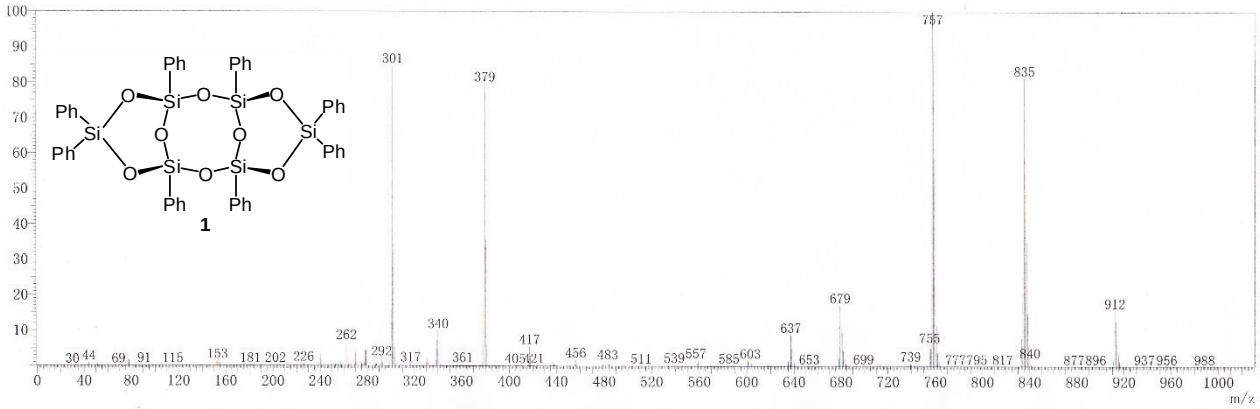

Figure 5. DIMS spectrum of **1**

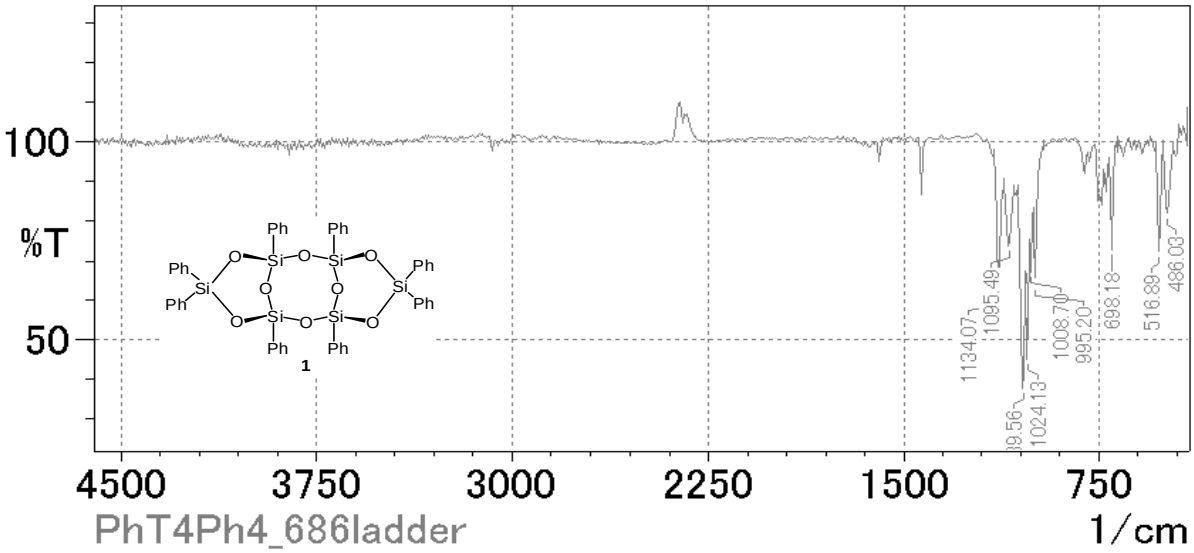

Figure 6. IR spectrum of **1**

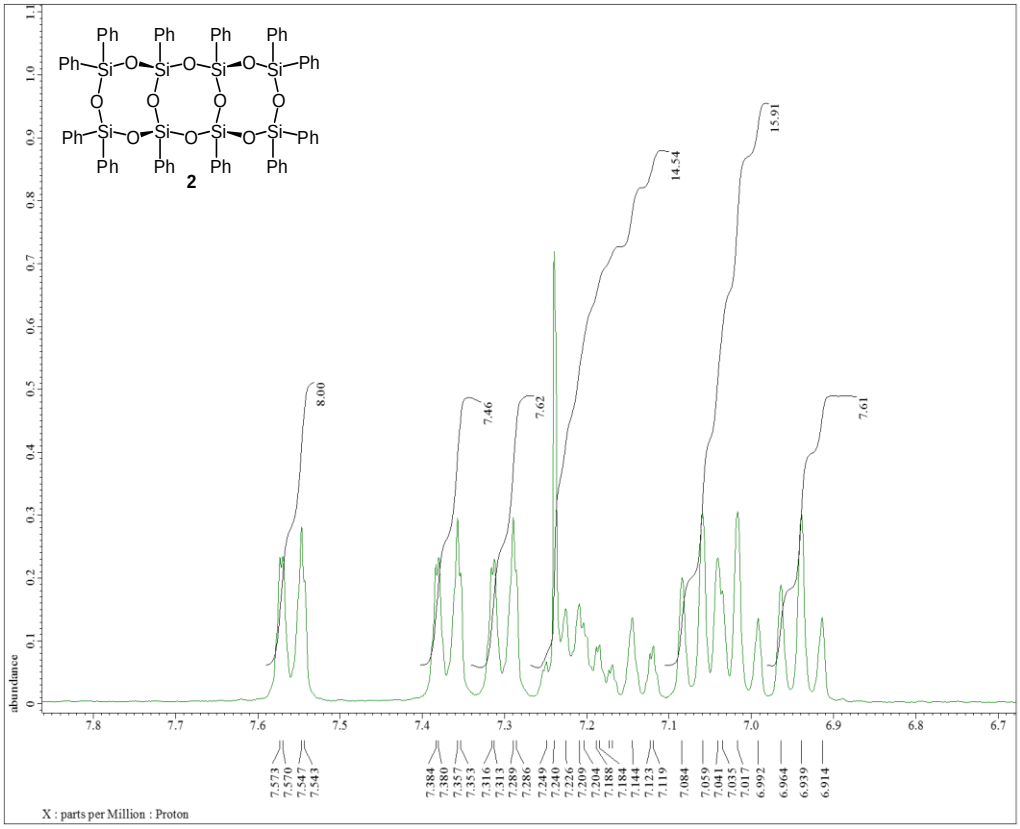

Figure 7. ^{1}H NMR spectrum of **2** (300.53 MHz, $CDCl_3$)

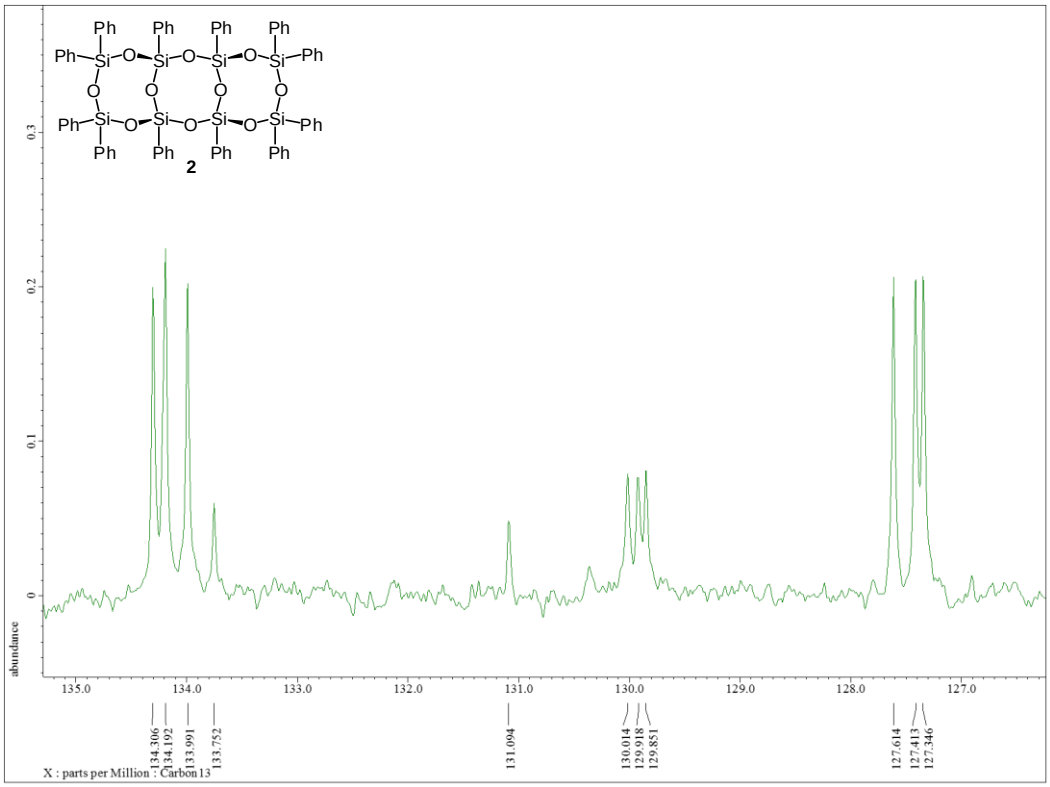

Figure 8.^{13}C NMR spectrum of **2** (75.57 MHz, $CDCl_3$)

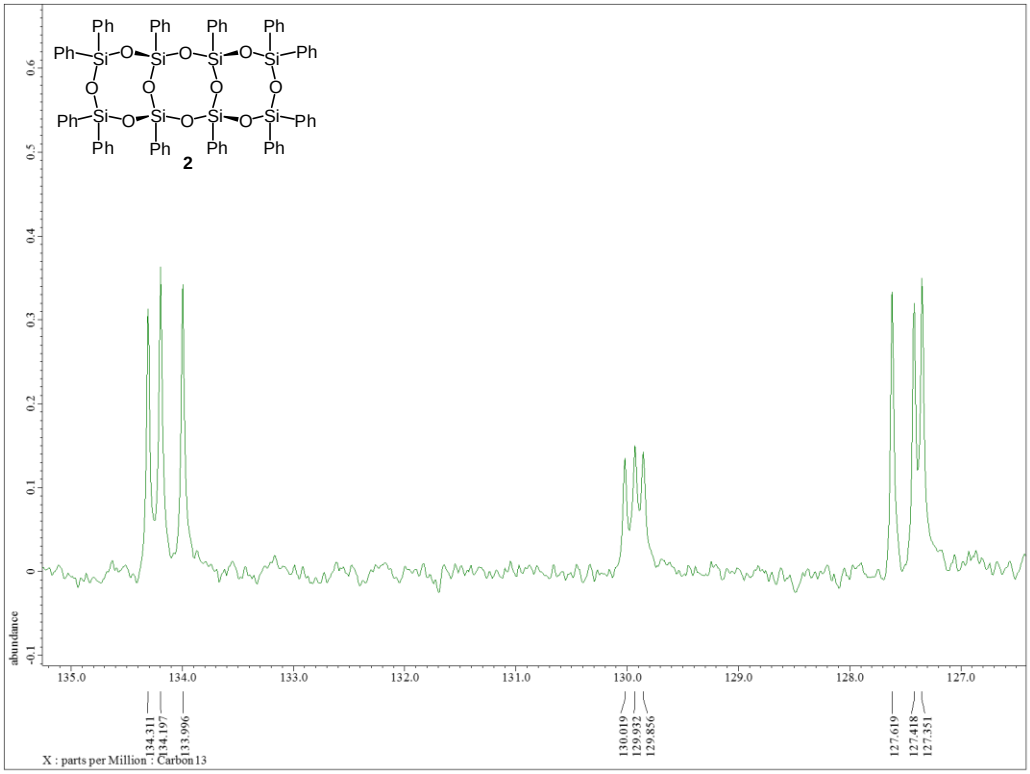

Figure 9. ^{13}C NMR (dept 135) spectrum of **2** (75.57 MHz, $CDCl_3$)

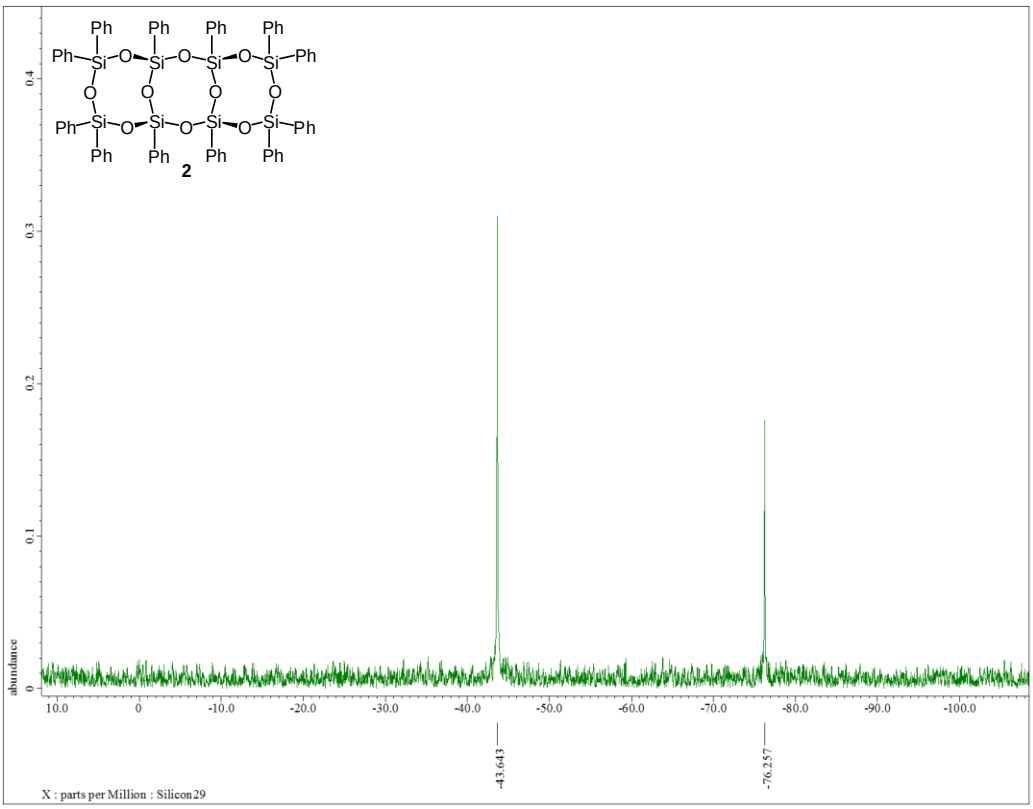

Figure 10. ^{29}Si NMR spectrum of **2** (59.71 MHz, $CDCl_3$)

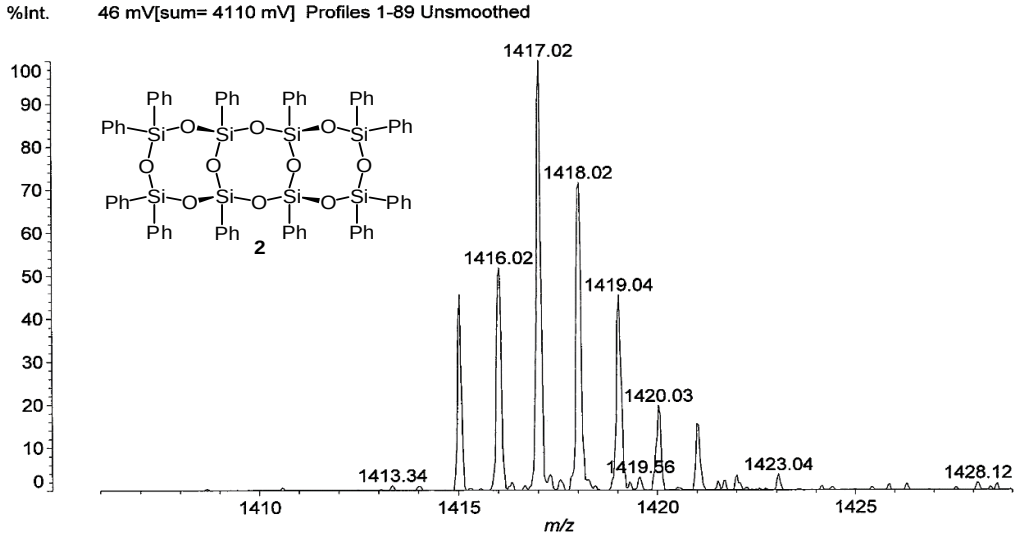

Figure 11. MALDITOFMS spectrum of **2**

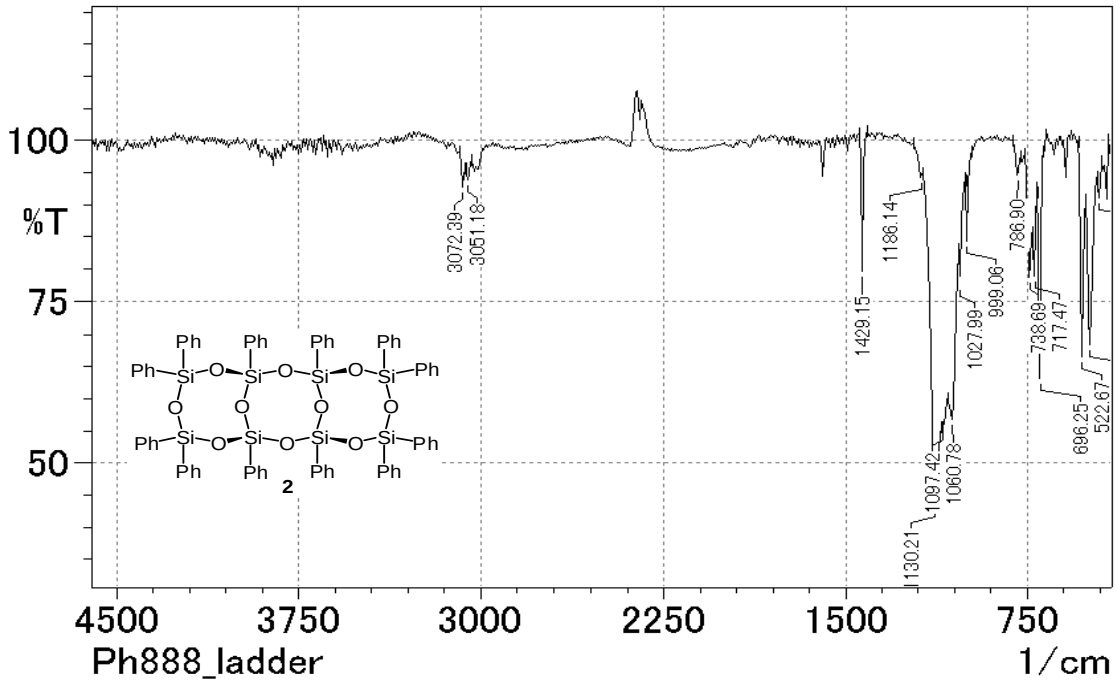

Figure 12. IR spectrum of **2**

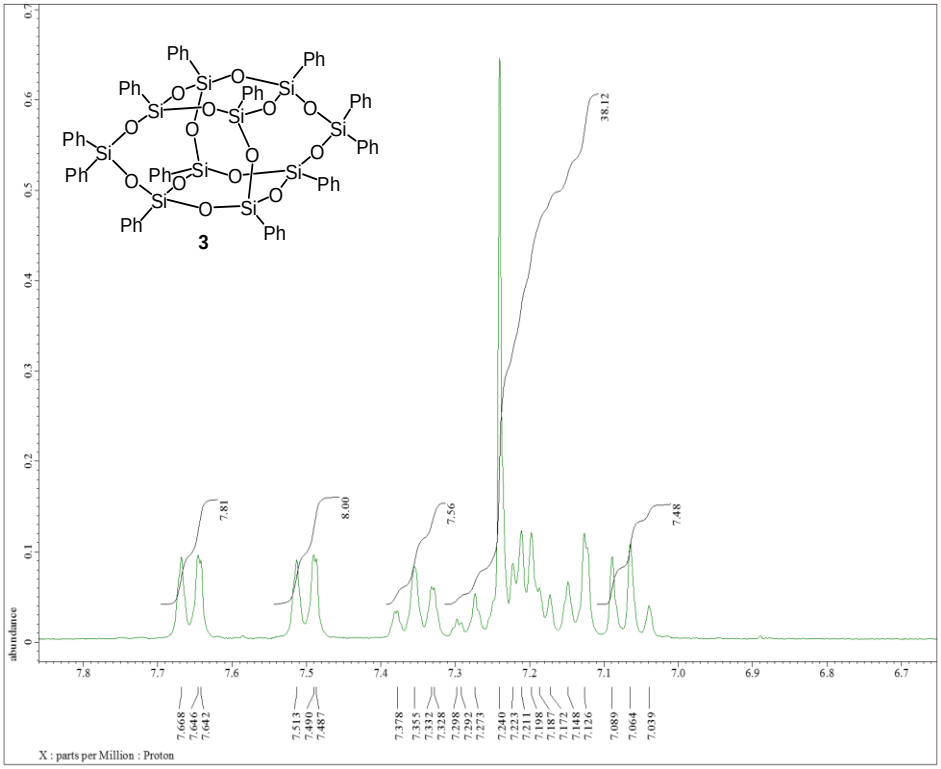

Figure 13. ^{1}H NMR spectrum of **3** (300.53 MHz, $CDCl_3$)

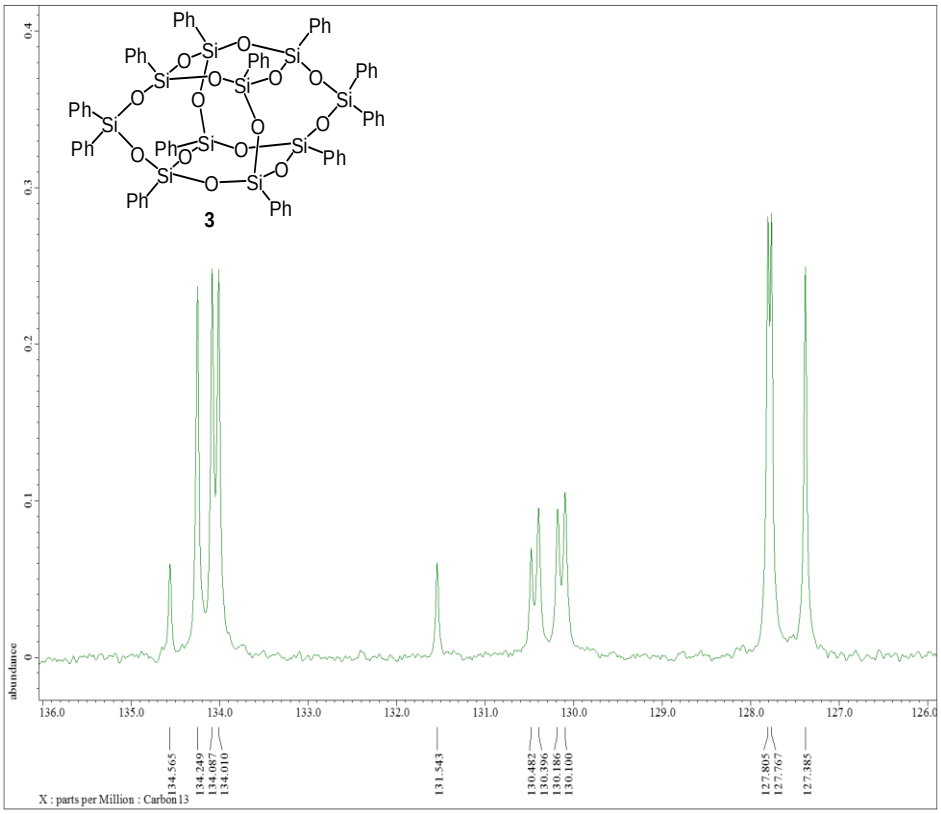

Figure 14. ^{13}C NMR spectrum of **3** (75.57 MHz, $CDCl_3$)

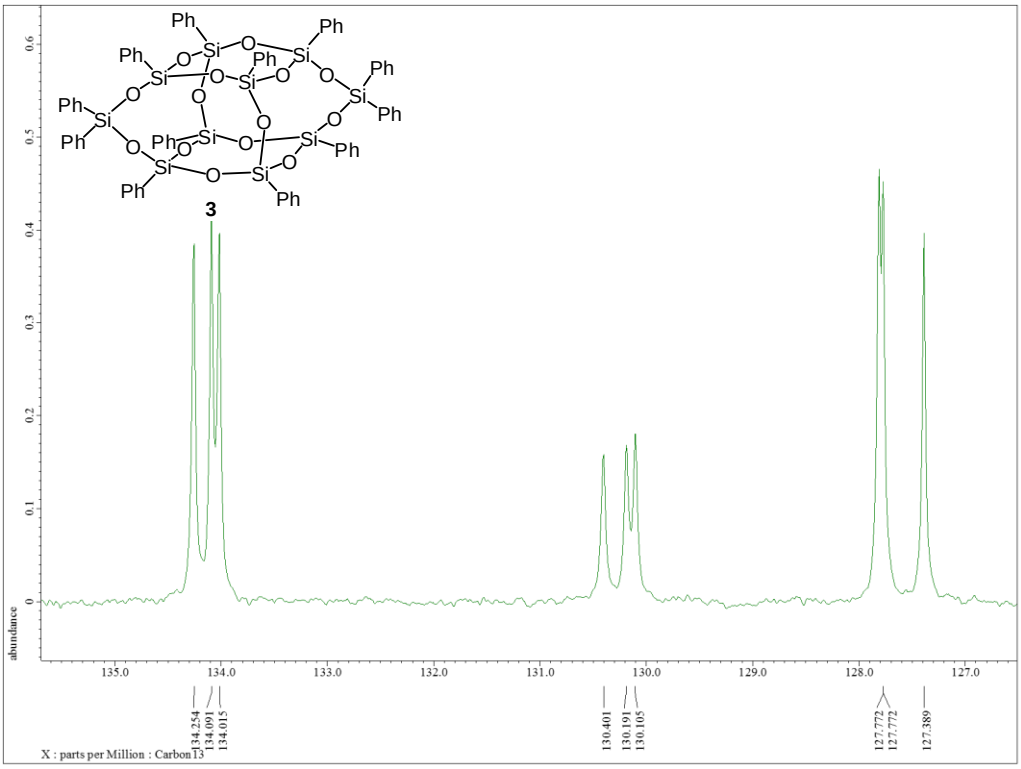

Figure 15. ^{13}C NMR (dept 135) spectrum of **3** (75.57 MHz, $CDCl_3$)

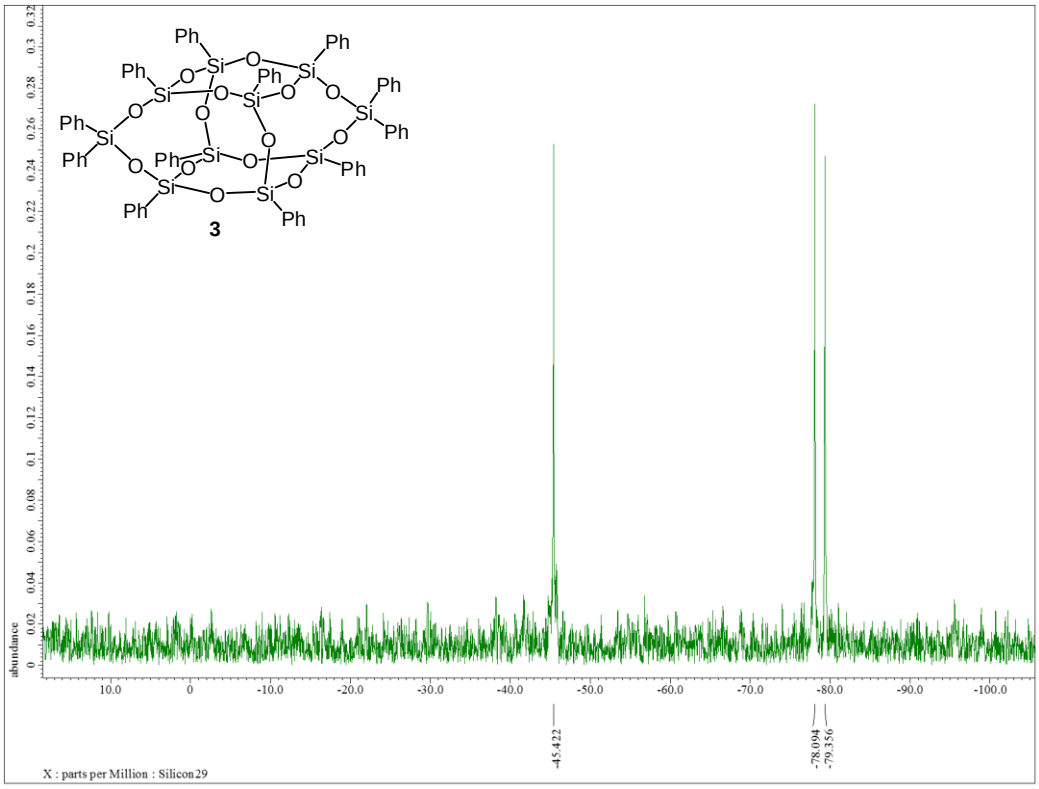

Figure 16. ^{29}Si NMR spectrum of **3** (59.71 MHz, $CDCl_3$)

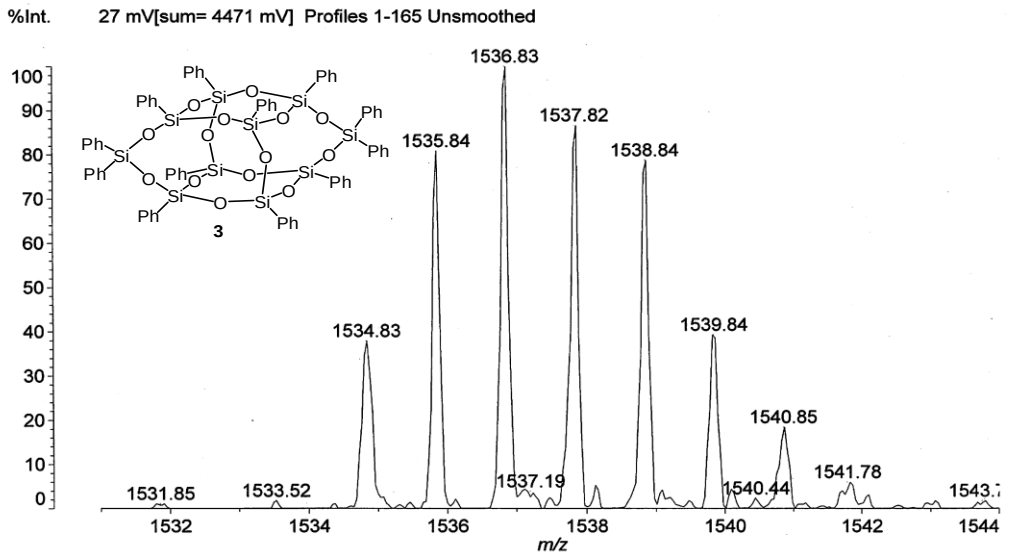

Figure 17. MALDITOFMS spectrum of **3**

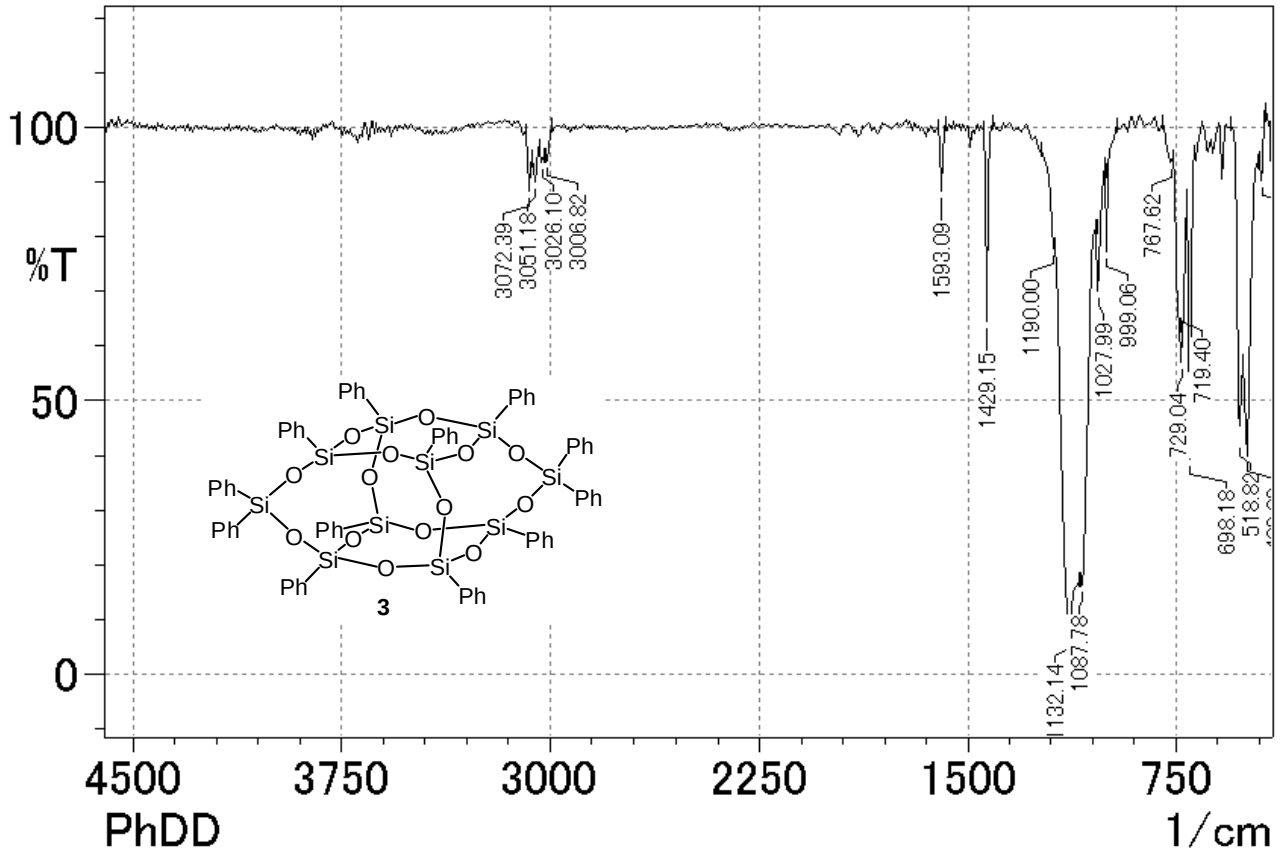

Figure 18. IR spectrum of **3**

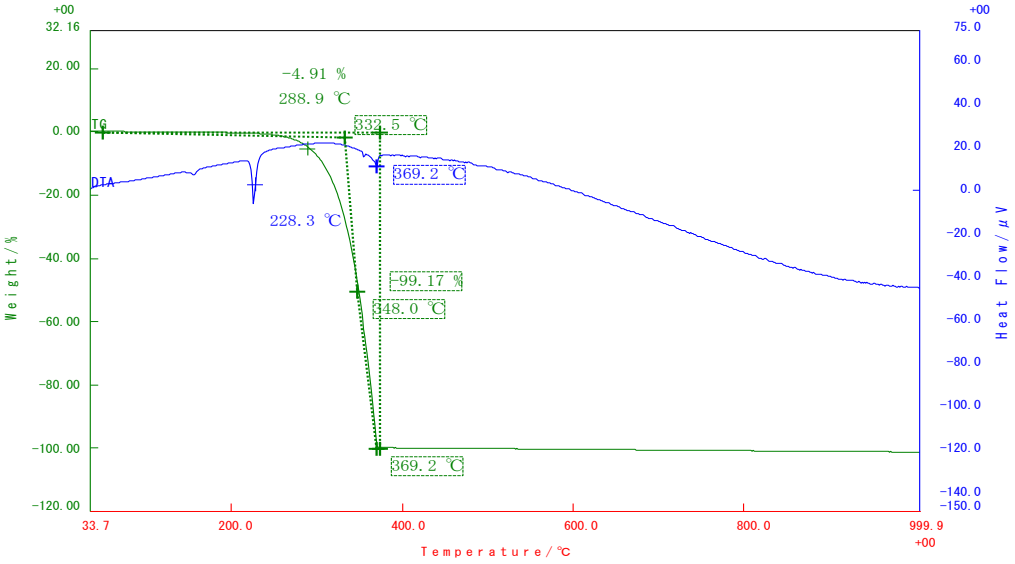

Figure 19. Tg-DTA analysis of $Ph_3SiOSiPh_3$ in N_2.

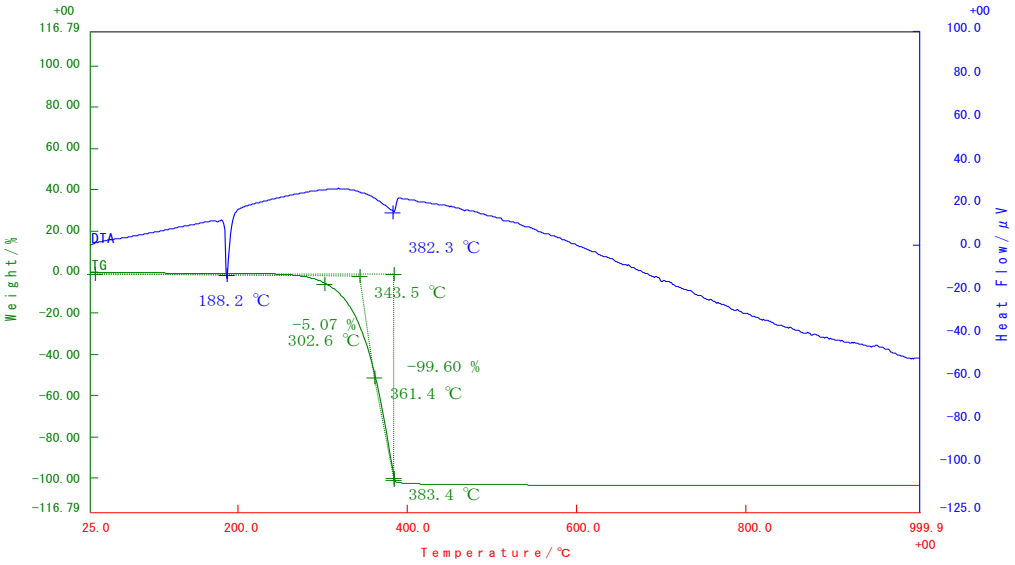

Figure 20. Tg-DTA analysis of $(Ph_2SiO)_3$ in N_2.

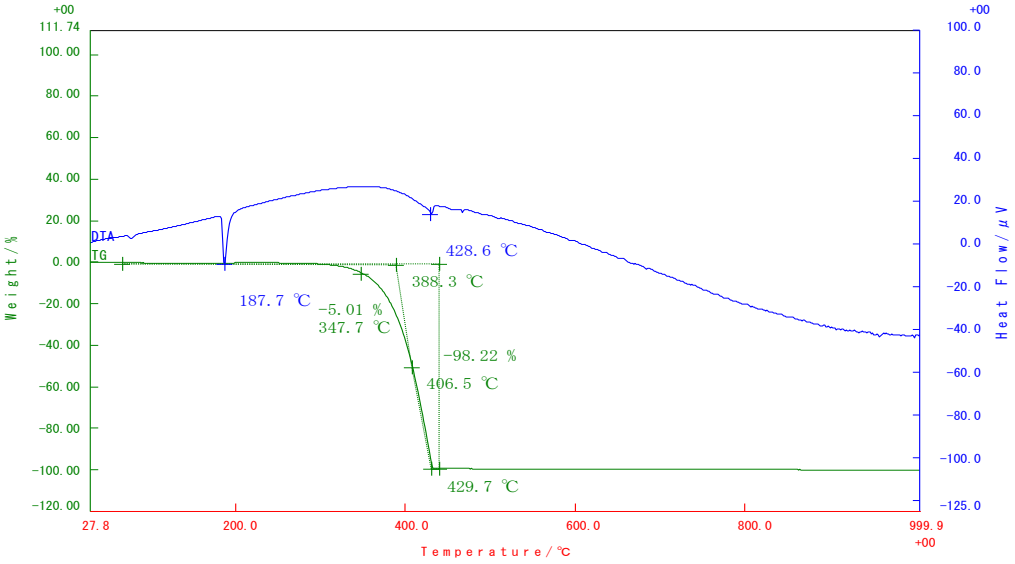

Figure 21. Tg-DTA analysis of $(Ph_2SiO)_4$ in N_2.

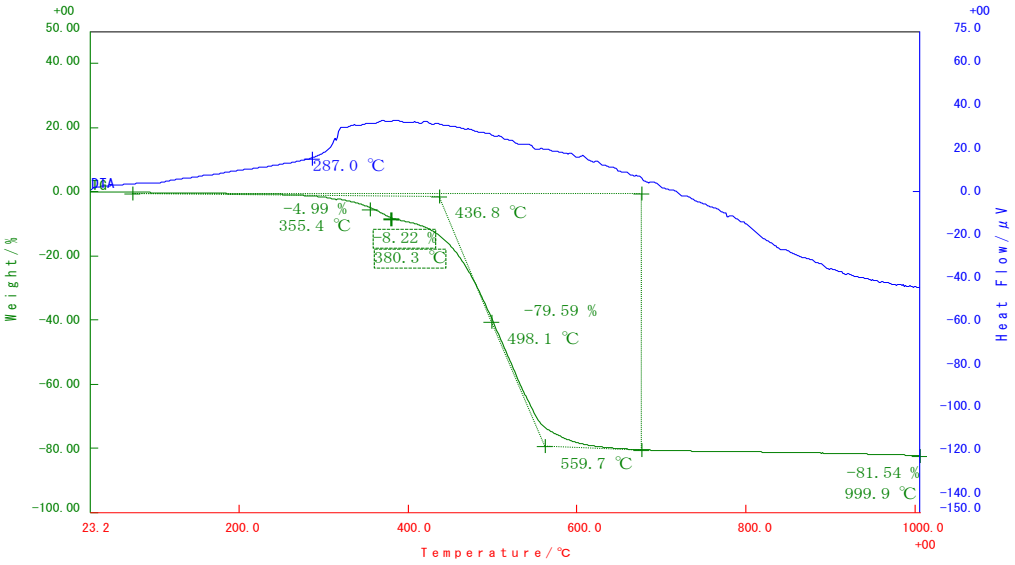

Figure 22. Tg-DTA analysis of **1** in N_2.

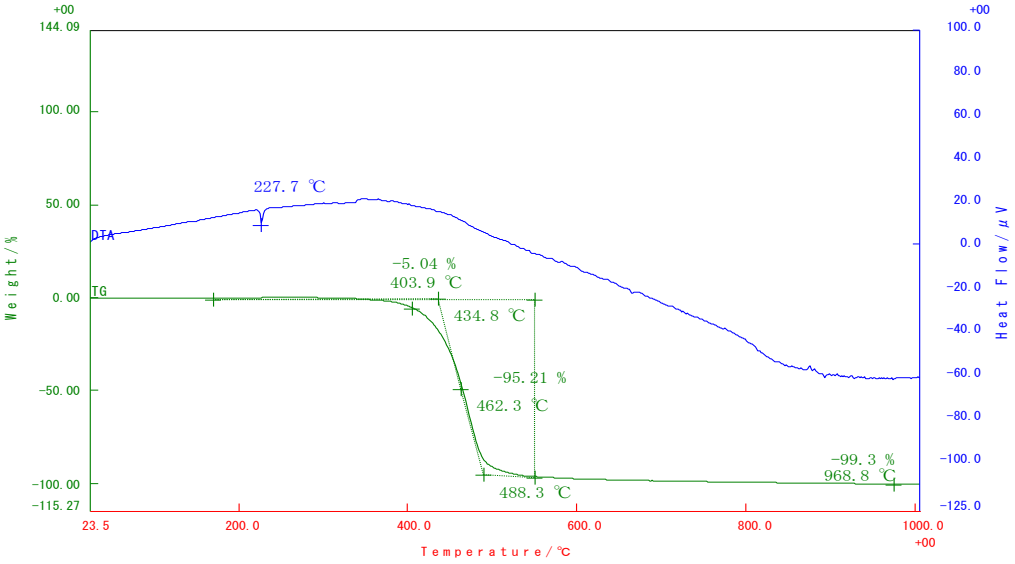

Figure 23. Tg-DTA analysis of **2** in N_2.

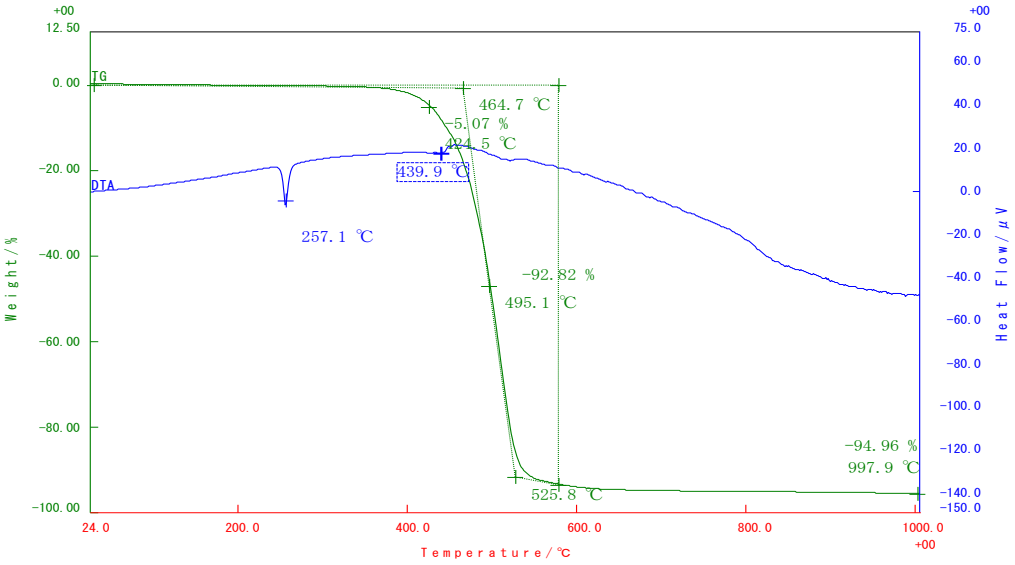

Figure 24. Tg-DTA analysis of **3** in N_2.

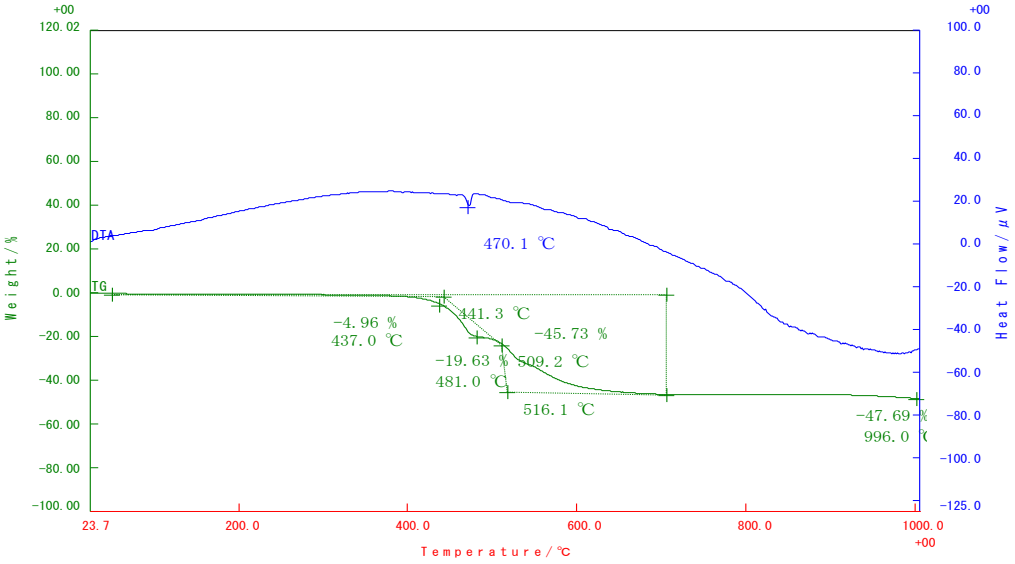

Figure 25. Tg-DTA analysis of $(PhSiO_{1.5})_8$ in N_2.

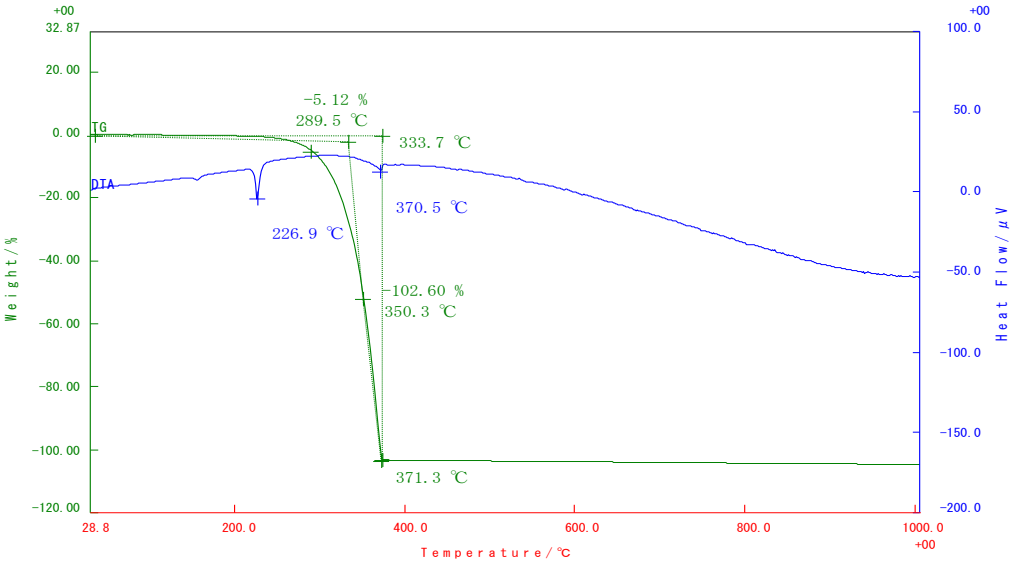

Figure 26. Tg-DTA analysis of $Ph_3SiOSiPh_3$ in air.

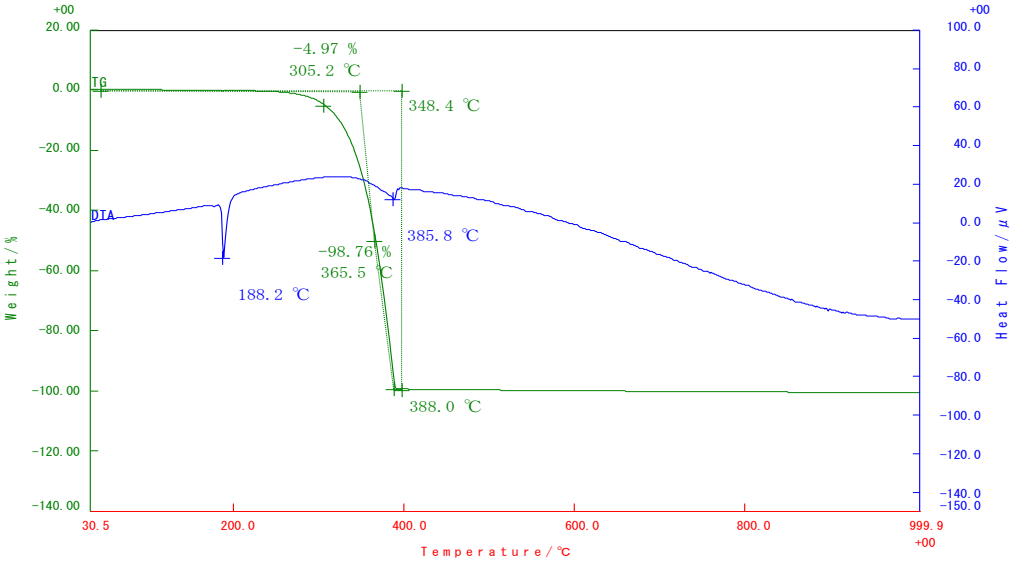

Figure 27. Tg-DTA analysis of $(Ph_2SiO)_3$ in air.

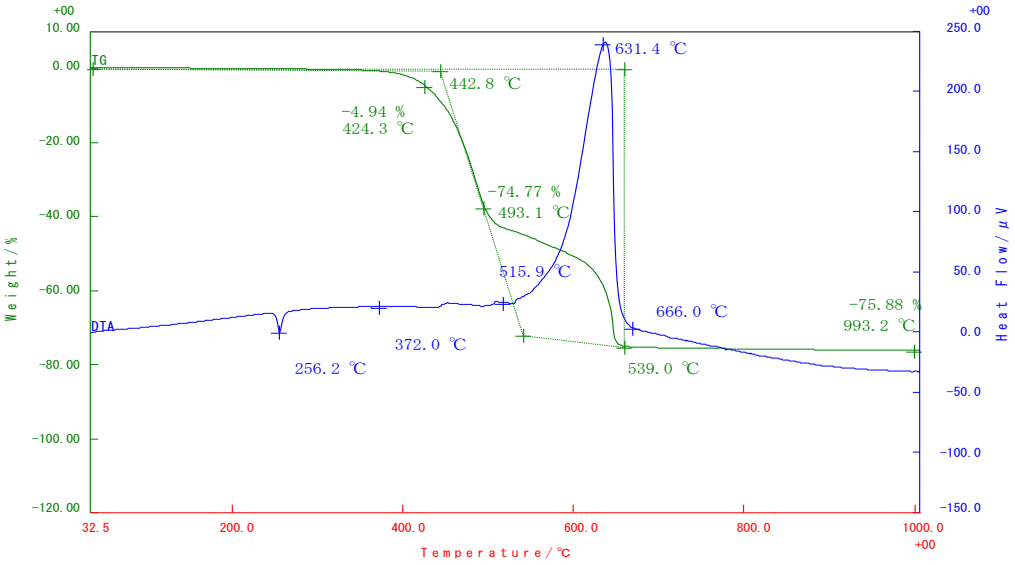

Figure 28. Tg-DTA analysis of $(Ph_2SiO)_4$ in air.

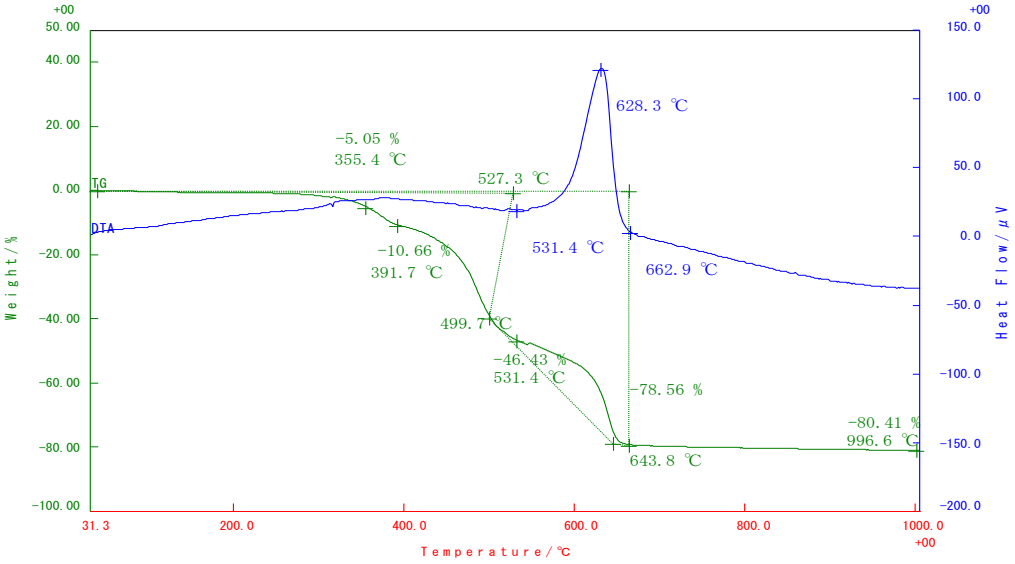

Figure 29. Tg-DTA analysis of **1** in air.

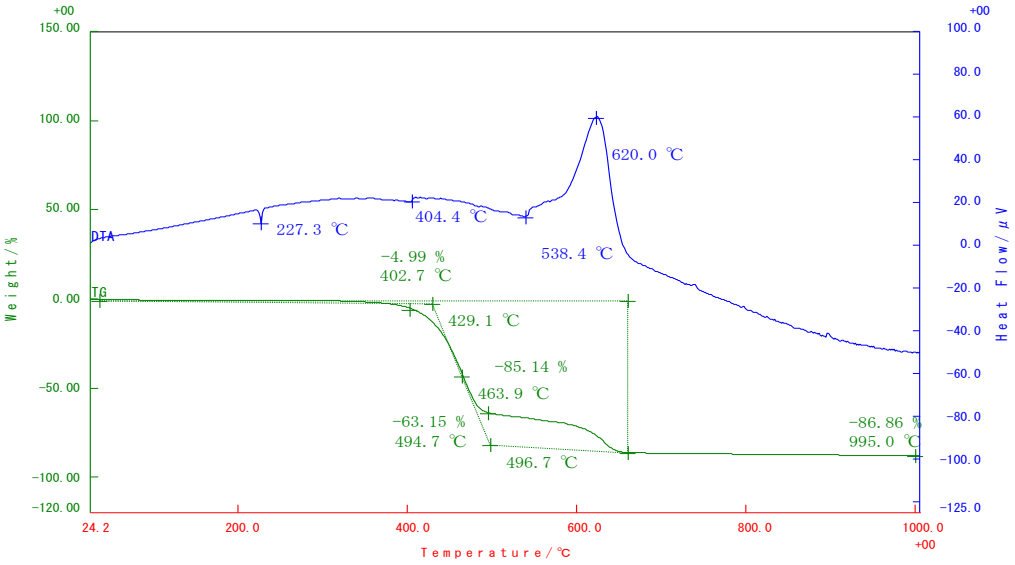

Figure 30. Tg-DTA analysis of **2** in air.

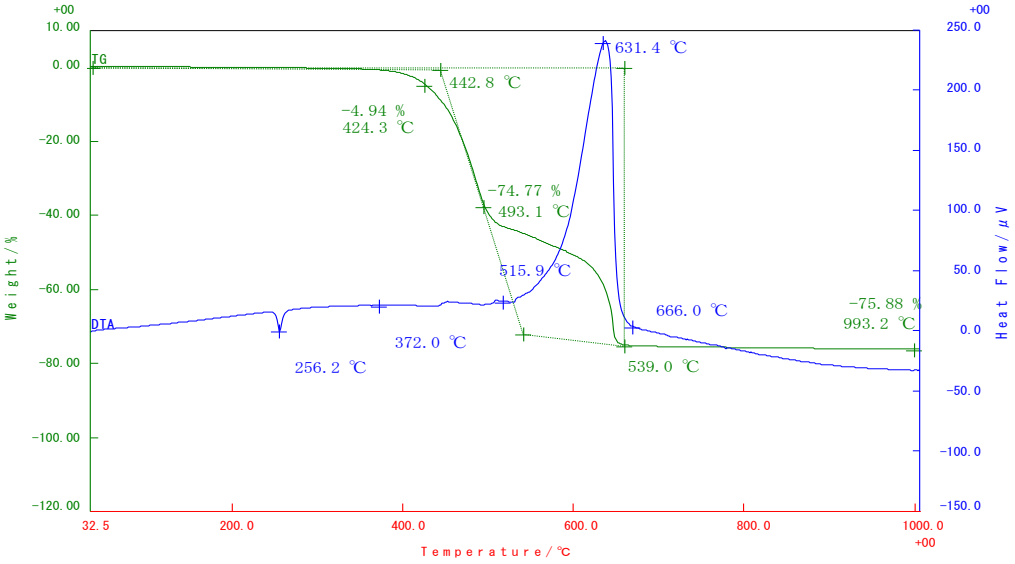

Figure 31. Tg-DTA analysis of **3** in air.

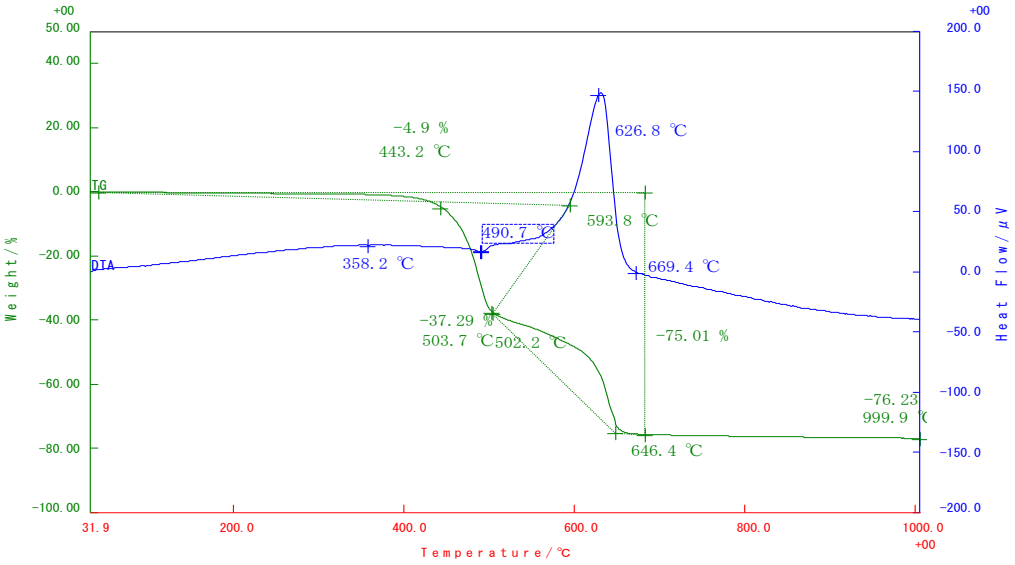

Figure 32. Tg-DTA analysis of $(PhSiO_{1.5})_8$ in air.

2. X-ray analysis

2-1 X-ray analysis of **1**.

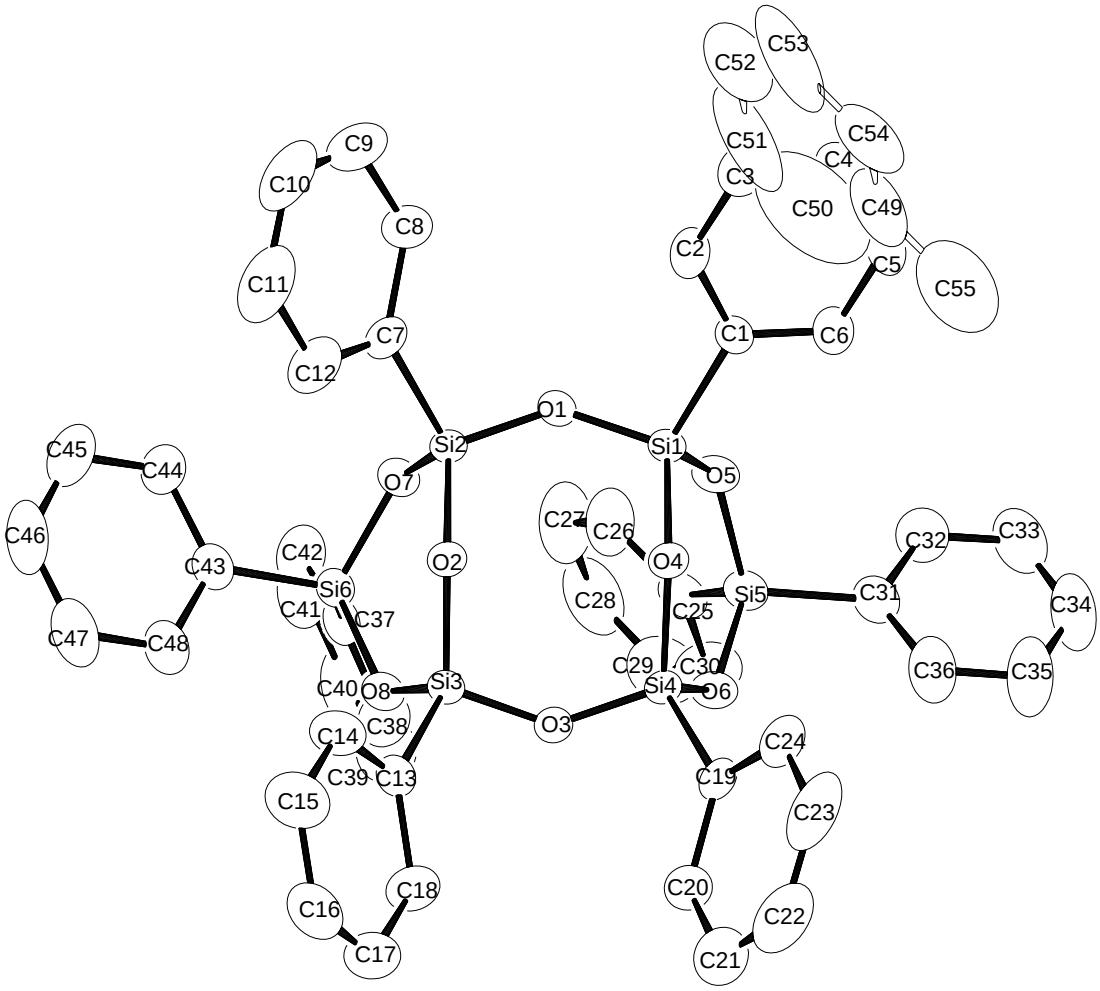

Figure 1. ORTEP drawing of **1**.

Table 1. Crystal data and structure refinement for **1**.

Empirical formula	$C_{51.50}H_{44}O_8Si_6$	
Formula weight	959.41	
Temperature	228.1500 K	
Wavelength	0.71070 Å	
Crystal system	Monoclinic	
Space group	*P* 21/n	
Unit cell dimensions	*a* = 18.4206(11) Å	α = 90.0000(7)°.
	b = 10.5744(7) Å	β = 90.4762(7)°.
	c = 25.4029(17) Å	γ = 90.0000(7)°.
Volume	4948.0(6) $Å^3$	
Z	4	
Density (calculated)	1.288 g/mL	
Absorption coefficient	0.221 mm^{-1}	
F(000)	2004	
Crystal size	0.3000 x 0.3000 x 0.2000 mm^3	
Theta range for data collection	2.22 to 25.50°.	
Index ranges	-22<=*h*<=22, -12<=*k*<=12, -30<=*l*<=30	
Reflections collected	33217	
Independent reflections	8836 [*R*(int) = 0.0255]	
Completeness to theta = 25.50°	96.0 %	
Absorption correction	Semi-empirical from equivalents	
Max. and min. transmission	1.0000 and 0.4258	
Refinement method	Full-matrix least-squares on F^2	
Data / restraints / parameters	8836 / 0 / 623	
Goodness-of-fit on F^2	1.152	
Final *R* indices [*I*>2sigma(*I*)]	*R*1 = 0.0437, *wR*2 = 0.1026	
R indices (all data)	*R*1 = 0.0468, *wR*2 = 0.1072	
Largest diff. peak and hole	0.307 and -0.291 e.$Å^{-3}$	

Table 2. Atomic coordinates (x 10^4) and equivalent isotropic displacement parameters ($Å^2$x 10^3) for **1**. U(eq) is defined as one third of the trace of the orthogonalized U^{ij} tensor.

	x	y	z	U(eq)
Si(1)	472(1)	6473(1)	1534(1)	23(1)
O(1)	736(1)	6828(1)	2126(1)	30(1)
Si(2)	907(1)	6217(1)	2699(1)	25(1)
O(2)	841(1)	4674(1)	2673(1)	26(1)
Si(3)	139(1)	3770(1)	2773(1)	25(1)
O(3)	-359(1)	3729(1)	2245(1)	29(1)
Si(4)	-329(1)	4066(1)	1623(1)	23(1)
O(4)	378(1)	4937(1)	1496(1)	25(1)
O(5)	-325(1)	7061(1)	1410(1)	31(1)
Si(5)	-1137(1)	6426(1)	1359(1)	29(1)
O(6)	-1043(1)	4907(1)	1479(1)	31(1)
O(7)	281(1)	6686(1)	3104(1)	30(1)
Si(6)	-183(1)	5810(1)	3519(1)	27(1)
O(8)	-331(1)	4439(1)	3233(1)	32(1)
C(1)	1127(1)	7092(2)	1055(1)	26(1)
C(2)	1836(1)	7389(3)	1195(1)	44(1)
C(3)	2313(2)	7864(3)	826(1)	60(1)
C(4)	2091(2)	8059(3)	317(1)	52(1)
C(5)	1394(1)	7762(2)	165(1)	44(1)
C(6)	918(1)	7283(2)	532(1)	35(1)
C(7)	1835(1)	6634(2)	2909(1)	35(1)
C(8)	2154(1)	7774(3)	2767(1)	49(1)
C(9)	2847(2)	8074(4)	2943(1)	74(1)
C(10)	3234(2)	7243(5)	3245(1)	84(1)
C(11)	2931(2)	6118(4)	3388(2)	85(1)
C(12)	2235(2)	5809(3)	3222(1)	62(1)
C(13)	434(1)	2169(2)	2962(1)	31(1)
C(14)	1119(1)	1953(2)	3170(1)	50(1)
C(15)	1334(2)	754(3)	3328(1)	64(1)
C(16)	868(2)	-246(2)	3279(1)	54(1)

C(17)	192(2)	-69(2)	3073(1)	57(1)
C(18)	-22(2)	1128(2)	2913(1)	50(1)
C(19)	-268(1)	2572(2)	1257(1)	28(1)
C(20)	-597(2)	1489(2)	1451(1)	47(1)
C(21)	-508(2)	327(3)	1215(1)	67(1)
C(22)	-85(2)	216(3)	786(1)	68(1)
C(23)	249(2)	1262(4)	581(1)	68(1)
C(24)	157(1)	2446(3)	813(1)	46(1)
C(25)	-1719(1)	7238(2)	1844(1)	36(1)
C(26)	-1429(2)	8017(3)	2230(1)	54(1)
C(27)	-1871(2)	8669(3)	2578(1)	70(1)
C(28)	-2604(2)	8551(3)	2542(1)	68(1)
C(29)	-2905(2)	7780(3)	2171(2)	72(1)
C(30)	-2469(1)	7126(3)	1822(1)	60(1)
C(31)	-1507(1)	6591(2)	683(1)	36(1)
C(32)	-1740(1)	7765(3)	494(1)	51(1)
C(33)	-2010(2)	7896(3)	-14(1)	65(1)
C(34)	-2071(2)	6864(4)	-338(1)	68(1)
C(35)	-1850(2)	5700(3)	-162(1)	69(1)
C(36)	-1566(2)	5570(3)	343(1)	52(1)
C(37)	-1076(1)	6520(2)	3657(1)	32(1)
C(38)	-1702(1)	5883(3)	3505(1)	49(1)
C(39)	-2381(2)	6342(3)	3622(1)	67(1)
C(40)	-2454(2)	7446(3)	3890(1)	65(1)
C(41)	-1850(2)	8099(3)	4051(1)	65(1)
C(42)	-1159(2)	7641(3)	3936(1)	49(1)
C(43)	386(1)	5537(2)	4113(1)	33(1)
C(44)	747(2)	6534(3)	4362(1)	49(1)
C(45)	1165(2)	6317(3)	4810(1)	63(1)
C(46)	1228(2)	5113(3)	5014(1)	60(1)
C(47)	881(2)	4128(3)	4773(1)	56(1)
C(48)	465(1)	4334(2)	4328(1)	43(1)
C(49)	4399(12)	4304(11)	-411(5)	80(4)
C(50)	4025(19)	4910(50)	50(30)	240(20)
C(51)	4480(20)	5400(30)	354(12)	121(8)
C(52)	5240(30)	5500(30)	282(15)	145(16)

C(53)	5625(17)	4950(20)	-95(9)	129(11)
C(54)	5119(15)	4350(20)	-480(13)	89(5)
C(55)	3920(7)	3690(11)	-795(5)	140(4)

Table 3. Bond lengths [Å] for **1**.

Si(1)-O(1)	1.6221(14)	C(5)-C(6)	1.381(3)
Si(1)-O(5)	1.6233(14)	C(7)-C(12)	1.388(4)
Si(1)-O(4)	1.6363(13)	C(7)-C(8)	1.390(3)
Si(1)-C(1)	1.840(2)	C(8)-C(9)	1.387(4)
O(1)-Si(2)	1.6193(15)	C(9)-C(10)	1.363(5)
Si(2)-O(7)	1.6295(15)	C(10)-C(11)	1.364(6)
Si(2)-O(2)	1.6376(13)	C(11)-C(12)	1.386(4)
Si(2)-C(7)	1.840(2)	C(13)-C(14)	1.382(3)
O(2)-Si(3)	1.6291(14)	C(13)-C(18)	1.390(3)
Si(3)-O(3)	1.6201(15)	C(14)-C(15)	1.387(3)
Si(3)-O(8)	1.6228(15)	C(15)-C(16)	1.368(4)
Si(3)-C(13)	1.841(2)	C(16)-C(17)	1.359(4)
O(3)-Si(4)	1.6205(15)	C(17)-C(18)	1.386(3)
Si(4)-O(6)	1.6269(14)	C(19)-C(24)	1.384(3)
Si(4)-O(4)	1.6290(14)	C(19)-C(20)	1.388(3)
Si(4)-C(19)	1.837(2)	C(20)-C(21)	1.377(4)
O(5)-Si(5)	1.6426(14)	C(21)-C(22)	1.351(5)
Si(5)-O(6)	1.6436(14)	C(22)-C(23)	1.370(5)
Si(5)-C(25)	1.850(2)	C(23)-C(24)	1.395(4)
Si(5)-C(31)	1.853(2)	C(25)-C(26)	1.385(4)
O(7)-Si(6)	1.6482(14)	C(25)-C(30)	1.387(3)
Si(6)-O(8)	1.6440(14)	C(26)-C(27)	1.390(4)
Si(6)-C(37)	1.844(2)	C(27)-C(28)	1.358(5)
Si(6)-C(43)	1.851(2)	C(28)-C(29)	1.359(5)
C(1)-C(2)	1.386(3)	C(29)-C(30)	1.387(4)
C(1)-C(6)	1.395(3)	C(31)-C(36)	1.387(4)
C(2)-C(3)	1.385(3)	C(31)-C(32)	1.396(3)
C(3)-C(4)	1.370(4)	C(32)-C(33)	1.385(4)
C(4)-C(5)	1.374(4)	C(33)-C(34)	1.371(5)

C(34)-C(35)	1.370(5)	C(45)-C(46)	1.378(5)
C(35)-C(36)	1.387(4)	C(46)-C(47)	1.364(4)
C(37)-C(38)	1.389(3)	C(47)-C(48)	1.378(4)
C(37)-C(42)	1.390(3)	C(49)-C(54)	1.34(3)
C(38)-C(39)	1.375(4)	C(49)-C(55)	1.46(2)
C(39)-C(40)	1.359(5)	C(49)-C(50)	1.50(8)
C(40)-C(41)	1.369(5)	C(50)-C(51)	1.25(6)
C(41)-C(42)	1.394(4)	C(51)-C(52)	1.41(4)
C(43)-C(48)	1.392(3)	C(52)-C(53)	1.33(6)
C(43)-C(44)	1.396(3)	C(53)-C(54)	1.49(5)
C(44)-C(45)	1.387(4)		

Table 4. Bond angles [°] for **1**.

O(1)-Si(1)-O(5)	110.77(8)	Si(3)-O(3)-Si(4)	141.06(10)
O(1)-Si(1)-O(4)	108.31(7)	O(3)-Si(4)-O(6)	107.76(8)
O(5)-Si(1)-O(4)	105.87(7)	O(3)-Si(4)-O(4)	110.52(7)
O(1)-Si(1)-C(1)	109.77(8)	O(6)-Si(4)-O(4)	107.00(7)
O(5)-Si(1)-C(1)	109.47(9)	O(3)-Si(4)-C(19)	107.87(9)
O(4)-Si(1)-C(1)	112.59(8)	O(6)-Si(4)-C(19)	114.13(8)
Si(2)-O(1)-Si(1)	142.72(9)	O(4)-Si(4)-C(19)	109.56(8)
O(1)-Si(2)-O(7)	108.19(8)	Si(4)-O(4)-Si(1)	129.39(8)
O(1)-Si(2)-O(2)	110.38(7)	Si(1)-O(5)-Si(5)	132.83(9)
O(7)-Si(2)-O(2)	105.98(7)	O(5)-Si(5)-O(6)	106.91(7)
O(1)-Si(2)-C(7)	109.79(9)	O(5)-Si(5)-C(25)	106.89(9)
O(7)-Si(2)-C(7)	113.87(9)	O(6)-Si(5)-C(25)	113.04(9)
O(2)-Si(2)-C(7)	108.57(9)	O(5)-Si(5)-C(31)	111.20(9)
Si(3)-O(2)-Si(2)	129.60(9)	O(6)-Si(5)-C(31)	107.52(9)
O(3)-Si(3)-O(8)	107.81(8)	C(25)-Si(5)-C(31)	111.23(10)
O(3)-Si(3)-O(2)	109.37(7)	Si(4)-O(6)-Si(5)	131.25(9)
O(8)-Si(3)-O(2)	106.57(7)	Si(2)-O(7)-Si(6)	127.36(9)
O(3)-Si(3)-C(13)	110.82(9)	O(8)-Si(6)-O(7)	107.29(7)
O(8)-Si(3)-C(13)	111.80(9)	O(8)-Si(6)-C(37)	107.34(9)
O(2)-Si(3)-C(13)	110.34(9)	O(7)-Si(6)-C(37)	111.12(9)

O(8)-Si(6)-C(43)	108.31(9)	C(26)-C(25)-C(30)	117.1(2)
O(7)-Si(6)-C(43)	108.44(9)	C(26)-C(25)-Si(5)	121.71(18)
C(37)-Si(6)-C(43)	114.09(10)	C(30)-C(25)-Si(5)	121.1(2)
Si(3)-O(8)-Si(6)	127.98(9)	C(25)-C(26)-C(27)	121.5(3)
C(2)-C(1)-C(6)	117.64(19)	C(28)-C(27)-C(26)	119.9(3)
C(2)-C(1)-Si(1)	122.16(16)	C(27)-C(28)-C(29)	120.0(3)
C(6)-C(1)-Si(1)	120.20(16)	C(28)-C(29)-C(30)	120.5(3)
C(3)-C(2)-C(1)	120.7(2)	C(25)-C(30)-C(29)	120.9(3)
C(4)-C(3)-C(2)	120.5(2)	C(36)-C(31)-C(32)	117.1(2)
C(3)-C(4)-C(5)	120.1(2)	C(36)-C(31)-Si(5)	122.08(18)
C(4)-C(5)-C(6)	119.5(2)	C(32)-C(31)-Si(5)	120.81(19)
C(5)-C(6)-C(1)	121.6(2)	C(33)-C(32)-C(31)	121.0(3)
C(12)-C(7)-C(8)	118.1(2)	C(34)-C(33)-C(32)	120.4(3)
C(12)-C(7)-Si(2)	120.22(19)	C(35)-C(34)-C(33)	119.7(3)
C(8)-C(7)-Si(2)	121.7(2)	C(34)-C(35)-C(36)	120.0(3)
C(9)-C(8)-C(7)	120.3(3)	C(31)-C(36)-C(35)	121.7(3)
C(10)-C(9)-C(8)	120.6(3)	C(38)-C(37)-C(42)	117.4(2)
C(9)-C(10)-C(11)	120.0(3)	C(38)-C(37)-Si(6)	119.31(18)
C(10)-C(11)-C(12)	120.3(3)	C(42)-C(37)-Si(6)	123.16(19)
C(11)-C(12)-C(7)	120.8(3)	C(39)-C(38)-C(37)	121.5(3)
C(14)-C(13)-C(18)	116.9(2)	C(40)-C(39)-C(38)	120.4(3)
C(14)-C(13)-Si(3)	121.17(17)	C(39)-C(40)-C(41)	119.9(3)
C(18)-C(13)-Si(3)	121.91(18)	C(40)-C(41)-C(42)	120.2(3)
C(13)-C(14)-C(15)	121.3(2)	C(37)-C(42)-C(41)	120.5(3)
C(16)-C(15)-C(14)	120.2(3)	C(48)-C(43)-C(44)	117.6(2)
C(17)-C(16)-C(15)	120.0(2)	C(48)-C(43)-Si(6)	121.28(18)
C(16)-C(17)-C(18)	119.8(2)	C(44)-C(43)-Si(6)	121.13(18)
C(17)-C(18)-C(13)	121.8(2)	C(45)-C(44)-C(43)	120.4(3)
C(24)-C(19)-C(20)	117.5(2)	C(46)-C(45)-C(44)	120.4(3)
C(24)-C(19)-Si(4)	122.13(17)	C(47)-C(46)-C(45)	119.9(3)
C(20)-C(19)-Si(4)	120.10(17)	C(46)-C(47)-C(48)	120.2(3)
C(21)-C(20)-C(19)	121.8(3)	C(47)-C(48)-C(43)	121.5(3)
C(22)-C(21)-C(20)	120.0(3)	C(54)-C(49)-C(55)	121.3(15)
C(21)-C(22)-C(23)	120.0(3)	C(54)-C(49)-C(50)	123(3)
C(22)-C(23)-C(24)	120.5(3)	C(55)-C(49)-C(50)	115(3)
C(19)-C(24)-C(23)	120.1(3)	C(51)-C(50)-C(49)	110(3)

C(50)-C(51)-C(52)	128(4)	C(52)-C(53)-C(54)	109(3)
C(53)-C(52)-C(51)	127(3)	C(49)-C(54)-C(53)	123(2)

Table 5. Anisotropic displacement parameters ($Å^2 x\ 10^3$) for **1**. The anisotropic displacement factor exponent takes the form: $-2\pi^2[h^2a^{*2}U^{11} + ... + 2hka^*b^*U^{12}]$

	U^{11}	U^{22}	U^{33}	U^{23}	U^{13}	U^{12}
Si(1)	22(1)	18(1)	29(1)	1(1)	4(1)	-2(1)
O(1)	40(1)	21(1)	28(1)	0(1)	4(1)	-8(1)
Si(2)	28(1)	18(1)	28(1)	-3(1)	3(1)	-5(1)
O(2)	26(1)	19(1)	31(1)	-3(1)	3(1)	-2(1)
Si(3)	30(1)	16(1)	28(1)	-1(1)	3(1)	-3(1)
O(3)	32(1)	24(1)	31(1)	0(1)	0(1)	-7(1)
Si(4)	22(1)	16(1)	31(1)	-1(1)	-1(1)	-1(1)
O(4)	22(1)	19(1)	34(1)	-2(1)	2(1)	0(1)
O(5)	24(1)	19(1)	48(1)	4(1)	4(1)	2(1)
Si(5)	22(1)	22(1)	43(1)	4(1)	3(1)	3(1)
O(6)	21(1)	23(1)	49(1)	5(1)	0(1)	0(1)
O(7)	38(1)	20(1)	32(1)	-3(1)	9(1)	-3(1)
Si(6)	31(1)	22(1)	27(1)	-2(1)	7(1)	-1(1)
O(8)	39(1)	24(1)	32(1)	-4(1)	11(1)	-6(1)
C(1)	29(1)	22(1)	29(1)	-1(1)	5(1)	-2(1)
C(2)	33(1)	67(2)	31(1)	-1(1)	2(1)	-14(1)
C(3)	38(2)	94(2)	47(2)	-5(2)	9(1)	-32(1)
C(4)	55(2)	63(2)	40(1)	1(1)	19(1)	-20(1)
C(5)	51(2)	50(2)	31(1)	5(1)	6(1)	-1(1)
C(6)	31(1)	40(1)	35(1)	0(1)	2(1)	-1(1)
C(7)	33(1)	36(1)	35(1)	-10(1)	1(1)	-9(1)
C(8)	46(2)	52(2)	48(1)	-6(1)	12(1)	-22(1)
C(9)	54(2)	99(3)	69(2)	-17(2)	15(2)	-50(2)
C(10)	40(2)	142(4)	69(2)	-27(2)	-6(2)	-34(2)
C(11)	57(2)	111(3)	87(3)	-4(2)	-38(2)	-3(2)
C(12)	52(2)	60(2)	72(2)	0(2)	-25(2)	-10(1)
C(13)	41(1)	22(1)	31(1)	1(1)	3(1)	-1(1)

C(14)	47(2)	30(1)	73(2)	13(1)	-6(1)	-4(1)
C(15)	51(2)	44(2)	98(2)	22(2)	-8(2)	6(1)
C(16)	76(2)	24(1)	63(2)	9(1)	8(2)	10(1)
C(17)	73(2)	25(1)	72(2)	5(1)	-9(2)	-9(1)
C(18)	57(2)	24(1)	69(2)	4(1)	-15(1)	-6(1)
C(19)	27(1)	23(1)	33(1)	-5(1)	-8(1)	1(1)
C(20)	68(2)	26(1)	46(1)	-5(1)	1(1)	-11(1)
C(21)	113(3)	25(1)	64(2)	-9(1)	-11(2)	-6(2)
C(22)	83(2)	39(2)	83(2)	-30(2)	-21(2)	16(2)
C(23)	49(2)	97(3)	58(2)	-46(2)	0(1)	11(2)
C(24)	44(1)	53(2)	40(1)	-14(1)	1(1)	-10(1)
C(25)	29(1)	30(1)	49(1)	10(1)	9(1)	7(1)
C(26)	47(2)	68(2)	46(2)	-6(1)	5(1)	12(1)
C(27)	74(2)	87(2)	51(2)	-13(2)	13(2)	24(2)
C(28)	72(2)	68(2)	66(2)	8(2)	32(2)	32(2)
C(29)	43(2)	69(2)	105(3)	6(2)	27(2)	16(2)
C(30)	35(1)	51(2)	93(2)	-9(2)	14(2)	4(1)
C(31)	28(1)	33(1)	47(1)	7(1)	3(1)	5(1)
C(32)	47(2)	39(1)	67(2)	9(1)	-11(1)	4(1)
C(33)	58(2)	63(2)	73(2)	30(2)	-13(2)	8(1)
C(34)	62(2)	95(3)	46(2)	15(2)	-5(1)	13(2)
C(35)	86(2)	78(2)	44(2)	-7(2)	-5(2)	20(2)
C(36)	62(2)	49(2)	47(2)	0(1)	0(1)	17(1)
C(37)	37(1)	33(1)	26(1)	3(1)	6(1)	4(1)
C(38)	37(1)	52(2)	58(2)	-3(1)	0(1)	1(1)
C(39)	40(2)	82(2)	80(2)	7(2)	0(2)	4(2)
C(40)	44(2)	96(3)	56(2)	8(2)	12(1)	27(2)
C(41)	71(2)	70(2)	53(2)	-17(2)	12(2)	32(2)
C(42)	52(2)	47(2)	47(1)	-13(1)	4(1)	10(1)
C(43)	30(1)	36(1)	32(1)	0(1)	10(1)	1(1)
C(44)	52(2)	50(2)	44(1)	1(1)	-7(1)	-13(1)
C(45)	51(2)	85(2)	52(2)	-10(2)	-10(1)	-15(2)
C(46)	43(2)	98(2)	38(1)	8(2)	-2(1)	10(2)
C(47)	55(2)	65(2)	49(2)	16(1)	4(1)	16(1)
C(48)	46(1)	42(1)	41(1)	4(1)	5(1)	3(1)
C(49)	110(10)	63(6)	67(7)	32(5)	8(8)	22(7)

C(50)	230(30)	160(20)	330(50)	180(30)	-50(50)	30(30)
C(51)	170(20)	118(18)	79(15)	53(13)	59(16)	58(16)
C(52)	190(40)	114(18)	130(30)	80(19)	-50(20)	-40(20)
C(53)	230(30)	93(10)	61(11)	26(9)	78(16)	52(13)
C(54)	94(15)	75(7)	100(14)	49(8)	13(9)	1(8)
C(55)	157(11)	122(9)	143(10)	47(8)	11(9)	5(8)

Table 6. Torsion angles [°] for **1**.

O(5)-Si(1)-O(1)-Si(2)	112.15(16)
O(4)-Si(1)-O(1)-Si(2)	-3.55(18)
C(1)-Si(1)-O(1)-Si(2)	-126.84(16)
Si(1)-O(1)-Si(2)-O(7)	-110.37(16)
Si(1)-O(1)-Si(2)-O(2)	5.17(19)
Si(1)-O(1)-Si(2)-C(7)	124.82(16)
O(1)-Si(2)-O(2)-Si(3)	-90.21(12)
O(7)-Si(2)-O(2)-Si(3)	26.70(13)
C(7)-Si(2)-O(2)-Si(3)	149.41(12)
Si(2)-O(2)-Si(3)-O(3)	81.24(12)
Si(2)-O(2)-Si(3)-O(8)	-35.05(13)
Si(2)-O(2)-Si(3)-C(13)	-156.61(11)
O(8)-Si(3)-O(3)-Si(4)	130.76(14)
O(2)-Si(3)-O(3)-Si(4)	15.27(17)
C(13)-Si(3)-O(3)-Si(4)	-106.59(16)
Si(3)-O(3)-Si(4)-O(6)	-130.10(15)
Si(3)-O(3)-Si(4)-O(4)	-13.51(17)
Si(3)-O(3)-Si(4)-C(19)	106.24(15)
O(3)-Si(4)-O(4)-Si(1)	-85.53(12)
O(6)-Si(4)-O(4)-Si(1)	31.53(14)
C(19)-Si(4)-O(4)-Si(1)	155.74(11)
O(1)-Si(1)-O(4)-Si(4)	88.58(12)
O(5)-Si(1)-O(4)-Si(4)	-30.27(13)
C(1)-Si(1)-O(4)-Si(4)	-149.85(11)
O(1)-Si(1)-O(5)-Si(5)	-106.19(13)
O(4)-Si(1)-O(5)-Si(5)	11.02(15)

C(1)-Si(1)-O(5)-Si(5)	132.63(13)
Si(1)-O(5)-Si(5)-O(6)	1.48(16)
Si(1)-O(5)-Si(5)-C(25)	122.80(14)
Si(1)-O(5)-Si(5)-C(31)	-115.61(14)
O(3)-Si(4)-O(6)-Si(5)	105.32(13)
O(4)-Si(4)-O(6)-Si(5)	-13.54(15)
C(19)-Si(4)-O(6)-Si(5)	-134.91(13)
O(5)-Si(5)-O(6)-Si(4)	-0.05(16)
C(25)-Si(5)-O(6)-Si(4)	-117.39(14)
C(31)-Si(5)-O(6)-Si(4)	119.45(14)
O(1)-Si(2)-O(7)-Si(6)	132.64(11)
O(2)-Si(2)-O(7)-Si(6)	14.27(14)
C(7)-Si(2)-O(7)-Si(6)	-105.01(13)
Si(2)-O(7)-Si(6)-O(8)	-36.23(14)
Si(2)-O(7)-Si(6)-C(37)	-153.28(12)
Si(2)-O(7)-Si(6)-C(43)	80.56(13)
O(3)-Si(3)-O(8)-Si(6)	-113.00(12)
O(2)-Si(3)-O(8)-Si(6)	4.33(14)
C(13)-Si(3)-O(8)-Si(6)	124.96(13)
O(7)-Si(6)-O(8)-Si(3)	25.11(14)
C(37)-Si(6)-O(8)-Si(3)	144.61(12)
C(43)-Si(6)-O(8)-Si(3)	-91.76(13)
O(1)-Si(1)-C(1)-C(2)	20.8(2)
O(5)-Si(1)-C(1)-C(2)	142.58(19)
O(4)-Si(1)-C(1)-C(2)	-99.9(2)
O(1)-Si(1)-C(1)-C(6)	-158.87(16)
O(5)-Si(1)-C(1)-C(6)	-37.09(19)
O(4)-Si(1)-C(1)-C(6)	80.38(18)
C(6)-C(1)-C(2)-C(3)	0.3(4)
Si(1)-C(1)-C(2)-C(3)	-179.4(2)
C(1)-C(2)-C(3)-C(4)	0.6(5)
C(2)-C(3)-C(4)-C(5)	-1.2(5)
C(3)-C(4)-C(5)-C(6)	0.8(4)
C(4)-C(5)-C(6)-C(1)	0.1(4)
C(2)-C(1)-C(6)-C(5)	-0.6(3)
Si(1)-C(1)-C(6)-C(5)	179.05(18)

O(1)-Si(2)-C(7)-C(12)	-148.5(2)
O(7)-Si(2)-C(7)-C(12)	90.0(2)
O(2)-Si(2)-C(7)-C(12)	-27.8(2)
O(1)-Si(2)-C(7)-C(8)	32.2(2)
O(7)-Si(2)-C(7)-C(8)	-89.3(2)
O(2)-Si(2)-C(7)-C(8)	152.96(19)
C(12)-C(7)-C(8)-C(9)	-1.0(4)
Si(2)-C(7)-C(8)-C(9)	178.3(2)
C(7)-C(8)-C(9)-C(10)	1.8(5)
C(8)-C(9)-C(10)-C(11)	-1.7(6)
C(9)-C(10)-C(11)-C(12)	0.7(6)
C(10)-C(11)-C(12)-C(7)	0.1(6)
C(8)-C(7)-C(12)-C(11)	0.0(5)
Si(2)-C(7)-C(12)-C(11)	-179.3(3)
O(3)-Si(3)-C(13)-C(14)	142.8(2)
O(8)-Si(3)-C(13)-C(14)	-96.9(2)
O(2)-Si(3)-C(13)-C(14)	21.5(2)
O(3)-Si(3)-C(13)-C(18)	-38.5(2)
O(8)-Si(3)-C(13)-C(18)	81.8(2)
O(2)-Si(3)-C(13)-C(18)	-159.8(2)
C(18)-C(13)-C(14)-C(15)	-0.9(4)
Si(3)-C(13)-C(14)-C(15)	177.9(2)
C(13)-C(14)-C(15)-C(16)	0.2(5)
C(14)-C(15)-C(16)-C(17)	0.2(5)
C(15)-C(16)-C(17)-C(18)	0.1(5)
C(16)-C(17)-C(18)-C(13)	-0.8(5)
C(14)-C(13)-C(18)-C(17)	1.2(4)
Si(3)-C(13)-C(18)-C(17)	-177.6(2)
O(3)-Si(4)-C(19)-C(24)	-141.81(18)
O(6)-Si(4)-C(19)-C(24)	98.48(19)
O(4)-Si(4)-C(19)-C(24)	-21.5(2)
O(3)-Si(4)-C(19)-C(20)	31.8(2)
O(6)-Si(4)-C(19)-C(20)	-87.9(2)
O(4)-Si(4)-C(19)-C(20)	152.17(18)
C(24)-C(19)-C(20)-C(21)	0.1(4)
Si(4)-C(19)-C(20)-C(21)	-173.8(2)

C(19)-C(20)-C(21)-C(22)	0.6(5)
C(20)-C(21)-C(22)-C(23)	-0.8(5)
C(21)-C(22)-C(23)-C(24)	0.2(5)
C(20)-C(19)-C(24)-C(23)	-0.7(4)
Si(4)-C(19)-C(24)-C(23)	173.1(2)
C(22)-C(23)-C(24)-C(19)	0.6(4)
O(5)-Si(5)-C(25)-C(26)	-12.1(2)
O(6)-Si(5)-C(25)-C(26)	105.2(2)
C(31)-Si(5)-C(25)-C(26)	-133.7(2)
O(5)-Si(5)-C(25)-C(30)	165.5(2)
O(6)-Si(5)-C(25)-C(30)	-77.2(2)
C(31)-Si(5)-C(25)-C(30)	43.9(2)
C(30)-C(25)-C(26)-C(27)	-0.6(4)
Si(5)-C(25)-C(26)-C(27)	177.1(2)
C(25)-C(26)-C(27)-C(28)	-0.2(5)
C(26)-C(27)-C(28)-C(29)	1.1(5)
C(27)-C(28)-C(29)-C(30)	-1.1(5)
C(26)-C(25)-C(30)-C(29)	0.6(4)
Si(5)-C(25)-C(30)-C(29)	-177.2(2)
C(28)-C(29)-C(30)-C(25)	0.3(5)
O(5)-Si(5)-C(31)-C(36)	107.9(2)
O(6)-Si(5)-C(31)-C(36)	-8.9(2)
C(25)-Si(5)-C(31)-C(36)	-133.1(2)
O(5)-Si(5)-C(31)-C(32)	-72.2(2)
O(6)-Si(5)-C(31)-C(32)	171.09(19)
C(25)-Si(5)-C(31)-C(32)	46.8(2)
C(36)-C(31)-C(32)-C(33)	-0.7(4)
Si(5)-C(31)-C(32)-C(33)	179.4(2)
C(31)-C(32)-C(33)-C(34)	1.5(4)
C(32)-C(33)-C(34)-C(35)	-1.2(5)
C(33)-C(34)-C(35)-C(36)	0.0(5)
C(32)-C(31)-C(36)-C(35)	-0.5(4)
Si(5)-C(31)-C(36)-C(35)	179.4(2)
C(34)-C(35)-C(36)-C(31)	0.9(5)
O(8)-Si(6)-C(37)-C(38)	-1.4(2)
O(7)-Si(6)-C(37)-C(38)	115.60(19)

C(43)-Si(6)-C(37)-C(38)	-121.4(2)
O(8)-Si(6)-C(37)-C(42)	174.72(19)
O(7)-Si(6)-C(37)-C(42)	-68.3(2)
C(43)-Si(6)-C(37)-C(42)	54.7(2)
C(42)-C(37)-C(38)-C(39)	0.3(4)
Si(6)-C(37)-C(38)-C(39)	176.7(2)
C(37)-C(38)-C(39)-C(40)	0.5(5)
C(38)-C(39)-C(40)-C(41)	-1.0(5)
C(39)-C(40)-C(41)-C(42)	0.7(5)
C(38)-C(37)-C(42)-C(41)	-0.6(4)
Si(6)-C(37)-C(42)-C(41)	-176.8(2)
C(40)-C(41)-C(42)-C(37)	0.1(5)
O(8)-Si(6)-C(43)-C(48)	-16.3(2)
O(7)-Si(6)-C(43)-C(48)	-132.45(18)
C(37)-Si(6)-C(43)-C(48)	103.14(19)
O(8)-Si(6)-C(43)-C(44)	163.99(19)
O(7)-Si(6)-C(43)-C(44)	47.9(2)
C(37)-Si(6)-C(43)-C(44)	-76.5(2)
C(48)-C(43)-C(44)-C(45)	-0.5(4)
Si(6)-C(43)-C(44)-C(45)	179.2(2)
C(43)-C(44)-C(45)-C(46)	0.2(4)
C(44)-C(45)-C(46)-C(47)	0.1(4)
C(45)-C(46)-C(47)-C(48)	-0.1(4)
C(46)-C(47)-C(48)-C(43)	-0.2(4)
C(44)-C(43)-C(48)-C(47)	0.5(4)
Si(6)-C(43)-C(48)-C(47)	-179.2(2)
C(54)-C(49)-C(50)-C(51)	-2(3)
C(55)-C(49)-C(50)-C(51)	179.6(17)
C(49)-C(50)-C(51)-C(52)	5(4)
C(50)-C(51)-C(52)-C(53)	-9(4)
C(51)-C(52)-C(53)-C(54)	8(3)
C(55)-C(49)-C(54)-C(53)	-179.1(13)
C(50)-C(49)-C(54)-C(53)	3(2)
C(52)-C(53)-C(54)-C(49)	-5(2)

2-2 X-ray analysis of **2**.

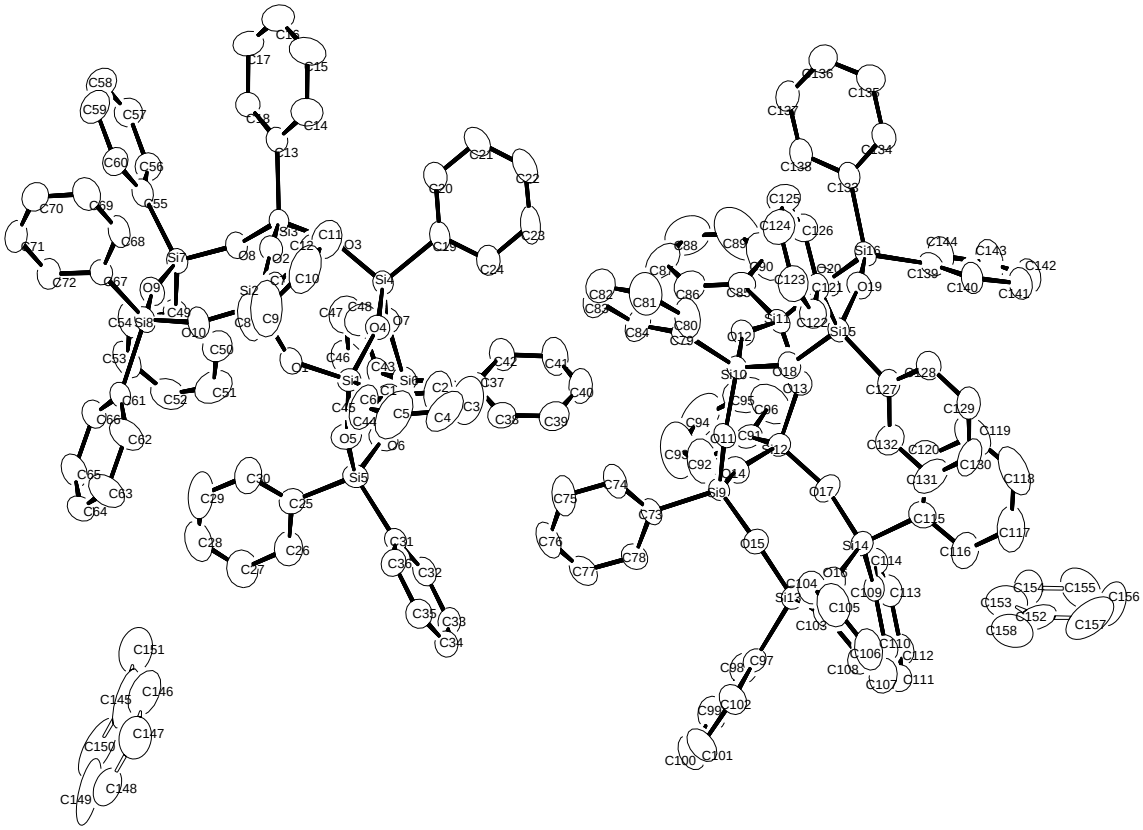

Figure 1. ORTEP drawing of **2**.

Table 1. Crystal data and structure refinement for **2**.

Empirical formula	$C_{75.50}H_{64}O_{10}Si_8$	
Formula weight	1355.99	
Temperature	180.1500 K	
Wavelength	0.71070 Å	
Crystal system	Triclinic	
Space group	*P* -1	
Unit cell dimensions	a = 10.7054(9) Å	α = 90.768(4)°.
	b = 13.9916(11) Å	β = 94.007(4)°.
	c = 47.955(4) Å	γ = 90.360(4)°.
Volume	7164.6(11) $Å^3$	
Z	4	
Density (calculated)	1.257 g/mL	
Absorption coefficient	0.207 mm^{-1}	
F(000)	2836	
Crystal size	0.3000 x 0.2000 x 0.1000 mm^3	
Theta range for data collection	1.92 to 25.50°.	
Index ranges	-12<=*h*<=12, -16<=*k*<=16, -58<=*l*<=58	
Reflections collected	47636	
Independent reflections	24775 [*R*(int) = 0.0363]	
Completeness to theta = 25.50°	93.0 %	
Absorption correction	Semi-empirical from equivalents	
Max. and min. transmission	1.0000 and 0.2821	
Refinement method	Full-matrix least-squares on F^2	
Data / restraints / parameters	24775 / 0 / 1717	
Goodness-of-fit on F^2	1.166	
Final *R* indices [*I*>2sigma(*I*)]	*R*1 = 0.0929, *wR*2 = 0.2166	
R indices (all data)	*R*1 = 0.1018, *wR*2 = 0.2228	
Largest diff. peak and hole	0.581 and -0.671 e.$Å^{-3}$	

Table 2. Atomic coordinates (x 10^4) and equivalent isotropic displacement parameters ($Å^2$x 10^3) for **2**. U(eq) is defined as one third of the trace of the orthogonalized U^{ij} tensor.

	x	y	z	U(eq)
Si(1)	5254(1)	7992(1)	1646(1)	32(1)
O(1)	4805(3)	8808(2)	1423(1)	37(1)
Si(2)	4781(1)	9959(1)	1388(1)	31(1)
O(2)	6173(3)	10391(2)	1458(1)	35(1)
Si(3)	7656(1)	10335(1)	1413(1)	28(1)
O(3)	8258(3)	9466(2)	1598(1)	35(1)
Si(4)	8077(1)	8530(1)	1782(1)	29(1)
O(4)	6604(3)	8279(2)	1794(1)	36(1)
O(5)	5365(3)	7014(3)	1471(1)	45(1)
Si(5)	6016(1)	6075(1)	1349(1)	36(1)
O(6)	7503(3)	6072(3)	1442(1)	45(1)
Si(6)	8841(1)	6510(1)	1564(1)	34(1)
O(7)	8731(3)	7648(2)	1632(1)	39(1)
O(8)	7868(3)	10101(2)	1092(1)	36(1)
Si(7)	7536(1)	10295(1)	759(1)	31(1)
O(9)	6034(3)	10413(3)	705(1)	38(1)
Si(8)	4557(1)	10459(1)	751(1)	33(1)
O(10)	4300(3)	10171(3)	1067(1)	41(1)
C(1)	4179(4)	7855(3)	1925(1)	37(1)
C(2)	4579(7)	7480(6)	2177(2)	72(2)
C(3)	3851(9)	7400(7)	2397(2)	95(3)
C(4)	2645(8)	7741(5)	2375(2)	84(3)
C(5)	2205(7)	8125(6)	2133(2)	89(3)
C(6)	2951(6)	8194(5)	1905(2)	71(2)
C(7)	3731(4)	10502(4)	1632(1)	37(1)
C(8)	2439(6)	10558(6)	1569(1)	71(2)
C(9)	1653(7)	10868(7)	1764(2)	94(3)
C(10)	2136(8)	11148(6)	2028(2)	79(2)
C(11)	3373(7)	11126(5)	2091(1)	65(2)
C(12)	4185(6)	10797(4)	1897(1)	47(1)

C(13)	8395(4)	11484(3)	1533(1)	35(1)
C(14)	8156(5)	11853(4)	1796(1)	50(1)
C(15)	8716(6)	12704(5)	1897(2)	64(2)
C(16)	9502(6)	13186(5)	1736(2)	63(2)
C(17)	9755(7)	12846(5)	1478(2)	69(2)
C(18)	9194(6)	11995(4)	1377(1)	53(2)
C(19)	8770(4)	8761(4)	2141(1)	34(1)
C(20)	9242(5)	9650(4)	2221(1)	47(1)
C(21)	9720(6)	9833(5)	2491(1)	59(2)
C(22)	9739(6)	9128(5)	2688(1)	59(2)
C(23)	9276(6)	8244(5)	2616(1)	58(2)
C(24)	8794(5)	8052(4)	2344(1)	45(1)
C(25)	5771(4)	6101(4)	959(1)	40(1)
C(26)	5899(7)	5276(5)	803(1)	65(2)
C(27)	5719(8)	5265(7)	515(1)	81(2)
C(28)	5361(7)	6110(7)	384(2)	80(2)
C(29)	5215(9)	6926(7)	531(2)	96(3)
C(30)	5413(7)	6916(6)	823(2)	72(2)
C(31)	5256(5)	4996(3)	1486(1)	35(1)
C(32)	5844(5)	4098(4)	1501(1)	45(1)
C(33)	5216(6)	3302(4)	1575(1)	53(2)
C(34)	3975(6)	3344(4)	1635(1)	52(1)
C(35)	3366(6)	4218(4)	1628(1)	49(1)
C(36)	3999(5)	5030(4)	1552(1)	43(1)
C(37)	9290(5)	5864(4)	1894(1)	39(1)
C(38)	8412(6)	5461(4)	2056(1)	50(1)
C(39)	8761(7)	5022(5)	2306(1)	67(2)
C(40)	10009(9)	4972(6)	2395(2)	82(2)
C(41)	10896(7)	5339(6)	2234(2)	76(2)
C(42)	10559(6)	5794(5)	1984(1)	54(2)
C(43)	10051(5)	6384(4)	1308(1)	39(1)
C(44)	10223(6)	5505(5)	1176(1)	55(2)
C(45)	11215(6)	5370(6)	1004(2)	70(2)
C(46)	12014(6)	6108(7)	962(2)	76(2)
C(47)	11852(7)	6980(6)	1085(2)	71(2)
C(48)	10877(6)	7121(5)	1258(1)	60(2)

C(49)	8063(4)	9260(4)	560(1)	38(1)
C(50)	8275(6)	8367(4)	679(1)	55(2)
C(51)	8605(7)	7592(5)	516(2)	73(2)
C(52)	8735(6)	7696(5)	235(2)	64(2)
C(53)	8557(6)	8585(5)	116(1)	61(2)
C(54)	8214(6)	9347(5)	275(1)	52(2)
C(55)	8326(5)	11406(4)	661(1)	37(1)
C(56)	9609(5)	11395(4)	620(1)	43(1)
C(57)	10284(6)	12217(5)	579(1)	52(2)
C(58)	9674(7)	13072(5)	572(2)	66(2)
C(59)	8412(7)	13118(5)	610(2)	69(2)
C(60)	7731(5)	12289(4)	655(1)	47(1)
C(61)	3709(4)	9599(4)	510(1)	36(1)
C(62)	2538(6)	9270(6)	569(1)	66(2)
C(63)	1841(7)	8655(7)	387(2)	86(3)
C(64)	2336(6)	8349(5)	145(1)	59(2)
C(65)	3504(6)	8655(5)	81(1)	58(2)
C(66)	4183(5)	9274(4)	264(1)	46(1)
C(67)	4009(4)	11700(4)	692(1)	36(1)
C(68)	3867(6)	12332(4)	912(1)	51(1)
C(69)	3526(7)	13275(5)	866(1)	63(2)
C(70)	3327(6)	13595(4)	597(1)	53(2)
C(71)	3455(5)	12994(4)	375(1)	48(1)
C(72)	3799(5)	12051(4)	421(1)	41(1)
Si(9)	7030(1)	3355(1)	3213(1)	30(1)
O(11)	6851(3)	4299(2)	3403(1)	35(1)
Si(10)	7442(1)	5192(1)	3585(1)	30(1)
O(12)	8923(3)	5266(2)	3546(1)	36(1)
Si(11)	10288(1)	4804(1)	3629(1)	32(1)
O(13)	10208(3)	3661(3)	3594(1)	39(1)
Si(12)	9832(1)	2851(1)	3357(1)	33(1)
O(14)	8486(3)	3114(3)	3202(1)	40(1)
O(15)	6346(3)	2477(3)	3356(1)	40(1)
Si(13)	6242(1)	1340(1)	3424(1)	35(1)
O(16)	7590(3)	932(3)	3542(1)	46(1)
Si(14)	9066(1)	931(1)	3641(1)	37(1)

O(17)	9747(3)	1852(3)	3519(1)	49(1)
O(18)	7195(3)	5002(2)	3906(1)	35(1)
Si(15)	7476(1)	5220(1)	4239(1)	31(1)
O(19)	8972(3)	5363(3)	4307(1)	40(1)
Si(16)	10455(1)	5385(1)	4264(1)	33(1)
O(20)	10720(3)	5057(3)	3950(1)	44(1)
C(73)	6377(4)	3596(4)	2852(1)	35(1)
C(74)	5885(6)	4489(5)	2784(1)	54(2)
C(75)	5425(7)	4695(6)	2512(1)	73(2)
C(76)	5466(6)	4019(6)	2308(1)	64(2)
C(77)	5948(6)	3133(5)	2369(1)	55(2)
C(78)	6393(5)	2925(4)	2640(1)	45(1)
C(79)	6721(5)	6329(4)	3456(1)	42(1)
C(80)	5884(7)	6836(5)	3608(2)	72(2)
C(81)	5333(9)	7673(6)	3499(2)	88(3)
C(82)	5620(8)	7983(5)	3240(2)	84(3)
C(83)	6430(7)	7504(6)	3090(2)	75(2)
C(84)	6992(6)	6651(5)	3196(2)	60(2)
C(85)	11422(5)	5289(4)	3398(1)	42(1)
C(86)	11063(7)	5682(5)	3143(1)	59(2)
C(87)	11952(9)	5975(5)	2963(2)	80(3)
C(88)	13192(9)	5863(7)	3033(2)	104(4)
C(89)	13540(9)	5480(11)	3278(2)	145(6)
C(90)	12693(6)	5206(8)	3462(2)	104(3)
C(91)	10970(5)	2804(4)	3087(1)	39(1)
C(92)	10589(7)	2787(6)	2808(2)	73(2)
C(93)	11478(10)	2821(8)	2608(2)	109(4)
C(94)	12704(9)	2854(6)	2681(2)	96(3)
C(95)	13099(7)	2835(7)	2952(2)	93(3)
C(96)	12250(6)	2812(7)	3154(2)	85(3)
C(97)	5758(5)	657(3)	3102(1)	36(1)
C(98)	6638(5)	297(4)	2927(1)	50(1)
C(99)	6265(7)	-167(5)	2674(1)	60(2)
C(100)	5006(7)	-285(5)	2597(1)	66(2)
C(101)	4114(6)	64(5)	2768(1)	65(2)
C(102)	4497(5)	531(5)	3016(1)	51(1)

C(103)	5052(5)	1242(4)	3687(1)	41(1)
C(104)	4342(6)	2016(5)	3760(1)	57(2)
C(105)	3373(7)	1903(7)	3939(2)	76(2)
C(106)	3117(6)	1025(7)	4045(1)	70(2)
C(107)	3835(7)	259(6)	3980(1)	68(2)
C(108)	4780(6)	372(5)	3803(1)	56(2)
C(109)	9841(5)	-151(4)	3509(1)	38(1)
C(110)	9234(5)	-1042(4)	3484(1)	46(1)
C(111)	9899(6)	-1850(4)	3409(1)	51(1)
C(112)	11146(6)	-1779(4)	3359(1)	54(2)
C(113)	11750(6)	-908(4)	3380(1)	49(1)
C(114)	11094(5)	-113(4)	3453(1)	44(1)
C(115)	9265(5)	997(4)	4028(1)	42(1)
C(116)	9119(7)	184(5)	4186(1)	66(2)
C(117)	9290(8)	224(7)	4478(2)	81(2)
C(118)	9639(8)	1077(8)	4609(2)	88(3)
C(119)	9795(10)	1870(8)	4454(2)	105(3)
C(120)	9638(8)	1837(6)	4165(2)	77(2)
C(121)	6662(4)	6337(4)	4327(1)	34(1)
C(122)	5389(5)	6325(4)	4366(1)	44(1)
C(123)	4730(6)	7166(5)	4405(1)	57(2)
C(124)	5338(7)	8015(5)	4408(2)	67(2)
C(125)	6606(7)	8060(5)	4371(2)	68(2)
C(126)	7268(5)	7229(4)	4332(1)	50(1)
C(127)	6921(4)	4196(4)	4438(1)	39(1)
C(128)	6751(6)	4312(5)	4723(1)	52(1)
C(129)	6415(6)	3546(5)	4882(1)	59(2)
C(130)	6243(6)	2674(5)	4764(2)	66(2)
C(131)	6385(7)	2540(5)	4485(2)	74(2)
C(132)	6717(6)	3294(4)	4319(1)	56(2)
C(133)	11013(4)	6633(4)	4318(1)	37(1)
C(134)	11241(5)	7018(4)	4586(1)	40(1)
C(135)	11589(5)	7966(4)	4627(1)	49(1)
C(136)	11694(6)	8548(4)	4403(1)	55(2)
C(137)	11459(7)	8202(5)	4135(1)	60(2)
C(138)	11137(6)	7247(5)	4094(1)	53(2)

C(139)	11287(4)	4546(4)	4511(1)	37(1)
C(140)	10795(5)	4231(4)	4753(1)	44(1)
C(141)	11476(6)	3628(4)	4933(1)	54(2)
C(142)	12640(7)	3332(5)	4872(1)	62(2)
C(143)	13147(7)	3622(6)	4633(2)	77(2)
C(144)	12474(6)	4246(5)	4455(1)	60(2)
C(145)	915(14)	5316(12)	53(3)	103(11)
C(146)	104(14)	5552(10)	257(2)	89(8)
C(147)	-1142(14)	5259(11)	226(2)	99(8)
C(148)	-1576(15)	4729(12)	-8(2)	91(8)
C(149)	-765(17)	4492(11)	-212(2)	200(30)
C(150)	480(16)	4786(12)	-181(2)	150(20)
C(151)	2239(19)	5641(16)	90(5)	98(7)
C(152)	4078(17)	257(14)	4957(3)	100(9)
C(153)	4851(16)	445(13)	4743(3)	103(9)
C(154)	6094(17)	156(15)	4766(3)	94(8)
C(155)	6562(18)	-321(16)	5003(3)	139(19)
C(156)	5789(18)	-509(15)	5217(3)	180(30)
C(157)	4546(18)	-220(15)	5194(3)	170(30)
C(158)	2790(20)	594(18)	4922(6)	116(9)

Table 3. Bond lengths [Å] for **2**.

Si(1)-O(5)	1.605(4)	C(2)-C(3)	1.360(10)
Si(1)-O(4)	1.612(3)	C(3)-C(4)	1.377(11)
Si(1)-O(1)	1.625(3)	C(4)-C(5)	1.341(12)
Si(1)-C(1)	1.839(5)	C(5)-C(6)	1.401(10)
O(1)-Si(2)	1.622(4)	C(7)-C(12)	1.384(8)
Si(2)-O(2)	1.616(3)	C(7)-C(8)	1.398(7)
Si(2)-O(10)	1.619(3)	C(8)-C(9)	1.369(10)
Si(2)-C(7)	1.840(5)	C(9)-C(10)	1.384(12)
O(2)-Si(3)	1.618(3)	C(10)-C(11)	1.337(11)
Si(3)-O(8)	1.603(3)	C(11)-C(12)	1.392(8)
Si(3)-O(3)	1.626(3)	C(13)-C(18)	1.376(7)
Si(3)-C(13)	1.853(5)	C(13)-C(14)	1.398(8)
O(3)-Si(4)	1.605(3)	C(14)-C(15)	1.395(9)
Si(4)-O(7)	1.606(3)	C(15)-C(16)	1.364(10)
Si(4)-O(4)	1.619(3)	C(16)-C(17)	1.365(10)
Si(4)-C(19)	1.853(5)	C(17)-C(18)	1.396(8)
O(5)-Si(5)	1.613(4)	C(19)-C(20)	1.379(8)
Si(5)-O(6)	1.623(3)	C(19)-C(24)	1.395(7)
Si(5)-C(31)	1.860(5)	C(20)-C(21)	1.378(8)
Si(5)-C(25)	1.869(6)	C(21)-C(22)	1.374(9)
O(6)-Si(6)	1.624(4)	C(22)-C(23)	1.360(9)
Si(6)-O(7)	1.628(4)	C(23)-C(24)	1.393(8)
Si(6)-C(43)	1.853(5)	C(25)-C(30)	1.366(8)
Si(6)-C(37)	1.867(5)	C(25)-C(26)	1.378(9)
O(8)-Si(7)	1.635(3)	C(26)-C(27)	1.382(9)
Si(7)-O(9)	1.620(3)	C(27)-C(28)	1.391(12)
Si(7)-C(49)	1.839(5)	C(28)-C(29)	1.350(12)
Si(7)-C(55)	1.848(5)	C(29)-C(30)	1.400(11)
O(9)-Si(8)	1.615(3)	C(31)-C(36)	1.405(7)
Si(8)-O(10)	1.613(4)	C(31)-C(32)	1.409(7)
Si(8)-C(61)	1.847(5)	C(32)-C(33)	1.362(8)
Si(8)-C(67)	1.855(5)	C(33)-C(34)	1.381(9)
C(1)-C(2)	1.366(8)	C(34)-C(35)	1.389(8)
C(1)-C(6)	1.397(7)	C(35)-C(36)	1.385(8)

C(37)-C(38)	1.384(7)	Si(9)-O(14)	1.602(3)
C(37)-C(42)	1.400(7)	Si(9)-O(15)	1.611(3)
C(38)-C(39)	1.380(9)	Si(9)-O(11)	1.615(4)
C(39)-C(40)	1.377(11)	Si(9)-C(73)	1.856(5)
C(40)-C(41)	1.365(11)	O(11)-Si(10)	1.614(4)
C(41)-C(42)	1.393(9)	Si(10)-O(18)	1.607(3)
C(43)-C(48)	1.389(8)	Si(10)-O(12)	1.613(3)
C(43)-C(44)	1.396(8)	Si(10)-C(79)	1.865(5)
C(44)-C(45)	1.398(8)	O(12)-Si(11)	1.628(3)
C(45)-C(46)	1.363(11)	Si(11)-O(13)	1.607(4)
C(46)-C(47)	1.366(11)	Si(11)-O(20)	1.610(3)
C(47)-C(48)	1.392(9)	Si(11)-C(85)	1.831(5)
C(49)-C(54)	1.392(7)	O(13)-Si(12)	1.623(4)
C(49)-C(50)	1.394(8)	Si(12)-O(17)	1.612(4)
C(50)-C(51)	1.388(9)	Si(12)-O(14)	1.621(3)
C(51)-C(52)	1.377(10)	Si(12)-C(91)	1.839(5)
C(52)-C(53)	1.385(10)	O(15)-Si(13)	1.633(4)
C(53)-C(54)	1.372(8)	Si(13)-O(16)	1.623(3)
C(55)-C(60)	1.395(7)	Si(13)-C(97)	1.845(5)
C(55)-C(56)	1.401(7)	Si(13)-C(103)	1.862(5)
C(56)-C(57)	1.378(8)	O(16)-Si(14)	1.618(3)
C(57)-C(58)	1.365(9)	Si(14)-O(17)	1.615(4)
C(58)-C(59)	1.377(10)	Si(14)-C(115)	1.851(6)
C(59)-C(60)	1.393(9)	Si(14)-C(109)	1.857(6)
C(61)-C(62)	1.381(8)	O(18)-Si(15)	1.629(3)
C(61)-C(66)	1.390(7)	Si(15)-O(19)	1.623(3)
C(62)-C(63)	1.392(9)	Si(15)-C(127)	1.848(5)
C(63)-C(64)	1.375(10)	Si(15)-C(121)	1.852(5)
C(64)-C(65)	1.375(9)	O(19)-Si(16)	1.615(3)
C(65)-C(66)	1.389(8)	Si(16)-O(20)	1.614(4)
C(67)-C(68)	1.385(8)	Si(16)-C(133)	1.852(5)
C(67)-C(72)	1.400(7)	Si(16)-C(139)	1.863(5)
C(68)-C(69)	1.387(8)	C(73)-C(78)	1.376(7)
C(69)-C(70)	1.376(9)	C(73)-C(74)	1.393(8)
C(70)-C(71)	1.364(9)	C(74)-C(75)	1.396(8)
C(71)-C(72)	1.388(8)	C(75)-C(76)	1.357(10)

C(76)-C(77)	1.373(10)	C(112)-C(113)	1.376(9)
C(77)-C(78)	1.389(8)	C(113)-C(114)	1.374(8)
C(79)-C(84)	1.380(8)	C(115)-C(120)	1.383(9)
C(79)-C(80)	1.388(9)	C(115)-C(116)	1.390(8)
C(80)-C(81)	1.406(9)	C(116)-C(117)	1.398(9)
C(81)-C(82)	1.374(12)	C(117)-C(118)	1.379(12)
C(82)-C(83)	1.341(12)	C(118)-C(119)	1.361(13)
C(83)-C(84)	1.424(9)	C(119)-C(120)	1.382(11)
C(85)-C(90)	1.379(8)	C(121)-C(122)	1.388(7)
C(85)-C(86)	1.380(9)	C(121)-C(126)	1.403(8)
C(86)-C(87)	1.393(9)	C(122)-C(123)	1.394(8)
C(87)-C(88)	1.356(13)	C(123)-C(124)	1.351(10)
C(88)-C(89)	1.330(15)	C(124)-C(125)	1.382(10)
C(89)-C(90)	1.363(11)	C(125)-C(126)	1.382(9)
C(91)-C(92)	1.373(9)	C(127)-C(132)	1.388(8)
C(91)-C(96)	1.385(8)	C(127)-C(128)	1.395(8)
C(92)-C(93)	1.399(11)	C(128)-C(129)	1.384(8)
C(93)-C(94)	1.335(13)	C(129)-C(130)	1.345(10)
C(94)-C(95)	1.339(13)	C(130)-C(131)	1.364(11)
C(95)-C(96)	1.371(10)	C(131)-C(132)	1.391(9)
C(97)-C(102)	1.392(7)	C(133)-C(138)	1.394(7)
C(97)-C(98)	1.399(7)	C(133)-C(134)	1.394(7)
C(98)-C(99)	1.400(9)	C(134)-C(135)	1.384(8)
C(99)-C(100)	1.380(9)	C(135)-C(136)	1.368(8)
C(100)-C(101)	1.389(10)	C(136)-C(137)	1.372(9)
C(101)-C(102)	1.385(8)	C(137)-C(138)	1.386(9)
C(103)-C(104)	1.382(8)	C(139)-C(144)	1.383(7)
C(103)-C(108)	1.382(8)	C(139)-C(140)	1.386(7)
C(104)-C(105)	1.401(9)	C(140)-C(141)	1.387(8)
C(105)-C(106)	1.372(11)	C(141)-C(142)	1.365(9)
C(106)-C(107)	1.368(11)	C(142)-C(143)	1.367(10)
C(107)-C(108)	1.376(9)	C(143)-C(144)	1.399(9)
C(109)-C(114)	1.387(7)	C(145)-C(146)	1.3900
C(109)-C(110)	1.403(7)	C(145)-C(150)	1.3900
C(110)-C(111)	1.396(8)	C(145)-C(151)	1.48(3)
C(111)-C(112)	1.376(9)	C(146)-C(147)	1.3900

C(147)-C(148)	1.3900	C(152)-C(158)	1.46(3)
C(148)-C(149)	1.3900	C(153)-C(154)	1.3900
C(149)-C(150)	1.3900	C(154)-C(155)	1.3900
C(152)-C(153)	1.3900	C(155)-C(156)	1.3900
C(152)-C(157)	1.3900	C(156)-C(157)	1.3900

Table 4. Bond angles [°] for **2**.

O(5)-Si(1)-O(4)	109.61(19)	Si(1)-O(4)-Si(4)	151.5(2)
O(5)-Si(1)-O(1)	106.9(2)	Si(1)-O(5)-Si(5)	157.9(3)
O(4)-Si(1)-O(1)	109.63(18)	O(5)-Si(5)-O(6)	110.5(2)
O(5)-Si(1)-C(1)	111.1(2)	O(5)-Si(5)-C(31)	108.7(2)
O(4)-Si(1)-C(1)	106.9(2)	O(6)-Si(5)-C(31)	109.7(2)
O(1)-Si(1)-C(1)	112.7(2)	O(5)-Si(5)-C(25)	107.6(2)
Si(2)-O(1)-Si(1)	141.2(2)	O(6)-Si(5)-C(25)	109.9(2)
O(2)-Si(2)-O(10)	110.61(18)	C(31)-Si(5)-C(25)	110.3(2)
O(2)-Si(2)-O(1)	109.53(18)	Si(5)-O(6)-Si(6)	156.7(3)
O(10)-Si(2)-O(1)	107.3(2)	O(6)-Si(6)-O(7)	110.90(19)
O(2)-Si(2)-C(7)	108.4(2)	O(6)-Si(6)-C(43)	111.5(2)
O(10)-Si(2)-C(7)	110.9(2)	O(7)-Si(6)-C(43)	106.6(2)
O(1)-Si(2)-C(7)	110.1(2)	O(6)-Si(6)-C(37)	107.0(2)
Si(2)-O(2)-Si(3)	148.4(2)	O(7)-Si(6)-C(37)	109.4(2)
O(8)-Si(3)-O(2)	110.11(18)	C(43)-Si(6)-C(37)	111.4(2)
O(8)-Si(3)-O(3)	107.55(18)	Si(4)-O(7)-Si(6)	151.2(3)
O(2)-Si(3)-O(3)	108.82(18)	Si(3)-O(8)-Si(7)	150.0(2)
O(8)-Si(3)-C(13)	112.1(2)	O(9)-Si(7)-O(8)	108.90(18)
O(2)-Si(3)-C(13)	108.4(2)	O(9)-Si(7)-C(49)	109.9(2)
O(3)-Si(3)-C(13)	109.8(2)	O(8)-Si(7)-C(49)	108.2(2)
Si(4)-O(3)-Si(3)	149.8(2)	O(9)-Si(7)-C(55)	109.4(2)
O(3)-Si(4)-O(7)	108.23(19)	O(8)-Si(7)-C(55)	109.2(2)
O(3)-Si(4)-O(4)	110.46(17)	C(49)-Si(7)-C(55)	111.2(2)
O(7)-Si(4)-O(4)	108.14(19)	Si(8)-O(9)-Si(7)	162.3(2)
O(3)-Si(4)-C(19)	108.8(2)	O(10)-Si(8)-O(9)	110.56(18)
O(7)-Si(4)-C(19)	112.2(2)	O(10)-Si(8)-C(61)	108.2(2)
O(4)-Si(4)-C(19)	109.0(2)	O(9)-Si(8)-C(61)	109.2(2)

O(10)-Si(8)-C(67)	108.5(2)	C(30)-C(25)-C(26)	118.4(6)
O(9)-Si(8)-C(67)	108.8(2)	C(30)-C(25)-Si(5)	121.5(5)
C(61)-Si(8)-C(67)	111.6(2)	C(26)-C(25)-Si(5)	120.1(4)
Si(8)-O(10)-Si(2)	151.6(2)	C(25)-C(26)-C(27)	121.8(7)
C(2)-C(1)-C(6)	115.8(5)	C(26)-C(27)-C(28)	118.0(8)
C(2)-C(1)-Si(1)	121.0(4)	C(29)-C(28)-C(27)	121.4(7)
C(6)-C(1)-Si(1)	123.0(4)	C(28)-C(29)-C(30)	119.1(8)
C(3)-C(2)-C(1)	124.0(7)	C(25)-C(30)-C(29)	121.1(8)
C(2)-C(3)-C(4)	119.5(8)	C(36)-C(31)-C(32)	116.9(5)
C(5)-C(4)-C(3)	119.0(7)	C(36)-C(31)-Si(5)	120.0(4)
C(4)-C(5)-C(6)	121.3(7)	C(32)-C(31)-Si(5)	122.8(4)
C(1)-C(6)-C(5)	120.3(6)	C(33)-C(32)-C(31)	121.2(6)
C(12)-C(7)-C(8)	117.4(5)	C(32)-C(33)-C(34)	121.2(6)
C(12)-C(7)-Si(2)	120.6(4)	C(33)-C(34)-C(35)	119.4(5)
C(8)-C(7)-Si(2)	121.9(5)	C(36)-C(35)-C(34)	119.6(6)
C(9)-C(8)-C(7)	121.2(7)	C(35)-C(36)-C(31)	121.5(5)
C(8)-C(9)-C(10)	120.0(7)	C(38)-C(37)-C(42)	118.4(5)
C(11)-C(10)-C(9)	119.9(6)	C(38)-C(37)-Si(6)	122.4(4)
C(10)-C(11)-C(12)	121.0(7)	C(42)-C(37)-Si(6)	119.2(4)
C(7)-C(12)-C(11)	120.6(6)	C(39)-C(38)-C(37)	121.5(6)
C(18)-C(13)-C(14)	117.5(5)	C(40)-C(39)-C(38)	119.7(6)
C(18)-C(13)-Si(3)	123.4(4)	C(41)-C(40)-C(39)	120.0(7)
C(14)-C(13)-Si(3)	119.1(4)	C(40)-C(41)-C(42)	121.1(7)
C(15)-C(14)-C(13)	121.1(6)	C(41)-C(42)-C(37)	119.4(6)
C(16)-C(15)-C(14)	119.4(6)	C(48)-C(43)-C(44)	117.6(5)
C(15)-C(16)-C(17)	121.0(6)	C(48)-C(43)-Si(6)	122.0(4)
C(16)-C(17)-C(18)	119.4(7)	C(44)-C(43)-Si(6)	120.2(4)
C(13)-C(18)-C(17)	121.6(6)	C(43)-C(44)-C(45)	120.9(7)
C(20)-C(19)-C(24)	117.6(5)	C(46)-C(45)-C(44)	120.0(7)
C(20)-C(19)-Si(4)	121.1(4)	C(45)-C(46)-C(47)	120.3(6)
C(24)-C(19)-Si(4)	121.3(4)	C(46)-C(47)-C(48)	120.3(7)
C(21)-C(20)-C(19)	121.3(5)	C(43)-C(48)-C(47)	120.9(7)
C(22)-C(21)-C(20)	120.5(6)	C(54)-C(49)-C(50)	117.7(5)
C(23)-C(22)-C(21)	119.7(5)	C(54)-C(49)-Si(7)	119.6(4)
C(22)-C(23)-C(24)	120.2(6)	C(50)-C(49)-Si(7)	122.7(4)
C(23)-C(24)-C(19)	120.7(6)	C(51)-C(50)-C(49)	120.7(6)

C(52)-C(51)-C(50)	120.4(7)	O(18)-Si(10)-O(11)	107.30(19)
C(51)-C(52)-C(53)	119.4(6)	O(12)-Si(10)-O(11)	109.50(19)
C(54)-C(53)-C(52)	120.1(6)	O(18)-Si(10)-C(79)	112.2(2)
C(53)-C(54)-C(49)	121.6(6)	O(12)-Si(10)-C(79)	107.3(2)
C(60)-C(55)-C(56)	117.5(5)	O(11)-Si(10)-C(79)	110.0(2)
C(60)-C(55)-Si(7)	122.5(4)	Si(10)-O(12)-Si(11)	145.2(2)
C(56)-C(55)-Si(7)	119.6(4)	O(13)-Si(11)-O(20)	108.3(2)
C(57)-C(56)-C(55)	122.4(5)	O(13)-Si(11)-O(12)	109.70(18)
C(58)-C(57)-C(56)	118.8(6)	O(20)-Si(11)-O(12)	110.12(19)
C(57)-C(58)-C(59)	120.9(6)	O(13)-Si(11)-C(85)	109.9(2)
C(58)-C(59)-C(60)	120.4(6)	O(20)-Si(11)-C(85)	110.1(2)
C(59)-C(60)-C(55)	119.9(6)	O(12)-Si(11)-C(85)	108.7(2)
C(62)-C(61)-C(66)	117.3(5)	Si(11)-O(13)-Si(12)	139.9(2)
C(62)-C(61)-Si(8)	119.8(4)	O(17)-Si(12)-O(14)	110.55(19)
C(66)-C(61)-Si(8)	122.9(4)	O(17)-Si(12)-O(13)	106.4(2)
C(61)-C(62)-C(63)	121.8(6)	O(14)-Si(12)-O(13)	109.02(19)
C(64)-C(63)-C(62)	119.5(7)	O(17)-Si(12)-C(91)	112.0(2)
C(65)-C(64)-C(63)	120.2(6)	O(14)-Si(12)-C(91)	107.3(2)
C(64)-C(65)-C(66)	119.5(6)	O(13)-Si(12)-C(91)	111.6(2)
C(65)-C(66)-C(61)	121.7(5)	Si(9)-O(14)-Si(12)	150.8(3)
C(68)-C(67)-C(72)	117.3(5)	Si(9)-O(15)-Si(13)	150.6(3)
C(68)-C(67)-Si(8)	121.6(4)	O(16)-Si(13)-O(15)	110.63(19)
C(72)-C(67)-Si(8)	121.0(4)	O(16)-Si(13)-C(97)	107.5(2)
C(67)-C(68)-C(69)	121.6(5)	O(15)-Si(13)-C(97)	110.2(2)
C(70)-C(69)-C(68)	119.5(6)	O(16)-Si(13)-C(103)	111.6(2)
C(71)-C(70)-C(69)	120.7(6)	O(15)-Si(13)-C(103)	105.8(2)
C(70)-C(71)-C(72)	119.7(5)	C(97)-Si(13)-C(103)	111.2(2)
C(71)-C(72)-C(67)	121.3(5)	Si(14)-O(16)-Si(13)	158.9(3)
O(14)-Si(9)-O(15)	108.68(19)	O(17)-Si(14)-O(16)	109.9(2)
O(14)-Si(9)-O(11)	110.33(19)	O(17)-Si(14)-C(115)	108.2(2)
O(15)-Si(9)-O(11)	107.78(19)	O(16)-Si(14)-C(115)	109.7(2)
O(14)-Si(9)-C(73)	108.4(2)	O(17)-Si(14)-C(109)	107.6(2)
O(15)-Si(9)-C(73)	113.2(2)	O(16)-Si(14)-C(109)	111.0(2)
O(11)-Si(9)-C(73)	108.4(2)	C(115)-Si(14)-C(109)	110.4(2)
Si(10)-O(11)-Si(9)	150.2(2)	Si(12)-O(17)-Si(14)	156.3(3)
O(18)-Si(10)-O(12)	110.51(18)	Si(10)-O(18)-Si(15)	151.4(2)

O(19)-Si(15)-O(18)	109.12(18)	C(88)-C(89)-C(90)	122.1(10)
O(19)-Si(15)-C(127)	109.5(2)	C(89)-C(90)-C(85)	121.5(9)
O(18)-Si(15)-C(127)	109.1(2)	C(92)-C(91)-C(96)	116.5(6)
O(19)-Si(15)-C(121)	109.4(2)	C(92)-C(91)-Si(12)	121.3(4)
O(18)-Si(15)-C(121)	108.10(19)	C(96)-C(91)-Si(12)	122.2(5)
C(127)-Si(15)-C(121)	111.6(2)	C(91)-C(92)-C(93)	119.9(8)
Si(16)-O(19)-Si(15)	160.3(3)	C(94)-C(93)-C(92)	121.6(9)
O(20)-Si(16)-O(19)	110.70(19)	C(93)-C(94)-C(95)	119.5(8)
O(20)-Si(16)-C(133)	108.0(2)	C(94)-C(95)-C(96)	120.2(8)
O(19)-Si(16)-C(133)	107.8(2)	C(95)-C(96)-C(91)	122.2(8)
O(20)-Si(16)-C(139)	108.0(2)	C(102)-C(97)-C(98)	117.4(5)
O(19)-Si(16)-C(139)	110.0(2)	C(102)-C(97)-Si(13)	121.1(4)
C(133)-Si(16)-C(139)	112.3(2)	C(98)-C(97)-Si(13)	121.4(4)
Si(11)-O(20)-Si(16)	153.0(2)	C(97)-C(98)-C(99)	121.3(6)
C(78)-C(73)-C(74)	117.3(5)	C(100)-C(99)-C(98)	119.6(6)
C(78)-C(73)-Si(9)	122.3(4)	C(99)-C(100)-C(101)	120.2(6)
C(74)-C(73)-Si(9)	120.4(4)	C(102)-C(101)-C(100)	119.5(6)
C(73)-C(74)-C(75)	121.3(6)	C(101)-C(102)-C(97)	122.0(6)
C(76)-C(75)-C(74)	119.8(7)	C(104)-C(103)-C(108)	117.2(5)
C(75)-C(76)-C(77)	120.0(6)	C(104)-C(103)-Si(13)	121.6(4)
C(76)-C(77)-C(78)	120.2(6)	C(108)-C(103)-Si(13)	121.1(5)
C(73)-C(78)-C(77)	121.3(6)	C(103)-C(104)-C(105)	120.5(7)
C(84)-C(79)-C(80)	119.2(6)	C(106)-C(105)-C(104)	120.6(7)
C(84)-C(79)-Si(10)	118.7(5)	C(107)-C(106)-C(105)	119.3(6)
C(80)-C(79)-Si(10)	122.0(5)	C(106)-C(107)-C(108)	119.8(7)
C(79)-C(80)-C(81)	120.1(7)	C(107)-C(108)-C(103)	122.5(7)
C(82)-C(81)-C(80)	119.8(8)	C(114)-C(109)-C(110)	117.6(5)
C(83)-C(82)-C(81)	121.0(7)	C(114)-C(109)-Si(14)	120.0(4)
C(82)-C(83)-C(84)	120.2(7)	C(110)-C(109)-Si(14)	122.2(4)
C(79)-C(84)-C(83)	119.8(7)	C(111)-C(110)-C(109)	119.8(5)
C(90)-C(85)-C(86)	116.3(6)	C(112)-C(111)-C(110)	120.6(5)
C(90)-C(85)-Si(11)	121.2(5)	C(111)-C(112)-C(113)	120.2(6)
C(86)-C(85)-Si(11)	122.3(4)	C(114)-C(113)-C(112)	119.2(6)
C(85)-C(86)-C(87)	120.9(7)	C(113)-C(114)-C(109)	122.6(5)
C(88)-C(87)-C(86)	120.6(8)	C(120)-C(115)-C(116)	118.3(6)
C(89)-C(88)-C(87)	118.6(7)	C(120)-C(115)-Si(14)	121.1(5)

C(116)-C(115)-Si(14)	120.5(5)	C(135)-C(136)-C(137)	120.7(6)
C(115)-C(116)-C(117)	120.9(7)	C(136)-C(137)-C(138)	119.0(6)
C(118)-C(117)-C(116)	119.4(8)	C(137)-C(138)-C(133)	122.0(6)
C(119)-C(118)-C(117)	119.6(8)	C(144)-C(139)-C(140)	118.1(5)
C(118)-C(119)-C(120)	121.5(9)	C(144)-C(139)-Si(16)	118.6(4)
C(119)-C(120)-C(115)	120.2(8)	C(140)-C(139)-Si(16)	123.2(4)
C(122)-C(121)-C(126)	117.5(5)	C(139)-C(140)-C(141)	120.6(5)
C(122)-C(121)-Si(15)	120.4(4)	C(142)-C(141)-C(140)	120.4(6)
C(126)-C(121)-Si(15)	121.9(4)	C(141)-C(142)-C(143)	120.4(6)
C(121)-C(122)-C(123)	121.5(5)	C(142)-C(143)-C(144)	119.3(6)
C(124)-C(123)-C(122)	119.6(6)	C(139)-C(144)-C(143)	121.1(6)
C(123)-C(124)-C(125)	120.7(6)	C(146)-C(145)-C(150)	120.0
C(124)-C(125)-C(126)	120.1(6)	C(146)-C(145)-C(151)	119.0(12)
C(125)-C(126)-C(121)	120.6(6)	C(150)-C(145)-C(151)	121.0(12)
C(132)-C(127)-C(128)	117.9(5)	C(147)-C(146)-C(145)	120.0
C(132)-C(127)-Si(15)	122.6(4)	C(146)-C(147)-C(148)	120.0
C(128)-C(127)-Si(15)	119.4(4)	C(149)-C(148)-C(147)	120.0
C(129)-C(128)-C(127)	121.0(6)	C(148)-C(149)-C(150)	120.0
C(130)-C(129)-C(128)	120.3(6)	C(149)-C(150)-C(145)	120.0
C(129)-C(130)-C(131)	120.2(6)	C(153)-C(152)-C(157)	120.0
C(130)-C(131)-C(132)	121.1(7)	C(153)-C(152)-C(158)	117.1(11)
C(127)-C(132)-C(131)	119.5(6)	C(157)-C(152)-C(158)	122.9(11)
C(138)-C(133)-C(134)	117.2(5)	C(152)-C(153)-C(154)	120.0
C(138)-C(133)-Si(16)	121.9(4)	C(153)-C(154)-C(155)	120.0
C(134)-C(133)-Si(16)	120.8(4)	C(156)-C(155)-C(154)	120.0
C(135)-C(134)-C(133)	121.0(5)	C(155)-C(156)-C(157)	120.0
C(136)-C(135)-C(134)	120.2(6)	C(156)-C(157)-C(152)	120.0

Table 5. Anisotropic displacement parameters ($Å^2 x 10^3$) for **2**. The anisotropic displacement factor exponent takes the form: $-2 \pi^2 [h^2 a^{*2} U^{11} + ... + 2 h k a^* b^* U^{12}]$

	U^{11}	U^{22}	U^{33}	U^{23}	U^{13}	U^{12}
Si(1)	23(1)	28(1)	44(1)	-2(1)	2(1)	3(1)
O(1)	31(2)	41(2)	38(2)	-1(2)	-2(1)	3(1)

Si(2)	22(1)	39(1)	31(1)	2(1)	2(1)	5(1)
O(2)	27(2)	37(2)	40(2)	-1(2)	2(1)	3(1)
Si(3)	23(1)	30(1)	31(1)	1(1)	0(1)	2(1)
O(3)	30(2)	36(2)	39(2)	3(2)	-3(1)	3(1)
Si(4)	23(1)	30(1)	32(1)	-2(1)	0(1)	5(1)
O(4)	24(2)	38(2)	47(2)	-1(2)	-1(1)	-1(1)
O(5)	35(2)	33(2)	68(2)	-11(2)	8(2)	6(2)
Si(5)	29(1)	31(1)	47(1)	-8(1)	1(1)	3(1)
O(6)	28(2)	44(2)	62(2)	-13(2)	-3(2)	3(2)
Si(6)	27(1)	34(1)	42(1)	-7(1)	3(1)	7(1)
O(7)	34(2)	33(2)	50(2)	-9(2)	2(2)	11(1)
O(8)	35(2)	38(2)	33(2)	-2(2)	4(1)	3(1)
Si(7)	25(1)	36(1)	30(1)	-2(1)	5(1)	3(1)
O(9)	24(2)	49(2)	42(2)	-4(2)	3(1)	6(1)
Si(8)	24(1)	41(1)	32(1)	-1(1)	-2(1)	4(1)
O(10)	26(2)	58(2)	39(2)	6(2)	-1(1)	6(2)
C(1)	27(2)	27(2)	57(3)	2(2)	9(2)	-2(2)
C(2)	56(4)	90(6)	72(5)	25(4)	16(3)	6(4)
C(3)	88(6)	118(8)	84(6)	33(5)	33(5)	0(5)
C(4)	100(6)	59(5)	101(6)	15(4)	59(5)	-1(4)
C(5)	46(4)	88(6)	139(8)	38(6)	49(4)	27(4)
C(6)	41(3)	81(5)	96(5)	40(4)	23(3)	22(3)
C(7)	29(2)	40(3)	44(3)	8(2)	10(2)	17(2)
C(8)	39(3)	121(7)	54(4)	17(4)	5(3)	26(4)
C(9)	48(4)	148(8)	90(6)	33(6)	30(4)	50(5)
C(10)	90(6)	78(5)	78(5)	16(4)	54(5)	40(4)
C(11)	88(5)	56(4)	55(4)	-3(3)	35(4)	15(3)
C(12)	53(3)	40(3)	47(3)	2(3)	10(2)	4(2)
C(13)	33(2)	31(3)	39(3)	-2(2)	-5(2)	7(2)
C(14)	33(3)	47(3)	70(4)	-14(3)	10(3)	4(2)
C(15)	56(4)	55(4)	81(5)	-32(4)	6(3)	-1(3)
C(16)	59(4)	37(3)	92(5)	-5(4)	-8(4)	-2(3)
C(17)	80(5)	47(4)	78(5)	2(4)	-10(4)	-25(3)
C(18)	65(4)	47(3)	45(3)	4(3)	-7(3)	-21(3)
C(19)	29(2)	44(3)	29(2)	0(2)	3(2)	10(2)
C(20)	45(3)	52(4)	44(3)	4(3)	-5(2)	-7(2)

C(21)	68(4)	64(4)	43(3)	-8(3)	-11(3)	-12(3)
C(22)	63(4)	77(5)	35(3)	-10(3)	-9(3)	3(3)
C(23)	73(4)	68(4)	33(3)	9(3)	-3(3)	18(3)
C(24)	50(3)	44(3)	43(3)	0(3)	0(2)	9(2)
C(25)	30(2)	40(3)	50(3)	0(2)	7(2)	-3(2)
C(26)	86(5)	62(4)	50(4)	-3(3)	12(3)	0(3)
C(27)	109(6)	94(6)	43(4)	-5(4)	23(4)	-21(5)
C(28)	69(5)	120(7)	50(4)	14(5)	-1(3)	-19(5)
C(29)	126(8)	94(7)	67(5)	31(5)	-4(5)	16(6)
C(30)	83(5)	63(5)	68(4)	13(4)	-4(4)	5(4)
C(31)	40(3)	29(3)	34(2)	-7(2)	-3(2)	4(2)
C(32)	49(3)	45(3)	40(3)	-6(2)	-5(2)	6(2)
C(33)	78(4)	32(3)	46(3)	1(3)	-11(3)	6(3)
C(34)	70(4)	43(3)	39(3)	1(3)	-7(3)	-11(3)
C(35)	47(3)	52(4)	49(3)	0(3)	4(2)	-4(3)
C(36)	43(3)	36(3)	50(3)	2(2)	4(2)	2(2)
C(37)	45(3)	30(3)	41(3)	-2(2)	2(2)	-3(2)
C(38)	55(3)	42(3)	52(3)	-7(3)	7(3)	-8(3)
C(39)	88(5)	57(4)	56(4)	-1(3)	12(4)	-22(4)
C(40)	119(7)	68(5)	55(4)	19(4)	-20(4)	-15(4)
C(41)	74(5)	84(5)	66(4)	15(4)	-17(4)	1(4)
C(42)	45(3)	62(4)	55(3)	6(3)	-7(3)	2(3)
C(43)	36(3)	45(3)	35(3)	-5(2)	1(2)	12(2)
C(44)	50(3)	55(4)	59(4)	-12(3)	11(3)	10(3)
C(45)	58(4)	83(5)	69(4)	-30(4)	15(3)	22(4)
C(46)	45(4)	123(7)	62(4)	-21(4)	16(3)	9(4)
C(47)	60(4)	84(5)	71(4)	-2(4)	27(3)	-5(4)
C(48)	57(4)	56(4)	68(4)	-4(3)	23(3)	-4(3)
C(49)	30(2)	42(3)	40(3)	-6(2)	2(2)	2(2)
C(50)	61(4)	48(4)	58(4)	-5(3)	17(3)	2(3)
C(51)	77(5)	43(4)	102(6)	-11(4)	27(4)	7(3)
C(52)	56(4)	63(5)	74(4)	-29(4)	8(3)	4(3)
C(53)	64(4)	74(5)	42(3)	-20(3)	-4(3)	20(3)
C(54)	56(3)	60(4)	40(3)	-7(3)	3(2)	22(3)
C(55)	37(3)	46(3)	27(2)	-2(2)	5(2)	0(2)
C(56)	41(3)	46(3)	43(3)	-5(2)	11(2)	-1(2)

C(57)	46(3)	60(4)	53(3)	1(3)	11(3)	-15(3)
C(58)	67(4)	55(4)	76(5)	9(4)	6(3)	-16(3)
C(59)	75(5)	47(4)	84(5)	14(4)	1(4)	1(3)
C(60)	50(3)	38(3)	53(3)	3(3)	1(3)	3(2)
C(61)	36(3)	37(3)	35(2)	1(2)	-5(2)	2(2)
C(62)	42(3)	97(6)	58(4)	-21(4)	6(3)	-20(3)
C(63)	62(5)	118(7)	76(5)	-10(5)	-7(4)	-41(5)
C(64)	69(4)	49(4)	56(4)	-6(3)	-20(3)	-12(3)
C(65)	62(4)	63(4)	47(3)	-6(3)	-9(3)	6(3)
C(66)	43(3)	50(3)	42(3)	-1(3)	-4(2)	-2(2)
C(67)	29(2)	38(3)	39(3)	0(2)	0(2)	0(2)
C(68)	67(4)	49(4)	35(3)	-2(3)	-7(3)	11(3)
C(69)	81(5)	48(4)	58(4)	-12(3)	-9(3)	16(3)
C(70)	58(4)	36(3)	64(4)	2(3)	-5(3)	6(3)
C(71)	42(3)	53(4)	50(3)	17(3)	1(2)	1(2)
C(72)	35(3)	49(3)	40(3)	4(2)	10(2)	6(2)
Si(9)	22(1)	34(1)	33(1)	-1(1)	-2(1)	-4(1)
O(11)	31(2)	40(2)	34(2)	-2(2)	-4(1)	-2(1)
Si(10)	26(1)	34(1)	31(1)	-1(1)	-1(1)	-1(1)
O(12)	26(2)	42(2)	40(2)	-1(2)	0(1)	0(1)
Si(11)	22(1)	44(1)	30(1)	-3(1)	2(1)	-6(1)
O(13)	31(2)	43(2)	42(2)	-1(2)	-1(1)	-4(1)
Si(12)	21(1)	33(1)	46(1)	3(1)	0(1)	-2(1)
O(14)	21(2)	47(2)	52(2)	-2(2)	-2(1)	1(1)
O(15)	31(2)	39(2)	50(2)	4(2)	2(2)	-6(1)
Si(13)	25(1)	37(1)	43(1)	4(1)	2(1)	-7(1)
O(16)	23(2)	53(2)	60(2)	12(2)	-3(2)	-3(2)
Si(14)	29(1)	35(1)	46(1)	7(1)	-2(1)	-4(1)
O(17)	38(2)	38(2)	69(3)	16(2)	-1(2)	-6(2)
O(18)	32(2)	42(2)	32(2)	-3(2)	6(1)	3(1)
Si(15)	25(1)	37(1)	31(1)	-1(1)	4(1)	0(1)
O(19)	26(2)	49(2)	45(2)	-2(2)	1(1)	-2(1)
Si(16)	25(1)	42(1)	32(1)	-2(1)	-2(1)	-3(1)
O(20)	34(2)	66(3)	33(2)	-9(2)	-1(1)	-5(2)
C(73)	28(2)	50(3)	28(2)	-1(2)	-1(2)	-4(2)
C(74)	65(4)	61(4)	34(3)	-8(3)	-5(3)	14(3)

C(75)	98(6)	69(5)	49(4)	5(3)	-13(4)	25(4)
C(76)	68(4)	88(5)	33(3)	-5(3)	-8(3)	-2(4)
C(77)	53(3)	70(4)	42(3)	-11(3)	1(3)	-13(3)
C(78)	46(3)	46(3)	43(3)	-9(3)	1(2)	-5(2)
C(79)	38(3)	33(3)	54(3)	0(2)	-14(2)	-3(2)
C(80)	100(6)	57(4)	56(4)	-6(3)	-13(4)	38(4)
C(81)	106(7)	65(5)	92(6)	-8(5)	-13(5)	41(5)
C(82)	86(6)	49(4)	110(7)	18(4)	-40(5)	8(4)
C(83)	59(4)	74(5)	90(5)	38(4)	-20(4)	-16(4)
C(84)	42(3)	60(4)	78(4)	30(4)	-4(3)	-7(3)
C(85)	40(3)	44(3)	43(3)	-8(2)	11(2)	-13(2)
C(86)	67(4)	55(4)	57(4)	-7(3)	24(3)	-10(3)
C(87)	135(8)	52(4)	60(4)	-3(3)	55(5)	-15(4)
C(88)	89(7)	118(8)	115(8)	-5(6)	68(6)	-46(6)
C(89)	60(6)	271(17)	107(8)	-8(9)	27(5)	-69(8)
C(90)	24(3)	202(11)	87(6)	11(6)	10(3)	-36(5)
C(91)	36(3)	28(3)	54(3)	-4(2)	9(2)	-1(2)
C(92)	65(4)	95(6)	60(4)	-4(4)	12(3)	33(4)
C(93)	123(8)	144(10)	66(5)	-11(5)	33(5)	55(7)
C(94)	97(7)	73(5)	128(8)	18(6)	74(6)	28(5)
C(95)	51(4)	97(7)	135(8)	-29(6)	45(5)	-18(4)
C(96)	27(3)	135(8)	93(6)	-15(5)	11(3)	-16(4)
C(97)	36(3)	29(3)	44(3)	3(2)	4(2)	-3(2)
C(98)	44(3)	47(3)	60(4)	2(3)	10(3)	5(2)
C(99)	72(4)	57(4)	51(3)	-6(3)	17(3)	12(3)
C(100)	79(5)	71(5)	45(3)	-11(3)	-8(3)	7(4)
C(101)	54(4)	82(5)	57(4)	-14(4)	-15(3)	-3(3)
C(102)	43(3)	58(4)	50(3)	-6(3)	0(2)	-1(3)
C(103)	31(3)	53(3)	37(3)	-2(2)	-2(2)	-9(2)
C(104)	55(4)	67(4)	49(3)	-1(3)	12(3)	-4(3)
C(105)	66(5)	105(7)	61(4)	-8(4)	21(3)	16(4)
C(106)	48(4)	115(7)	50(4)	13(4)	12(3)	-8(4)
C(107)	64(4)	81(5)	60(4)	17(4)	10(3)	-19(4)
C(108)	55(4)	57(4)	58(4)	8(3)	12(3)	-10(3)
C(109)	39(3)	39(3)	35(2)	4(2)	-4(2)	0(2)
C(110)	44(3)	50(3)	42(3)	1(3)	-5(2)	-8(2)

C(111)	63(4)	40(3)	47(3)	0(3)	-4(3)	-3(3)
C(112)	70(4)	46(4)	45(3)	-7(3)	-6(3)	11(3)
C(113)	49(3)	53(4)	45(3)	-3(3)	5(2)	7(3)
C(114)	44(3)	46(3)	41(3)	1(2)	-2(2)	-7(2)
C(115)	29(2)	42(3)	54(3)	-8(3)	2(2)	3(2)
C(116)	96(5)	57(4)	46(3)	0(3)	18(3)	7(4)
C(117)	102(6)	96(6)	49(4)	9(4)	22(4)	25(5)
C(118)	76(5)	139(9)	47(4)	-23(5)	-2(4)	32(5)
C(119)	132(9)	112(8)	68(5)	-25(6)	-13(5)	-11(6)
C(120)	97(6)	66(5)	68(5)	-9(4)	-9(4)	-10(4)
C(121)	32(2)	44(3)	28(2)	-1(2)	5(2)	1(2)
C(122)	41(3)	44(3)	48(3)	-6(3)	10(2)	7(2)
C(123)	45(3)	65(4)	63(4)	-3(3)	14(3)	15(3)
C(124)	77(5)	46(4)	78(5)	-7(4)	6(4)	19(3)
C(125)	79(5)	41(4)	82(5)	-12(4)	3(4)	-2(3)
C(126)	42(3)	51(4)	57(3)	-6(3)	4(3)	-3(2)
C(127)	30(2)	47(3)	41(3)	7(2)	2(2)	-4(2)
C(128)	54(3)	55(4)	45(3)	4(3)	-1(3)	-11(3)
C(129)	57(4)	72(5)	47(3)	17(3)	-3(3)	-16(3)
C(130)	56(4)	66(5)	76(5)	37(4)	4(3)	-2(3)
C(131)	80(5)	46(4)	100(6)	10(4)	24(4)	-2(3)
C(132)	64(4)	48(4)	57(4)	0(3)	14(3)	-2(3)
C(133)	29(2)	45(3)	35(2)	2(2)	-2(2)	-3(2)
C(134)	37(3)	48(3)	36(3)	-4(2)	4(2)	-3(2)
C(135)	48(3)	47(3)	52(3)	-11(3)	7(3)	-2(2)
C(136)	52(3)	44(3)	67(4)	1(3)	0(3)	-5(3)
C(137)	81(5)	48(4)	49(3)	9(3)	-6(3)	-6(3)
C(138)	58(4)	58(4)	41(3)	7(3)	-7(3)	-8(3)
C(139)	28(2)	41(3)	39(3)	-8(2)	-6(2)	-2(2)
C(140)	45(3)	54(3)	34(3)	3(2)	1(2)	6(2)
C(141)	61(4)	54(4)	45(3)	2(3)	-9(3)	6(3)
C(142)	77(5)	52(4)	52(4)	-2(3)	-20(3)	18(3)
C(143)	56(4)	104(6)	71(5)	10(4)	-5(3)	40(4)
C(144)	41(3)	83(5)	56(4)	10(3)	5(3)	12(3)
C(145)	180(20)	69(14)	67(12)	42(12)	72(17)	84(16)
C(146)	141(17)	45(13)	86(16)	5(11)	37(14)	48(12)

C(147)	160(20)	53(12)	81(15)	-9(11)	-2(15)	34(12)
C(148)	140(30)	45(13)	83(16)	17(12)	-9(17)	7(12)
C(149)	500(90)	63(17)	35(11)	17(12)	30(30)	90(30)
C(150)	350(60)	39(16)	87(19)	10(14)	110(30)	60(30)
C(151)	89(15)	101(18)	107(18)	30(14)	10(12)	8(11)
C(152)	190(30)	43(12)	68(13)	-24(10)	31(16)	-49(14)
C(153)	125(18)	100(20)	88(18)	-26(15)	26(14)	-45(15)
C(154)	160(20)	63(13)	60(12)	3(11)	-14(14)	-13(12)
C(155)	200(40)	70(17)	140(30)	-38(18)	-70(30)	30(20)
C(156)	420(90)	69(19)	40(12)	7(12)	-10(20)	-50(30)
C(157)	380(70)	60(20)	90(20)	-26(17)	100(30)	-60(30)
C(158)	130(20)	100(20)	110(20)	-19(15)	-8(16)	-48(17)

Table 6. Torsion angles [°] for **2**.

O(5)-Si(1)-O(1)-Si(2)	-159.7(3)
O(4)-Si(1)-O(1)-Si(2)	-41.0(4)
C(1)-Si(1)-O(1)-Si(2)	78.0(4)
Si(1)-O(1)-Si(2)-O(2)	52.1(4)
Si(1)-O(1)-Si(2)-O(10)	172.2(3)
Si(1)-O(1)-Si(2)-C(7)	-67.0(4)
O(10)-Si(2)-O(2)-Si(3)	-70.3(5)
O(1)-Si(2)-O(2)-Si(3)	47.8(5)
C(7)-Si(2)-O(2)-Si(3)	168.0(4)
Si(2)-O(2)-Si(3)-O(8)	40.9(5)
Si(2)-O(2)-Si(3)-O(3)	-76.7(5)
Si(2)-O(2)-Si(3)-C(13)	163.9(4)
O(8)-Si(3)-O(3)-Si(4)	-106.6(5)
O(2)-Si(3)-O(3)-Si(4)	12.6(5)
C(13)-Si(3)-O(3)-Si(4)	131.1(5)
Si(3)-O(3)-Si(4)-O(7)	119.4(5)
Si(3)-O(3)-Si(4)-O(4)	1.2(6)
Si(3)-O(3)-Si(4)-C(19)	-118.4(5)
O(5)-Si(1)-O(4)-Si(4)	57.2(5)
O(1)-Si(1)-O(4)-Si(4)	-59.8(5)

C(1)-Si(1)-O(4)-Si(4)	177.8(5)
O(3)-Si(4)-O(4)-Si(1)	61.3(5)
O(7)-Si(4)-O(4)-Si(1)	-57.0(5)
C(19)-Si(4)-O(4)-Si(1)	-179.2(5)
O(4)-Si(1)-O(5)-Si(5)	2.6(8)
O(1)-Si(1)-O(5)-Si(5)	121.3(7)
C(1)-Si(1)-O(5)-Si(5)	-115.4(7)
Si(1)-O(5)-Si(5)-O(6)	-4.4(8)
Si(1)-O(5)-Si(5)-C(31)	116.1(7)
Si(1)-O(5)-Si(5)-C(25)	-124.5(7)
O(5)-Si(5)-O(6)-Si(6)	-13.9(8)
C(31)-Si(5)-O(6)-Si(6)	-133.9(7)
C(25)-Si(5)-O(6)-Si(6)	104.7(7)
Si(5)-O(6)-Si(6)-O(7)	-4.2(8)
Si(5)-O(6)-Si(6)-C(43)	-122.9(7)
Si(5)-O(6)-Si(6)-C(37)	115.0(7)
O(3)-Si(4)-O(7)-Si(6)	-152.3(5)
O(4)-Si(4)-O(7)-Si(6)	-32.6(6)
C(19)-Si(4)-O(7)-Si(6)	87.7(5)
O(6)-Si(6)-O(7)-Si(4)	53.0(6)
C(43)-Si(6)-O(7)-Si(4)	174.6(5)
C(37)-Si(6)-O(7)-Si(4)	-64.8(5)
O(2)-Si(3)-O(8)-Si(7)	45.9(5)
O(3)-Si(3)-O(8)-Si(7)	164.3(4)
C(13)-Si(3)-O(8)-Si(7)	-74.9(5)
Si(3)-O(8)-Si(7)-O(9)	-41.9(5)
Si(3)-O(8)-Si(7)-C(49)	-161.3(4)
Si(3)-O(8)-Si(7)-C(55)	77.5(5)
O(8)-Si(7)-O(9)-Si(8)	-2.9(9)
C(49)-Si(7)-O(9)-Si(8)	115.4(8)
C(55)-Si(7)-O(9)-Si(8)	-122.2(8)
Si(7)-O(9)-Si(8)-O(10)	-4.1(9)
Si(7)-O(9)-Si(8)-C(61)	-123.0(8)
Si(7)-O(9)-Si(8)-C(67)	115.0(8)
O(9)-Si(8)-O(10)-Si(2)	12.6(6)
C(61)-Si(8)-O(10)-Si(2)	132.1(6)

C(67)-Si(8)-O(10)-Si(2)	-106.6(6)
O(2)-Si(2)-O(10)-Si(8)	17.5(6)
O(1)-Si(2)-O(10)-Si(8)	-101.9(6)
C(7)-Si(2)-O(10)-Si(8)	137.8(5)
O(5)-Si(1)-C(1)-C(2)	83.5(6)
O(4)-Si(1)-C(1)-C(2)	-36.1(6)
O(1)-Si(1)-C(1)-C(2)	-156.6(5)
O(5)-Si(1)-C(1)-C(6)	-102.0(6)
O(4)-Si(1)-C(1)-C(6)	138.4(5)
O(1)-Si(1)-C(1)-C(6)	17.9(6)
C(6)-C(1)-C(2)-C(3)	2.0(12)
Si(1)-C(1)-C(2)-C(3)	176.8(7)
C(1)-C(2)-C(3)-C(4)	-2.3(15)
C(2)-C(3)-C(4)-C(5)	1.5(15)
C(3)-C(4)-C(5)-C(6)	-0.6(14)
C(2)-C(1)-C(6)-C(5)	-0.9(11)
Si(1)-C(1)-C(6)-C(5)	-175.6(6)
C(4)-C(5)-C(6)-C(1)	0.3(13)
O(2)-Si(2)-C(7)-C(12)	-29.1(5)
O(10)-Si(2)-C(7)-C(12)	-150.7(4)
O(1)-Si(2)-C(7)-C(12)	90.7(5)
O(2)-Si(2)-C(7)-C(8)	156.4(5)
O(10)-Si(2)-C(7)-C(8)	34.8(6)
O(1)-Si(2)-C(7)-C(8)	-83.8(5)
C(12)-C(7)-C(8)-C(9)	-1.9(10)
Si(2)-C(7)-C(8)-C(9)	172.8(7)
C(7)-C(8)-C(9)-C(10)	1.2(13)
C(8)-C(9)-C(10)-C(11)	0.7(13)
C(9)-C(10)-C(11)-C(12)	-1.9(11)
C(8)-C(7)-C(12)-C(11)	0.6(8)
Si(2)-C(7)-C(12)-C(11)	-174.1(5)
C(10)-C(11)-C(12)-C(7)	1.3(10)
O(8)-Si(3)-C(13)-C(18)	-9.6(5)
O(2)-Si(3)-C(13)-C(18)	-131.3(4)
O(3)-Si(3)-C(13)-C(18)	109.9(5)
O(8)-Si(3)-C(13)-C(14)	171.6(4)

O(2)-Si(3)-C(13)-C(14)	49.9(4)
O(3)-Si(3)-C(13)-C(14)	-68.9(4)
C(18)-C(13)-C(14)-C(15)	-0.4(8)
Si(3)-C(13)-C(14)-C(15)	178.5(5)
C(13)-C(14)-C(15)-C(16)	0.4(10)
C(14)-C(15)-C(16)-C(17)	-0.4(11)
C(15)-C(16)-C(17)-C(18)	0.4(11)
C(14)-C(13)-C(18)-C(17)	0.4(9)
Si(3)-C(13)-C(18)-C(17)	-178.4(5)
C(16)-C(17)-C(18)-C(13)	-0.4(10)
O(3)-Si(4)-C(19)-C(20)	5.0(5)
O(7)-Si(4)-C(19)-C(20)	124.7(4)
O(4)-Si(4)-C(19)-C(20)	-115.5(4)
O(3)-Si(4)-C(19)-C(24)	-177.2(4)
O(7)-Si(4)-C(19)-C(24)	-57.5(4)
O(4)-Si(4)-C(19)-C(24)	62.2(4)
C(24)-C(19)-C(20)-C(21)	0.0(8)
Si(4)-C(19)-C(20)-C(21)	177.8(5)
C(19)-C(20)-C(21)-C(22)	0.0(10)
C(20)-C(21)-C(22)-C(23)	-0.3(10)
C(21)-C(22)-C(23)-C(24)	0.5(10)
C(22)-C(23)-C(24)-C(19)	-0.4(9)
C(20)-C(19)-C(24)-C(23)	0.2(8)
Si(4)-C(19)-C(24)-C(23)	-177.6(4)
O(5)-Si(5)-C(25)-C(30)	15.9(6)
O(6)-Si(5)-C(25)-C(30)	-104.5(5)
C(31)-Si(5)-C(25)-C(30)	134.4(5)
O(5)-Si(5)-C(25)-C(26)	-161.3(5)
O(6)-Si(5)-C(25)-C(26)	78.3(5)
C(31)-Si(5)-C(25)-C(26)	-42.8(5)
C(30)-C(25)-C(26)-C(27)	2.4(10)
Si(5)-C(25)-C(26)-C(27)	179.6(6)
C(25)-C(26)-C(27)-C(28)	-2.0(11)
C(26)-C(27)-C(28)-C(29)	1.3(13)
C(27)-C(28)-C(29)-C(30)	-0.8(14)
C(26)-C(25)-C(30)-C(29)	-1.9(11)

Si(5)-C(25)-C(30)-C(29)	-179.2(6)
C(28)-C(29)-C(30)-C(25)	1.2(13)
O(5)-Si(5)-C(31)-C(36)	29.1(5)
O(6)-Si(5)-C(31)-C(36)	150.1(4)
C(25)-Si(5)-C(31)-C(36)	-88.7(4)
O(5)-Si(5)-C(31)-C(32)	-157.8(4)
O(6)-Si(5)-C(31)-C(32)	-36.8(5)
C(25)-Si(5)-C(31)-C(32)	84.5(5)
C(36)-C(31)-C(32)-C(33)	0.2(8)
Si(5)-C(31)-C(32)-C(33)	-173.2(4)
C(31)-C(32)-C(33)-C(34)	0.7(8)
C(32)-C(33)-C(34)-C(35)	-1.9(9)
C(33)-C(34)-C(35)-C(36)	2.1(9)
C(34)-C(35)-C(36)-C(31)	-1.2(9)
C(32)-C(31)-C(36)-C(35)	0.1(8)
Si(5)-C(31)-C(36)-C(35)	173.6(4)
O(6)-Si(6)-C(37)-C(38)	-26.8(5)
O(7)-Si(6)-C(37)-C(38)	93.4(5)
C(43)-Si(6)-C(37)-C(38)	-148.9(5)
O(6)-Si(6)-C(37)-C(42)	154.2(4)
O(7)-Si(6)-C(37)-C(42)	-85.6(5)
C(43)-Si(6)-C(37)-C(42)	32.1(5)
C(42)-C(37)-C(38)-C(39)	1.8(9)
Si(6)-C(37)-C(38)-C(39)	-177.2(5)
C(37)-C(38)-C(39)-C(40)	-0.6(10)
C(38)-C(39)-C(40)-C(41)	-1.4(12)
C(39)-C(40)-C(41)-C(42)	2.2(12)
C(40)-C(41)-C(42)-C(37)	-1.0(11)
C(38)-C(37)-C(42)-C(41)	-1.0(9)
Si(6)-C(37)-C(42)-C(41)	178.0(5)
O(6)-Si(6)-C(43)-C(48)	136.5(5)
O(7)-Si(6)-C(43)-C(48)	15.3(5)
C(37)-Si(6)-C(43)-C(48)	-104.1(5)
O(6)-Si(6)-C(43)-C(44)	-48.8(5)
O(7)-Si(6)-C(43)-C(44)	-170.0(4)
C(37)-Si(6)-C(43)-C(44)	70.6(5)

C(48)-C(43)-C(44)-C(45)	1.6(9)
Si(6)-C(43)-C(44)-C(45)	-173.3(5)
C(43)-C(44)-C(45)-C(46)	-1.2(11)
C(44)-C(45)-C(46)-C(47)	-0.1(12)
C(45)-C(46)-C(47)-C(48)	0.8(12)
C(44)-C(43)-C(48)-C(47)	-0.9(10)
Si(6)-C(43)-C(48)-C(47)	173.9(5)
C(46)-C(47)-C(48)-C(43)	-0.3(11)
O(9)-Si(7)-C(49)-C(54)	79.0(5)
O(8)-Si(7)-C(49)-C(54)	-162.2(4)
C(55)-Si(7)-C(49)-C(54)	-42.3(5)
O(9)-Si(7)-C(49)-C(50)	-98.3(5)
O(8)-Si(7)-C(49)-C(50)	20.5(5)
C(55)-Si(7)-C(49)-C(50)	140.5(5)
C(54)-C(49)-C(50)-C(51)	-1.0(9)
Si(7)-C(49)-C(50)-C(51)	176.3(5)
C(49)-C(50)-C(51)-C(52)	0.4(11)
C(50)-C(51)-C(52)-C(53)	1.2(11)
C(51)-C(52)-C(53)-C(54)	-2.1(10)
C(52)-C(53)-C(54)-C(49)	1.5(10)
C(50)-C(49)-C(54)-C(53)	0.1(9)
Si(7)-C(49)-C(54)-C(53)	-177.4(5)
O(9)-Si(7)-C(55)-C(60)	24.0(5)
O(8)-Si(7)-C(55)-C(60)	-95.1(5)
C(49)-Si(7)-C(55)-C(60)	145.5(4)
O(9)-Si(7)-C(55)-C(56)	-163.4(4)
O(8)-Si(7)-C(55)-C(56)	77.5(4)
C(49)-Si(7)-C(55)-C(56)	-41.9(5)
C(60)-C(55)-C(56)-C(57)	0.8(8)
Si(7)-C(55)-C(56)-C(57)	-172.2(4)
C(55)-C(56)-C(57)-C(58)	-1.2(9)
C(56)-C(57)-C(58)-C(59)	0.9(10)
C(57)-C(58)-C(59)-C(60)	-0.2(11)
C(58)-C(59)-C(60)-C(55)	-0.3(10)
C(56)-C(55)-C(60)-C(59)	0.0(8)
Si(7)-C(55)-C(60)-C(59)	172.7(5)

O(10)-Si(8)-C(61)-C(62)	38.2(5)
O(9)-Si(8)-C(61)-C(62)	158.5(5)
C(67)-Si(8)-C(61)-C(62)	-81.2(5)
O(10)-Si(8)-C(61)-C(66)	-143.5(4)
O(9)-Si(8)-C(61)-C(66)	-23.1(5)
C(67)-Si(8)-C(61)-C(66)	97.2(5)
C(66)-C(61)-C(62)-C(63)	-1.4(11)
Si(8)-C(61)-C(62)-C(63)	177.1(7)
C(61)-C(62)-C(63)-C(64)	1.2(13)
C(62)-C(63)-C(64)-C(65)	-0.6(12)
C(63)-C(64)-C(65)-C(66)	0.2(10)
C(64)-C(65)-C(66)-C(61)	-0.3(9)
C(62)-C(61)-C(66)-C(65)	0.9(9)
Si(8)-C(61)-C(66)-C(65)	-177.5(4)
O(10)-Si(8)-C(67)-C(68)	21.4(5)
O(9)-Si(8)-C(67)-C(68)	-98.9(5)
C(61)-Si(8)-C(67)-C(68)	140.6(5)
O(10)-Si(8)-C(67)-C(72)	-162.7(4)
O(9)-Si(8)-C(67)-C(72)	76.9(4)
C(61)-Si(8)-C(67)-C(72)	-43.6(5)
C(72)-C(67)-C(68)-C(69)	0.3(9)
Si(8)-C(67)-C(68)-C(69)	176.3(5)
C(67)-C(68)-C(69)-C(70)	-0.3(10)
C(68)-C(69)-C(70)-C(71)	0.4(10)
C(69)-C(70)-C(71)-C(72)	-0.5(9)
C(70)-C(71)-C(72)-C(67)	0.6(8)
C(68)-C(67)-C(72)-C(71)	-0.5(8)
Si(8)-C(67)-C(72)-C(71)	-176.5(4)
O(14)-Si(9)-O(11)-Si(10)	5.3(5)
O(15)-Si(9)-O(11)-Si(10)	123.8(4)
C(73)-Si(9)-O(11)-Si(10)	-113.3(5)
Si(9)-O(11)-Si(10)-O(18)	-111.4(5)
Si(9)-O(11)-Si(10)-O(12)	8.6(5)
Si(9)-O(11)-Si(10)-C(79)	126.3(5)
O(18)-Si(10)-O(12)-Si(11)	43.1(5)
O(11)-Si(10)-O(12)-Si(11)	-74.9(4)

C(79)-Si(10)-O(12)-Si(11)	165.8(4)
Si(10)-O(12)-Si(11)-O(13)	46.7(5)
Si(10)-O(12)-Si(11)-O(20)	-72.3(4)
Si(10)-O(12)-Si(11)-C(85)	167.0(4)
O(20)-Si(11)-O(13)-Si(12)	177.7(3)
O(12)-Si(11)-O(13)-Si(12)	57.5(4)
C(85)-Si(11)-O(13)-Si(12)	-62.0(4)
Si(11)-O(13)-Si(12)-O(17)	-168.2(3)
Si(11)-O(13)-Si(12)-O(14)	-49.0(4)
Si(11)-O(13)-Si(12)-C(91)	69.3(4)
O(15)-Si(9)-O(14)-Si(12)	-58.4(6)
O(11)-Si(9)-O(14)-Si(12)	59.5(6)
C(73)-Si(9)-O(14)-Si(12)	178.1(5)
O(17)-Si(12)-O(14)-Si(9)	61.1(6)
O(13)-Si(12)-O(14)-Si(9)	-55.6(6)
C(91)-Si(12)-O(14)-Si(9)	-176.6(5)
O(14)-Si(9)-O(15)-Si(13)	-29.5(6)
O(11)-Si(9)-O(15)-Si(13)	-149.1(5)
C(73)-Si(9)-O(15)-Si(13)	91.0(5)
Si(9)-O(15)-Si(13)-O(16)	49.1(6)
Si(9)-O(15)-Si(13)-C(97)	-69.6(5)
Si(9)-O(15)-Si(13)-C(103)	170.1(5)
O(15)-Si(13)-O(16)-Si(14)	-0.2(9)
C(97)-Si(13)-O(16)-Si(14)	120.2(8)
C(103)-Si(13)-O(16)-Si(14)	-117.7(8)
Si(13)-O(16)-Si(14)-O(17)	-18.7(9)
Si(13)-O(16)-Si(14)-C(115)	100.1(8)
Si(13)-O(16)-Si(14)-C(109)	-137.6(8)
O(14)-Si(12)-O(17)-Si(14)	-8.0(9)
O(13)-Si(12)-O(17)-Si(14)	110.3(8)
C(91)-Si(12)-O(17)-Si(14)	-127.5(8)
O(16)-Si(14)-O(17)-Si(12)	5.2(9)
C(115)-Si(14)-O(17)-Si(12)	-114.5(8)
C(109)-Si(14)-O(17)-Si(12)	126.2(8)
O(12)-Si(10)-O(18)-Si(15)	44.5(5)
O(11)-Si(10)-O(18)-Si(15)	163.8(4)

C(79)-Si(10)-O(18)-Si(15)	-75.3(5)
Si(10)-O(18)-Si(15)-O(19)	-40.8(5)
Si(10)-O(18)-Si(15)-C(127)	-160.4(5)
Si(10)-O(18)-Si(15)-C(121)	78.1(5)
O(18)-Si(15)-O(19)-Si(16)	-8.0(8)
C(127)-Si(15)-O(19)-Si(16)	111.4(8)
C(121)-Si(15)-O(19)-Si(16)	-126.1(8)
Si(15)-O(19)-Si(16)-O(20)	0.2(8)
Si(15)-O(19)-Si(16)-C(133)	118.2(8)
Si(15)-O(19)-Si(16)-C(139)	-119.0(8)
O(13)-Si(11)-O(20)-Si(16)	-100.4(6)
O(12)-Si(11)-O(20)-Si(16)	19.5(7)
C(85)-Si(11)-O(20)-Si(16)	139.4(6)
O(19)-Si(16)-O(20)-Si(11)	12.1(7)
C(133)-Si(16)-O(20)-Si(11)	-105.8(6)
C(139)-Si(16)-O(20)-Si(11)	132.5(6)
O(14)-Si(9)-C(73)-C(78)	60.0(5)
O(15)-Si(9)-C(73)-C(78)	-60.6(5)
O(11)-Si(9)-C(73)-C(78)	179.8(4)
O(14)-Si(9)-C(73)-C(74)	-117.7(5)
O(15)-Si(9)-C(73)-C(74)	121.6(5)
O(11)-Si(9)-C(73)-C(74)	2.1(5)
C(78)-C(73)-C(74)-C(75)	0.2(9)
Si(9)-C(73)-C(74)-C(75)	178.0(5)
C(73)-C(74)-C(75)-C(76)	-0.8(11)
C(74)-C(75)-C(76)-C(77)	0.7(12)
C(75)-C(76)-C(77)-C(78)	0.1(10)
C(74)-C(73)-C(78)-C(77)	0.6(8)
Si(9)-C(73)-C(78)-C(77)	-177.2(4)
C(76)-C(77)-C(78)-C(73)	-0.7(9)
O(18)-Si(10)-C(79)-C(84)	171.6(4)
O(12)-Si(10)-C(79)-C(84)	50.0(5)
O(11)-Si(10)-C(79)-C(84)	-69.1(5)
O(18)-Si(10)-C(79)-C(80)	-11.2(6)
O(12)-Si(10)-C(79)-C(80)	-132.8(5)
O(11)-Si(10)-C(79)-C(80)	108.2(5)

C(84)-C(79)-C(80)-C(81)	-0.7(11)
Si(10)-C(79)-C(80)-C(81)	-177.9(6)
C(79)-C(80)-C(81)-C(82)	0.5(13)
C(80)-C(81)-C(82)-C(83)	-0.7(13)
C(81)-C(82)-C(83)-C(84)	1.1(12)
C(80)-C(79)-C(84)-C(83)	1.2(9)
Si(10)-C(79)-C(84)-C(83)	178.5(5)
C(82)-C(83)-C(84)-C(79)	-1.4(11)
O(13)-Si(11)-C(85)-C(90)	-75.5(7)
O(20)-Si(11)-C(85)-C(90)	43.7(7)
O(12)-Si(11)-C(85)-C(90)	164.4(6)
O(13)-Si(11)-C(85)-C(86)	99.0(5)
O(20)-Si(11)-C(85)-C(86)	-141.8(5)
O(12)-Si(11)-C(85)-C(86)	-21.1(6)
C(90)-C(85)-C(86)-C(87)	-0.1(10)
Si(11)-C(85)-C(86)-C(87)	-174.9(5)
C(85)-C(86)-C(87)-C(88)	1.3(11)
C(86)-C(87)-C(88)-C(89)	-1.0(15)
C(87)-C(88)-C(89)-C(90)	-0.5(19)
C(88)-C(89)-C(90)-C(85)	2(2)
C(86)-C(85)-C(90)-C(89)	-1.3(14)
Si(11)-C(85)-C(90)-C(89)	173.5(9)
O(17)-Si(12)-C(91)-C(92)	108.4(6)
O(14)-Si(12)-C(91)-C(92)	-13.0(6)
O(13)-Si(12)-C(91)-C(92)	-132.4(5)
O(17)-Si(12)-C(91)-C(96)	-73.5(6)
O(14)-Si(12)-C(91)-C(96)	165.0(6)
O(13)-Si(12)-C(91)-C(96)	45.7(6)
C(96)-C(91)-C(92)-C(93)	-2.7(11)
Si(12)-C(91)-C(92)-C(93)	175.4(7)
C(91)-C(92)-C(93)-C(94)	1.1(15)
C(92)-C(93)-C(94)-C(95)	1.3(16)
C(93)-C(94)-C(95)-C(96)	-2.0(15)
C(94)-C(95)-C(96)-C(91)	0.2(15)
C(92)-C(91)-C(96)-C(95)	2.1(12)
Si(12)-C(91)-C(96)-C(95)	-176.0(7)

O(16)-Si(13)-C(97)-C(102)	152.7(4)
O(15)-Si(13)-C(97)-C(102)	-86.7(5)
C(103)-Si(13)-C(97)-C(102)	30.2(5)
O(16)-Si(13)-C(97)-C(98)	-31.4(5)
O(15)-Si(13)-C(97)-C(98)	89.2(5)
C(103)-Si(13)-C(97)-C(98)	-153.8(4)
C(102)-C(97)-C(98)-C(99)	0.3(8)
Si(13)-C(97)-C(98)-C(99)	-175.8(5)
C(97)-C(98)-C(99)-C(100)	-0.8(9)
C(98)-C(99)-C(100)-C(101)	0.7(11)
C(99)-C(100)-C(101)-C(102)	0.0(11)
C(100)-C(101)-C(102)-C(97)	-0.6(11)
C(98)-C(97)-C(102)-C(101)	0.5(9)
Si(13)-C(97)-C(102)-C(101)	176.6(5)
O(16)-Si(13)-C(103)-C(104)	128.5(5)
O(15)-Si(13)-C(103)-C(104)	8.1(5)
C(97)-Si(13)-C(103)-C(104)	-111.5(5)
O(16)-Si(13)-C(103)-C(108)	-56.1(5)
O(15)-Si(13)-C(103)-C(108)	-176.5(4)
C(97)-Si(13)-C(103)-C(108)	63.9(5)
C(108)-C(103)-C(104)-C(105)	-1.5(9)
Si(13)-C(103)-C(104)-C(105)	174.0(5)
C(103)-C(104)-C(105)-C(106)	0.4(11)
C(104)-C(105)-C(106)-C(107)	1.3(11)
C(105)-C(106)-C(107)-C(108)	-1.8(11)
C(106)-C(107)-C(108)-C(103)	0.6(11)
C(104)-C(103)-C(108)-C(107)	1.1(9)
Si(13)-C(103)-C(108)-C(107)	-174.5(5)
O(17)-Si(14)-C(109)-C(114)	29.8(5)
O(16)-Si(14)-C(109)-C(114)	150.1(4)
C(115)-Si(14)-C(109)-C(114)	-88.1(4)
O(17)-Si(14)-C(109)-C(110)	-155.7(4)
O(16)-Si(14)-C(109)-C(110)	-35.4(5)
C(115)-Si(14)-C(109)-C(110)	86.5(5)
C(114)-C(109)-C(110)-C(111)	0.9(7)
Si(14)-C(109)-C(110)-C(111)	-173.8(4)

C(109)-C(110)-C(111)-C(112)	0.0(8)
C(110)-C(111)-C(112)-C(113)	-0.8(9)
C(111)-C(112)-C(113)-C(114)	0.6(9)
C(112)-C(113)-C(114)-C(109)	0.3(8)
C(110)-C(109)-C(114)-C(113)	-1.1(8)
Si(14)-C(109)-C(114)-C(113)	173.7(4)
O(17)-Si(14)-C(115)-C(120)	15.4(6)
O(16)-Si(14)-C(115)-C(120)	-104.4(5)
C(109)-Si(14)-C(115)-C(120)	132.9(5)
O(17)-Si(14)-C(115)-C(116)	-160.5(5)
O(16)-Si(14)-C(115)-C(116)	79.7(5)
C(109)-Si(14)-C(115)-C(116)	-43.0(5)
C(120)-C(115)-C(116)-C(117)	2.8(10)
Si(14)-C(115)-C(116)-C(117)	178.8(6)
C(115)-C(116)-C(117)-C(118)	-1.6(12)
C(116)-C(117)-C(118)-C(119)	0.9(13)
C(117)-C(118)-C(119)-C(120)	-1.4(15)
C(118)-C(119)-C(120)-C(115)	2.7(15)
C(116)-C(115)-C(120)-C(119)	-3.3(11)
Si(14)-C(115)-C(120)-C(119)	-179.3(7)
O(19)-Si(15)-C(121)-C(122)	-161.3(4)
O(18)-Si(15)-C(121)-C(122)	80.0(4)
C(127)-Si(15)-C(121)-C(122)	-40.0(5)
O(19)-Si(15)-C(121)-C(126)	24.4(5)
O(18)-Si(15)-C(121)-C(126)	-94.3(4)
C(127)-Si(15)-C(121)-C(126)	145.8(4)
C(126)-C(121)-C(122)-C(123)	0.6(8)
Si(15)-C(121)-C(122)-C(123)	-173.9(4)
C(121)-C(122)-C(123)-C(124)	-0.4(9)
C(122)-C(123)-C(124)-C(125)	0.2(11)
C(123)-C(124)-C(125)-C(126)	-0.3(11)
C(124)-C(125)-C(126)-C(121)	0.6(10)
C(122)-C(121)-C(126)-C(125)	-0.7(8)
Si(15)-C(121)-C(126)-C(125)	173.7(5)
O(19)-Si(15)-C(127)-C(132)	-99.4(5)
O(18)-Si(15)-C(127)-C(132)	20.0(5)

C(121)-Si(15)-C(127)-C(132)	139.3(5)
O(19)-Si(15)-C(127)-C(128)	77.5(5)
O(18)-Si(15)-C(127)-C(128)	-163.1(4)
C(121)-Si(15)-C(127)-C(128)	-43.7(5)
C(132)-C(127)-C(128)-C(129)	1.3(9)
Si(15)-C(127)-C(128)-C(129)	-175.8(5)
C(127)-C(128)-C(129)-C(130)	-0.2(10)
C(128)-C(129)-C(130)-C(131)	-0.8(10)
C(129)-C(130)-C(131)-C(132)	0.6(11)
C(128)-C(127)-C(132)-C(131)	-1.5(9)
Si(15)-C(127)-C(132)-C(131)	175.5(5)
C(130)-C(131)-C(132)-C(127)	0.6(11)
O(20)-Si(16)-C(133)-C(138)	23.2(5)
O(19)-Si(16)-C(133)-C(138)	-96.5(5)
C(139)-Si(16)-C(133)-C(138)	142.2(5)
O(20)-Si(16)-C(133)-C(134)	-161.5(4)
O(19)-Si(16)-C(133)-C(134)	78.8(4)
C(139)-Si(16)-C(133)-C(134)	-42.5(5)
C(138)-C(133)-C(134)-C(135)	-0.7(8)
Si(16)-C(133)-C(134)-C(135)	-176.3(4)
C(133)-C(134)-C(135)-C(136)	1.2(8)
C(134)-C(135)-C(136)-C(137)	-0.1(9)
C(135)-C(136)-C(137)-C(138)	-1.3(10)
C(136)-C(137)-C(138)-C(133)	1.7(10)
C(134)-C(133)-C(138)-C(137)	-0.7(9)
Si(16)-C(133)-C(138)-C(137)	174.8(5)
O(20)-Si(16)-C(139)-C(144)	40.2(5)
O(19)-Si(16)-C(139)-C(144)	161.1(5)
C(133)-Si(16)-C(139)-C(144)	-78.8(5)
O(20)-Si(16)-C(139)-C(140)	-142.0(4)
O(19)-Si(16)-C(139)-C(140)	-21.1(5)
C(133)-Si(16)-C(139)-C(140)	99.0(5)
C(144)-C(139)-C(140)-C(141)	-0.3(9)
Si(16)-C(139)-C(140)-C(141)	-178.1(4)
C(139)-C(140)-C(141)-C(142)	-0.3(9)
C(140)-C(141)-C(142)-C(143)	-0.3(11)

C(141)-C(142)-C(143)-C(144)	1.6(12)
C(140)-C(139)-C(144)-C(143)	1.6(10)
Si(16)-C(139)-C(144)-C(143)	179.5(6)
C(142)-C(143)-C(144)-C(139)	-2.2(12)
C(150)-C(145)-C(146)-C(147)	0.0
C(151)-C(145)-C(146)-C(147)	179.7(12)
C(145)-C(146)-C(147)-C(148)	0.0
C(146)-C(147)-C(148)-C(149)	0.0
C(147)-C(148)-C(149)-C(150)	0.0
C(148)-C(149)-C(150)-C(145)	0.0
C(146)-C(145)-C(150)-C(149)	0.0
C(151)-C(145)-C(150)-C(149)	-179.7(12)
C(157)-C(152)-C(153)-C(154)	0.0
C(158)-C(152)-C(153)-C(154)	179.0(16)
C(152)-C(153)-C(154)-C(155)	0.0
C(153)-C(154)-C(155)-C(156)	0.0
C(154)-C(155)-C(156)-C(157)	0.0
C(155)-C(156)-C(157)-C(152)	0.0
C(153)-C(152)-C(157)-C(156)	0.0
C(158)-C(152)-C(157)-C(156)	-178.9(17)

2-2 X-ray analysis of **3**.

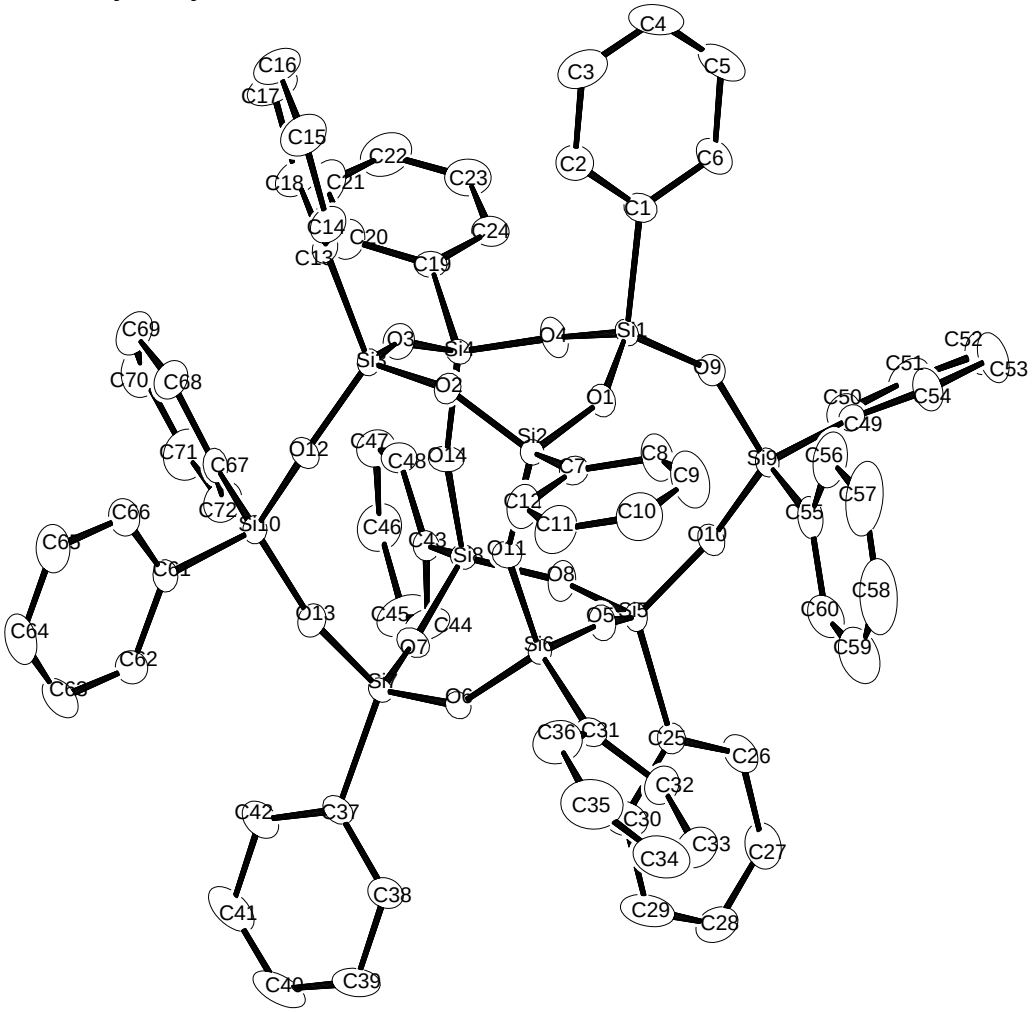

Figure 1. ORTEP drawing of **3**.

Table 1. Crystal data and structure refinement for **3**.

Empirical formula	$C_{72}H_{60}O_{14}Si_{10}$	
Formula weight	1430.10	
Temperature	173.1500 K	
Wavelength	0.71070 Å	
Crystal system	Triclinic	
Space group	*P* -1	
Unit cell dimensions	a = 12.3673(11) Å	α = 101.281(2)°.
	b = 15.8156(15) Å	β = 103.206(2)°.
	c = 18.8138(19) Å	γ = 95.940(2)°.
Volume	3470.8(6) $Å^3$	
Z	2	
Density (calculated)	1.368 g/mL	
Absorption coefficient	0.255 mm^{-1}	
F(000)	1488	
Crystal size	0.3000 x 0.2000 x 0.1000 mm^3	
Theta range for data collection	2.28 to 25.50°.	
Index ranges	$-14<=h<=14$, $-19<=k<=19$, $-22<=l<=21$	
Reflections collected	24294	
Independent reflections	12048 [R(int) = 0.0210]	
Completeness to theta = 25.50°	93.3%	
Absorption correction	Semi-empirical from equivalents	
Max. and min. transmission	1.0000 and 0.3176	
Refinement method	Full-matrix least-squares on F^2	
Data / restraints / parameters	12048 / 0 / 865	
Goodness-of-fit on F^2	1.118	
Final R indices [I>2sigma(I)]	$R1$ = 0.0426, $wR2$ = 0.1043	
R indices (all data)	$R1$ = 0.0454, $wR2$ = 0.1061	
Largest diff. peak and hole	0.377 and -0.389 e.$Å^{-3}$	

Table 2. Atomic coordinates (x 10^4) and equivalent isotropic displacement parameters ($Å^2$x 10^3) for **3**. U(eq) is defined as one third of the trace of the orthogonalized U^{ij} tensor.

	x	y	z	U(eq)
Si(1)	5939(1)	3839(1)	1992(1)	16(1)
O(1)	7294(1)	4085(1)	2185(1)	23(1)
Si(2)	8523(1)	4149(1)	2740(1)	15(1)
O(2)	8446(1)	4322(1)	3604(1)	20(1)
Si(3)	8027(1)	3809(1)	4180(1)	15(1)
O(3)	6833(1)	3194(1)	3780(1)	24(1)
Si(4)	5873(1)	2598(1)	3086(1)	15(1)
O(4)	5616(1)	3090(1)	2408(1)	26(1)
Si(5)	6779(1)	1378(1)	869(1)	16(1)
O(5)	7888(1)	2070(1)	1343(1)	22(1)
Si(6)	9091(1)	2413(1)	1939(1)	14(1)
O(6)	9459(1)	1653(1)	2370(1)	19(1)
Si(7)	9079(1)	1053(1)	2899(1)	15(1)
O(7)	7763(1)	651(1)	2568(1)	22(1)
Si(8)	6483(1)	817(1)	2291(1)	15(1)
O(8)	6252(1)	912(1)	1431(1)	25(1)
O(9)	5430(1)	3462(1)	1106(1)	26(1)
Si(9)	5569(1)	2853(1)	336(1)	19(1)
O(10)	5863(1)	1904(1)	461(1)	22(1)
O(11)	8966(1)	3221(1)	2572(1)	20(1)
O(12)	8950(1)	3203(1)	4450(1)	21(1)
Si(10)	9151(1)	2215(1)	4514(1)	17(1)
O(13)	9285(1)	1625(1)	3741(1)	23(1)
O(14)	6348(1)	1715(1)	2812(1)	24(1)
C(1)	5347(2)	4828(1)	2306(1)	22(1)
C(2)	5712(2)	5274(2)	3056(1)	36(1)
C(3)	5296(3)	6028(2)	3315(2)	48(1)
C(4)	4507(3)	6337(2)	2827(2)	50(1)
C(5)	4144(2)	5913(2)	2088(2)	47(1)
C(6)	4560(2)	5163(2)	1824(2)	32(1)

C(7)	9500(2)	5018(1)	2593(1)	20(1)
C(8)	9210(2)	5398(2)	1988(2)	38(1)
C(9)	9983(3)	5998(2)	1840(2)	53(1)
C(10)	11060(2)	6207(2)	2290(2)	44(1)
C(11)	11369(2)	5846(2)	2898(2)	39(1)
C(12)	10595(2)	5258(2)	3051(1)	31(1)
C(13)	7783(2)	4644(1)	4936(1)	20(1)
C(14)	8419(2)	5474(1)	5167(1)	29(1)
C(15)	8160(2)	6128(2)	5677(2)	41(1)
C(16)	7238(3)	5968(2)	5951(2)	45(1)
C(17)	6598(2)	5152(2)	5741(2)	46(1)
C(18)	6866(2)	4497(2)	5233(1)	34(1)
C(19)	4576(2)	2320(1)	3365(1)	21(1)
C(20)	4621(2)	2165(2)	4076(1)	32(1)
C(21)	3656(2)	1835(2)	4249(2)	45(1)
C(22)	2638(2)	1650(2)	3713(2)	46(1)
C(23)	2572(2)	1804(2)	3015(2)	37(1)
C(24)	3529(2)	2141(1)	2842(1)	27(1)
C(25)	7185(2)	550(1)	178(1)	21(1)
C(26)	6516(3)	201(2)	-536(1)	49(1)
C(27)	6843(3)	-437(2)	-1026(2)	70(1)
C(28)	7858(3)	-728(2)	-808(2)	46(1)
C(29)	8517(2)	-402(2)	-99(2)	47(1)
C(30)	8188(2)	232(2)	392(2)	41(1)
C(31)	10181(2)	2727(1)	1476(1)	23(1)
C(32)	10070(2)	2435(2)	715(2)	39(1)
C(33)	10926(3)	2663(2)	395(2)	59(1)
C(34)	11903(3)	3189(2)	831(2)	63(1)
C(35)	12025(3)	3492(2)	1585(2)	63(1)
C(36)	11170(2)	3270(2)	1902(2)	44(1)
C(37)	9878(2)	130(1)	2860(1)	20(1)
C(38)	10384(2)	-107(2)	2274(1)	28(1)
C(39)	10902(2)	-849(2)	2211(2)	42(1)
C(40)	10918(2)	-1355(2)	2730(2)	49(1)
C(41)	10433(2)	-1132(2)	3311(2)	49(1)
C(42)	9911(2)	-398(2)	3375(2)	34(1)

C(43)	5513(2)	-102(1)	2377(1)	18(1)
C(44)	5548(2)	-956(2)	2032(2)	36(1)
C(45)	4786(3)	-1647(2)	2056(2)	49(1)
C(46)	3961(2)	-1492(2)	2425(2)	39(1)
C(47)	3914(2)	-654(2)	2786(1)	32(1)
C(48)	4683(2)	31(1)	2762(1)	26(1)
C(49)	4210(2)	2680(1)	-385(1)	24(1)
C(50)	3368(2)	1976(2)	-498(1)	31(1)
C(51)	2374(2)	1869(2)	-1052(1)	44(1)
C(52)	2201(2)	2454(2)	-1500(2)	51(1)
C(53)	3020(3)	3156(2)	-1403(2)	53(1)
C(54)	4010(2)	3268(2)	-848(1)	37(1)
C(55)	6711(2)	3452(2)	54(1)	28(1)
C(56)	6876(3)	4363(2)	206(2)	44(1)
C(57)	7701(3)	4826(2)	-15(2)	63(1)
C(58)	8395(3)	4388(3)	-384(2)	68(1)
C(59)	8249(3)	3484(3)	-539(2)	67(1)
C(60)	7411(2)	3018(2)	-328(2)	44(1)
C(61)	10464(2)	2303(1)	5254(1)	21(1)
C(62)	11114(2)	1625(2)	5243(1)	27(1)
C(63)	12038(2)	1658(2)	5830(2)	38(1)
C(64)	12338(2)	2357(2)	6439(2)	43(1)
C(65)	11704(2)	3029(2)	6461(1)	40(1)
C(66)	10781(2)	3002(2)	5878(1)	29(1)
C(67)	7951(2)	1689(1)	4796(1)	22(1)
C(68)	7636(2)	2138(2)	5417(1)	32(1)
C(69)	6809(2)	1747(2)	5687(2)	43(1)
C(70)	6284(2)	906(2)	5345(2)	47(1)
C(71)	6567(2)	461(2)	4725(2)	47(1)
C(72)	7397(2)	846(2)	4455(1)	34(1)

Table 3. Bond lengths [Å] for **3**.

Si(1)-O(9)	1.6060(15)	Si(9)-C(55)	1.854(2)
Si(1)-O(4)	1.6078(15)	Si(9)-C(49)	1.859(2)
Si(1)-O(1)	1.6198(15)	O(12)-Si(10)	1.6296(14)
Si(1)-C(1)	1.846(2)	Si(10)-O(13)	1.6206(15)
O(1)-Si(2)	1.6168(14)	Si(10)-C(61)	1.854(2)
Si(2)-O(11)	1.6181(14)	Si(10)-C(67)	1.858(2)
Si(2)-O(2)	1.6199(15)	C(1)-C(6)	1.393(3)
Si(2)-C(7)	1.840(2)	C(1)-C(2)	1.395(3)
O(2)-Si(3)	1.6169(15)	C(2)-C(3)	1.391(3)
Si(3)-O(3)	1.6135(15)	C(3)-C(4)	1.378(4)
Si(3)-O(12)	1.6230(14)	C(4)-C(5)	1.368(4)
Si(3)-C(13)	1.845(2)	C(5)-C(6)	1.390(3)
O(3)-Si(4)	1.6066(15)	C(7)-C(8)	1.381(3)
Si(4)-O(14)	1.6079(14)	C(7)-C(12)	1.398(3)
Si(4)-O(4)	1.6089(15)	C(8)-C(9)	1.388(4)
Si(4)-C(19)	1.836(2)	C(9)-C(10)	1.372(4)
Si(5)-O(8)	1.6153(16)	C(10)-C(11)	1.372(4)
Si(5)-O(10)	1.6164(14)	C(11)-C(12)	1.382(3)
Si(5)-O(5)	1.6193(14)	C(13)-C(18)	1.391(3)
Si(5)-C(25)	1.850(2)	C(13)-C(14)	1.392(3)
O(5)-Si(6)	1.6120(14)	C(14)-C(15)	1.383(3)
Si(6)-O(11)	1.6128(14)	C(15)-C(16)	1.375(4)
Si(6)-O(6)	1.6230(14)	C(16)-C(17)	1.375(4)
Si(6)-C(31)	1.841(2)	C(17)-C(18)	1.388(3)
O(6)-Si(7)	1.6123(14)	C(19)-C(20)	1.395(3)
Si(7)-O(13)	1.6134(15)	C(19)-C(24)	1.399(3)
Si(7)-O(7)	1.6157(15)	C(20)-C(21)	1.385(4)
Si(7)-C(37)	1.845(2)	C(21)-C(22)	1.385(4)
O(7)-Si(8)	1.6154(14)	C(22)-C(23)	1.367(4)
Si(8)-O(14)	1.6080(14)	C(23)-C(24)	1.380(3)
Si(8)-O(8)	1.6181(15)	C(25)-C(26)	1.378(3)
Si(8)-C(43)	1.842(2)	C(25)-C(30)	1.392(3)
O(9)-Si(9)	1.6312(15)	C(26)-C(27)	1.386(4)
Si(9)-O(10)	1.6279(15)	C(27)-C(28)	1.383(4)

C(28)-C(29)	1.362(4)	C(50)-C(51)	1.390(3)
C(29)-C(30)	1.384(3)	C(51)-C(52)	1.369(4)
C(31)-C(32)	1.386(3)	C(52)-C(53)	1.377(5)
C(31)-C(36)	1.394(3)	C(53)-C(54)	1.386(4)
C(32)-C(33)	1.383(4)	C(55)-C(56)	1.396(3)
C(33)-C(34)	1.378(5)	C(55)-C(60)	1.397(4)
C(34)-C(35)	1.373(5)	C(56)-C(57)	1.382(4)
C(35)-C(36)	1.376(4)	C(57)-C(58)	1.381(5)
C(37)-C(42)	1.394(3)	C(58)-C(59)	1.385(5)
C(37)-C(38)	1.396(3)	C(59)-C(60)	1.387(4)
C(38)-C(39)	1.391(3)	C(61)-C(66)	1.396(3)
C(39)-C(40)	1.378(4)	C(61)-C(62)	1.404(3)
C(40)-C(41)	1.366(4)	C(62)-C(63)	1.385(3)
C(41)-C(42)	1.385(3)	C(63)-C(64)	1.377(4)
C(43)-C(44)	1.388(3)	C(64)-C(65)	1.383(4)
C(43)-C(48)	1.396(3)	C(65)-C(66)	1.381(3)
C(44)-C(45)	1.382(3)	C(67)-C(72)	1.390(3)
C(45)-C(46)	1.377(4)	C(67)-C(68)	1.401(3)
C(46)-C(47)	1.379(3)	C(68)-C(69)	1.385(4)
C(47)-C(48)	1.382(3)	C(69)-C(70)	1.379(4)
C(49)-C(50)	1.391(3)	C(70)-C(71)	1.376(4)
C(49)-C(54)	1.398(3)	C(71)-C(72)	1.384(4)

Table 4. Bond angles [°] for **3**.

O(9)-Si(1)-O(4)	107.64(9)	O(5)-Si(5)-C(25)	108.78(9)
O(9)-Si(1)-O(1)	110.34(8)	Si(6)-O(5)-Si(5)	156.82(10)
O(4)-Si(1)-O(1)	109.45(8)	O(5)-Si(6)-O(11)	108.87(8)
O(9)-Si(1)-C(1)	110.05(9)	O(5)-Si(6)-O(6)	109.65(8)
O(4)-Si(1)-C(1)	110.49(9)	O(11)-Si(6)-O(6)	106.41(8)
O(1)-Si(1)-C(1)	108.86(9)	O(5)-Si(6)-C(31)	111.29(9)
Si(2)-O(1)-Si(1)	150.28(10)	O(11)-Si(6)-C(31)	111.24(9)
O(1)-Si(2)-O(11)	109.32(8)	O(6)-Si(6)-C(31)	109.26(8)
O(1)-Si(2)-O(2)	110.29(8)	Si(7)-O(6)-Si(6)	142.80(9)
O(11)-Si(2)-O(2)	106.07(7)	O(6)-Si(7)-O(13)	110.24(8)
O(1)-Si(2)-C(7)	109.36(9)	O(6)-Si(7)-O(7)	109.54(8)
O(11)-Si(2)-C(7)	110.36(8)	O(13)-Si(7)-O(7)	109.55(8)
O(2)-Si(2)-C(7)	111.39(8)	O(6)-Si(7)-C(37)	107.86(9)
Si(3)-O(2)-Si(2)	140.14(9)	O(13)-Si(7)-C(37)	112.24(9)
O(3)-Si(3)-O(2)	110.76(8)	O(7)-Si(7)-C(37)	107.34(8)
O(3)-Si(3)-O(12)	108.80(8)	Si(8)-O(7)-Si(7)	148.41(10)
O(2)-Si(3)-O(12)	108.71(8)	O(14)-Si(8)-O(7)	107.76(8)
O(3)-Si(3)-C(13)	106.50(9)	O(14)-Si(8)-O(8)	109.21(8)
O(2)-Si(3)-C(13)	106.84(9)	O(7)-Si(8)-O(8)	108.88(8)
O(12)-Si(3)-C(13)	115.21(8)	O(14)-Si(8)-C(43)	110.77(9)
Si(4)-O(3)-Si(3)	155.48(11)	O(7)-Si(8)-C(43)	109.38(8)
O(3)-Si(4)-O(14)	107.13(8)	O(8)-Si(8)-C(43)	110.78(8)
O(3)-Si(4)-O(4)	110.24(8)	Si(5)-O(8)-Si(8)	142.92(10)
O(14)-Si(4)-O(4)	109.09(8)	Si(1)-O(9)-Si(9)	147.19(10)
O(3)-Si(4)-C(19)	111.29(9)	O(10)-Si(9)-O(9)	111.25(8)
O(14)-Si(4)-C(19)	109.10(8)	O(10)-Si(9)-C(55)	110.99(9)
O(4)-Si(4)-C(19)	109.92(9)	O(9)-Si(9)-C(55)	106.91(10)
Si(1)-O(4)-Si(4)	151.63(10)	O(10)-Si(9)-C(49)	108.30(9)
O(8)-Si(5)-O(10)	108.76(8)	O(9)-Si(9)-C(49)	108.07(8)
O(8)-Si(5)-O(5)	109.57(8)	C(55)-Si(9)-C(49)	111.31(10)
O(10)-Si(5)-O(5)	108.43(8)	Si(5)-O(10)-Si(9)	146.17(10)
O(8)-Si(5)-C(25)	109.92(9)	Si(6)-O(11)-Si(2)	146.27(10)
O(10)-Si(5)-C(25)	111.36(9)	Si(3)-O(12)-Si(10)	145.12(10)

O(13)-Si(10)-O(12)	112.90(8)	C(21)-C(20)-C(19)	120.6(2)
O(13)-Si(10)-C(61)	108.40(9)	C(22)-C(21)-C(20)	119.9(3)
O(12)-Si(10)-C(61)	107.61(9)	C(23)-C(22)-C(21)	120.5(2)
O(13)-Si(10)-C(67)	109.80(9)	C(22)-C(23)-C(24)	119.8(2)
O(12)-Si(10)-C(67)	108.73(9)	C(23)-C(24)-C(19)	121.2(2)
C(61)-Si(10)-C(67)	109.32(9)	C(26)-C(25)-C(30)	117.7(2)
Si(7)-O(13)-Si(10)	165.23(11)	C(26)-C(25)-Si(5)	123.19(17)
Si(4)-O(14)-Si(8)	160.48(11)	C(30)-C(25)-Si(5)	119.05(16)
C(6)-C(1)-C(2)	118.0(2)	C(25)-C(26)-C(27)	121.0(2)
C(6)-C(1)-Si(1)	122.91(17)	C(28)-C(27)-C(26)	120.3(3)
C(2)-C(1)-Si(1)	119.05(17)	C(29)-C(28)-C(27)	119.4(2)
C(3)-C(2)-C(1)	120.9(2)	C(28)-C(29)-C(30)	120.3(2)
C(4)-C(3)-C(2)	119.7(3)	C(29)-C(30)-C(25)	121.3(2)
C(5)-C(4)-C(3)	120.3(2)	C(32)-C(31)-C(36)	117.9(2)
C(4)-C(5)-C(6)	120.3(3)	C(32)-C(31)-Si(6)	122.73(18)
C(5)-C(6)-C(1)	120.7(2)	C(36)-C(31)-Si(6)	119.41(19)
C(8)-C(7)-C(12)	117.9(2)	C(33)-C(32)-C(31)	120.8(3)
C(8)-C(7)-Si(2)	121.17(17)	C(34)-C(33)-C(32)	120.1(3)
C(12)-C(7)-Si(2)	120.73(16)	C(35)-C(34)-C(33)	120.0(3)
C(7)-C(8)-C(9)	121.0(2)	C(34)-C(35)-C(36)	119.9(3)
C(10)-C(9)-C(8)	119.9(3)	C(35)-C(36)-C(31)	121.3(3)
C(9)-C(10)-C(11)	120.3(2)	C(42)-C(37)-C(38)	117.9(2)
C(10)-C(11)-C(12)	119.7(2)	C(42)-C(37)-Si(7)	121.09(16)
C(11)-C(12)-C(7)	121.1(2)	C(38)-C(37)-Si(7)	120.79(16)
C(18)-C(13)-C(14)	117.5(2)	C(39)-C(38)-C(37)	120.7(2)
C(18)-C(13)-Si(3)	120.56(16)	C(40)-C(39)-C(38)	119.8(2)
C(14)-C(13)-Si(3)	121.53(17)	C(41)-C(40)-C(39)	120.5(2)
C(15)-C(14)-C(13)	121.5(2)	C(40)-C(41)-C(42)	119.9(2)
C(16)-C(15)-C(14)	119.7(2)	C(41)-C(42)-C(37)	121.2(2)
C(17)-C(16)-C(15)	120.3(2)	C(44)-C(43)-C(48)	117.18(19)
C(16)-C(17)-C(18)	119.7(3)	C(44)-C(43)-Si(8)	121.18(16)
C(17)-C(18)-C(13)	121.3(2)	C(48)-C(43)-Si(8)	121.58(15)
C(20)-C(19)-C(24)	118.0(2)	C(45)-C(44)-C(43)	121.9(2)
C(20)-C(19)-Si(4)	120.64(16)	C(46)-C(45)-C(44)	119.6(2)
C(24)-C(19)-Si(4)	120.82(17)	C(45)-C(46)-C(47)	120.2(2)

C(46)-C(47)-C(48)	119.7(2)	C(59)-C(60)-C(55)	120.5(3)
C(47)-C(48)-C(43)	121.4(2)	C(66)-C(61)-C(62)	117.5(2)
C(50)-C(49)-C(54)	117.3(2)	C(66)-C(61)-Si(10)	121.16(16)
C(50)-C(49)-Si(9)	123.05(17)	C(62)-C(61)-Si(10)	121.03(17)
C(54)-C(49)-Si(9)	119.68(18)	C(63)-C(62)-C(61)	120.8(2)
C(51)-C(50)-C(49)	120.8(2)	C(64)-C(63)-C(62)	120.6(2)
C(52)-C(51)-C(50)	120.7(3)	C(63)-C(64)-C(65)	119.4(2)
C(51)-C(52)-C(53)	119.9(2)	C(66)-C(65)-C(64)	120.5(2)
C(52)-C(53)-C(54)	119.5(3)	C(65)-C(66)-C(61)	121.2(2)
C(53)-C(54)-C(49)	121.8(3)	C(72)-C(67)-C(68)	118.0(2)
C(56)-C(55)-C(60)	118.0(3)	C(72)-C(67)-Si(10)	123.44(18)
C(56)-C(55)-Si(9)	120.1(2)	C(68)-C(67)-Si(10)	118.42(17)
C(60)-C(55)-Si(9)	121.8(2)	C(69)-C(68)-C(67)	120.7(2)
C(57)-C(56)-C(55)	121.4(3)	C(70)-C(69)-C(68)	120.1(3)
C(58)-C(57)-C(56)	120.0(3)	C(71)-C(70)-C(69)	119.9(3)
C(57)-C(58)-C(59)	119.7(3)	C(70)-C(71)-C(72)	120.3(3)
C(58)-C(59)-C(60)	120.4(3)	C(71)-C(72)-C(67)	120.9(2)

Table 5. Anisotropic displacement parameters ($Å^2 x 10^3$)for **3**. The anisotropic displacement factor exponent takes the form: $-2 \pi^2 [h^2 a^{*2} U^{11} + ... + 2 h k a^* b^* U^{12}]$

	U^{11}	U^{22}	U^{33}	U^{23}	U^{13}	U^{12}
Si(1)	17(1)	16(1)	17(1)	5(1)	4(1)	6(1)
O(1)	18(1)	30(1)	23(1)	10(1)	6(1)	6(1)
Si(2)	16(1)	14(1)	16(1)	4(1)	6(1)	4(1)
O(2)	27(1)	16(1)	19(1)	4(1)	9(1)	5(1)
Si(3)	16(1)	15(1)	14(1)	3(1)	4(1)	2(1)
O(3)	21(1)	25(1)	23(1)	1(1)	4(1)	-1(1)
Si(4)	14(1)	13(1)	18(1)	3(1)	4(1)	3(1)
O(4)	24(1)	25(1)	31(1)	16(1)	3(1)	3(1)
Si(5)	17(1)	16(1)	15(1)	4(1)	3(1)	3(1)
O(5)	22(1)	19(1)	22(1)	5(1)	2(1)	0(1)
Si(6)	15(1)	13(1)	16(1)	4(1)	6(1)	3(1)

O(6)	21(1)	18(1)	22(1)	10(1)	10(1)	8(1)
Si(7)	15(1)	14(1)	19(1)	6(1)	6(1)	5(1)
O(7)	16(1)	20(1)	32(1)	7(1)	7(1)	5(1)
Si(8)	14(1)	13(1)	18(1)	4(1)	6(1)	2(1)
O(8)	25(1)	26(1)	21(1)	7(1)	4(1)	-3(1)
O(9)	29(1)	29(1)	20(1)	3(1)	3(1)	13(1)
Si(9)	20(1)	22(1)	17(1)	6(1)	3(1)	8(1)
O(10)	22(1)	23(1)	23(1)	7(1)	3(1)	8(1)
O(11)	22(1)	17(1)	23(1)	2(1)	7(1)	7(1)
O(12)	20(1)	17(1)	26(1)	7(1)	4(1)	5(1)
Si(10)	19(1)	17(1)	17(1)	6(1)	6(1)	4(1)
O(13)	28(1)	23(1)	21(1)	6(1)	9(1)	5(1)
O(14)	25(1)	16(1)	35(1)	5(1)	16(1)	7(1)
C(1)	20(1)	17(1)	32(1)	6(1)	10(1)	4(1)
C(2)	43(1)	31(1)	35(1)	2(1)	11(1)	14(1)
C(3)	62(2)	30(1)	52(2)	-7(1)	28(2)	8(1)
C(4)	56(2)	25(1)	83(2)	10(1)	39(2)	21(1)
C(5)	45(2)	33(1)	73(2)	21(1)	20(2)	24(1)
C(6)	30(1)	26(1)	41(1)	12(1)	9(1)	11(1)
C(7)	24(1)	16(1)	23(1)	5(1)	11(1)	4(1)
C(8)	32(1)	45(2)	43(1)	26(1)	10(1)	6(1)
C(9)	50(2)	58(2)	70(2)	49(2)	24(2)	10(1)
C(10)	45(2)	31(1)	62(2)	16(1)	26(1)	-4(1)
C(11)	33(1)	37(1)	40(1)	1(1)	10(1)	-11(1)
C(12)	32(1)	31(1)	27(1)	6(1)	6(1)	-4(1)
C(13)	23(1)	22(1)	17(1)	4(1)	7(1)	6(1)
C(14)	34(1)	23(1)	30(1)	3(1)	14(1)	1(1)
C(15)	57(2)	20(1)	45(2)	-4(1)	23(1)	0(1)
C(16)	61(2)	32(1)	44(2)	-5(1)	29(1)	11(1)
C(17)	47(2)	43(2)	53(2)	-1(1)	35(1)	5(1)
C(18)	36(1)	28(1)	39(1)	-2(1)	21(1)	-3(1)
C(19)	19(1)	17(1)	26(1)	0(1)	8(1)	4(1)
C(20)	27(1)	37(1)	31(1)	7(1)	10(1)	2(1)
C(21)	44(2)	54(2)	42(2)	13(1)	24(1)	-3(1)
C(22)	30(1)	48(2)	61(2)	3(1)	26(1)	-7(1)

C(23)	20(1)	35(1)	50(2)	-3(1)	10(1)	0(1)
C(24)	21(1)	25(1)	33(1)	-2(1)	6(1)	5(1)
C(25)	23(1)	18(1)	22(1)	5(1)	6(1)	4(1)
C(26)	61(2)	53(2)	27(1)	-4(1)	-6(1)	38(2)
C(27)	107(3)	68(2)	25(1)	-8(1)	-5(2)	57(2)
C(28)	68(2)	36(1)	42(2)	4(1)	27(2)	23(1)
C(29)	28(1)	36(1)	70(2)	-7(1)	12(1)	12(1)
C(30)	29(1)	36(1)	45(2)	-13(1)	-4(1)	11(1)
C(31)	24(1)	21(1)	33(1)	14(1)	15(1)	9(1)
C(32)	41(1)	51(2)	37(1)	20(1)	24(1)	17(1)
C(33)	72(2)	78(2)	61(2)	42(2)	52(2)	40(2)
C(34)	57(2)	57(2)	115(3)	54(2)	65(2)	26(2)
C(35)	38(2)	50(2)	109(3)	20(2)	40(2)	-4(1)
C(36)	34(1)	39(2)	62(2)	7(1)	24(1)	-4(1)
C(37)	13(1)	17(1)	28(1)	6(1)	4(1)	4(1)
C(38)	25(1)	26(1)	34(1)	5(1)	9(1)	10(1)
C(39)	33(1)	38(1)	57(2)	0(1)	17(1)	18(1)
C(40)	41(2)	26(1)	89(2)	20(1)	21(2)	21(1)
C(41)	46(2)	36(2)	84(2)	40(2)	25(2)	21(1)
C(42)	32(1)	32(1)	50(2)	24(1)	18(1)	14(1)
C(43)	17(1)	17(1)	20(1)	5(1)	4(1)	2(1)
C(44)	45(1)	20(1)	48(2)	2(1)	31(1)	4(1)
C(45)	68(2)	17(1)	67(2)	-1(1)	41(2)	-2(1)
C(46)	41(1)	25(1)	54(2)	10(1)	20(1)	-10(1)
C(47)	29(1)	29(1)	43(1)	11(1)	19(1)	2(1)
C(48)	26(1)	21(1)	35(1)	6(1)	15(1)	6(1)
C(49)	25(1)	32(1)	15(1)	2(1)	5(1)	14(1)
C(50)	25(1)	43(1)	25(1)	4(1)	7(1)	6(1)
C(51)	25(1)	69(2)	30(1)	-5(1)	7(1)	3(1)
C(52)	29(1)	89(2)	29(1)	5(2)	-5(1)	23(2)
C(53)	48(2)	73(2)	36(2)	20(2)	-5(1)	28(2)
C(54)	37(1)	44(1)	31(1)	14(1)	2(1)	14(1)
C(55)	26(1)	35(1)	24(1)	15(1)	3(1)	4(1)
C(56)	58(2)	38(1)	32(1)	10(1)	8(1)	-6(1)
C(57)	83(3)	54(2)	45(2)	23(2)	6(2)	-23(2)

C(58)	45(2)	97(3)	65(2)	54(2)	5(2)	-18(2)
C(59)	40(2)	111(3)	83(2)	69(2)	33(2)	30(2)
C(60)	39(2)	57(2)	56(2)	37(2)	25(1)	22(1)
C(61)	21(1)	25(1)	22(1)	12(1)	8(1)	5(1)
C(62)	27(1)	28(1)	31(1)	10(1)	11(1)	8(1)
C(63)	29(1)	45(2)	50(2)	26(1)	12(1)	18(1)
C(64)	29(1)	60(2)	38(1)	21(1)	-2(1)	8(1)
C(65)	39(1)	42(2)	29(1)	4(1)	-3(1)	3(1)
C(66)	30(1)	28(1)	28(1)	7(1)	5(1)	7(1)
C(67)	21(1)	28(1)	22(1)	12(1)	5(1)	5(1)
C(68)	32(1)	37(1)	28(1)	6(1)	12(1)	5(1)
C(69)	38(1)	65(2)	35(1)	17(1)	22(1)	11(1)
C(70)	33(1)	62(2)	54(2)	27(2)	22(1)	-2(1)
C(71)	43(2)	40(2)	59(2)	14(1)	22(1)	-8(1)
C(72)	35(1)	30(1)	38(1)	8(1)	16(1)	-1(1)

Table 6. Torsion angles [°] for **3**.

O(9)-Si(1)-O(1)-Si(2)	-145.03(19)
O(4)-Si(1)-O(1)-Si(2)	-26.8(2)
C(1)-Si(1)-O(1)-Si(2)	94.1(2)
Si(1)-O(1)-Si(2)-O(11)	86.0(2)
Si(1)-O(1)-Si(2)-O(2)	-30.2(2)
Si(1)-O(1)-Si(2)-C(7)	-153.03(19)
O(1)-Si(2)-O(2)-Si(3)	75.01(16)
O(11)-Si(2)-O(2)-Si(3)	-43.26(17)
C(7)-Si(2)-O(2)-Si(3)	-163.37(14)
Si(2)-O(2)-Si(3)-O(3)	-42.97(17)
Si(2)-O(2)-Si(3)-O(12)	76.52(16)
Si(2)-O(2)-Si(3)-C(13)	-158.57(14)
O(2)-Si(3)-O(3)-Si(4)	27.9(3)
O(12)-Si(3)-O(3)-Si(4)	-91.6(3)
C(13)-Si(3)-O(3)-Si(4)	143.7(2)
Si(3)-O(3)-Si(4)-O(14)	70.2(3)
Si(3)-O(3)-Si(4)-O(4)	-48.4(3)
Si(3)-O(3)-Si(4)-C(19)	-170.6(2)
O(9)-Si(1)-O(4)-Si(4)	148.8(2)
O(1)-Si(1)-O(4)-Si(4)	28.9(3)
C(1)-Si(1)-O(4)-Si(4)	-91.0(2)
O(3)-Si(4)-O(4)-Si(1)	16.2(3)
O(14)-Si(4)-O(4)-Si(1)	-101.2(2)
C(19)-Si(4)-O(4)-Si(1)	139.2(2)
O(8)-Si(5)-O(5)-Si(6)	49.6(3)
O(10)-Si(5)-O(5)-Si(6)	168.2(2)
C(25)-Si(5)-O(5)-Si(6)	-70.6(3)
Si(5)-O(5)-Si(6)-O(11)	-120.2(3)
Si(5)-O(5)-Si(6)-O(6)	-4.1(3)
Si(5)-O(5)-Si(6)-C(31)	116.9(3)
O(5)-Si(6)-O(6)-Si(7)	-60.19(17)
O(11)-Si(6)-O(6)-Si(7)	57.40(17)
C(31)-Si(6)-O(6)-Si(7)	177.60(15)

Si(6)-O(6)-Si(7)-O(13)	-74.26(17)
Si(6)-O(6)-Si(7)-O(7)	46.35(17)
Si(6)-O(6)-Si(7)-C(37)	162.88(15)
O(6)-Si(7)-O(7)-Si(8)	-54.3(2)
O(13)-Si(7)-O(7)-Si(8)	66.7(2)
C(37)-Si(7)-O(7)-Si(8)	-171.14(19)
Si(7)-O(7)-Si(8)-O(14)	-35.6(2)
Si(7)-O(7)-Si(8)-O(8)	82.7(2)
Si(7)-O(7)-Si(8)-C(43)	-156.10(19)
O(10)-Si(5)-O(8)-Si(8)	-126.09(17)
O(5)-Si(5)-O(8)-Si(8)	-7.7(2)
C(25)-Si(5)-O(8)-Si(8)	111.76(17)
O(14)-Si(8)-O(8)-Si(5)	71.49(19)
O(7)-Si(8)-O(8)-Si(5)	-45.92(19)
C(43)-Si(8)-O(8)-Si(5)	-166.24(16)
O(4)-Si(1)-O(9)-Si(9)	-80.0(2)
O(1)-Si(1)-O(9)-Si(9)	39.3(2)
C(1)-Si(1)-O(9)-Si(9)	159.49(19)
Si(1)-O(9)-Si(9)-O(10)	48.0(2)
Si(1)-O(9)-Si(9)-C(55)	-73.4(2)
Si(1)-O(9)-Si(9)-C(49)	166.7(2)
O(8)-Si(5)-O(10)-Si(9)	117.13(18)
O(5)-Si(5)-O(10)-Si(9)	-1.9(2)
C(25)-Si(5)-O(10)-Si(9)	-121.59(18)
O(9)-Si(9)-O(10)-Si(5)	-67.3(2)
C(55)-Si(9)-O(10)-Si(5)	51.6(2)
C(49)-Si(9)-O(10)-Si(5)	174.09(17)
O(5)-Si(6)-O(11)-Si(2)	-49.92(19)
O(6)-Si(6)-O(11)-Si(2)	-168.02(16)
C(31)-Si(6)-O(11)-Si(2)	73.07(19)
O(1)-Si(2)-O(11)-Si(6)	43.3(2)
O(2)-Si(2)-O(11)-Si(6)	162.16(16)
C(7)-Si(2)-O(11)-Si(6)	-77.06(19)
O(3)-Si(3)-O(12)-Si(10)	-4.2(2)
O(2)-Si(3)-O(12)-Si(10)	-124.91(17)
C(13)-Si(3)-O(12)-Si(10)	115.26(18)

Si(3)-O(12)-Si(10)-O(13)	82.27(19)
Si(3)-O(12)-Si(10)-C(61)	-158.16(16)
Si(3)-O(12)-Si(10)-C(67)	-39.8(2)
O(6)-Si(7)-O(13)-Si(10)	97.1(4)
O(7)-Si(7)-O(13)-Si(10)	-23.5(4)
C(37)-Si(7)-O(13)-Si(10)	-142.7(4)
O(12)-Si(10)-O(13)-Si(7)	-69.4(4)
C(61)-Si(10)-O(13)-Si(7)	171.5(4)
C(67)-Si(10)-O(13)-Si(7)	52.1(4)
O(3)-Si(4)-O(14)-Si(8)	-162.4(3)
O(4)-Si(4)-O(14)-Si(8)	-43.1(3)
C(19)-Si(4)-O(14)-Si(8)	77.0(3)
O(7)-Si(8)-O(14)-Si(4)	156.6(3)
O(8)-Si(8)-O(14)-Si(4)	38.5(3)
C(43)-Si(8)-O(14)-Si(4)	-83.8(3)
O(9)-Si(1)-C(1)-C(6)	1.0(2)
O(4)-Si(1)-C(1)-C(6)	-117.69(19)
O(1)-Si(1)-C(1)-C(6)	122.09(19)
O(9)-Si(1)-C(1)-C(2)	-177.88(19)
O(4)-Si(1)-C(1)-C(2)	63.4(2)
O(1)-Si(1)-C(1)-C(2)	-56.8(2)
C(6)-C(1)-C(2)-C(3)	0.4(4)
Si(1)-C(1)-C(2)-C(3)	179.3(2)
C(1)-C(2)-C(3)-C(4)	0.5(4)
C(2)-C(3)-C(4)-C(5)	-1.0(5)
C(3)-C(4)-C(5)-C(6)	0.7(5)
C(4)-C(5)-C(6)-C(1)	0.2(4)
C(2)-C(1)-C(6)-C(5)	-0.7(4)
Si(1)-C(1)-C(6)-C(5)	-179.64(19)
O(1)-Si(2)-C(7)-C(8)	-11.5(2)
O(11)-Si(2)-C(7)-C(8)	108.80(19)
O(2)-Si(2)-C(7)-C(8)	-133.66(19)
O(1)-Si(2)-C(7)-C(12)	174.37(17)
O(11)-Si(2)-C(7)-C(12)	-65.34(19)
O(2)-Si(2)-C(7)-C(12)	52.20(19)
C(12)-C(7)-C(8)-C(9)	0.1(4)

Si(2)-C(7)-C(8)-C(9)	-174.2(2)
C(7)-C(8)-C(9)-C(10)	1.3(5)
C(8)-C(9)-C(10)-C(11)	-1.9(5)
C(9)-C(10)-C(11)-C(12)	1.0(4)
C(10)-C(11)-C(12)-C(7)	0.4(4)
C(8)-C(7)-C(12)-C(11)	-1.0(3)
Si(2)-C(7)-C(12)-C(11)	173.37(19)
O(3)-Si(3)-C(13)-C(18)	21.9(2)
O(2)-Si(3)-C(13)-C(18)	140.33(18)
O(12)-Si(3)-C(13)-C(18)	-98.82(19)
O(3)-Si(3)-C(13)-C(14)	-150.36(18)
O(2)-Si(3)-C(13)-C(14)	-31.9(2)
O(12)-Si(3)-C(13)-C(14)	88.91(19)
C(18)-C(13)-C(14)-C(15)	0.5(4)
Si(3)-C(13)-C(14)-C(15)	173.0(2)
C(13)-C(14)-C(15)-C(16)	-1.6(4)
C(14)-C(15)-C(16)-C(17)	2.3(5)
C(15)-C(16)-C(17)-C(18)	-1.9(5)
C(16)-C(17)-C(18)-C(13)	0.8(5)
C(14)-C(13)-C(18)-C(17)	-0.1(4)
Si(3)-C(13)-C(18)-C(17)	-172.7(2)
O(3)-Si(4)-C(19)-C(20)	-35.9(2)
O(14)-Si(4)-C(19)-C(20)	82.14(19)
O(4)-Si(4)-C(19)-C(20)	-158.29(17)
O(3)-Si(4)-C(19)-C(24)	152.98(16)
O(14)-Si(4)-C(19)-C(24)	-89.02(18)
O(4)-Si(4)-C(19)-C(24)	30.55(19)
C(24)-C(19)-C(20)-C(21)	0.7(3)
Si(4)-C(19)-C(20)-C(21)	-170.7(2)
C(19)-C(20)-C(21)-C(22)	0.5(4)
C(20)-C(21)-C(22)-C(23)	-1.1(4)
C(21)-C(22)-C(23)-C(24)	0.5(4)
C(22)-C(23)-C(24)-C(19)	0.8(4)
C(20)-C(19)-C(24)-C(23)	-1.3(3)
Si(4)-C(19)-C(24)-C(23)	170.04(17)
O(8)-Si(5)-C(25)-C(26)	97.8(2)

O(10)-Si(5)-C(25)-C(26)	-22.8(3)
O(5)-Si(5)-C(25)-C(26)	-142.2(2)
O(8)-Si(5)-C(25)-C(30)	-79.3(2)
O(10)-Si(5)-C(25)-C(30)	160.06(19)
O(5)-Si(5)-C(25)-C(30)	40.6(2)
C(30)-C(25)-C(26)-C(27)	-0.9(5)
Si(5)-C(25)-C(26)-C(27)	-178.1(3)
C(25)-C(26)-C(27)-C(28)	-0.7(6)
C(26)-C(27)-C(28)-C(29)	1.9(5)
C(27)-C(28)-C(29)-C(30)	-1.6(5)
C(28)-C(29)-C(30)-C(25)	0.0(5)
C(26)-C(25)-C(30)-C(29)	1.2(4)
Si(5)-C(25)-C(30)-C(29)	178.6(2)
O(5)-Si(6)-C(31)-C(32)	-19.9(2)
O(11)-Si(6)-C(31)-C(32)	-141.52(18)
O(6)-Si(6)-C(31)-C(32)	101.29(19)
O(5)-Si(6)-C(31)-C(36)	161.07(18)
O(11)-Si(6)-C(31)-C(36)	39.5(2)
O(6)-Si(6)-C(31)-C(36)	-77.7(2)
C(36)-C(31)-C(32)-C(33)	1.3(4)
Si(6)-C(31)-C(32)-C(33)	-177.7(2)
C(31)-C(32)-C(33)-C(34)	-0.3(4)
C(32)-C(33)-C(34)-C(35)	-0.3(5)
C(33)-C(34)-C(35)-C(36)	-0.1(5)
C(34)-C(35)-C(36)-C(31)	1.1(5)
C(32)-C(31)-C(36)-C(35)	-1.7(4)
Si(6)-C(31)-C(36)-C(35)	177.4(2)
O(6)-Si(7)-C(37)-C(42)	166.43(18)
O(13)-Si(7)-C(37)-C(42)	44.8(2)
O(7)-Si(7)-C(37)-C(42)	-75.6(2)
O(6)-Si(7)-C(37)-C(38)	-19.36(19)
O(13)-Si(7)-C(37)-C(38)	-140.98(17)
O(7)-Si(7)-C(37)-C(38)	98.60(18)
C(42)-C(37)-C(38)-C(39)	0.0(3)
Si(7)-C(37)-C(38)-C(39)	-174.36(18)
C(37)-C(38)-C(39)-C(40)	-0.1(4)

C(38)-C(39)-C(40)-C(41)	-0.3(4)
C(39)-C(40)-C(41)-C(42)	0.7(5)
C(40)-C(41)-C(42)-C(37)	-0.7(4)
C(38)-C(37)-C(42)-C(41)	0.3(4)
Si(7)-C(37)-C(42)-C(41)	174.7(2)
O(14)-Si(8)-C(43)-C(44)	-174.10(18)
O(7)-Si(8)-C(43)-C(44)	-55.5(2)
O(8)-Si(8)-C(43)-C(44)	64.6(2)
O(14)-Si(8)-C(43)-C(48)	8.7(2)
O(7)-Si(8)-C(43)-C(48)	127.30(17)
O(8)-Si(8)-C(43)-C(48)	-112.68(18)
C(48)-C(43)-C(44)-C(45)	1.0(4)
Si(8)-C(43)-C(44)-C(45)	-176.3(2)
C(43)-C(44)-C(45)-C(46)	0.5(5)
C(44)-C(45)-C(46)-C(47)	-1.7(5)
C(45)-C(46)-C(47)-C(48)	1.3(4)
C(46)-C(47)-C(48)-C(43)	0.2(4)
C(44)-C(43)-C(48)-C(47)	-1.4(3)
Si(8)-C(43)-C(48)-C(47)	175.99(18)
O(10)-Si(9)-C(49)-C(50)	29.3(2)
O(9)-Si(9)-C(49)-C(50)	-91.30(19)
C(55)-Si(9)-C(49)-C(50)	151.60(18)
O(10)-Si(9)-C(49)-C(54)	-149.85(18)
O(9)-Si(9)-C(49)-C(54)	89.53(19)
C(55)-Si(9)-C(49)-C(54)	-27.6(2)
C(54)-C(49)-C(50)-C(51)	0.2(3)
Si(9)-C(49)-C(50)-C(51)	-179.00(18)
C(49)-C(50)-C(51)-C(52)	0.0(4)
C(50)-C(51)-C(52)-C(53)	0.1(4)
C(51)-C(52)-C(53)-C(54)	-0.5(4)
C(52)-C(53)-C(54)-C(49)	0.7(4)
C(50)-C(49)-C(54)-C(53)	-0.6(4)
Si(9)-C(49)-C(54)-C(53)	178.7(2)
O(10)-Si(9)-C(55)-C(56)	-154.12(18)
O(9)-Si(9)-C(55)-C(56)	-32.6(2)
C(49)-Si(9)-C(55)-C(56)	85.2(2)

O(10)-Si(9)-C(55)-C(60)	27.5(2)
O(9)-Si(9)-C(55)-C(60)	148.94(19)
C(49)-Si(9)-C(55)-C(60)	-93.3(2)
C(60)-C(55)-C(56)-C(57)	0.2(4)
Si(9)-C(55)-C(56)-C(57)	-178.3(2)
C(55)-C(56)-C(57)-C(58)	-1.1(5)
C(56)-C(57)-C(58)-C(59)	0.9(5)
C(57)-C(58)-C(59)-C(60)	0.1(5)
C(58)-C(59)-C(60)-C(55)	-0.9(5)
C(56)-C(55)-C(60)-C(59)	0.8(4)
Si(9)-C(55)-C(60)-C(59)	179.2(2)
O(13)-Si(10)-C(61)-C(66)	155.60(17)
O(12)-Si(10)-C(61)-C(66)	33.2(2)
C(67)-Si(10)-C(61)-C(66)	-84.7(2)
O(13)-Si(10)-C(61)-C(62)	-30.8(2)
O(12)-Si(10)-C(61)-C(62)	-153.20(17)
C(67)-Si(10)-C(61)-C(62)	88.87(19)
C(66)-C(61)-C(62)-C(63)	-0.3(3)
Si(10)-C(61)-C(62)-C(63)	-174.16(18)
C(61)-C(62)-C(63)-C(64)	0.0(4)
C(62)-C(63)-C(64)-C(65)	0.3(4)
C(63)-C(64)-C(65)-C(66)	-0.3(4)
C(64)-C(65)-C(66)-C(61)	0.0(4)
C(62)-C(61)-C(66)-C(65)	0.3(3)
Si(10)-C(61)-C(66)-C(65)	174.16(19)
O(13)-Si(10)-C(67)-C(72)	10.1(2)
O(12)-Si(10)-C(67)-C(72)	134.13(19)
C(61)-Si(10)-C(67)-C(72)	-108.7(2)
O(13)-Si(10)-C(67)-C(68)	-174.45(16)
O(12)-Si(10)-C(67)-C(68)	-50.47(19)
C(61)-Si(10)-C(67)-C(68)	66.75(19)
C(72)-C(67)-C(68)-C(69)	1.0(3)
Si(10)-C(67)-C(68)-C(69)	-174.69(19)
C(67)-C(68)-C(69)-C(70)	-0.1(4)
C(68)-C(69)-C(70)-C(71)	-1.2(4)
C(69)-C(70)-C(71)-C(72)	1.6(5)

C(70)-C(71)-C(72)-C(67)	-0.7(4)
C(68)-C(67)-C(72)-C(71)	-0.6(4)
Si(10)-C(67)-C(72)-C(71)	174.9(2)

Conclusion of part 3

3.3.1. Conclusion of part 3

Siloxane compounds containing T structure are called silsesquioxanes. In siloxane polymer, T structure is very important to control degree of crosslinking. It is very difficult to synthesize well-defined polymer including silsesquioxanes (T type) because silsesquioxane has possible structures as random structure, ladder structure, and cage structure as illustrated in Figure 1 [1]. Therefore relationship with well-defined structure and properties are almost unknown. In previous ladder-type silsesquioxane polymers, there has been no unequivocal evidence of real ladder structure. Our laboratory reported synthesis, structure determination of up to nonacyclic laddersiloxane [2]. And we also reported thermal stability of these compounds increases with the numbers of rings. If relationship with well-defined siloxane structure and several properties are elucidated, it is very useful to apply to design siloxane monomer and polymer.

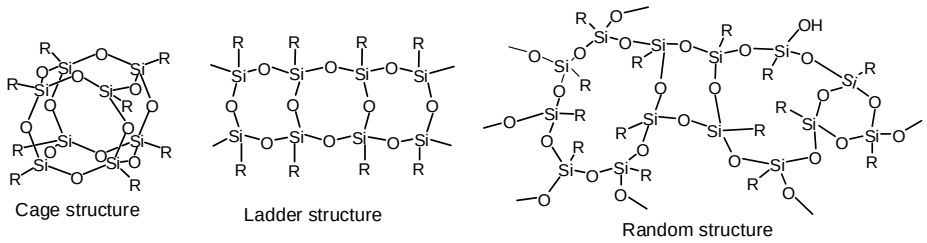

Figure 1

Therefore, in this part, we attempted to elucidate relationship with well-defined siloxane structure and several properties (refractive index and thermal stability).

We elucidated that RI (refractive index) values of these siloxane compounds slightly increase as ring number increases (Figure 2). However, the RI values is almost unchanged by changing siloxane structure. Therefore, it is better to change substituents to high RI.

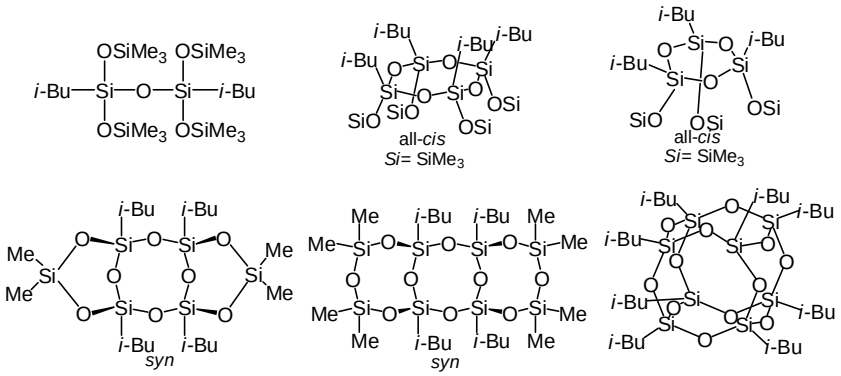

Figure 2

Thermal analysis of the phenyl-substituted siloxane compounds showed their high thermal stability (Figure 3). The results show that a higher Td_5 (5% weight loss) temperature was observed with a higher inorganic component ratio (Si and O % ratio). And phenyl substituted siloxane compound is more stable than alkyl substituted siloxane.

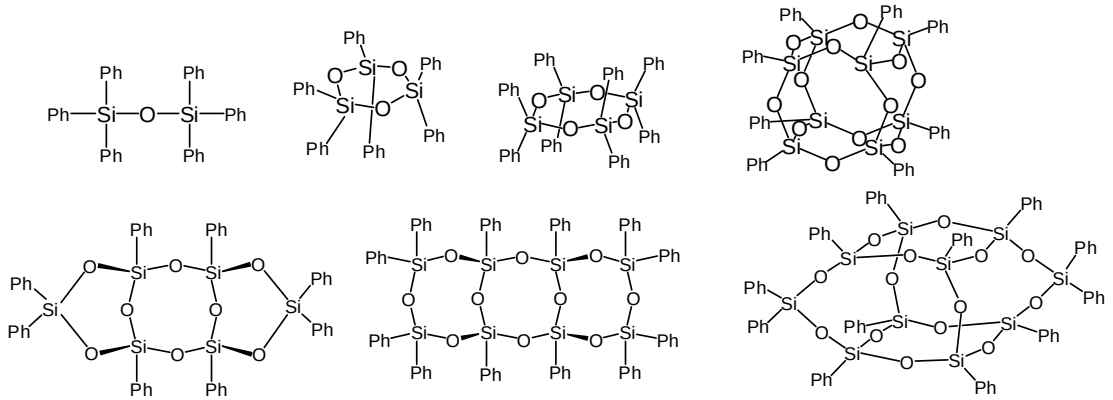

Figure 3

Information of RI and thermal stability are very useful to apply to LED encapsulate. LED (light emitting diode) is used as illumination lamp [3].

In our results, RI was almost similar by different siloxane structures. However changing substituents was effective for increase RI values. For example, RI of organic polymer is about 1.4–1.6, however RI of TiO_2 is 2.45–2.70, ZrO is 2.2, ZnO is 2.2 [4]. Therefore silicone polymer introduced Ti atom is promising as next generation LED encapsulate.

Previously, Ti atom introduced double-decker type polysilsesquioxane is reported (Scheme 1) [5]. In this method, the polymer precipitated as insoluble solid in organic solvent. Insoluble solid is difficult to apply LED encapsulate. And in the reaction, isopropyl alcohol is generated. It is caused harmful effect.

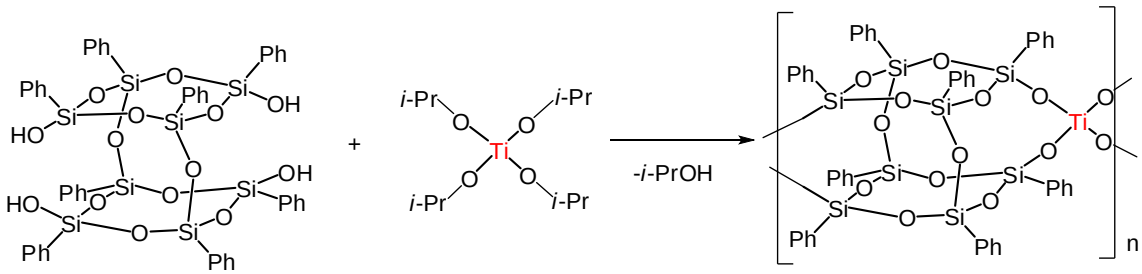

Scheme 1

We propose new titanium siloxane polymer by hydrosilylation (Scheme 2). The new polymer has Ti atom, many phenyl group, and double-decker structure. The polymer is maybe high refractive index and high thermal stability.

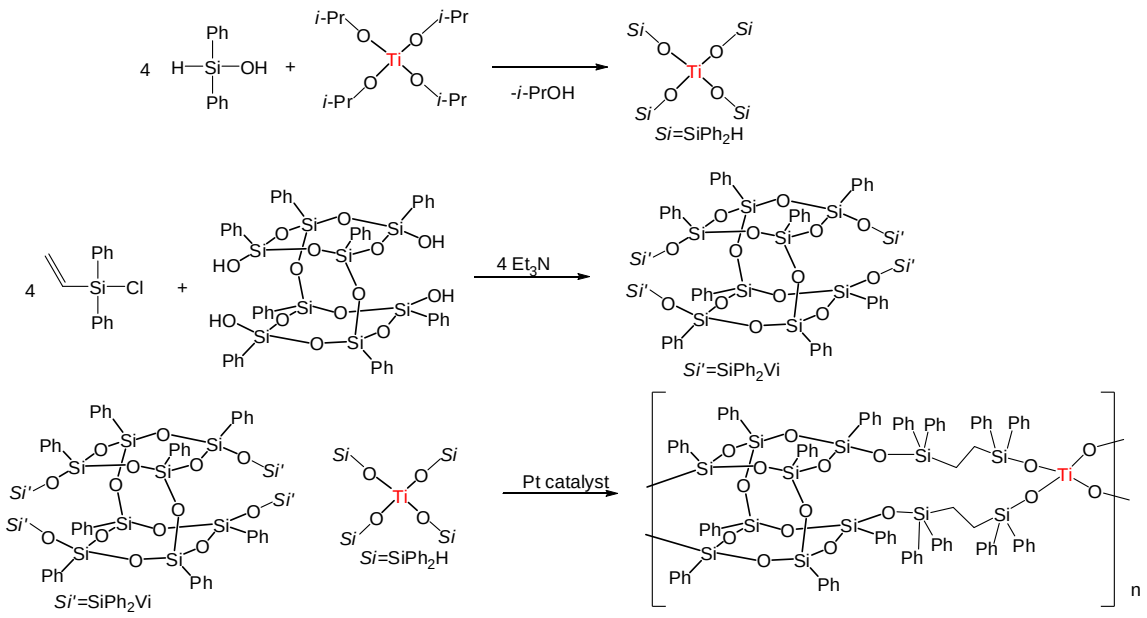

Scheme 2

3.3.2. References

[1] 技術情報協会 “ケイ素化合物の選定と最適利用技術 -応用事例集- <上巻>” 技術情報協会 (2006). *Gijyutu Jyouhou Kyoukai Ed.*, “*Keiso kagoubutsu no sentei to saiteki riyo gijyutsu –ouyou jirei shu jyoukan*”, *Gijyutu Jjyouhou Kyoukai*, Tokyo, Japan, **2006**.

[2] M. Unno, A. Suto, T. Matsumoto, *Russ. Chem. Rev.*, **2013**, *82*, 289.

[3] E. F. Schubert, “Light-emitting diodes, second edition”, Cambridge University Press, Cambridge, **2006**.

[4] 渡辺敏行，魚津吉弘 “光学材料の屈折率制御技術の最前線”，株式会社シーエムシー出版 (2009). T. Watanabe, and Y. Uozu, Ed, “Frontiers of refractive index control in optical materials (*Kogaku zairyo no kussetsuritsu seigyo gijutsu no saizensen*)”, *CMC Shuppan*, Tokyo, Japan, **2009.**

[5] M. T. Hay, B. Seurer, D. Holmes, A. Lee, Macromolecules, **2010**, *43*, 2108.

Acknowledgement

This thesis summarizes my study that has been carried out under the direction of Prof. Masafumi Unno at Gunma University, during the period of April 2012 to December 2014.

I would like to express my sincere gratitude to my supervisor, Prof. Masafumi Unno for providing me this precious study opportunity as a Ph.D student in his laboratory.

I especially would like to express my deepest appreciation to Prof. Nobuhiro Takeda at Gunma University for his elaborated guidance, considerable encouragement and invaluable discussion that make my research of great achievement and my study life unforgettable.

To Prof. Soichiro Kyushin, Prof. Hideki Amii, Prof. Takako Kudo, Prof. Minoru Yamaji at Gunma University, their meticulous comments were an enormous help to me.

I am grateful to Momentive Performance Materials Japan for measuring refractive indices.

Prof. Shinichi Kondo at Yamagata University gives me constructive comments and warm encouragement.

I would like to thanks to all members of Unno Laboratory for their supports and communication.

I would like to thank to Mr. Hiroshi Nishizawa who was my teacher of elementary school and junior high school, and Mr. Hideshi Shinoyama who was my teacher of senior high school for guiding me to chemistry world.

Finally I would like to extend my indebtedness to my mother, Mrs. Sayoko Endo for her endless love, understanding, support, encouragement, and sacrifice throughout my study.

Hisayuki Endo

Department of Chemistry and Chemical Biology
Graduate School of Engineering
Gunma University
2014

List of publications

[Part 2, chapter 3]

[1] “Effective Synthesis and Isomerization of Cyclotetrasiloxanetetraol"
Hisayuki Endo and Masafumi Unno, *Key Eng. Mater.*, **2013**, *534*, 66.

[Part 3, chapter 1]

[2] “Refractive Indices of Silsesquioxanes with Various Structures”
Hisayuki Endo, Nobuhiro Takeda, Masanori Takanashi, Takafumi Imai, Masafumi Unno, *Silicon, in press* **2014**.

[Part 3, chapter 2]

[3] “Synthesis and Properties of Phenylsilsesquioxanes with Ladder and Double-Decker Structures”
Hisayuki Endo, Nobuhiro Takeda, and Masafumi Unno, *Organometallics*, **2014**, *33*, 4148.

[Other publication]

[4] “Synthesis and Structures of Extended Cyclic Siloxanes”
Masafumi Unno, Hisayuki Endo, and Nobuhiro Takeda, *Heteroatom Chem.*, **2014**, *25*, 525.

[5] “Effects of Organic Silicon Compounds as Additives on Charge–discharge Cycling Efficiencies of Lithium in Nonaqueous Electrolytes for Rechargeable Lithium Cells”
Ryota Yanagisawa, Hisayuki Endo, Masafumi Unno, Hideyuki Morimoto, and Shin-ichi Tobishima, *J. Power Sources*, **2014**, *266*, 232.

Contribution to conferences and meetings

In master course

[Domestic conference]

[1] Hisayuki Endo, Nobuhiro Takeda, and Masafumi Unno, Poster presentation, ”かご状シルセスキオキサンの選択的合成”, 日本化学会 第 91 春季年会, Kanagawa Japan, Mar. 2011.

[2] Hisayuki Endo, Nobuhiro Takeda, and Masafumi Unno, Oral presentation, “T4 骨格を有する新規シルセスキオキサンの立体異性化反応の検討”, 日本化学会 第 92 春季年会, Kanagawa Japan, Mar. 2012.

[International conference]

[1] Hisayuki Endo, and Masafumi Unno, Poster presentation, “Approach to Molecule Encapsulated Cage Silsesquioxane”, 6th International Symposium on Silicon Science, Gunma Japan, Dec. 2010.

[2] Hisayuki Endo, and Masafumi Unno, Poster presentation, “Syntheses and Reactivity of Cyclic Tetrasiloxanetetraols Containing Various Organic Substituents”, 16th International Symposium on Silicon Chemistry (ISOS XVI), Hamilton Canada, Aug. 2011.

[3] Hisayuki Endo, and Masafumi Unno, Short oral presentation, “Syntheses and Reactivity of Cyclic Tetrasiloxanetetraols Containing Various Organic Substituents”, 16th International Symposium on Silicon Chemistry (ISOS XVI), Hamilton Canada, Aug. 2011.

[4] Hisayuki Endo, Yoshiteru Kawakami, Nobuhiro Takeda, and Masafumi Unno, Poster presentation, “Syntheses and Reactivity of Cyclic Tetrasiloxanetetraols Containing Various Organic Substituents” The First International Symposium on Element Innovation, Gunma Japan, Dec. 2011.

[Poster prize]

[1] Hisayuki Endo, and Masafumi Unno, Poster presentation, “Syntheses and Reactivity of Cyclic Tetrasiloxanetetraols Containing Various Organic Substituents”, 16th International Symposium on Silicon Chemistry (ISOS XVI), Hamilton Canada, Aug. 2011.

In doctoral course

[Domestic conference]

[1]Hisayuki Endo, Nobuhiro Takeda, and Masafumi Unno, Poster presentation, “様々な構造を持つシルセスキオキサンの合成と物性”, 第 17 回ケイ素化学協会シンポジウム, Kanagawa Japan, Oct. 2013.

[2]Hisayuki Endo, Nobuhiro Takeda, and Masafumi Unno, Poster presentation, “環状シラノールの異性化反応の検討、およびメカニズムの解明”, 第 18 回ケイ素化学協会シンポジウム, Tochigi Japan, Oct. 2014.

[3]Hisayuki Endo, Nobuhiro Takeda, and Masafumi Unno, Poster presentation, ”環状シラノールの異性化反応の詳細”, 日本化学会関東支部群馬地区地域懇談会, Gunma Japan, Dec. 2014.

[International conference]

[1]Hisayuki Endo, Nobuhiro Takeda, and Masafumi Unno, Poster presentation, “Synthesis and reactivity of new silsesquioxanes with T_4 framework”, THE 10TH INTERNATIONAL CONFERENCE ON HETEROATOM CHEMISTRY (ICHAC-10), Kyoto Japan, May 2012.

[2]Hisayuki Endo, Nobuhiro Takeda, and Masafumi Unno, Poster presentation, “Approach to Novel Silsesquioxanes”, 6TH EUROPEAN SILICON DAYS, Lyon France, Sep. 2012.

[3]Hisayuki Endo, Nobuhiro Takeda, and Masafumi Unno, Poster presentation, “Stereoisomerization Reaction of Cyclotetrasiloxanes”, The Second International Symposium on Element Innovation, Gunma Japan, Oct. 2012.

[4]Hisayuki Endo, Nobuhiro Takeda, and Masafumi Unno, Poster presentation, “Selective Synthesis of Disiloxanetetraol and New Cyclic Silanol”, The 4th Asian Silicon Symposium (ASiS-4), Ibaraki Japan, Oct. 2012.

[5]Hisayuki Endo, Nobuhiro Takeda, and Masafumi Unno, Poster presentation, ”Facile Synthesis of Disiloxanetetraol”, 45th Silicon Symposium, Texas The United States of America, May 2013.

[6]Hisayuki Endo, Nobuhiro Takeda, and Masafumi Unno, Poster presentation, “Synthesis of Various Cyclotrisiloxanetriols”, 45th Silicon Symposium, Texas The United States of America, May 2013.

[7]Hisayuki Endo, Nobuhiro Takeda, and Masafumi Unno, Poster presentation, “Reflective Index of Siloxane Compounds Having Various Structures”, The Third International Symposium on Element Innovation, Gunma Japan, Sep. 2013.

[8]Hisayuki Endo, Nobuhiro Takeda, and Masafumi Unno, Poster presentation, “Chemistry of cyclotetrasiloxanetetraols”, ISOS XVII BERLIN 2014 (The 17th International Symposium on Silicon Chemistry), Berlin Germany, Aug. 2014.
[9]Hisayuki Endo, Nobuhiro Takeda, and Masafumi Unno, Short oral presentation, “Chemistry of cyclotetrasiloxanetetraols”, ISOS XVII BERLIN 2014 (The 17th International Symposium on Silicon Chemistry) Berlin, Germany, Aug. 2014.
[10]Hisayuki Endo, Nobuhiro Takeda, and Masafumi Unno, Poster presentation, “Relationship between physical properties and siloxane structures”, ISOS XVII BERLIN 2014 (The 17th International Symposium on Silicon Chemistry), Berlin Germany, Aug. 2014.
[11]Hisayuki Endo, Nobuhiro Takeda, and Masafumi Unno, Poster presentation, “Stereoisomerization of Cyclic Silanols”, The Fourth International Symposium on Element Innovation, Gunma Japan, Oct. 2014.